

www.büronauten.pc-ware.de

Intelligente Prozesse. Die Büronauten. PC-WARE

www.ijceronline.com

International Journal of Computational Engineering Research (IJCER)

Frequency: 12 issues per year

Volume 3, Issue 4, April, 2013



IJCER

ISSN: 2250-3005



Editorial Board

Editor-In-Chief

Prof. Chetan Sharma

Specialization: Electronics Engineering, India
Qualification: Ph.d, Nanotechnology, IIT Delhi, India

Editorial Committees

DR.Qais Faryadi

Qualification: PhD Computer Science
Affiliation: USIM(Islamic Science University of Malaysia)

Dr. Lingyan Cao

Qualification: Ph.D. Applied Mathematics in Finance
Affiliation: University of Maryland College Park,MD, US

Dr. A.V.L.N.S.H. HARIHARAN

Qualification: Phd Chemistry
Affiliation: GITAM UNIVERSITY, VISAKHAPATNAM, India

DR. MD. MUSTAFIZUR RAHMAN

Qualification: Phd Mechanical and Materials Engineering
Affiliation: University Kebangsaan Malaysia (UKM)

Dr. S. Morteza Bayareh

Qualificatio: Phd Mechanical Engineering, IUT
Affiliation: Islamic Azad University, Lamerd Branch
Daneshjoo Square, Lamerd, Fars, Iran

Dr. Zahéra Mekkioui

Qualification: Phd Electronics
Affiliation: University of Tlemcen, Algeria

Dr. Yilun Shang

Qualification: Postdoctoral Fellow Computer Science
Affiliation: University of Texas at San Antonio, TX 78249

Lugen M.Zake Sheet

Qualification: Phd, Department of Mathematics
Affiliation: University of Mosul, Iraq

Mohamed Abdellatif

Qualification: PhD Intelligence Technology
Affiliation: Graduate School of Natural Science and Technology

Meisam Mahdavi

Qualification: Phd Electrical and Computer Engineering
Affiliation: University of Tehran, North Kargar st. (across the ninth lane), Tehran, Iran

Dr. Ahmed Nabih Zaki Rashed

Qualification: Ph. D Electronic Engineering
Affiliation: Menoufia University, Egypt

Dr. José M. Merigó Lindahl

Qualification: Phd Business Administration
Affiliation: Department of Business Administration, University of Barcelona, Spain

Dr. Mohamed Shokry Nayle

Qualification: Phd, Engineering
Affiliation: faculty of engineering Tanta University Egypt

CONTENTS :

S.No	Title Name	Page No.
1.	Development of Software-Based University Research Tools for Metocean Engineering Applications: A Reflective Case Study E.S.Lim , M.S.Liew, G.Dinis Jr.	01-5
2.	A RELIABLE NODE-DISJOINT MULTIPATH ROUTING PROTOCOL FOR MANET A.Monisha , K.Vijayalakshmi	6-10
3.	Mining Temporal Patterns for Interval-Based and Point-Based Events S.Kalaivani , M.Gomathi , R.Sethukkarasi	11-16
4.	Application of Matrix Iterative-Inversion in Solving Eigenvalue Problems in Structural Engineering O. M. Ibearugbulem , L. O. Ettu, J. C. Ezeh , U. C. Anya	17-22
5.	Path Planning Optimization Using Genetic Algorithm – A Literature Review Er. Waghoo Parvez , Er. Sonal Dhar	23-28
6.	Low Cost and Simple Management and Security System for Hospitals and Hotels Adnan Affandi , Mubashshir Husain	29-40
7.	Standardization of Systems and Processes for CDR Based Billing System in Telecom Companies K.V.V.Satyanarayana , Hashmi Vallipalli , A.Shivarama rao	41-44
8.	Integral Solutions of the Non Homogeneous Ternary Quintic Equation S.Vidhyalakshmi , K.Lakshmi , M,A.Gopalan	45-50
9.	Integral Solutions of Non-Homogeneous Biquadratic Equation With Four Unknowns M.A.Gopalan , G.Sumathi , S.Vidhyalakshmi	51-56
10.	Prediction of Number of Faults And Time To Remove Errors Nirvikar Katiyar , Dr. Raghuraj Singh	57-65
11.	Enhancement of Error Detection and Correction Capability Using Orthogonal Code Convolution Mukesh Gholase , L.P.Thakare, Dr. A.Y. Deshmukh	66-71
12.	Improving Features of Media Player Mr. Juned A. Khan , Prof . V. S. Gulhane	72-76
13.	Analysis Of Metal Cutting Tools Reliability During Processing By Turning In Laboratory Conditions And Exploitation Roshan Patel, Urvish Patel	77-80

14.	Numerical Statistic Approach for Expert System in Rainfall Prediction Based On Data Series Indrabayu , Nadjamuddin Harun , M. Saleh Pallu, Andani Achmad	81-87
15.	Study of Two Different Methods for Iris Recognition Support Vector Machine and Phase Based Method Gaganpreet kaur , Dilpreet kaur , Dheerendra singh	88-94
16.	Study Of Hybrid Genetic Algorithm Using Artificial Neural Network In Data Mining For The Diagnosis Of Stroke Disease Mr. Deepak Dhanwani , Prof. Avinash Wadhe	95-100
17.	Structural Analysis of a Milling Cutter Using FEA Chittibomma. Tirumalaneelam, Tippa Bhimasankara Rao	101-105
18.	A Review Paper on Various Approaches for Image Mosaicing Ms. Parul M.Jain , Prof. Vijaya K.Shandliya	106-109
19.	The Distance Measurement by Using RSSI of Wireless Sensor Network Yi-Jen Mon	110-112
20.	A Distributed Decisive Support Disease Prediction Algorithm for E-Health Care with the Support of JADE O.Saravanan , Dr.A.Nagappan	113-118
21.	DC Motor Control by ARM-Based Developer Suite Yi-Jen Mon	119-122
22.	Analysis of Lossless Data Compression Techniques Dalvir Kaur , Kamaljeet Kaur	123-127
23.	Removal of Fluoride Ion from Aqueous Solution Neelo Razbe1, Rajesh Kumar, Pratima, Rajat Kumar	128-133
24.	Physio- Chemical Properties of the Water of River Ganga at Kanpur Anjum Praveen , Rajesh Kumar , Pratima, Rajat Kumar	134-137
25.	Novel Encoding and Decoding Algorithm for Block Turbo Codes over Rayleigh Fading Channel M.Christhu Raju, Dr. Ch. D.V. Paradesi Rao	138-144
26.	Design of Contact Stress Analysis in Straight Bevel Gear N.Mohan Raj , M.Jayaraj	145-148
27.	Web Mining: Summary Sonia Gupta , Neha Singh	149-154
28.	A Study on User Future Request Prediction Methods Using Web Usage Mining Dilpreet kaur, Sukhpreet Kaur	155-159
29.	A Study on Image Indexing and Its Features Rajni Rani, Kamaljeet Kaur	160-163
30.	Reactive Power Reserve Management by Using Improved Particle Swarm Optimization Algorithm S. Sakthivel , A. Subramanian ,S. Gajendran ,P. Viduthalai Selvan	164-171

31.	On The Zeros of Polynomials and Analytic Functions M. H. Gulzar	172-180
32.	Using Novel, Flexible Benchmarking Tool for Robustness Evaluation of Image Watermarking Techniques Sweta .S. Palewar , Ranjana Shende	181-185
33.	Performance Comparison of Uncoded & Coded Adaptive OFDM System over AWGN Channel Swati M. Kshirsagar , A. N. Jadhav	186-189
34.	Mathematical Model By Using Mixture Weibull Distribution For Finding The Combination Of Gad65 And Gaba For Modulation Of Spasticity S.Lakshmi , P.Gomathi Sundari	190-195
35.	Mobile Phone Radiation Effects on Human Health Bhargavi K , KE Balachandrudu , Nageswar P	196-203
36.	Gsm Based Controlled Switching Circuit Between Supply Mains and Captive Power Plant Mr.S.Vimalraj , Gausalya.R.B , Samyuktha.V, Shanmuga Priya , M,Minuramya.B	204-209
37.	Review: Soft Computing Techniques (Data-Mining) On Intrusion Detection Shilpa Batra ,Pankaj Kumar, Sapna Sinha	210-217
38.	Dielectric Properties of Irradiated and Non Irradiated Muga (Antheraea Assama) Silk Fibre in Presence of Oxygen at Elevated Temperature Manoranjan Talukdar	218-221
39.	Dynamic Topology Control In Manet's To Mitigate Spam Attacks Using Secure Communication Protocols N.Nimitha ,V.Nirmala	222-229
40.	Graphical Password Authentication System with Integrated Sound Signature Anu Singh , Kiran Kshirsagar, Lipti Pradhan	230-234
41.	Fault Management in Wireless Sensor Networks S.Irfan , K.Sravani, K.Manohar	235-245
42.	Managing Order Batching Issue of Supply Chain Management with Multi-Agent System Manoj Kumar , Dr. S Srinivasan , Dr. Gundeep Tanwar	246-251
43.	Study of the Effect of Substrate Materials on the Performance of UWB Antenna D.Ujwala , D.S.Ramkiran , N.Brahmani , D.Sandhyarani , K.Nagendrababu	252-257
44.	A Phased Approach to Solve the University Course Scheduling System Rohini V,	258-261
45.	Dynamic Neighbor Positioning In Manet with Protection against Adversarial Attacks K. Priyadharshini , V. Kathiravan , S.Karthiga , A.Christopher Paul	262-266

46.	Solving Optimal Linear Time-Variant Systems via Chebyshev Wavelet Hatem Elaydi , Atya A. Abu Haya	267-273
47.	Effect of Process Parameters on Performance Measures of Wire EDM for AISI A2 Tool Steel S. B. Prajapati , N. S. Patel	274-278
48.	Design Evaluation of a Two Wheeler Suspension System for Variable Load Conditions Kommalapati. Rameshbabu , Tippa Bhimasankara Rao	279-283
49.	Analysis of Image Registration Using RANSAC Method Riddhi J Ramani , Kanan P Patel	284-286

(IJCER) Volume 3, Issue 4, version, 2 April, 2013

1.	Energy Conservation in Wireless Sensor Networks Using Data Reduction Approaches: A Survey Ms. Pallavi R , Shreya Animesh , Preetesh Shivam , Raghunandana Alse Airody Niraj Kumar Jha	01-7
2.	Ethnomedicinal Investigation of Medicinal Plants Used By the Tribes of Pedabayalu Mandalam, Visakhapatnam District, Andhra Pradesh, India S. B. Padal , Chandrasekhar P. , K. Satyavathi	08-13
3.	Enhancing Productivity by Using Adjustable Multi-Spindle Attachment M. Narasimha , M. Hailu Shimels , R. Reji Kumar , Achameyeh Aemro Kassie	14-22
4.	Analysis of Rivets Using Finite Element Analysis Arumulla. Suresh, Tippa Bhimasankara Rao	23-27
5.	Modeling and Analysis of Hydrant Clutch Gudavalli. Baby Theresa , Tippa Bhimasankara Rao	28-31
6.	Comparative Study of Image Enhancement and Analysis of Thermal Images Using Image Processing and Wavelet Techniques Ms. Shweta Tyagi , Mr. Hemant Ambia. Mr Shivdutt Tyagi	32-38
7.	Survey Paper Based On Hand Gesture Hex Color Matrix Vector Sukrit Mehra, Prashant Verma , Harshit Bung , Deepak Bairagee	39-42
8.	Token Based Contract Signing Protocol using OTPK Bhagyashree Bodkhe , Ms. Pallavi Jain	43-46
9.	State of Art on Yarn Manufacturing Process & its defects in Textile Industry Neha Gupta, Prof. Dr. P. K. Bharti	47-60
10.	Analyzing Stability of a Dam using MATLAB Manikanta Kotti , J K Chaitanya , Bh Vamsi Varma , K Bharat Venkat	61-64

11.	Design and Analysis of Microstrip-Fed Band Notch Uwb Antennas G.Karthikeyan, C.Nandagopal.M.E	65-70
12.	Strength of Binary Blended Cement Composites Containing Afikpo Rice Husk Ash L. O. Ettu, I. O. Onyeyili, U. C. Anya, C. T. G. Awodiji, A. P. C. Amanze	71-76
13.	Advanced Tracking System with Automated Toll Pritam Mhatre , Parag Ippar , Vinod Hingane , Yuvraj Sase , Sukhadev Kamble	77-79
14.	Association Rule Mining by Using New Approach of Propositional Logic Prof. M.N.Galphade, Pratik P. Raut, Sagar D. Savairam,Pravin S. Lokhande Varsha B. Khese	80-84
15.	On a Probabilistic Approach to Rate Control for Optimal Color Image Compression and Video Transmission Evgeny Gershikov	85-98

(IJCER) Volume 3, Issue 4, version,3 April, 2013

1.	Fault Impact Assessment on Indirect Field Oriented Control for Induction Motor R.Senthil kumar, R.M.Sekar, L.Hubert Tony Raj, I.Gerald Christopher Raj	01-10
2.	Brain Tumor Detection Using Clustering Method Suchita Yadav, Sachin Meshram	11-14
3.	Evaluation of Routing Protocols based on Performance Ms. Pallavi R , TanviAggarwal, Ullas Gupta	15-19
4.	Invention of the plane geometrical formulae - Part II Mr. Satish M. Kaple	20-27
5.	Modeling and Simulation of Different Gas Flows Velocity and Pressure in Catalytic Converter with Porous K.Mohan Laxmi , V.Ranjith Kumar , Y.V.Hanumantha Rao	28-41
6.	Heat transfer enhancement in domestic refrigerator using R600a/mineral oil/nano-Al ₂ O ₃ as working fluid R. Reji Kumar , K. Sridhar , M.Narasimha	42-51
7.	Geoidal Map and Three Dimension Surface Model Part of Port Harcourt Metropolis from "Satlevel" Collocation Model Olaleye J. B. , J. O. Olusina , O. T. Badejo and K. F. Aleem	52-58
8.	Server Based Dora in Vanets and Its Applications R.Thenamuthan , A.Manikandan	59-64
9.	Design and development of Optical flow based Moving Object Detection and Tracking (OMODT) System Ms. Shamshad Shirgeri , Ms. Pallavi Umesh Naik, Dr.G.R.Udupi , Prof.G.A.Bidkar	65-72

10.	Design and Development of Medium Access Control Scheduler in LTE eNodeB Ms. Pallavi Umesh Naik , Ms. Shamshad Shirgeri , Dr.G.R.Udupi , Prof. Plasin Francis Dias	73-79
11.	Development, Carbonation and Characterization of Local Millet Beverage (Kunu) Otaru, A.J., Ameh, C.U., Okafor, J.O., Odigure, J.O., Abdulkareem, A.S ,Ibrahim, S	80-86
12.	Study on the Effectiveness of Phytoremediation in the Removal of Heavy Metals from Soil Using Corn Otaru, A.J., Ameh, C.U., Okafor, J.O.,Odigure, J.O., Abdulkareem , A.S ,Ibrahim, S.	87-93
13	Design of Vibration Isolator for Machine-tool Komma.Hemamaheshbabu , Tippa Bhimasankara Rao ,D.Muralidhar yadav	94-98
14.	Power Systems Generation Scheduling and Optimization Using Fuzzy Logic Techniques Yogesh Sharma , Kuldeep Kumar Swarnkar	99-106
15.	Static and Modal Analysis of Leaf Spring using FEA Meghavath. Peerunaik , Tippa Bhimasankara Rao , K.N.D.Malleswara Rao	107-110
16.	Facial Emotion Recognition in Videos Using Hmm Rani R. Pagariya , Mahip M. Bartere	111-118
17.	Unique and Low Cost Airport Multi-Application Control System Adnan Affandi , Mubashshir Husain	124-136

Development of Software-Based University Research Tools for Metocean Engineering Applications: A Reflective Case Study

E.S.Lim¹, M.S.Liew¹, G.Dinis Jr.¹
¹Universiti Teknologi PETRONAS, Perak, Malaysia

Abstract:

The oil and gas industry has traditionally been one of the most demanding forms of engineering as the lucrative returns form the basis of global development. As such, oil operators have made it a norm to reinvest a significant portion of their profits into research and development (R&D). This stemmed as a result of depleting natural resources which has forced operators to go further and deeper to explore for hydrocarbons. To balance the economics of such ventures, R&D plays a critical role in optimization and defining standards in which to operate safely with economical consideration. As such, various software tools for various disciplines have been developed for this purpose, i.e. SESAM, SACS and etc. However, there has been a lack of R&D tools that have been tailor-made for metocean operations; most of those that are currently in existence are not open to public use/sales. This has created a demand by Malaysian oil operators to have such tools being readily available for in-house use. The paper herein will discuss the framework and development of an integrated and tailor-made metocean software, namely Blue Hive (BH).

Index term –Statistical analysis, metocean, software development, .NET, Blue Hive

I. INTRODUCTION

Metocean is an integral part of offshore engineering and has always been significantly more complex in design compared to land-based civil engineering works due to the fact that it is based in conditions where fluid dynamics develop dominant forces on the structure. The stochastic nature of wave conditions are coupled with the effect of ocean currents on top of the more extreme wind conditions prevalent in open seas. As such, a strong understanding or fundamental of these environmental metocean loads at sea form a critical component in almost every stage of an offshore facility's life cycle. These stages include the design of facilities and forecasting of operations for offshore vessels. The understanding of these metocean loads will be critical from two ends of the engineering consideration, which is to prevent loss of life as a result of structural failure or capsizing (underdesign) and to prevent the overdesign of offshore structures (which results in excessive usage of steel in fabrication).

Strong understanding of metocean loads is essential in aiding the optimization of engineering design and definitions. This can only be achieved via investment into dedicated R&D divisions or institutions. For example, multinational operators such as Shell has a R&D division known as Shell Global Solutions which have a running contract with Fugro GEOS to conduct metocean studies and redefinitions. There are however also operators in the region who do not have extensive metocean research units and as such would have to leverage on existing codes and standards that may not be optimized for the region. For example, most of South East Asian (SEA) operations are very much dependent on the American Petroleum Institute (API) standard which bases itself on Gulf of Mexico conditions (which are far more conservative than SEA). What compounds the situation is that there is little sharing of developed metocean knowledge amongst operators which makes individualized research efforts critical to establishing optimized metocean standards.

This case study is based upon the efforts of Universiti Teknologi PETRONAS (UTP), Malaysia in particular to develop localized metocean definitions for one of the biggest oil operators in SEA, PETRONAS. The effort is a fast-track initial research that spans approximately 1-year long in which the deliverables are to develop the following metocean tools, a) correlation factoring between measured and hindcast data, b) joint density analysis of metocean parameters, c) spectral analysis and modeling of metocean parameters and d) ARIMA modeling and forecasting of metocean parameters. In order to undertake the research, there was a need to perform extensive statistical data analysis and time series analysis. Throughout the initial phases of the research, there was a need to constantly interoperate between software, i.e. SPSS PASW, Excel and MATLAB.

While this may be acceptable to some, efficiency of research works can be greatly enhanced if there is an integrated platform that combined the benefits of each program such as MATLAB's powerful scripting options and the user-friendly interface of SPSS PASW which makes the input-output process seamless. Since the format of data being input into the software is standardized across PETRONAS' operating units, there was room for improved efficiency by cutting down steps required during the data import process. Moreover, it was envisioned that there would be a need to materialize the algorithms and methodologies employed in research into commercially usable software. As such, the gears of motion were set in place to develop Blue Hive (BH) which is intended to integrate metocean analysis specific tools under a seamless input-output process. BH is also intended to be the precursor to future and continually evolving research in metocean engineering such as transfer function modeling.

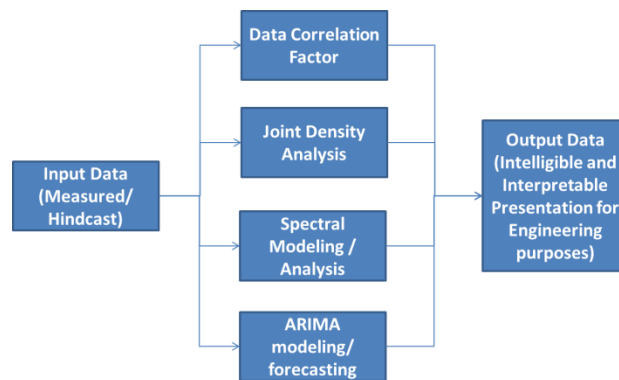


Fig. 1. Proposed process flow for BH

II. FRAMEWORK, METHODOLOGY AND MODEL

The buzzwords framework, methodology, model and even process, are not alien to any development effort. Despite being routinely used, these terms do not always carry the same meaning for everyone that uses them. Based on common definition, the terms are defined as follows:

2.1 Framework: an architectural skeleton of what should be done, or stages that should be walked through without defining any activities or tasks within them.

2.2 Methodology: the definition of what should be done in each stage of a development effort, without defining how to do it.

2.3 Process: a step by step guide on how to perform a task.

2.4 Model: the representation or simulation of a software process.

Building software, i.e. software engineering, is a highly debated topic in the industry. Although software engineering was created based on the foundation of common engineering, development of software systems is influenced by unique factors that require special attention apart from traditional engineering concepts based on sequential procedures which are not always able to address these factors effectively (Bern, et al., 2007). The customer, the business environment, and the organizational structures are examples of such factors, as they influence software projects in a non-sequential or structured manner (Bern, et al, 2007). Thus, the emergence of new frameworks and models, i.e. Agile models, for the past twenty years can be seen as an attempt to try and address these issues (Mnkandla, 2009 and Bernetal., 2007); large scale projects do however still work better with older methodologies.

Metocean engineering is highly statistical in nature and requires extensive data analysis tools. The purpose of BH is to incorporate whatever methodologies for data analysis that are developed by the team of researchers into a simplified User Experience (UX), that brings about results for immediate usage in an industrial environment situation, such as the ones mentioned in *Section I*. Software engineering can be a volatile process, where the needs of the customers rapidly change, and either new components need to be added or removed to accommodate new features or completely remove an existing one (Qureshi & Hussain, 2008). Adding to this complexity is the fact that research in itself is not a static process in nature, thus existing components are also liable to frequent modification and adaption, as experienced during the developmental cycle of this project. This trend is prevalent in almost all fields of research as progress in research will constantly see improvements and redefinitions to the engineering technique in which the software is to replicate. Despite all of these, there is still a need to have a framework defined that will allow developers to know what

the end goal is, or at least what it should look like, while maintaining the flexibility of development demanded by the nature of their work. To achieve this, the team opted to follow the Agile framework, using eXtreme Programming (XP) programming methodology, with a component based modeling approach.

The Agile framework, developed by the Agile Alliance back in 2001 in response to the growing demands of the software market, was set to value individuals and interactions, working software, customer collaboration and responding to change; as opposed to processes and tools, comprehensive documentation, contract negotiation and following a plan, respectively (Agile Alliance, 2001). The framework permits construction of a system architecture that is fixed in terms of its structure while being highly flexible in terms of its internal components. This is very suitable for the development environment where in-situ change is pertinent, as opposed to traditional frameworks which demanded a fixed software structure, components definition, procedures and end goals. Traditional frameworks are complemented by extensive documentation on what was done throughout each stage, making accommodation to changes virtually impossible (Munassar & Govardhan, 2010).

XP, a methodology originally designed for usage by small teams in projects with non-clearly defined and mutating requirements, was chosen to be used, because of its main core elements: communication, feedback, simplicity, and courage, and the fact that is highly suitable for small development teams, as is the case in this project, where there is more emphasis on customer communication compared to anything else. Now, XP defines that projects should be carried out in periodic cycles, of three (3) weeks, and at each cycle a different component or feature is addressed (Wolak, 2003). In research, such periodicity is not easy to achieve, nonetheless, the separation of each feature-cycle is desirable as at each cycle, each feature implemented has some degree of independency from the others and the irregularity of time frames between each feature-cycle does not affect the objectives of the project. Contrarily, it helps suit the dynamic and irregular schedule of research work which is very much reliant on the dynamic requirements of clients in which they are recipients of the deliverables. A research was conducted to quantify the results of XP usage in several fields of development across Europe, USA, Asia, and Australia, in companies both young and mature, and found an almost one hundred percent satisfaction rating from a total of 45 respondents (Rumpe and Schroder, 2001). This pattern was seen even for large teams, i.e. teams with more than 10 people. It is also worth mentioning is the fact that 73% of the projects interviewed were new, and made use of high level languages, as in this project's case, where the main language in use is C#. When asked to rate the factors of time delivery, costs to last minute changes and quality, the respondents gave ratings between 3.77 and 4.44 on a -5 to 5 scale for finished and running projects, indicating positive perceptions of XP's effectiveness.

The nature of this project is based on constant exchange and feedback between customers, i.e. the researchers, and the developers. On-site customer presence is one of the main principles of XP. In the same study by Rumpe and Schroder, it was found that the absence of on-site customer was reported as the second highest risk factor to XP projects. Studies on performance of XP by researchers were able to adopt this principle and reported it to work "extremely well" (Ganeshan and Ganesham, 2003). Primavera Software, a project management portfolio vendor now owned by Oracle Corporation, managed to successfully increase their customers satisfaction base, establish a highly motivated development environment and produce working and reliable software by adopting Scrum and XP agile practices back in 2003, which helped save the company from its low productivity and customer satisfaction ratings at the time (Object Mentor, Inc. and Advanced Development Methods, 2004).

Finally, the component based approach is chief for the entire purpose of BH. As a standalone application package being developed to address various analytical needs in the field of metocean data analysis, BH needs to have a solid foundation that allows it to support different modules that are independent of each other for operation. In section III, the architecture of the system will illustrate this better. Here, we will limit the discussion to the need of using this approach, as well as its advantages and drawbacks. As previously mentioned, BH was designed to support a variety of metocean data analysis computational needs, without much binding in between different modules, so that each module could be setup and used without requiring the others to be present. This would permit both concurrent development of different modules and distribution or release of different modules at different stages for either testing or usage. The concept is widely adopted, not only by statistical software package vendors such as MathWorks, but by other industry area software providers, such as Adobe Systems. This is one of the main development goals in the project, along with having each module capable of producing ready to use interpreted results from the analysis processes they perform. Looking at generic analysis software packages such as IBM's Statistical Package for the Social Sciences (SPSS) and Microsoft Excel, they have the distinct characteristic of providing a basic platform for analysts to define

procedures based on their needs. The issue with such approach is that there is learning curve required for each package, and in some cases, the users have to familiarize themselves with defining computational procedures on a machine due to these packages offering powerful and elaborate scripting options. This is seen in software such as MATLAB that requires comprehensive control and knowledge of the scripts where BH would only be a matter of point-and-click the required options. This advantage nests itself when there is a need to shorten the project duration by the client; it however comes at the cost of inability to create customized scripts. This was a compromise that was accepted by BH as the multitude of metocean research projects that it serves had a lifecycle of no more than 1 year. As such, rapid mastery and development of software is required. Another issue that arises is that, more than often, a single package simply does not provide all the functionality required, as it was in the application of the aforementioned metocean projects. In order to perform the required analysis processes required for the studies being carried out, there was a constant need to be interchanging between one package and the other. In an environment where results are demanded at a fast rate, there is a need to shorten the time it takes for one to obtain intelligible results that can be interpreted and utilized almost immediately.

III. SOFTWARE ARCHITECTURE

BH was designed as a .NET application, to take full advantage of the software framework developed by Microsoft for Windows. The .NET is cited by some as the best Windows development framework (Magenic, 2012) for the variety of advantages that it offers to businesses and developers. Its most prominent features of interest to the development are the (1) extensive number of classes readily available for usage, (2) the short time span required from development under any of its languages, with interoperability among all of them, (3) the fact that it allows applications to be designed for divergent purposes at the same time, without requiring much effort to make them run on different environments, i.e. desktop, web-based and mobile apps, and (4) the existence of an open source community supported by Microsoft, that is dedicated to building .NET projects (Magenic, 2012). What follows is the description of how these features were used in relevance to the project. First, the .NET offers many classes for basic and low level program control requirements such as data management, network connectivity, and UX design. As mentioned previously, BH needed to be built on a solid platform that would allow it to define the lower level features required by all components in such a way that independent modules could be built on top of this platform without much effort. With the .NET, the team did not have many difficulties in this process, given the wide array of predefined classes and data structures already available in the framework, e.g. *System.IO* module and the *DataTable* class.

Second, one of the most time consuming, yet required, development activities are those carried out in the stages of coding and debugging, and currently, there is no other framework that delivers a better system for both, than the .NET combined with the Visual Studio (Magenic). From this project, this was easily verified, as most debugging environments lack the high level user communication efficiency of Visual Studio. With the Visual Studio Debugger, present in VS2005 onwards, useful functions such as code stepping in, stepping out and over, and parallel code debugging are intuitively available, apart from the standard functions such as break-points and value modification.

Third, as team's intents of usage environment for BH is still in the process of redefinition as the research progresses, there was a need for a framework that would allow the team to build application logic that could easily be ported onto any environment of choice. Obviously, this is possible with other languages such as C and C++ through binding. However, with the .NET, binding would be virtually unnecessary, as the framework natively supports a desktop, web application, and mobile environment. Finally, given that team's needs were to develop a solid foundation that could support independent modules, the possibility of using existing open source libraries to shorten development time and costs on non-critical system modules could not be ignored. Microsoft currently supports an open source community for .NET projects, i.e. Codeplex, where useful resources were found and adopted to shorten the time spent on some system modules so focus could be given to more critical ones.

Each component shown in Fig. 2 was built as a standalone library. We have the option of building our needed libraries using any of the .NET languages (F#, C#, VB), and use them all for any system component. The level of abstraction for each computing module is given by the Application Processing Logic (APL) component which interfaces with the REPORT, UX and CORE components of the system. As for the remaining components, they were built on top of one another to provide those four (4) components with the services they need. On the top of diagram, we have the UX component, which provides a layer of abstraction for the application's environment. Currently, BH is being developed as a desktop-application; however porting it into a web-based system in ASP.NET would be feasible, requiring only changes to be made to the upper layer, i.e. the design of new interfaces for the target environment. It is believed that this architecture design addresses both the

current and future needs of BH, as it sets a robust framework for the addition, removal and modification of any specific application analysis module without the need to modify the lower level layers of the system. Additionally, the architecture model allows for ease of integration with third party libraries, which provides us with considerable savings in terms of time and costs.

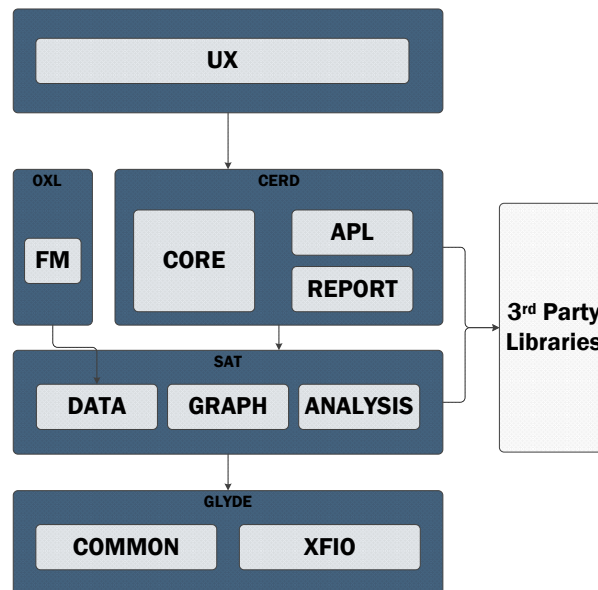


Fig. 2. Software architecture model of BH

IV. CONCLUSION

The BH software in essence is targeted to be a fast-track research tool that serves the purpose of fulfilling the deliverables of university-industry collaborations. As such, the utilization of Agile frameworks and XP is essential to achieving such goals in short term. This is needed as the nature of such research projects are dynamic in nature as methodologies of research and algorithms employed may evolve as the deliverables reach maturity. Moreover, BH is intended to be the precursor to long-term development of commercially useable software for oil operators in SEA by providing alternative figures to existing metocean practices on top of BH also potentially evolving into more advanced research tools in similar areas.

REFERENCES

- [1] Mnkandla, E. (2009). About Software Engineering Frameworks and Methodologies. IEEE AFRICON 2009. September 23-25, 2009. Retrieved 5th September, 2012
- [2] Bern, A., Nikula, U., Pasi, S. J. A., Smolander, K. (2007) Contextual Factors Affecting the Software Development Process. Proceedings of the 2nd AIS SIGSAND European Symposium on Systems Analysis and Design, Gdansk, Poland, June 5, 2007
- [3] Munassar, N. M. A., and Govardhan, A. (September, 2010). A Comparison Between Five Models Of Software Engineering. IJCSI International Journal of Computer Science Issues. Vol 7(5). pp94-101
- [4] Qureshi, M. R. J., & Hussain, S.A. (2008). A reusable software component-based development model. Advances in Engineering Software. Vol 39(2). pp88-94
- [5] Agile Alliance. (2001). Manifesto for Agile Software Development. Retrieved 5th September, 2012. From <http://www.agilealliance.org/the-alliance/the-agile-manifesto/>
- [6] Ganeshan, K., Ganesham, V. (2003). Extreme Programming - A Success Story. Poster Paper in Proceedings of the 16th Annual NACCQ, Palmerston North New Zeland, July 2003. Retrieved 5th September, 2012. From www.naccq.ac.nz/conferences/2003/papers/483.pdf
- [7] Magenic. (2012). Why .NET. Retrieved 5th September, 2012. From <http://magenic.com/Portals/0/Magenic-White-Paper-Why-NET.pdf>
- [8] Object Mentor, Inc. and Advanced Development Methods. (2004) Best Practices in Scrum Project Management and XP Agile Software Development. Retrieved 5th September, 2012. From <http://www.objectmentor.com/resources/articles/Primavera.pdf>
- [9] Rumpe, B., Schroder, A. (2001). Quantitative Survey on Extreme Programming Projects. Munich University of Technology. Retrieved 6th September, 2012. From <http://www.se-rwth.de/~rumpe/publications/ps/XP02.RumpeSchroeder.Study.pdf>
- [10] Wolak, R. G. (2001). DISS 725 - System Development: Research Paper 1 SDLC on a Diet. Nova Southeastern University. Retrieved 5th September, 2012. From <http://scisstudyguides.addr.com/papers/rwDISS725researchpaper1.pdf>

A RELIABLE NODE-DISJOINT MULTIPATH ROUTING PROTOCOL FOR MANET

A.Monisha¹K.Vijayalakshmi²

¹PG Scholar,S.K.P Engineering College, Thiruvannamalai.

²Asst professor, S.K.P Engineering College,Thiruvannamalai

Abstract:

Frequent link failures are caused in mobile ad-hoc networks due to node's mobility and use of unreliable wireless channels for data transmission. Due to this, multipath routing protocols become an important research issue. In this paper, we propose and implement a reliable node-disjoint multipath routing protocol. The main goal of the proposed method is to determine all available reliable node-disjoint routes from source to destination with minimum routing control overhead. In the route discovery method, the routes with good link quality and route expiration time are selected as the primary and backup routes. If there is any route failure during the data transmission through primary path, the next available backup route with good link quality and route expiration time is selected from the list. The performance of the proposed protocol will be evaluated using NS-2 and will be shown that it reduces the packet drop and delay there by increasing the packet delivery ratio.

Keywords: Average End-to-End Delay, Node-disjoint, Packet drop, Primary and Backup Routes, Routing protocols.

INTRODUCTION:

A mobile ad-hoc network (MANET) is a self-configuring infrastructure less network of mobile devices connected by wireless. Ad hoc is Latin and means "for this purpose". Each device in a MANET is free to move independently in any direction, and will therefore change its links to other devices frequently. Each must forward traffic unrelated to its own use, and therefore be a router. The primary challenge in building a MANET is equipping each device to continuously maintain the information required to properly route traffic. Such networks may operate by themselves or may be connected to the larger Internet.

MANETs are a kind of wireless ad hoc networks that usually has a routable networking environment on top of a Link Layer ad hoc network. The growth of laptops and 802.11/Wi-Fi wireless networking has made MANETs a popular research topic since the mid-1990s. Many academic papers evaluate protocols and their abilities, assuming varying degrees of mobility within a bounded space, usually with all nodes within a few hops of each other. Different protocols are then evaluated based on measure such as the packet drop rate, the overhead introduced by the routing protocol, end-to-end packet delays, network throughput etc. Routing protocols that discover and store more than one route in their routing table for each destination node are referred to as multipath routing protocols. In wireless scenarios, routes are broken due to node movement. Also, the wireless links used for data transmission are inherently unreliable and error prone. Therefore, multipath routing protocols are used to overcome the disadvantages of shortest path routing protocols. Multipath routing protocols are used to increase the reliability (by sending the same packet on each path) and fault tolerance (by ensuring the availability of backup routes at all times). It can also be used to provide load balancing, which reduces the congestion on a single path caused by bursty traffic [9]. The remainder of the paper is structured as follows. In Section II, we present related work in our area by providing a brief description of existing multipath extensions of AODV routing protocol. The proposed method AOMDV used for discovering multiple paths is presented in Section III. In Section IV, we present the experimental setup details and provide results with analysis obtained through various simulations. Finally, the conclusions and directions for future work are provided in Section V.

II.EXTENSION WORK:

In this section, we discuss the previous work done on multipath routing methods on AODV. Ad hoc On-Demand Distance Vector (AODV) Routing is a routing protocol for mobile ad hoc networks (MANETs) and other wireless ad-hoc networks. It is a reactive routing protocol, meaning that it establishes a route to a destination only on demand. In contrast, the most common routing protocols of the Internet are proactive,

meaning they find routing paths independently of the usage of the paths. AODV is, as the name indicates, a distance-vector routing protocol. AODV avoids the counting-to-infinity problem of other distance-vector protocols by using sequence numbers on route updates, a technique pioneered by DSDV. AODV is capable of both unicast and multicast routing.

In AODV, the network is silent until a connection is needed. At that point the network node that needs a connection broadcasts a request for connection. Other AODV nodes forward this message, and record the node that they heard it from, creating an explosion of temporary routes back to the needy node. When a node receives such a message and already has a route to the desired node, it sends a message backwards through a temporary route to the requesting node. The needy node then begins using the route that has the least number of hops through other nodes. Unused entries in the routing tables are recycled after a time. Much of the complexity of the protocol is to lower the number of messages to conserve the capacity of the network. For example, each request for a route has a sequence number. Nodes use this sequence number so that they do not repeat route requests that they have already passed on. Another such feature is that the route requests have a "time to live" number that limits how many times they can be retransmitted. Another such feature is that if a route request fails, another route request may not be sent until twice as much time has passed as the timeout of the previous route request.

The advantage of AODV is that it creates no extra traffic for communication along existing links. Also, distance vector routing is simple, and doesn't require much memory or calculation. However AODV requires more time to establish a connection, and the initial communication to establish a route is heavier than some other approaches [3]. In this section, the existing NDMP-AODV protocol is described [4]. The main goal of NDMP-AODV is to find all available node-disjoint routes between a source-destination pair with minimum routing overhead. When a source node has a data packet to send, it checks its routing table for the next-hop towards the destination of the packet. If there is an active entry for the destination in the routing table, the data packet is forwarded to the next hop. Otherwise, the route discovery phase begins. In route discovery phase, routes are determined using two types of control messages: (i) Route request messages (RREQs) and (ii) Route reply messages (RREPs). The source node floods the RREQ message into the network. Each intermediate node that receives a RREQ, checks whether it is a duplicate or a fresh one by searching an entry in the Seen Table. Seen Table stores two entries (i.e. source IP address and RREQ flooding ID (*f id*)) that uniquely identifies a RREQ message in the network. If an entry is present in the Seen Table for the received RREQ message, it is considered a duplicate RREQ message and discarded without further broadcasting. Otherwise, the node creates an entry in the Seen Table and updates its routing table for forward path before broadcasting the RREQ message.

Source IP Address	Flooding ID	Seen Flag
---	---	---

Fig. 1. NDMP-AODV Seen Table structure

Type	R	A	Reserved	Prefix Size	Hop Count
Destination IP Address					
Destination Sequence Number					
Source IP Address					
Source Sequence Number					
Broadcasting ID					

Fig. 2. NDMP-AODV RREP structure

In NDMP-AODV, only the destination node can send RREPs upon reception of a RREQ message. The intermediate nodes are forbidden to send RREPs even if they have an active route to destination. This is done so as to get the node-disjoint routes. In NDMP-AODV, the destination node has to send a RREP message for each RREQ received, even if the RREQ is a duplicate one. We add an extra field that works as a flag known as seenflag. This flag is set to FALSE at start i.e. when an entry is first inserted in the Seen Table after a node gets its first RREQ message. The RREP messages initiated by destination node in NDMP-AODV contain one extra field known as broadcast ID (*b id*). The route discovery method used to discover node-disjoint paths. When a destination node receives a RREQ message, it creates the corresponding RREP message. The destination node copies the *f id* from the received RREQ message into the *b id* field of sent RREP message.

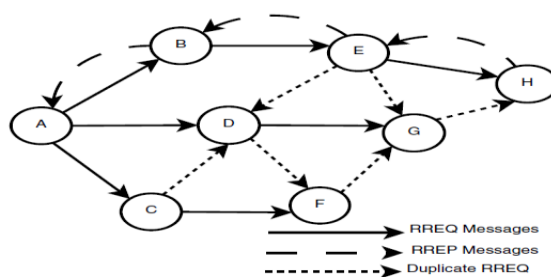


Fig. 3. Traditional AODV route discovery process

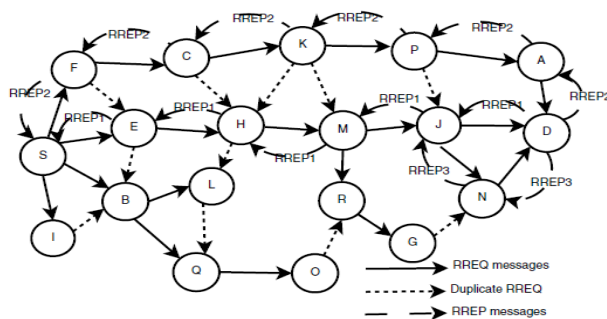


Fig. 4. NDMP-AODV route discovery process

Figure shows the route discovery process of traditional AODV protocol. In Figure we demonstrate with an example how the route discovery process in NDMP-AODV gets all node-disjoint routes between a source-destination pair. Suppose, node S is the source node and node D is the destination node. When node S has data to send, it initiates the route discovery process by flooding RREQ in the network. Let us assume that destination D receives its first RREQ from intermediate node J at time $t1$ and D initiates the RREP1 message. RREP1 is unicast towards source S by creating the reverse path $D \rightarrow J \rightarrow M \rightarrow H \rightarrow E \rightarrow S$. When RREP1 is received by an intermediate node along the reverse route each intermediate node resets the value of seenflag in their Seen Table. Suppose, D receives the first duplicate RREQ message from A at time $t2$. Again node D initiates a RREP2 for this duplicate RREQ and sends it back towards node S through the same path it came to D (i.e. $S \rightarrow F \rightarrow C \rightarrow K \rightarrow P \rightarrow D \rightarrow D$) to make the reverse route $D \rightarrow A \rightarrow P \rightarrow K \rightarrow C \rightarrow F \rightarrow S$. This helps to create a forward route towards node D . Finally, say at time $t3$, node D receives the third duplicate RREQ message from node N . Node D initiates RREP3 for this duplicate RREQ and sends it towards S through N . The RREP3 reaches node J through N . Node J checks the value of seenflag for RREP3 before forwarding it to next hop. Node J determines that the seenflag is set to TRUE. So node J considers RREP3 as a duplicate message and drops it. This helps to maintain the node-disjoint property of our method.

III. RESULTS

In this section, we discuss the results obtained from intensive simulations that have been performed to show the effectiveness of proposed route discovery and route maintenance methods. The simulation results include the average packet delivery ratio (PDR), average end-to-end delay (EED), percentage availability of backup routes and routing control overhead caused by route discovery and route maintenance processes. The effectiveness of proposed methods are checked against the effect of node mobility.

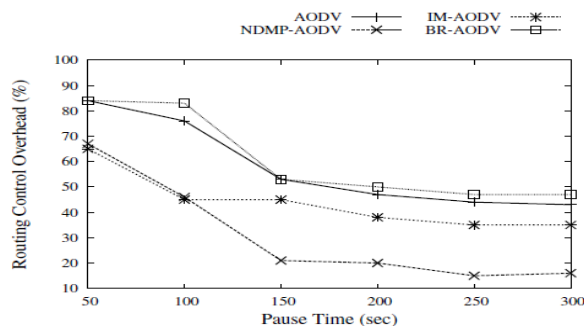


Fig.5. Routing control packet overhead with change in mobility

Figure 5 shows the overhead caused by routing control messages during route discovery process. Routing overhead created during transmission of one video stream are calculated and plotted in Figure 5. The routing overhead is calculated by dividing the total number of routing control messages with the total number of packets in the network (i.e. control messages plus data packets). As we can see in Figure 5, AODV causes approximately 50% more routing overhead in moderate or low mobility networks (i.e. when node pause time is greater than 100 sec) as compared to NDMP-AODV. This is due to the fact that NDMP-AODV uses one RREQ flooding to calculate all node-disjoint routes as compared to AODV which uses one RREQ flooding for each route discovery.

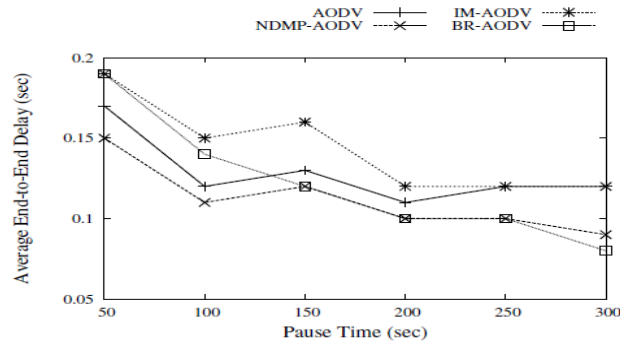


Fig.6. Average End-to-End delay with change in node mobility.

The number of RREP messages in NDMP-AODV is greater than AODV but they are very few in number because the RREPs are unicast towards source. Also, the intermediate nodes will not forward the duplicate RREPs. Low routing overhead saves the scarce network bandwidth, thus increasing the network capacity. The number of routes stored in routing table for a destination from the available node-disjoint routes greatly depends on the mobility of network. If the network mobility is high, the probability that the secondary route is expired with the primary route is high. As shown in Figure 5, BR-AODV has the highest routing overhead because only two routes for destination are stored in the routing table. Due to this, BRAODV has to flood the RREQ messages whenever anyone route is broken to maintain the backup route at all times. In this case, the overhead for route maintenance is approximately more or equal to AODV protocol.

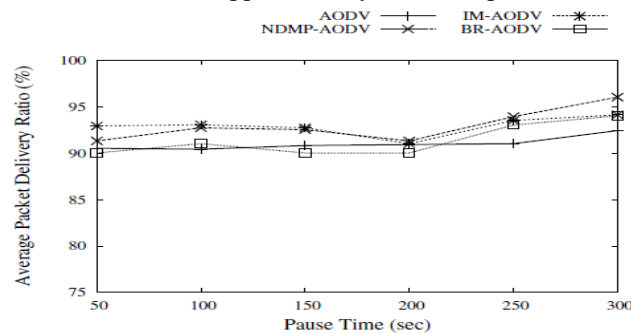


Fig.7. Packet delivery ratio with change in node Mobility.

Effect of mobility on EED and PDR are shown in Figure 6 and Figure 7. The delay in NDMP-AODV is less as compared to other protocols. This is because NDMP-AODV keeps a backup routing path more than 50% of the time when the primary route fails with the lowest routing overhead. We can observe from Figure 6, that EED of all routing protocols decreases with increase in node pause time. NDMP-AODV EED again increases at the end of simulation due to increase in its PDR. Also, IM-AODV causes the highest delay because it uses the backup route from the point the link is broken. We compare the performance of AODV and AOMDV according to the following performance metrics:

Packet delivery fraction: the ratio of data packets delivered to the destinations to those generated by the constant bit rate. Average End-to-End delay of data packets: this includes all possible delays caused by buffering during route discovery, queuing at the interface queue, retransmission delays at the MAC, propagation and transfer times. Routing Overhead: the total number of routing packets transmitted during the simulation. For packets sent over multiple hops, each transmission of the packet (each hop) counts as one transmission.

IV. CONCLUSION

In this we propose method known as an on-demand, multipath distance vector routing protocol for mobile ad hoc networks. Specifically, we propose multipath extensions to a well-studied single path routing protocol known as ad hoc on-demand distance vector (AODV). The resulting protocol is referred to as ad hoc on-demand multipath distance vector (AOMDV). The protocol guarantees loop freedom and disjoint ness of alternate paths. Performance comparison of AOMDV with AODV using ns-2 simulations shows that AOMDV is able to effectively cope with mobility-induced route failures.

A new class of on-demand routing protocols (e.g., DSR, TORA, AODV) for mobile ad hoc networks has been developed with the goal of minimizing the routing overhead. These protocols reactively discover and maintain only the needed routes, in contrast to proactive protocols (e.g., DSDV) which maintain all routes regardless of their usage. The key characteristic of an on-demand protocol is the source-initiated route discovery procedure. Whenever a traffic source needs a route, it initiates a route discovery process by sending a route request for the destination (typically via a network-wide flood) and waits for a route reply. Each route discovery flood is associated with significant latency and overhead. This is particularly true for large networks. Therefore, for on-demand routing to be effective, it is desirable to keep the route discovery frequency low. Comparison was based on of packet delivery fraction, routing overhead incurred, average end-to-end delay and number of packets dropped, we conclude that AOMDV is better than AODV. AOMDV is a better on-demand routing protocol than AODV since it provide better statistics for packet delivery and number of packets dropped. But if routing overhead is a concern, then AODV is preferred over AOMDV.

REFERENCES

- [1] CHHAGAN LAL , V.LAXMI, M.S.GAUR, A Node Disjoint Multipath Routing Method based on AODV protocol for MANETs, 2012 26th IEEE International Conference on Advanced Information Networking and Applications.
- [2] S. R. Biradar, Koushik Majumder, Subir Kumar Sarkar, Puttamadappa C. Performance Evaluation and Comparison of AODV and AOMDV, (IJCSE) International Journal on Computer Science and Engineering Vol. 02, No. 02, 2010, 373- 377.
- [3] Fubao Yang and Baolin Sun. Ad hoc on-demand distance vector multipath routing protocol with path selection entropy. In Consumer Electronics, Communications and Networks (CECNet), 2011 International Conference on, pages 4715 –4718, april 2011.
- [4] Chang-Woo Ahn, Sang-Hwa Chung, Tae-Hun Kim, and S Young Kang. A node-disjoint multipath routing protocol based on aodv in mobile ad hoc networks. In Information Technology: New Generations (ITNG), 2010 Seventh International Conference on, pages 828 –833, april 2010.
- [5] Shunli Ding and Liping Liu. A node-disjoint multipath routing protocol based on aodv. In Distributed Computing and Applications to Business Engineering and Science (DCABES), 2010 Ninth International Symposium on, pages 312 –316, aug. 2010
- [6] MOHAMMED TARIQUE, KEMAL E. TAPE, SASAN ADIBI AND SHERVIN ERFANI. SURVEY OF MULTIPATH ROUTING PROTOCOLS OF MOBILE AD HOC NETWORKS, JOURNAL OF COMPUTER AND NETWORKS, 32(6):1125-1143,2009.
- [7] S. Rimac-Drlje, O. Nemicic, and M. Vranjes. Scalable coding extension of the h.264/avc standard. In ELMAR,2008 50th International Symposium, volume 1, pages 9 –12, sept. 2008.
- [8] C. Perkins and E. Royer. Ad hoc on-demand distance vector routing.1999.
- [9] YuHua Yuan, HuiMin Chen, and Min Jia. An optimized ad-hoc ondemand multipath distance VECTOR (aomdv) routing protocol. In Communications, 2005 Asia-Pacific Conference on pages 569 –573, oct. 2005.
- [10] Z.Ye, S.V. Krishnamurthy, and S.K. Tripathi. A framework for reliable routing in mobile ad hoc networks. In INFOCOM 2003.Twenty-Second Annual Joint CONFERENCES of the IEE Computer and Communications. IEEE Societies, volume 1, pages 270 – 280 vol.1, march-3 april 2003.
- [11] S.Corson, J. Macker, Mobile Ad Hoc Networking (MANET): Routing Protocols Performance Issues and evaluation, RFC2501,1999

Mining Temporal Patterns for Interval-Based and Point-Based Events

^{1, 2, 3} S.Kalaivani, ² M.Gomathi, ³ R.Sethukkarasi

^{1,2,3}Department of Computer Science and Engineering, R.M.K. Engineering College,
Kavaraipettai, Tamil Nadu, India.

Abstract

Previous research on mining sequential patterns mainly focused on discovering patterns from point-based event data and interval-based event data, where a pair of time values is associated with each event. Since many areas of research includes data on a snapshot of time points as well as time intervals, it is necessary to define a new temporal pattern. In this work, based on the existing thirteen temporal relationships, a new variant of temporal pattern is defined for interval-based as well as point-based event data. Then, a hybrid pattern mining technique is proposed. Experimental results show that the completeness and accuracy of the proposed hybrid technique are more efficient than the existing algorithm.

Keywords: Data mining, temporal pattern, sequential pattern, interval-based event, point-based event.

I. INTRODUCTION

Data mining (also called knowledge discovery) is useful in various domains such as market analysis, decision support, fraud detection, business management, and so on [1], [2], [3]. Many approaches have been proposed to extract information and sequential pattern mining is one of the most important methods. The sequential pattern mining problem was first proposed by Agrawal and Srikant [4]. Data mining software is one of a number of analytical tools for analyzing data. It allows users to analyze data from many different dimensions or angles, categorize it, and summarize the relationships identified. Technically, data mining is the process of finding correlations or patterns among dozens of fields in large relational databases. Temporal Data Mining is a single step in the process of Knowledge Discovery in Temporal Databases that enumerates structures (temporal patterns or models) over the temporal data. Any algorithm that enumerates temporal patterns from, or fits models to, temporal data is a Temporal Data Mining Algorithm.

Temporal data mining tasks include:

- Temporal data characterization and comparison,
- Temporal clustering analysis,
- Temporal classification,
- Temporal association rules,
- Temporal pattern analysis,
- Temporal prediction and trend analysis.

Sequence Data Mining provides balanced coverage of the existing results on sequence data mining, as well as pattern types and associated pattern mining methods. While there are several research on data mining and sequence data analysis, currently there are no research that balance both of these topics. This paper fills in the gap, allowing readers to access state-of-the-art results in one place.

II. LITERATURE SURVEY

In [1] Shin-Yi Wu et al proposed a new kind of non ambiguous temporal pattern for interval-based event data. Then, the TPrefixSpan algorithm is developed to mine the new temporal patterns from interval-based events. W.J. Frawley et al. in [2] discussed the use of domain knowledge within Data Mining and defined three classes of domain knowledge such as Hierarchical Generalization Trees (HG-Trees), Attribute Relationship Rules (AR-rules) and Environment Based Constrains (EBC). Jiawei Han et al [3] proposed a novel Sequential Pattern Mining Method named FreeSpan (Frequent Pattern-Projected Sequential Pattern mining). The general idea of this method is integration of mining frequent sequences with that of frequent

patterns and use projected sequence databases to confine the search and the growth of subsequent fragments. Jian Pei et al [4] proposed a novel sequential pattern mining method, called PrefixSpan (**Prefix**-projected **Sequential pattern** mining), which explores prefix projection in sequential pattern mining. PrefixSpan mines the complete set of patterns but greatly reduces the efforts of candidate subsequence generation. R. Agrawal and R. Srikant in [5] proposed an algorithm MS-PISA, which stands for Multi Support Progressive mIning of Sequential pAttens, which discovers sequential patterns in, by considering different multiple minimum support threshold values for every possible combinations of item or item set.

C.-C. Yu and Y.-L. Chen in [6] discovered frequently occurred sequential patterns from databases and also two efficient algorithms are developed to mine frequent sequential patterns from multi-dimensional sequence data. J. Pei et al in [7] proposed a novel sequential pattern mining method called PrefixSpan, which explores prefix-projection in sequential pattern mining. Prefixspan mines the complete set of patterns but generally rduces the efforts of candidate subsequence generation. R. Srikant and R. Agrawal in [8] proposed the use of constraint approximations to guide the mining process, reduce the number of discovered patterns. J. Pei, J. Han, and W. Wang in [9] proposed a general model of sequential pattern mining with a progressive database while the data in the database may be static, inserted or deleted. In addition to a progressive algorithm PISA, standing for Progressive mIning of Sequential pAttens, to progressively discover sequential patterns in defined time period of interest was presented. P.S. Kam and A.W.C. Fu in [10] considered an interval-based events where the duration of events is expressed in terms of endpoint values, and these are used to form temporal constraint in the discovery process. introduce the notion of temporal representation which is capable of expressing the relationships between interval-based events. We develop new methods for finding such interesting patterns.

III. EXISTING SYSTEM

3.1Point-based event is represented by one end point. It has three possible projection methods between two events. Prefix Span algorithm is used for this event. The advantages of this algorithm are novel, scalable and efficient.

Example : (*PrefixSpan*) Let the sequence database S given in Table1 an min-support =2. The set of items in the database is {a,b,c,d,e,f,g}.

Table 1: A Sequence Database.

Sequence_No	Sequence
01	< a (abc) (ac) d (cf) >
02	< (ad) c (bc) (ae) >
03	< (ef) (ab) (df) cb >
04	< eg (af) cbc >

Step 1: Find length-1 sequential pattern.

Scan S once to find all frequent items in sequences. Each of these frequent items is a length-1 sequential pattern. They are as follows:

$$\langle a \rangle : 4, \langle b \rangle : 4, \langle c \rangle : 4, \quad \langle d \rangle : 3, \langle e \rangle : 3, \text{ and } \langle f \rangle : 3.$$

Step: 2 Divide search space.

The sequential patterns can be partitioned into the following six subsets according to the six prefixes. Table 2 represents the projected database.

Table 2: Projected database.

Prefix	Projected (Postfix) Database
< a >	< (abc) (ac) d (cf) >, < (_d) c (bc) (ae) >, < (_b) (df) cb >, < (_f) (cbc) >
< b >	< (_c) (ac) d (cf) >, < (_c) (ae) >, < (df) cb >, < c >
< c >	< (ac) d (cf) >, < (bc) (ae) >, < b >, < bc >
< d >	< (cf) >, < c (bc) (ae) >, < (_f) cb >
< e >	< (_f) (ab) (df) cb >, < (af) cbc >
< f >	< (ab) (df) cb >, < cbc >

Step 3: Find subsets of sequential patterns.

The subsets of sequential patterns can be mined by constructing corresponding projected databases and mine each recursively. Table 3 represents the sequential database.

Table 3: Sequential patterns.

Prefix	Sequential patterns
< a >	< a >, < aa >, < a (bc) >, < a (bc) a >, < aba >, < abc >, < (ab) c >, < (ab) d >, < (ab) f >, < (ab) dc >, < ac >, < aca >, < acb >, < acc >, < ad >, < adc >, < af >
< b >	< b >, < ba >, < bc >, < (bc) >, < (bc) a >, < bd >, < bdc >, < bf >
< c >	< c >, < ca >, < cb >, < cc >
< d >	< d >, < db >, < dc >, < dcb >
< e >	< e >, < ea >, < eab >, < eac >, < each >, < eb >, < ebc >, < ec >, < ecb >, < ef >, < efb >, < efc >, < efcb >
< f >	< f >, < fb >, < fbc >, < fc >, < fcb >

3.2. Interval-based event is represented by two end points. It has thirteen possible projection methods between two events according to the classification scheme proposed by Allen [32]: “before”, “after”, “during”, “contain”, “meet”, “met by”, “overlap”, “overlapped by”, “start”, “started by”, “finish”, “finished by”, and “equal”. Based on these relationships, the patterns that they find may look like “(a during b),” which means that “event a occurs during event b.”

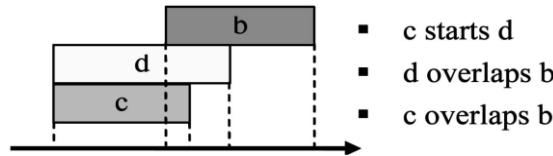


Fig.1. The temporal relationship of three event: b, c and d.

Definition 1: Event end points and order relations

An event e_i has two end points e_i^+ and e_i^- , called event end points, where e_i^+ is the starting point (esp) and e_i^- is the ending point (eep) of e_i . Let the time of an event end point, either esp or eep, be denoted as $time(u)$. Then the order relation $Rel(u, v)$ of two event end points u and v can be denoted as “<” if $time(u) < time(v)$ and as “=” if $time(u) = time(v)$.

Definition 2: Temporal sequence

The temporal sequence in Fig. 1 can be arranged in the following order: $c^+, d^+, b^+, c^-, d^-,$ and b^- . A temporal sequence can be constructively defined as follows:

1. A temporal sequence of one event, called a 1-event temporal sequence, can be written as $(e_i^+ \oplus e_i^-)$, where $e_i \in \{1, \dots, t\}$, and $\oplus \in \{<, =\}$ is the order relation of e_i^+ and e_i^- .
2. Let $p = (p_1 \oplus_1 p_2 \oplus_2 \dots \oplus_{i-1} p_i \oplus_i p_{i+1} \oplus_{i+1} \dots \oplus_{j-1} p_j \oplus_j p_{j+1} \oplus_{j+1} \dots \oplus_{2k-1} p_{2k})$ denote a temporal sequence of k -event (with $2k$ event end points), called a k -event temporal sequence where p_i is an end point, and $\oplus_i \in \{<, =\}$ for all i . suppose p' is the temporal sequence obtained by inserting event e_a into p . Assume that e_a^+ must be placed between p_i and p_{i+1} and e_a^- must be placed between p_j and p_{j+1} . Then we have,

$$p' = (p_1 \oplus_1 p_2 \oplus_2 \dots \oplus_{i-1} p_i \oplus_i e_a^+ \oplus_{i+1} p_{i+1} \oplus_{i+1} \dots \oplus_{j-1} p_j \oplus_j e_a^- \oplus_{j+1} p_{j+1} \oplus_{j+1} \dots \oplus_{2k-1} p_{2k}),$$

where,

$$Rel(p_i, e_a^+) = \oplus_i, Rel(e_a^+, p_{i+1}) = \oplus_{i+1}, Rel(p_j, e_a^-) = \oplus_j, \text{ and } Rel(e_a^-, p_{j+1}) = \oplus_{j+1}.$$

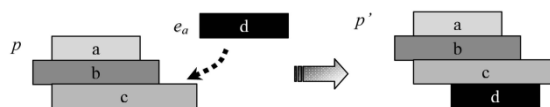


Fig.2. Construction of Temporal sequence.

3.3 TprefixSpan Algorithm:

TPrefixSpan is very similar to *PrefixSpan*. However, the input sequences and output patterns for these two methods are totally different. For example, the process to append a large 1-pattern to an original prefix in *TPrefixSpan* is much more complicated than that in *PrefixSpan*. The main reason for these differences is due to the fact that the input events and output patterns become interval-based instead of point-based, but in this paper the point-based events are also used as input. Therefore, “temporal prefix”, “projection”, and temporal Postfix” are used in the algorithm to design temporal patterns using *TPrefixSpan*.

3.4 Definition : (Temporal prefix)

Suppose we have two temporal sequences $\alpha = (p_1 \oplus_1 p_2 \oplus_2 \dots \oplus_{n-1} p_n)$ and $\beta = (p'_1 \oplus'_1 p'_2 \oplus'_2 \dots \oplus'_{m-1} p'_m)$, where $m \leq n$. Let p'_x denote the last esp in β . Then, β is called a temporal prefix of α if and only if 1) β is contained in α , that is β is subset of α , 2) $p'_i = p_i$ (for $1 \leq i \leq x$), and 3) $\oplus'_i = \oplus_i$ (for $1 \leq i \leq x-1$).

3.5 Definition : (Projection)

Let $\alpha = (p_1 \oplus_1 p_2 \oplus_2 \dots \oplus_{lastp-1} p_{lastp} \oplus_{lastp} p_{lastp+1} \oplus_{lastp+1} \dots \oplus_{n-2} p_{n-1} \oplus_{n-1} p_n)$ and $\beta = (p'_1 \oplus'_1 p'_2 \oplus'_2 \dots \oplus'_{x-1} p'_x \oplus'_x \dots \oplus'_{m-1} p'_m)$ be two temporal sequence satisfying β is subset of α , where p'_x is the last esp in β , and p_{lastp} is the end point in α that matches p'_x . A projection of α with respect to temporal prefix β is temporal sequence α' is subset of α , which can be constructed by the following steps:

- 1) Set $\alpha' = (p'_1 \oplus'_1 p'_2 \oplus'_2 \dots \oplus'_{x-1} p'_x \oplus_{lastp} p_{lastp+1} \oplus_{lastp+1} \dots \oplus_{n-2} p_{n-1} \oplus_{n-1} p_n)$.
- 2) If p_i , where $(lastp+1) \leq i \leq n$, is an eep and its corresponding esp is not in α' then delete p_i .
- 3) After deleting p_i set the order relation between p_{i-1} and p_{i+1} as small (\oplus_{i-1}, \oplus_i).

3.6 Definition: (Temporal postfix)

Let $\alpha' = (p'_1 \oplus'_1 p'_2 \oplus'_2 \dots \oplus'_{x-1} p'_x \oplus_{lastp} p_{lastp+1} \oplus_{lastp+1} \dots \oplus_{n-2} p_{n-1} \oplus_{n-1} p_n)$. be the projection of α with respect to β . Then temporal sequence $\gamma = (p'_x \oplus_{lastp} p_{lastp+1} \oplus_{lastp+1} \dots \oplus_{n-2} p_{n-1} \oplus_{n-1} p_n)$ is called the temporal postfix of α with respect to temporal prefix β , denoted as $\gamma = \alpha / \beta$. If γ contains only one esp, that is p'_x , then we set $\gamma = \phi$. The fig.3 illustrates the generation of projection and temporal postfix.

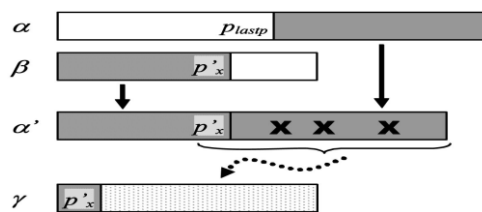


Fig.3.Illustrations for projection and postfix

IV. PROPOSED SYSTEM

4.1 HTPrefixSpan algorithm

Let us apply the HTPrefixSpan algorithm (which is given below) to the temporal sequence database S in Table 4. This table has both interval-based and point-based as an input.

Table 4: Temporal Sequence Database S

Patient	Temporal sequence
01	$(a^+ < e < b^+ < a^- < c^+ < f < b^- < g < c^-)$
02	$(a^+ < a^- < f < g < b^+ < c^+ < c^- < d^+ < h < d^- < b^-)$
03	$(a^+ < b^+ < e < f < b^- < c^+ < d^+ < c^- < g < d^- < a^-)$

The terms a^+ , b^+ , c^+ d^+ and a^- , b^- , c^- , d^- are the starting and ending events of the interval-based event respectively. Whereas, e , f , g , h are the point-based events. Initially we need to find,

$$L_1 = \{ (a^+ < a^-), (b^+ < b^-), (c^+ < c^-), (d^+ < d^-), (e), (f), (g), (h) \}$$

Consider $\alpha = (a^+ < b^+ < d^+ < e < g < c^+ < b^- < h < d^- < a^- < c^-)$ and $\beta = (a^+ < b^+ < d^+ < e < g < c^+ < b^- < h)$.

Then the projection and temporal postfix for the above database S is given below respectively,

$$\alpha = (a^+ < b^+ < d^+ < e < g < c^+ < b^- < h < a^- < c^-)$$

$$\gamma = (c^+ < b^- < h < a^- < c^-)$$

After projecting S with respect to every frequent 1-pattern in L_1 , we obtain eight projected databases, as shown in Table 5.

Table 5: Projected Database of L_1

Prefix	Projected Database
$(a^+ < a^-)$	$(a^+ < e < b^+ < a^- < c^+ < f < b^- < g < c^-)$ $(a^+ < a^- < f < g < b^+ < c^+ < c^- < d < h < d^- < b^-)$ $(a^+ < b^+ < e < f < b^- < c^+ < d^+ < c^- < g < d < a^-)$
$(b^+ < b^-)$	$(b^+ < c^+ < f < b^- < g < c^-)$ $(b^+ < c^+ < c^- < d^+ < h < d^- < b^-)$ $(b^+ < e < f < b^- < c^+ < d^+ < c^- < g < d^-)$
$(c^+ < c^-)$	$(c^+ < f < g < c^-)$ $(c^+ < c^- < d^+ < h < d^-)$ $(c^+ < d^+ < c^- < g < d^-)$
$(d^+ < d^-)$	$(d^+ < h < d^-), (d^+ < c^- < g < d^-)$
(e)	$(e < b^+ < c^+ < f < b^- < g < c^-)$ $(e < f < c^+ < d^+ < c^- < g < d^-)$
(f)	$(f < g)$ $(f < g < b^+ < c^+ < c^- < d^+ < h < d^- < b^-)$ $(f < c^+ < d^+ < c^- < g < d^-)$
(g)	$(g), (g < b^+ < c^+ < c^- < d < h < d^- < b^-)$
(h)	(h)

Then the candidates can be generated by inserting the prefixes with one another.

For an example $\alpha = (a^+ < a^-)$ with $L_1 \{ (b^+ < b^-), (c^+ < c^-), (d^+ < d^-), (e), (f), (g), (h) \}$

Repeat the process till $\alpha = (g)$ with $L_1 \{ h \}$

Consider $(a^+ < a^-)$ with $(b^+ < b^-)$ the possible insertion places are as follows:

$$\begin{aligned} (a^+ < b^+ < a^- < b^-) &\longrightarrow 1 \\ (a^+ < b^+ < b^- < a^-) &\longrightarrow 2 \\ (a^+ < a^- < b^+ < b^-) &\longrightarrow 3 \end{aligned}$$

From the above example 1, 2 and 3 are present in the database so they are consider as frequent temporal patterns. By repeating the process the following temporal patterns has been generated.

$$\begin{aligned} (a^+ < c^+ < a^- < c^-) \\ (a^+ < a^- < c^+ < c^-) \\ (a^+ < d^+ < d^- < a^-) \\ (a^+ < a^- < d^+ < d^-) \\ (a^+ < e < a^-) \\ (a^+ < f < a^-) \\ (a^+ < a^- < e) \end{aligned}$$

$(a^+ < g < a^-)$
 $(a^+ < a^- < g)$
 $(a^+ < a^- < h)$
 $(b^+ < c^+ < b^- < c^-)$
 $(b^+ < c^+ < c^- < b^-)$
 $(b^+ < d^+ < d^- < b^-)$
 $(b^+ < b^- < d^+ < d^-)$
 $(b^+ < e < b^-)$
 $(b^+ < f < b^-)$
 $(b^+ < b^- < g)$
 $(b^+ < h < b^-)$
 $(c^+ < d^+ < c^- < d^-)$
 $(c^+ < c^- < d^+ < d^-)$
 $(c^+ < f < c^-)$
 $(c^+ < g < c^-)$
 $(c^+ < c^- < g)$
 $(c^+ < c^- < h)$
 $(d^+ < g < d^-)$
 $(d^+ < h < d^-)$
 $(e < f)$
 $(e < g)$
 $(f < g)$
 $(f < h)$
 $(g < h)$

4.2 HTPrefixSpan Algorithm

Step1: Scan the database S to identify the interval-based and point-based inputs.

Step2: Find the projection and temporal postfix patterns using the above mentioned definition.

Step3: Using the prefix of length-1 generate projected database.

Step4: Generate the set of patterns using all the prefix combinations.

Step5: The generated patterns from step4 are compared with the database.

Step6: The coinciding patterns with the database are considered as the Temporal Patterns.

V. APPLICATIONS

This temporal pattern mining is applicable to various fields like financial services, census, stock fluctuations, library management, hospital management etc.,

VI. CONCLUSION AND FUTURE WORK

In this paper, a new algorithm Hybrid TPrefixSpan is proposed and implemented. This technique uses the approach of Tprefix span and extends the algorithm by including point based events also in the temporal sequence. Thus the proposed algorithm can be used for both interval-based and point-based events. This makes an efficient way of mining the exact data from the database. This work can be extended to find time span between frequent temporal patterns. The ambiguous problem of temporal pattern representation can also be considered in the future work.

REFERENCES

- [1] Shin-Yi Wu and Yen-Liang Chen, "Mining Nonambiguous Temporal Patterns for Interval-Based Events", IEEE Transactions on Knowledge and Data Engineering, Vol.19, No.6, June 2007.
- [2] W.J. Frawley, G. Piatetsky-Shapiro, and C.J. Matheus, Knowledge Discovery in Database: An Overview. AAAI/MIT Press, 1991.
- [3] Jiawei Han, Jian Pei, Behzad Mortazavi-Asl, Qiming Chen Umeshwar Dayal, Mei-Chun Hsu, "FreeSpan: Frequent Pattern-Projected Sequential Pattern Mining",
- [4] Jian Pei, Jiawei Han, Behzad Mortazavi-Asl, Helen Pinto, Qiming Chen Umeshwar Dayal Mei-Chun Hsu, "PrefixSpan: Mining Sequential Patterns Efficiently by Prefix-Projected Pattern Growth".
- [5] R. Agrawal and R. Srikant, "Mining Sequential Patterns", Proc. 11th Int'l Conf. Data Eng. (ICDE '95), pp. 3-14, Mar. 1995.
- [6] C.-C. Yu and Y.-L. Chen, "Mining Sequential Patterns from Multi-Dimensional Sequence Data", IEEE Trans. Knowledge and Data Eng., vol. 17, no. 1, pp. 136-140, Jan. 2005.
- [7] J. Pei, J. Han, B. Mortazavi-Asl, H. Pinto, Q. Chen, U. Dayal, and M.-C. Hsu, "PrefixSpan: Mining Sequential Patterns Efficiently by Prefix-Projected Pattern Growth", Proc. 17th Int'l Conf. Data Eng.(ICDE '01), pp. 215-224, 2001.
- [8] R. Srikant and R. Agrawal, "Mining Sequential Patterns: Generalizations and Performance Improvements," Proc. Fifth Int'l Conf. Extending Database Technology (EDBT '96), pp. 3-17, 1996.
- [9] J. Pei, J. Han, and W. Wang, "Mining Sequential Patterns with Constraints in Large Databases," Proc. 11th Int'l Conf. Information and Knowledge Management (CIKM '02), 2002.
- [10] P.S. Kam and A.W.C. Fu, "Discovering Temporal Patterns for Interval-Based Events," Proc. Second Int'l Conf. Data Warehousing and Knowledge Discovery (DaWaK '00), 2000.

Application of Matrix Iterative-Inversion in Solving Eigenvalue Problems in Structural Engineering

¹O. M. Ibearugbulem, ²L. O. Ettu, J. C. Ezeh, ³U. C. Anya
^{1,2,3,4}Civil Engineering Department, Federal University of Technology, Owerri, Nigeria

Abstract:

There are many methods of solving eigenvalue problems, including Jacobi method, polynomial method, iterative methods, and Householder's method. Unfortunately, except the polynomial method, all of these methods are limited to solving problems that have lump mass matrices. It is difficult to use them when solving problems that have consistent mass or stiffness matrix. The polynomial method also becomes very difficult to use when the size of the matrix exceeds 3×3 . There is, therefore, a need for a method that can be used in solving all types of eigenvalue problems for all matrix sizes. This work provides such a method by the application of matrix iterative-inversion, Iteration-Matrix Inversion (I-MI) method, consisting in substituting a trial eigenvalue, λ into $(A - \lambda B) = 0$, and checking if the determinant of the resultant matrix is zero. If the determinant is zero then the chosen eigenvalue is correct; but if not, another eigenvalue will be chosen and checked, and the procedure continued until a correct eigenvalue is obtained. A QBASIC program was written to simplify the use of the method. Five eigenvalue problems were used to test the efficiency of the method. The results show that the newly developed I-MI method is efficient in convergence to exact solutions of eigenvalues. The new I-MI method is not only efficient in convergence, but also capable of handling eigenvalue problems that use consistent mass or stiffness matrices. It can be used without any limit for problems whose matrices are of $n \times n$ order, where $2 \leq n \leq \infty$. It is therefore recommended for use in solving all the various eigenvalue problems in structural engineering.

Keywords: Eigenvalue, Matrix, Consistent mass, Consistent Stiffness, Determinant

I. INTRODUCTION

The dynamic equation in structural dynamics is given by Fullard (1980) as in equation (1).

$$\{F(t)\} = [M]\{X''\} + [C]\{X'\} + [K]\{X\} \quad (1)$$

where $\{F(t)\}$ is the time-dependent loading vector; $[M]$ is the mass matrix; $\{X''\}$ and $\{X'\}$ are the first and second time derivatives of the response vector, $\{X\}$; $[C]$ is the damping matrix; and $[K]$ is the stiffness matrix. For the case of free vibration in nature where $\{F(t)\} = \{c\} = 0$, the dynamic equation reduces to equation (2).

$$[M]\{X''\} + [K]\{X\} = 0 \quad (2)$$

When a static stability case is considered, the equation further reduces to equation (3).

$$\{F\} = [K - K_g]\{X\} \quad (3)$$

Where K is the material stiffness and K_g is the geometric stiffness. $\{F\}$ is the vector of bending forces (shear force and bending moment). The continuum (beam or plate) can buckle in cases of axial forces only with no bending forces; the equation becomes as written in equation (4).

$$0 = [K - K_g]\{X\} \quad (4)$$

Equation (2) is used in finding the natural frequencies in structural dynamics, while equation (4) is used to determine the buckling loads in structural stability. The solutions in both cases are called eigenvalue or characteristic value solutions.

In structural mechanics, shape functions are usually assumed to approximate the deformed shape of the continuum. If the assumed shape function is the exact one, then the solution will converge to exact solution. The stiffness matrix $[K]$ is formulated using the assumed shape function. In the same way, the mass matrix $[M]$ and the geometric stiffness matrix $[K_g]$ will be formulated. The mass matrix and the geometric stiffness matrix formulated in this way are called consistent mass matrix and consistent geometric stiffness matrix respectively (Paz, 1980 and Geradin, 1980).

Owen (1980) transformed equation (2) to into the form expressed in equations (5a) and (5b).

$$[K]\{X\} = \omega^2[M]\{X\} \text{----- (5a)}$$

$$([K] - \omega^2[M])\{X\} = 0 \text{----- (5b)}$$

It is easy to determine the eigenvalues of equations (4) and (5) when the size of the square matrix is not more than 3 x 3. Geradin (1980) noted that significant amount of computational effort is required for the eigenvalue problems using consistent mass matrix. Because of this difficulty, many analysts preferred using lump mass matrix to consistent mass matrix. The works of Key and Krieg (1972) and Key (1980) showed that the difference between the solutions from lump mass and consistent mass is very significant. Since the difference in the solutions is high, analysts need not stick to the use of lump mass just because it is easy to solve. Sheik et al. (2004) recommended efficient mass lumping scheme to form a mass matrix having zero mass for the internal nodes. This, according to them, would help facilitate condensation of the structural matrix. The use of lump mass matrix will transform equation (5) into the form written in equation (6).

$$([K] - \omega^2m[I])\{X\} = 0 \text{----- (6)}$$

where [I] is the identity matrix. Equation (6) can simply be written as shown in equation (7).

$$(A - \lambda I)X = 0 \text{----- (7)}$$

where A is a square matrix, λ is a scalar number called eigenvalue or characteristic value of matrix A, I is identity matrix, and X is the eigenvector (Stroud, 1982 and James, Smith and Wolford, 1977). There are many methods of solving equations (6) and (7). Some of the methods include Jacobi method, polynomial method, iterative methods, and Householder’s method (Greenstadt, 1960; Ortega, 1967; and James, Smith and Wolford, 1977). Iterative methods are based on matrix–vector multiplication. Some of the iterative methods include power method, inverse iteration method (Wilkinson, 1965), Lanczos method (Lanczos, 1950), Arnoldi method (Arnoldi, 1951; Demmel, 1997; Bai et al., 2000; Chatelin, 1993; and Trefethen and Bau, 1997), Davidson method, Jacobi-Davidson method (Hochstenbach and Notay, 2004; and Sleijpen and van der Vorst, 1996), minimum residual method, generalized minimum residual method (Barrett et al., 1994), multilevel preconditioned iterative eigensolvers (Arbenz and Geus, 2005), block inverse-free preconditioned Krylov subspace method (Quillen and Ye, 2010), Inner-outer iterative method (Freitag, 2007), and adaptive inverse iteration method (Chen, Xu and Zou, 2010). Unfortunately, except the polynomial method, all of these methods can only be used for equations (6) and (7); they cannot handle equations (4) and (5); and as previously noted, Polynomial method also becomes very difficult to use when the size of the matrix exceeds 3 x 3.

There is, therefore, a need for a method that can be used in solving eigenvalue problems of equations (6) and (7) as well as equations (4) and (5) for any size of matrix. This work provides such a method by the application of matrix iterative-inversion, consisting in substituting a trial eigenvalue, λ into (A – λB) = 0, and checking if the determinant of the resultant matrix is zero. If the determinant is zero then the chosen eigenvalue is correct; but if not, another eigenvalue will be chosen and checked, and the procedure continued until a correct eigenvalue is obtained.

II. MATRIX ITERATIVE-INVERSION

Trivial solutions will exist for both equations (4) and (5) if and only if {X} = 0. To avoid trivial solutions, equations (4) and (5) will respectively satisfy equations (8) and (9).

$$|[K - Kg]| = 0 \text{----- (8)}$$

$$|[K] - \omega^2[M]| = 0 \text{----- (9)}$$

Equations (8) and (9) can simply be written as in equation (10).

$$|[A] - \lambda[B]| = 0 \text{----- (10)}$$

$$\text{Let } [C] = [A] - \lambda[B] \text{----- (11)}$$

$$\text{That is to say } |C| = 0 \text{----- (12)}$$

The inverse of matrix [C] is denoted as [C]⁻¹. From elementary mathematics,

$$[C]^{-1} = \frac{[D]^T}{|C|} \text{----- (13)}$$

Where [D] is the matrix of the cofactors of the elements of . The implication of equation (13) is that the inverse of matrix C, [C]⁻¹ will be infinity (and this does not exist) as long as its determinant is equal to zero. The approach used in this work is to deal with the inverse matrix because it is easier to evaluate the inverse of a matrix using row operation rather than the determinant of the same matrix. The iteration process can start with taking the value of λ as zero and checking if the inverse [C]⁻¹ exists or not. If the inverse exists then zero is not the eigenvalue; λ will then be increased (say by 0.1) and used to test if the inverse of C matrix exists. If the inverse still exists, λ will again be increased and the process repeated until the inverse matrix ceases to exist as it

becomes infinity. The value of λ at which the inverse matrix becomes infinity is the lowest eigenvalue. The next eigenvalue will be a slight increment of this lowest eigenvalue, say $\lambda+0.1$.

III. QBASIC PROGRAM FOR THE METHOD

A simple user-friendly and interactive QBASIC program which requires no special training to be used was written in order to simplify the use of this method (see appendix to this work). The program was used to test the following problems.

$$[1] \quad \begin{bmatrix} 2 & 0 & 1 \\ -1 & 4 & -1 \\ -1 & 2 & 0 \end{bmatrix} - \lambda \begin{bmatrix} 1 & 0 \\ 0 & 1 \\ 0 & 0 \end{bmatrix} \quad (\text{Stroud, 1982})$$

$$[2] \quad \begin{bmatrix} 0.1 & 0.1 & 0.1 \\ 0.1 & 0.2 & 0.2 \\ 0.1 & 0.2 & 0.3 \end{bmatrix} - \lambda \begin{bmatrix} 1 & 0 \\ 0 & 1 \\ 0 & 0 \end{bmatrix} \quad (\text{James, Smith and Wolford, 1977})$$

$$[3] \quad \begin{bmatrix} 5.143 & 3.863 & 3.543 \\ 3.863 & 6.05 & 6.857 \\ 3.543 & 6.857 & 8.341 \end{bmatrix} - \lambda \begin{bmatrix} 0.324 & 0.194 & 0.1 \\ 0.194 & 0.139 & 0.1 \\ 0.162 & 0.121 & 0.1 \end{bmatrix}$$

$$[4] \quad \begin{bmatrix} 1.8844 & 4.7212 & 4.7212 \\ 4.7212 & 11.8316 & 11.80294 \\ 4.7212 & 11.80294 & 11.91948 \end{bmatrix} - \lambda \begin{bmatrix} 0.0478 & 0.1195 & 0.1195 \\ 0.1195 & 0.29904 & 0.299 \\ 0.1195 & 0.299 & 0.3 \end{bmatrix}$$

$$[5] \quad \begin{bmatrix} 0.60953 & 0.3962 & 0.34287 & 0.30477 \\ 0.3962 & 0.4039 & 0.40964 & 0.41738 \\ 0.34287 & 0.40964 & 0.44353 & 0.4777 \\ 0.30477 & 0.41738 & 0.4777 & 0.53884 \end{bmatrix} - \lambda \begin{bmatrix} 0.0127 & 0.00762 & 0.00635 & 0.00544 \\ 0.00762 & 0.00544 & 0.00476 & 0.00423 \\ 0.00635 & 0.00476 & 0.00423 & 0.00381 \\ 0.00544 & 0.00423 & 0.00381 & 0.003 \end{bmatrix}$$

IV. RESULTS, DISCUSSION, AND CONCLUSION

The resulting lowest eigenvalues obtained for the above five problems by use of the developed QBASIC program are as shown in Table 1. When these lowest eigenvalues are substituted into their respective problems, and the determinants of the problems calculated, the resulting values of the determinants are as shown in Table 2. It is a common knowledge that the determinant of an eigenvalue matrix is zero when the exact eigenvalue is substituted into it. Hence, if the eigenvalues in table 1 were exact or approximate eigenvalues of matrices 1, 2, 3, 4 and 5, the determinants would be exactly or approximately equal to zero upon substituting the eigenvalues into the matrices. Table 2 shows that the determinants from the Iteration-Matrix Inversion (I-MI) method are approximately zero. It can also be seen from table 2 that the determinant for matrix 2 from power method (James, Smith and Wolford, 1977) is far from being zero. The results show that the newly developed I-MI method is efficient in convergence to exact solutions of eigenvalues. The new I-MI method is not only efficient in convergence, but also capable of handling eigenvalue problems that use consistent mass or stiffness matrices. It can be used without any limit for problems whose matrices are of $n \times n$ order, where $2 \leq n \leq \infty$. It is therefore recommended for use in solving all the various eigenvalue problems in structural engineering.

Table 1: Results of Eigenvalue Problems

Problem	Eigenvalues from Matrix Iterative-Inversion method				1st Eigenvalues from Reference
	1st eigenvalue	2nd eigenvalue	3rd eigenvalue	4th eigenvalue	
1	1	2	3		1 ¹
2	0.031	0.2618	0.5049		1.98 ²
3	15.113	15.8732	63.2421		No reference
4	10.089	10.189	10.289		No reference
5	47.2399	47.9867	116.9181	117.0181	No reference

1:(Stroud, 1982); 2: (James, Smith and Wolford, 1977)

Table 2: Determinants of Eigenvalue Problems

Problem	Determinant from Matrix Iterative-Inversion method				Determinant from Reference
	From 1st eigenvalue	From 2nd eigenvalue	From 3rd eigenvalue	From 4th eigenvalue	
1	0	0	0		0^1
2	-3.2E-06	0.01109	-0.0000017		-5.50815^2
3	5.67E-06	-0.18079	-0.00285		No reference
4	-0.011196	-0.011067	-0.01093784		No reference
5	3.967E-13	-1.91E-08	-9.701E-09	-5.9579E-09	No reference

1:(Stroud, 1982), 2: (James, Smith and Wolford, 1977)

V. APPENDIX (VISUAL BASIC PROGRAM)

```

Private Sub STARTMNU_Click()
ReDim AA(40, 100, 100), AANS(100, 100), ANS(100, 100)
ReDim MROW(100), MCOLUMN(100), MM(40, 100, 100), MMANS(100, 100), EMMANS(100, 100)
ReDim INVM(100, 200), INVAM(200, 200), INVRM(200, 200), INVABM(100, 200), A(200, 200), B(200, 200)
Dim VROW As Variant, VCOLUMN As Variant
Cls
FontSize = 11: OWUS = 0
2220 OWUS = 0: OW = 1
' THIS AREA IS FOR MATRIX INVERSION
' HERE IS THE INPUT FOR INVERSION
10 VROW = InputBox("WHAT'S THE NO. OF ROWS OF THIS MATRIX ?"): NR = 1 * VROW
If VROW = 0 Then Notice = InputBox("IT IS NOT POSSIBLE", "ROW OF MATRIX CAN'T BE ZERO", "Click O.K. for me"): GoTo 10
20 VCOLUMN = InputBox("WHAT'S THE NO OF COLUMNS OF THIS MATRIX?")
If VCOLUMN = 0 Then Notice = InputBox("IT IS NOT POSSIBLE", "COLUMN OF MATRIX CAN'T BE ZERO", "Click O.K. for me"): GoTo 20
If VROW <> VCOLUMN Then MsgBox (IMPOSSIBLE), , "IMPOSSIBLE" Else GoTo 2221
2221 For X = 1 To VROW
For Y = 1 To VCOLUMN
A(X, Y) = InputBox([Y], [X], "ENTER A")
Next Y
Next X
For X = 1 To VROW
For Y = 1 To VCOLUMN
B(X, Y) = InputBox([Y], [X], "ENTER B")
Next Y
Next X
T = 0
2255 For I = 1 To VROW
For J = 1 To VCOLUMN
INVM(I, J) = A(I, J) - T * B(I, J)
Next J
Next I
' THE INVERSE IS CARRIED OUT HERE
' THE PREAMBLE OF INVERSION
For I = 1 To VROW
For J = 1 To 2 * VCOLUMN
INVAM(I, J) = 0
Next J
Next I
For I = 1 To VROW

```

```

For J = 1 To 2 * VCOLUMN
INVAM(I, J) = INVAM(I, J) + INVM(I, J)
Next J
Next I
For I = 1 To VROW
INVAM(I, I + VCOLUMN) = INVAM(I, I + VCOLUMN) + 1
Next I
For I = 1 To VROW
For J = 1 To VCOLUMN
INVABM(I, J) = INVAM(I, J)
Next J
Next I
ZZ = 1
'THIS IS THE PLACE FOR INVERSION PROPER
For I = 1 To VROW
OWUSS = INVAM(I, I)
3333 If OWUSS > -0.0001 And OWUSS < 0.0001 Then GoTo 2222
For J = 1 To 2 * VCOLUMN
INVAM(I, J) = INVAM(I, J) / OWUSS
Next J
For J = 1 To VROW
If (J = I) Then GoTo 77777
OWUSS = INVAM(J, I)
For K = 1 To 2 * VCOLUMN
INVAM(J, K) = INVAM(J, K) - OWUSS * INVAM(I, K)
Next K
77777 Next J
Next I
' If T > 40 Then GoTo 1111111
T = T + 0.0001
GoTo 22555
2222 ' HERE IS THE PLACE INTERCHANGE OF ROWS
If I + ZZ = 3 * VROW Then GoTo 1111111: MsgBox (IMPOSSIBLE), , "THIS MATRIX HAS NO
INVERSE":
For W = 1 To 2 * VCOLUMN
INVRM(I, W) = INVAM(I, W): INVRM(I + ZZ, W) = INVAM(I + ZZ, W)
INVAM(I, W) = INVRM(X + ZZ, W): INVAM(I + ZZ, W) = INVRM(I, W)
Next W
OWUSS = INVAM(I, I)
If OWUSS = 0 Then ZZ = ZZ + 1: GoTo 6666
Z = 1: GoTo 3333
6666 For W = 1 To 2 * VCOLUMN
INVRM(I, W) = INVAM(I, W): INVRM(I + ZZ, W) = INVAM(I + ZZ, W)
INVAM(I, W) = INVRM(I + ZZ, W): INVAM(I + ZZ, W) = INVAM(I, W)
Next W
If I + ZZ = 3 * VROW Then: GoTo 1111111: MsgBox (IMPOSSIBLE), , "THIS MATRIX HAS NO
INVERSE":
ZZ = ZZ + 1: GoTo 2222
'this is the end of inversion
1111111
Print "RESULT"
Print " H = "; Format(T, "0.###0");
If OW = NR Then GoTo 1111112
OW = OW + 1: T = T + 0.1
GoTo 22555
1111112
WWW = InputBox(" Press OK or Cancele to Stop")
End Sub

```

REFERENCES

- [1] Arnoldi, W. E. (1951). The principle of minimized iteration in the solution of the matrix eigenvalue problem. *Quarterly of Applied Mathematics*, 9: 17– 29.
- [2] Arbenz, P., and Geus, R. (2005). Multilevel preconditioned iterative eigensolvers for maxwell eigenvalue problems. *Applied numerical mathematics*, 54(2): 107 – 121.
- [3] Bai, Z. D. J., Dongarra, J. R. A., and Van-der Vorst, H. (2000). *Templates for the Solution of Algebraic Eigenvalue Problems - A Practical Guide*. Philadelphia, PA:SIAM.
- [4] Barrett, R.; Berry, M.; Chan, T. F.; Demmel, J.; Donato, J.; Dongarra, J.; Eijkhout, V.; Pozo, R.; Romine, C.; and Van-der Vorst, H. A. (1994). *Templates for the Solution of Linear Systems: Building Blocks for Iterative Methods*, 2nd ed. Philadelphia, PA:SIAM.
- [5] Chatelin, F. (1993). *Eigenvalues of matrices*, Chichester, West Sussex: JohnWiley&Sons Ltd.
- [6] Demmel, J. W. (1997). *Applied Numerical Linear Algebra*. Philadelphia, PA:SIAM.
- [7] Freitag, M. (2007). *Inner-outer Iterative Methods for Eigenvalue Problems - Convergence and Preconditioning* (Unpublished doctoral dissertation). University of Bath.
- [8] Fullard, K. (1980). The Modal Method for Transient Response and its Application to Seismic Analysis. In Donea, J. (ed.), *Advanced Structural Dynamics* (pp.43-70).
- [9] Geradin, M. (1980). Variational Methods of Structural Dynamics and their Finite Element Implementation. In Donea, J. (ed.), *Advanced Structural Dynamics*(pp.1-42)
- [10] Greenstadt, J. (1960). *Mathematical Methods for Digital Computers*. Vol. 1(ed. A. Ralston and H. S. Wilf). New York: John Wiley & sons. Pp. 84-91.
- [11] Hochstenbach, M. E. and Notay, Y. (2004). The Jacobi-Davidson method, GAMM Mitt.
- [12] James, M. L., Smith, G. M. and Wolford, J. C. (1977). *Applied Numerical Methods for Digital Computation: withFORTRAN and CSMP*. New York: Harper and Row Publishers.
- [13] Key, S. W. (1980). Transient Response by Time Integration: Review of Implicit and Explicit Operators. In Donea, J. (ed.), *Advanced Structural Dynamics*.
- [14] Key, S. W. and Krieg, R. D. (1972) Transient Shell Response by numerical Time Integration. 2nd US-JAPAN Seminar on Matrix Methods in Structural Analysis. Berkeley, California.
- [15] Lanczos, C. (1950). An iterative method for the solution of the eigenvalue problem of linear differential and integral operators. *Journal of Research of the National Bureau of Standards*, 45: 255–282.
- [16] Ortega, J. (1967). *Mathematical Methods for Digital Computers*. Vol. 2(ed. A. Ralston and H. S. Wilf). New York: John Wiley & sons. Pp. 94-115.
- [17] Owen, D. R. J. (1980). Implicit Finite Element Methods for the Dynamic Transient Analysis of Solids with Particular Reference to Non-linear Situations. In Donea, J. (ed.), *Advanced Structural Dynamics* (pp. 123-152).
- [18] Paz, M. (1980). *Structural Dynamics: Theory and Computation*. New York: Litton Education Publishers.
- [19] Quillen, P. and Ye, Q. (2010). A block inverse-free preconditioned Krylov subspace method for symmetric generalized eigenvalue problems. *Journal of Computational and Applied Mathematics*, 233 (5): 1298-1313
- [20] Sheikh, A. H.; Haldar, S.; and Sengupta, D. (2004). Free flexural vibration of composite plates in different situations using a high precision triangular element. *Journal of Vibration and Control*, 10 (3): 371-386.
- [21] Sleijpen, G. L. G., and Van-der Vorst, H. A. (1996). A Jacobi-Davidson iteration method for linear eigenvalue problems. *SIAM J. Matrix Anal. Appl.*, 17: 401–425.
- [22] Stroud, K. A. (1982). *Engineering Mathematics*, 2nd ed. London: MacMillan Press.
- [23] Trefethen, L. N., and Bau, D. I. (1997). *Numerical Linear Algebra*. Philadelphia, PA: SIAM.
- [24] Wilkinson, J. H. (1965). *The Algebraic Eigenvalue Problem*. Oxford, UK: Oxford University Press.

Path Planning Optimization Using Genetic Algorithm – A Literature Review

¹Er. Waghoo Parvez , ²Er. Sonal Dhar

¹. (Department of Mechanical Engg , Mumbai University, MHSSCOE , Mumbai - 400008.

². (Department of Production Engg, Mumbai University, DJSCOE, Mumbai – 410206.

Abstract

This paper presents a review to the path planning optimization problem using genetic algorithm as a tool. Path planning is a term used in robotics for the process of detailing a task into discrete motions. It is aimed at enabling robots with capabilities of automatically deciding and executing a sequence motion in order to achieve a task without collision with other objects in a given environment. Genetic algorithms are considered as a search process used in computing to find exact or an approximate solution for optimization and search problems. There are also termed as global search heuristics. These techniques are inspired by evolutionary biology such as inheritance mutation, selection and cross over.

Keywords - Chromosome, Genetic Algorithm (GA) , Mutation, Optimization, Path Planning.

I. INTRODUCTION

Motion planning is a term used in robotics for the process of detailing a task into discrete motions. It is a process to compute a collision-free path between the initial and final configuration for a rigid or articulated object (the "robot") among obstacles. It is aimed at enabling robots with capabilities of automatically deciding and executing a sequence motion in order to achieve a task without collision with other objects in a given environment. Typically the obstacles and the mobile objects are modeled. Given a source position & orientation for mobile object and goal position & orientation, a search is made for a path from source to goal that is collision free and perhaps satisfied additional criteria such as a short path, a path which can be found quickly or a path which does not wander too close to any one of the obstacles. The general path planning problem requires a search in six dimensional spaces since the mobile object can have three translational and three rotational degrees of freedom. But still there are three dimensional search problems which have two translational and one rotational degrees of freedom. [10]The Genetic algorithm is an adaptive heuristic search method based on population genetics. Genetic algorithm were introduced by John Holland in the early 1970s [1].Genetic algorithm is a probabilistic search algorithm based on the mechanics of natural selection and natural genetics. Genetic algorithm is started with a set of solutions called population. A solution is represented by a chromosome. The population size is preserved throughout each generation. At each generation, fitness of each chromosome is evaluated, and then chromosomes for the next generation are probabilistically selected according to their fitness values. Some of the selected chromosomes randomly mate and produce offspring. When producing offspring, crossover and mutation randomly occurs. Because chromosomes with high fitness values have high probability of being selected, chromosomes of the new generation may have higher average fitness value than those of the old generation. The process of evolution is repeated until the end condition is satisfied. The solutions in genetic algorithms are called chromosomes or strings [2].

A genetic algorithm is a search technique used in computing to find exact or approximate solutions to optimization and search problems. Genetic algorithms are categorized as global search heuristics. Genetic algorithms are a particular class of evolutionary algorithms (EA) that use techniques inspired by evolutionary biology such as inheritance, mutation, selection, and crossover [7]. Genetic algorithms have been used to find optimal solutions to complex problems in various domains such as biology, engineering, computer science, and social science. Genetic algorithms fall under the heading of evolutionary algorithm. Evolutionary algorithms are used to solve problems that do not already have a well defined efficient solution. Genetic algorithm have been used to solve optimization problems (scheduling, shortest path, etc), and in modeling systems where randomness is involved (e.g., the stock market).

II. GENETIC ALGORITHM

2.1. Initialization

Initially many individual solutions are randomly generated to form an initial population. The population size depends on the nature of the problem, but typically contains several hundreds or thousands of possible solutions. Traditionally, the population is generated randomly, covering the entire range of possible solutions (the search space).

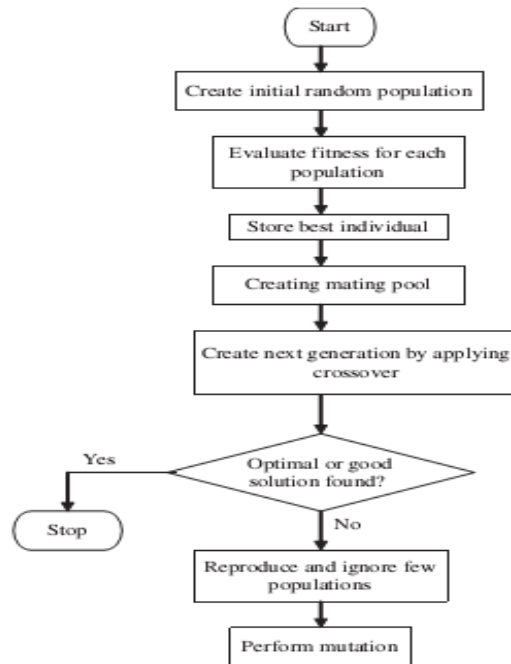


Figure No.1 Flowchart of GA [9]

2.2. Selection

During each successive generation, a proportion of the existing population is selected to breed a new generation. Individual solutions are selected through a fitness-based process, where fitter solutions (as measured by a fitness function) are typically more likely to be selected. Certain selection methods rate the fitness of each solution and preferentially select the best solutions.

Most functions are stochastic and designed so that a small proportion of less fit solutions are selected. This helps keep the diversity of the population large, preventing premature convergence on poor solutions. Popular and well-studied selection methods include roulette wheel selection and tournament selection.

2.3. Reproduction

The next step is to generate a second generation population of solutions from those selected through genetic operators: crossover (also called recombination), and/or mutation. For each new solution to be produced, a pair of “parent” solutions is selected for breeding from the pool selected previously.

By producing a “child” solution using the above methods of crossover and mutation, a new solution is created which typically shares many of the characteristics of its “parents”. New parents are selected for each new child, and the process continues until a new population of solutions of appropriate size is generated.

These processes ultimately result in the next generation population of chromosomes that is different from the initial generation. Generally the average fitness will have increased by this procedure for the population, since only the best or genetic algorithm from the first generation are selected for breeding, along with a small proportion of less fit solutions.

2.4. Termination

This generational process is repeated until a termination condition has been reached. Common terminating conditions are:

- A solution is found that satisfies minimum criteria;
- Fixed number of generations reached;
- Allocated budget (computation time/money) reached;
- The highest ranking solution’s fitness is reaching or has reached a plateau such that successive iterations no longer produce better results;
- Manual inspection.

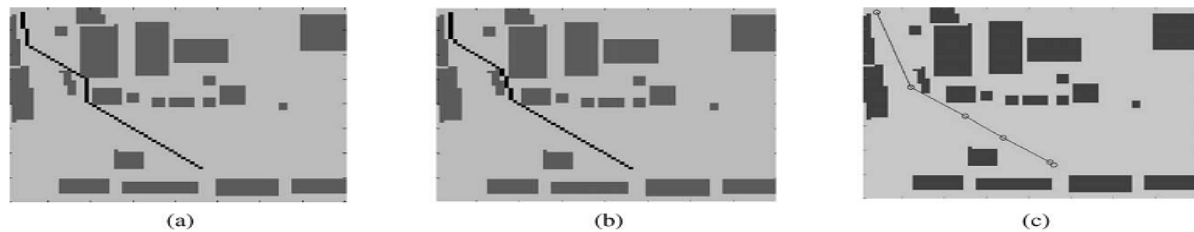
2.5 APPLICATIONS OF GENETIC ALGORITHM [8]

- Nonlinear dynamical systems–predicting, data analysis
- Robot trajectory planning
- Evolving LISP programs (genetic programming)
- Strategy planning
- Finding shape of protein molecules
- TSP and sequence scheduling
- Functions for creating images
- Control–gas pipeline, pole balancing, missile evasion, pursuit
- Design–semiconductor layout, aircraft design, keyboard configuration, communication networks
- Scheduling–manufacturing, facility scheduling, resource allocation
- Machine Learning–Designing neural networks, both architecture and weights.
- Signal Processing–filter design

III. LITERATURE REVIEW

3.1 Path planning in construction sites: performance evaluation of the Dijkstra, A*, and GA search algorithms A.R. Soltani, H. Tawfik, J.Y. Goulermas, T. Fernando [2] says:

The study illustrated the potential of deterministic and probabilistic search algorithms in addressing the site path planning issues with multiple objectives. The application generate the shortest path, low risk path, most visible path, and finally the path that reflects a combination of low risks, short distance, and high visibility between two site locations. Dijkstra algorithm can find optimal solutions to problems by systematically generating path nodes and testing them against a goal, but becoming inefficient for large-scale problems. A* can find optimal and near to optimal solutions more efficiently by directing search towards the goal by means of heuristic functions, reducing the time complexity substantially. These algorithms suffer from the curse of dimensionality effect, which limits the Dijkstra and A* operation to small and medium problems.



Comparison of the algorithms path cost solution

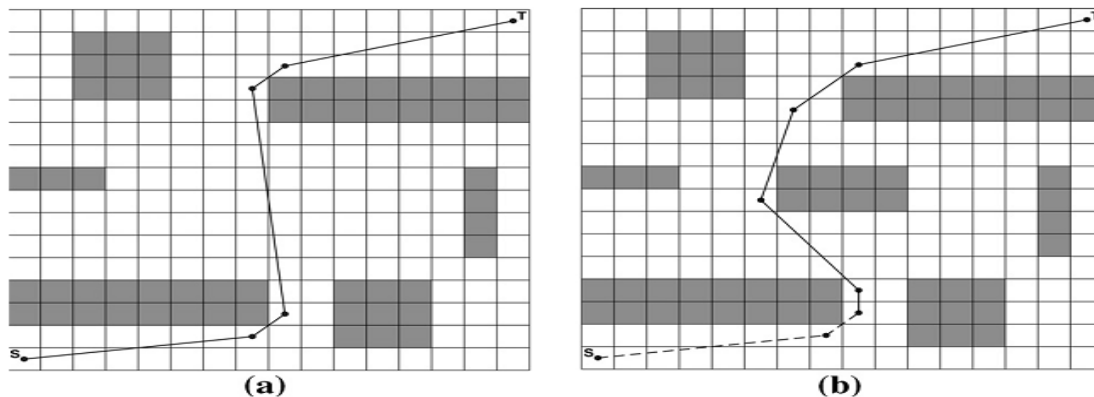
Path evaluation criteria	Dijkstra path cost solution	A* path cost solution	GA path cost solution
Distance minimisation	80.4	80.4	78.6
Safety minimisation	41.5	41.6	43.3
Visibility maximisation	43.5	43.7	42.5
Combined optimisation via G ₁	35.3	43.2	39.5
Combined optimisation via G ₂	29.7	38.9	30.2

Figure No.2 Courtesy [2] environment for research

Probabilistic optimization approach based on GA generates a set of feasible, optimal, and close-to-optimal solutions that captures globally optimal solutions. GA operators exploit the similarities in string structures to make an effective search. Good regions of the search space get exponentially more copies and get combined with each other by the action of GA operators and finally form the optimum or a near-optimum solution in substantially less time. The GA's performance limitations are mainly related to obtaining less accurate solutions and the time-consuming fine-tuning process to guide the search. The future avenues for this work include investigation of the applicability of fuzzy based multi-criteria evaluation, and hybrid optimization search algorithms.

3.2 Dynamic path planning of mobile robots with improved genetic algorithm Adem Tuncer , Mehmet Yildirim [3] says:

They have improved a new mutation operator for the GA and applied it to the path planning problem of mobile robots. The improved mutation method simultaneously checks all the free nodes close to mutation node instead of randomly selecting a node one by one. The method accepts the node according to the fitness value of total path instead of the direction of movement through the mutated node. It is clearly seen from the results that the GA with the proposed mutation operator can find the optimal path far too many times than the other methods do. The average fitness values and the average generation numbers of the proposed method are better than the other methods.



Experimental results for the initial environment in Fig. 5a.

	# of optimal solution	# of near optimal solution	# of infeasible solution	Fitness value	Generation number	Solution time (s)
Random mutation	1	86	13	31.78	21	0.28
Mutation in Ref. [14]	3	69	28	29.25	23	0.31
Mutation in Ref. [20]	2	69	29	29.91	22	0.46
Mutation in this study	54	44	2	27.82	11	0.89

Experimental results for the modified environment in Fig. 5b.

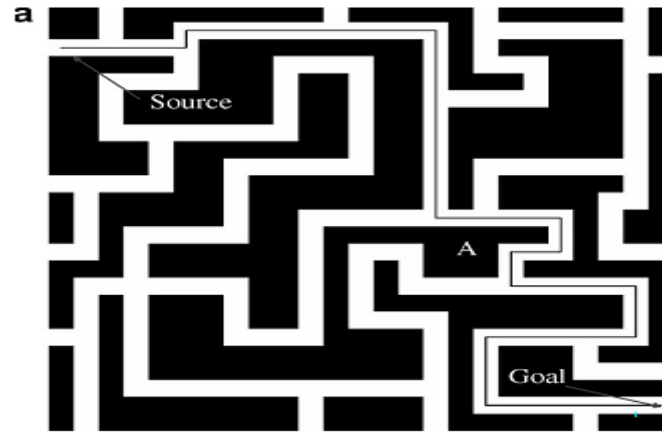
	# of optimal solution	# of near optimal solution	# of infeasible solution	Fitness value	Generation number	Solution time (s)
Random mutation	0	95	5	35.37	23	0.20
Mutation in Ref. [14]	0	95	5	31.21	22	0.26
Mutation in Ref. [20]	0	89	11	30.87	23	0.41
Mutation in this study	44	56	0	29.08	11	0.86

Figure No.3 Courtesy [3] environment for research

3.3 Multi-robot path planning using co-evolutionary genetic programming Rahul Kala [4] says:

Motion planning for multiple mobile robots must ensure the optimality of the path of each and every robot, as well as overall path optimality, which requires cooperation amongst robots. The paper proposes a solution to the problem, considering different source and goal of each robot. Each robot uses genetic programming for figuring the optimal path in a maze-like map, while a master evolutionary algorithm caters to the needs of overall path optimality. Co-operation amongst the individual robots, evolutionary algorithms ensures generation of overall optimal paths. Experiments are carried out with a number of maps, scenarios, and different speeds. Experimental results confirm the usefulness of the algorithm in a variety of scenarios. The modeling scenario has a maze like map where the different robots are initially located at distinct places and are given their own goals that they are supposed to reach. It further assumes that each robot moves with its own

speed. The algorithm makes use of co evolutionary genetic programming. At the first level a linear representation of genetic programming is used. The individual in this case consists of instructions for movement whenever a cross is encountered. The other level consists of a genetic algorithm instance. This algorithm selects the individuals from the genetic programming and tries to generate a combination such that the overall path of all the robots combined is optimal.



Summary of situation and results for simulation with 2 robots.

S. No.	Factor	Robot 1	Robot 2
1	Source	(0,2)	(24,23)
2	Goal	(24,23)	(0,2)
3	Speed	0.5	0.3
4	Reached Goal	Yes	Yes
5	Collision	No	No
6	Time	142	383
7	Path Length	66	115

Figure No.4 Courtesy [4] environment for research

3.4 A new vibrational genetic algorithm enhanced with a Voronoi diagram for path Planning of autonomous UAV Y. Volkan Pehlivanoglu [5] says:

The algorithm emphasizes a new mutation application strategy and diversity variety such as the global random and the local random diversity. Clustering method and Voronoi diagram concepts are used within the initial population phase of mVGA process. The new algorithm and three additional GA's in the paper are applied to the path planning problem in two different three-dimensional (3D) environments such as sinusoidal and city type terrain models and their results are compared. The first mutation operator is applied to all genes of the whole population and this application provided global but random diversity in the population. The global diversity afforded a chance for the population to escape from all local optima. The second mutation operator was specifically applied to the genes of an elite individual in the population. This application provided local diversity leading to a fast convergence. From the results obtained, it is concluded that a Voronoi supported multi frequency vibrational genetic algorithm is an efficient and fast algorithm since it avoided all local optima within relatively short optimization cycles.

3.5 Path planning on a cuboid using genetic algorithms Aybars UG~UR [6] says:

Optimization on a cuboid has potential applications for areas like path planning on the faces of buildings, rooms, furniture, books, and products or simulating the behaviors of insects. This paper, addresses a variant of the TSP in which all points (cities) and paths (solution) are on the faces of a cuboid. They developed an effective hybrid method based on genetic algorithms and 2-opt to adapt the Euclidean TSP to the surface of a cuboid. The aim is to develop a simple and efficient method to find the optimum route visiting all items on a cuboid, one of the most common man-made object shapes. They selected a good TSP solving hybrid method based on GA and 2-opt that has been used for many years. They integrated it with an algorithm developed to calculate the distances of any two points on a cuboid; this implementation allows the hybrid method to be replaced by faster TSP solvers. In accordance with the main goal of this study, the first TSP optimization results were obtained and presented for different point densities in the cuboid environment. A second contribution is the presentation approach of the solution and environment. The user can rotate or scale the cuboid and trace the

optimum path easily.

GA Parameters			
GA parameter	Default	Min	Max
Generation Size	100	1	65,535
Population Size	250	3	65,535
Crossover Rate	0.80	0.0	1.0
Mutation Rate	0.05	0.0	1.0

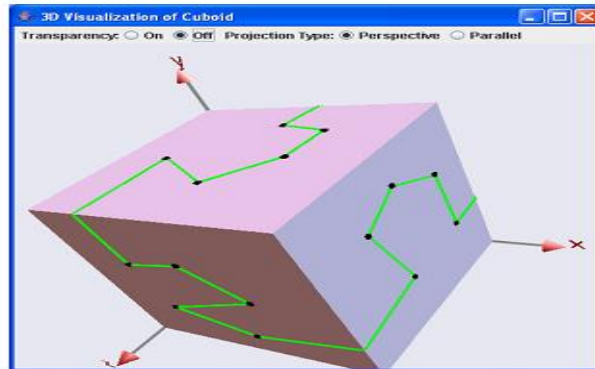


Figure No.5 Courtesy [6] environment for research

IV. CONCLUSION

Based on the various papers studied and textbooks referred it can be concluded that for multi objective optimisation problems genetic algorithms find variety of applications in different fields. Optimal path planning is one of the important factors in scheduling, moving, transporting, etc. Various factors considered for optimal path planning includes avoiding obstacles, minimum path finding, multi objectives constraining, safe distance travelling, etc. For finding the optimal path various optimization techniques are used out of which genetic algorithm finds extreme applications as it gives optimum results considering global population. If proper mathematical model is formed it can give the optimum results in optimum time for path planning/motion planning in the field of robotics.

REFERENCES

- [1] Manoj Kumar, Mohammad Husian, Naveen Upreti, & Deepti Gupta "Genetic Algorithm: Review & Application" International Journal of Information Technology and Knowledge Management July-December 2010, Volume 2, No. 2, pp. 451-454.
- [2] A. R Soltani, H Tawfik, et al" Path planning in construction sites: performance evaluation of the Dijkstra, A* and GA search Algorithm", Advanced Engineering Informatics pg 291-303.
- [3] Adem Tuncer, Mehmet Yildirim "Dynamic path planning of mobile robots with improved genetic algorithm" Computers & Electrical Engineering submitted for publication.
- [4] Rahul Kala "Multi-robot path planning using co-evolutionary genetic programming" Expert Systems with Applications 39 (2012) 3817-3831.
- [5] Y. Volkan Pehlivanoglu "A new vibrational genetic algorithm enhanced with a Voronoi diagram for path planning of autonomous UAV" Aerospace Science and Technology 16 (2012) 47-55.
- [6] Aybars UGUR "Path planning on a cuboid using genetic algorithms" Information Sciences 178 (2008) 3275-3287.

Books:

- [7] David E. Goldberg , Genetic Algorithms in search, optimization & Machine Learning" (Pearson Education Twelfth Impression 2013).
- [8] Melanie Mitchell, An Introduction to Genetic Algorithms (Prentice Hall of India Edition 2005).
- [9] S.N.Sivanandam S.N.Deepa Introduction to Genetic Algorithms (Springer Edition 2008)

Website:

- [10] http://en.wikipedia.org/wiki/Motion_

Low Cost and Simple Management and Security System for Hospitals and Hotels

¹Adnan Affandi , ²Mubashshir Husain

^{1,2}Electrical and Computer Engineering Department, King Abdul Aziz University P.O. BOX: 80204, Jeddah 21589

Abstract

In this paper we designed and built an automatic parking lot management system that keeps track of vehicles entering and leaving a parking lot. Another system was designed and built to record (using a camera) activities of cars entering and leaving the parking lot. Secondly we designed and built an automatic service request management system. This system keeps track of all requests from different rooms and keeps a record of them. Thirdly we designed and built an automatic phone call management system that utilizes the existing power lines as the phone call carrier medium. For all systems we developed programs and employ a visual interface design.

I. INTRODUCTION

1.1 Parking Lot Management and Security System

With all events taking place around the world, security concerns are continuously on the rise. As a consequence of wars, conflicts, or social problems, security concerns must be thoroughly evaluated and necessary measures must be taken in order to reduce risks and improve the safety of people, assets, and facilities. Many places need to be kept secure from intruders or suspects. Parking Lots are provided for visitors of all government buildings, hotels, hospitals, and large buildings. They have been a prime security concern, as many incidents of terrorism were carried out by implanting cars with bombs in parking lots of important buildings. Management and security of parking lots is a continuous challenge. It would be a great idea if an automatic management and security system is designed to continuously manage and watch a parking lot. Cameras are utilized extensively for security solutions. Due to technological advances in manufacturing, cameras are very affordable, abundant, and being used nowadays to monitor and record all activities within certain places. For example banks, airports, government facilities, and even supermarkets are equipped with different cameras that keep recording and tracking activities inside and outside those facilities.

Normally, a camera and a video recording system is installed at the gate of the building to take photographs or a slow motion video and record them along with a timing stamp which tells the reviewer of these records the time and date information. Such systems will allow retrieving the photographs taken within a defined period of time. A drawback is that current security systems employ cameras that keep running and recording continuously regardless of activity taking place or not. Such practice produces huge amount of recorded data and requires huge storage capacity especially when high resolution cameras are used. As a result the captured data quickly fills the storage devices being used. [1]

1.2 Service Request Management

Modern hospitals and hotels are of great importance for nowadays civilized communities. Hospitals extend their medical services to all people, adults and children. Hotels extend their services to most travelers from within the country or from outside the country. Millions of people use the services of hotels and hospitals throughout the world daily. Modern hospitals and hotels of nowadays have high tech equipments that are used for many different purposes. These equipments integrate advanced electronics and computer systems to provide extremely useful tools. Nurses in hospitals continuously watch patients that stay at different rooms. These patients require some assistance at certain times. The on duty nurse is supposed to answer the requests from different patients and address their demands or concerns. Similarly in hotels many rooms are occupied by hundreds of guests daily. These guests have different demands that need to be answered in order to keep the service quality of the hotel at a higher class. Current service request management systems located at hospitals produce an audio and a visual alarm at the nurse desk indicating that requests have been issued. The nurse should keep track manually of the requests. Work stress can cause the nurse to miss some of the requests or answer some requests before others. Similarly in hotels requests are in general placed by the guests via telephone. The help desk staff record the requests manually in order to answer them. It would be a great idea if

an automatic management system is designed to watch multiple rooms and continuously monitor their requests until answered.[4]

1.3 Phone over Power Line Management System

Phone services in hospitals and hotels are extended to patients and guests at an extra charge. Wiring of phone lines in a hotel can be cumbersome. Monitoring of the phone calls and durations need to be done for each guest (room). It would also be a very good idea if the existing power lines are used to extend the phone service to every room in a hospital or hotel. In addition it would be very helpful if the automatic system continues to watch phone call requests and monitor the length of established calls and calculate the total cost of each call for billing.

II. SECURITY AND PARKING LOT MANAGEMENT SYTEM

2.1 Security

Due to technological advances in manufacturing, cameras are very affordable, abundant, and being used nowadays to monitor and record all activities within certain places. For example banks, airports, government facilities, and even supermarkets are equipped with different cameras that keep recording and tracking activities inside and outside those facilities. Normally, a camera and a video recording system is installed at the gate of the building to take photographs or a slow motion video and record them along with a timing stamp which tells the reviewer of these records the time and date information. Such systems will allow retrieving the photographs taken within a defined period of time. The cost for such systems is divided into two parts: the cost of the camera which is usually not very high and the cost of the recording system which contributes more to the total cost. Also, the recording media might be an analog media such as video tape or a digital media such as a hard disk or a compact disk.

Generally, the cost of digital media continues to decrease with advances in digital technology. So, it might be a very cost effective solution to use a personal computer with all of its capabilities to perform the function of a video or photographs recorder. This is possible because of two specific features in new personal computers which are used nowadays. The first feature is the large hard disk which can run up to several hundreds of Gigabytes. This feature makes the computer capable of holding large amounts of digital information required for the application of digital photographs recording. The second feature is the USB cameras that can be interfaced to the USB port which is now standard port in all personal computers. [2]

2.2 Alternative Solutions

A draw back is that current security systems employ cameras that keep running and recording continuously regardless of activity taking place or not. Such practice produces huge amount of recorded data and requires huge storage capacity especially when high resolution cameras are used. As a result the captured data quickly fills the storage devices being used. In order to provide a solution for this problem, three things can be done.

- a) Keep increasing storage capacity to provide enough space for the new captured data.
- b) Use lower resolution cameras whose images are smaller, less clear, and thus require less storage capacity.
- c) Recycle data by erasing older data and replacing it with newly captured data.

Although such solutions help tremendously in providing storage space for storing new captured data, they possess certain disadvantages. First, continuously increasing storage capacity requires continuous purchasing of new storage media and is cost ineffective. Secondly, using lower resolution cameras require less storage capacity however such cameras capture images that do not provide clear pictures of persons that might need to be identified in case of problems. Thirdly, recycling data removes the need for providing new storage media or the need to use lower resolution cameras but requires erasing older recorded data that might be needed at a much later time.

III. PARKING LOT MANAGEMENT

Any parking lot has limited capacity. When the number of cars in a parking lot exceeds its designated capacity, illegal parking starts becoming an issue that causes many further problems. It is very hard for a parking lot manager to keep track of the number of vehicles that entered the parking lot and the number of cars that left the parking lot especially in parking lots that operate over extended time periods and cover large areas. When parking lot supervisors change shifts, the new supervisor has no information to the number of cars in the parking lot. In addition if the supervisor leaves his desk for prayer for example, he would not be able to know the number of cars that entered and left the parking lot during that time. This would mean that each incident such as the one mentioned will cause a problem in counting. [3]

3.1 Alternative solution

The supervisor can close the parking lot entrance and exist until he is done with prayer. Or the supervisor can recount the cars in the parking lot. Or two supervisors need to be on duty all the time. All of those solutions are not practical.

3.2 Proposed Solution

The problem definition suggests designing an automatic counting system that can help tremendously in managing the parking lot. This allows the supervisor to close the parking lot when the number of cars inside the parking lot reaches the maximum capacity. Also the system needs to employ a security camera that will take pictures of cars entering the parking lot or leaving it. The system should be smart on saving storage space. The Parking Lot Control and Security System is described best by the following list of actions:

- [1] The system will be interfaced to the computer.
- [2] Will monitor vehicle entrance.
- [3] Will monitor vehicle exit.
- [4] Keep count of number of empty spaces in the parking lot.
- [5] Upon car entry or exit the camera will be turned on to take a picture.
- [6] All pictures will be time stamped for easy filing.

Following is a block diagram that best describes the functionality of the two systems integrated together.

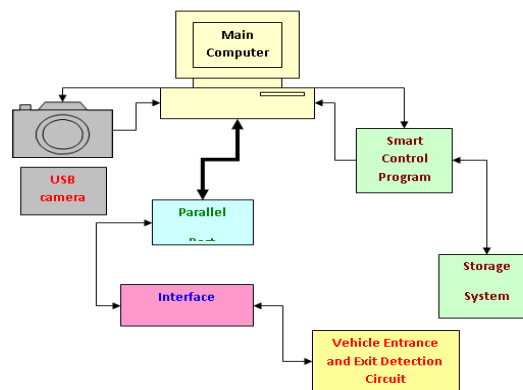


Figure 2 1: Computer-Based parking Lot control and security system

IV. SERVICE REQUEST MANAGEMENT AND TRACKING SYSTEM

Service request management systems generally employ manual recording of requests from different rooms. When handling many rooms and under work stress, service personnel tend to miss some requests unanswered. An alternative solution to this problem is to employ dedicated supervisors that can be costly.

4.1 Proposed Solution

The proposed solution is to design and build a control and monitoring system that can be used for hospitals and hotels. The system will be designed to perform the following functions.

- [1] This system will be designed to serve a total of 5 rooms simultaneously.
- [2] Each room is to be equipped with a service request button.
- [3] Calls or requests from all rooms are to be monitored simultaneously via a main computer that is located at the nurse monitoring room or service desk.
- [4] Upon receiving a request a visual notification and audio alarm is to be turned on to attract the attention of the service desk personnel or the nurses.
- [5] The monitoring computer will display a message showing the room number that requested the service.
- [6] The message window is to provide a button that can be clicked to acknowledge that a nurse or service team member is going to attend the call.
- [7] The system will track all events by recording all calls and requests initiation times, the acknowledgment times, and answer times.
- [8] A status report is to be available via network at the supervisor computer.
- [9] The system will allow the supervisor to monitor the service desk computer via the network.

Following is a block diagram that best describes the functionality of the service request management system.

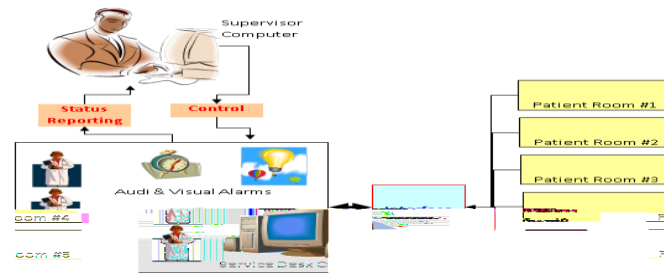


Figure 2 2: Block Diagram of service request management and tracking System

V. TELEPHONE OVER POWER LINE MANAGEMENT SYSTEM

Telephone service need to be extended to guests in hotels and hospitals. Designated (numbers) phone lines can be extended to every room. However the incurred subscription cost can get outrageously high. In addition sophisticated monitoring system needs to be employed to keep track of carried out calls for billing purposes. Cost of such systems is in general very high. Since phone lines in hotel and hospital rooms are not used a lot, there is no need to subscribe to many services from the phone company. Rather a small number of lines can be shared and extended for all rooms. The service can be extended to a room only upon request. When the phone call is done the phone service is free to be extended to other rooms. Selectively extending the phone service to many rooms in the building can be done in different ways.[5]

5.1 Alternative Solutions

Dedicated lines can be laid from the service desk to every room in the building. This requires extensive labor and construction work. Wireless connections can also be employed to every room. However the cost can be very high.

5.2 Proposed Solution

The proposed solution is to utilize the existing power lines that extend to multiple points in every room to carry the phone service. The control system will connect the phone line signal to the room that requests external calling via power lines. When the guest at the requesting room starts the phone call the system will keep track of the time. When the guest hangs up the phone the system will stop the timer and calculate the appropriate charge.

- [1] The system will monitor a request signal from the guest room.
- [2] The system will use a transmitter and receiver to carry phone conversation over power lines.
- [3] A control circuit will be designed to connect the phone line to the intercom module.
- [4] Upon connection of call a timer will be started.
- [5] The timer will be stopped automatically when the guest hangs up.
- [6] The system will display the total charge and records it in a log file.
- [7] The system will be built and tested.

Following is a block diagram that best describes the functionality of the telephone over power line management system.

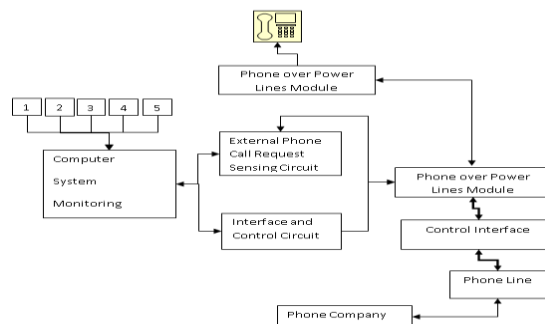


Figure 2 3: Block Diagram of the calling system control and charging

VI. SECURITY AND PARKING LOT MANAGEMENT

The hardware requirement for this paper consists of the following elements:

- [1] A parallel port connection that gives access to the different lines of the parallel port. This will allow the outside circuits to be interfaced to the parallel port.
- [2] A USB camera along with its software. The camera will be used to capture the images.
- [3] Dual infrared detection circuits that will be used to detect the presence of a car entering the parking lot or leaving it.

The infrared detection circuit will be discussed in the following section.

6.1 Car Detection Circuit

Each car detection circuit is used in our paper in to detect the event when an object crosses a certain line. The detection circuit consists of two parts. The first part is an infra red transmitter that continuously transmits infra red light in the direction of an infra red receiver. The second part is an infra red receiver that is aligned with the transmitter for best performance. A block diagram of the transmitter and receiver with no obstruction is shown below in the following figure.

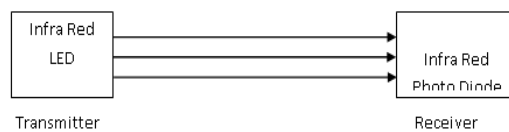


Figure 4 2: Block Diagram of the intrusion detection circuit with no obstruction.

When an object crosses the door or line, the infra red light is obstructed from reaching the receiver. A block diagram of the transmitter and receiver in the presence of an object is shown in the following figure.



Figure 4 3: Block Diagram of the Vehicle detection Circuit with obstruction

6.2 Transmitter

To implement the transmitter we require a light source. The most economical choice of light sources is a light emitting diode. There are two types of light emitting diodes. They are Infra Red Light Emitting Diodes (IRLED) and Visible Light Emitting Diodes (VLED). For most through applications the infrared light emitting diode (IRLED) is the most common choice. Although visible light emitting devices do exist, the infrared parts are generally chosen for their higher efficiency and more favorable wavelength, especially when used with silicon photo diode light detectors. Samples of Light emitters are shown in the following figure.

The transmitter in our paper uses an Infra Red LED that is connected through a 100 ohm resistor to VCC (7V). The circuit diagram is shown in Figure 12. The transmitter is continuously transmitting and is supplied with 7V through an external power supply. The IR transmitter used in this paper is the LD271.

6.3 Receiver

The receiver that will receive the infra red light is designed using a photo diode that connects when infra red light falls on it. The IR receiver used is the BPW42 and its wavelength matches the wavelength of the LD271 transmitter. When no light falls on the photo diode it doesn't conduct. The red LED is used to indicate the presence of an object. When no object is present, the IR receiver conducts current and the Red LED turns on. When an object obstructs the IR source from reaching the IR receiver, the IR diode stops conducting and the current becomes zero. When the current is zero, the Red LED turns off. The voltage between the resistor and the IR receiver diode is zero when there is an object obstructing the IR rays and around one volt when there are no obstacles. The one volt value changes according to the distance between the transmitter and receiver, strength of the transmitter, and other elements in the circuit. In our case the high voltage at the point is one volt. This voltage is too low and would be considered zero by the computer port since it is way lower than 5 volts that defines logic one. Thus an interface circuit is to be designed to perform level shifting from 1 volt to 5 volt.

6.4 Car entering or Exiting

We need to differentiate between cars entering the parking lot and exiting it. This section demonstrates the scenarios of each case.

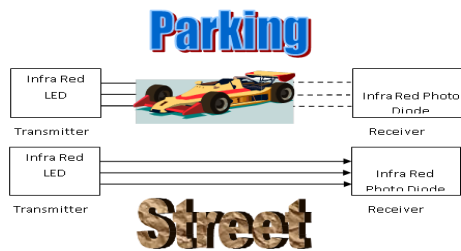


Figure 4 6: Sequence of car entering the parking lot

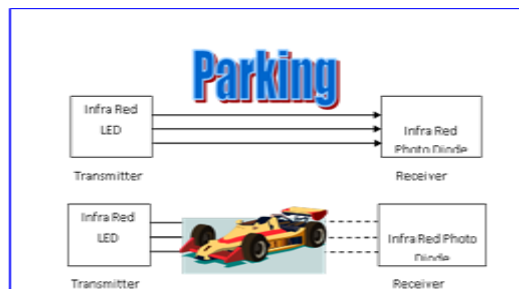


Figure 4 6: Sequence of car exiting the parking lot

6.5 Car detection Circuit

The system requires two car detection circuits placed sequential at the parking lot entrance. The following circuit diagram shows the design we implemented twice to perform the required function.

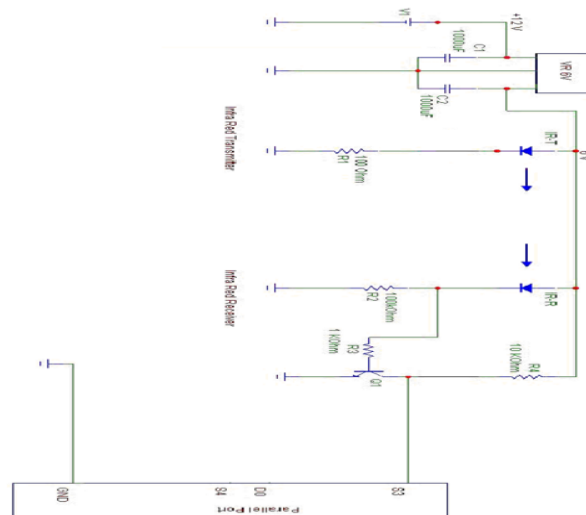


Figure 4 7: Car detection circuit with connection to parallel port

The circuit that is shown above performs a level shifting task by utilizing a transistor to amplify the small signal. The transistor used is an NPN transistor (2N2222). When the voltage at the output of the IR receiver diode is zero (object present), the voltage at the base of the transistor Q1 is zero. This causes the transistor to turn off and the voltage at its collector is equal to VCC. Thus the presence of an object is indicated by a logic one at the input pins of the parallel port of the computer. When no object is present, the voltage at the output of the IR receiver diode is around 1 volt. This voltage will be present at the base of the transistor causing it to turn on. When the transistor turns on, the voltage at its collector drops down close to zero. Thus the absence of an object is indicated by logic zero at the input of the parallel port.

	IR Detector Output
Car Present	High
Car not present	Low

VII. SERVICE REQUEST MANAGEMENT

The hardware requirement for this system consists of the following elements:

- [1] A parallel port connection that gives access to the different lines of the parallel port. This will allow the outside circuits to be interfaced to the parallel port.
- [2] Sensing circuits that will be placed at different rooms.
- [3] Multiplexing circuit.

The total number of input pins available in the parallel port is 5. Since two of those ports need to be used for the car detection circuits and we need 5 more for this system. It is necessary to increase the capacity of the parallel port. This is done by multiplexing the signals. This is done using a multiplexer with select line. The multiplexer to be used is the 74ls157. The 74LS157 is shown in the next figure.

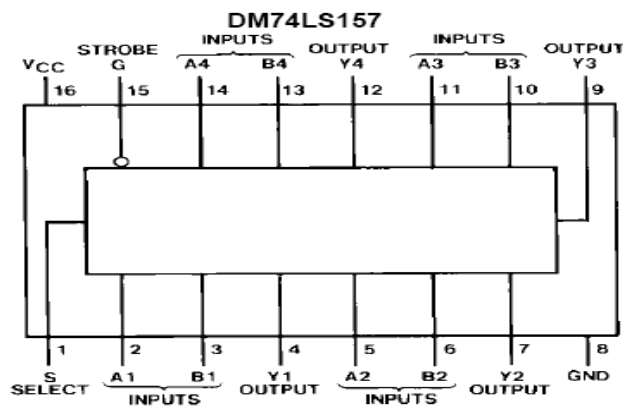


Figure 4 8: Block diagram of 74LS157

The next figure shows the logic diagram of the used multiplexer with select line (74LS157)

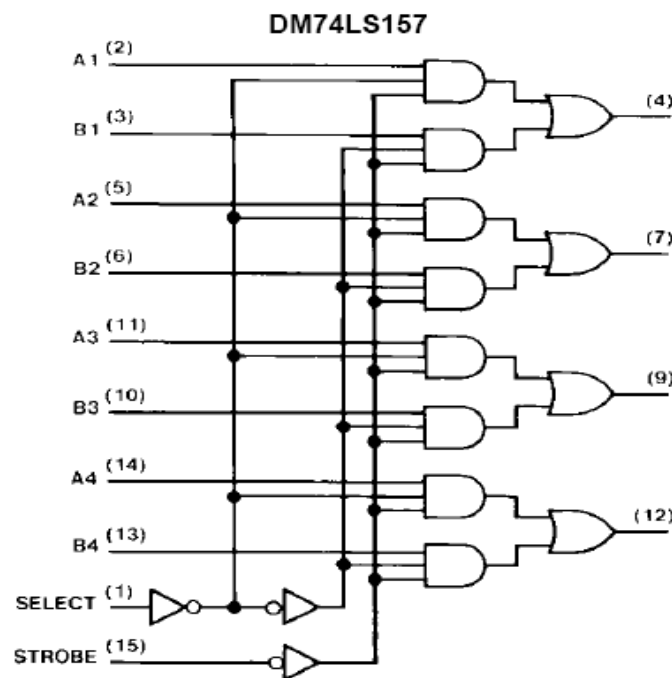


Figure 4 9: Block diagram of 74LS157

The operation of the 74LS157, Quad 2 line to 1 line multiplexer is quite simple. It simply acts as four switches. When the A/B input is low, the A inputs are selected. E.g. 1A passes through to 1Y, 2A passes through to 2Y etc. When the A/B is high, the B inputs are selected. The Y outputs are connected up to the Parallel Port's status port, in such a manner that it represents the MSnibble of the status register. While this is not necessary, it makes the software easier.

To use this circuit, first we must initialize the multiplexer to switch either inputs A or B. We will read the LSnibble first, thus we must place A/B low. The strobe is hardware inverted, thus we must set Bit 0 of the control port to get a low on Pin 1.

7.1 Service Request Detection Circuit

The system requires five service request detection circuits placed at each room. The system needs to check all rooms continuously and simultaneously. The following circuit diagram shows the design we implemented to perform the required function.

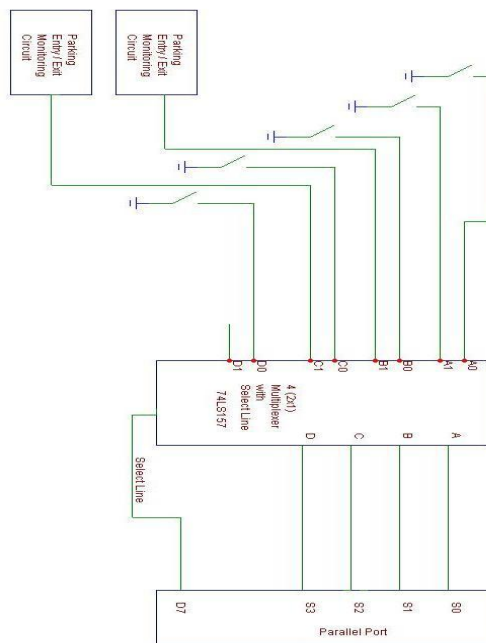


Figure 4 10: Service request monitoring circuit diagram

7.2 Phone over power Line System

It is possible to communicate audio signals from telephone to another using the power lines as the communication medium or channel. However, since AC voltage is also present on the power lines, some sort of isolation will be required between the AC voltage and the audio signal. This can be achieved using modulation and coupling. Since power lines are running everywhere in houses and buildings, it is very convenient to use the power lines as communication medium. Audio over power lines is used in wireless intercom systems. They are called wireless because the audio signal does not need special wires to be transmitted on. These intercoms are not only popular in households, but are also becoming common in the workplace. A wireless intercom allows people to communicate instantly with each other through the push of a button. Business owners and homeowners alike are realizing many uses for these intercom systems. Some wireless intercom can be used as two-way communication.

A wireless intercom system has the advantage of simple installation, while traditional intercom systems require wires to connect each intercom placed throughout the building or home. The cost of installing wires to run throughout the walls and ceilings of a building far surpasses the cost of purchasing the intercom system itself, and a wireless intercom requires no installation. Wireless intercoms need only be plugged into AC power outlets throughout the home or office. Battery operated wireless intercom systems don't even require this step, have had much success, and perform just as well as their AC counterparts. The only downside of battery operated systems is that the batteries must be replaced regularly.

Once your wireless intercoms are in place, a person in the basement of a house, for example, can speak to someone on the second floor with just the push of a button. Utilizing an intercom system prevents the need to shout or run up and down stairs to communicate. Many wireless intercom systems have a range of nearly 1,000 feet (304.8 meters), making them ideal for the home or workplace. But some systems can communicate up to 6,500 feet (2KM) [6]

VIII. DEVELOPMENT OF SOFTWARE IN MATLAB

8.1 Main Interface Program Logic

The software functionality is outlined in the following list.

- [1] Start Main Interface window
- [2] Monitor User Selection
- [3] If selection is for Parking system, Start Parking program
- [4] If selection is for Room service monitoring, start room service program
- [5] If selection is for phone over power line, start phone program
- [6]



Figure 5 1: Main Program Interface

8.2 Security and Parking System

The software functionality is outlined in the following list.

- [1] Read start time and stop time
- [2] Create Parallel Port object
- [3] Add hardware lines
- [4] Create Video Object
- [5] Create Sound Alarm tone
- [6] Check Sound System and waves
- [7] Initialize all data fields
- [8] Read Parallel port values
- [9] Determine if car is entering
- [10] Increase car count display field
- [11] Take picture
- [12] Determine time
- [13] Generate image name
- [14] Save image
- [15] Determine if car is exiting
- [16] Decrease car count display field
- [17] Take picture
- [18] Determine time
- [19] Generate image name
- [20] Save image
- [21] Open log file
- [22] Update Information and record activity
- [23] Close file
- [24] Go back to step 8



Figure 5 2: Security and Parking Interface

8.3 Room Service Request System for Hospitals and Hotels

The software functionality is outlined in the following list.

- [1] Read start time and stop time
- [2] Create Parallel Port object
- [3] Add hardware lines
- [4] Create Sound Alarm tone
- [5] Check Sound System and waves
- [6] Initialize all data fields
- [7] Read Parallel port values
- [8] Determine if service is being requested
- [9] Find the room number requesting service
- [10] Display control to answer service and room number requesting service
- [11] If service request is answered close the previous control
- [12] Open log file
- [13] Update Information and record activity
- [14] Close file
- [15] Go back to step 7

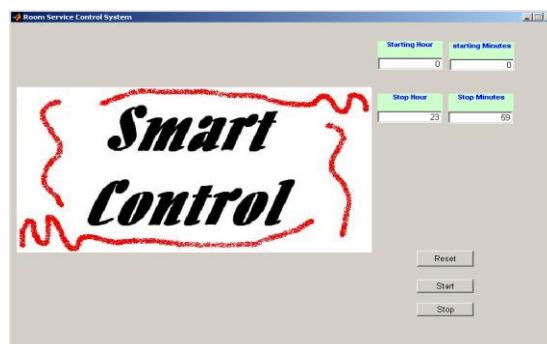


Figure 5 3(a): Room service Interface

INFO ROOM NO.1	
INFORMATION FOR PATIENT OF ROOM NO.1	
NAME	عبدالله
NATIONALITY	السعودية
AGE	25
GENDER	MALE
CASE	إجراحة
SAVE INFORMATION	

Figure 5-3(b): Informations about Room No.1

8.4 Phone Service System For Hospitals & Hotels

The software functionality is outlined in the following list.

- [1] Read start time and stop time
- [2] Create Parallel Port object
- [3] Add hardware lines
- [4] Create Sound Alarm tone
- [5] Check Sound System and waves
- [6] Initialize all data fields
- [7] Read Parallel port values
- [8] Determine if service is being requested
- [9] Find the room number requesting service
- [10] Display control to answer service and room number requesting service
- [11] Start timer when call starts
- [12] determine if phone call ended
- [13] stop timer
- [14] calculate total fee
- [15] Open log file
- [16] Update Information and record activity
- [17] Close file
- [18] Go back to step 7

By using software, we can get information about rooms in Hospitals and Hotels . In Fig.5-3(a) we can see Room No.1 has a patient named Abdullah and he is suffering from eye problem. We have all his details about his problems. Both Patient and Nurse can communicate easily any time.

ROOM NO.	NAME	CASE	ALARM	CALL	DETAILS	CONNECT
ROOM NO.1	عبدالله	العيون	ALARM	CALL	DETAILS	CONNECT
ROOM NO.2	عبد العزيز	العيون	ALARM	CALL	DETAILS	CONNECT
ROOM NO.3	عبد الرزاق	الاسنان	ALARM	CALL	DETAILS	CONNECT
ROOM NO.4	عبد الوهاب	الجراحة	ALARM	CALL	DETAILS	CONNECT
ROOM NO.5	عبد الكريم	الجراحة	ALARM	CALL	DETAILS	CONNECT
ROOM NO.6	عبد القوي	البيطنية	ALARM	CALL	DETAILS	CONNECT
ROOM NO.7	عبد الملك	البيطنية	ALARM	CALL	DETAILS	CONNECT
ROOM NO.8	عبد ايله	انف و اذن وحجره	ALARM	CALL	DETAILS	CONNECT
ROOM NO.9	عبد الحقيق	انف و اذن وحجره	ALARM	CALL	DETAILS	CONNECT

Figure 5-3(a): Phone Service System for Hospitals

IX . IMPLEMENTATION OF PAPER

9.1 Built Model

The system was built and tested numerous times. The following figures show the different circuits and model that was built.



Figure 6 1(b): Model Picture

X. CONCLUSION

With all events taking place around the world, security concerns are continuously on the rise. As a consequence of wars, conflicts, or social problems, security concerns must be thoroughly evaluated and necessary measures must be taken in order to reduce risks and improve the safety of people, assets, and facilities. Many places need to be kept secure from intruders or suspects. Parking Lots are provided for visitors of all government buildings, hotels, hospitals, and large buildings. They have been a prime security concern, as many incidents of terrorism were carried out by implanting cars with bombs in parking lots of important buildings. Management and security of parking lots is a continuous challenge. It would be a great idea if an automatic management and security system is designed to continuously manage and watch a parking lot.

Modern hospitals and hotels are of great importance for nowadays civilized communities. Hospitals extend their medical services to all people, adults and children. Hotels extend their services to most travelers from within the country or from outside the country. Millions of people use the services of hotels and hospitals throughout the world daily. Modern hospitals and hotels of nowadays have high tech equipments that are used for many different purposes. These equipments integrate advanced electronics and computer systems to provide extremely useful tools. Nurses in hospitals continuously watch patients that stay at different rooms. These patients require some assistance at certain times. The on duty nurse is supposed to answer the requests from different patients and address their demands or concerns. Similarly in hotels many rooms are occupied by hundreds of guests daily. These guests have different demands that need to be answered in order to keep the service quality of the hotel at a higher class. Current service request management systems located at hospitals produce an audio and a visual alarm at the nurse desk indicating that requests have been issued. The nurse should keep track manually of the requests. Work stress can cause the nurse to miss some of the requests or answer some requests before others. Similarly in hotels requests are in general placed by the guests via telephone. The help desk staff record the requests manually in order to answer them. It would be a great idea if an automatic management system is designed to watch multiple rooms and continuously monitor their requests until answered.

Phone services in hospitals and hotels are extended to patients and guests at an extra charge. Wiring of phone lines in a hotel can be cumbersome. Monitoring of the phone calls and durations need to be done for each guest (room). It would also be a very good idea if the existing power lines are used to extend the phone service to every room in a hospital or hotel. In addition it would be very helpful if the automatic system continues to watch phone call requests and monitor the length of established calls and calculate the total cost of each call for billing. In this paper we designed and built an automatic parking lot management system that keeps track of vehicles entering and leaving a parking lot. Another system was designed and built to record (using a camera) activities of cars entering and leaving the parking lot. Developed programs are simple to use and employ a visual interface design. Secondly we designed and built an automatic service request management system. This system keeps track of all requests from different rooms and keeps a record of them. The system was developed to run using a personal computer. Developed programs are simple to use and employ a visual interface design. Thirdly we designed and built an automatic phone call management system that utilizes the existing power lines as the phone call carrier medium. The system is able to detect automatically the phone call request from the room and indicate this on the computer interface. Upon establishing the phone call, the system keeps track of the time period of the call and generates and save the total cost of the call. The system automatically detects the end of conversation. The system was developed to run using a personal computer. Developed programs are simple to use and employ a visual interface design.

REFERENCES

- [1] Lugang Guo, Peng Li, Huaqiao Lv, & Chunheng Wang Research on the Automatic Vehicle Monitoring Methods Based on Image Sequence 2010 International Conference on Educational and Information Technology (ICEIT 2010)
- [2] Wang Lixia & Jiang Dalin A method of Parking space detection based on image
- [3] segmentation and LBP 2012 Fourth International Conference on Multimedia Information Networking and Security
- [4] HUA-CHUN TAN, JIE ZHANG, XIN-CHEN YE, HUI-ZE LI, PEI ZHU, QING-HUA ZHAO INTELLIGENT CAR-SEARCHING SYSTEM FOR LARGE PARK Proceedings of the Eighth International Conference on Machine Learning and Cybernetics, Baoding, 12-15 July 2009
- [5] Ludwig, Heiko Catalog-based service request management IBM Systems Journal 2007
- [6] Ma Yuchun, Huang Yinghong (corresponding author), Zhang Kun, Li Zhuang
- [7] Hainan Key Telephone Clients Management System with Short Messages 2011 International Conference on Internet Computing and Information Services
- [8] Md. Mahmud Hasan, Lim Hooi Jiun, Ng Wei Chuen and Md. Shahjahan Shahid Smart Telephone Design -
- [9] Caller Identification and Answering Machine ICSE'98 Proc., Nov. 1998, Bangi, Malaysia
- [10] Matlab 7.0 Help Notes and Libraries". Mathworks Inc. June 18 2002.

Standardization of Systems and Processes for CDR Based Billing System in Telecom Companies

K.V.V.Satyanarayana¹, Hashmi Vallipalli¹, A.Shivarama rao²

¹, Dept of C.S.E K L University, Vaddeswaram, Vijayawada, India

², Sasi Institute of Technology & Engineering Tadeppligudem, West Godavari District, India

Abstract:

In olden days the telephone system we have used the Meter Based (MB) System for billing process. The Meter Based system having the online recording of metered units in which it is having instant unit conversion according to the charge bands stored in the switch. The meter system is based on the manual process and it is not having the decentralized database. So, it is making that Inflexible billing system and Insufficient call details. So, here there is a new system in proposal that is CDR system (Call Detail Record System) for billing purpose. There is a centralized database for having centralized customer services. The CDR system is having 4-Data Centers all over India. The 4-Data Centers are connected to each other, Exchange Routers, and their respective Backbone Routers. The CDR system consisting of the application software's like Customer Relationship Management, Customer Care & Convergent Billing, Clarity Check, Payment Management System, Enterprise Reports, Integrated Voice Recognition System, Web self-care, Oracle DBMS. The CDR based Billing system in mainly proposed for online services, online query and prompt customer response. It supports for different tariffs, different billing cycles and different discounting schemes for different category of subscribers. It also helps for Accurate and timely invoicing of call details to generate error free bills. It is useful for Pre-paid and Post Paid system integration.

Keywords: Meter Based system, Customer Relationship Management, Convergent Billing, Enterprise Reports, Integrated Voice Recognition System, and CDR based Billing system.

I. INTRODUCTION

1.1. DATA CENTER:

The Data Center plays a very important role in the telecom systems. The Data Center has the centralized system by connecting varieties of systems. A single effortless integrated standard operation system will support all the operational activities providing the associated advantages. The overall quality of billing and payment accrual systems should improve. The unspoiled integration of system will make possible single point high quality customer care.

The Billing was the last function in Telecom operations coming after Commercial System, Fault tracking and management system and Directory Enquiry system. New connections along with Shift and other such functions were dealt in Commercial system. This system maintained a database of existing customers for dealing with Shift, Transfer, Safe custody and other such requests from existing customers. The Fault tracking and management system specifically catered to the management of line faults and while doing so had to maintain another database on existing customers. The third system of Directory Enquiry was an important system for informing the customers about the name and address for a telephone in a fast changing landline environment. That was the period when landline network grew and was reshaped at an excited speed. The Directory Enquiry system also needed to have its own structured database.

The four core Telecom operation systems separately maintained four different databases. A single event like a request for a new connection needed four update transactions at different times for updating the four systems. The usual error content in transactions and asynchronous updates resulted finally in accumulated mismatch of the four databases. Apart from the mismatch, as the operation systems were not interlinked with each other, changing any procedure was manageable needing changes to be made separately in all the four systems.

1.2. METER BASED SYSTEM:

Online Recording of metered units with instant unit conversion according to the charge bands, stored in the switch. Limited number of charge bands. Credit limit threshold setting possible for certain percentage of subs. Fault Repair System (FRS) implemented at exchange level without any interface with billing or commercial systems. SSA wise DQ and exchange wise Interactive Voice Response Systems. No single data model for Billing, Commercial, Directory enquiry & Fault Repair System.

1.3. CDR BASED BILLING SYSTEM:

The CDR based system is mainly used for landline operations and it consists mainly of the subsystem like Directory enquiry, mediation and billing. Online mediation of CDRs eliminates the need of bill data transportation, eliminating fraud on this account. Proper accounting of payments & receivables for better financial management. Standard and ad-hoc reporting on all aspects of the business. Facilitate market studies and analyses for forming optimal sales strategies and assess business performance of self and partners and prevention. Minimization of internal and external frauds. System consolidation resulting in reduction of O&M cost.

Apart from integration, a very important aspect of these systems was the basis of Billing. In these new systems, billing was based on Call Detail Records (CDRs) for a customer accumulated over a period instead of call meters. A CDR contained details such as calling number, called number, time of call, duration of call etc. It didn't contain the call charge. This made possible the flexible rating or charging a CDR according to where the call was made, when the call was made and by whom the call was made. Time dependent, destination dependent, plan dependent flexible charging became possible. In competitive telecom business arena this flexibility of charging gained crucial importance and all operators without exception, according to their capability adopted this new concept.

The incumbent operators were in the field of landline operations where growth slowed down all over the world and mobile market exploded. The mobile systems invariably brought in these new CDR based billing systems. The quality and maturity of these billing systems in many cases determined the success of a mobile operator. Some operators needed to change their ineffective CDR based billing system for a better system within only a few years. The CDR based Billing and Customer Care systems gained a central importance in mobile operations because of their capability to support flexible and quick introduction of new customer schemes and plans, quickly activate or deactivate a connection while updating all the relevant information of a customer and finally providing high quality Customer Care.

1.4. LINUX BASH SHELL SCRIPTING:

BASH (Bourne Again Shell) is a scripting language as well as the default command interpreter in most Linux distributions, including Red Hat Linux. The ability to create quality scripts is arguably the most time and error saving aspect of Linux Systems Administration. The fact that the default shell or user environment in Linux is BASH makes learning to create scripts both very valuable as well as simple. Shell scripts can be very simple or extremely complex involving dozens of support files, but regardless of the complexity, they should be created in a consistent, self-explanatory and easy to read format. These scripts are used for making work easy in the corporate life. These Scripting and automation are the keys to consistency and reliability. By using these scripts we make scheduling processes. Scripts are mainly for having the log files, system performance, and port status.

II. EXISTING SYSTEM

OSS and BSS modules implemented in decentralized manner .No system to consolidate meter readings at one place .Billing process depends upon collection and transfer of subscriber wise exchange meter reading (OMR and CMR).Deployment of various Integrated packages. Fault Repair System (FRS) implemented at exchange level without any interface with billing or commercial systems. SSA wise DQ and exchange wise Interactive Voice Response Systems No single data model for Billing, Commercial, Directory enquiry & Fault Repair System.

2.1. FEATURES OF METER BASED SYSTEM:

- Online Recording of metered units with instant unit conversion according to the charge bands, stored in the switch.
- Limited number of charge bands.
- Credit limit threshold setting possible for certain percentage of subs.

2.2. DRAWBACKS OF METER BASED SYSTEM:

- Inflexible billing system. Insufficient call details which cannot be used for future processing and analysis.
- Tariff change involves huge effort
- Corporate level data consolidation not possible due to distributed databases.
- Subscription level fraud – Not possible to rate or impose credit limits against individual subscribers
- No standard system for payment and Receivables management.
- Decentralized database – Cannot provide Nationwide customer services over telephone or web like:
 - bill inquiry
 - directory inquiry
 - Connection status, Complaint Handling information about new/special services etc.

III. PROPOSED SYSTEM

It is about Standardization of the Systems and Processes over all the south BSNL Exchanges at the single Data center. It is mainly used for Call Detail Record system in the server tapes. It is also having tariff based Billing System and providing efficient customer care service.

In this system we are having different applications for different purposes. Some of those are IVRS, Mediation, Billing, Accounting, and Security. These applications are to be maintained under the servers. So, those servers are to be maintained and managed by having backups, error logs etc...

3.1. BENEFITS OF PROPOSED SYSTEM:

- Move from telephone based system to Customer based system
- Accurate and timely invoicing of call details to generate error free bills.
- Supports different tariffs, different Billing cycles, and different discounting schemes for different category of subscribers.
- Pre-paid and Post Paid integration possible
- Easy implementation of change in business policies and rules.
- Host of online services, online query and prompt customer response
-

IV. DESIGN OF CDR SYSTEM

4.1. DATA FLOW FROM LOCAL EXCHANGE TO DATA CENTER

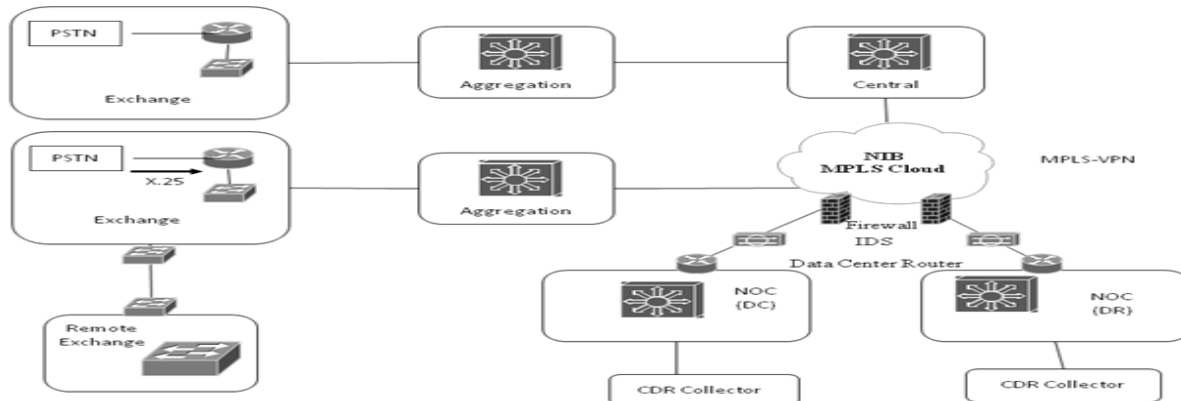


Fig: 1 Data Flow from Local Exchange to Data Center

V. METHODOLOGY

The varieties of systems in all over BSNL exchanges are integrated to a single standard operation system at Data Center. By having the secure routing of network using IPSec, Network based IDS and SACS. The overall quality of billing and payment management systems are improved by IVRS and managed at Database servers. By the integration systems the total Call Record system and the Customer Detail record system is centralized and should be maintained at the server tapes. It is used to make different bill rating for different tariffs, different Billing cycles and different discounting schemes for different category of subscribers through their Databases. These are to be given secure by taking backup.

VI. CONCLUSION

The CDR system is mainly used as up-gradation of the Meter Based Billing System. The CDR System used to support for bill rating purpose of different tariffs. It helps for Accurate and timely invoicing of call details to generate error free bills. Having backups for the purpose of the disaster recovery.

REFERENCES

- [1] Security and Virtualization in the Data Center
http://www.cisco.com/en/US/docs/solutions/Enterprise/Data_Center/DC_3_0/dc_sec_design.html
- [2] Integrating the Virtual Switching System in Cisco Data Center Infrastructure
http://www.cisco.com/en/US/docs/solutions/Enterprise/Data_Center/vssdc_integrate.html
- [3] J. Ousterhout, "Scripting: Higher-Level Programming for the 21st Century," IEEE Computer, Vol. 31, No. 3, March 1998, pp. 23-30.
- [4] http://www.linuxconfig.org/Bash_scripting_Tutorial
- [5] <http://www.thegeekstuff.com/2010/06/bash-array-tutorial/>
- [6] <http://www.panix.com/~elflord/unix/bash-tute.html>
- [7] <http://www.codecoffee.com/tipsforlinux/articles2/043.html>
- [8] <http://tldp.org/LDP/abs/html/>
- [9] http://linuxsig.org/files/bash_scripting.html
- [10] <http://mywiki.woledge.org/BashGuide>
- [11] <http://www.regular-expressions.info/> Alexander Bernstein

Integral Solutions of the Non Homogeneous Ternary Quintic Equation

$$ax^2 - by^2 = (a-b)z^5, a, b > 0$$

S.Vidhyalakshmi¹, K.Lakshmi², M,A.Gopalan³

¹Professor, Department of Mathematics, SIGC, Trichy

²Lecturer, Department of Mathematics, SIGC, Trichy,

³Professor, Department of Mathematics, SIGC, Trichy,

Abstract:

We obtain infinitely many non-zero integer triples (x, y, z) satisfying the ternary quintic equation $ax^2 - by^2 = (a-b)z^5, a, b > 0$. Various interesting relations between the solutions and special numbers, namely, polygonal numbers, Pyramidal numbers, Star numbers, Stella Octangular numbers, Pronic numbers, Octahedral numbers, Four Dimensional Figurative numbers and Five Dimensional Figurative numbers are exhibited.

Keywords: Ternary quintic equation, integral solutions, 2-dimentional, 3-dimentional, 4- dimensional and 5- dimensional figurative numbers.

MSC 2000 Mathematics subject classification: 11D41.

NOTATIONS:

$$T_{m,n} = n \left(1 + \frac{(n-1)(m-2)}{2} \right) \text{-Polygonal number of rank } n \text{ with size } m$$

$$P_n^m = \frac{1}{6} n(n+1)((m-2)n+5-m) \text{- Pyramidal number of rank } n \text{ with size } m$$

$$SO_n = n(2n^2 - 1) \text{-Stella octangular number of rank } n$$

$$S_n = 6n(n-1) + 1 \text{-Star number of rank } n$$

$$PR_n = n(n+1) \text{-Pronic number of rank } n$$

$$OH_n = \frac{1}{3} (n(2n^2 + 1)) \text{- Octahedral number of rank } n$$

$$F_{5,n,3} = \frac{n(n+1)(n+2)(n+3)(n+4)}{5!} = \text{Five Dimensional Figurative number of rank } n$$

whose generating polygon is a triangle.

$$F_{4,n,3} = \frac{n(n+1)(n+2)(n+3)}{4!} = \text{Four Dimensional Figurative number of rank } n$$

whose generating polygon is a triangle

1. INTRODUCTION

The theory of diophantine equations offers a rich variety of fascinating problems. In particular, quintic equations, homogeneous and non-homogeneous have aroused the interest of numerous mathematicians since antiquity [1-3]. For illustration, one may refer [4-10] for homogeneous and non-homogeneous quintic equations with three, four and five unknowns. This paper concerns with the problem of determining non-trivial integral solution of the non- homogeneous ternary quintic equation given by $ax^2 - by^2 = (a-b)z^5, a, b > 0$. A few relations between the solutions and the special numbers are presented.

II. METHOD OF ANALYSIS

The Diophantine equation representing the quintic equation with three unknowns under consideration is

$$ax^2 - by^2 = (a-b)z^5, a, b > 0 \tag{1}$$

Introduction of the transformations

$$x = X + bT, y = X + aT \tag{2}$$

in (1) leads to

$$X^2 - abT^2 = z^5 \tag{3}$$

The above equation (3) is solved through different approaches and thus, one obtains distinct sets of solutions to (1)

2.1. Case1:

Choose a and b such that ab is not a perfect square.

Assume $z = p^2 - abq^2$ (4)

Substituting (4) in (3) and using the method of factorisation, define

$$(X + \sqrt{ab}T) = (p + \sqrt{ab}q)^5 \tag{5}$$

Equating real and imaginary parts in (5) we get,

$$\left. \begin{aligned} X &= p^5 + 10abp^3q^2 + 5(ab)^2pq^4 \\ T &= 5qp^4 + 10abp^2q^3 + (ab)^2q^5 \end{aligned} \right\} \tag{6}$$

In view of (2) and (4), the corresponding values of x, y are represented by

$$x = p^5 + 10abp^3q^2 + 5(ab)^2pq^4 + b(5qp^4 + 10abp^2q^3 + (ab)^2q^5) \tag{7}$$

$$y = p^5 + 10abp^3q^2 + 5(ab)^2pq^4 + a(5qp^4 + 10abp^2q^3 + (ab)^2q^5) \tag{8}$$

Thus (7) and (4) represent the non-zero distinct integral solutions to (1)

A few interesting relations between the solutions of (1) are exhibited below:

- $\left[2 \frac{a(x(p,1) - by(p,1))}{a-b} \right] - 8T_{3,p-1} \times P_p^5 - (1+10ab)SO_p \equiv p \pmod{10}$

2. The following are nasty numbers;

- $60p \left\{ 2 \frac{a(x(p,1) - by(p,1))}{a-b} - 8T_{3,p-1} \times P_p^5 - (1+10ab)SO_p + (9+10ab)p \right\}$

- $30p \left[\frac{ax(p,1) - by(p,1)}{a-b} - 120F_{5,p,3} + 240F_{4,p,3} - (2ab+5)30P_p^3 + 15PR_p + 12T_{4,p} - 8T_{5,p} + 60abT_{3,p} \right]$

- $2ab \left\{ 5(T_{4,p} + ab)^2 - \left[\frac{x(p,1) - y(p,1)}{b-a} \right] \right\}$ is a cubical integer.

- $ax(p,1) - by(p,1) + (a-b)\{3840F_{4,p,3} - 1920F_{5,p,3} - 1200P_p^4 - 720T_{3,p} - 48T_{4,p} + 32T_{5,p}\} \equiv 0 \pmod{5}$

- $\left[2 \frac{a(x(p,1) - by(p,1))}{a-b} \right] - 8T_{3,p-1} \times P_p^5 - 3(1+10ab)OH_p + 11(2T_{3,p} - T_{4,p}) \equiv 0 \pmod{10}$

- $S_p - 6z(p,1) + 18(OH_p) - 6SO_p - 12T_{3,p} + 6T_{4,p} - 6ab = 1$

Now, rewrite (3) as,

$$X^2 - abT^2 = 1 \times z^5 \tag{9}$$

Also 1 can be written as

$$1 = \frac{(a+b+2\sqrt{ab})(a+b-2\sqrt{ab})}{(a-b)^2} \tag{10}$$

Substituting (4) and (10) in (9) and using the method of factorisation, define,

$$(X + \sqrt{ab}T) = \frac{(a+b+2\sqrt{ab})}{a-b} (p + \sqrt{ab}q)^5 \tag{11}$$

Equating real and imaginary parts in (11) we obtain,

$$X = \frac{1}{a-b} \left[(a+b)(p^5 + 10abp^3q^2 + 5(ab)^2 pq^4) + 2ab(5qp^4 + 10abq^3p^2 + (ab)^2 q^5) \right]$$

$$T = \frac{1}{a-b} \left[(a+b)(5qp^4 + 10abq^3p^2 + (ab)^2 q^5) + 2(p^5 + 10abp^3q^2 + 5(ab)^2 pq^4) \right]$$

In view of (2) and (4), the corresponding values of x, y and z are obtained as,

$$\left. \begin{aligned} x &= (a-b)^4 [(a+3b)(p^5 + 10abp^3q^2 + 5(ab)^2 pq^4) + \\ &\quad b(3a+b)(5qp^4 + 10abp^2q^3 + (ab)^2 q^5)] \\ y &= (a-b)^4 [(3a+b)(p^5 + 10abp^3q^2 + 5(ab)^2 pq^4) + \\ &\quad a(a+3b)(5qp^4 + 10abp^2q^3 + (ab)^2 q^2)] \\ z &= (a-b)^2 (p^2 - abq^2) \end{aligned} \right\} \tag{12}$$

Further 1 can also be taken as

$$1 = \frac{(ab + \alpha^2 + 2\alpha\sqrt{ab})(ab + \alpha^2 - 2\alpha\sqrt{ab})}{(ab - \alpha^2)^2} \tag{13}$$

For this choice, after performing some algebra the value of x, y and z are given by

$$\left. \begin{aligned} x &= (ab - \alpha^2)^4 [(ab + \alpha^2 - 2\alpha b)(p^5 - 10abp^3q^2 + 5(ab)^2 pq^4) + \\ &\quad (2\alpha ab - b(ab + \alpha^2))(5qp^4 - 10abp^2q^3 + (ab)^2 q^5)] \\ y &= (ab - \alpha^2)^4 [(ab + \alpha^2 - 2\alpha a)(p^5 - 10abp^3q^2 + 5(ab)^2 pq^4) + \\ &\quad (2\alpha ab - a(ab + \alpha^2))(5qp^4 - 10abp^2q^3 + (ab)^2 q^5)] \\ z &= (ab - \alpha^2)^2 (p^2 - abq^2) \end{aligned} \right\} \tag{14}$$

Remark1:

Instead of (2), the introduction of the transformations, $x = X - bT, y = X - aT$ in (1) leads to (3). By a similar procedure we obtain different integral solutions to (1).

2.2. Case2:

Choose a and b such that ab is a perfect square, say, d^2 .

\therefore (3) is written as $X^2 - (dT)^2 = z^5$ (15)

To solve (15), we write it as a system of double equations which are solved in integers for X, T and z in view of (2), the corresponding integral values of x, y are obtained. The above process is illustrated in the following table:

System of double equations	Integral values of z	Integral values of x, y
$X + dT = z^4$ $X - dT = z$	$z = 2dk$	$x = 8k^4 d^3 (d + b) + k(d - b)$ $y = 8k^4 d^3 (d + a) + k(d - a)$
$X + dT = z$ $X - dT = z^4$	$z = 2dk$	$x = 8k^4 d^3 (d - b) + k(d + b)$ $y = 8k^4 d^3 (d - a) + k(d + a)$

$X + dT = z^3$ $X - dT = z^2$	$z = 2dk$	$x = 4k^3d^2(d + b) + 2dk^2(d - b)$ $y = 4k^3d^2(d + a) + 2dk^2(d - a)$
$X + dT = z^2$ $X - dT = z^3$	$z = 2dk$	$x = 4k^3d^2(d - b) + 2dk^2(d + b)$ $y = 4k^3d^2(d - a) + 2dk^2(d + a)$
$X + dT = z^5$ $X - dT = 1$	$z = 2dk + 1$	$x = (16k^5d^4 + 40k^4d^3 + 40k^3d^2 + 20k^2d + 5k)(d + b) + 1$ $y = (16k^5d^4 + 40k^4d^3 + 40k^3d^2 + 20k^2d + 5k)(d + a) + 1$
$X + dT = z^5$ $X - dT = 1$	$z = 2dk + 1$	$x = (16k^5d^4 + 40k^4d^3 + 40k^3d^2 + 20k^2d + 5k)(d - b) + 1$ $y = (16k^5d^4 + 40k^4d^3 + 40k^3d^2 + 20k^2d + 5k)(d - a) + 1$

2.3. Case3:

Take $z = \alpha^2$ (16)

Substituting (16) in (15) we get,

$$X^2 = (dT)^2 + (\alpha^5)^2 \tag{17}$$

which is in the form of Pythagorean equation and is satisfied by

$$\alpha^5 = 2rs, dT = r^2 - s^2, X = r^2 + s^2, r > s > 0 \tag{18}$$

Choose r and s such that $rs = 16d^5k^5$ (19)

and thus $\alpha = 2dk$.

Knowing the values of r, s and using (18) and (2), the corresponding solutions of (1) are obtained. For illustration, take

$$r = 2^3d^4k^4, s = 2dk, r > s > 0$$

The corresponding solutions are given by

$$\left. \begin{aligned} x &= 64d^7k^8(d + b) + 4dk^2(d - b) \\ y &= 64d^7k^8(d + a) + 4dk^2(d - a) \\ z &= 4d^2k^2 \end{aligned} \right\} \tag{20}$$

Taking the values of r, s differently such that $rs = 16d^5k^5$, we get different solution patterns.

It is to be noted that, the solutions of (17) may also be written as

$$X = r^2 + s^2, dT = 2rs, \alpha^5 = r^2 - s^2, r > s > 0 \tag{21}$$

Choose $r = \frac{\alpha^3 + \alpha^2}{2}, s = \frac{\alpha^3 - \alpha^2}{2}$

Substituting the values of r, s in (21) and performing some algebra using (2) we get the corresponding solutions as

$$\left. \begin{aligned} x &= 32d^5k^6(d + b) + 8d^3k^4(d - b) \\ y &= 32d^5k^6(d + a) + 8d^3k^4(d - a) \\ z &= 4d^2k^2 \end{aligned} \right\} \tag{22}$$

Taking the values of r, s differently such that $\alpha^5 = r^2 - s^2$, we get different solution patterns.

2.4. Case4:

Also, introducing the linear transformations

$$X = 2dk + u, dT = 2dk - u$$

in (15) and performing a few algebra, we have

$$X = 4k^4 d^4 + 2dk, T = 2k - 4k^4 d^3 \quad (23)$$

In view of (2) and (23) the corresponding integral solutions of (1) are obtained as

$$\left. \begin{aligned} x &= 4k^4 d^3 (d - b) + 2k(d + b) \\ y &= 4k^4 d^3 (d - a) + 2k(d + a) \\ z &= 2dk \end{aligned} \right\} \quad (24)$$

It is to be noted that, in addition to the above choices for X and dT , we have other choices, which are illustrated below:

Illustration1:

The assumption $X = zX, dT = zdT$ (25)

in (15) yields

$$X = md^3(m^2 - n^2), T = nd^2(m^2 - n^2), z = d^2(m^2 - n^2) \quad (26)$$

From (25), (26) and (2), the corresponding integral solutions of (1) are

$$\left. \begin{aligned} x &= d^4(m^2 - n^2)^2(md + nb) \\ y &= d^4(m^2 - n^2)^2(md + na) \\ z &= d^2(m^2 - n^2) \end{aligned} \right\} \quad (26)$$

Illustration2:

The assumption $X = z^2X, dT = z^2dT$ (27)

in (15) yields to $X^2 - (dT)^2 = z$ (28)

Taking $z = 4m^2n^2d^2$ (29)

and performing some algebra, we get

$$X = 16m^4n^4d^{10}(m^2 + n^2), T = 16m^4n^4d^9(n^2 - m^2) \quad (30)$$

From (29), (30) and (2), the corresponding integral solutions of (1) are

$$\left. \begin{aligned} x &= 16m^4n^4d^9[d(m^2 + n^2) + b(n^2 - m^2)] \\ y &= 16m^4n^4d^9[d(m^2 + n^2) + a(n^2 - m^2)] \\ z &= 4m^2n^2d^2 \end{aligned} \right\} \quad (31)$$

Illustration3:

Instead of (29), taking $z = 2dk + 1$ (32)

in (28) we get

$$X = (2dk + 1)^2(dk + 1), T = -k(2k + 1)^2 \quad (33)$$

From (30), (31) and (2), the corresponding integral solutions of (1) are

$$\left. \begin{aligned} x &= (2dk + 1)^2(dk - bk + 1) \\ y &= (2dk + 1)^2(dk - ak + 1) \\ z &= 2dk + 1 \end{aligned} \right\} \quad (34)$$

Illustration4:

In (28), taking $z = -t^2$ and arranging we get (35)

$$X^2 + t^2 = (dT)^2 \quad (36)$$

which is in the form of Pythagorean equation and is satisfied by

$$X = 2pq, dT = p^2 + q^2, t = p^2 - q^2, r > s > 0 \quad (37)$$

From (35), (37) and (2) we get the corresponding solutions as

$$\left. \begin{aligned} x &= (p^2 - q^2)^4 d^9 [2pqd + b(p^2 + q^2)] \\ y &= (p^2 - q^2)^4 d^9 [2pqd + a(p^2 + q^2)] \\ z &= -(p^2 - q^2)^2 d^4 \end{aligned} \right\} \quad (38)$$

It is to be noted that, the solutions of (36) may also be written as

$$X = p^2 - q^2, t = 2pq, dT = p^2 + q^2, p > q > 0 \tag{39}$$

From (33),(37) and (2) we get the corresponding solutions as

$$\left. \begin{aligned} x &= 16p^4q^4d^9[d(p^2 - q^2) + b(p^2 + q^2)] \\ y &= 16p^4q^4d^9[d(p^2 - q^2) + a(p^2 + q^2)] \\ z &= -4p^2q^2d^4 \end{aligned} \right\} \tag{40}$$

III. Remarkable observations:

I: If (x_0, y_0, z_0) be any given integral solution of (1), then the general solution pattern is presented in the matrix form as follows:

Odd ordered solutions:

$$\begin{pmatrix} x_{2m-1} \\ y_{2m-1} \\ z_{2m-1} \end{pmatrix} = (a-b)^{4m-2} \begin{pmatrix} -(a+b)(a-b)^{6m-4} & +2a(a-b)^{6m-4} & 0 \\ -2a(a-b)^{6m-4} & (a+b)(a-b)^{6m-4} & 0 \\ 0 & 0 & 1 \end{pmatrix} \begin{pmatrix} x_0 \\ y_0 \\ z_0 \end{pmatrix}$$

Even ordered solutions:

$$\begin{pmatrix} x_{2m} \\ y_{2m} \\ z_{2m} \end{pmatrix} = (a-b)^{4m} \begin{pmatrix} -(a+b)(a-b)^{6m} & +2b(a-b)^{6m} & 0 \\ -2a(a-b)^{6m} & (a+b)(a-b)^{6m} & 0 \\ 0 & 0 & 1 \end{pmatrix} \begin{pmatrix} x_0 \\ y_0 \\ z_0 \end{pmatrix}$$

II: The integral solutions of (1) can also be represented as,

$$\begin{aligned} x &= (m + bN)Z^2 \\ y &= (m + aN)Z^2 \\ z &= m^2 + abN^2, a, b > 0 \end{aligned}$$

IV. CONCLUSION

In conclusion, one may search for different patterns of solutions to (1) and their corresponding properties.

REFERENCES:

- [1]. L.E.Dickson, History of Theory of Numbers, Vol.11, Chelsea Publishing company, New York (1952).
- [2]. L.Mordell, Diophantine equations, Academic Press, London (1969).
- [3]. Carmichael ,R.D.,The theory of numbers and Diophantine Analysis,Dover Publications, New York (1959)
- [4]. M.A.Gopalan & A.Vijayashankar, *An Interesting Diophantine problem $x^3 - y^3 = 2z^5$* Advances in Mathematics, Scientific Developments and Engineering Application, Narosa Publishing House, Pp 1-6, 2010.
- [5]. M.A.Gopalan & A.Vijayashankar, *Integral solutions of ternary quintic Diophantine equation $x^2 + (2k + 1)y^2 = z^5$* , International Journal of Mathematical Sciences 19(1-2), 165-169, (jan-june 2010)
- [6]. M.A..Gopalan,G.Sumathi & S.Vidhyalakshmi, *Integral solutions of non-homogeneous ternary quintic equation in terms of pells sequence $x^3 + y^3 + xy(x + y) = 2Z^5$* , accepted for Publication in JAMS(Research India Publication)
- [7]. S.Vidhyalakshmi, K.Lakshmi and M.A.Gopalan, *Observations on the homogeneous quintic equation with four unknowns $x^5 - y^5 = 2z^5 + 5(x + y)(x^2 - y^2)w^2$* ,accepted for Publication in International Journal of Multidisciplinary Research Academy. (IJMRA)
- [8]. M.A.Gopalan & A.Vijayashankar, *Integral solutions of non-homogeneous quintic equation with five unknowns $xy - zw = R^5$* , Bessel J.Math, 1(1),23-30,2011.
- [9]. M.A.Gopalan & A.Vijayashankar, *solutions of quintic equation with five unknowns $x^4 - y^4 = 2(z^2 - w^2)P^3$* ,Accepted for Publication in International Review of Pure and Applied Mathematics.
- [10] M.A.Gopalan,G.Sumathi & S.Vidhyalakshmi, *On the non-homogenous quintic equation with five unknowns $x^3 + y^3 = z^3 + w^3 + 6T^5$* ,accepted for Publication in International Journal of Multidisciplinary Research Academy (IJMRA).

Integral Solutions of Non-Homogeneous Biquadratic Equation With Four Unknowns

M.A.Gopalan¹, G.Sumathi², S.Vidhyalakshmi³

¹. Professor of Mathematics, SIGC,Trichy

². Lecturer of Mathematics, SIGC,Trichy,

³. Professor of Mathematics, SIGC,Trichy

Abstract

The non-homogeneous biquadratic equation with four unknowns represented by the diophantine equation

$$x^3 + y^3 = (k^2 + 3)^n z^3 w$$

is analyzed for its patterns of non-zero distinct integral solutions and three different methods of integral solutions are illustrated. Various interesting relations between the solutions and special numbers, namely, polygonal numbers, pyramidal numbers, Jacobsthal numbers, Jacobsthal-Lucas number, Pronic numbers, Stella octangular numbers, Octahedral numbers, Gnomonic numbers, Centered triangular numbers, Generalized Fibonacci and Lucas sequences are exhibited.

Keywords: Integral solutions, Generalized Fibonacci and Lucas sequences, biquadratic non-homogeneous equation with four unknowns

M.Sc 2000 mathematics subject classification: 11D25

NOTATIONS

- $t_{m,n}$: Polygonal number of rank n with size m
- P_n^m : Pyramidal number of rank n with size m
- S_n : Star number of rank n
- Pr_n : Pronic number of rank n
- SO_n : Stella octangular number of rank n
- j_n : Jacobsthal lucas number of rank n
- J_n : Jacobsthal number of rank n
- OH_n : Octahedral number of rank n
- $Gnomic_n$: Gnomonic number of rank n
- GF_n : Generalized Fibonacci sequence number of rank n
- GL_n : Generalized Lucas sequence number of rank n
- $Ct_{m,n}$: Centered Polygonal number of rank n with size m

I. INTRODUCTION

The biquadratic diophantine (homogeneous or non-homogeneous) equations offer an unlimited field for research due to their variety Dickson. L. E. [1], Mordell.L.J. [2], Carmichael R.D[3]. In particular, one may refer Gopalan.M.A.et.al [4-13] for ternary non-homogeneous biquadratic equations. This communication concerns with an interesting non-homogeneous biquadratic equation with four unknowns represented by

$$x^3 + y^3 = (k^2 + 3)^n z^3 w$$

for determining its infinitely many non-zero integral points. Three different methods are illustrated. In method 1, the solutions are obtained through the method of factorization. In method 2, the binomial expansion is introduced to obtain the integral solutions. In method 3, the integral solutions are expressed in terms of Generalized Fibonacci and Lucas sequences along with a few properties in terms of the above integer sequences. Also, a few interesting relations among the solutions are presented.

II. METHOD OF ANALYSIS

The Diophantine equation representing a non-homogeneous biquadratic equation with four unknowns is

$$x^3 + y^3 = (k^2 + 3)^n z^3 w \tag{1}$$

Introducing the linear transformations

$$x = u + v, y = u - v, w = 2u \tag{2}$$

in (1), it leads to

$$u^2 + 3v^2 = (k^2 + 3)^n z^3 \tag{3}$$

The above equation (3) is solved through three different methods and thus, one obtains three distinct sets of solutions to (1).

2.1. Method:1

Let
$$z = a^2 + 3b^2 \tag{4}$$

Substituting (4) in (3) and using the method of factorization, define

$$\begin{aligned} (u + i\sqrt{3}v) &= (k + i\sqrt{3})^n (a + i\sqrt{3}b)^3 \\ &= r^n \exp(in\theta)(a + i\sqrt{3}b)^3 \end{aligned} \tag{5}$$

where
$$r = \sqrt{k^2 + 3}, \quad \theta = \tan^{-1} \frac{\sqrt{3}}{k} \tag{6}$$

Equating real and imaginary parts in (5) we get

$$\begin{aligned} u &= (k^2 + 3)^{\frac{n}{2}} \left\{ \cos n\theta (a^3 - 9ab^2) - \sqrt{3} \sin \theta (3a^2b - 3b^3) \right\} \\ v &= (k^2 + 3)^{\frac{n}{2}} \left\{ \cos n\theta (3a^2b - 3b^3) + \frac{1}{\sqrt{3}} \sin \theta (a^3 - 9ab^2) \right\} \end{aligned}$$

Substituting the values of u and v in (2), the corresponding values of x, y, z and w are represented by

$$x(a, b, k) = (k^2 + 3)^{\frac{n}{2}} \left\{ \cos n\theta (a^3 - 9ab^2 + 3a^2b - 3b^3) + \frac{\sin \theta}{\sqrt{3}} (a^3 - 9ab^2 - 9a^2b + 9b^3) \right\}$$

$$y(a, b, k) = (k^2 + 3)^{\frac{n}{2}} \left\{ \cos n\theta (a^3 - 9ab^2 - 3a^2b + 3b^3) - \frac{\sin \theta}{\sqrt{3}} (9a^2b - 9b^3 + a^3 - 9ab^2) \right\}$$

$$z(a, b) = a^2 + 3b^2$$

$$w(a, b, k) = 2(k^2 + 3)^{\frac{n}{2}} \left\{ \cos n\theta (a^3 - 9ab^2) - \sqrt{3} (3a^2b - 3b^3) \right\}$$

Properties:

- $$x(a, b, k) - y(a, b, k) = (k^2 + 3)^{\frac{n}{2}} \left\{ \cos n\theta (Ct_{12,a} + S_a + 2Gnomic_a - 4Pr_a - 2t_{4,a}) + \frac{\sin \theta}{\sqrt{3}} (So_a - t_{4,a} + t_{38,a}) \right\}$$

2. $x(b, b, k) + y(b, b, k) + (k^2 + 3)^{\frac{n}{2}} (\cos n\theta(32P_b^5 - 16t_{4,b}) = 0$

4. Each of the following is a nasty number

(a) $6 \cos n\theta \left[\frac{32(k^2 + 3)^{\frac{n}{2}} P_b^5 \cos n\theta + x(b, b, k) + y(b, b, k)}{(k^2 + 3)^{\frac{n}{2}}} \right]$

(b) $6 \cos(4\alpha\theta) [32(k^2 + 3)^{2\alpha} P_b^5 \cos(4\alpha\theta) + x(b, b, k) + y(b, b, k)]$

3. $4[z(a^2, a^2)]$ is a biquadratic integer.

4. $w(a, 1, k) = 2(k^2 + 3)^{\frac{n}{2}} [\cos n\theta(2P_a^5 - 9Pr_a + 8t_{4,a}) - \sqrt{3} \sin \theta(t_{8,a} + Gnomic_a - 2Ct_{6,a} + 6t_{3,a})]$

5. $x(a, a, k) = \frac{w(a, a, k)}{2} \left[1 + \frac{\tan \theta}{\sqrt{3}} \right]$

2.2. Method 2:

Using the binomial expansion of $(k + i\sqrt{3})^n$ in (5) and equating real and imaginary parts, we have

$$u = f(\alpha)(a^3 - 9ab^2) - 3g(\alpha)(3a^2b - 3b^3)$$

$$v = f(\alpha)(3a^2b - 3b^3) + g(\alpha)(a^3 - 9ab^2)$$

Where

$$\left. \begin{aligned} f(\alpha) &= \sum_{r=0}^{\left[\frac{n}{2}\right]} (-1)^r n C_{2r} k^{n-2r} (3)^r \\ g(\alpha) &= \sum_{r=1}^{\left[\frac{n+1}{2}\right]} (-1)^{r-1} n C_{2r-1} k^{n-2r+1} (3)^{r-1} \end{aligned} \right\} \dots \dots \dots (7)$$

In view of (2) and (7) the corresponding integer solution to (1) is obtained as

$$x = (f(\alpha) + g(\alpha))(a^3 - 9ab^2) + (f(\alpha) - 3g(\alpha))(3a^2b - 3b^3)$$

$$y = (f(\alpha) - g(\alpha))(a^3 - 9ab^2) - (f(\alpha) + 3g(\alpha))(3a^2b - 3b^3)$$

$$z = a^2 + 3b^2$$

$$w = 2f(\alpha)(a^3 - 9ab^2) - 6g(\alpha)(3a^2b - 3b^3)$$

2.3. Method 3:

Taking $n = 0$ in (3), we have,

$$u^2 + 3v^2 = z^3 \tag{8}$$

Substituting (4) in (8), we get

$$u^2 + 3v^2 = (a^2 + 3b^2)^3 \tag{9}$$

whose solution is given by

$$u_0 = (a^3 - 9ab^2)$$

$$v_0 = (3a^2b - 3b^3)$$

Again taking $n = 1$ in (3), we have

$$u^2 + 3v^2 = (k^2 + 3)(a^2 + 3b^2)^3 \tag{10}$$

whose solution is represented by

$$u_1 = ku_0 - 3v_0$$

$$v_1 = u_0 + kv_0$$

The general form of integral solutions to (1) is given by

$$\begin{pmatrix} u_s \\ v_s \end{pmatrix} = \begin{pmatrix} \frac{A_s}{2} & -\frac{\sqrt{3}B_s}{2i} \\ \frac{B_s}{2i\sqrt{3}} & \frac{A_s}{2} \end{pmatrix} \begin{pmatrix} u_0 \\ v_0 \end{pmatrix}, s = 1, 2, 3, \dots$$

Where $A_s = (k + i\sqrt{3})^s + (k - i\sqrt{3})^s$

$$B_s = (k + i\sqrt{3})^s - (k - i\sqrt{3})^s$$

Thus, in view of (2), the following triples of integers x_s, y_s, w_s in terms of Generalized Lucas and fibonacci sequence satisfy (1) are as follows:

Triples:

$$x_s = \frac{1}{2}GL_n(2k, -k^2 - 3)(a^3 - 9ab^2 + 3a^2b - 3b^3) + GF_n(2k, -k^2 - 3)(a^3 - 9ab^2 - 9a^2b + 9b^3)$$

$$y_s = \frac{1}{2}GL_n(2k, -k^2 - 3)(a^3 - 9ab^2 - 3a^2b + 3b^3) - GF_n(2k, -k^2 - 3)(a^3 - 9ab^2 + 9a^2b - 9b^3)$$

$$w_s = GL_n(2k, -k^2 - 3)(a^3 - 9ab^2) - 6GF_n(2k, -k^2 - 3)(3a^2b - 3b^3)$$

The above values of x_s, y_s, w_s satisfy the following recurrence relations respectively

$$x_{s+2} - 2kx_{s+1} + (k^2 + 3)x_s = 0$$

$$y_{s+2} - 2ky_{s+1} + (k^2 + 3)y_s = 0$$

$$w_{s+2} - 2kw_{s+1} + (k^2 + 3)w_s = 0$$

Properties

1. $x_s(a, a, k) + y_s(a, a, k) + 16A_s t_{3,a} = 8A_s t_{4,a}$

2. $x_s(a, a + 1, k) - \frac{A_s}{2} (6P_a^5 - 9P_{a+1}^5 + 18t_{4,a+1} - 3Ct_{6,a} - 24P_a^3 + 4t_{4,a})$

$$\frac{B_s}{2i\sqrt{3}} (6Ct_{6,a} - 18P_a^5 + 42P_a^3 - 14Pr_a - 7t_{4,a})$$

3. $\frac{i\sqrt{3}(x_s(a, a, k) - y_s(a, a, k))}{B_s}$ is a biquadratic integer.

4. $x_s(a, a, k) - y_s(a, a, k) + \frac{B_s}{2i\sqrt{3}} (24(OH_a) + t_{20,a} - 9t_{4,a}) = 0$

5. $x_s(a, a, k) + w_s(a, a, k) + \frac{4B_s}{i\sqrt{3}} (2P_a^5 - t_{4,a}) + A_s(18(OH_a) + S_a - Ct_{4,a} + 2CT_{6,a} - 6t_{4,a}) = 0$

6. $x_s(2a, a, k) + y_s(2a, a, k) + \frac{B_s}{2i\sqrt{3}} (10P_a^5 + 5t_{4,a}) = 5A_s(t_{4,a} - So_a - Pr_a)$

7. $x_s(a,1,k) + y_s(a,1,k) + \frac{B_s}{2i\sqrt{3}}(4P_a^5 - 2Ct_{36,a} + 36t_{4,a})$
 $= \frac{A_s}{2}(4P_a^5 t_{4,a} - G_{nomic}_a - Ct_{4,a} + 4t_{3,a})$
8. $w_s(2^a, 2^a, k) + 24A_s J_{3a} = \begin{cases} 8, & \text{if } a \text{ is odd} \\ -8, & \text{if } a \text{ is even} \end{cases}$
9. $x_s(2^a, 2^a, k) + y_s(2^a, 2^a, k) + 8A_s j_{3a} = \begin{cases} 8, & \text{if } a \text{ is odd} \\ -8, & \text{if } a \text{ is even} \end{cases}$
10. $x_s(a,b,k) + y_s(a,b,k) = w_s(a,b,k)$
11. $x_s^3(a,b,k) + y_s^3(a,b,k) + 3x_s(a,b,k)y_s(a,b,k)w_s(a,b,k) = w_s^3(a,b,k)$
12. $(9A_s)^2 \left(x_s(a,2a,k) - y_s(a,a,k) + \frac{5B_s}{2i\sqrt{3}}(2P_a^5 - t_{4,a}) \right)$ is a cubic integer
13. Each of the following is a nasty number
- (a) $3A_s(x_s(a,a,k) + y_s(a,a,k) + 16A_s t_{3,a})$
- (b) $6(z(a,a))$
- (c) $4A_s \left\{ x_s(a,a,k) + w_s(a,a,k) + \frac{4B_s}{i\sqrt{3}}(2P_a^5 - t_{4,a}) + A_s(18(OH_a) + S_a - 3Ct_{4,a} + 2Ct_{6,a}) \right\}$
- (d) $6[(x_s(a,a,k) + y_s(a,a,k))(w_s(a,a,k))]$
- (e) $30A_s \left\{ x_s(a,a,k) + w_s(a,a,k) + \frac{B_s}{2i\sqrt{3}}(10P_a^5 + 5t_{4,a}) + 5A_s(So_a + Pr_a) \right\}$
14. $x_s(a,b,k) + y_s(a,b,k) = GL_n(2k, -k^2 - 3)u_0 - 6GF_n(2k, -k^2 - 3)v_0$
15. $x_{s+1}(a,b,k) + y_{s+1}(a,b,k) = \left[2k(GL_n(2k, -k^2 - 3)) - (k^2 - 3)(GL_{n-1}(2k, -k^2 - 3)) \right] u_0 - \left[(12k)GF_n(2k, -k^2 - 3) - 6(k^2 + 3)GF_{n-1}(2k, -k^2 - 3) \right] v_0$
16. $x_{s+2}(a,b,k) + y_{s+2}(a,b,k) = \left[(3k^2 - 1)(GL_n(2k, -k^2 - 3)) - (2k^3 + 6k)(GL_{n-1}(2k, -k^2 - 3)) \right] u_0 - \left[(18k^2 - 1)GF_n(2k, -k^2 - 3) - (12k^3 + 36k)GF_{n-1}(2k, -k^2 - 3) \right] v_0$

III. CONCLUSION:

To conclude, one may search for other pattern of solutions and their corresponding properties.

REFERENCES:

- [1] Dickson. L. E. "History of the Theory of Numbers", Vol 2. Diophantine analysis, New York, Dover, 2005.
- [2] Mordell L. J., "Diophantine Equations Academic Press", New York, 1969.
- [3] Carmichael. R.D. "The Theory of numbers and Diophantine Analysis", New York, Dover, 1959.
- [4] Gopalan.M.A., Manjusomnath and Vanith N., "Parametric integral solutions of $x^2 + y^3 = z^4$ ", Acta Ciencia Indica, Vol. XXXIII(No.4)Pg.1261-1265(2007).
- [5] Gopalan.M.A., and Pandichelvi .V., "On Ternary biquadratic Diophantine equation $x^2 + ky^3 = z^4$ ", Pacific- Asian Journal of Mathematics, Vol-2.No.1-2, 57-62, 2008.
- [6] Gopalan.M.A., and Janaki.G., "Observation on $2(x^2 - y^2) + 4xy = z^4$ ", Acta Ciencia Indica, Vol. XXXVM(No.2)Pg.445-448,(2009).

- [8] Gopalan.M.A., Manjusomnath and Vanith N., “Integral solutions of $x^2 + xy + y^2 = (k^2 + 3)^n z^4$ ”, Pure and Applied Mathematika Sciences, Vol.LXIX,NO.(1-2):149-152,(2009).
- [9] Gopalan.M.A., and Sangeetha.G., “Integral solutions of ternary biquadratic equation $(x^2 - y^2) + 2xy = z^4$ ”, Antartica J.Math.,7(1)Pg.95-101,(2010).
- [10] Gopalan.M.A.,and Janaki.G., “Observations on $3(x^2 - y^2) + 9xy = z^4$ ”, Antartica J.Math.,7(2)Pg.239-245,(2010).
- [11] Gopalan.M.A., and Vijayasankar.A., “Integral Solutions of Ternary biquadratic equation $x^2 + 3y^2 = z^4$ ”, Impact.J.Sci.Tech.Vol.4(No.3)Pg.47-51,2010.
- [12] Gopalan.M.A,Vidhyalakshmi.S., and Devibala.S., “Ternary biquadratic diophantine equation $2^{4n+3}(x^3 - y^3) = z^4$ ”,Impact. J.Sci.Tech.Vol(No.3) Pg.57-60,2010.
- [13] 12.Gopalan.M.A,Vidhyalakshmi.S., and SumathiG., “ Integral Solutions of Ternary biquadratic Non-homogeneous Equation $(\alpha + 1)(x^2 + y^2) + (2\alpha + 1)xy = z^4$ ”,JARCEvol(6),No.2, Pg.97-98,July-Dec 2012.
- [14] 13. Gopalan.M.A, SumathiG.,and Vidhyalakshmi.S., “ Integral Solutions of Ternary biquadratic Non-homogeneous Equation $(k + 1)(x^2 + y^2) - (2k + 1)xy = z^4$ ”,Archimedes J.Math,3(1),67-71,2013.
- [15]
- [16]
- [17]
- [18]
- [19]

Prediction of Number of Faults And Time To Remove Errors

¹Nirvikar Katiyar ²Dr. Raghuraj Singh

¹Ph.D. SCHOLAR J.J.T.U. RAJASTHAN

²Prof. C.S. Department HBTI KANPUR

Abstract:

Advance knowledge of which files in the next release of a large software system are most likely to contain the largest numbers of faults can be a very valuable asset. To accomplish this, a negative binomial regression model has been developed and used to predict the expected number of faults in each file of the next release of a system. The predictions are based on the code of the file in the current release, and fault and modification history of the file from previous releases. The model has been applied two large industrial systems, one with a history of 17 consecutive quarterly releases over 4 years, and the other with nine releases over 2 years. The predictions were quite accurate: for each release of the two systems, the 20 percent of the files with the highest predicted number of faults contained between 71 percent and 92 percent of the faults that were actually detected, with the overall average being 83 percent. The same model was also used to predict which files of the first system were likely to have the highest fault densities (faults per KLOC). In this case, the 20 percent of the files with the highest predicted fault densities contained an average of 62 percent of the system's detected faults. However, the identified files contained a much smaller percentage of the code mass than the files selected to maximize the numbers of faults. The model was also used to make predictions from a much smaller input set that only contained fault data from integration testing and later. The prediction was again very accurate, identifying files that contained from 71 percent to 93 percent of the faults, with the average being 84 percent. Finally, a highly simplified version of the predictor selected files containing, on average, 73 percent and 74 percent of the faults for the two systems. Defect tracking using computational intelligence methods is used to predict software readiness in this study. By comparing predicted number of faults and number of faults discovered in testing, software managers can decide whether the software are ready to be released or not. In this paper the predictive models can predict: (i) the total number of faults (defects), (ii) the number of code lines changes required to correct a fault and (iii) the amount of time calculated (in minutes) to make the changes in respective object classes using software metrics as independent variables. The use of neural network model with a genetic training strategy is introduced to improve prediction results for estimating software readiness in this study. Our prediction model is divided into three parts: (1) prediction model for Presentation Logic Tier software components (2) prediction model for Business Tier software components and (3) prediction model for Data Access Tier software components. Existing object-oriented metrics and complexity software metrics are used in the Business Tier neural network based prediction model. New sets of metrics have been defined for the Presentation Logic Tier and Data Access Logic Tier. These metrics are validated using two sets of real world application data, one set was collected from a warehouse management system and another set was collected from a corporate information system.

Keywords :Software Readiness, Predictive model, Defect Tracking, N-tier Application, Prediction of number of faults, software fault analysis and data accumulation.

I. INTRODUCTION:

Reliability is a significant factor in quantitatively characterizing quality and determining when to stop testing and release software on the basis of predetermined reliability objectives. Our works belong to a class of software reliability models that estimate software readiness through gauging on the amount of unresolved

residual defects. In highly competitive commercial software market, software companies feel compelled to release the completely ready software. Their task is treacherous, treading the line between releasing poor quality software early and high quality software late [26]. If software is released too early, then customers will be sent poor quality code; if it takes too long before releasing software, it can avoid the problems of low quality, but run the risk of exceeding deadlines and being penalized for the late delivery. Therefore, the ability to predict software readiness is essential to any software for optimizing development resources usage and project planning. A variety of traditional statistical techniques are used in software reliability modeling. Models are often based on statistical relationships between measures of quality and measures of software metrics. However, relationships between static software metrics and quality factors are often complex and nonlinear, limiting the accuracy of conventional approaches [31]. Artificial neural networks and genetic training strategy are adept at modeling nonlinear functional relationships that are difficult to model with other techniques, and thus are attractive for software quality modeling. The use of neural network model with a genetic training strategy is introduced to improve prediction results for estimating software readiness in this study. With many variables, it is quite difficult to find the exact combination of contributions of each of the variables that creates the best predictions [23]. Genetic algorithm provides the solution to overcome this difficulty [4]. It finds the best set of importance of input values on an arbitrary scale of 0 to 1. The importance of input values are a relative measure of how significant each of the inputs is in the predictive model. We can then decide to remove the variables with the lowest Relative importance of inputs values. Most software today is developed so as to be integrated into existing systems. New software components are replaced or added into existing system. They use N-tier application architecture which produces flexible and reusable application for distribution to any number of client interfaces. Since all tiers have clear separation, this allows the developers to plug each layer in and out without too much hassles and without limiting the technology used at each tier [24]. For example, re-definition of the storage strategy or changing of DBMS middleware will not cause disruption to the other tiers. Our predictive model is targeting at software that is designed and written using this type of architecture. Our research team has analyzed the fault reports of a Warehouse Application System (WAS) and an Information Management System (IMS) and classified the faults. These software fault reports are recorded by CAIB GmbH, Murrhardt Company and Hwafuh, Myanmar software development team respectively during system test and maintenance stages in recent years for the Warehouse Application System and the Hwafuh Information System. The classification scheme was based on the nature of these faults and their relevance to the application architecture. For example, the faults coming from the Business Tier are strongly related to object oriented features and are introduced by features such as inheritance and polymorphism. In the Data Access Tier, the faults are strongly related to the code are used to interface with the database. Therefore, our prediction model is divided into three parts: (1) prediction model for Presentation Logic Tier (2) prediction model for Business Tier and (3) prediction model for Data Access Tier. Although N-tire application architectures are widely used, currently none of the existing research studies on the prediction of number of software development faults is based on architecture layers. Our model was built on an application tier basis using neural network model with a genetic training strategy and the trained system is used to predict the number of software development faults to help the software managers in deciding whether their software is ready to be released or not.

II. RELATED WORKS:

One of the methods to predict software readiness is defect tracking. McConnell describe four methods in [26]. Residual defects are one of the most important factors that allow one to decide if a piece of software is ready to be released. In theory, one can find all the defects and count them; however it is impossible to find all the defects within a reasonably short amount of time. One possible technique that a software manager can use is to apply the software reliability models and thus estimate the total number of defects present at the beginning of testing [35]. According to [1], there are essentially two types of software reliability models: those attempts to predict: (i) from design parameters and (ii) from test data. Both types of models aim to predict residual errors of software under development. The first type of models are usually called “defect density” models and use code characteristics in traditional software codes such as lines of code, nesting of loops, external references, input/outputs, cyclomatic complexity and so forth to estimate the number of defects in the software. Our model belongs to this category. However, instead of using conventional software parameters, our model focuses on objected-oriented code characteristics and N-tier application architecture. Nowadays, software houses widely adopted N-tier architecture approach in software development and have successfully implemented software systems using current technologies such as .NET and J2EE [24]. The second type of models is usually called software reliability growth models. These models attempt to statistically correlate defect detection data with known functions (such as an exponential function) using parametric methods. If the correlation is good, the known function can be used to predict future behavior. Both reliability models are used to estimate software readiness by gauging on the residual defects. Software development faults are predicted using various types of

software metrics in various studies [8, 11, 13, 17 and 21]. In our earlier studies, software development faults were predicted using Object-Oriented Design Metrics and SQL Metrics [32, 33]. The results from these studies showed that neural network models had better prediction accuracy than regression models. Our research set out to answer three questions: (i) how many faults are remaining in the programs, (ii) how many lines are required to be changed in order to correct these errors and (iii) how much time is required for the above activities. By comparing predicted number of faults and number of faults discovered in testing, software managers can decide whether the software are ready to be released or not. Most of the software quality models such as [18, 29, 6, 23 and 19] for object-oriented systems predict whether a software module contain faults by using traditional statistical models. However, only identifying faulty modules is not enough to estimate the software readiness.

III. SOFTWARE FAULT ANALYSIS:

Previous work in software fault modeling can be classified into prediction of number of faults remaining in the system and accounting for the number of faults found in the system. Most of the work on prediction is done in connection with software reliability studies in which one first estimates the number of remaining faults in a software system, then uses this estimate as a predictor of the number of faults in some given time interval. (See Musa, et al. [27] for an introduction to software reliability.) Classic models of software faults [29, 31] are discussed in a survey of the early work on measuring software quality by Mohanty [26] which has a section on estimation of fault content. There are also many recently proposed models [30, 32]. These models estimate the number of faults that are already in the software. Our work differs from these studies in that we assume new faults are continuously being added to the system as changes are made. Our research is similar to previous empirical studies of software faults, e.g. [12, 17, 30, 34], where the aim is to understand the nature and causes of faults. In these studies, explanatory variables are identified in order to account for the number of faults found. Our work extends this by attempting to understand how the process of software evolution could have an effect on the number of faults found over time. In several of the cited studies, no actual model is articulated. Our goal is to build fault models based on these explanatory variables that are reasonably accurate and interpretable. Below we list some of the factors, cited in previous work, which were thought to be predictors of number of faults. These factors can be classified into two groups: product related and process-related measures. Within each group, we will list the measurements in that group that we used to try to predict fault potential, and describe how successful these measurements were.

IV. SOFTWARE METRICS:

In this paper prediction model is divided into three parts, therefore software metrics are defined for different three levels as:

4.1 DATA ACCESS TIER:

We have analyzed the Data Access Tier source code of N-tier applications. SQL commands are mainly composed in the Data Access Tier classes to perform these database operations. It allows the creation of a set of useful and specific routines to be able to perform insert, select, delete and update actions on database tables. It does not usually contain business logic or presentation items. Therefore, the metrics for the Data Access Tier are different from other tiers. For source code of this tier, the number of database operations statements which are invoked from Data Access Tier classes and the error corresponding with these operations are more involved than other operations. For example, retrieving wrong database records, insertion fail error, cannot update error etc. In such cases developers need to check and modify the corresponding SQL statements to correct the error. To measure the size of Data Access Tier source code, we should measure the number of database operations statements instead of other LOC metrics for the Data Access Tier. The following Data Access Tier metrics are proposed and used in this study. Metrics having weak relationship with fault occurrence, such as the number of Data Definition Language (DDL) commands and Data Control Language (DCL) commands, are omitted in this study. Therefore we have measured three types of database operations, the statements given as (Table-1):

- [1] The number of delete operations (TNDO) for deleting database records.
- [2] The number of Select statements (TNSC) for data retrieval.
- [3] The number of Insert/Update operations (TNIUO) for updating database records.

We have measured the complexity of SQL statements instead of other complexity metrics such as cyclomatic complexity because the Data Access Tier does not control the logic and flow of the application. These are controlled in Business Tier. The Data Access Tier codes only contain the specific routines to perform database operations. We have measured the complexity of SQL commands by using following construct that contain in SQL statements:

- [1] The number of sub queries.
- [2] The number of search condition criteria.
- [3] The number of group by clauses.

Complexity of SQL statement is likely to increase following the increase in the number of these constructs because the latter can specify rows of data from a table or group of tables by joining such tables. As such, these are important in measuring the complexity of SQL statements as (Table-1).

Metrics	Description
TNDO	Total number of delete operations
TNSQ	Total number of sub-queries in data retrieval statements
TNIUO	Total number of insert/update operations
TNGB	Total number of group-by-clause in data retrieval statements
TNSC	Total number of select-SQL commands
ANSC	Average number of search condition criteria of where-clause in data manipulation statements

Table-1. List of Data Access Tier metrics

4.2 BUSINESS TIER:

It controls the logic and flow of the application. This layer does not have codes to access the database or codes for the user interface. Business Tier is the brain of applications since it basically contains elements such as business rules, data manipulation, etc. As this layer mainly contains object-oriented codes, object-oriented metrics are used for this tier. There is great interest in the use of the object-oriented approach to software engineering these days. Many measures have been proposed and evaluated in the literature to capture the structural quality of object-oriented code and design [6, 18, 19, 23, and 29]. The following existing traditional complexity metrics and object-oriented metrics are used in the prediction model for the Business Tier as (Table-2).

Metrics	Description
CBO	Coupling between objects
NOP	Number of parents
NA	Number of Attributes
AMC	Average Method Complexity
NOC	Number of Children
RFC	Response for a class
WMC	Weighted Methods per Class
LCOM	Lack of cohesion in methods
NMA	Number of methods added
DIT	Depth of inheritance tree

Table-2. List of metrics for the Business Tier

4.3 PRESENTATION LOGIC TIER:

Presentation logic tier works with the results/output of the Business Tier and handle the transformation into something usable and readable by the end user. It consists of windows forms, dialogs and ASP documents etc. We have found that some errors in this tier are strongly related to the interface objects. For example, improper display of edit box value, showing some buttons which should be hidden until some specific events have occurred, wrong adjustment of width of objects for some output values etc. In such cases developers need to check and modify the corresponding controls of these interface objects to correct the error. Therefore the number of user interface objects (NUIO) should be measured for predicting these kinds of errors instead of using other metrics such as LOC. Another metrics that has used in this tier is the total number of messages (TNM). This metric measures the total number of interface objects' messages of presentation layer classes. For example, BN_CLICKED message, LBN_DBCLICKED message of C list Box and C Button interface objects. When the user clicks a button, BN_CLICKED method is invoked. If an error occurred, the developers need to check the corresponding method to correct the error. A larger number of these methods are likely to correlate to

a higher number of fault occurrences. We use the following metrics for this tier of object-oriented applications instead of using metrics such as count of bytes, lines, language keywords, comment bytes, semicolons, block length, and nesting depth etc. (Halstead's metrics) – which are designed mainly for conventional applications with procedural flows.

4.4 Number of user interface objects (NUIO):

The NUIO is the measure of user interface objects or controls which handle input operations from user and output operation to users. For example, text box objects, button objects and label objects etc. The NUIO is defined as:

$$\text{NUIO}(c) = |\text{Interface Objects}(c)|$$

Where Interface Objects (c) is the set of interface objects which are declared in the Presentation Logic Tier class c.

4.5 Total Number of Messages (TNM):

This metric measures the total number of interface objects' messages of presentation layer classes. The TNM is defined as:

$$\text{TNM}(c) = |\text{Messages}(c)|$$

Where Message (c) is the set of messages which are handled by interface objects of the Presentation Logic Tier class c.

V. DEXTEROUS STUDY:

The genetic training strategy of Neuro Shell Predictor is used in this study. The genetic net combines a genetic algorithm with a statistical estimator to produce a model which also shows the usefulness of inputs. The genetic algorithm tests many weighting schemes until it finds the one that gives the best predictions for the training data. The genetic method produces a set of relative importance factors that is more reliable than those produced by the neural method. Genetic algorithms (GAs) seek to solve optimization problems using the methods of evolution, specifically survival of the fittest. The functioning of the genetic estimator is built upon the General Regression Neural Net (GRNN) [5]. Genetic learning stores every set of inputs and related output in the training data. When predicting an output (e.g. defects) of particular input pattern, it is compared to every other pattern. Depending upon how close the match is, the output for each training row is weighted. Closer matches receive higher weights, and inputs that are farther away from the training inputs receive lower weights. The predicted output for the particular set of inputs is a "weighted" average of all of the other outputs (e.g. defects) with which the network was trained. As the genetic method uses a "one hold out" strategy during both training using current data set and afterwards when evaluating new data set, all available data sets can be used [25]. As such, out of sample evaluation set is not necessary when using genetic method. If the method is called upon to produce an output from a particular pattern of inputs T, then it never looks at T if T is in the training set, as long as "enhanced generalization" feature is turned on. This is true at all times during training. The genetic method is much like a "nearest neighbor" predictor or classifier. Its output is a kind of weighted average of the closest neighbors' outputs in the training set. In other words, if evaluating T, T is never considered to be in the neighborhood. Most other neural networks do not work this way. They look at the entire training set when being trained for each data set in the training set. Therefore, they are essentially looking at the entire training set when being applied to new data set later [23, 25].

5.1 Data Collection:

The experiment data is collected from two application systems. The first application is the warehouse management applications (WMA) that is developed using C, JAM (JYACC Application Manager) and PL/SQL languages. This set of applications has more than a thousand source files of C, JAM (JYACC Application Manager) and PL/SQL codes and uses the Oracle database. The warehouse system has been customized and used by many companies. Data Access Tier faults were collected from the journal files that contain the documentation of all changes in source files such as status of module, start date, end date, developer, nature of changes, etc. Data on software metrics were extracted from 102 PL/SQL files of the warehouse application. The second application used in this prediction is subsystems of an application system which is used in the Hwafuh (Myanmar) company, which is a fully networked information system. The Hwafuh Information System (HIS) contains more than 300 classes and approximately 1,000,000 lines of codes. The experiment data was collected from the payroll subsystem, time record subsystem, human resource function subsystem and piece calculation subsystems.

5.2 Experiments for the Data Access Tier:

Experiment Analysis 1:

The warehouse application system data was used for the experiment on prediction of data access faults of Data Access Tier. Six software metrics were extracted from 103 PL/SQL files. It contains TNSQ, TNSC, TNDO, ANSC, TNGB, and TNIUO metrics. The dependent variable was the number of Data Access Tier faults and the independent variables were the six software metrics identified above. First, each data pattern was examined for erroneous entries, outliers, blank entries and redundancy. A threshold value was set at 1000 for maximum number of generations without improvement. After 1621 generations, the optimized coefficient of multiple determination (R-square) value 0.737046 was arrived at. Therefore, about 74% of the variation in the number of faults can be accounted by the six predictors. To measure the goodness of fit of the model, coefficient of multiple determination (R-square), coefficients of correlation(r), mean square error (MSE) and root mean square error (RMSE) were used. The correlation of the predicted variable and the observed variable is represented by the coefficient of correlation (r). An r value of 0.861246 represents high correlations for cross-validation. The number of observations is 104. The significance level of a cross-validation is indicated by the p value. A commonly accepted p value is 0.06. In our experiment, a two tailed probability p value is less than 0.0001. This shows a high degree of confidence for the successful validations. The results clearly indicate a close relationship between Data Access Tier metrics (independent variables) and the number of Data Access Tier faults (dependent variable).

r (correlation coefficient)	0.860796
MSE	0.191002
t values	16.95783
R-square	0.768120
RMSE	0.4297
Avg error	0.267628
p values	< 0.0001

Table-3 Experimental result for the WMA system

5.3 Experiment Analysis 2:

The Hwafuh Information System (HIS) was used for prediction of data access faults, the number of line changed per class and required time (in minutes) to correct these data access tier faults. Six software metrics were extracted from 36 Data Access Tier classes.

5.4 Selection of Metrics for Data Access Tier:

Four Data Access Tier metrics (TNIUO, TNSC, ANSC and TNDO) from proposed six Data Access Tier metrics are selected in this experiment. TNGB and TNSQ metrics could not be collected because corresponding SQL constructs are seldom used in the HIS system.

5.5 Prediction of number of faults:

Average number of search condition criteria of where-clause (ANSC) and Number of insert /update operations (TNIUO) are found to be more important for number of faults prediction for the Data Access Tier. That shows the complexity of search condition criteria is highly related to occurrence of faults in this Tier.

5.6 Prediction of number of lines changed per class:

In this prediction, the TNSC metric is the most important inputs in this model. The amount of Select operation containing in Data Access Tier class is highly related to number of lines changes in that class. The ANSC and the TNIUO metrics are also important for prediction of number of lines changed.

5.7 Prediction of required time (in minutes) to change:

The TNIUO and the ANSC metrics are also most important for prediction of required time (in minutes) to change. Although only 36 rows of data have been tested in Experiment 2 the two-tailed P values are less than 0.0001. By conventional criteria, these p values are considered to be statistically significant. Experiment results show that r values are 0.788908 for prediction of the number of faults, 0.793297 for prediction of the number of lines changed per class and 0.818494 for prediction of required time (in minutes) to change. These results show a close relationship between Data Access Tier metrics (independent variables) and dependent variables (the number of faults per class and the maintenance cost). The values of squared multiple correlation are 0.732894 for prediction of the number of faults, 0.623987 for the prediction of the number of lines changed per class and

0.663987 for prediction required time (in minutes) to change. Therefore, about 72%, 63% and 67% of the variance, respectively, in the number of faults and the maintenance cost can be accounted for by these predictors.

5.8 Experiment for Business Tier:

The Hwafuh Information System (HIS) was used for prediction of data access faults, the number of line changed per class and required time (in minutes) to correct these Business Tier faults. Software metrics were extracted from 178 Business Tier classes.

5.9 Selection of Metrics:

As discussed in Section IV, we have selected the Chidamber and Kemerer object oriented metrics [29] and complexity metrics. After testing several combinations of models using Business Tier software metrics using subsystems of the Hwafuh Information system data, the following models achieved the best prediction for number of faults, number of line changes and required time (in minutes) respectively.

5.10 Prediction of number of faults:

The model used in this experiment contains NOP, RFC, DIT, LCOM, NMA, NOC, NA and CBO metrics. From Business Tier metrics, inheritance metrics (NOP, DIT), Response for a class (RFC) and cohesion metrics (LCOM) are the important ones for number of faults prediction in this tier.

5.11 Prediction of number of lines changed per class:

The model used in this experiment contains LCOM, DIT, NMA, RFC, NOC, WMC, CBO, NA, and NOP metrics. The cohesion metric (LCOM) is most important metric and other metrics is about equal importance.

5.12 Prediction model for required time (in minutes):

This model contains LCOM, DIT, NMA, RFC, NOC, WMC, CBO, NA, and NOP metrics. As in fault prediction experiment, LCOM, NOP, RFC and DIT are the most important. For 178 observations, the two-tailed p values are less than 0.0001. By conventional criteria, these p values are considered to be statistically significant. Experiment results show that r values are 0.838913 for prediction of the number of faults, 0.867894 for prediction of the number of lines changed per class and 0.748748 for prediction of required time (in minutes) to change the code. These results show a close relationship between Business Tier metrics (independent variables) and dependent variables (the number of faults per class and the maintenance cost / effort). The values of squared multiple correlation are 0.701936 for prediction of the number of faults, 0.747582 for the prediction of the number of lines changed per class and 0.548946 for prediction of required time (in minutes) to change the erroneous code. Therefore about 70 %, 74% and 55% of the variance, respectively, in the number of faults and the maintenance cost can be accounted for by these predictors.

5.13 Experiments for Presentation Logic Tier:

Presentation tier classes (58 classes) were collected from the Hwafuh Information System.

5.14 Selection of Metrics:

As they mainly include dialog classes, form classes and view classes etc, the number of user interface objects (NUIO) metrics and the total number of messages (TNM) metrics were proposed and used in this study. Their relative importance is roughly equal for experiments of Presentation Logic Tier.

5.15 Prediction of number of faults:

After performing 380 generations, an R square value of 0.67399 was received using the genetic learning strategy of Neuro Shell predictor. Therefore about 67% in the number of faults can be explained by the two selected predictors. An r value of 0.828206 represents high correlations for cross-validation for 58 observations.

5.16 PREDICTION OF NUMBER OF LINES CHANGED PER CLASS:

After performing 156 generations, an R square value of 0.53185 was received. Therefore about 52% in the number of lines changed per class can be explained by the two selected predictors. An r value of 0.740297 represents high correlations for cross-validation for 58 observations.

5.17 Prediction model for required time (in minutes):

After performing 116 generations, an R square value of 0.589987 was received. Therefore about 61% in required time (in minutes) to change per class can be explained by the two selected predictors. An r value of 0.800102 represents high correlations for cross-validation for 58 observations. From the experiment results, the Presentation Logic Tier metrics in this study appear to be useful in predicting software readiness. About 68%, 52% and 61% of the variance, respectively, in the number of faults and the maintenance cost can be accounted for by these predictors. The relative importance both Presentation Logic Tier metrics are about the same. Equal care should be taken when designing interface objects and messages of Presentation Logic Tier classes.

VI. CONCLUSION FOR COMPARATIVE STUDY USING REGRESSION MODEL:

We run the whole set of experiment using a regression model once again after execution. The superiority of the neural network model with genetic training algorithm in predicting software readiness using metrics is undisputable as it consistently performed the regression model.

VII. RESULTS:

In this section we present various models of modules' fault potential. First we discuss the stable model, which predicts numbers of future faults using numbers of past faults. Next we list out most successful generalized linear models, which construct predictors in terms of variables measuring the static properties of the code or comprising simple summaries of the change history using different models as: stable model and weighted time damped model etc.

VIII. CONCLUSION:

Our research extended currently software quality prediction models by including structural/architecture considerations into software quality metrics. The genetic training strategy of Neuro Shell Predictor is used in our study. The Genetic Training Strategy uses a "genetic algorithm" or survival of the fittest technique to determine a weighting scheme for the inputs. The genetic algorithm tests many weighting schemes until it finds the one that gives the best predictions for the training data. Data patterns from WMS (103 patterns) were used for the prediction of the number of faults in the Data Access Tier prediction model. This study used 36 Data Access Tier classes, 178 Business Tier classes and 58 for Presentation Logic Tier classes from HIS to predict the number of faults, the number of lines changed and time required (in minutes). For these numbers of patterns, the genetic training method is much better because the evaluation set is not necessary in the genetic training method. We have compared this approach to a multiple regression analysis approach. The comparative performance data for the models are define by comparing empirical results including R2 and RMSE, Genetic Nets give better prediction results than Regression analysis. Regression analysis was done by using SPSS software. We intend to extend this investigation to a wide range of applications and also to propose a new set of Presentation Logic Tier metrics related to various types of user interface objects. For example, by separating pure display interface objects from interface objects that are able to perform both input/output functions. Also, it may be useful to separate control interface objects from interface objects which can be control objects as well as holding values.

REFERENCES:

- [1] Alen Wood, "Software Reliability Growth Models", hp Technological Report, TR-96.1, September 1996.
- [2] Bellini, P. (2005), "Comparing Fault-Proneness Estimation Models", 10th IEEE International Conference on Engineering of Complex Computer Systems (ICECCS'05), vol. 0, 2005, pp. 205-214.
- [3] D. A. Christenson and S. T. Huang, Estimating the fault content of software using the $_x\text{-on-}_x$ model," Bell Labs Technical Journal, vol. 1, no. 1, pp. 130{137, Summer 1996.
- [4] D. E Goldberg, "Genetic Algorithms in Search, Optimization, and Machine Learning", Reading, Mass: Addison-Wesley, 1989.
- [5] D.F, Specht, "A general regression neural network", IEEE Transactions on Neural Networks, vol. 2, Issue: 6, pp. 568-576, 1991.
- [6] El Emam, W. Melo, C.M. Javam, "The Prediction of Faulty Classes Using Object-Oriented Design Metrics", Journal of Systems and Software, Elsevier Science, 2001, pp. 63-75.
- [7] Fenton, N. E. and Neil, M. (1999), "A Critique of Software Defect Prediction Models", Bellini, I. Bruno, P. Nesi, D. Rogai, University of Florence, IEEE Trans. Softw. Engineering, vol. 25, Issue no. 5, pp. 675- 689.
- [8] Giovanni Denaro (2000), "Estimating Software Fault-Proneness for Tuning Testing Activities" Proceedings of the 22nd International Conference on Software Engineering (ICSE2000), Limerick, Ireland, June 2000.
- [9] G. J. Schick and R. W. Wolverton, An analysis of competing software reliability models," IEEE Trans. on Software Engineering, vol. SE-4, no. 2, pp. 104{120, March 1978.
- [10] J. D. Musa, A. Iannino, and K. Okumoto, Software Reliability, McGraw-Hill Publishing Co., 1990.
- [11] J. Jelinski and P. B. Moranda, Software reliability research," in Probabilistic Models for Software, W. Freiberger, Ed., pp. 485{502. Academic Press, 1972.
- [12] K. H. An, D. A. Gustafson, and A. C. Melton, A model for software maintenance," in Proceedings of the Conference on Software Maintenance, Austin, Texas. September 1987, pp. 57{ 62, IEEE Computer Society Press.
- [13] Khoshgoftaar, T. M. and J. C. Munson, (1990). "Predicting Software Development Errors using Complexity Metrics", IEEE Journal on Selected Areas in Communications, 8(2): 253 -261.

- [14] Khoshgoftaar, T.M., K. Gao and R. M. Szabo (2001), "An Application of Zero-Inflated Poisson Regression for Software Fault Prediction. Software Reliability Engineering", ISSRE 2001. Proceedings of 12th International Symposium on, 27-30 Nov. (2001), pp: 66 -73.
- [15] L Briand, W.L Melo, J. Wust, "Assessing the applicability of fault-proneness models across object-oriented software projects", IEEE Transactions on Software Engineering, vol. 28 pp. 706 –720, 2002.
- [16] Lanubile F., Lonigro A., and Visaggio G. (1995) "Comparing Models for Identifying Fault-Prone Software Components", Proceedings of Seventh International Conference on Software Engineering and Knowledge Engineering, June 1995, pp. 12-19.
- [17] L. Hatton, "Reexamining the fault density{component size con- nexion," IEEE Software, pp. 89{97, March/April 1997.
- [18] M. Cartwright and M. Shepperd, "An Empirical Investigation of Object-Oriented Software System", IEEE Transactions on Software Engineering, vol. 26, pp. 786-796, 2000.
- [19] Mei-Huei Tang, Ming-Hung Kao, Mei-Hwa Chen,"An empirical study on object-oriented metrics", Proceedings of the Sixth IEEE International Symposium on Software Metrics, pp. 242-249, 1999.
- [20] Manasi Deodhar (2002), "Prediction Model and the Size Factor for Fault-proneness of Object Oriented Systems", MS Thesis, Michigan Tech. University, Dec. 2002.
- [21] Menzies, T., K. Ammar, A. Nikora, and S. Stefano, (2003), "How Simple is Software Defect Prediction?", Journal of Empirical Software Engineering, October (2003).
- [22] Munson, J. C. and T. M. Khoshgoftaar, (1992), "The detection of faultprone programs", IEEE Transactions on Software Engineering, 18(5): 423- 433.
- [23] NeuroShell Predictor Reference Manual, Ward Sysms Group, Inc. <http://www.wardsystems.com>.
- [24] Robert Chartier, "Application Architecture: An N-Tier Approach ", <http://www.15seconds.com>.
- [25] C.H. Chen, "Fuzzy Logic and Neural Network Handbook", New York, N.Y.: McGraw-Hill, Inc., 1996.
- [26] S. McConnell, "Gauging software readiness with defect tracking", IEEE Software, Vol. 14, no. 3, pp. 136, 135,1997.
- [27] S. G. Eick, C. R. Loader, M. D. Long, L. G. Votta, and S. Van- derWiel, Estimating software fault content before coding," in Proceedings of the 14th International Conference on Software Engineering, Melbourne, Australia, May 1992, pp. 59{65.
- [28] S. N. Mohanty, "Models and measurements for quality assessment of software," ACM Computing Surveys, vol. 11, no. 3, pp. 251{275, September 1979.
- [29] S.R. Chidamber, and C.F. Kemerer, "A Metrics Suite for Object Oriented Design", IEEE Transactions on Software Engineering, vol. 20, pp. 476-493, 1994.
- [30] T. J. Yu, V. Y. Shen, and H. E. Dunsmore, An analysis of several software defect models," IEEE Trans. on Software Engineering, vol. 14, no. 9, pp. 1261{1270, September 1988.
- [31] T. M. Khoshgoftaar, E. B. Allen, J. P. Hudepohl, S. J. Aud, "Application of neural networks to software quality modeling of a very large telecommunications system", Neural Networks, IEEE Transactions on ,Vol. 8, Issue 4, July 1997, pp. 902 – 909.
- [32] Tong-Seng Quah, Mie Mie Thet Thwin, "Prediction of Software Development Faults in PL/SQL Files Using Neural Network Models", Information and Software Technology, vol. 46, No.8, pp. 519-523, 2004.
- [33] Tong-Seng Quah and Mie Mie Thet Thwin, "Application of neural networks for software quality prediction using object-oriented metrics", Proceedings of International Conference on Software Maintenance, ICSM 2003, 22-26 Sept., 2003, pp. 116 – 125.
- [34] V. R. Basili and B. T. Perricone, Software errors and complex- ity: An empirical investigation," Communications of the ACM, vol. 27, no. 1, pp. 42{52, January 1984.
- [35] Y.K. Malaiya and J. Denton, 'Estimating the number of Residual Defects', HASE '98, 3rd IEEE Int'l High-Assurance Systems Engineering Symposium, Maryland, USA, November 13-14, 1998.

Enhancement of Error Detection and Correction Capability Using Orthogonal Code Convolution

¹Mukesh Gholase , ²L.P.Thakare, ³Dr. A.Y. Deshmukh
^{1,2,3}Dept. Of Electronics Engineering, G.H.Raisoni College of Engineering,
Nagpur, India.

Abstract

In this paper, The Orthogonal Codes has been developed and realized by means of Field Programmable Gate Array (FPGA). The proposed techniques map a k-bit data block into an n-bit Orthogonal code block (n>k) and transmit the coded block across the channel. Construction of orthogonal coded modulation schemes are realised by means of FPGA. The result shows that the proposed technique enhances both error detection and correction capabilities of Orthogonal Codes Convolution with a detection rate of 99.99%

Index Terms - Error detection and correction, FPGA, Orthogonal Code Antipodal Code.

I. INTRODUCTION

When data is stored, compressed, or communicated through a media such as cable or air, sources of noise and other parameters such as EMI, crosstalk, and distance can considerably affect the reliability of these data. Error detection and correction techniques are therefore required. Some of those techniques can only detect errors, such as the Cyclic Redundancy Check; (CRC) [1-3]; others are designed to detect as well as correct errors, such as Solomon Codes [4,5], Hamming Codes [6], and Orthogonal Codes Convolution (OCC) [7,8].

However, the existing techniques are not able to achieve high efficiency and to meet bandwidth requirements especially with the increase in the quantity of data transmitted. Orthogonal Code is one of the codes that can detect errors and correct corrupted data. The objective of this paper is to enhance the error control capability of orthogonal code by means of Field Programmable Gate Array (FPGA) implementation.

II. ORTOGONAL CODES

Orthogonal codes are binary valued, and they have equal number of 1's and n/2 0's; i.e., there are n/2 positions where 1's and 0's differ [7,8]. Therefore, all orthogonal codes will generate zero parity bits. The concept is illustrated by 16-bit orthogonal codes as shown in Fig. 1. It has 16- orthogonal codes and 16- antipodal codes for a total of 32-bi-orthogonal codes. Antipodal codes are just the inverse of orthogonal codes; they have the same properties. A notable distinction in this method is that the transmitter does not have to send the parity bit for the code, since it is known to be always zero [8,9]. Therefore, if there is a transmission error, the receiver may be able to detect it by generating a parity bit at the receiving end. Before transmission, a k-bit data set is mapped into a unique n-bit orthogonal code. For example, a 5-bit data set is represented by a unique 16-bit orthogonal code, which is transmitted without the parity bit. When received, the data are decoded based on code correlation. It can be done by setting a threshold between two orthogonal codes. This is set by the following equation

$$d_{th} = \frac{n}{4} \quad (1)$$

Where n is the code length and d_{th} is the threshold, which is midway between two orthogonal codes. Therefore, for the 16-bit orthogonal code (Fig. 2), we have $d_{th} = 16/4 = 4$

This mechanism offers a decision process in error correction, where the incoming impaired orthogonal code is examined for correlation with the codes stored in a look-up table, for a possible match. The acceptance criterion for a valid code is that an n-bit comparison must yield a good cross correlation value; otherwise, a false detection will occur. This is governed by the following correlation process, where a pair of n-bit codes $x_1x_2...x_n$ and $y_1y_2...y_n$ is compared to yield,

A counter is used to count the number of 1's in the resulting signal. For example, for 16-bit orthogonal code, the operation will lead to thirty-two counter results. If one of the results is zero, it means there is no error. Otherwise, the code is corrupted. The corrected code is associated with minimum count. If the minimum count is associated with one combination, the received and corrected code will be this combination. However, if the minimum count is associated with more than one combination of the orthogonal codes, it is not possible to correct the corrupted code.

III. METHODOLOGY

An orthogonal code is having equal number of 1's and 0's so it will generate zero parity all time except that code received is erroneous. We need not to send any extra parity bit while transmitting data. In case if, after the transmission the data received is erroneous then it will generate parity error. In this process of detecting and correcting the errors code received is split into two equal parts. Each part will be checked for parity bit, if generated parity is zero then code is error free and if one then the received code is considered to be the erroneous. By orthogonal code method we can detect the part of the incoming or received system data that is containing the errors and along with the correction of code we can also improve trans-reception system by using effective means to reduce the error in that particular area and over all reception system will become more effective.

TABLE II
Orthogonal Codes and the Corresponding Detection rate.

Code length (<i>n</i>)	Detection Rate (%)
8	93.57
16	99.95
32	99.99
64	100.00

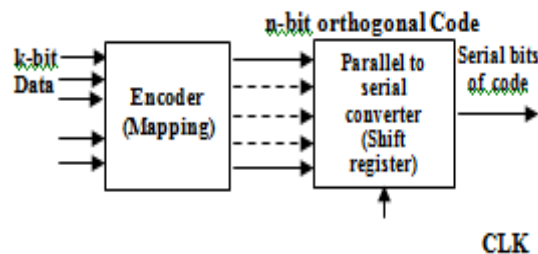


Fig.3 Block diagram of 5-bit transmitter

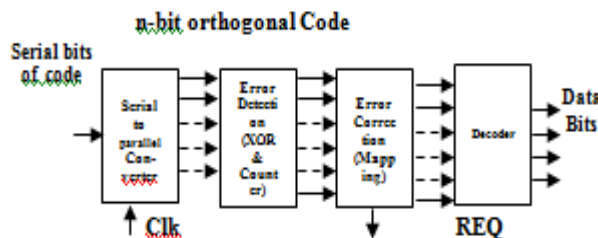


Fig.4. Block Diagram of Receiver

3.1 Transmitter

The Transmitter consists of two blocks (a) encoder (b) shift register

- (a) The encoder encodes a k-bit data set to $n=2^{k-1}$ bits of the orthogonal code.
- (b) The Shift Register transforms this code to a serial data in order to be transmitted as shown in Fig.3.

For example, 5-bit data is encoded to 16-bit (2^4) orthogonal code according to the lookup table shown in Fig.2. The generated orthogonal code is then transmitted serially using a shift register with the rising edge of the clock.

3.2 Receiver

The received code is processed through the sequential steps, as shown in Fig.4. The incoming serial bits are converted into n-bit parallel codes. The received code is compared with all the codes in the lookup table for error detection. This is done by counting the number of ones in the signal resulting from 'XOR' operation between the received code and each combination of the orthogonal codes in the lookup table. A bit signal and also searches for the minimum count. However a value rather than zero shows an error in the received code. The orthogonal code in the lookup table which is associated with the minimum count is the closest match for the corrupted received code. The matched orthogonal code in the lookup table is the corrected code, which is then decoded to k-bit data. The receiver is able to correct up to $(n/4-1)$ bits in the received impaired code. However, if the minimum count is associated with more than one combination of orthogonal code then a signal, REQ, goes high

IV. IMPLEMENTATION AND RESULTS

A Spartan-3 hardware board and ISE. Xilinx software has been used for code testing. The simulation has been performed using modelSim XE software. The Simulation Result were verified for most of the combination 16-bit Orthogonal Code, ISE Xilinx Software have use for synthetics.

The detection rate for k block of n-bit code is

$$(2^n - 2^k)/2^n\%$$

This gives for 8-bit detection

$$\frac{2^8 - 2^4}{2^8} \times 100 \qquad \frac{128 - 8}{128} \times 100 = 93.75$$

This gives for 16-bit detection

$$\frac{2^{16} - 2^5}{2^{16}} \times 100 \qquad \frac{65536 - 32}{65536} \times 100 = 99.95$$

This gives for 32-bit detection

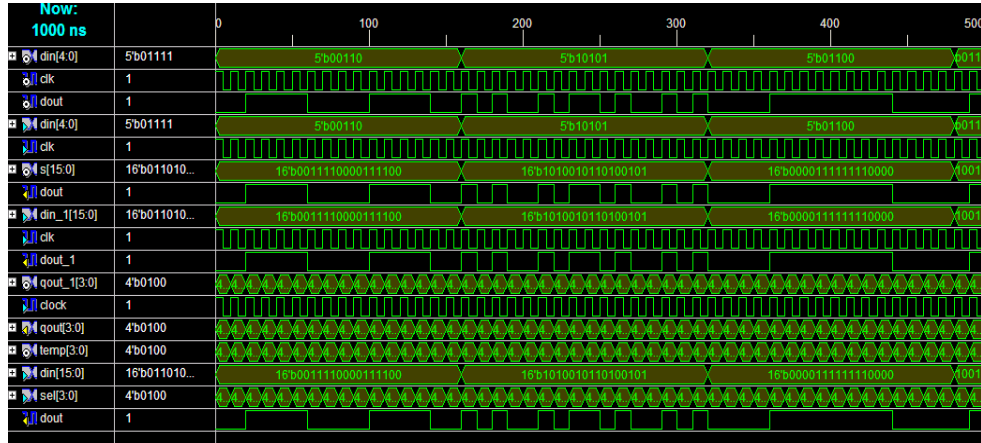
$$\frac{2^{32} - 2^6}{2^{32}} \times 100 \qquad \frac{4294967296 - 64}{4294967296} \times 100 = 99.99$$

This gives for 64-bit detection

$$\frac{2^{64} - 2^7}{2^{64}} \times 100 \qquad \frac{1.84 \times 10^{19} - 128}{1.84 \times 10^{19}} \times 100 \\ = 1 \times 100 = 100$$

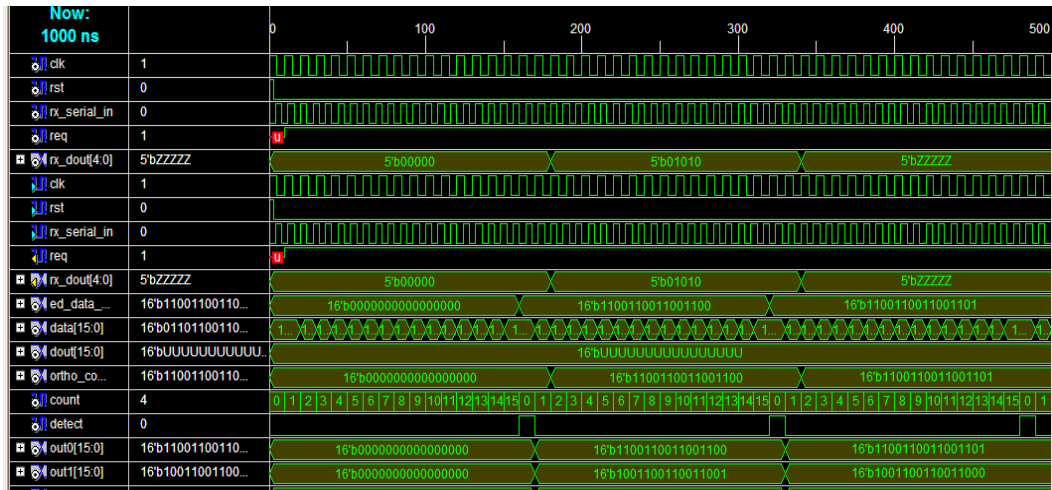
4.1 Transmitter

Fig. 5 shows an example of the results of the transmitter simulation corresponding to the input data value 00010 labelled as 'data'. This data has been encoded to the associated orthogonal code "0110011001100110" labelled 'ortho'. The signal 'EN' is used to enable the transmission of the serial bits 'txcode' of the orthogonal code with every rising edge of the clock.



4.2 Receiver

Upon reception, the incoming serial data is converted into 16-bit parallel code ‘rxcode’. Counter is used to count the number of 1st after XOR operation between the received code and all combinations of orthogonal code in the lookup table. Fig.6, the received code is rxcode=“0110011001100110”, count=’0’ and hence the received code is not corrupted. The code is then decoded to the corresponding final data 00010.



The results of the simulation show that for a k-bit data, the corresponding n-bit orthogonal code is able to detect any faulty combination other than the combinations of orthogonal code in the lookup table.

TABLE III

Correction Capabilities Between Orthogonal Codes Convolution

Codes length (Bit)	Techniques OCC
8	1
16	3
32	7
64	15
N	(n/4-1)

V. CONCLUSION

FPGA implementation of orthogonal code convolution is presented to ensure the efficient digital communication. This work involved the implementation of the transmitter and receiver using VHDL to detect and correct the errors. A fully synthesizable HDL code was written to ensure that the design was feasible. This orthogonal code implementation has improved the error detection up to 99.9% for 16-bit coding. It is noted that with this method, the transmitter does not have to send the parity bit since the parity bit is known to be always zero. Therefore, if there is a transmission error, the receiver will be able to detect it by generating a parity bit at the receiving end. Finally, this work has the future scope of further improvement in orthogonal coding for large digital data processing.

REFERENCES

- [1] N. Kaabouch, A. Dhirde, and S. Faruque, "Improvement of the Orthogonal Code Convolution Capabilities using FPGA Implementation", IEEE Electro/Information Technology Proceedings. Pp. 380-384, 2007.
- [2] S. Faruque, N. Kaabouch, and A. Dhirde, "Forward error control coding based on orthogonal code and its implementation using FPGA" Wireless and Optical Communication Proceedings, PP 565-630, ACTA Press, June 2007.
- [3] U. K. Kumar, and B. S. Umashankar, "Improved hamming code for error detection and correction", 2007 2nd International Symposium on Wireless Pervasive Computing, pp. 498-500.
- [4] Z. Cai, J. Hao, S. Sun, and F. P. Chin, "A high-speed reed-solomon decoder for correction of both errors and erasures", 2006 IEEE International Symposium on Circuits and Systems, pp. 281-284.
- [5] S. Faruque, "Error Control Coding based on Orthogonal Codes", Wireless Proceedings, Vol. 2, pp. 608-615, 2004.
- [6] S. Shukla, N.W. Bergmann, "Single bit error correction implementation in CRC-16 on FPGA", in Conf. Rec. 2004 IEEE Int. Conf. on Field-Programmable Technology, pp. 319-322.
- [7] T. Baicheva, S. Dodunekov, and P. Kazakov, "Undetected error probability performance of cyclic redundancy-check codes of 16-bit redundancy", IEEE Proceedings. Communications, Vol. 147, No. 5, pp. 253-256, Oct. 2000.
- [8] A. Hokanin, H. Delic, and S. Sarin, "Two dimensional CRC for efficient transmission of ATM Cells over CDMA", IEEE Communications Letters, Vol. 4, No. 4, pp. 131-133, April 2000.
- [9] V. Stylianakis, S. Toptchiyski, "A Reed - Solomon coding/decoding structure for an ADS modem", in Conf. Rec. 1999 IEEE Int. Conf. on Electronics, Circuits and Systems, pp. 473 - 476.

Improving Features of Media Player

¹Mr. Juned A. Khan , ²Prof . V. S. Gulhane
^{1,2}M.E.(CSE)⁴th Sem SIPNA College Of Engineering, Amravati.

Abstract

Media Player Are One Of The Most Used And Important Software Application In Today's World. Maximum Computer Users Switch On To The Media Player As Soon As They Start The Computers And Then Move To Their Respective Woks. Today's Era Is To Do Work With High Efficiency But At The Same Time It Should Consume Very Less Time. And Thus Answer To The Problems Arising In The Use Of Traditional Media Players And The Lack Of Features In Proposed Media Players Is "Versatile Media Player" Versatile Media Player Is A Unique Player Developed To Fulfill Maximum Requirements Of User Regarding Audio And Video Songs. This Player Gives Numerous Facilities Which Differentiate It From The Conventional Media Players. The Various Features Included In The Versatile Media Player Are Shut-Down Facility, Alarm Facility, Lyrics Display, Splitting Windows, Access To More Than One Media File Simultaneously

I. INTRODUCTION

Media player have grabbed huge attention over a past decade and attracted majority of computer users thus making the users addicted to videos and music. Over the last decade, human computer interaction has become an active research area, which releases people from inactive, inflexible communication with machine [1]. Maximum computer users switch on to the media player as soon as they start the computers and then move to their respective woks. Also, many have a habit of dragging the songs into the list pane of media player, tune into music and then work. So we know how much are the media player used and required . Interacting with computers intelligently makes a significant contribution to the future application of human computer interaction [1]. Today's era is to do work with high efficiency but at the same time it should consume very less time. And thus answer to the problems arising in the use of traditional media players and the lack of features in available media players is the designing and development of the Versatile Media Player. In this paper we aim to develop a Versatile Media Player which will fulfill maximum requirements of user regarding audio and videos. This player gives numerous facilities which differentiate it from the conventional media players. The various features included in the Versatile Media Player are Shut-down facility, Alarm facility, Lyrics display, Splitting windows, Access to more than one media file simultaneously. Thus we can say Versatile Media Player is a fully loaded media player and a better option over the traditional media players. Versatile Media Player is a good and dynamic option for music lovers, computer users and all those people who are dynamic and love changes.

II. LITERATURE REVIEW AND RELATED WORK

There are various media player available in this world developed and manufactured by various other companies. The variety of players provide user with the plenty of features and characteristics. As it goes the saying that you cannot have happiness without sorrows, applies here. Every player has a drawback which pulls it back from the race. The pros and cons of the various media players are given in details here. And to overcome these problems we are devising the versatile media player.

A. Windows Media Player

Windows Media Player (abbreviated WMP)[10] is a media player and media library application developed by Microsoft that is used for playing audio, video and viewing images on personal computers running the Microsoft Windows operating system, as well as on pocket PC and Windows Mobile-based devices. Editions of Windows Media Player were also released for Mac OS, Mac OS X and Solaris but development of these has since been discontinued. The various advantages[13] WMP are Customizable appearance, Good compatibility with several different MP3 devices, Easy enough to track down album artwork, automatically detects which codecs are required to play certain types of video files. The various limitations[13] of WMP are Menus and program themselves require a bit of a learning curve, Does not always determine which codecs are needed should they be lacking in order to play a video file properly, Doesn't sync with the iPod, nor does it support Podcasts, Has a long way to go before it catches up with the features and usability of iTunes.

B. Flash

Flash[9] is another media player available in the market. In moderation and used for specific purposes such as delivering video content is good and most computers come off the line with the latest "Flash Player" installed. Flash is installed in some form on roughly 95% of all computers. Just beware not to make too much of the site out of flash. It simply isn't an efficient way of delivering content especially if that content changes often. Never ever use flash for the navigation of a site.

C. Winamp

Winamp[12] appeared to be more user friendly among the media players. The various advantages[13] of Winamp are Customizable appearance by downloading (designing for yourself) different skins, easy enough to use, access to several online radio stations, such as XM radio, Sufficient video playback. There are some limitations[13] of Winamp and they are flimsy design; poor organization of different windows, audio controls, etc, Could use better access to online stores, Free version only allows 2x burning and ripping, Pro needed in order to encode MP3s, WMAs, etc

D. RealPlayer

Some advantages[13,11] of Real Player are Has made significant strides to create a far more usable product, 5.1 surround sound playback for DVDs, Cleaner, more organized menus allow for users to effectively build up a video playlist, Those who are familiar with iTunes will navigate through RealPlayer's menus with relative ease. Apart from the advantages there are some limitations[13] also and they are as Extra features such as burning DVDs requires purchasing RealPlayer Plus, Difficult to find the Basic player on the website; download links automatically take you to the Plus player, May be too little, too late for Real Player? Poor, buggy programming has left this company with a bad reputation in the past

E. Adobe Media Player

In the list of frequently used media player one more name is Adobe Media Player[8]. The various advantages[13] of Adobe Media Player are its Clean design, Access to different streaming content. Some limitations of Adobe Media Player are that it runs on Flash, so expect to do more downloading if you don't have it installed already (which isn't unlikely), Loading streaming video can be very sluggish, Expect to see plenty of advertisements while using this player, Managing video downloads is frustrating, Could use a better variety of content, but more will certainly be added in the future, When downloading, it doesn't give the status of how the download is coming along.

F. VLC Media Player

VLC Media Player[7] is the most popular media player. It's the most frequently used media player due to some of its incomparable features like it is Open source, which allows for endless customization, It is Powerful tool, fully featured for free, It plays a variety of media, including OGG, MP3, WMA, AVI, MPEG, etc But It is also having some limitations such as Its appearance needs a bit of tweaking, Skin selection could be better, For Preference changes to be made to the program, it must be restarted, Playlist is limited and buggy, something which will hopefully be fixed in later versions, No sync support Apart from the limitations enlisted above, the common disadvantage of all the players is that they cannot play multiple files at a single time. Also other players do not have the facilities like player shut down, system shut down, timer, alarm, splitting windows and sliding screen. Considering all these demerits of various players we are trying to incorporate the facilities in our player which will overcome these demerits and thus will prove really versatile. The facility of shut down will help the user to automatically shut down the player as well as system. The user can set the timer and be relaxed as it will automatically get switched off. The splitting window will enable the user to watch the different videos at the same time. Sliding screen is the function inserted in the designing of this player to avail the user with showing of desired file at central position.

III. ANALYSIS OF PROBLEM

The media player is an important application in the time of modern world. Every user either it may be a naïve to computer or even a computer expert is highly inclined to the use of the media player. But every different media player has different feature. All the features are not found to be available at one place in one media player. Some media players are found to be efficient in playing different file formats. Some are having 'Timer' enabled in them and other are having 'shut down facility' with it. But no such application is there which is having all the features embedded in it. Today's era is to do work with high efficiency but at the same time it should consume very less time. So in order to resolve this problem one such application is needed which integrates the features of all the previous applications along with the successful implementation of all the features. Such development will surely improve the efficiency and consume less time as was required with the previous applications.

Thus the particular project of designing and development of the Versatile Media Player is undertaken in order to resolve the problem which is being faced as explained above.

IV. PROPOSED WORK AND OBJECTIVES

A. Main objectives of project

The various facilities and features have been planned to be incorporated in the Versatile Media Player to differentiate it from traditional media players. We will attempt to attain some of the following listed issues related to versatile media player.

- [1] Splitting Windows: This feature is used to split the windows of player according to the requirement. We can split the windows of media player into as many as parts as we require.
- [2] Sliding Screen: This feature is used to show the desired file at central positions.
- [3] Switching: This feature provides us the facility to switch between two or more than two songs simultaneously at regular interval of time given by the user.
- [4] Playlist: To store audio or video files for further processes.
- [5] Lyrics: This player displays the lyrics for audio or video files and shows that onto the bottom part of the media player.
- [6] Play Maximum format: It is capable to play any format of audio or video files.
- [7] Login screen: It also provide a high-tech login screen for security purpose.
- [8] Feedback: This is the part of back-end which stores a feedback given by user for further modification.
- [9] Virtual DJ: For better sound facility[2].
- [10] Cheat Code Section : To modify the content of media player if any problem persists at run time (this is for admin use only)
- [11] Shut Down: It provides the facility through which we can shut down our system at stimulated time maintained by the user.
- [12] Alarm: It provides the facility to listen a song st particular time maintained by the user.

V. PROJECT ARCHITECTURE

Architecture provides a basic idea about a particular concept. In the same way this section “Project Architecture” describes a blueprint of conceptual framework of the project undertaken. The tentative ideas related with the project and its working are specified here. We have divided our project “Versatile Media Player” into number of modules. The modules are:

A. Login Screen

For authentication purpose we can use this feature of our project. Through this login you can change your password too. The password is stored in database and when you change your password the current password comes into existence. The default user name would be “scott” and password would be “tiger” that is stored in database. If user wants to change the password then they could use “change password” option of login screen . If they click on “change password” button then another window appears onto screen. When you enter the old password then another screen or form will be appearing to confirm the new one. When the new password will be confirmed then the new password is set in the place of old one.

B. Welcome Screen

The Welcome Screen is the main window or form of this project through which we can use all the features of this player. Through this window we can watch up to 15 videos at the same time and listen the audio of any screen as per our requirement.

C. Multiple Screen

Through this screen you can maximize any screen by double clicking on the required screen. The screen is transparent enough so that the desktop of your screen is clearly visible.

D. Splitting Window

This feature plays a vital role in this player. Through this user can split the screen into number of parts as per their requirements.

E. Sliding Screen

This feature is used to show the desired screen at central position by just a single click.

F. Shut Down

This feature of media player provides the facility through which we can shut down the system at specified time maintained by the user.

G. Alarm

It provides the facility to listen the song at particular time maintained by the user.

H. Feedback Section

This is part of Back End which store feedback given by the user for further modification. For editing feedback there is one admin feedback screen.

The Data Flow Diagram of this project is shown below for better understanding of the topic.

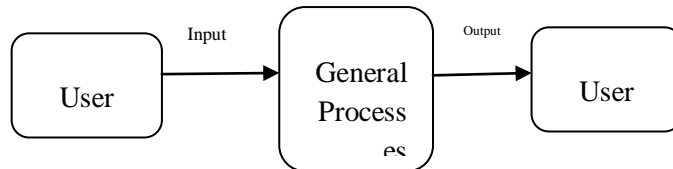


Fig. 1. General DFD

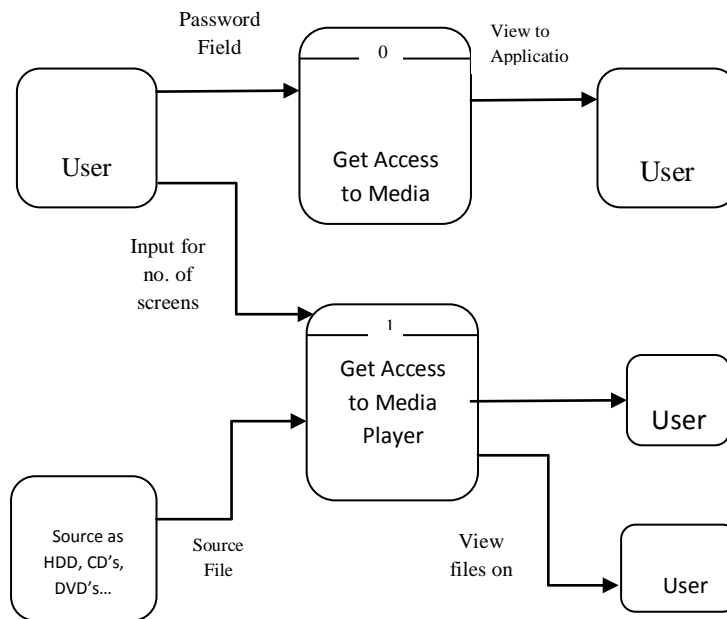


Fig. 2. Project DFD

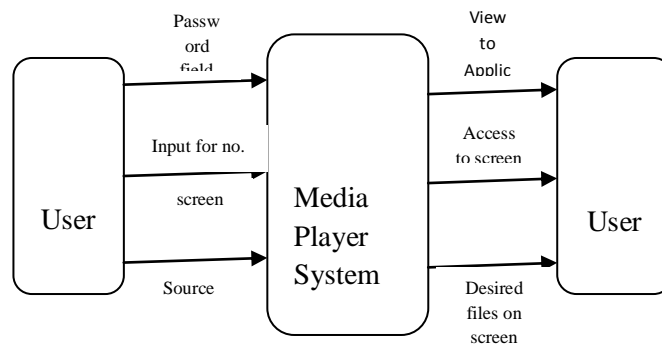


Figure. 3. Context level diagram for Media Player

VI. CONCLUSION AND FUTURE WORK

Our effort is to obtain efficiency with the consumption of less time also, by using this player users save their time. By using this media player we can access number of media files at the same time. This application provides the GUI interface and reduces the access time. This project “Versatile Media Player” has been designed as per required specification of user. A worth analysis of designing principle has been followed in the development of this project. In the near future some new and enhanced features will be added to the above mentioned media player such as Speech to text conversion will be implemented, File format converter will be added to it, Video encryption will also be implemented.

REFERENCES

- [1]. Wang Ruihu, Bi Hongwei, Liu Jiachen, Wu Lingguo, Fang Bin ,Interactive Intelligent Media Player Based on Head Motion Recognition, 2009 Second International Symposium on Electronic Commerce and Security.
- [2]. Michael Westermann, digitalklang sonification services, Interactive Sound Player (ISP): Enabling interactive sound in Digital Media Proceedings of the Third International Conference WEB Delivering of Music (WEDELMUSIC'03) 0-7695-1935-0/03 \$17.00 © 2003 IEEE.
- [3]. Hinckley, K.J., Sinclair, M.P., and Horvitz E., Sensing techniques for mobile interaction. ACM Symposium on User Interface Software and Technology. p91 – 100. 2000.
- [4]. Korde, K., Jondhale K. C., Hand Gesture Recognition System Using Standard Fuzzy C-Means Algorithm for Recognizing Hand Gesture with Angle Variations for Unsupervised Users. Emerging Trends in Engineering and Technology, International Conference. p681-685. 2008.
- [5]. Miners, B.W. Basir, O.A. Kamel, M.S., Understanding Hand Gestures Using Approximate Graph Matching. IEEE Volume35 Issue 2. p239- 248. 2005 90.
- [6]. Strachan, S. and Murray-Smith, R. and O'Modhrain, S. BodySpace: inferring body pose for natural control of a music player. 2003.
- [7]. <http://vlc-media.wikidot.com/>
- [8]. <http://www.adobe.com/products/mediaplayer/>
- [9]. <http://www.adobe.com/software/flash/about/>
- [10]. <http://windows.microsoft.com/en-IN/windows/windows-media>
- [11]. <http://in.real.com/>
- [12]. <http://www.winamp.com/>
- [13]. http://www.ehow.com/about_5379113_types-media-players.html

Analysis Of Metal Cutting Tools Reliability During Processing By Turning In Laboratory Conditions And Exploitation

Roshan Patel¹, Urvish Patel²

^{1,2} Dept. of Mechanical Engg., Bhagwant University, Ajmer, India,

Abstract:

In this paper the possible differences in reliability of the metal cutting tools during in vitro (in laboratory) processing and exploitation conditions has been analyzed. The estimation of reliability of metal cutting tools in volume productions is done on the bases of monitoring failure rates of metal cutting tools in a long period of time in order to obtain a large number of samples possible. Investigations have been realized in theoretical and experimental ways, hereby to get approximately data about failure occurrence of the instrument while metal cutting process from the aspect of consumption, crack and fracture. In laboratory conditions research as the criteria for determining of reliability the flank wear width consumption of instrument is used, while during the research on exploitation conditions the technological criteria of consumption method is explored.

Keywords: cutting, tool, reliability, failure, consumption, turning, laboratory, exploitation.

I. INTRODUCTION

The reliability of the metal cutting tools is a relatively new scientific field. This field includes study, analysis and development of the cutting edge characteristics in the definite conditions and time interval of exploitation that will not change the used parameters of the allowed limits. The aim of the paper is to research, identify and analysis the factors which bring to the failure of the instrument during the cutting process. If we are limited on the investigation of the reliability of the metal cutting tools, within the processing system one can conclude that its depend the several factors and presents very complex phenomena because the tool could fail during the work. These failures mostly happen cause of consumption, crack and fracture of the cutting instrument. The cutting process characterized by; material of working piece, the material of instrument and the conditions of the realized processing (cutting regime, geometry of instrument, cooling equipment and lubricators and the dynamic state of system: machine–instrument–equipment–working piece). The current researches indicate that the probability functions of the cutting instruments failure will relied on the We bulls disperse.

$$F(t) = 1 - \exp[-(t/\eta_0)^\beta] \quad (1)$$

The reliability is the compliment of the probability;

$$R(t) = 1 - F(t) = \exp[-(t/\eta_0)^\beta] \quad (2)$$

Frequency of failures is defined as follows:

$$f(t) = dR(t)/dt \quad (3)$$

The intensity of failures:

Investigations have been realized in theoretical and experimental ways, hereby to get approximately data about failure occurrence of the instrument while metal cutting process from the aspect of consumption, crack and fracture. The problem that has been considered in this paper was the determination of reliability of the metal cutting tool at small and medium series by applying the medium rank method.

Table 1 Measured values of instrument consumption

	Order of measurements						
	No.	1	2	3	4	5	6
	T[s]	60	180	300	420	600	900
SCM 105	H[mm]						
	1	0,16	0,24	0,29	0,30	0,31	0,33
	2	0,12	0,20	0,26	0,27	0,29	0,30
	3	0,10	0,15	0,19	0,23	0,24	0,26
	4	0,11	0,18	0,21	0,24	0,26	0,28
	5	0,10	0,17	0,23	0,27	0,29	0,32
	6	0,80	0,15	0,20	0,23	0,25	0,28
Cutting plate							
	Order of measurements						
	No.	7	8	9	10	11	12
	T[s]	1200	1500	1800	2100	2520	2640
SCM 105	H[mm]						
	1	0,16	0,24	0,29	0,30	0,31	0,33
	2	0,12	0,20	0,26	0,27	0,29	0,30
	3	0,10	0,15	0,19	0,23	0,24	0,26
	4	0,11	0,18	0,21	0,24	0,26	0,28
	5	0,10	0,17	0,23	0,27	0,29	0,32
	6	0,80	0,15	0,20	0,23	0,25	0,28

Table 2 Resistance of the cutting plate edge

	Resistance of cutting plate T [s]	5%	MR%	95%
	SCM 105			
1	2570	0,9	10,9	39,3
2	2620	6,3	26,4	48,2
3	2650	15,3	42,1	72,9
4	2680	27,1	57,9	84,7
5	2700	41,8	73,6	93,7
6	2750	60,7	89,1	99,1

II. EXPERIMENTAL CONDITION

2.1. Laboratory Conditions

The reference material for work piece is rolled steel CM45 (according to ISO). The initial work piece diameter is 20.2 mm and the length is 360 mm. The experiments have been performed by using the similar processing parameters in volume productions of the piston of shock absorber. During the experiment there have been used the hard metal plates TNMGS04 10 FR according the ISO standard No.1832 the product from "Syntel"-Zagreb, of the quality SCM-105 (covered by three layers TiC-Al2O3-TiN on the hard metal base P25) . The plate is attached mechanically to the holder PSBNR2020K12 with the fastening system PROMAX-C. The testing has been realized on PA 22 machine Moran do.

2.2. Exploitation Conditions

The research has been realized on processing conditions of the piston, where the data for the technologic consumption, crack and fracture of the instrument failure are gathered. Data is gathered:

- verifying the number of processed pieces between two instrument substitution, 679
- The good pieces are identified measuring control dimensions (in every 5 pieces),
- The processing process is interrupted after identification of the first piece over the allowed tolerances after what the instrument is replaced,
- the work of the instrument is monitored visually estimating the reasons for replacement of the cutting plate; normal consumption of the edge, cracks or instrument fractures, The criteria for defining the effective duty of the instruments:
- The exactness of dimensions in the work part (it is realized through special control metering) serves as principal criteria,
- monitoring the edge (it is done in a visual way) and serves as preventive criteria,
- The form of the chip (monitoring in a visual way) and serves as preventive criteria,
- The conditions for monitoring the instruments are the same for all instruments,
- The examinations are done through regular technological process in conditions of exploitation. The change of instruments:

- The change of instruments is done one by one, in the moment of failure of any crack, fracture or consumption according to the criteria mentioned above,
- The sharpening is done in the tool room, for the cases of normal consumption or if the instrument is cracked or fractured,
- If the edge is broken the entire instrument should be changed, when there should be done the repair of the base handler,
- The machine paused during the sharpening of the instrument. The plan for executing the instrument:
- The monitoring of duty of instrument is realized according to the existing state and the existing technological process,
- The lowest number of the monitored samples between two cuttings is 36; the data of monitoring of the work of instruments are done in (Tab.1. During the experiment there have been used approximately the same hard metal plates of the quality SCM-105. The testing has been realized on automatic 6 axis machine Wickman.

III. EXPERIMENTAL RESULTS

3.1. Laboratory Conditions

In laboratory conditions research as the criteria for determining of reliability the flank wear width consumption of instrument is used ($VB=0.30$ mm). The recovered data from the sustained average lifetime of the cutting edge between two changed instruments, from the monitored samples according to the experimental conditions, ordered in 6 value groups, medial rank and the reliability limit of exactness $\alpha z = 0.05$ (5% and 95% respectively), are shown in (Tab. 2). The graphical presentation of Waybill functions according to the results based on the graphic -analytical calculations are shown in (Fig.1.).

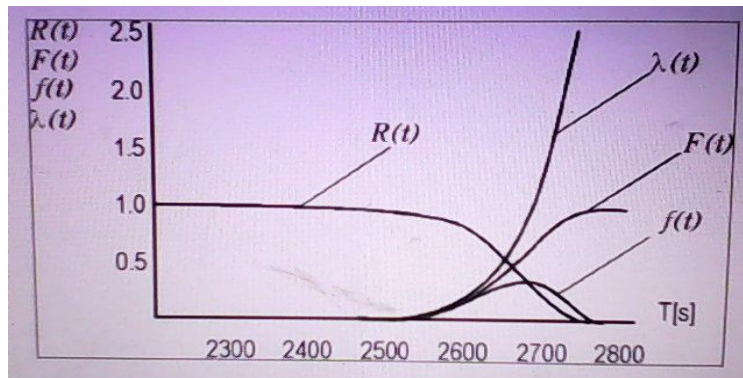


Figure 1 Graphical presentation of Weibull's functions

3.2. Exploitation Conditions

The recovered data from the sustained average lifetime of the cutting edge between two changed instruments, from the monitored samples according to the experimental conditions, ordered in 9 value groups, medial rank and the reliability limit of exactness $\alpha z = 0.05$ (5% and 95% respectively), are shown in (Tab.1). The graphical presentation of Weibull functions according to the results based of the graphic -analytical calculations is shown in (Fig. 2).

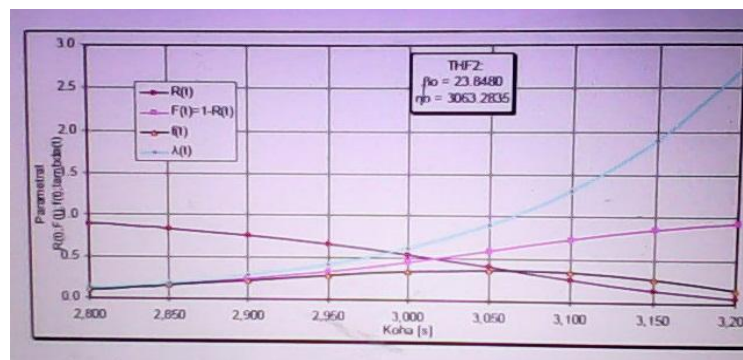


Figure 2 Graphical presentation of Weibull's function

IV. CONCLUSION

According to the theoretical researches and experiments carried earlier and the analysis based on diagram in fig.1, can be concluded that the reliability of cutting tool during the work under exploitation conditions is 10-15% higher comparing to laboratory/vitro conditions. This difference is supposed to be for these reasons:

- During the work in laboratory conditions the expedients for cooling and lubrication are not used;
 - The working period of cutting blade has been longer for several hundred of seconds, compared to the exploitation conditions of tens of seconds, so the cutting blade has been overloaded in terms of temperature;
 - Cutting chips, during labor in vitro conditions have been longer influencing the durability of cutting blade;
- The working machine under exploitation conditions has been newer and had smooth work.

REFERENCES

- [1] Sekulic S. Odredjivanje ouzdanosti reznog alata skracenim postupkom, Zbornik radova XVIII. Savjetovanje proizvodnog masinstva Jugoslavije, Budva, 1983.
- [2] Daiic P. Determination of reliability of ceramic cutting tools on the basis of comparative analysis of different functions distribution, International Journal of Quality & Reliability Management, Vol. 18 Iss: 4, pp.431 – 443, 2001.
- [3] Z. Klim, E. Ennajimi, M. Balazinski and C. Fortin, Cutting tool reliability analysis for variable feed milling of 17-4PH stainless steel, *Wear, Volume 195, Issues 1-2, July 1996, Pages 206-213*, Science direct.com.
- [4] Qehaja, N. Zavistnost reznih alata i produktivnosti rada u procesu eksploatacije, magistarski rad, FSB Zagreb, 1989.
- [5] Qehaja N. "The reliability of the metal cutting tools on the bases on method of consumption", The 13th International DAAAM Symposium, Vienna, 2002.

Numerical Statistic Approach for Expert System in Rainfall Prediction Based On Data Series

Indrabayu¹, Nadjamuddin Harun², M. Saleh Pallu³, Andani Achmad⁴

¹ Student of Doctoral Program Civil Engineering Hasanuddin University, Makassar Indonesia

^{1,2,4} Department of Electrical Engineering, Hasanuddin University, Makassar, Indonesia

³ Department of Civil Engineering, Hasanuddin University, Makassar, Indonesia

Abstract

The potential of statistical approach in predicting rain fall is discussed in this paper. Two most implemented methods i.e. Auto-Regressive Integrated Moving Average (ARIMA) and Adaptive Splines Threshold Autoregressive (ASTAR) are compared in term of accuracy in prediction. Both methods are constructed to predict daily rainfall in the area of Makassar, Indonesia. Rain problem in Indonesia increasingly complex due to climate shifts that result in high intensity rainfall in the dry season so it is very influential on the development of many aspect of social-economy sector. A ten years daily data (2001-2010) obtained from BMKG (the Meteorology, Climatology and Geophysics). Several complementary data is also obtained from LAPAN (Government Space Agent). From various meteorological variables, four variables are selected for predicting rainfall- There are temperature, humidity, wind speed, and previous precipitation based on their high correlation to rain event.. These four variables are then input to the ARIMA and ASTAR. The accuracy of prediction is measured based on root mean square error (RMSE). ASTAR outperformed ARIMA with less RMSE which is 0.02 to 0.24.

Keywords: ARIMA, ASTAR, Expert System, Rain Prediction,

I. INTRODUCTION

Indonesia is a tropical country which has a high rainfall intensity. Rainfall is a stochastic process, which upcoming event depends on some other meteorology precursors. Many research have revealed these meteorology precursors especially those region affected by monsoonal. [1,2,3,4]. These precursors are sea surface temperature, land surface temperature, relative humidity, winds, geo potential height, and the surface pressure. A common methodology used in predicting daily rainfall intensity is harvesting abundant of previous daily rainfall data [5,6]. A statistical method is worth trying method for rain fall forecasting. This is due to the fact that statistical method can harvesting abundant of data and transform it into a simple line outlook i.e. auto regressive, moving average, and several other forms. A research has conducted in modelling ARIMA to forecast daily power consumption [7]. Though data forecast is highly deterministic but very complex since inflation rate is influenced by many parameters. Preliminary research on Daily Rainfall prediction has been conducted for Makassar which shows a promising results [8,9]. In this paper, ARIMA and ASTAR are compared in term of special advantage in dealing stochastic data, in this case rainfall data, and future development for better predicting result. The paper is outline into 5 parts, i.e. (1) Introduction, (2)ARIMA modelling, (3) ASTAR Modelling, (4) Results and Discussion, and (5) Conclusions.

II. ARIMA MODELLING

ARIMA is used to predict a value in a response time series as a linear combination of its own past values, past errors, and current and past values of other time series. The ARIMA procedure provides a comprehensive set of tools for uni-variate time series model identification, parameter estimation, and forecasting, and it offers great flexibility in the kinds of ARIMA or ARIMA X models that can be analyzed. The ARIMA procedure supports seasonal, subset, and factored ARIMA models;; multiple regression analysis with ARMA errors; and rational transfer function models of any complexity. In general, the ARIMA procedure can be subtle as follows [8]:

- Step 0) A class of models is formulated assuming certain hypotheses.
- Step 1) A model is identified for the observed data.
- Step 2) The model parameters are estimated.
- Step 3) If the hypotheses of the model are validated, go to Step 4, otherwise go to Step 1 to refine the model.
- Step 4) The model is ready for forecasting.

A. Step 0

In this step, a general ARIMA formulation is selected to model the rain fall data. This selection is carried out by careful inspection and selection of the main characteristics of the daily rain fall and other meteorological data. The corresponding data are: humidity, air pressure, surface land temperature and wind velocity (corresponding to daily respectively), among others.

B. Step 1

A trial model must be identified for the rain fall data. First, in order to make the underlying process stationary (a more homogeneous mean and variance), a transformation of the original rain fall data and the inclusion of factors of the form may be necessary. In this step, the checking process can be done using Autocorrelation function (ACF) or unit root test. A further check for lag residual and lag dependent tested from partial ACF.

C. Step 2

After the functions of the model have been specified, the parameters of these functions must be estimated. Good estimators of the parameters can be computed by assuming the data are observations of a stationary time series (Step 1). If a Moving Average (MA) pattern is identified then further optimization process needed by using maximum likelihood or least square estimation. A conditional likelihood function is selected in order to get a good starting point to obtain an exact likelihood function. Also, an option to detect and adjust possible unusual observations is selected. As these events are not initially known, a procedure that detects and minimizes the effect of the outliers is necessary. With this adjustment, a better understanding of the series, a better modeling and estimation, and, finally, a better forecasting performance is achieved.

D. Step 3

In this step, a diagnosis check is used to validate the model assumptions of Step 0. This diagnosis checks if the hypotheses made on the residuals (actual prices minus fitted prices, as estimated in Step 1) are true. Residuals must satisfy the requirements of a white noise process: zero mean, constant variance, uncorrelated process and normal distribution. These requirements can be checked by taking tests for randomness, such as the autocorrelation and partial autocorrelation plots. If the hypotheses on the residuals are validated by tests and plots, then, the model can be used to forecast prices. Otherwise, the residuals contain a certain structure that should be studied to refine the model in Step 1.

E. Step 4

In Step 4, the model from Step 2 can be used to predict future values of daily rainfall data. Due to this requirement, difficulties may arise because predictions can be less certain as the forecast lead time becomes larger. Based on the natural of data, time series forecasting is suit to short term forecasting (hourly or daily). For a long term period, a structural forecaster is more comply for the situation. The flowchart of corresponding steps above can be seen in Figure 1. Several historical daily data is collected from BMKG Makassar over 10 years periods (2001 -2010).

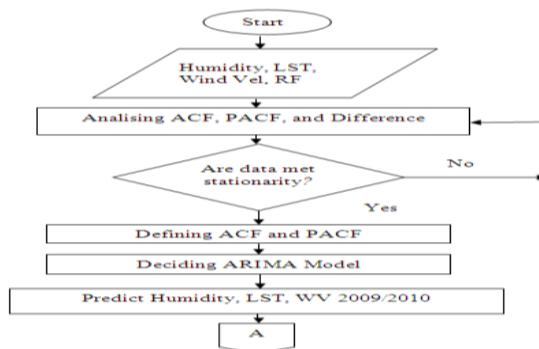


Figure 1. ARIMA process

2.1. DOUBLE REGRESSION

Double regression as part of multivariate analysis aiming on revealing the substantial relationship between two variable. A dependent variable Y is influenced by subsequent independent variable X. General view of process is shown in Figure 2.

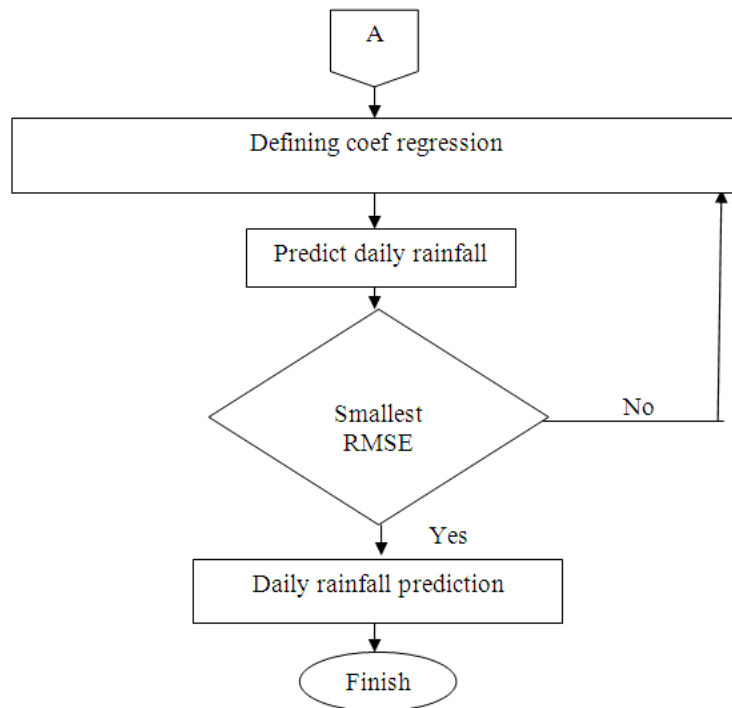


Figure 2. Double Regression Steps

The coefficient of independent variable Y (rain fall) and subsequent dependent variables Xn are formulated as follows:

$$Y = \beta_0 + \beta_1X_1 + \beta_2X_2 + \beta_3X_3... + \beta_nX_n \quad (1)$$

- Y : Dependent/response Variable
- X1 : Independence parameter 1
- X2 : Independence parameter 2
- Xn : Independence parameter n
- β : Regression Coefficient

III. ASTAR Modelling

In modelling ASTAR several software are used and integrated to process the ASTAR result, I.e. Microsoft Excel, SPSS 16 and MARS 2.0 are the software for ASTAR planning system. Rain fall forecasting, as response variable (Y), Input variable, as predictor variable (X), is wind speed, humidity and temperature with X1, X2, and X3 respectively. All of predictor variables are applied to attain the best model of rain fall forecasting. The significant variable, influenced the next day condition with importance variable, is processed using MARS 2.0 Software.

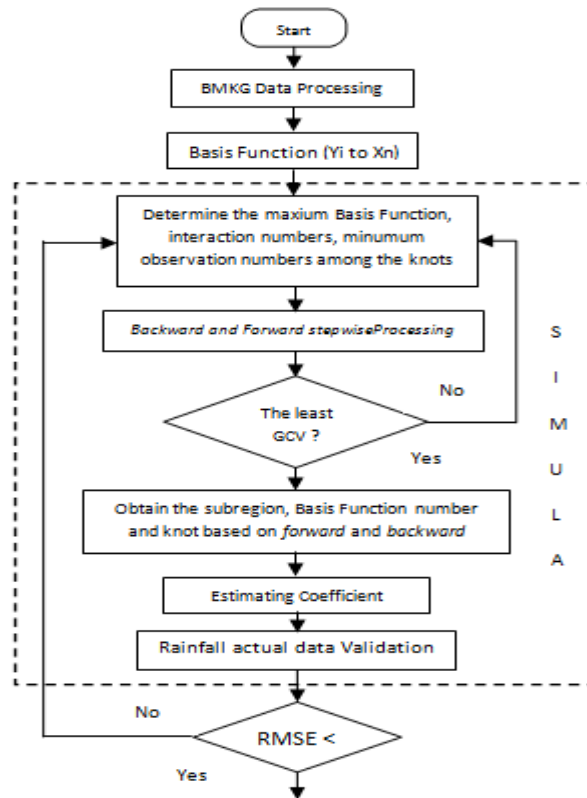


Figure 3. Flowchart of ASTAR Methodology

Fuction Base

A Basis Function is distance between sequence knots. In ASTAR, Basis Function is a set of function to describe information that consist of one or two variables.

$\text{Max}(0, x - t)$ or $\text{Min}(0, t - x)$ is Basis Function value with t as a value to illustrate knot position and x as predictor variable. Every 1 knot will produce a couple of Basis Function.

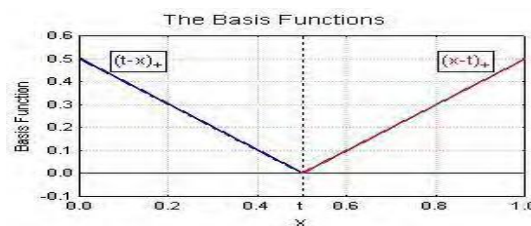


Figure 4. Basis Function

ASTAR Methods as data analysis technique to find the best model from a set of data. It is using past and present data to predict the short-term forecasting.

Modelling Stage of ASTAR

- [1] Determine maximum Basis Function, maximum interaction numbers and minimum observation numbers between knots.
- [2] Forward Stepwise Processing to obtain maximum number of Basis Function using MARS 2.0
- [3] Backward Stepwise Processing to obtain Basis Function numbers from forward stepwise by minimizing the least GCV (Generalized Cross Validation) value.
- [4] Knots selection using forward and backward algorithm.
- [5] Estimating the coefficient of chosen Basis Function as a stage of response variable (Y) prediction (Y) to predictor variable (X).

Linearity on predictor variables is modelling main problem. One of MARS strategy to solve this problem, is reducing the modelling variable, thus it will diminish fake interaction due to its colinearity and will produce more stable forecasting. Variable declining could be completed by adding fine value in lack of-fit of knot selection. It is using forward algorithm. Model verification is applying RMSE (Root Mean Square Error) and MAE (Mean Absolut Error). This research is using RMSE to compare the accuracy of rain fall forecasting with observation data.

RMSE formula is shown bellow :

$$RMSE = \frac{\sqrt{\frac{1}{N} \sum_{t=h}^N (y_t - \hat{y}_t)^2}}{y \text{ max} - y \text{ min}} \quad (2)$$

- Where, y_i = Observation value
- \hat{y}_i = Forecasting value
- n = Observation number
- y_{maks} = maksimum observation data
- y_{min} = minimum observation data

IV. RESULTS AND DISCUSSION

4.1. ARIMA

Stationary condition is checked for each variable. If variable does not meet the term, differencing process commencing. Figure 3 shows ACF of humidity from 2001-2008.

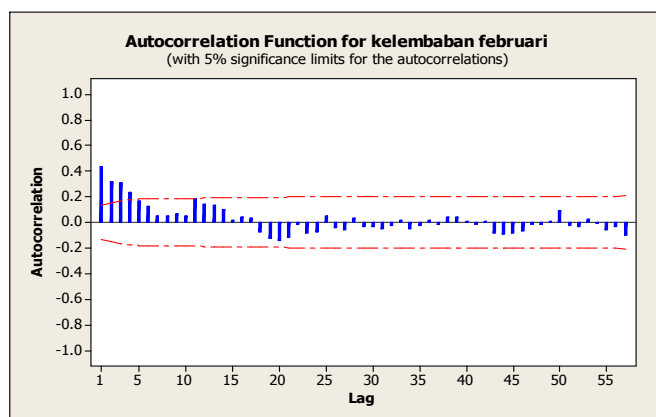


Figure 5. ACF of Humidity 2001-2008

The figures describe following terms:

- [1] Time Lag 1-4 gain significance since out of range $-0.130377 < r_k < 0.130377$.
- [2] The ACF for humidity shows a not-stationary condition, hence differencing is needed.

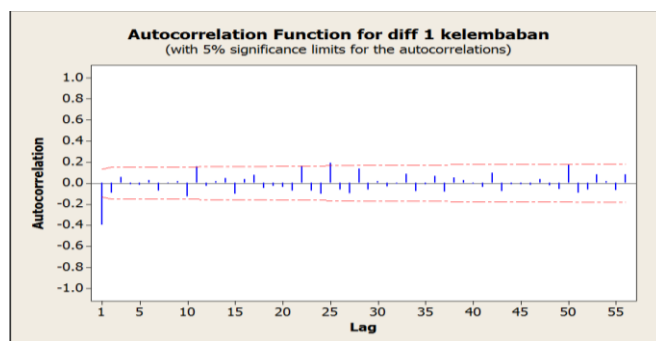


Figure 6. ACF Diff 1 of Humidity 2001-2008

Output of ACF diff 1 concluded points are:

[1] Time Lag 1,11, 25 gain significance since out of range $-0.130377 < r_k < 0.130377$.

[2] As rule of thumbs, if the number of out of range time lags ≤ 3 , then the ACF consider to be stationary.

Similar procedure imply for LST and Winds. When first differencing failed then next differencing need to be considered. The same procedure also conducted for PACF to find the MA value. The Mini Tab Software is used for calculating the coefficient of double regression. The outcome of processing is:

$$\text{Rain fall} = 1055 - 2.72 H - 32.4 \text{LST} + 3.53W \quad (3)$$

From the formula above, daily rainfall can be predicted for 2009 and 2010.

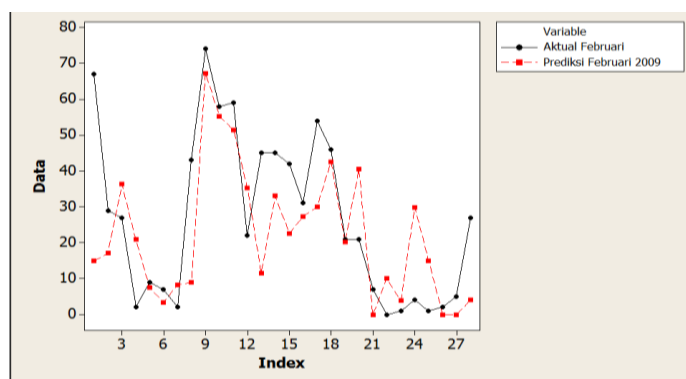


Figure 7. The actual vs prediction rainfall in february 2009

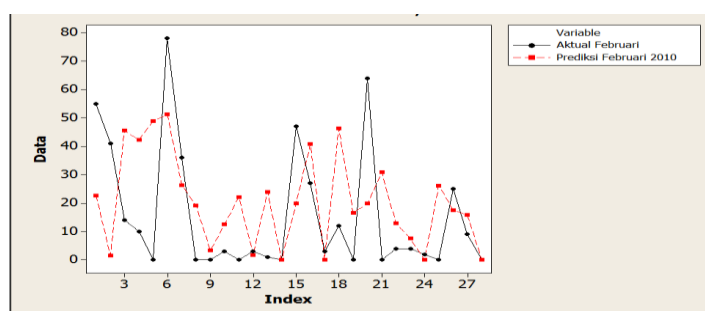


Figure 8. The actual vs prediction rainfall in february 2010

From both fig. 7 and fig 8, the prediction quite follow the actual data. The deviation range from 0-25 mm/hr which is acceptable if base on classification of rain by WMO. The root mean square (RMSE) calculated for year 2009 and 2010 are 0,242 and 0,301 respectively. A little drawback in 2010 is due to the fact that in 2010 the La Nina event occurred. There are also some disadvantages in the system since some data obtained from BMKG, particularly 2001-2003 periods has some blank events.

4.2. ASTAR

Before input parameter is determined, calculation of input variables correlation is important to know how those variables affect the rain fall. Input variable to rain fall condition is a variable with high correlation, thus the product could be used to forecast the rain fall. There are wind speed (knot), humidity (%) and temperature (C) as predictor variables. Rain fall forecasting for the year 2009 is using 2004 – 2008 BMKG Region IV, Makassar, data and forecasting of rain fall for the year 2010 is using 2004 – 2009 data. Relation of humidity, temperature and wind speed to rain fall is determined with MARS software. It will form a equation model to February 2009 prediction as follow:

$$Y = -9.296 + 36.493*BF2 + 5.351*BF4 + 1.302*BF5$$

While for Februari 2010 prediction has formulation model:

$$Y = -12.204 + 32.570*BF2 + 4.995*BF4 + 1.493*BF5 \quad \text{Where,}$$

BF2 = $\max(0, 24.200 - \text{Temperature});$

BF4 = $\max(0, 12.000 - \text{Wind, X1});$

BF5 = $\max(0, \text{Humidity} - 69.000);$

Rainfall modelling_FE = BF2 BF4 BF5

The next step is using Microsoft Excel to attain the nest modelling of rain fall forecasting for the year 2009 and 2010.

$$Y_{2009} = -9.296 + 36.493 * (24,2 - \text{Temp}) + 5.351 * (12 - \text{Wind}) + 1.302 * (\text{Humidity}-69) = 115,298 \text{ mm}$$

$$Y_{2010} = (-12.204 + (32.570 * (24.3 - \text{Temperture})) + (4.995 * (12 - \text{WInd})) + (1.493 * (\text{Humidity}-69))) = 60.374 \text{ mm}$$

Therefore, rain fall forecasting per 1 February 2009 and 2010 is 115,298 mm and 60,374 mm.

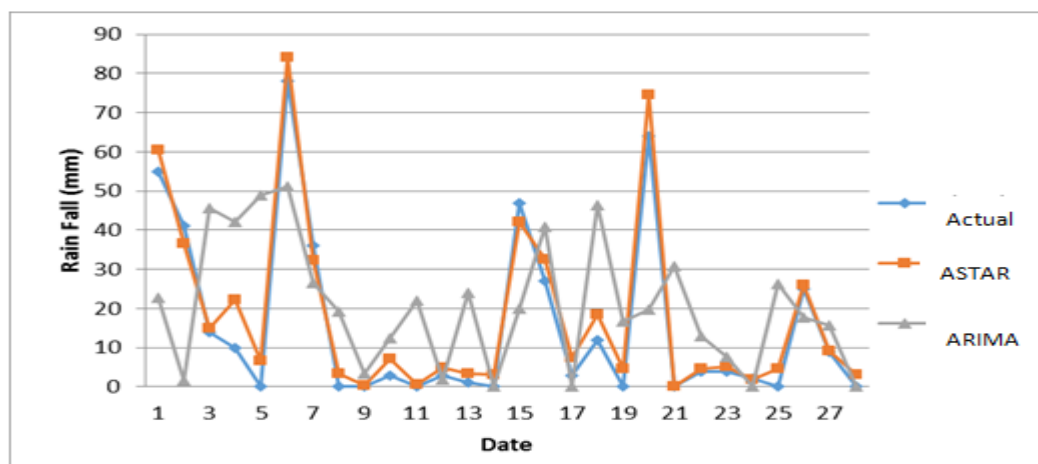


Figure 9. The actual vs prediction rainfall ARIMA and ASTAR in february 2010

From Fig. 9 it can be seen that ASTAR has better prediction compare to ARIMA. ASTAR also shows following trend to the actual data. It seem ARIMA cannot perform well in dealing stochastic data.

V. CONCLUSION

ASTAR method has a better prediction compare to ARIMA in general. It can be seen from the lower RMSE between 0,060757012 to 0,335681565 with average 0,1373 in year 2010 compare to ARIMA with RMSE from 0,19331303 to 0,440727825 with average 0,2942. ASTAR also shows a better following trend to the actual data since its feature in dealing with stochastic data.

REFERENCES

- [1] E. Aldrian and Y.S Djamil, Application of Multivariate Anfis For Daily Rainfall Prediction: Influences Of Training Data Size, MAKARA, SAINS, VOLUME 12, NO. 1, APRIL 2008: 7-14.
- [2] H. Wu, X. Lin, "Application of Fuzzy Neural Network to the Flood Season Precipitation Forecast", International Joint Conference on Computational Sciences and Optimization IEEE, 2009.
- [3] J.F. Nong, "Application of Nonparametric Methods in Short-range Precipitation Forecastng", International Joint Conference on Computational Sciences and Optimization IEEE, 2009.
- [4] Fangqiong Luo, Chunmei Wu and Jiansheng Wu, "A Novel Neural Network Ensemble Model Based on Sample Reconstruction and Projection Pursuit for Rainfall Forecasting", ICNC, IEEE, 2010.
- [5] I. Sonjaya, T. Kurniawan, "Uji Aplikasi HyBMG Untuk Prakiraan Curah Hujan Pola Monsunal", Ekuatorial dan Lokal. BULETIN METEOROLOGI KLIMATOLOGI DAN Vol. 5 No. 3 SEPTEMBER 2009.
- [6] Indrabayu, "Jaringan Sarat Tiruan dan Fuzzy Untuk Memprediksi Hujan", Pertemuan Tahunan Nasional Teknik Elektro, FORTEI, 2011.
- [7] J. Contreras, "ARIMA Models to Predict Next-Day Electricity Prices", IEEE TRANSACTIONS ON POWER SYSTEMS, VOL. 18, NO. 3, AUGUST 2003.
- [8] Indrabayu, N. Harun, M. S. Pallu, and A. Ahmad, Constructing Auto-Regressive Integrated Moving Average (ARIMA) as Expert System for Daily Precipitation Forecasting, The 2nd MICEEI International Conference, Makassar, Indonesia, 2011, pp.89.
- [9] Indrabayu, N. Harun, M. S. Pallu, and A. Ahmad, Performance of ASTAR for Rainfall Forecasting, Proc. The 3rd MICEEI, Makassar, Indonesia, 2012, pp.327.

Study of Two Different Methods for Iris Recognition Support Vector Machine and Phase Based Method

Gaganpreet kaur¹, Dilpreet kaur², Dheerendra singh³

¹A.P. Deptt. Of C.S.E., Sggsu, Punjab, India.

²Research Scholar, Deptt. Of C.S.E., Sggsu, Punjab, India.

³Prof & Head, Deptt. Of C.S.E., Suscet, Tangori, Punjab, India.

Abstract:

The iris recognition is a kind of the biometrics technologies based on the physiological characteristics of human body, compared with the feature recognition based on the fingerprint, palm-print, face and sound etc, the iris has some advantages such as uniqueness, stability, high recognition rate, and non-infringing etc. The iris recognition consists of iris localization, normalization, encoding and comparison. In this paper two different methods of iris recognition mechanism are analyzed. One is support vector machine and other is the Phase based method. Experimental results and data sets of both methods are also discussed. This paper also showed the table for the performance result iris methodologies.

Keywords: Biometric recognition system, Phase based method, Support vector machine (SVM).

1. INTRODUCTION

Iris recognition is a biometric-based method of identification. This method has many advantages, such as unique, stability, can be collected, non aggressive, etc. The iris recognition's error rate is the lowest in most biometric identification method. Now many research organizations at home and abroad spend a lot of time and energy to do research of iris recognition [13]. Biometric recognition refers to the process of matching an input biometric to stored biometric information. In particular, biometric verification refers to matching the live biometric input from an individual to the stored biometric template about that individual [1]. Examples of biometrics include face images, fingerprint images, iris images, retinal scans, etc. Thus, image processing techniques prove useful in the biometric recognition. The field of biometrics utilizes computer models of the physical and behavioral characteristics of human beings with a view to reliable personal identification. The human characteristics of interest include visual images, speech, and indeed anything which might help to uniquely identify the individual.

Most current authentication systems are password based making them susceptible to problems such as forgetting the password and passwords being stolen. One way to overcome these problems is to employ biometrics (e.g., fingerprints, face, iris pattern, etc.) for authentication. Another important application is to match an individual's biometrics against a database of biometrics. An example application of biometric identification is the matching of fingerprints found at a crime scene to a set of fingerprints in a database [11]. Authentication problem has narrower scope, but the matching technologies are applicable to both verification and identification problems [10]. Many biometric sensors output images and thus image processing plays an important role in biometric authentication. Image preprocessing is important since the quality of a biometric input can vary significantly. For example, the quality of a face image depends very much on illumination type, illumination level, detector array resolution, noise levels, etc [3]. Preprocessing methods that take into account sensor characteristics must be employed prior to attempting any matching of the biometric images. The use of biometric systems has been increasingly encouraged by both government and private entities in order to replace or increase traditional security systems. The word iris is generally used to denote the colored portion of the eye. It is a complex structure comprising muscle, connective tissues and blood vessels. The image of a human iris thus constitutes a plausible biometric signature for establishing or confirming personal identity [6]. Further properties of the iris that makes it superior to finger prints for automatic identification systems include, among others, the difficulty of surgically modifying its texture without risk, its inherent protection and isolation from the physical environment, and it's easily monitored physiological response to light [5]. Additional technical advantages over fingerprints for automatic recognition systems include the ease of registering the iris optically without physical contact beside the fact that its intrinsic polar geometry does make the process of feature

extraction easier [4]. Boles and Boashash [2] proposed a novel iris recognition algorithm based on zero crossing detection of the wavelet transform, this method has only obtained the limited results in the small samples, and this algorithm is sensitive to the grey value changes, thus recognition rate is lower. In another method followed by Jie Wang [7] the iris texture extraction is performed by applying wavelet packet transform (WPT) using Haar wavelet. The iris image is decomposed in to sub images by applying WPT and suitable sub images are selected and WPT coefficients are encoded. One more technique to extract the feature is Haar wavelet decomposition. Tze Weng Ng, Thein Lang Tay, Siak Wang Khor [8], has proposed Haar wavelet decomposition method for feature extraction. It acquires an accuracy using complex neural network matching method. Coefficients obtained from the decomposition of are then converted to binary codes to be used on calculation of hamming distance for matching purpose. Zhonghua Lin, Bibo Lu [9], has proposed iris recognition based on the optimized Gabor filters. The recognition rate is high, the recognition speed is guaranteed. Iris recognition will need in future for security. Iris recognition has many advantages comparing other biometric techniques:

1.1 Uniqueness

Dissector F. H. Adler suggested the uniqueness of iris originally in 1965. The visible features in an iris include the trabecular meshwork of connective tissue, collagenous stromal fibres, ciliary processes, contraction, and freckle. These textures ensure that different persons have distinct iris. The probability of two persons' irises being the same is lower than 10^{-35} . Even though they are twins, their irises are quite different. This fact is the reason why we use iris to recognize personal identity.

1.2 Reliability

Iris is an inner organ in our eyes and protected by eyelid, lash and cornea. Unlike finger and palm, it is seldom hurt and the error of recognition caused by scar will never happen. In this sense, iris recognition is much better than fingerprint and palm-print recognition. Furthermore, our irises matured when we were one year old and would not change in our life.

1.3 Against artifice

A living eye's pupillary diameter relative to iris diameter in a normal eye is constantly changing, even under steady illumination. The pupillomotor response could provide a test against artifice.

II. STEPS OF IRIS RECOGNITION SYSTEM

It is the process of acquiring high definition iris images either from iris scanner or precollected images. These images should clearly show the entire eye especially iris and pupil part. Then Major steps are followed:-

2.1 Segmentation

A technique is required to isolate and exclude the artifacts as well as locating the circular iris region. The inner and the outer boundaries of the iris are calculated.

2.2 Normalization

Iris of different people may be captured in different size, for the same person also size may vary because of the variation in illumination and other factors. The normalization process will produce iris regions, which have the same constant dimensions, so that two photographs of the same iris under different conditions will have characteristic features at the same spatial location.

2.3 Feature extraction

The significant features of the iris must be encoded so that comparisons between templates can be made. Most iris recognition systems make use of a band pass decomposition of the iris image to create a biometric template. Iris provides abundant texture information. A feature vector is formed which consists of the ordered sequence of features extracted from the various representation of the iris images.

2.4 Matching of an Image

To authenticate via identification (one-to-many template matching) or verification (one to- one template matching), a template created by imaging the iris is compared to a stored value template in a database. If the Hamming distance is below the decision threshold, a positive identification has effectively been made e.g. a hamming distance of 0 would result in a perfect match.

III. SUPPORT VECTOR MACHINE (SVM)

Support Vector Machines (SVMs) [19] as pattern classification techniques which are based on iris code model which the feature vector size is transformed to one-dimension vector which reduces to 1 x 480 by using averaging techniques contains the average value to recognize an authorized user and unauthorized user. SVM is a relatively new learning machine technique, which is based on the principle of Structural risk minimization (minimizing classification error). A SVM is binary classifier that optimally separates the two classes of data. There are two important aspects in the development of SVM as classifier. The first aspect is determination of the optimal hyper plane which will optimally separate the two classes and the other aspect is transformation of non-linearly separable classification problem into linearly separable Fig1 shows linearly separable binary classification problem with no possibility of miss-classification data. Let x and y be a set of input feature vector and the class label respectively. The pair of input feature vectors and the class label can be represented as tuples $\{x_i, y_i\}$ where $i = 1, 2, \dots, N$ and $y = \pm 1$. In the case of linear separable problem, there exists a separating hyper plane which defines the boundary between class 1 (labeled as $y = 1$) and class 2 (labeled as $y = -1$). The separating hyper plane is:

$$w \cdot x + b = 0 \tag{1}$$

Which implies

$$y_i(w \cdot x_i + b) \geq 1, i = 1, 2, \dots, N \tag{2}$$

Basically, there are numerous possible values of $\{w, b\}$ that create separating hyper plane. In SVM only hyper plane that maximizes the margin between two sets is used. Margin is the distance between the closest data to the hyper plane.

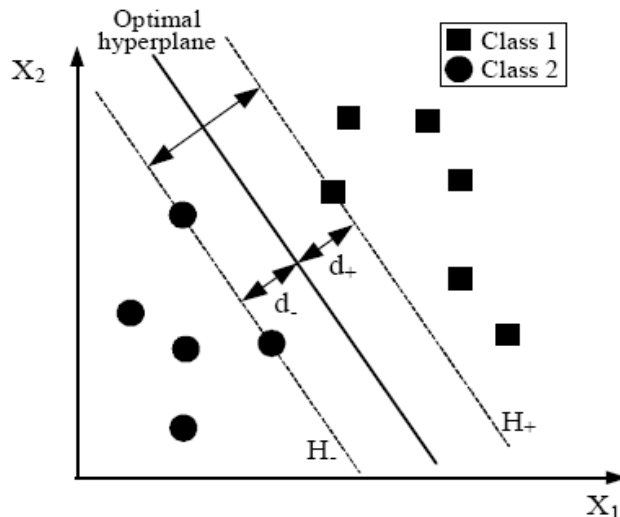


Figure1. SVM with linear separable

The margins are defined as $d+$ and $d-$. The margin will be maximized in the case $d+ = d-$. Moreover, training data in the margins will lie on the hyper planes $H+$ and $H-$.

$$(d+) + (d-) = \frac{2}{\|w\|} \tag{3}$$

As $H+$ and $H-$ are the hyper planes in which the closest training data to the optimal hyper plane, then there is no training data which fall between $H+$ and $H-$. This means the hyper plane that separates optimally the training data is the hyper plane which minimizes $\|w\|^2$, the minimization of $\|w\|^2$ is constrained by equation(1). When the data is non-separable, slack variables, ϵ_j , are introduced into the inequalities for relaxing them slightly so that some points allow lying within the margin or even being misclassified completely. The resulting problem is then to minimize,

$$\frac{1}{2}\|w\|^2 + \left(\sum_i L(\epsilon_j)\right) \tag{4}$$

Where C is the adjustable penalty term and L is the loss function. The most common used loss function is linear loss function, $L(\varepsilon_i) = (\varepsilon_i)$ The optimization of (3) with linear loss function using Lagrange multipliers approach is to maximize,

$$L_D(w, b, a) = \sum_i^N a_i - \frac{1}{2} \sum_{i=1}^N \sum_{j=1}^N a_i a_j \cdot y_i y_j \langle x_i, x_j \rangle \quad (5)$$

Subject to

$$0 \leq a_i \leq C \quad (6)$$

And

$$\sum_i^N a_i y_i = 0 \quad (7)$$

Where a_i is the Lagrange multipliers. This optimization problem can be solved by using standard quadratic programming technique. Once the problem is optimized, the parameters of optimal hyper plane are,

$$w = \sum_i^N a_i y_i x_i \quad (8)$$

As matter of fact, a_i is zero for every x_i except the ones that lie on the margin. The training data with non-zero a_i are called as support vectors. In the case of a non-linear separable problem, a kernel function is adopted to transform the feature space into higher dimensional feature space in which the problem become linearly separable. Typical kernel functions commonly used are listed in table 1.

Kernel	$K(X, X_i)$
Linear	$X^T \cdot X_j$
Polynomial	$(X^T \cdot X_j + 1)^d$
Gaussian RBF	$\exp \left[- \frac{\ x_i - x_j\ ^2}{2\sigma^2} \right]$

Table1. Formulation for kernel function

3.1 Performance measurement

This system in general makes four possible decisions; the authorized person is accepted, the authorized person is rejected, the unauthorized person (impostor) is accepted and the unauthorized person (impostor) is rejected. The accuracy of the proposed system is then specified based on the rate in which the system makes the decision to reject the authorized person and to accept the unauthorized person. False Rejection Rates (FRR) is used to measure the rate of the system to reject the authorized person and False Acceptance Rates (FAR) used to measure the rates of the system to accept the unauthorized person. Both performances are can be expressed as:

$$FRR = \frac{NFR}{NAA} \times 100\% \quad (9)$$

$$FAR = \frac{NFA}{NIA} \times 100\% \quad (10)$$

NFR is referred to the numbers of false rejections and NFA is referred to the number of false acceptance, while NAA and NIA are the numbers of the authorized person attempts and the numbers of impostor person attempts respectively. Furthermore, low FRR and low FAR is the main objective in order to achieve both high usability and high security of the system.

3.2 Data sets and experimental results

The Chinese Academy of Sciences–Institute of Automation (CASIA) eye image database is used in the experiment. To evaluate the effectiveness of the proposed system, a database of 42 grayscale eye images (7 eyes with 6 different images for each eye) was employed. About 30 grayscale eye images with 5 unique eyes are

considered as authorized users and the others are impostors. For each eye, 6 eye images were captured in two different sessions with one month interval between sessions (three samples are collected in the first session and others three in second sessions) using specialized digital optics developed by the National Laboratory of Pattern Recognition, China. Infra-red lighting was used in acquiring the images, hence features in the iris region are highly visible and there is good contrast between pupil, iris and sclera regions.

The performance of biometric systems is usually described by two error rates: FRR and FAR. Hence, the effectiveness of the proposed system in testing phase is evaluated based upon FRR and FAR values. The FAR is calculated based on the close set and open set. In the close set, the typing biometric of an authorized person uses other authorized person identity. On other hand, the open set is referred as typing biometric of the impostors use authorized person. The obtained feature vector of iris code comprises matrix of 20 x 480. This feature vector consists of bits 0 and 1. It was observed in all the experiments conducted that the feature vector size which containing high dimensionality often contributed to high FRR and FAR values with long processing time. To overcome this problem, feature vector size is transformed to one-dimension vector which reduces to 1 x 480 by using averaging techniques contains the average value. SVMs are classifiers which have demonstrated high capability in solving variety of problems that include the object recognition problems. Experimental results of training and testing based on iris code using SVMs are discussed. In developing user models based on iris code, a SVM with polynomial kernel function of order 8 is used. Each authorized user has its own SVM-based model characterized by a set of support vectors. By using quadratic programming in the MATLAB environment, appropriate support vectors are determined. The penalty term C of 10^{15} is used to anticipate misclassified data. Table 2 shows the training performance when the SVM is employed to develop user's models based on their iris code.

Authorized User	Training Time(sec)	Classification Results (%)
User1	0.0781	100
User2	0.0781	100
User3	0.0625	100
User4	0.1094	100
User5	0.0781	100
Average	0.0812	100

Table2. Training performance of iris code

These results indicate that all of the SVM-based user models give perfect classifications as there are no errors in recognizing all the users. Besides, all of the SVM-based models can be trained in a very short time of about 0.1 second. A series of experiments is conducted using the testing data which have not been used during the training phase. Table 3 shows the testing performances of the SVM-based authorized user models. The SVM-based authentication gives very good results for FAR of close set and open set conditions. This implies that the proposed system is well protected from attacking by impostors. In contrast, the FRR values are very high percentage with an average value of about 19.80%. Hence, the system seems to have poor usability. Experimental results show that the first, second and fourth users produce maximum FRR values of about 33%.

Authorized User	FRR (%)	FAR (%) Close set	FAR (%) Open set
User1	33	0	0
User2	33	0	0
User3	0	0	0
User4	33	0	0
User5	0	0	0
Average	19.80	0	0

Table3. Testing performance of iris code

IV. PHASE BASED METHOD

4.1 Daugman integrodifferential operator

The phase based method recognize iris patterns based on phase information. Phase information is independent of imaging contrast and illumination. J.Daugman [12, 14] designed and patented the first complete, commercially available phase-based iris recognition system in 1994. The eye images with resolution of 80-130 pixels iris radius were captured with image focus assessment performed in real time. The pupil and iris boundary was found using integrodifferential operator given in following Equation:

$$\max_{x_0, y_0} \left| G(r) * \frac{d}{dr} \int_{x_0, y_0} \frac{I(x, y)}{2\pi r} ds \right| \quad (11)$$

Where $I(x, y)$ is the image in spatial coordinates r is the radius, (x_0, y_0) are centre coordinates, the symbol $*$ denotes convolution and $G_\sigma(r)$ is a Gaussian smoothing function of scale σ . The centre coordinates and radius are estimated for both pupil and iris by determining the maximum partial derivative of the contour integral of the image along the circular arc. The eyelid boundaries are localized by changing the path of contour integration from circular to actuate. The iris portion of the image $I(x)$ is normalized to the polar form by the mapping function $I(x(r, \theta), y(r, \theta)) \rightarrow I(r, \theta)$ where r lies on the unit interval $[0, 1]$ and θ is the angular quantity in the range $[0, 2\pi]$. The representation of iris texture is binary coded by quantizing the phase response of a texture filter using quadrature 2D Gabor wavelets into four levels. Each pixel in the normalized iris pattern corresponds to two bits of data in the iris template. A total of 2,048 bits are calculated for the template, and an equal number of masking bits are generated in order to mask out corrupted regions within the iris. This creates a compact 256-byte template, which allows for storage and comparison of iris.

The recognition in this method is the failure of a test of statistical independence involving degrees of freedom. Iris codes are different for two different samples. The test was performed using Boolean XOR operator applied to 2048 bit phase vectors to encode any two iris patterns, masked by both of their bit vectors. From the resultant bit vector and mask bit vectors, the dissimilarity measure between any two iris patterns is computed using Hamming Distance (HD), given in the following equation:

$$HD = \frac{(codeA \oplus codeB) \odot maskA \odot maskB}{maskA \odot maskB} \quad (11)$$

Where code A, code B are two phase code bit vectors and mask A, mask B are mask bit vectors. The HD is a fractional measure of dissimilarity with 0 representing a perfect match. A low normalized HD implies strong similarity of iris codes. The work by Xianchao Qui [15] used 2D Gabor filters for localization. The filter response vectors were clustered using vector quantization algorithms like k-means. The experiments were conducted on CASIA-Biosecure iris database consisting of images captured from Asian and non-Asian race groups. In Martin's method, the iris circumference parameters are obtained by maximizing the average intensity differences of the five consecutive circumferences.

In Masek's method, the segmentation was based on the Hough transform. The phase data from 1D Log-Gabor filters was extracted and quantized to four levels to encode the unique pattern of the iris into a bit-wise biometric template. Xiaomei Liu [16] reimplemented Masek's algorithm in C that was originally written in Matlab. Continuing the Daugman's method, Karen Vollingsworth [17] has developed a number of techniques for improving recognition rates. These techniques include fragile bit masking, signal-level fusion of iris images, and detecting local distortions in iris texture. The bits near the axes of the complex plane shift the filter response from one quadrant to adjacent quadrant in presence of noise. In the fragile bit masking method, such bits called as the fragile bits are identified and masked to improve the accuracy. The signal-level fusion method uses image averaging of selected frames from a video clip of an iris. Local texture distortions occurs with contact lenses with a logo, poor-fit contacts and edges of hard contact lenses, segmentation inaccuracies and shadows on the iris. These are detected by analyzing iris code matching results. The 20x240 normalized images were covered with 92 windows each of size 8x20. Fractional HD was computed for each window. The location of windows with highest fractional HD was identified and removed from further calculations. The effect of dilation was studied by collecting datasets of images with varying degrees of dilation. The data was divided into subsets with small pupils, medium pupils and large pupils. The subset of data with large pupils showed worst performance with EER at an order of magnitude greater compared to that of small pupil data set. The visibility in the iris area is reduced and greater part of iris is occluded by eyelids which provide less information for iris code generation. Following table shows the performance result of Daugman's algorithm and other algorithms of iris recognition.

Group	EER	FAR/FRR	Overall accuracy
Wides et al	1.76	2.4/2.9	95.10
Avila	3.38	0.03/2.08	97.89
Tisse	5.94	1.84/8.79	96.61
Li Ma	4.73	0.02/1.98	98.00
Daugman	0.95	0.01/0.09	99.9
Boles	8.13	0.02/1.98	94.33
Hamed Ranjzad	2.1	1.6/1.2	98.1
Kaushik Rai	0.92	0.03/0.02	99.5

Table4. Performance results of Iris recognition methods

V. CONCLUSION

This paper concluded that the Support Vector Machine was adopted as classifier in order to develop the user model based on his/her iris code data. Experimental study using CASIA database is carried out to evaluate the effectiveness of the proposed system. Based on obtained results, SVM classifier produces excellent FAR value for both open and close set condition. Thus, the proposed system seems in a good level of security. Phase based method recognize the iris pattern based on the phase information. Phase information is independent of imaging contrast and illumination. Continuing Daugman's method, Karen Vollingsworth has developed a numbers of techniques for improving the recognition rates. In fragile bit masking method, fragile bits are identified and masked to improve the accuracy. The signal level fusion method uses image averaging of selected frames from video clip of an iris. Local texture distortions occurs with contact lenses with a logo, poor-fit contacts and edges of hard contact lenses, segmentation inaccuracies and shadows on the iris. These are detected by analyzing iris code matching results. The experiments were conducted on CASIA-Biosecure iris database consisting of images captured from Asian and non-Asian race groups. The performance results are based on the error rates: False Acceptance Rate (FAR) and False Rejection Rate (FRR); Equal Error Rate (EER) and the overall accuracy. Table 4 shows that Daugman's method gives the maximum accuracy with respect to FRR and FAR, 0.01/0.09 and overall accuracy 99.9%.

REFERENCES

- [1] J. G. Daugman, "High Confidence Visual Recognition of Persons by a Test of Statistical Independence", IEEE Trans. Pattern Analysis and Machine Intelligence, vol. 15, pp. 1148-1161, Nov. 1993.
- [2] W. Boles, B. Boashash, "A human identification technique using images of the iris and wavelet transform", IEEE Transaction on Signal Processing, vol.46 (4), pp.1185-1188, 1998.
- [3] Lye Wil Liam, Ali Chekima, Liau Chung Fan, "Iris recognition using self-organizing neural network", IEEE, 2002.
- [4] Daugman G., "How Iris Recognition Works", IEEE Transaction on Circuits and System for Video Technology, vol.14, no. I, pp. 21-30, 2004.
- [5] U.M. Chaskar, M.S. Suataone, "A Novel Approach for Iris Recognition", IEEE, 2010.
- [6] Lin Zhonghua, Lu Bibo, "Iris Recognition Method Based on the Coefficients of Morlet Wavelet Transform", IEEE, 2010.
- [7] Jie Wang, Xie Mei, "Iris Feature extraction based on wavelet packet analysis", IEEE, 2006.
- [8] Tze Weng Ng, Thien Lang Tay, Siak Wang Khor, "Iris Recognition using Rapid Haar Wavelet Decomposition", IEEE, 2010.
- [9] Zhonghua Lin, Bibo Lu, "Iris Recognition Method Based on the Optimized Gabor Filters", IEEE, 2010.
- [10] L.Masek., "Recognition of human iris patterns for biometric identification", [Online].Available: <http://www.csse.uwa.edu.au/~pk/studentprojects/libor/LiborMasekThesis.pdf>. 2003.
- [11] R. P. Wildes, "Iris recognition: an emerging biometric technology", Proc IEEE, vol. 85, pp. 1348-1363, 1997.
- [12] Daugman J., "How iris recognition works", IEEE Transactions CSV, Vol.14, No.1, pp. 21-30, 2004.
- [13] Institute of Automation Chinese Academy of Sciences. Database of CASIA iris image [EB/OL].
- [14] Li Ma, Tieniu Tan, Yunhong Wang, Dexin Zhang, "Personal Identification based on Iris Texture Analysis", IEEE Transactions on Pattern Analysis and Machine Intelligence, Vol.25, No.12, pp. 1519 - 1533, 2003.
- [15] J. Daugman, "High Confidence Visual Recognition by a test of Statistical Independence", IEEE Trans. Pattern Analysis and Machine Intelligence, Vol.15, No.11, pp.1148-1161, 1993.
- [16] L. Ma, Y. Wang, and T. Tan, "Iris Recognition Using Circular Symmetric Filters", Proc. 16th Int'l Conf. Pattern Recognition, vol. II, pp. 414-417, 2002.
- [17] Kaushik Roy, Prabir Bhattacharya and Ramesh Chandra Debnath, "Multi-Class SVM Based Iris Recognition", international conference on computer and information technology.
- [18] Martin-Roche D., Sanchez-Avila C. and Sanchez-Reillo R., "Iris recognition for biometric identification using dyadic wavelet transform zero-crossing", IEEE Aersp. Electron. Syst. Mag., Vol. 17, Issue 10, pp. 3-6, 2002.
- [19] Burges, C. J. C., "A tutorial on support vector machines for pattern recognition", Data Mining and Knowledge Discovery, Vol.2, pp. 121-167, 1998.

Study Of Hybrid Genetic Algorithm Using Artificial Neural Network In Data Mining For The Diagnosis Of Stroke Disease

Mr. Deepak Dhanwani¹, Prof. Avinash Wadhe²
¹,ME (CSE) 2nd Semester Department Of CSE G.H.R.C.E.M, Amravati
²M-Tech (CSE) Department Of CSE G.H.R.C.E.M., Amravati

Abstract:

The main purpose of data mining is to extract knowledge from large amount of data. Artificial Neural network (ANN) has already been applied in a variety of domains with remarkable success. This paper presents the application of hybrid model for stroke disease that integrates Genetic algorithm and back propagation algorithm. Selecting a good subset of features, without sacrificing accuracy, is of great importance for neural networks to be successfully applied to the area. In addition the hybrid model that leads to further improvised categorization, accuracy compared to the result produced by genetic algorithm alone. In this study, a new hybrid model of Neural Networks and Genetic Algorithm (GA) to initialize and optimize the connection weights of ANN so as to improve the performance of the ANN and the same has been applied in a medical problem of predicting stroke disease for verification of the results.

Keywords: ANN, Back Propagation algorithm, data mining, Feed Forward Network, Genetic algorithm, Hybrid model, Neuron.

I. INTRODUCTION

Data mining is the process of discovering useful knowledge in data and also finding the inter-relation pattern among the data [7]. It is an automated discovery of strategic hidden patterns (useful information) in large amounts of raw data using intelligent data analysis methods [8]. For the past few years, there have been a lot of studies focused on the classification problem in the field of data mining [9, 10]. The general goal of data mining is to extract knowledge from large amount of data. The discovered knowledge should be predictive and comprehensible classification is given an equal importance to both predictive accuracy and comprehensibility. Neural Network is used for the classification of diseases based on the features of the patients.

A stroke is the sudden death of brain cells in a localized area due to inadequate blood flow. The sudden death of brain cells due to lack of oxygen, caused by blockage of blood flow or rupture of an artery to the brain. Sudden loss of speech, weakness, or paralysis of one side of the body can be symptoms. In medical diagnosis, the information provided by the patients may include redundant and interrelated symptoms and signs especially when the patients suffer from more than one type of disease of same category. The physicians may not be able to diagnose it correctly. So it is necessary to identify the important diagnostic features of a disease and this may facilitate the physicians to diagnosis the disease early and correctly. The expert go for computer aided diagnosis (CAD) for confirming their prediction. The CAD helps to improve their prediction efficiency and accuracy. It should also be user friendly, so that expert can have the classification with explanation.

II. RELATED WORK

In August 2012, Dharmistha.D.Vishwakarma, presented paper on Genetic based weight optimization of Artificial Neural network. This papers shows the weights in different layers of the network are optimized using genetic algorithm comparison results for the ANN trained without GA and GA based ANN. [1] In July 2012, P.Venkateshan and V.Premlatha, presented paper on Genetic–Nero approach for disease classification ,which shows genetic neuro classification system performs better than the conventional neural network.[2] In June 2012, Kafka Khan and Ashok Sahai presented the comparison of BA ,BP,GA,PSO and LM algorithms for training feed forward neural network in e-Learning context was done.[3] In May 2011,Asha Karegowada,A..S.Manjunath, M.A.Jayaram presented the Application of Hybrid model that integrates Genetic

algorithm and Back Propagation network.[4].In 2009,D.Shanthi,Dr.G.Sahoo,Dr.N. Saravanan presented the paper on Evolving Connection Weights of Artificial Neural Networks Using Genetic Algorithm with Application to the Prediction of Stroke Disease , the real output and desired output of ANN and Hybrid ANN-GA were compared. The classification accuracy for all surfaces were improved. Evolving Connection Weights of Artificial Neural Networks Using Genetic Algorithm with Application to the Prediction of Stroke Disease.[5] In December 2008, D.Shanthi, Dr.G.Sahoo, and Dr.N.Saravanan paper on Input Feature Selection using Hybrid Neuro-Genetic Approach in the Diagnosis of Stroke Disease. In this paper, they proposed a neuro-genetic approach to feature selection in disease classification in this paper, a new hybrid neuro-genetic approach has been proposed and the same has been used for the selection of input features for the neural network. Experimental results showed the performance of ANN can be improved by selecting good combination of input variables. [6]

III. ARTIFICIAL NEURAL NETWORK

A Neural Network (NN) consists of many Processing Elements (PEs), loosely called “neurons” and weighted interconnections among the PEs. Each PE performs a very simple computation, such as calculating a weighted sum of its input connections, and computes an output signal that is sent to other PEs. The training (mining) phase of a NN consists of adjusting the weights (real valued numbers) of the interconnections, in order to produce the desired output. [10] The Artificial Neural Network (ANN) is a technique that is commonly applied to solve data mining applications. The previous neuron doesn't do anything that conventional computers don't do already. A more sophisticated neuron is the McCulloch and Pitts model (MCP). The difference from the previous model is that the inputs are ‘weighted’; the effect that each input has at decision making is dependent on the weight of the particular input. The weight of an input is a number which when multiplied with the input gives the weighted input. These weighted inputs are then added together and if they exceed a pre-set threshold value, the neuron fires. In any other case the neuron does not fire.

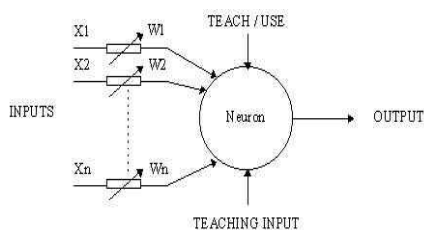


Figure 1 A MCP neuron

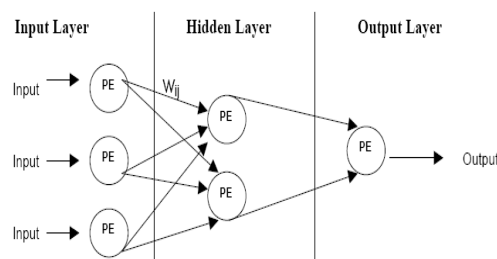


Figure 2. An example of a simple feed- forward network

IV. BACK PROPAGATION ALGORITHM

The back propagation algorithm (BP) [11] is a classical domain-dependent technique for supervised training. It works by measuring the output error, calculating the gradient of this error, and adjusting the ANN weights (and biases) in the descending gradient direction. Hence, BP is a gradient-descent local search procedure (expected to stagnate in local optima in complex landscapes). The squared error of the ANN for a set of patterns i The actual value of the previous expression depends on the weights of the network. The basic BP algorithm calculates the gradient of E (for all the patterns) and updates the weights by moving them along the gradient-descent direction. This can be summarized with the expression $\Delta w = -\eta \nabla E$, where the parameter $\eta > 0$ is the learning rate that controls the learning speed. The pseudo-code of the BP algorithm is shown (cf. Figure 3).

```

Initialize Weights;
While not Stop-Criterion do
  For all i, j do
     $w_{ij} = w_{ij} - \eta \frac{\partial E}{\partial w_{ij}}$ 
  End For
End While
    
```

Figure 3. Pseudo code of back propagation algorithm

V. GENETIC ALGORITHM

A GA is a stochastic general search method. It proceeds in an iterative manner by generating new populations of individuals from the old ones. Every individual is the encoded (binary, real, etc.) version of a tentative solution. [13] The canonical algorithm applies stochastic operators such as selection, crossover, and mutation on an initially random population in order to compute a new population. In generational GAs all the population is replaced with new individuals. In steady-state GAs (used in this work) only one new individual is created and it replaces the worst one in the population if it is better.

The total process is described as follows:

- 1- Generate randomly an initial population;
- 2- Evaluate this population using the fitness function;
- 3- Apply genetic operators such selection, crossover, and mutation;
- 4- Turn the process "Evaluation Crossover mutation" until reaching the stopped criteria fixed in prior.

```

t = 0
Initialize: P(0) = {a1(0), ..., aμ(0)} ∈ Iμ
Evaluate: P(0): {Φ(a1(0)), ..., Φ(aμ(0))}
While L (P(t)) ≠ true //Reproductive loop
    Select: P'(t) = sθz {P(t)}
    Recombine: P''(t) = ⊗θz {P'(t)}
    Mutate: P'''(t) = mθm {P''(t)}
    Evaluate: P'''(t): {Φ(a1'''(t)), ..., Φ(aλ'''(t))}
    Replace: P(t+1) = rθr (P'''(t) ∪ Q)
t = t + 1
End While
    
```

Figure 4. Pseudo code of genetic algorithm

VI. HYBRID MODEL OF GENETIC AND BACK PROPAGATION ALGORITHM

Back propagation learning works by making modifications in weight values starting at the output layer then moving backward through the hidden layers of the network. BPN uses a gradient method for finding weights and is prone to lead to troubles such as local minimum problem, slow convergence pace and convergence unsteadiness in its training procedure. Unlike many search algorithms, which perform a local, greedy search, GAs performs a global search. GA is an iterative procedure that consists of a constant-size population of individuals called chromosomes, each one represented by a finite string of symbols, known as the genome, encoding a possible solution in a given problem space. The GA can be employed to improve the performance of BPN in different ways. GA is a stochastic general search method, capable of effectively exploring large search spaces, which has been used with BPN for determining the number of hidden nodes and hidden layers, select relevant feature subsets, the learning rate, the momentum, and initialize and optimize the network connection weights of BPN. GA has been used for optimally designing the ANN parameters including, ANN architecture, weights, input selection, activation functions, ANN types, training algorithm, numbers of iterations, and dataset partitioning ratio [13]. The new hybrid Neuro-Genetic approach is depicted in figure 5 and the same has been applied for the diagnosis of stroke disease. The result show this hybrid approach has the potential to eventually improve the success rate better than traditional ANN monolithic design

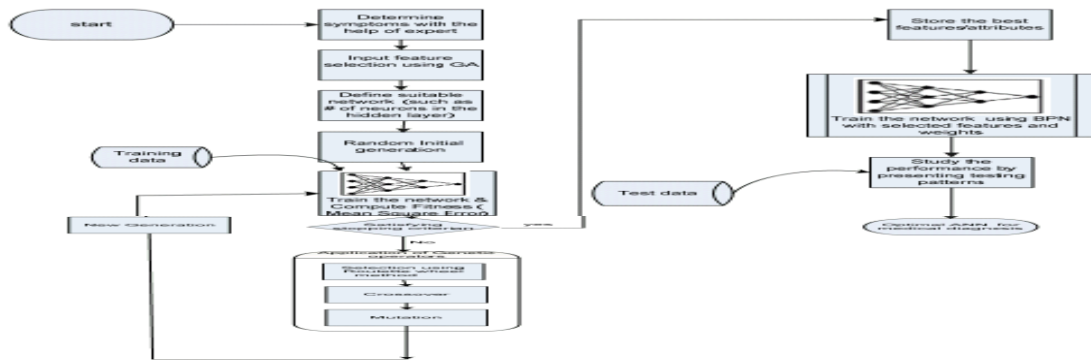


Figure 5: Hybrid Neuro- Genetic Approach

The process of GA-NN algorithm is presented below:

- [1] Determine the symptoms with help of Expert
- [2] Initialize count=0, fitness=0, number of cycles
- [3] Generation of Initial Population. The chromosome of an individual is formulated as a sequence of consecutive genes, each one coding an input.
- [4] Design suitable network (input layer, hidden Layer, output layer)
- [5] Assign weights for each link
- [6] Train the network using BP algorithm
- [7] Find cumulative error and the fitness value. The genotypes are evaluated on the basis of the fitness function.
- [8] If (previous fitness < current fitness value) Then store the current features
- [9] count = count +1
- [10] Selection: Two parents are selected by using the roulette wheel mechanism
- [11] Genetic Operations: Crossover, Mutation and Reproduction to generate new features set (Apply new weights to each link)
- [12] If (number of cycles <= count) go to 4
- [13] Train the network with the selected features
- [14] Study the performance with test data.

VII. STUDY OF PREVIOUS RESULTS AND DISCUSSION FOR DIAGNOSIS OF STROKE DISEASE

The data for this work have been collected from 150 Patients who have symptoms of stroke disease. The data have been standardized so as to be error free in nature. Table 1 below shows the various input parameters for the Prediction of stroke disease.

Table 1: Input Parameters

Sr..No	Attributes
1	Hypertensive
2	Diabetes
3	Myocardial
4	Cardiac failure
5	Atrial fibrillation
6	Smoking
7	Blood cholesterol
8	Left arm and leg
9	Right arm and leg
10	Slurring
11	Giddiness
12	Headache
13	Vomiting
14	Memory deficits
15	Swallowing
16	Vision
17	Double vision
18	Vertigo
19	Numbness
20	Dizziness

7.1 Neural Network based Feature Selection

Data are analyzed in the dataset to define column Parameters and data anomalies. Data analysis information needed for correct data preprocessing. After data analysis, the values have been identified as missing, wrong type values or outliers and which columns were rejected as unconvertible for use with the neural network . Feature selection methods are used to identify input columns that are not useful and do not contribute significantly to the performance of neural network. The removal of insignificant inputs will improve the generalization performance of a neural network. In this study, first Backward stepwise method is used for input feature selection. This method begins with all inputs and it works by removing one input at each step. At each step, the algorithm finds an input that least deteriorates the network performance and becomes the candidate for removal from the input set. The architecture of the neural network designed with 20 input nodes, 10 hidden nodes, and 10 output nodes. This ANN is trained using Back propagation algorithm and tested with the data and overall predictive accuracy was shown in table 10 against different datasets.

7.2 GA Based Feature Selection

In this neuro-genetic approach all the 20 symptoms are taken in to account. GA optimizes the 20 inputs in to 14. The genotype is represented by a sequence of symptoms. The number of individual in the initial population is 20. The fitness function is represented by means of root mean square error. The maximum number of generations are fixed at 20. The rest of the paper describes pre-processing, analysis, design, training and testing of ANN.

Table 2: Parameters used in GA

Search Method	Genetic Algorithm
Population size	20
Number of generations	20
Probability of crossover	0.6
Probability of mutation	0.033
Random number seed	1

In this work, the probability of crossover is 0.6 and the probability of mutation is 0.033. These probabilities are chosen by trial and error through experiments for good performance. The data is partitioned are done randomly and the following table shows the no of records in the training set, validation set and test set.

Table 3: Data Partition Set

Sl.No	Data Partition set	Records	Percentage
1.	Training set	104	69.33%
2.	Validation set	23	15.33%
3.	Test set	23	15.34%
4.	Ignored set	0	0%
	Total	150	100%

The average prediction accuracy by the traditional Neural Network approach and the new hybrid Neuro-Genetic approaches are depicted in table 4 below:

Table 4: Average Prediction Accuracy

Approach	Training	Validation	Testing
Neural Networks	78.52%	82.43%	90.61%
GA-NN	79.17%	83.88%	98.67%

The result shows clearly that our new hybrid neuro-genetic method provides better accuracy and faster convergence due to the complexity of the network. The prediction accuracy is 98.67% with the reduced features. Sometimes reduction of features yields the drop in accuracy. So the input parameters should be chosen without compromising the accuracy.

VIII. CONCLUSION

In this paper, a new hybrid neuro genetic approach has been used for the selection of input features for the neural network. results showed the performance of ANN can be improved by selecting good combination of input variables from the results; GA-NN approach gives better average prediction accuracy than the traditional ANN.

REFERENCES

- [1] Ms. Dharmistha D.Vishwakarma “Genetic Algorithm based Weights Optimization of Artificial Neural Network” International Journal of Advanced Research in Electrical ,Electronics and Instrumentation Engineering(2278-8875),Volume1,Issue 3,August 2012.
- [2] P.Venkatesan ,V.Premlatha,” Genetic Neuro Approach for classification”, International Journal of Science and Technology (2224-3577)Volume 2 No.7,July 2012
- [3] Kafka Khan ,Ashok Sahai ,” A Comparison of BA,GA,PSO,BP and LM for Training Feed Forward Neural Networks in e-Learning Context”I.J.Intelligent System and applications,2012,7,23-29.
- [4] Asha Gowanda Karegowada,A.S.Manjunath ,” Application of Genetic algorithm optimized Neural Network Connection Weights for medical diagnosis of PIMA Indian Diabetes “International Journal on SoftComputing(IJSC),Volume2,No.2,May 2011
- [5] D.Shanthi, Dr.G.Sahoo, Dr.N.Saravanan “Evolving Connection Weights of Artificial Neural Networks Using Genetic Algorithm with Application to the Prediction of Stroke Disease”, International Journal of Soft Computing Year: 2009 | Volume: 4 | Issue: 2 | Page No.: 95-102
- [6] D.Shanthi, Dr.G.Sahoo, Dr.N.Saravanan,” Input Feature Selection using Hybrid Neuro-Genetic Approach in he Diagnosis of Stroke Disease “,IJCSNS International Journal of Computer Science and Network Security, VOL.8 No.12, December 2008
- [7] S.Kalaiarasi Anbananthen, Fabian H.P. Chan, K.Y. Leong. Data Mining Using Decision Tree Induction of Neural Networks, 3rd Seminar on Science and Technology. Kota Kinabalu: SST. 2004.
- [8] Kriegel, H.-P., et al.: Future Trends in Data Mining. Data Mining and Knowledge Discovery (5): 113-134, 2008.
- [9] . Kalaiarasi Anbananthen, Fabian H.P. Chan, K.Y. Leong. Data Mining Using Decision Tree Induction of Neural Networks, 3rd Seminar on Science and Technology. Kota Kinabalu: SST. 2004.
- [10] An introduction to neural computing. Aleksander, I. and Morton, H. 2nd edition.
- [11] Koohang, A. Foundations of Informing Science. T. Grandon Gill & Eli Cohen (eds.), (5): 113-134, 2008.
- [12] A. Kusiak, K.H. Kernstine, J.A. Kern, K A. McLaughlin and T.L. Tseng, (2000) “Data mining: Medical and Engineering Case Studies”, Proceedings of the Industrial Engineering Research Conference, Cleveland, Ohio, May21-23, pp.1-7.
- [13] Larranaga, P., Sierra, B., Gallego, M.J., Michelena,M.J., Picaza, J.M.,(1997). Learning Bayesian networks by genetic algorithms: a case study in the rediction of survival in malignant skin melanoma. Proc. Artificial Intelligence in Medicine Europe .

Structural Analysis of a Milling Cutter Using FEA

Chittibomma. Tirumalaneelam¹, Tippa Bhimasankara Rao²

¹PG Student, Department Of Mechanical Engineering, Nimra Institute Of Science And Technology

² HOD, Department Of Mechanical Engineering, Nimra Institute Of Science And Technology, Vijayawada, AP, INDIA

Abstract:

Milling is a process of producing flat and complex shapes with the use of multi-tooth cutting tool, which is called a milling cutter and the cutting edges are called teeth. The axis of rotation of the cutting tool is perpendicular to the direction of feed, either parallel or perpendicular to the machined surface. The machine tool that traditionally performs this operation is a milling machine. Milling is an interrupted cutting operation: the teeth of the milling cutter enter and exit the work during each revolution. This interrupted cutting action subjects the teeth to a cycle of impact force and thermal shock on every rotation. The tool material and cutter geometry must be designed to withstand these conditions. Cutting fluids are essential for most milling operations. In this Paper the design aspects of milling cutter is analyzed. The objective considered is the design and modeling of milling cutter and to analyse various stress components acting on it. Various designing strategies are considered to design the effective milling cutter like outer diameter, inner diameter, radius, teeth angle etc. The design and analysis is carried out using the softwares like CATIA V5 and ANSYS.

Keywords: ANSYS, CATIA, cutting fluids, cutting edges, High Speed Steel, Milling Speed, machined surfaces, surface milling cutter.

I. INTRODUCTION

Milling, for example, has its own particularities, such as variation on the unreformed chip thickness (h), interrupted cuts, etc. Models developed for turning and adapted to milling, working with average chip thickness, can yield reasonable results in terms of force. There are operations, however, where a more accurate result is needed and then, the discrepancies may become unacceptable. That is the case with high speed milling, which uses very low chip thickness. In this case, the cutting edge radius almost equals the unreformed chip thickness and the rake angle tends to be highly negative. The material seems to be removed like in abrasive processes (Shaw 1996). Additionally, the main parameters describing the models are a function of other ones related to the tool (material, geometry, coating, etc.) and the machine (rigidity, speed, position control, etc.). In order to investigate the end milling process in some cutting conditions, at any particular combination tool-machine-work piece, a simple and fast method is needed to find the main parameters of the classical existing models and study some new ones. Milling is a process of producing flat and complex shapes with the use of multi-tooth cutting tool, which is called a milling cutter and the cutting edges are called teeth. The axis of rotation of the cutting tool is perpendicular to the direction of feed, either parallel or perpendicular to the machined surface. The machine tool that traditionally performs this operation is a milling machine. Milling is an interrupted cutting operation: the teeth of the milling cutter enter and exit the work during each revolution. This interrupted cutting action subjects the teeth to a cycle of impact force and thermal shock on every rotation. The tool material and cutter geometry must be designed to withstand these conditions. Cutting fluids are essential for most milling operations.

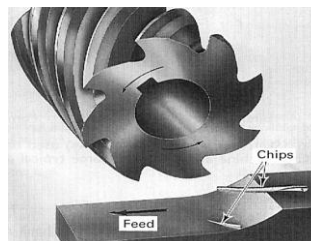


Fig 1: Milling Cutter

1.1 Types of milling

There are two basic types of milling, are as follows

- Down (climb) milling: It is type of milling in which the cutter rotation is in the same direction as the motion of the work piece being fed. In down milling, the cutting force is directed into the work table, which allows thinner work parts to be machined. Better surface finish is obtained but the stress load on the teeth is abrupt, which may damage the cutter. In conventional milling, friction and rubbing occur as the insert enters into the cut, resulting in chip welding and heat dissipation into the insert and work piece. Resultant forces in conventional milling are against the direction of the feed. Work-hardening is also likely to occur.

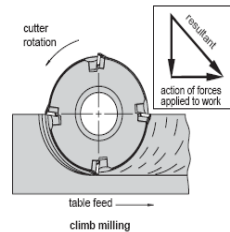


Fig 2: Climb Milling

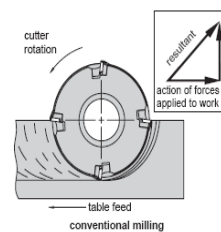


Fig 3: Conventional Milling

- Up (conventional) milling: It is the type of milling in which the work piece is moving towards the cutter, opposing the cutter direction of rotation. In up milling, the cutting force tends to lift the work piece. The work conditions for the cutter are more favorable. Because the cutter does not start to cut when it makes contact (cutting at zero cut is impossible), the surface has a natural waviness. The insert enters the work piece material with some chip load and produces a chip that thins as it exits the cut. This reduces the heat by dissipating it into the chip. Work-hardening is minimized. Climb milling is preferred over conventional milling in most situations.

1.2 Milling of complex surfaces

Milling is one of the few machining operations, which are capable of machining complex two and three-dimensional surfaces, typical for dies, molds, cams, etc. Complex surfaces can be machined either by means of the cutter path (profile milling and surface contouring), or the cutter shape (form milling).

- Form milling: In form milling, the cutting edges of the peripheral cutter (called form cutter) have a special profile that is imparted to the work piece. Cutters with various profiles are available to cut different two-dimensional surfaces. One important application of form milling is in gear manufacturing.
- Profile milling: In profile milling, the conventional end mill is used to cut the outside or inside periphery of a flat part. The end mill works with its peripheral teeth and is fed along a curvilinear path equidistant from the surface profile.
- Surface contouring: The end mill, which is used in surface contouring has a hemispherical end and is called ball-end mill. The ball-end mill is fed back and forth across the work piece along a curvilinear path at close intervals to produce complex three-dimensional surfaces. Similar to profile milling, surface contouring require relatively simple cutting tool but advanced, usually computer-controlled feed control system.

II. Classification of milling cutters according to their design

- HSS cutters: Many cutters like end mills, slitting cutters, slab cutters, angular cutters, form cutters, etc., are made from high-speed steel (HSS).
- Brazed cutters: Very limited numbers of cutters (mainly face mills) are made with brazed carbide inserts. This design is largely replaced by mechanically attached cutters.
- Mechanically attached cutters: The vast majority of cutters are in this category. Carbide inserts are either clamped or pin locked to the body of the milling cutter.

III. Geometry of milling cutter

The milling cutter is a multiple point cutting tool. The cutting edge may be straight or in the form of various contours that are to be reproduced upon the work piece. The relative motion between the work piece and the cutter may be either axial or normal to the tool axis. In some cases a combination of the two motions is used. For example, form-generating milling cutters involve a combination of linear travel and rotary motion. The figure below shows the various angles and geometry of a milling cutter.

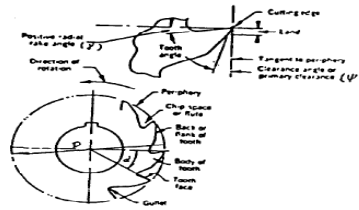


Fig 4: A Plain Milling Cutter

IV. THE GENERATED MODEL OF A MILLING CUTTER USING CATIA

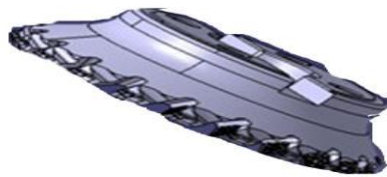


Fig 5: 3D-Model of milling cutter

V. ANALYSIS OF MILLING CUTTER

The basic steps for performing analysis are listed below:

- Create the model geometry and mesh
- Identify the contact pairs
- Designate contact and target surfaces
- Define the target surface
- Define the contact surface
- Set the element KEYOPTS and real constants
- Define/control the motion of the target surface (rigid-to-flexible only)
- Apply necessary boundary conditions
- Define solution options and load steps
- Solve the contact problem
- Review the results

VI. RESULTS & DISCUSSION

- CASE 1: Analysis of High Speed Steel Milling cutter for $W=10000$ N

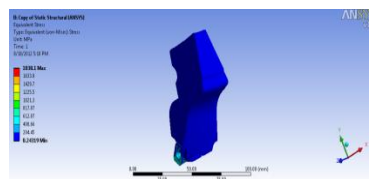


Fig 6: Stress values

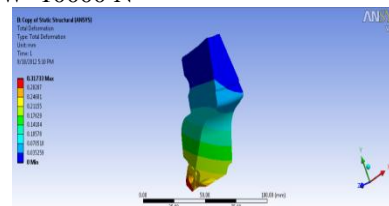


Fig 7: Deformation

- CASE 2: Analysis of High Speed Steel Milling cutter for $W=250$ N

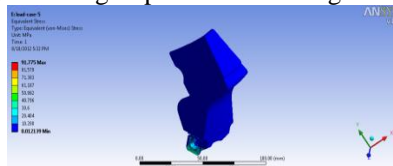


Fig 8: Stress values

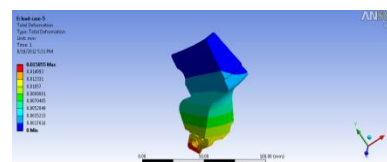


Fig 9: Deformation

- CASE 3: Analysis of Tungsten Carbide Milling cutter for $W=10000$ N

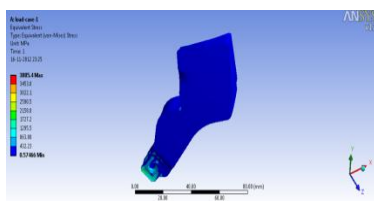


Fig 10: Stress value

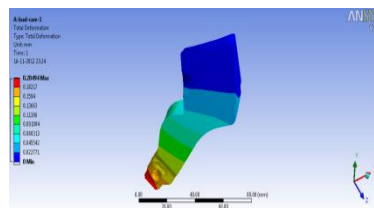


Fig 11: Deformation

- CASE 4: Analysis of Tungsten Carbide cutter for W=250 N
-

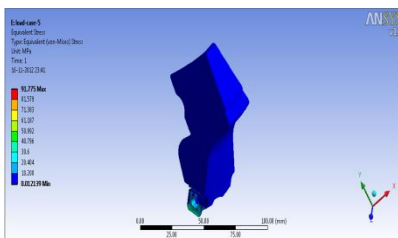


Fig 12: Stress values

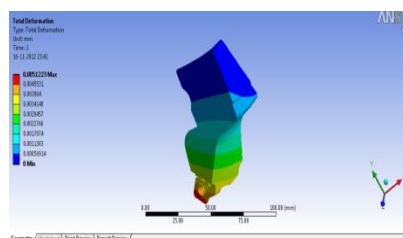


Fig 13: Deformation

SR.NO.	LOAD	STRESS	STRAIN
1	10000	3885.4	0.20494
2	250	91.775	0.005122

Table 1: Load vs Stress for High Speed steel

SR.NO.	LOAD	STRESS (Model)	STRESS (Theoretical)
1	10000	3676.4	2209.4
2	250	91.775	55.04

Table 2: Load vs Stress for Tungsten Carbide

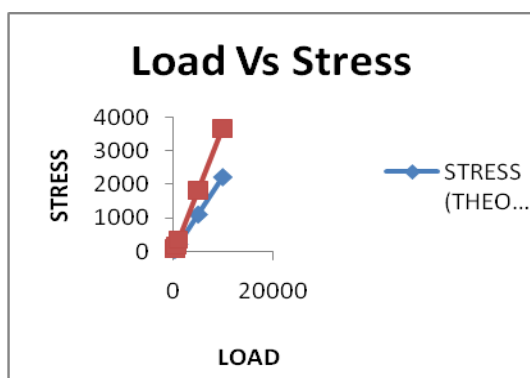


Fig 14: Load vs Stress for High Speed steel.

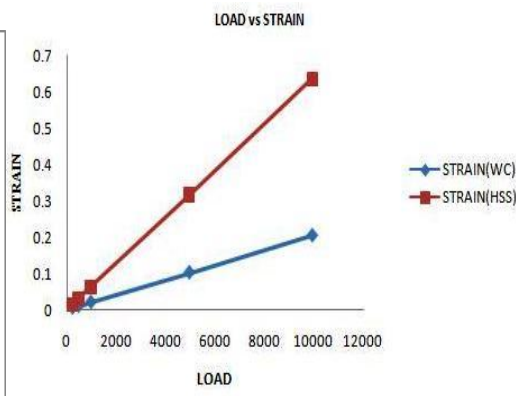


Fig 15: Load vs Stress for Tungsten Carbide

VII. Conclusion

In this study the design and analysis is carried out for two different cutter materials and they are High Speed Steel and Tungsten Carbide. In this analysis the loads acting on the cutter and speed is varied and the results obtained are compared. Finally the design and analysis is carried out using the software's CATIA V5, ANSYS. It could even be ventured that this approach can be used to design any complex mechanical component or system. Specifically for the cutter design, it produced the cutting variables that yield the minimum cost of manufacturing. The different design activities, such as design, solid modelling, and finite element analysis, have been integrated. As is evident, approach presented in this paper is flexible and easy to use.

REFERENCES

- [1]. Mr. John L. Yang & Dr. Joseph C. Chen; 'A Systematic Approach for Identifying Optimum Surface Roughness Performance in End-Milling Operations'. Journal of Industrial Technology, Volume 17, Number 2-February 2001 to April 2001.
- [2]. Abdel Badie Sharkawy, "Prediction of Surface Roughness in End Milling Process Using Intelligent Systems": A Comparative Study Hindawi Publishing Corporation Applied Computational Intelligence and Soft Computing Volume 2011, Article ID 183764, 18 pages.
- [4]. Abbas Fadhel Ibraheem, Saad Kareem Shather & Kasim A. Khalaf, "Prediction of Cutting Forces by using Machine Parameters in end Milling Process", Eng.&Tech. Vol.26.No.11, 2008.
- [5]. S. Abainia, M. Bey, N. Moussaoui and S. Gouasmia." Prediction of Milling Forces by Integrating a Geometric and a Mechanistic Model", Proceedings of the World Congress on Engineering 2012 Vol III WCE 2012, July 4 - 6, 2012, London, U.K.
- [6]. Md. Anayet u patwari, a.k.m. nurul amin, waleed f. Faris, 'prediction of tangential cutting force in end milling of Medium carbon steel by coupling design of experiment and Response surface methodology'. Journal of mechanical engineering, vol. Me 40, no. 2, December 2009 Transaction of the mech. Eng. Div., the institution of engineers, Bangladesh.
- [7]. Smaoui, M.; Bouaziz, z. & Zghal, A., 'Simulation of cutting forces for complex surfaces in Ball-End milling', Int j simul model 7(2008) 2,93-105.
- [8]. F. CUS, U. ZUPERL and M. MILFELNER, "Dynamic Neural Network Approach for Tool Cutting Force Modelling of End Milling Operations. Journal of Material Processing and Technology 95 pp. 30 – 39.
- [9]. Mohan, L. V. Profile Corrections for relieving tool for form relieved milling cutters. *Proceedings of the 12th All India Machine Tool Design and Research Conference 1986*, Dec. 1&12, pp. 2255228.
- [10]. Davies, R. Bonding cemented carbide milling cutter inserts. *Proceedings of Materials Selection & Design*, London, July, 1985..
- [11]. Granger, C. Never too old to pick up milling tips. *Machinery Prod, Eng. 1991,149(3797), 1617, 19-20*
- [12]. Agullo-Bathe, J., Cardona-Foix, S. and Vinas-Sanz, C. *On the design of milling cutters or grinding wheels for twist drill manufacture: A CAD approach*. Proceedings of the 25th International Machine Tool Design and Research Conference, April 22-24, 1985, pp. 315-320.

A Review Paper on Various Approaches for Image Mosaicing

Ms. Parul M.Jain¹, Prof. Vijaya K.Shandliya²

¹, M.E. (C.S.E.) First Year, Sipna College Of Engineering & Technology, Amravati.¹

²Professor, Computer Science & Engineering Department, Sipna College Of Engineering & Technology, Amravati

Abstract

Image mosaicing is one of the most important subject of research in computer vision. Image mosaicing requires the integration of direct methods and feature based methods. Direct methods are found to be useful for mosaicing large overlapping regions, small translations and rotations while feature based methods are useful for small overlapping regions. Feature based image mosaicing is combination of corner detection, corner matching, motion parameters estimation and image stitching. In this paper we present a review on different approaches for image mosaicing and the literature over the past in the field of image mosaicing methods. We take an overview on the various methods for image mosaicing.

Keywords: Direct method, feature based method, homography, image registration, image wrapping, image compositing, pixel blending.

I. INTRODUCTION

An Image mosaic is a synthetic composition generated from a sequence of images and it can be obtained by understanding geometric relationships between images. The geometric relations are coordinate transformations that relate the different image coordinate systems. By applying the appropriate transformations via a warping operation and merging the overlapping regions of warped images, it is possible to construct a single image indistinguishable from a single large image of the same object, covering the entire visible area of the scene. This merged single image is the motivation for the term mosaic. Various steps in mosaicing are feature extraction and registration, stitching and blending. Image registration refers to the geometric alignment of a set of images. The set may consist of two or more digital images taken of a single scene at different times, from different sensors, or from different viewpoints. The goal of registration is to establish geometric correspondence between the images so that they may be transformed, compared, and analyzed in a common reference frame. This is of practical importance in many fields, including remote sensing, medical imaging, and computer vision [1]. Registration methods can be loosely divided into the following classes: algorithms that use image pixel values directly, e.g., correlation methods [2]; algorithms that use the frequency domain, e.g., fast Fourier transform based (FFT-based) methods [3]; algorithms that use low-level features such as edges and corners, e.g., feature based methods [1]; and algorithms that use high-level features such as identified (parts of) objects, or relations between features, e.g., graph-theoretic methods [1]. The registration method presented uses the Fourier domain approach to match images that are translated and rotated with respect to one another. The algorithm uses the property of phase correlation which gives the translation parameters between two images if there is no other transformation between the images other than translation, by showing a distinct peak at the point of the displacement [4]. The next step, following registration, is image stitching. Image integration or image stitching is a process of overlaying images together on a bigger canvas. The images are placed appropriately on the bigger canvas using registration transformations to get the final mosaic.

II. LITERATURE REVIEW

Registration and mosaicing of images have been in practice since long before the age of digital computers. Shortly after the photographic process was developed in 1839, the use of photographs was demonstrated on topographical mapping [5]. Images acquired from hill-tops or balloons were manually pieced together. After the development of airplane technology (1903) aerophotography became an exciting new field. The limited flying heights of the early airplanes and the need for large photo-maps, forced imaging experts to construct mosaic images from overlapping photographs. This was initially done by manually mosaicing [6] images which were acquired by calibrated equipment. The need for mosaicing continued to increase later in history as satellites started sending pictures back to earth. Improvements in computer technology became a natural motivation to develop computational techniques and to solve related problems. The construction of

mosaic images and the use of such images on several computer vision/graphics applications have been active areas of research in recent years. There have been a variety of new additions to the classic applications mentioned above that primarily aim to enhance image resolution and field of view. Image-based rendering [7] has become a major focus of attention combining two complementary fields: computer vision and computer graphics [8]. In computer graphics applications images of the real world have been traditionally used as environment maps. These images are used as static background of synthetic scenes and mapped as shadows onto synthetic objects for a realistic look with computations which are much more efficient than ray tracing. In early applications such environment maps were single images captured by fish-eye lenses or a sequence of images captured by wide-angle rectilinear lenses used as faces of a cube. Mosaicing images on smooth surfaces (e.g. cylindrical or spherical) allows an unlimited resolution also avoiding discontinuities that can result from images that are acquired separately. Such immersive environments (with or without synthetic objects) provide the users an improved sense of presence in a virtual scene. A combination of such scenes used as nodes allows the users to navigate through a remote environment. Computer vision methods can be used to generate intermediate views between the nodes. As a reverse problem the 3D structure of scenes can be reconstructed from multiple nodes. Among other major applications of image mosaicing in computer vision are image stabilization, resolution enhancement, video processing (e.g. video compression, video indexing).

III. IMAGE MOSAICING METHODS

Image mosaicing methods can be classified broadly into direct method and feature based method. Direct Method uses information from all pixels. It iteratively updates an estimate of homography so that a particular cost function is minimized. Sometimes Phase-Correlation is used to estimate the a few parameters of the homography. In Feature Based Method a few corresponding points are selected on the two images and homography is estimated using these reliable points only. Feature Based Methods are in general more accurate. It can handle large disparities. Direct methods, may not converge to the optimal solution is the presence of local minima. For reliable performance direct methods rely on feature based initialization. Feature based methods [9] mosaic the images by first automatically detecting and matching the features in the source images, and then warping these images together. Normally it consists of three steps: feature detection and matching, local and global registration, and image composition.

Feature detection and matching aims to detect features and then match them. Local and global registration starts from these feature matches, locally registers the neighboring images and then globally adjusts accumulated registration error so that multiple images can be finely registered. Image composition blends all images together into a final mosaic. Direct methods [10] attempt to iteratively estimate the camera parameters by minimizing an error function based on the intensity differences in the area of overlap. But this type of methods needs initialization, either by correlation or by manually setting some corresponding points. It is hard for the user to manually set the corresponding points correctly especially when the photographed scene does not have planar faces while Feature Based Methods mosaic the images by detecting the features in the images automatically, matching these features, and then creating the final mosaic image by warping other images related to one base image. Direct methods are useful for mosaicing large overlapping regions, small translations and rotations. Feature based methods can usually handle small overlapping regions and in general tend to be more accurate but computationally intensive.

IV. IMAGE MOSAICING PROCESS

The image mosaicing procedure generally includes three steps. First, we register input images by estimating the homography, which relates pixels in one frame to their corresponding pixels in another frame. Second, we warp input frames according to the estimated homographies so that their overlapping regions align. Finally, we paste the warped images and blend them on a common mosaicing surface to build the panorama result.

- 4.1. Image Registration:** given a set of N images $\{I_1, I_2, \dots, I_N\}$ with a partial overlap between at least two images, compute an image-to-image transformation that will map each image I_2, \dots, I_N into coordinate system of I_1 .
- 4.2. Image Warping:** warp each image I_2, \dots, I_N using the computed transformation.
- 4.3. Image Interpolation:** resample the warped image.
- 4.4. Image Compositing:** blend images together to create a single image on the reference coordinate system.

4.5 Image Registration

Image registration is the task of matching two or more images. It has been a central issue for a variety of problems in image processing [11] such as object recognition, monitoring satellite images, matching stereo images for reconstructing depth, matching biomedical images for diagnosis, etc. Registration is also the central task of image mosaicing procedures. Carefully calibrated and prerecorded camera parameters may be used to eliminate the need for an automatic registration. User interaction also is a reliable source for manually registering images (e.g. by choosing corresponding points and employing necessary transformations on screen with visual feedback). Automated methods for image registration used in image mosaicing literature can be categorized as follows:

Feature based [12] methods rely on accurate detection of image features. Correspondences between features lead to computation of the camera motion which can be tested for alignment. In the absence of distinctive features, this kind of approach is likely to fail.

Exhaustively searching for a best match for all possible motion parameters can be computationally extremely expensive. Using hierarchical processing (i.e. coarse-to-fine [13]) results in significant speed-ups. We also use this approach also taking advantage of parallel processing for additional performance improvement.

Frequency domain approaches for finding displacement and rotation/scale are computationally efficient but can be sensitive to noise. These methods also require the overlap extent to occupy a significant portion of the images (e.g. at least 50%).

Iteratively adjusting camera-motion parameters leads to local minimums unless a reliable initial estimate is provided. Initial estimates can be obtained using a coarse global search or an efficiently implemented frequency domain approach.

4.6 Warping in the Discrete Domain

Forward and reverse mapping

In the forward mapping the source image is scanned pixel by pixel, and copies them to the appropriate location in the destination image. The reverse mapping goes through the destination image, pixel by pixel, and samples the corresponding pixel from the source image. The main advantage of the reverse mapping is that every pixel in the destination image will have assigned an intensity value. In the forward mapping case, some of the pixels in the destination images may not be coloured, and would have to be interpolated [15].

Expansion and contraction problems

When working with digital images, we deal with a discrete space and quantized intensities. Warping an image in the discrete space has as a consequence dilations and contractions of the rectangular pixels, originating, in general, quadrilaterals. This expansion/contractions demands the use of convenient methods for estimating pixel intensities on the image result. Two different problems may arise. In the case of expansion some pixels have no intensity assigned. In the case of contraction, several original pixel may converge to a single one. In both cases we need to estimate the new pixel intensities. These two problems are two typical instances of image resampling. In the first case, expansion, we have to use interpolation techniques to estimate the intermediate pixel intensities. The contraction may originate aliasing problems. To limit its effect we can use anti-aliasing filters [16].

4.7 Image Compositing

Images aligned after undergoing geometric corrections most likely require further processing to eliminate remaining distortions and discontinuities. Alignment of images may be imperfect due to registration errors resulting from incompatible model assumptions, dynamic scenes, etc. Furthermore, in most cases images that need to be mosaiced are not exposed evenly due to changing lighting conditions, automatic controls of cameras, printing/scanning devices, etc. These unwanted effects can be alleviated during the compositing process. The main problem in image compositing is the problem of determining how the pixels in an overlapping area should be represented. Finding the best separation border between overlapping images has the potential to eliminate remaining geometric distortions. Such a border is likely to traverse around moving objects avoiding double exposure. The uneven exposure problem can be solved by histogram equalization, by iteratively distributing the edge effect on the border to a large area, or by a smooth blending function [14].

A particular case of image combination is the function *dissolve* characterised by

$$I = \text{Dissolve } a(I_1 I_2) = (1 - a)I_1 + aI_2.$$

where a is in the interval $[0, 1]$. We may notice that for $a = 0$, we have

$$I = \text{Dissolve } 0 (I_1 I_2) = I_1$$

and for $a = 1$

$$I = \text{Dissolve } 1 (I_1 I_2) = I_2$$

For other values of a , the image result is the weighted average of the two images, as illustrated in Figure below. The value of a is constant, being independent of the position of the pixel to be combined.

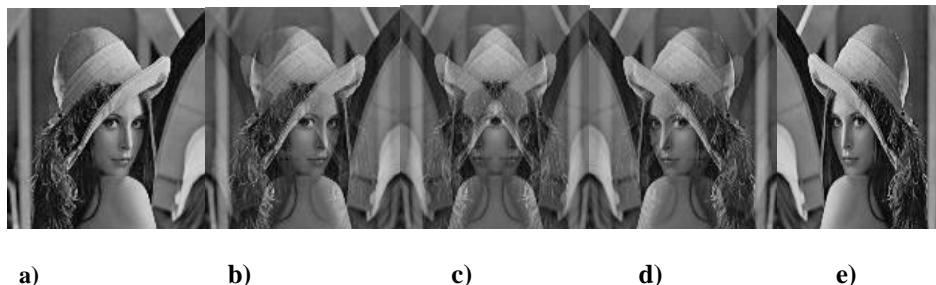


Image dissolving: a) Image(I_1); b) Dissolve 0.25($I_1 I_2$); c) Dissolve 0.5($I_1 I_2$); d) Dissolve 0.75($I_1 I_2$); e) Image (I_2).

4.8 Pixel Blending

Once the correspondences between input images have been correctly aligned, inputs are warped onto the common mosaicing image surface according to the estimated homographies and then merged to build the output panorama. However, due to exposure differences, misregistrations or even movement of objects in the scene, merging warped inputs is not simply an averaging process between overlapping pixels. A better approach is to take a weighted averaging that assigns pixels closer to the center of the image higher weights before blending them. Such a technique of blending pixels by a weighted averaging is called feathering [14], and is helpful in overcoming the exposure differences between inputs. When integrated with the high dynamic range (HDR) radiance map and the exposure invariant feature-based image alignment method, it can even construct panoramas over tremendous exposure differences. Feathering can be performed within pixel color spaces, or in the gradient domain.

V. CONCLUSION

Image mosaicing is useful for a variety of tasks in vision and computer graphics. Due to the wide range of applications, image mosaicing is one of the important research area in the field of image processing. Here we have presented some of the very fundamental and basic techniques used in image mosaicing. This paper presents a complete process for image mosaicing.

REFERENCES

- [1] Lisa G. Brown. A survey of image registration techniques. *ACM Computing Surveys*, 24(4):325–376, December 1992.
- [2] D. I. Barnea and H. F. Silverman, "A class of algorithms for fast digital registration," *IEEE Trans. Comput.*, vol. C-21, pp. 179-186, 1972.
- [3] C. D. Kuglin and D. C. Hines, "The phase correlation image alignment method," in *Proc. IEEE 1975 Int. Conf. Cybernet. Society.*, New York, NY, pp. 163-165.
- [4] Q. Chen, M. Defrise, and F. Deconinck, "Symmetric phase-only matched filtering of Fourier- Mellin transforms for Image Registration and Recognition," *IEEE Transactions on Pattern Analysis and Machine Intelligence*, vol 16 No. 12 pp 1156-1168
- [5] P.R. Wolf. *Elements of Photogrammetry*. McGraw-Hill, 2 edition, 1983.
- [6] P. Kolonia. When more is better. *Popular Photography*, 58(1):30-34, Jan 1994.
- [7] S.B. Kang. A survey of image-based rendering techniques. Technical Report CRL 97/4, Digital Equipment Corp. Cambridge Research Lab, Aug 1997.
- [8] J. Lengyel. The convergence of graphics and vision. *Computer, IEEE Computer Society Magazine*, pages 46-53, July 1998.
- [9] Soo-Hyun CHO, Yun-Koo CHUNG and Jae Yeon LEE, Automatic Image Mosaic System Using Image Feature Detection and Taylor Series, In Proceedings of the 7th International Conference on Digital Image Computing: Techniques and Applications, Sydney, Australia, 2003, pp. 549-556.
- [10] R. Szeliski, Image Alignment and Stitching: A Tutorial, Technical Report MSR-TR- 2004-92, Microsoft Research (2004).
- [11] L. G. Brown. A survey of image registration techniques. *ACM Computing Surveys*, 24(4):325-376, 1992.
- [12] P. Dani S. Chaudhuri. Automated assembling of images: Image montage preparation. *Pattern Recognition*, 28(3):431-445, 1995.
- [13] P.J. Burt. Smart sensing within a pyramid vision. *Proceedings of the IEEE*, 76(8):1006- 1015, 1988.
- [14] P.J. Burt E.H. Adelson. A multiresolution spline with application to image mosaics. *ACM Transactions on Graphics*, 2(4):217-236, 1983.
- [15] R. Szeliski, "Video Mosaics for Virtual Environments", *IEEE Computer Graphics and Applications*, Vol 16, No 2, 1996.
- [16] S. Kang, "A Survey of Image-Based Rendering Techniques," *Tech. Report CRL 97/4, Digital Equipment Cooperation, Cambridge Research Lab, August 1997.*

The Distance Measurement by Using RSSI of Wireless Sensor Network

Yi-Jen Mon

Department of Computer Science and Information Engineering, Taoyuan Innovation Institute of Technology,
Chung-Li, Taoyuan, 320, Taiwan

Abstract

In this paper, the measurement of received signal strength indication (RSSI) is demonstrated by using wireless sensor network (WSN). This measurement is a basic technology which is varied according to distance of command device and client device. Many algorithms are developed based on this measurement of RSSI such as to develop many useful WSN's applications. The experimental results of WSN are demonstrated in this paper. Good effectiveness of distance measurements by using RSSI is achieved.

Keywords: Wireless sensor network (WSN), ZigBee, RSSI, Distance measurement.

I. INTRODUCTION

The low cost and low power consumption is main advantages of wireless sensor network (WSN). WSN is based on technologies of radio transceivers and receivers such as to achieve some useful information around the environment to develop many control techniques such as vehicle/building automation, home security, environmental monitoring, indoor location awareness/identification, etc. When many WSNs are deployed in large field, they can be automatically organized to form an ad hoc network to communicate with each other by means of some network topologies such as star, mesh and tree communication topologies [1, 2]. The standard of WSN is followed the standard of IEEE 802.15.4/ZigBee. So many people can also call WSN as ZigBee. The ZigBee builds upon the IEEE 802.15.4 standard which defines the physical and medium access control (MAC) layers for low cost, low rate personal area networks and provides a framework for application programming in the application layer [3, 4].

Many indoor applications of distance measurement such as monitors, identifications, etc. are based on ZigBee. Many distance measurement algorithms are developed such as to estimate the location of client device. Among some conventional distance measurement techniques, the received signal strength indication (RSSI) is most interested [5]. In particular, RSSI can be measured in the 802.15.4 physical standard which reports the signal strength associated with a received packet to higher layers. The RSSI values of the transmitted signals recorded at different client devices. In this paper, the good performances of distance measurement by RSSI of WSN are demonstrated. Meanwhile, the values of RSSI are shown in computer's screen.

II. INTRODUCTION TO WSN

The ZigBee Alliance is an association of companies working together to develop standards (and products) for reliable, cost-effective, low-power wireless networking. ZigBee technology will probably be embedded in a wide range of products and applications across consumer, commercial, industrial and government markets worldwide. ZigBee builds upon the IEEE 802.15.4 standard which defines the physical and Medium Access Control (MAC) layers for low cost, low rate personal area networks. ZigBee defines the network layer specifications for star, tree and mesh network topologies and provides a framework for application programming in the application layer. In this paper, the subroutines are provided by *Jennic Inc.* to develop the distance measurement applications. All these subroutines include different type of application program interface (API). For example, the Queue API provides a queue-based interface between an application and both the IEEE 802.15.4 stack and the peripheral hardware drivers. The API interacts with the IEEE 802.15.4 stack via the *Jennic* 802.15.4 Stack API (which sits on top of the 802.15.4 stack). The most important part of APIs is Application Queue API. The Application Queue API handles interrupts coming from the MAC sub-layer of the IEEE 802.15.4 stack and from the integrated peripherals of the wireless microcontroller, saving the application from dealing with interrupts such as MAC Common Part Sublayer (MCPS) interrupts, MAC sub-Layer Management Entity (MLME) interrupts and Hardware interrupts [6, 7]. A variety of network topologies are possible with IEEE 802.15.4. A network must consist of a minimum of two devices, one is command device and some client devices. The basic type of network topology is the Star topology. A Star topology consists of a central personal area network (PAN) command device surrounded by the other client devices of the network [6, 7].

III. EXPERIMENTAL RESULTS FOR DISTANCE MEASUREMENT

The free Code::Blocks software is used in distance measurement of RSSI of WSN. At first, the program of command device is developed then the program of client device is developed consequently. Every network must have one and only one PAN command device, and one of the tasks in setting up a network is to select and initialize this command device. The personal area network identification (PAN-ID) must be set adequately in program. The development board can provide all the software tools and hardware required to get the first-hand experience with WSN. For the software, free Application Programming Interface (API) packages is provided to the peripheral devices on the single-chip IEEE 802.15.4 compliant wireless microcontrollers. It details the calls that may be made through the API in order to set up, control and respond to events generated by the peripheral blocks, such as UART, GPIO lines and Timers among others. The software invoked by this API is present in the on-chip ROM. This API does not include support for the ZigBee WSN MAC hardware built into the device; this hardware is controlled using the MAC software stack that is built into the on-chip ROM [6, 7]. In this paper, the ZigBee WSNs are used to design for the distance measurement by means of RSSI of WSN.

At first, the program of RSSI test is demonstrated and shown in Fig. 1. From the results, the values of RSSI will be varied according to the distance between the command and client device. In Fig. 2 (a), the near distance test shows the value of RSSI transformed into digital value of LQI as 255. In Fig. 2 (b), the long distance test shows the value of RSSI as 102. In the programs, the actual analogue to digital values are normalized from 0 to 255. From this example, it demonstrates that the RSSI based WSN is successfully established, meanwhile, the good distance measurement performance is also possessed.

```

261
262
263 /* Check for anything on the MCPS upward queue */
264 do
265 {
266     psMcpsInd = psAppQApiReadMcpsInd();
267     if (psMcpsInd != NULL)
268     {
269         vProcessIncomingData(psMcpsInd);
270         vAppQApiReturnMcpsIndBuffer(psMcpsInd);
271     } while (psMcpsInd != NULL);
272
273 /* Check for anything on the MLME upward queue */
274 do
275 {
276     psMlmeInd = psAppQApiReadMlmeInd();
277     if (psMlmeInd != NULL)
278     {
279         vProcessIncomingMlme(psMlmeInd);
280         vAppQApiReturnMlmeIndBuffer(psMlmeInd);
281     } while (psMlmeInd != NULL);
282
283 /* Check for anything on the AHI upward queue */
284 do
285 {
286     psAHI_Ind = psAppQApiReadHwInd();
287     if (psAHI_Ind != NULL)
288     {
289         vProcessIncomingHwEvent(psAHI_Ind);
290         vAppQApiReturnHwIndBuffer(psAHI_Ind);
291     } while (psAHI_Ind != NULL);
292
293
294
    
```

Fig. 1. The program of RSSI for distance measurement

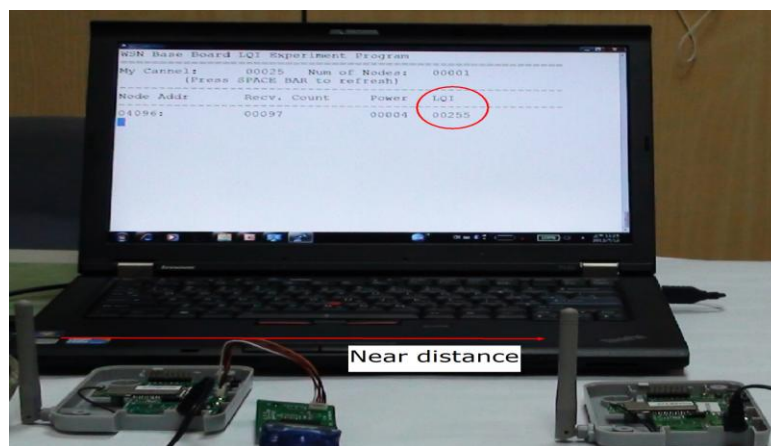


Fig. 2 (a) The near distance test of RSSI

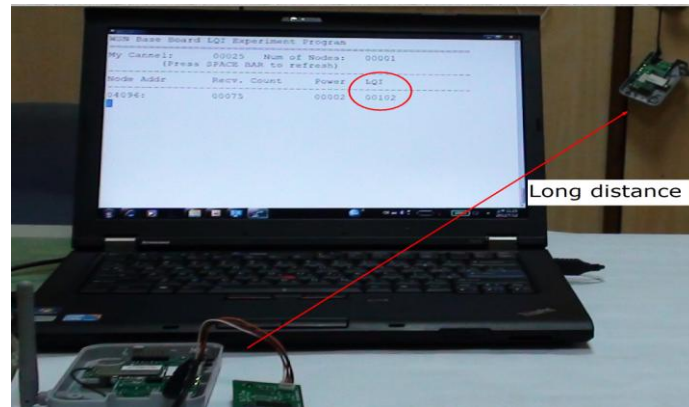


Fig. 2 (b) The long distance test of RSSI

IV. CONCLUSION

In this paper, the design method for the application of distance measurement is established by using the measurement programs of received signal strength indicator (RSSI) of IEEE 802.15.4/ZigBee wireless sensor network (WSN). It demonstrates that the RSSI based WSN is successfully established, meanwhile, the good distance measurement performance is also possessed.

ACKNOWLEDGMENTS:

This paper is partially funded by teacher's research project of Taoyuan Innovation Institute of Technology.

REFERENCES

- [1]. Y. C. Hu, D. B. Johnson and A. Perrig, "SEAD: secure efficient distance vector routing for mobile wireless ad hoc networks," *Ad Hoc Networks*, vol. 1, pp. 175-192, 2003.
- [2]. M. Abolhasan, T. Wysocki and E. Dutkiewicz, "A review of routing protocols for mobile ad hoc networks," *Ad Hoc Networks*, vol. 2, pp. 1-22, 2004.
- [3]. I. J. Su, C. C. Tsai and W. T. Sung, "Area temperature system monitoring and computing based on adaptive fuzzy logic in wireless sensor networks," *Applied Soft Computing*, vol. 12, pp. 1532-1541, 2012.
- [4]. L. Aguilar, G. Licea and J. A. García-Macías, "An experimental wireless sensor network applied in engineering courses," *Computer Applications in Engineering Education*, vol. 19, pp. 777-786, 2011.
- [5]. K. Lu, X. Xiang, D. Zhang, R. Mao and Y. Feng, "Localization algorithm based on maximum a posteriori in wireless sensor networks," *International Journal of Distributed Sensor Networks*, Article ID 260302, 2012. ([doi:10.1155/2012/260302](https://doi.org/10.1155/2012/260302))
- [6]. Y. J. Mon, C. M. Lin and I. J. Rudas, "Wireless Sensor Network (WSN) Control for Indoor Temperature Monitoring," *Acta Polytechnica Hungarica*, vol. 9, no. 6, pp. 17-28, 2012.
- [7]. Jennic Application Queue API Reference Manual (JN-RM-2025), Jennic Inc., 2006.

A Distributed Decisive Support Disease Prediction Algorithm for E-Health Care with the Support of JADE

O.Saravanan¹, Dr.A.Nagappan²

¹research Scholar, Vinayaka Missions University, Salem, TN, India

²research Guide & Principal, V.M.K.V Engineering College, Salem, TN, India

Abstract:

A Distributed decisive support disease prediction system for E-Health Care with the support of JADE (java agent development environment). The proposed solution supports the doctors to access the patient details from anywhere in the world easily. Due to the data diversity, it is not possible to maintain all the patient details in a single location. This solution makes easier to access the patient details independent of location and it produces decisive support information for doctors. Sometimes the doctor may not be sure about any disease that the patient get affected, in such situations the doctor need some assistance about other patient history with similar symptoms. For example cough and cold may be a symptom for fever but those symptoms also supports for other unfamiliar diseases also. So that the doctor can't take any decision by simply seeing few symptoms, on that stage the doctor may need to access patient histories of other hospitals or branches. The Jade framework makes easier to access the data instantly within short time. This framework maintains many containers and different agents to fetch different data from different location. Using those mobile agents all the data from remote locations is fetched and we use modern support and count methods to make decision. For the purpose of decision support, this methodology proposes a new support and count methods. It maintains a different patient database, whenever a new query is made then use database initially and also whenever fetch data from remote location it will be updated to related database also. Using the patterns or symptoms of the patient framework calculates probability value for each disease in order to predict by which the patient has affected. This solution reduces the time of moving agent from and to and increases the efficiency of the system.

Keywords: Mobile Agents, Agent Creation, E-Health Care, Agent Management, Decisive Support algorithm, FIPA, JADE.

I. INTRODUCTION

Nowadays there are various researches for medical solutions due to the increase of population and also the incoming of new kind of diseases. Day to day people are suffering with new diseases which cannot be identified by the doctor for prolong period. Still there are researches to identify diseases in a faster manner and to find solutions to them. In many cases the doctor's were find difficulty in identifying a disease or concluding a disease with the symptoms the patient have, because same set of symptoms may be support to more than one disease. For example cough and cold are symptoms of ordinary fever and also that are symptoms for tuberculosis. With these problems the doctors could not take a decision with the patient symptoms to proceed with treatment. Here, propose a decisive support disease prediction system for E-Health care using JADE environment. Java Agent Development Environment provides various features to create multiple agents using which an application can perform remote computation. It acts as a middleware between the application layer and data base layer. It is very useful in peer to peer and distributed environment where the data is distributed in many places. The agents developed using this environment can communicate with other agents and control them as necessary. The agent management system is used to control the lifecycles of other agents in the platform. The jade has functionalities to handle the events to be generated and handled, according to the event generated there are message can be fetched from the event and based on the generated message agent communication between other agents is carried out. Basically the environment has a main container where all agents are created and registered. The agents in the main container are controlled by another agent so it is launched very first and has a graphical user interface. The other containers in the distributed environment have to be registered first, so that

the distributed environment can be formed. The other containers can be registered using a command Boot with parameters container, host which specifies the internet protocol address of the machine where the main container runs. Once all other containers are registered with the main container then everything is ready for computation. Each ACL message contains agent id and other persistent values used by the agent to perform computation in the remote location. The agent location is identified by the location parameter using which the agent can distinguish between its home container and remote container. The agent performs the specified computation by identifying its location. The mobility behavior provided by the Jade environment makes easier to reduce the processing load in huge data processing environments and it reduces the time and scalability of the application. There may be any number of agents can be generated depend on the work load of the application and sent for remote execution.

The Agent Management System is responsible for the movement of agents from one location to other location with the help of ACL messages. Whenever an agent wants to move from one location it has to generate an ACL message, so that the agent will be moved to remote location by the Agent Management System. Decision support algorithm provides the benefit of getting into a conclusion about a patient by which he affected. It generates a probability value by which the decision is taken and it uses support and count methods to calculate the probability. There are various methods for decision support like apriori, frequent pattern etc. We propose a new one which generates probability with the support of frequent patterns.

II. LITERATURE REVIEW

Java agent Development environment has been used for various purposes. Its main area of application is networking and network security. There have been many publications with the help of JADE. Also the applications of jade extended to the area of data mining also. A Distributed framework using jade mobile agent environment is proposed to support the administrators to manage the network from the intrusions which are coming from inter and intranet [13]. The administrator will be able to analyze the kind of network threat coming to the network and according to that he can change the rules. It uses snort intrusion detection system and used alert database to store alerts.

New mobile agent based intrusion detection system is proposed which contains Intrusion Detection System on every network location [12]. It has a mobile agent environment to support distributed computing and each segment in the network has a sensor which captures the packets coming to the network and mobile agents move from different location and captured packets are delivered to the IDS using the agents. The intrusion detection system identifies the correctness of the packet. Spynet: This framework provides a solution to investigate crimes initiated by genuine users of the network [14]. It uses scattered network traffic data to identify the crimes. It uses the agents as a design unit in the distributed environment, so that the processing time, usage of bandwidth and overhead generated by communication. In this system additional agents can be created to reduce the work load, so that it reduces the scalability and increases the efficiency.

Web server with multi agent for medical practitioners by jade technology is proposed to support processing of bio signals like ECG, EMG, and EEG [19]. It helps the practioners to interact with other specialist to come to a conclusion. In this a multi agent system is proposed for content based retrieval of multimedia data [5]. It uses existing agent software components to fulfill the client requirements by adapting retrieved components. It has various levels as group, agent, module and code. Each level has its own responsibility and used for various purposes. Agent Based Software Engineering [7], proposed a method for Multi Agent System design, to reduce the time complexity in designing the multi agent system. It uses domain ontology and internal structure of the agents to design the multi agent system. By using this design of multi agent system will become easier with reduced cost. It reduces overall time and internal structure.

Multi agent Systems: A Modern Approach to Distributed Artificial Intelligence [2] is proposed, to get an intelligence using multiple agents which works in distributed manner. The evaluation of trust and reputation is computed with the interacting agents with dynamic behavior [15]. Here trust computation is performed dynamically and the agent should pass the trust computation process to perform its process in the remote location. This methodology reduces the risk of malicious agents attack, and also a load balancing algorithm is specified. With the help of mobile agents a distributed intrusion detection system is proposed in [18]. Here intrusion detection system runs on various locations of the network and captures the attack and logs to the database. The mobile agents are responsible for initializing the intrusion detection system, and fetching the log data from remote location. The administrator could control the IDS remotely with the help of mobile agents and he can infer some knowledge to improve the performance of the network.

III. EXISTING SYSTEM

There are various existing methodologies for the prediction of medical diseases, few of them have been discussed here. Prediction of medical diseases using radial basis function [20] is proposed by Hannan. They used artificial neural network and they trained 300 patient's symptoms. The radial basis function is used to predict the heart disease. A cardiovascular disease prediction system using genetic algorithm and neural network [21], used multilayered feed forward neural networks are used and genetic algorithm is used to determine the weight in less number of iterations. Improving the disease prediction using ontology [22], perform disease prediction based on crisp DRG features and fuzzy membership of patient diagnoses in the DRG groups. ICD-9 ontological similarity approach is used to compute fuzzy membership. In [23], an intelligent disease prediction system using data mining is discussed, using decision tree, naïve bayes and neural network. The methodologies here discussed are centralized in nature and more time consuming due to the amount of data to be processed. Keeping all those data in a single location makes the system scalable and more chance for single point failure. To overcome all those factors, here propose a distributed decisive support system for E-Health Care.

3.1 Proposed System

The proposed system contains four parts namely web server, web container, main agent container, remote container. The input to the web server through the web page symptoms given by the practitioner and output is through the web page as disease and probability values from the web server forwards the query and data to the main web container.

3.2 Multi-Agent Controller

Whenever a query rises, it identifies the location information about the other agent containers and number of agents necessary to process the query, to avoid unnecessary movement of agents to and from where no relevant data available.

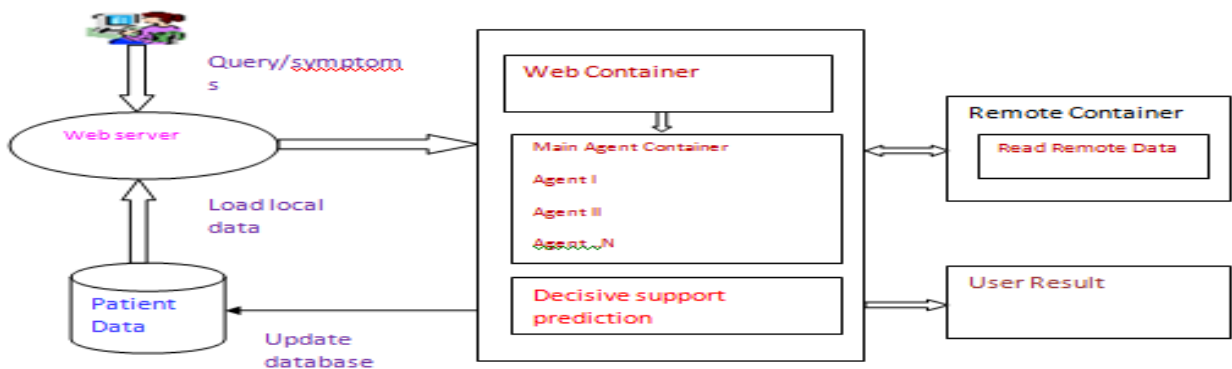


Figure1: System Architecture

The agent controller moves the agent only to the location where relevant data about the query is available. It generates the agents and moves them to remote container. The mobile agent reads the data from the remote data base when it reaches the remote container. After reading it once again returns to the main container and returns the data it read from the remote location.

3.3 Query Submission

The medical practitioner generates a query to the web server to get the disease probability for submitted query. He enters the set of symptoms and values of symptoms to through the web interface to the web server. For example if the patient affected by fever, it generates the temperature value ,and ECG details in case of chest pain , urine culture details in case of urinary tract infection (UTI) etc. Upon receiving such a query the web server reads the patient details and data from its local data base.

IV. DECISIVE SUPPORT PREDICTION ALGORITHM

The proposed algorithm reads both the agent fetched data and local data from the web server. First it identifies unique diseases from the dataset and unique pattern P_i from the whole data set D_s . For each pattern P_i in the data set D_s , It computes the number of matches N_i the pattern of symptoms with the whole data set D_s . The support value is the number of pattern matches it has with the whole data set. For each disease K_i , the probability is calculated as follows.

$$P(K_i) = (N_i/T_i) * n * \log 0$$

N_i - the support value ie Number of pattern matches for a particular disease pattern.
 T_i - total number of pattern for a particular disease pattern.
 n - Number of agent locations we used.

2.1 Algorithm

Step1: Read all patterns from local and remote fetched.

Step2: Identify Unique Disease K_i .

Step3: For each Disease K_i Select patterns (M_i) from the whole set affected by Disease K_i . Match the symptoms with the pattern set (M_i). Count number of matches as support N_i . Count total number of patterns T_i . Calculate probability as

$$P(K_i) = (N_i/T_i) * n * \log 0. \text{ End}$$

Step 4: Sort the Disease probability values.

Step5: select the highest probability valued disease.

Step6: Stop.

2.2 Results and Discussion

The proposed methodology used many number of mobile agents and generates good results compared to other algorithms and methodologies. Here set of values provided as input for prediction and the results returned by the framework.

Table 1: Shows the efficiency of algorithms according to number of records used

No. of Patterns/Inputs	Prediction quality
1 million	78 %
2 million	85 %
3 million	92 %
More	95.5 %

widal	tiredness	tr	pressure	sugar	colastrol
2	2	102	0		33
3	4	100	0	158	
4	3	101			
1	2	102	0	168	43
3	4	100	0	156	
4	1	101		320	
2	2	102	0		21
3	4	100	0	158	
4	3	101			35
1	2	102	0	168	
3	4	100	0	156	25
4	1	101		320	
2	2	102	0		45
3	4	100	0	158	

Figure 2: Shows the data set used for prediction.

Multi Agent Based Disease Prediction Using (JADE)
 SPECIFY SYMPTOMS VALUES

Widal	<input type="text" value="123"/>
Tirednes	<input type="text" value="12"/>
Temperature	<input type="text" value="102"/>
Blood Pressure	<input type="text" value="0"/>
Sugar	<input type="text" value="0"/>
Collastrol	<input type="text" value="0"/>
HP count	<input type="text" value="0"/>

Figure 3: Shows the web interface for input

Figure 3. Shows a part of web interface input and the remaining parameters has shown in the following Figure

Puzz Cell Count	0
Salt	0
Albumin	0
Vomiting	0
Headache	0
Stomach Pain	0
Wheezing	0
Cold	123

Predict

Figure 4: Shows the web input interface

Resultant Disease Probability Values

Disease	Probability
typhoid	1.0
fever	0.0
uti	0.0
tubor	0.0
diaria	0.0
sugar	0.0
BP	0.0

Figure 5: Shows the result of generated probability values

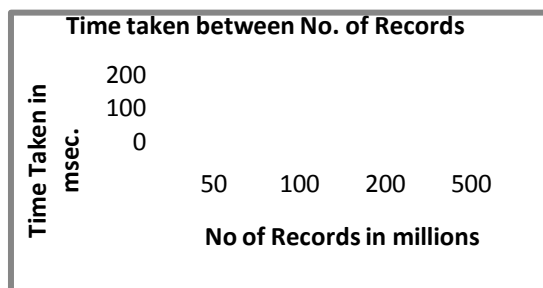


Figure 6: Graph shows the efficiency of algorithm

V. CONCLUSION

The proposed algorithm generates very good results. Here, 5 million records are used from 50 remote locations. This algorithm works faster even though more locations and containers and agents due to the reason why the main container maintains the meta data about the data exists in other locations, so that it moves only to particular locations where more data is relevant. This solution reduces the time and increases the efficiency of predicting disease.

REFERENCES

- [1]. Chiung-Hon Leon Lee, An agent-based software development method for developing an agent-based multimedia system, Multimedia Software Engineering, 2003.
- [2]. G. Weiss, A Modern Approach to Distributed Artificial Intelligence, pp. 79-120, MIT Press, 1999.
- [3]. J.D. Bronzino, A Distributed Computer System for Pediatric Primary Care, Ph.D. The Hartford Primary Care Consortium, Hartford, CT, IEEE 1997.
- [4]. Boston, MA, Pearson Education, Inc, The Tao of Network Security Monitoring Beyond Intrusion Detection, August 2005.
- [5]. Richard Bejtlich. Eoghan Casey, Handbook of Computer Crime Investigation –Forensic Tools and Technology, San Diego, California, Academic Press, 2002.
- [6]. Java Agents for Meta learning over Distributed Databases in AAA197 Workshop on AI Methods in Fraud and Risk Management, 1997.
- [7]. Margus oja, Agentbased Software Design, Proceedings of the Estonian Academy of Science Engineering, March 2001.
- [8]. JADE Graphical Interfaces, April 2004.
- [9]. Emerson F.A.Lima, An Approach to Modeling and Applying Mobile Agent Design Patterns, ACM Software Engineering, May 2004.

- [10]. Yang Kun, Security in mobile agent system, January 2000.
- [11]. JADE A FIPA compliant agent Framework, 1999.
- [12]. N.J. Prentice, Intrusion detection systems with Snort: Advanced IDS techniques using Snort, 2003.
- [13]. Asha Nagesh, Distributed Network Forensics using JADE Mobile Agent Framework, 2008.
- [14]. SpyNet: Network Intrusion Detection System, 2012
- [15]. Anupam Das, Secured Trust: A Dynamic Trust Computation Model for Secured Communication in Multiagent Systems, IEEE transaction on dependable and secure computing, 2012.
- [16]. Building Open Source Network Security Tools Components and Techniques, Mike D. Schiffman, 2003.
- [17]. Advanced IDS techniques using Snort, Rehman, 2003.
- [18]. Kannadiga, P, A distributed intrusion detection system using mobile agents, Software Engineering, Artificial Intelligence, Networking and Parallel/Distributed Computing, 2005.
- [19]. Saravanan.O, Web server with multi agent for medical practitioners by jade technology, 2012.
- [20]. Prediction of heart disease medical prescription using radial basis function, IEEE, 2010.
- [21]. Amma, Cardiovascular disease prediction system using genetic algorithm and neural network, ICCCA, 2012.
- [22]. Popeseu, Improving disease prediction using ICD-9 ontological features, IEEE, 2011.
- [23]. Palaniappan, Intelligent heart disease prediction system using data mining techniques, AICCSA, 2008.

DC Motor Control by ARM-Based Developer Suite

Yi-Jen Mon

Department of Computer Science and Information Engineering, Taoyuan Innovation Institute of Technology, Chung-Li, Taoyuan, 320, Taiwan, R. O. C.

Abstract

In this paper, the Advanced RISC Machine 9 (ARM9) based software of ARM developer suite (ADS) is utilized to control speed of DC motor. The educational kit of DMA 2440 is used to demonstrate the theoretical and experimental performances. The development procedure of ADS will be illustrated at first then an example of DC motor speed control is verified. The experimental result reveals that good DC motor speed control performance is possessed in this paper.

Keywords: ARM, DC motor, Speed control, ARM developer suite (ADS)

I. INTRODUCTION

Non-operation system (NOS) is easy to be implemented. Many industrial researches are developed which are based on central processing unit (CPU) of Advanced RISC Machine (ARM). For example, the research of face recognition technology based on ARM9 and Linux operating system can be found in [1]. The method of designing the control of an energy-efficient, knee-less, essentially planar, four-legged bipedal robot system based on ARM9 has been developed in [2].

In this paper, the ARM9 based Samsung S3C2440A CPU [3], ARM developer suite (ADS) [4] and educational development kit of DMA 2440 manufactured by DMATEK Ltd, Taiwan [5] are used to do experimental and educational DC motor control. The experimental results reveal that the good performances of DC motor speed control are possessed.

II. THE ARM DEVELOPER SUITE (ADS)

The ARM developer suite (ADS) is developed and is an integrated development environment (IDE) supported to us to compile a C program such as to achieve an optimized machine code of ARM target. The ADS is based on Metrowerks CodeWarrior IDE version 4.2. It has been tailored to support the ADS tool-chain. It includes ARM-specific configuration panels that enable us to configure the ARM development tools from the ADS IDE; and ARM-targeted project stationery that enables us to create basic ARM and Thumb projects from the ADS IDE. Although most of the ARM tool-chain is tightly integrated with the ADS IDE, there are a number of areas of functionality that are not implemented by the ARM version of the ADS IDE. In most cases, these are related to debugging, because the ARM debuggers are provided separately [4]. The diagram of ADS project window is shown in Fig. 1. The Editor window for C program of this paper is shown in Fig. 2. The Compile window for C program of this paper is shown in Fig. 3.

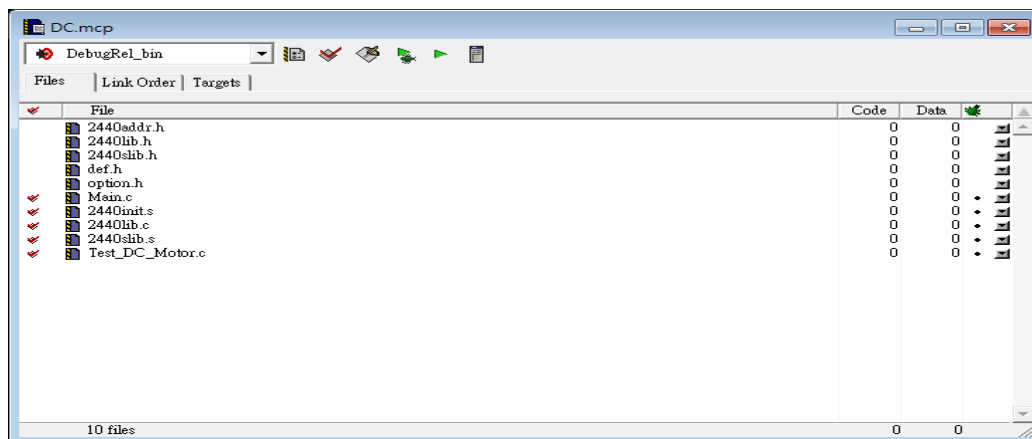


Fig. 1 The ADS project window diagram for DC motor control

```

Test_DC_Motor.c
{
    U16 HiRatio = 50;
    Uart_Printf("DC motor control Press +/- to adjust the speed\n");
    Set_PWM3(HiRatio);

    while(1)
    {
        U8 key;
        key = Uart_GetKey();

        if( key == '+' )
            HiRatio += (HiRatio<95)?5:(100-HiRatio);
        if( key == '-' )
            HiRatio -= (HiRatio>=5)?5:HiRatio;

        if( key == ESC_KEY ) break ;

        Set_PWM3(HiRatio);

        Uart_Printf("HiRatio%d\n",HiRatio);
    }

    Uart_Printf("DC Motor test end\n");
    rTCON = rTCON & ~(0xf<<16); // clear manual update bit, stop Timer3

    rGPBCON &= ~(3<<6);
    rGPBCON |= 1<<6; //output 0
    rGPBDAT &= ~(1<<3);
}
Line 22 Col 20

```

Fig. 2 The Editor window of C program for DC motor control

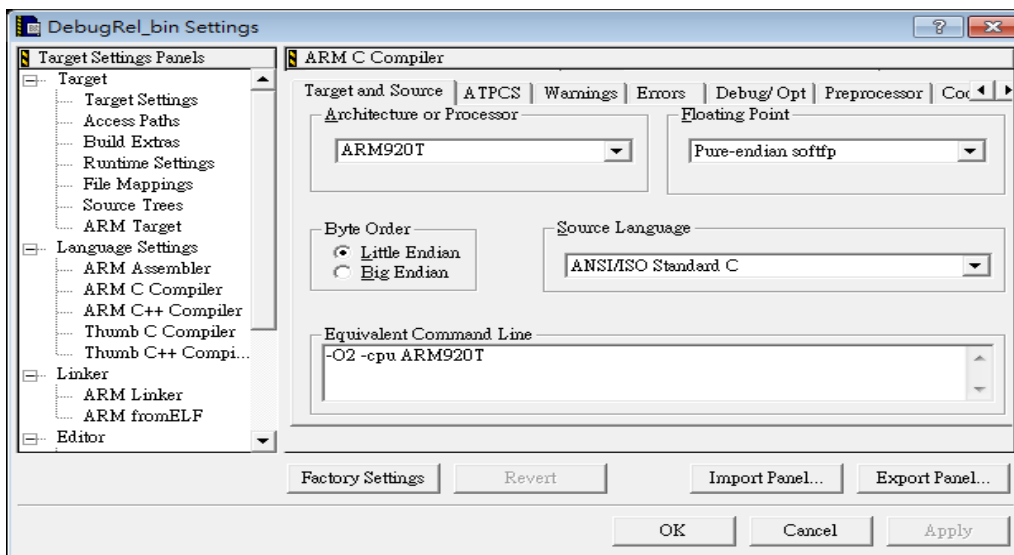


Fig. 3 The Compile window of C program for DC motor control

III. EXPERIMENTAL RESULTS

The main specification of SAMSUNG S3C2440 CPU is using 16/32 bit ARM920T RISC core CPU technology designed by Advanced RISC Machines (ARM). It can reach frequency of 400M Hz. It has core of ARM920T with 0.13um CMOS standard cells and a memory complier. It possesses advantages of lower power consumption and easy design so it is particularly suitable for mobile applications of power saving and low cost. Its new bus architecture is developed by a well known as Advanced Micro controller Bus Architecture (AMBA). The S3C2440A CPU implements MMU, AMBA BUS, and Harvard cache architecture with separate 16KB instruction and 16KB data caches, each with an 8-word line length [4]. Photo of DMA 2440 educational kit [5] is shown in Fig. 4. It provides a DC motor interface to support DC motor applications. The PC control panel diagram is shown in Fig. 5. This panel can control the speed of DC motor.

In this paper, the DC motor is controlled by keyboard of personal computer (PC) and the digital vales of control will be shown in control panel. The digital values of low speed control for DC motor shown in PC screen and the DC motor photo are shown in Fig. 6. The digital values of high speed control for DC motor shown in PC screen and the DC motor photo are shown in Fig. 7. From the experimental results, good performances of DC motor speed control are possessed in this paper.



Fig. 4 The photo of DMA 2440



Fig. 5 The Diagram of PC control panel for DMA 2440



Fig. 6 (a) The low speed diagram of PC control panel

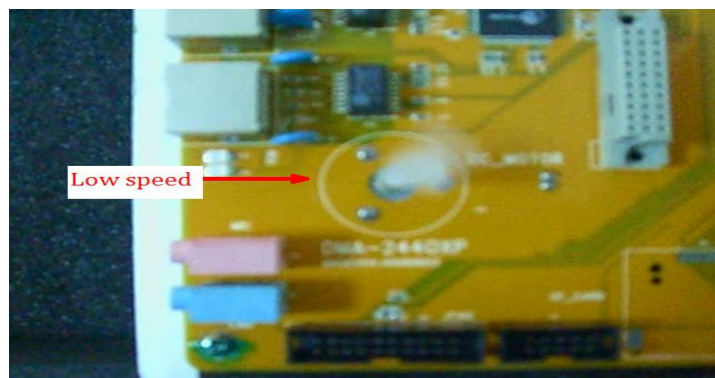


Fig. 6 (b) The low speed photo of DC motor



Fig. 7 (a) The high speed diagram of PC control panel

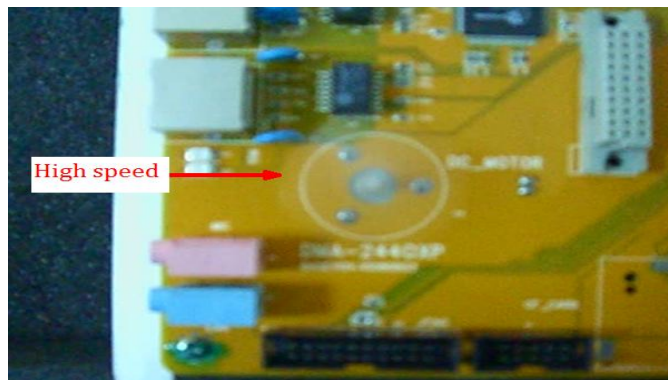


Fig. 7 (b) The high speed photo of DC motor

IV. CONCLUSION

In this paper, the ARM developer suite (ADS) have been installed successfully to develop DC motor control applications. This is verified by the ARM9 based DMA 2440 kit. The development of DC motor control applications can be used to develop other different industrial applications. The experimental results demonstrate that good performances of DC motor control are possessed in this paper.

ACKNOWLEDGMENTS

This research is partially funded by the teachers' research project of Taoyuan Innovation Institute of Technology and supported by the SOC project of the Ministry of Education, Taiwan, R. O. C.

References

- [1]. J. N. Elipe, M. Patil, S. Tejaswi and R. P. Nraiah, "Implementation of embedded face recognition system based on Linux and ARM9," World Journal of Science and Technology, vol. 2, no. 10, pp. 79-82, 2012.
- [2]. P. A. Bhounsule, J. Cortell and A. Ruina, "Design and Control of Ranger: an energy-efficient, dynamic walking robot," Proceedings of the Fifteenth International Conference on Climbing and Walking Robots and the Support Technologies for Mobile Machines, pp. 441-448, 2012.
- [3]. Samsung 2440 CPU data sheet, <http://www.samsung.com>.
- [4]. ARM Ltd. User guide, <http://www.arm.com>
- [5]. DMA 2440 user guide, <http://www.dmatek.com.tw>

Analysis of Lossless Data Compression Techniques

Dalvir Kaur¹ , Kamaljeet Kaur²

¹Master of Technology in Computer Science & Engineering, Sri Guru Granth Sahib World University, Fatehgarh Sahib, Punjab, India.

²Assistant Professor, Department Of Computer Science & Engineering, Sri Guru Granth Sahib World University, Fatehgarh Sahib, Punjab, India.

Abstract:

Compression is useful to reduce the size of data .There are different compression algorithms which are available in different formats.Data compressions are generally lossless and lossy data compression. In this paper, we study different methods of lossless data compression algorithms like-Shanon-Fano coding, Huffman Encoding, Run-Length Encoding (RLE), Lempel-Ziv-Welch (LZW).

Keywords: Data compression, Huffman Coding, Lempel-Ziv, Lossless Compression, Lossy Compression, Shanon-fano coding.

I. INTRODUCTION

Compression is the reduction in size of data by converting it to a format that requires fewer bits. Most often compression is used to minimize storage space (on a hard drive, for example) or for reducing transmitted data over a network. In other words, Compression is the art of representing the information in a compact form rather than its original run compressed form. In other words, using the data compression, the size of a particular file can be reduced.[2] Data compression refers to reducing the amount of space needed to store data or reducing the amount of time needed to transmit data. The size of data is reduced by removing the excessive Information. Data compression can be *lossless*, only if it is possible to exactly reconstruct the original data from the compressed version [4]. To compress something means that you have a piece of data and you decrease its size. There are different data compression techniques who to do that and they all have their own advantages and disadvantages. Examples of such source data are medical images, text and images Preserved for legal reason, some computer executable files, etc. The general principle of data compression algorithms on text files is to transform string of characters into a new string which contains the same information but with new length as small as possible. The efficient data compression algorithm is chosen according to some scales like: compression size, compression ratio, processing time or speed, and entropy. [1]

1.1. Lossless compression vs lossycompression:

Lossless compression: Reduces bits by identifying and eliminating statistical redundancy. no information is lost in lossless compression. In these schemes before the compression after the compression data must be same.

1.2 Lossy compression:

Reduces bits by identifying marginally important information and removing it. In these schemes some loss of information is acceptable depending upon the application [2].

$$\text{Compression ratio} = \frac{B1}{B0} * 100\%.$$

B0=no. of bits before compression.

B1= no. of bits after compression

II. Lossless data Compression Algorithm:

Lossless data compression is the size reduction of a file, such that a decompression function can restore the original file exactly with no loss of data. Lossless data compression is used ubiquitously in computing, from saving space on your personal computer to sending data over the web, communicating over a secure shell, or viewing a PNG or GIF image. The basic principle that lossless compression algorithms work on is that any non-random file will contain duplicated information that can be condensed using statistical modeling techniques that determine the probability of a character or phrase appearing. These statistical models can then be used to generate codes for specific characters or phrases based on their probability of occurring, and assigning the shortest codes to the most common data. Such techniques include Huffman coding , run-length encoding

Lempel-ziv Algorithm,Shanon-fano coding and, . Using these techniques and others, an 8-bit character or a string of such characters could be represented with just a few bits resulting in a large amount of redundant data being removed.[8]

III. SHANON-FANO CODING

In Shannon–Fano coding, the procedure is done by a more frequently occurring string which is encoded by a shorter encoding vector and a less frequently occurring string is encoded by longer encoding vector. Shannon-Fano coding. Relied on the occurrence of each character or symbol with their frequencies in a list and is also called as a variable length coding. The Shannon-Fano Algorithm This is a basic information theoretic algorithm [3].

IV. RUN-LENGTH ENCODING (RLE)

Run Length Encoding (RLE) is a simple and popular data compression algorithm. It is based on the idea to replace a long sequence of the same symbol by a shorter sequence and is a good introduction into the data compression field for newcomers. RLE requires only a small amount of hardware and software resources. Therefore RLE was introduced very early and a large range of derivatives have been developed up to now. Run-length encoding is a data compression algorithm that is supported by most bitmap file formats, such as TIFF, BMP, and PCX[2].

V. Huffman Coding

Huffman Encoding Algorithms use the probability distribution of the alphabet of the source to develop the code words for symbols. The frequency distribution of all the characters of the source is calculated in order to calculate the probability distribution. According to the probabilities, the code words are assigned. Shorter code words for higher probabilities and longer code words for smaller probabilities are assigned. For this task a binary tree is created using the symbols as leaves according to their probabilities and paths of those are taken as the code words. Two families of Huffman Encoding have been proposed: Static Huffman Algorithms and Adaptive Huffman Algorithms. Static Huffman Algorithms calculate the frequencies first and then generate common tree for both the compression and decompression processes . Details of this tree should be saved or transferred with the compressed file. The Adaptive Huffman algorithms develop the tree while calculating the frequencies and there will be two trees in both the processes. In this approach, a tree is generated with the flag symbol in the beginning and is updated as the next symbol is read[1].

VI. LEMPEL-ZIV ALGORITHM:

Data compression up until the late 1970’s mainly directed towards creating better methodologies for Huffman coding. An innovative, radically different method was introduced in 1977 by Abraham Lempel and Jacob Ziv. This technique (called Lempel-Ziv) actually consists of two considerably different algorithms, LZ77 and LZ78[7].

Due to patents, LZ77 and LZ78 led to many variants:

LZ77 Variants	LZR	LZSS	LZB	LZH		
LZ78 Variants	LZW	LZC	LZT	LZMW	LZJ	LZFG

6.1 LZ77 Sliding Window Algorithms

Published in 1977, LZ77 is the algorithm that started it all. It introduced the concept of a 'sliding window' for the first time which brought about significant improvements in compression ratio over more primitive algorithms. LZ77 maintains a dictionary using triples representing offset, run length, and a deviating character. The offset is how far from the start of the file a given phrase starts at, and the run length is how many characters past the offset are part of the phrase. The deviating character is just an indication that a new phrase was found, and that phrase is equal to the phrase from offset to offset+length plus the deviating character. The dictionary used changes dynamically based on the sliding window as the file is parsed. For example, the sliding window could be 64MB which means that the dictionary will contain entries for the past 64MB of the input data[7]. Given an input "abbadabba" the output would look something like "abb(0,1,'d')(0,3,'a')"

as in the example below:

Symbol	Output
a	a
b	b
b	b
a	(0, 1, 'd')
d	
a	(0, 3, 'a')
b	
b	
a	

While this substitution is slightly larger than the input, it generally achieves a considerably smaller result given longer input data.

6.2 LZR

LZR is a modification of LZ77 invented by Michael Rodeh in 1981. The algorithm aims to be a linear time alternative to LZ77. However, the encoded pointers can point to any offset in the file which means LZR consumes a considerable amount of memory. Combined with its poor compression ratio (LZ77 is often superior) it is an unfeasible variant[7].

6.3 LZSS

The LZSS, or Lempel-Ziv-Storer-Szymanski algorithm was first published in 1982 by James Storer and Thomas Szymanski. LZSS improves on LZ77 in that it can detect whether a substitution will decrease the filesize or not. If no size reduction will be achieved, the input is left as a literal in the output. Otherwise, the section of the input is replaced with an (offset, length) pair where the offset is how many bytes from the start of the input and the length is how many characters to read from that position. Another improvement over LZ77 comes from the elimination of the "next character" and uses just an offset-length pair[7]. Here is a brief example given the input " these theses" which yields " these(0,6)s" which saves just one byte, but saves considerably more on larger inputs.

Index	0	1	2	3	4	5	6	7	8	9	10	11	12
Symbol		t	h	e	s	e		t	h	e	s	e	s
Substituted		t	h	e	s	e	(0	,	6)	s	

LZSS is still used in many popular archive formats, the best known of which is RAR. It is also sometimes used for network data compression.

6.4 LZH

LZH was developed in 1987 and it stands for "Lempel-Ziv Huffman." It is a variant of LZSS that utilizes Huffman coding to compress the pointers, resulting in slightly better compression. However, the improvements gained using Huffman coding are negligible and the compression is not worth the performance hit of using Huffman codes[7].

6.5 LZB

LZB was also developed in 1987 by Timothy Bell et al as a variant of LZSS. Like LZH, LZB also aims to reduce the compressed file size by encoding the LZSS pointers more efficiently. The way it does this is by gradually increasing the size of the pointers as the sliding window grows larger. It can achieve higher compression than LZSS and LZH, but it is still rather slow compared to LZSS due to the extra encoding step for the pointers[7].

6.6 LZ78 Dictionary Algorithms:

LZ78 was created by Lempel and Ziv in 1978, hence the abbreviation. Rather than using a sliding window to generate the dictionary, the input data is either preprocessed to generate a dictionary with infinite scope of the input, or the dictionary is formed as the file is parsed. LZ78 employs the latter tactic. The dictionary size is usually limited to a few megabytes, or all codes up to a certain number of bytes such as 8; this is done to reduce memory requirements. How the algorithm handles the dictionary being full is what sets most LZ78 type algorithms apart. While parsing the file, the LZ78 algorithm adds each newly encountered character or string of characters to the dictionary. For each symbol in the input, a dictionary entry in the form (dictionary index,

unknown symbol) is generated; if a symbol is already in the dictionary then the dictionary will be searched for substrings of the current symbol and the symbols following it. The index of the longest substring match is used for the dictionary index. The data pointed to by the dictionary index is added to the last character of the unknown substring. If the current symbol is unknown, then the dictionary index is set to 0 to indicate that it is a single character entry. The entries form a linked-list type data structure.

An input such as "abbadabbaabaad" would generate the output "(0,a)(0,b)(2,a)(0,d)(1,b)(3,a)(6,d)". You can see how this was derived in the following example:

Input:		a	b	ba	d	ab	baa	baad
Dictionary Index	0	1	2	3	4	5	6	7
Output	NULL	(0,a)	(0,b)	(2,a)	(0,d)	(1,b)	(3,a)	(6,d)

6.7 LZW

LZW is the Lempel-Ziv-Welch algorithm created in 1984 by Terry Welch. It is the most commonly used derivative of the LZ78 family, despite being heavily patent-encumbered. LZW improves on LZ78 in a similar way to LZSS; it removes redundant characters in the output and makes the output entirely out of pointers. It also includes every character in the dictionary before starting compression, and employs other tricks to improve compression such as encoding the last character of every new phrase as the first character of the next phrase. LZW is commonly found in the Graphics Interchange Format, as well as in the early specifications of the ZIP format and other specialized applications. LZW is very fast, but achieves poor compression compared to most newer algorithms and some algorithms are both faster and achieve better compression.

6.8 LZC

LZC, or Lempel-Ziv Compress is a slight modification to the LZW algorithm used in the UNIX compress utility. The main difference between LZC and LZW is that LZC monitors the compression ratio of the output. Once the ratio crosses a certain threshold, the dictionary is discarded and rebuilt.

6.9 LZT

Lempel-Ziv Tischer is a modification of LZC that, when the dictionary is full, deletes the least recently used phrase and replaces it with a new entry. There are some other incremental improvements, but neither LZC nor LZT is commonly used today.

6.10 LZMW

Invented in 1984 by Victor Miller and Mark Wegman, the LZMW algorithm is quite similar to LZT in that it employs the least recently used phrase substitution strategy. However, rather than joining together similar entries in the dictionary, LZMW joins together the last two phrases encoded and stores the result as a new entry. As a result, the size of the dictionary can expand quite rapidly and LRUs must be discarded more frequently. LZMW generally achieves better compression than LZT, however it is yet another algorithm that does not see much modern use.

6.11 LZAP

LZAP was created in 1988 by James Storer as a modification to the LZMW algorithm. The AP stands for "all prefixes" in that rather than storing a single phrase in the dictionary each iteration, the dictionary stores every permutation[7].

6.12 LZWL

LZWL is a modification to the LZW algorithm created in 2006 that works with syllables rather than than single characters. LZWL is designed to work better with certain datasets with many commonly occurring syllables such as XML data. This type of algorithm is usually used with a preprocessor that decomposes the input data into syllables [8].

6.13 LZJ

Matti Jakobsson published the LZJ algorithm in 1985 and it is one of the only LZ78 algorithms that deviates from LZW. The algorithm works by storing every unique string in the already processed input up to an arbitrary maximum length in the dictionary and assigning codes to each. When the dictionary is full, all entries that occurred only once are removed[8].

VII. LEMPEL–ZIV–WELCH (LZW)

LZW is a universal lossless data compression algorithm [10] created by Abraham Lempel, Jacob Ziv, and Terry Welch. It was published by Welch in 1984 as an improved implementation of the LZ78 algorithm published by Lempel and Ziv in 1978. The algorithm is simple to implement, and has the potential for very high throughput in hardware implementations. LZW is referred to as a *dictionary-based encoding algorithm*. The algorithm builds a *data dictionary* (also called a *translation table* or *string table*) of data occurring in an uncompressed data stream. Patterns of data (*substrings*) are identified in the data stream and are matched to entries in the dictionary. If the substring is not present in the dictionary, a code phrase is created based on the data content of the substring, and it is stored in the dictionary. The phrase is then written to the compressed output stream[2].

VIII. CONCLUSION

Lossless Data Compression Algorithms are help to compress a huge amount of data as to carry from one place to another or in a storage format. Compression techniques are improved the efficiency compression on text data. Lempel-Ziv Algorithm is best of these Algorithms.

REFERENCES

- [1] Haroon A, Mohammed A. Data Compression Techniques on Text Files: A Comparison Study International Journal of Computer Applications (0975 –8887) Volume 26– No.5, July 2011.
- [2] P.Yellamma Dr.Narasimham Challa. Performance Analysis Of Different Data Compression Techniques On Text File October-2012.
- [3] Mamta Sharma. Compression Using HuffmanCoding IJCSNS International Journal of ComputerScience and Network Security, VOL.10 No.5, May 2010
- [4] Senthil Shanmugasundaram, Robert Lourdasamy. A Comparative Study Of Text Compression Algorithm International Journal of Wisdom Based Computing, Vol.1 (3),
- [5] Draft Lecture Note compression Algorithms: Huffman and Lempel-Ziv-Welch (Lzw) Last Update: February 13, 2012.
- [6] S.R. Kodituwakku. U. S.Amarasinghe Comparison Of Lossless Data Compression Algorithms For Text Data.
- [7] Bell, T., Witten, I. Cleary, J. Modeling for Text Compression ACM Computing Surveys, Vol. 21, No. 4 1989.
- [8] http://www.ieeeeghn.org/wiki/index.php/Historyof_Lossless_Data_Compression_Algorithms
- [9] Data compression Wikipedia.

Removal of Fluoride Ion from Aqueous Solution

Neelo Razbe¹, Rajesh Kumar², Pratima³ and Rajat Kumar⁴

¹Reseach Scholar of Singhania University, Jhunjhunu Rajasthan, India

²Department of Chemical Engg. HBTI Kanpur, India

^{3,4} Department of Chemistry DAV-PG College Kanpur, India

Abstract

High concentrations of fluoride in drinking water had caused widespread fluorosis. A simple, precise, rapid and reliable technique has been developed for removal of fluoride in drinking water. The innovative technique employs activated alumina for defluoridation of drinking water. Alumina is inert in nature, hence it is safe to use and handle. The innovation in regeneration of alumina makes the technique cost effective. The reliability of the newly developed technique has been established by analyzing spiked water samples of high concentrations of fluoride (upto 50 ppm) and levels of fluoride has been brought down to less than 1 ppm. The method is superior to currently employed techniques and is recommended to the laboratories where a huge volume of water is to be defluoridated.

Key words: Fluoride, Fluorosis, Water pollution, Activated alumina, Regenerative technique.

I. INTRODUCTION

High fluoride levels in drinking water has become a critical health hazard of this century as it induces intense impact on human health including skeletal and dental fluorosis. Fluoride in minute quantity is an essential component of normal mineralization of bones and formation of dental enamel [1]. However, its excessive intake may result in slow, progressive crippling scourge known as fluorosis. The world health organization (WHO) had recommended values of fluoride in drinking water: 0.1 to 0.5 ppm [2]. There is a minor aberration from this standard as U.S. standard recommends that the fluoride content in drinking water should be between 0.6 and 0.9 ppm. The bureau of Indian standard which is the main regulatory agency for drinking water in India specify that the maximum desirable limit of fluoride in drinking water is 0.5 ppm but in absence of alternatives, the maximum permissible limit is 1.5 ppm [3]. The fluorosis is caused by oral intake of fluoride when drinking water contains more than the permitted concentration of fluoride. Fluorosis may be life threatening in particular fluoride affected area if proper defluoridation techniques are not employed to curtail the levels of fluoride in drinking water. In India, endemic fluorosis effects more than one million population and is a major problem in 17 of the 25 states. The most affected states in India are Rajasthan, Andhra Pradesh, Orissa, Gujarat, Madhya Pradesh and Chhattisgarh states [4]. Similar health problems due to high fluoride content in ground water have also been reported worldwide and it is estimated that around 260 million people are adversely affected in 30 countries of the world especially from China, Sri Lanka, Spain, Holland, Italy, Mexico and North and South American Countries⁵.

II. HEALTH AFFECTS

Fluoride in drinking water is beneficial at low concentrations, but presents health concerns at higher concentrations [19]. There are many sources of fluoride in the diet. Dentists apply fluoride to teeth; some municipal water systems add fluoride to the water supply; and some toothpastes have fluoride as an additive; and some foods also have elevated fluoride such as fish and tea. The Centers for Disease Control (CDC) have recommended 1.0 to 1.2 milligrams per liter (mg/L) as the optimum beneficial concentration of fluoride in drinking water for dental protection in state of New Hampshire. At higher concentration however, there are health concerns. The US EPA has developed standards that limit the presence of fluoride in public drinking water supplies. These health standards are called maximum contaminant levels (MCLs). In addition, there are non-health related standards (that relate to aesthetics) called secondary maximum contaminant levels (SMCLs) which pertain to fluoride. These important ranges of fluoride in drinking water are explained below.

2.1 Fluoride concentration of approximately 1.1 mg/L

Fluoride has been shown to reduce tooth decay in children if they receive an adequate level. The optimal concentration, as recommended by CDC for New Hampshire, is approximately 1.1 mg/L. (1.1 mg/L is

the same as saying 1.1 parts per million parts (ppm)). Below 0.5 mg/L there is little tooth decay protection. Above 1.5 mg/L, there is little additional tooth decay benefit.

2.3 Fluoride concentration over 2.0 mg/L

In the range of 2.0-4.0 mg/L of fluoride, staining of tooth enamel is possible. EPA categorizes staining as an aesthetic concern, and thus only requires that customers of public water systems be notified of the elevated fluoride level. EPA does not require fluoride removal when the concentration exceeds 2.0 mg/L but is less than 4.0 mg/L. Approximately 5% of New Hampshire bedrock wells have fluoride that exceeds 2.0 mg/L.

2.4 Fluoride concentration over 4.0 mg/L

At concentrations above 4.0 mg/L, studies have shown the possibility of skeletal fluorosis as well as the staining of teeth. In its most severe form, skeletal fluorosis is characterized by irregular bone deposits that may cause arthritis and crippling when occurring at joints. EPA recognizes skeletal fluorosis as a health concern, and thus requires that public water systems not only **notify** their customers, but also **treat** the water to lower the fluoride concentration. Less than 1% of New Hampshire bedrock wells have fluoride that exceeds 4.0 mg/L of fluoride. Specific health questions concerning fluoride's effects should be directed to a physician or dentist. For general health information concerning fluoride, please call the Environmental Health Risk Assessment Bureau of the New Hampshire Division of Public Health Services at 271- 4608.

III. FACTORS AFFECTING FLUOROSIS

The severity of fluorosis is influenced by concentration of fluoride in water and period of its usage. Nutritional status and physical strain also play vital role in deciding total effects of fluoride pollution. A diet poor in calcium, for example, increases the body's retention capacity of fluoride⁶. Environmental factors include annual mean temperature, humidity, rainfall, tropical climate, duration of exposure etc. Besides, other factors such as pH in terms of alkalinity, age, calcium in diet, fresh fruits and vitamin-C reduces fluoride toxicity. Whereas, trace elements like molybdenum enhances the fluoride toxicity. Defluoridation of drinking water is the only pragmatic approach to solve the fluoride pollution problem as the use of alternate water sources and improvement of nutritional status of population at risk have their own limitations and are expensive affairs [7]. Generally, methods reported in literature are based on adsorption, ion exchange, precipitation and miscellaneous. All these methods, their principle of operation, advantages, disadvantages, limitations and applications have been critically reviewed [8,9]. Adsorption techniques are advantageous for defluoridation as the processes are capable of removing fluoride up to 90% and are cost effective [10-12]. However, these processes are highly dependent on pH and efficient at narrow pH range (pH between 5 and 6). High concentration of total dissolved solids (TDS) may pose fouling problems and also presence of sulfate, phosphate and carbonate results in ionic competition impairing the efficiency of the fluoride removal system. Ion exchange resins technology is advantageous as it retains the taste and colour of the treated water intact and is capable of removing 90 – 95% of fluoride¹³. Regeneration of resins generally pose problem as it leads to fluoride rich waste, which necessitates separate treatment before final disposal. The Nalgonda technique, which is a well established process and has been adopted in India and Tanzania¹ [4, 15]. The method comprises of addition, in sequence, of sodium aluminate or lime, bleaching powder and alum to the water samples, followed by flocculation, sedimentation and filtration. The technique can be used both for domestic as well as for community water supplies [7]. However, the process is not automatic. It requires a regular attendant for addition of chemicals and look after the treatment process. Requirement of large space for drying of sludge and maintenance cost are the other notable limitations. Bone, bone char and synthetic bone materials have shown good efficiency for curtailment of fluoride in water samples [16, 17]. However, high costs, non-acceptability on moral and ethical grounds are the notable limitations.

IV. METHODS TO REDUCE FLUORIDE IN YOUR WATER SUPPLY

Commonly used domestic defluoridation processes various defluoridation methods are used for removal of fluoride from drinking water. These exiting methods for defluoridation of drinking water is expensive, slow, in efficient, unhygienic and highly technical.

- [1] Nalgonda technique (Flocculation and Sedimentation)
- [2] Activated alumina process (Adsorption)
- [3] KRASS Process
- [4] Other processes (Bio-remedial, Ion exchange, R.O. etc.)

4.1 New defluoridation method by- green chemical approach

A comparative study of degree of toxicity of NaF, NaSiF₆, CaF₂, CaSiF₆, MgF₂, ZnF₂, AlF₃ and CuF₂ showed that calcium and aluminum fluoride are less toxic than other fluoride³. Therefore, in present paper authors used aluminum oxalate as defluoridation agents in soil pots and developed a new defluoridation method. The following investigations were conducted to find out the fluoride minimizing capacity of aluminum oxalate in the water samples kept in the soil pots.

4.2 Determination of different physical and chemical parameters of water samples

The pH, TDS and Al ion concentration were determined by the standard procedures. Result of these parameters shows that the values of all parameters in water samples are in their desirable limits.

4.3 Preparation of soil pots

Four soil pots (A, B, C and D) were prepared after incorporation of aluminum oxalate (2 g., 4 g., 6 g and 8 g.) in 500 g. of soil respectively as shown in flow chart given below^{2,5-7}.

4.4 Determination of fluoride concentration

Fluoride concentration of untreated sample and the treated fluoride water samples was determined as per the standard procedure by ion selective method by Orion 720+ after time interval of 3, 24, 48 and 72 hours. Results are given in Fig. 1.

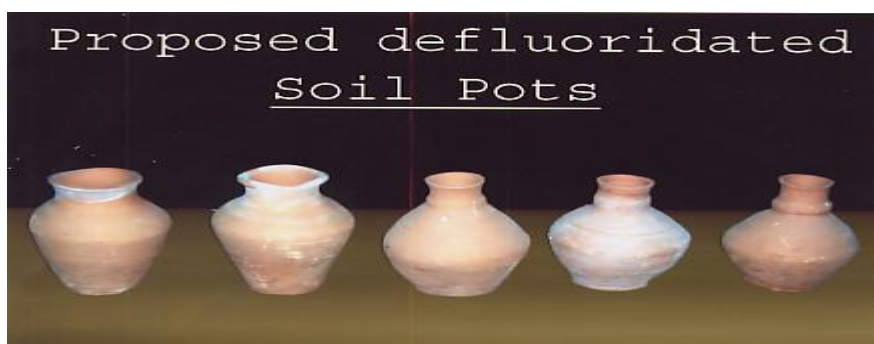


Fig. 1: Proposed soil pots

Investigation pertaining to the effect of increasing of aluminum oxalate in the soil pot on the fluoride concentration in Fig. 2 shows that the fluoride concentration of water sample (10 mg/L fluoride) decreases in the all soil pots with increasing amounts of aluminum oxalate at contact time periods. It is noticed that soil pot No-1 (having 2 g C₆Al₂O₁₂), decreases the fluoride concentration of the water sample about 20% but in case of soil pot No. 3 (having 6 g C₆Al₂O₁₂), the concentration of fluoride decreases about 70% at time interval 72 hours. This can be explained on the basis of surface chemistry. It is a general phenomena of surface chemistry that more the surface area of adsorbent more the adsorbate are adsorbed on the surface of adsorbent to form a unimolecular layer (Langmuir isotherm limitation) of adsorbent during chemisorption process. Result shows that a certain amount of aluminum oxalate reduces the fluoride concentration in the water sample.

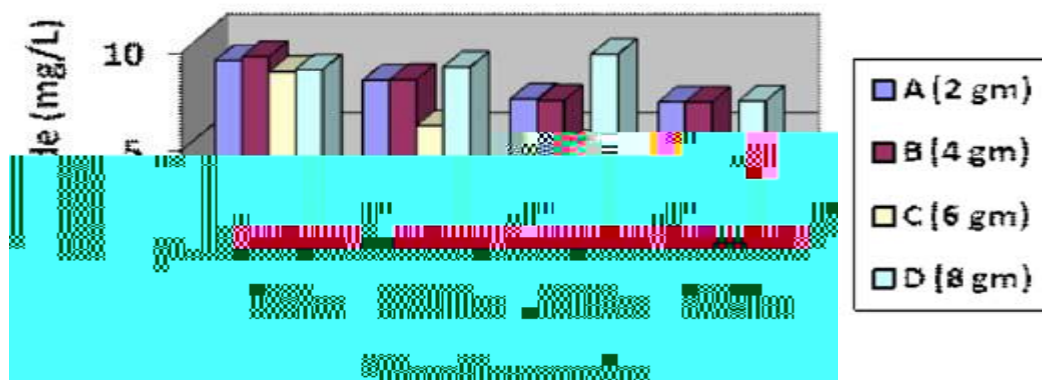
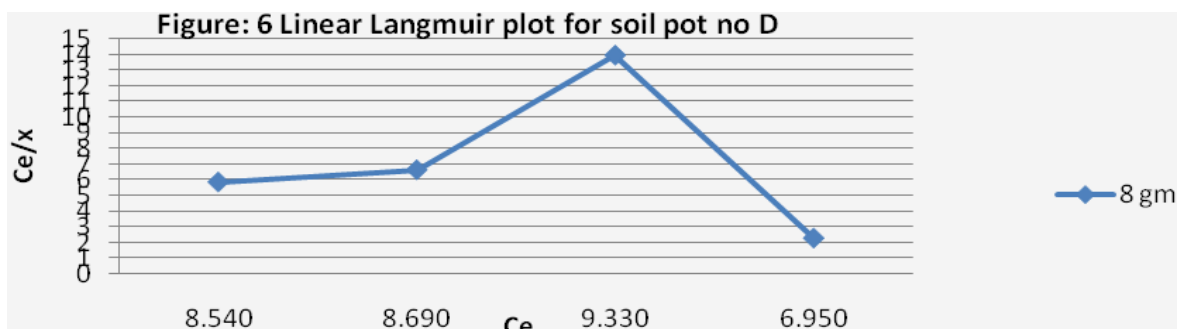
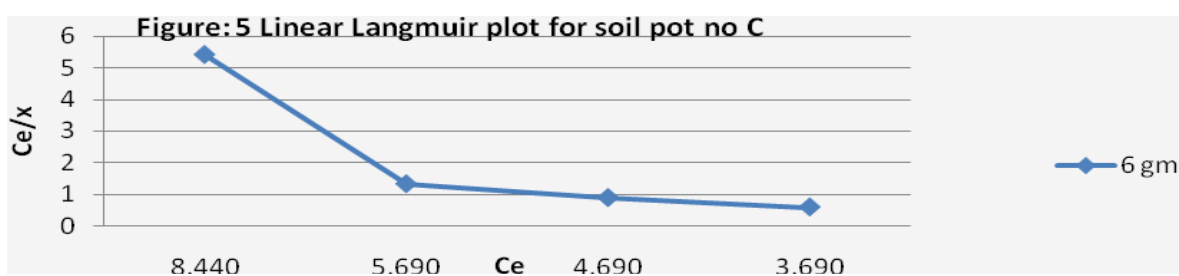
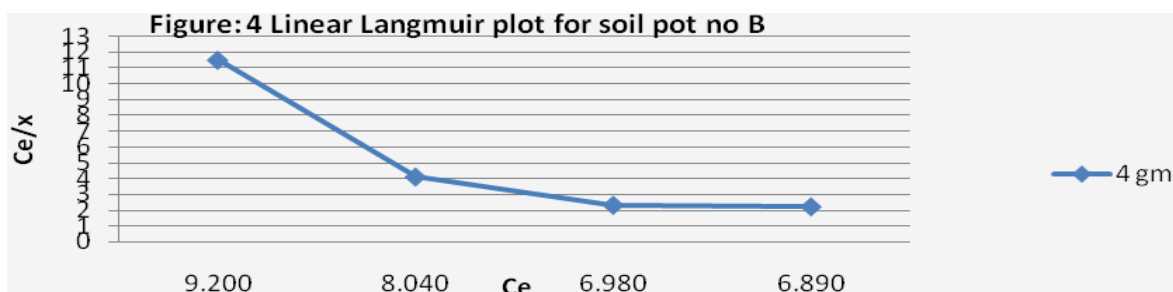
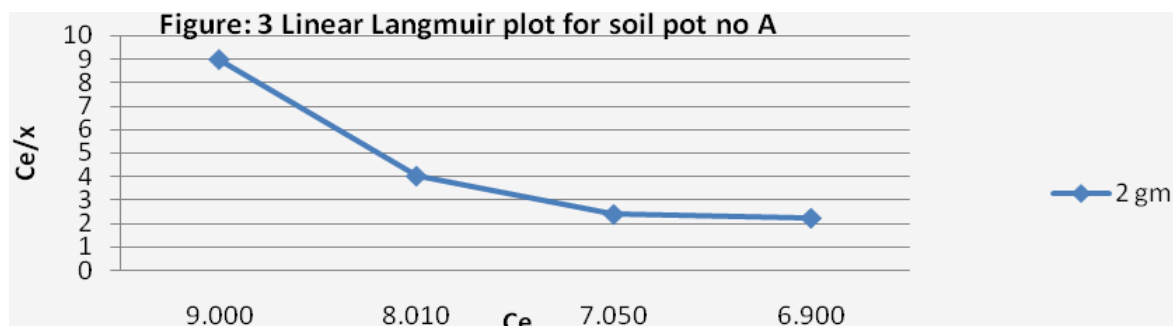


Fig. 2: Concentration of fluoride ions in different soil pots

The removal of fluoride from water sample (10 mg/L) is expected due to the formation of polyhydroxide aluminum complex (e.g. $[Al(H_2O)_3(OH)_3]$ $[Al(H_2O)_2(OH)_4]$ etc.) with fluoride and adsorption of fluoride on polymeric aluminum oxalate. The linear Langmuir plots between C_e/x and C_e are shown in the Fig. 3-6. The linear Freundlich isotherm models are shown in the Fig. 7-10 by plotting $\log x/\log C_e$. The constant values of the both isotherms for each soil pot are given in the Table 1. It is observed from the curves and the correlation coefficient data that the fluoride adsorption follows neither Langmuir isotherm nor Freundlich isotherm in a perfect way. However, it follows Langmuir isotherm in a better way. The value of n is always less than unity, which indicates that, none of the soil pots have completely energetically homogeneous surface. This can be explained that all the four soil pots are associated with certain amounts of aluminum oxalate at certain specific sites having different activation energy. The adsorption involves attractive electrostatic interaction between the negative sites created by the ionization of the sodium fluoride and the positively charged Al^{3+} cations.



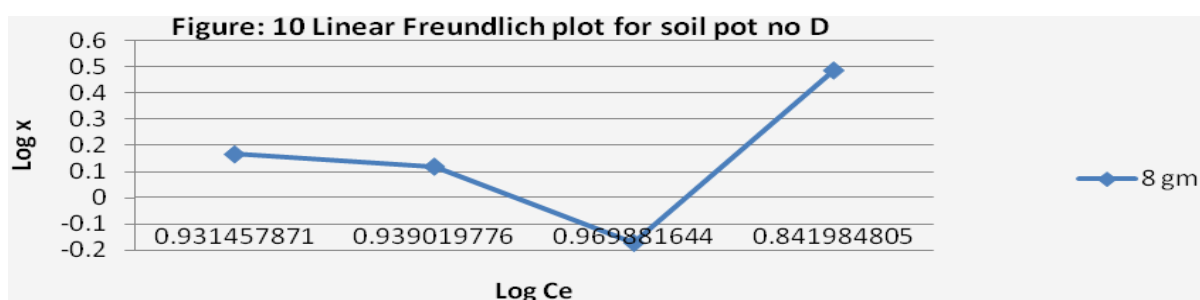
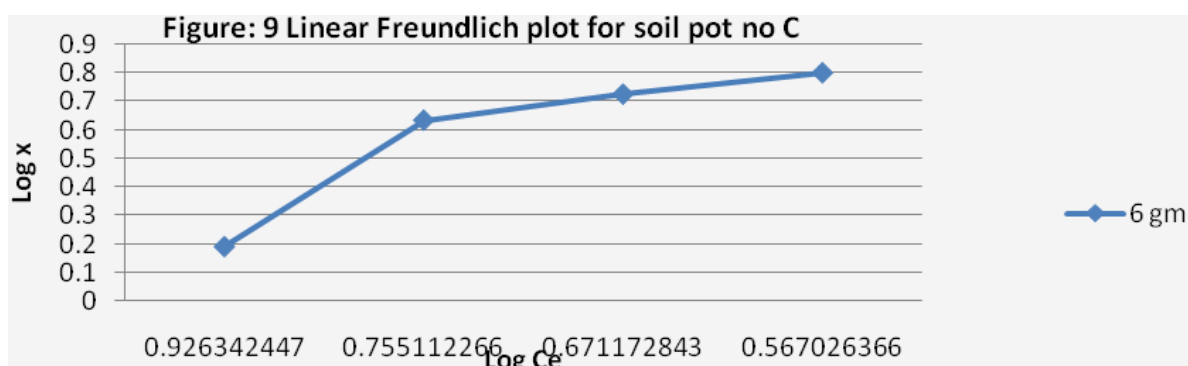
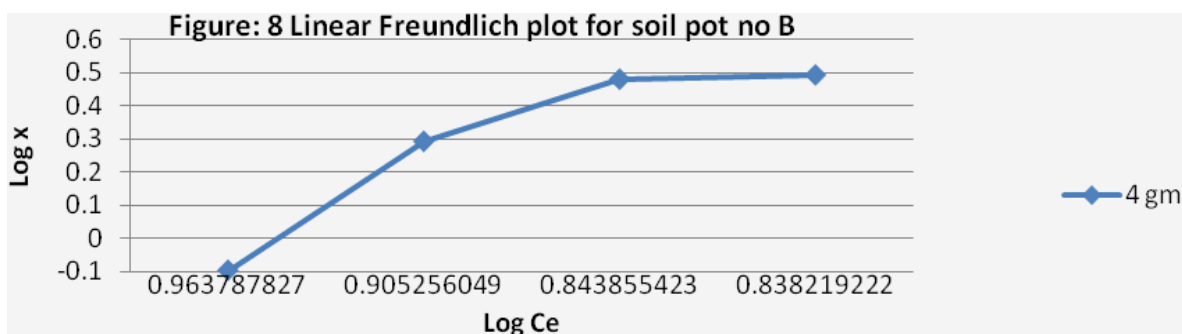
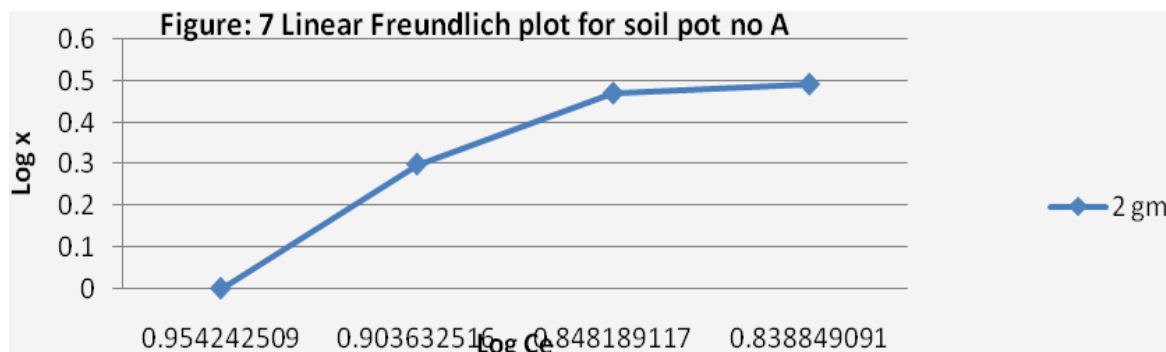


Table 1: Langmuir and Freundlich equation constants for adsorption of fluoride ions on different soil pots.

Soil Pots No.	C6Al2O12 in soil pots (g/500 g soil)	Langmuir equation constants		Freundlich equation constants	
		xm (mg/g)	k	N	kf
1	2g	0.487075	-0.17016	-3.82577	3.736795
2	4g	0.46465	-0.16922	-4.07778	3.954843
3	6g	1.807318	-0.36847	-1.5051	1.736619
4	8g	0.203617	-0.13747	-6.16173	5.881287

V. CONCLUSION

Activated alumina after pretreatment with aluminium sulphate has given promising results for removal of fluoride from drinking water. An adsorption capacity of regenerated activated alumina was found to be 4.06 g/Kg at pH 7. It has been observed that the adsorption capacity of activated alumina is strongly dependant on the flow rate, inlet fluoride ion concentration and bed length and the fluoride removal is greater under condition of high contact time and lower concentration of fluoride. The regeneration of activated alumina bed was investigated and results revealed excellent performance of regenerated activated alumina for removal of fluoride in drinking water. This innovation of regeneration makes the system economical on one hand and also avoids the logistic requirement of changing the adsorbent after every cycle of saturation on the other hand. Hence, activated alumina sorbent clearly seems to be viable option for defluoridation methods due to its significant specific sorption.

- [1] Adsorption isotherm of fluoride ions follows the mixed model of the Langmuir and Freundlich isotherm. The adsorption does not depend on the BET surface area of the pots and takes place on certain specific site.
- [2] Aluminum oxalate can be used as defluoridating agent in soil pots without effecting the environment as a Green Chemical Approach.

REFERENCES

- [1] M. C. Bell and T. G. Luwig, The Supply of Fluoride to Man: Ingestion from Water, in Fluorides and Human Health, WHO Monograph, Series 59, World Health Organisation, Geneva (1970).
- [2] WHO, International Standards for Drinking Water, 3rd Ed., Geneva (2008) pp. 375-377.
- [3] BIS 10500, Indian Standard Drinking Water Specification, Bureau of Indian Standards, New Delhi (1991).
- [4] B. K. Shrivastava and A.Vani, Comparative Study of Defluoridation Technologies in India, *Asian J. Exp. Sci.*, 23(1), 269-274 (2009).
- [5] N. Mameri, A. R. Yeddou, H. Lounici, H. Girb, D. Belhocine and B. Bariou, Defluoridation of Septentrional Sahara Water of North Africa by Electro-coagulation Process using Bipolar Aluminium Electrodes, *Water Res.*, 32(5), 1604-1610 (1998).
- [6] UNICEF, Fluoride in Water: An Overview, (2003), URL: <http://www.unicef.org/fluoride.Pdf>.
- [7] Meenakshi and R. C. Maheshwari, Fluoride in Drinking Water and its Removal, *J. Hazad. Mater.*, B137, 456-463 (2006).
- [8] A. K. Shrivastava, Fluoride Pollution: A Review, *Int. J. Environ. Sci.*, 3(1), 55-76 (2012).
- [9] M. Mohapatra, S. Anand, B. K. Mishra, D. E. Giles and P. Singh, Review of Fluoride Removal from Drinking Water, *J. Environ. Manag.*, 91, 67-77 (2009).
- [10] C. D. Nava, M. S. Rios and M. T. Olguin, Sorption of Fluoride Ions from Aqueous Solutions and Well Drinking Water by Thermally Heated Hydrocalcite, *Sept. Sci. Technol.*, 38(1), 131-147 (2003).
- [11] P. K. Gogoi and R. Baruah, Fluoride Removal from Water by Adsorption on Acid Activated Kaolinite Clay, *Ind. Jour. Chem. Tech.*, 15, 500-503 (2008).
- [12] S. G. Rao, A Study on the Removal of Fluoride from Water using Carbonized Coconut Coir, *J. IPHE, India*, 3, 5-81 (2003).
- [13] G. Sing, B. Kumar, P. K. Sen and J. Majumdar, Removal of Fluoride from Spent Pot Liner Lechate using Ion Exchange, *Water Environ. Res.*, 71, 36-42 (1999).
- [14] W. G. Nawlakhe, D. N. Kulkarni, B. N. Pathak and K. R. Bulusu, Defluoridation of Water by Nalgonda Technique, *Ind. J. Env. Hlth.*, 17(1), 25-26 (1975).
- [15] S. N. Ahemad, Evaluation of Defluoridation Technique and Innovative Domestic Defluoridation for Water Treatment, M. Tech. Dissertation, Centre for Environmental Science and Engineering IIT Bombay, India (2001).
- [16] M. J. Larsen, E. I. Pearce and S. J. Jensen, Defluoridation of Water at High pH with use of Brushite, Calcium Hydroxide and Bone Char, *J. Dental Res.*, 72(1), 1519-1525 (1993).
- [17] D. J. Killedar and D. S. Bhargava, Fluoride Adsorption on Fish Bone Charcoal Through a Moving Media Adsorption Column, *Water Resources*, 20(6), 781-788 (1992).
- [18] R. N. YADAV*, RAJDEEP YADAV, NAVIN KUMAR DAGAR, PRIYANKA GUPTA, O. P. SINGH and M. P. S. HANDRAWAT, REMOVAL OF FLUORIDE IN DRINKING WATER BY GREEN CHEMICAL APPROACH. *J. Curr. Chem. Pharm. Sc.*: 2(1), 2012, 69-75
- [19] ISSN 2277-2871. Department of Environmental Services web site (<http://www.des.state.nh.us/ws.htm>).

Physio- Chemical Properties of the Water of River Ganga at Kanpur

Anjum Praveen¹, Rajesh Kumar², Pratima³ And Rajat Kumar⁴

¹Reseach Scholar of Singhania University, Jhunjhunu Rajasthan, India

²Department of Chemical Engg. HBTI Kanpur, India

^{3,4} Department of Chemistry DAV-PG College Kanpur, India

Abstract:

We present an extensive investigation of physico-chemical parameters of water samples of Ganga River at Kanpur. Water samples under investigations were collected from Jalsanstan Benajhawar Kanpur sampling station during pre monsoon (April - May), monsoon (July - August) and post monsoon (October - November) seasons in the year 2012. Correlation coefficients were calculated between different pairs of parameters to identify the highly correlated and interrelated water quality parameters and t-test was applied for checking significance. The observed values of different physico-chemical parameters like pH, temperature, turbidity, total hardness (TH), Iron, Chloride, total dissolved solids (TDS), Ca²⁺, Mg²⁺, SO₄²⁻, NO₃⁻, F⁻¹, total alkalinity (TA), Oxygen consumption (OC), Suspended solids (SS) of samples were compared with standard values recommended by world health organization (WHO). It is found that significant positive correlation holds for TA with Cl⁻, Mg²⁺, Ca²⁺, TH, TDS, fluoride and OC. A significant negative correlation was found between SS with chloride, Mg²⁺, TDS, fluoride and OC. All the physico-chemical parameters for pre monsoon, monsoon and post monsoon seasons are within the highest desirable or maximum permissible limit set by WHO except turbidity which was high while NO₃⁻, Cl⁻¹ and F⁻ are less than the values prescribed by WHO.

Keywords: Physico-chemical parameters, correlation, t-test.

I. INTRODUCTION

Water is the principal need of life on earth, and is an essential component for all forms of lives, from micro-organism to man. The unplanned urbanization and industrialization (Singh et al¹, 2002) has resulted in over use of environment (Petak², 1980) in particular of water resource. A kind of crises situation has made getting clean water a serious problem. It is a known fact that when pure water is polluted its normal functioning and properties are affected. Ganges is a sacred river of India. The increased anthropogenic activities due to industrialization have contributed to decline in water quality of Ganges. Several works have been reported on water quality of river Ganges at Kanpur (Sinha et al³, 2000; Pandey and Pandey⁴, 19803 and Tare et al⁵, 2003) and other parts of country (Pahwa, and Mehrotra, 1966). The authors studied river Ganges from Kanpur city, west state UP, to Rajmahal city east state Jharkhand, covering total length of about 1090 kms. The maximum turbidity (1100-2170 ppm) was observed in monsoon and minimum (less than 100 ppm) during January to June. The minimum value Ph of the river water ranged between 7.45 (minimum) observed during June to August and 8.30 (maximum) during January to May. A comprehensive study of physico-chemical properties of Ganga water at Buxar (Unnao) UP (Sinha⁶, 1986), Narora and Kannauj, U.P (Khan et. Al⁸, 1984)6, in and around Haridwar (Kaur and Joshi⁹, 2003) has also been reported. The seasonal analysis of Kanpur (Zafer and Sultana¹⁰, 2007)8 water showed that extent of pollution varied in different seasons.

It is a fact that good water quality produces healthier humans than one with poor water quality. Ganga River is life line of Kanpur and its water is used for domestic and agriculture purposes therefore, effective maintenance of water quality is required through appropriate measurements. Physico-chemical and microbiological characteristics may describe the quality of water (Sinha¹¹, 1986), therefore, an analysis on physico-chemical parameters of Ganga water was made by many workers (Mehrotra¹², 1990; Sinha et.al¹³. 2000) regular monitoring of all the parameters is very difficult and laborious task even if adequate manpower and laboratory facilities are available. Therefore, statistical correlation technique has been used for comparison of physico-chemical parameters.

The present work deals with the study of 15 physico-chemical parameters like pH, temperature, turbidity, TH, Fe, Cl⁻, TDS, Ca²⁺, SO₄²⁻, NO₃⁻, F⁻, TA, Mg²⁺, OC, SS of Ganga river water in Kanpur. The observed values of various physico-chemical parameters of water samples were compared with standard values recommended by World Health Organization (WHO¹⁷) and are given in Table-2. The objective is to minimize the complexity and dimensionality of large set of data. Systematic calculation of correlation coefficient between physico-chemical parameters has been carried out and significant correlation has been further verified by using t- test. (Bhandari and Nayal¹⁴, 2008; Garg et.al¹⁵, 1990; Sarkar et. Al¹⁶. 2006)

II. EXPERIMENTAL

Water samples were collected from Jalsansthan Benajhawar Kanpur sampling station during pre monsoon (April - May), monsoon (July - August) and post monsoon (October - November) phase in year 2012. During sampling pH, temperature, and turbidity were determined using digital pH meter, thermometer and turbidimeter respectively. F⁻ And nitrate was estimated using colorimetric method. The laboratory analysis of samples was done using standard methods (APHA¹⁸, 1998), titrimetric method was used for the determination of total alkalinity and gravimetric method for total dissolved solid and total suspended solids Mohr's argentometric titration method was used for chloride (Vogel, 1978). Sulphate was estimated using turbidometric method. (Vogel¹⁹, 1978) Where as Ca²⁺, Mg²⁺ and TH was determined by EDTA titrimetric method (Vogel, 1978). Atomic absorption spectrophotometer was used for determination of Fe and Cr contents. All the chemical used were of AR grade. Shows water quality parameters in Table 1.

Table-1: Water quality parameters and analytical methods used in analysis of water samples.

Parameter Analytical method	
WT (°C)	Mercury thermometer
Tu (NTU)	Turbidimeter[10b]
pH	pH-meter
TA (CaCO ₃ mg/l)	Titrimetric
Cl ⁻ (mg/l)	Argentometric Method [10a](Silver nitrate method)
NO ₃ ⁻ (mg/l)	Colorimetric method
TH (CaCO ₃ mg/l)	EDTA Titrimetric Method[10c]
Ca ²⁺ (mg/l)	EDTA Titrimetric Method[10c]
Mg ²⁺ (mg/l)	EDTA Titrimetric Method[10c]
TDS (mg/l)	Gravimetric method
SO ₄ ²⁻ (mg/l)	Aplab turbidity meter[10b]
Cr (mg/l)	Atomic absorption spectrophotometer
Fe (mg/l)	Atomic absorption spectrophotometer
F ⁻ (mg/l)	Colorimetric method
* WT: temperature; Tu: turbidity; TA: alkalinity; Cl ⁻ : chloride;NO ₃ ⁻ : nitrate; TH: total hardness; TDS :Total dissolved Solids,	

Table 2. The average values of physico- chemical parameters of Ganga River water at Kanpur. HDL: Highest Desirable Limit; MPL; Maximum Permissible Limit]

NO.	PARAMETERS	UNITS	DRINKING WATER WHO Standard		Experimental Values (Range)
			HDL	MPL	
1	Temperature	°C	----	-----	21-30
2	Turbidity	NTU	5	10	18-471
3	pH value	-	6.5 to 8.5	No relaxation	8.3-8.8

4	Total hardness (as CaCO ₃)	mg/l	300	600	123-213
5	Iron	mg/l	0.3	1.0	0.2-0.7
6	Chlorides	mg/l	250	1000	6.9-26.8
7	Dissolved Solids	mg/l	500	2000	255-501
8	Calcium	mg/l	75	200	27.8-47.9
9	Sulphate	mg/l	200	400	51-90
10	Nitrate	mg/l	50	No relaxation	0-1.763
11	Fluoride	mg/l	1.0	1.5	0-0.39
12	Total Alkalinity	mg/l	200	600	12.7-245
13	Magnesium	mg/l	30	150	9.24-27.12
14	Oxygen Observed from KMnO ₄ at 370C in 3 hrs.	mg/l	3.0	No relaxation	2.3-7.9
15	Suspended Solids	mg/l	20	150	69-281

III. RESULTS AND DISCUSSION:

The observed pH value ranging from 8.3 to 8.8 show that the present water samples are slightly alkaline in pre-monsoon season. These values are within maximum permissible limit prescribed by WHO (www.lenntech.com/drinking-water-standards.htm.) Other parameters like turbidity (18 - 471 NTU), TH (123 - 213 mg/l), Fe contents (0.2 - 0.7 mg/l), Chloride (6.9- 26.8 mg/l), TDS (255 - 501 mg/l), The Ca²⁺ (27.8 – 47.9 mg/l, SO₄-2 (51 – 90 mg/l), NO₃-(0-1.763 mg/l), F-1 (0-0.039 mg/l), TA (12.7 -245 mg/l) , Mg⁺² (9.24-27.24 mg/), OC (2.3-7.9 mg/l), SS (69 -281 mg/l) are found within the highest desirable or maximum permissible limit set by WHO.(Trivedi and Goel²⁰, 1986 and Trivedi et al²¹, 2009) However, turbidity and Fe contents are observed to be on higher side in all seasons and pre-monsoon and monsoon seasons respectively.

IV. CONCLUSIONS

A large number of factors and geological conditions influence the correlations between different pairs of physico - chemical parameters of water samples directly or indirectly. All the physico-chemical parameters of Ganga river water at Kanpur for pre monsoon, monsoon and post monsoon for year 2012 are within the highest desirable limit or maximum permissible limit prescribed by WHO except turbidity, Fe contents and pH which recorded high values in all seasons, pre monsoon and monsoon season and pre monsoon season respectively . From the results of present study we conclude that Ganga water of Kanpur is though fit for drinking purposes yet it need treatment to minimize the contamination especially turbidity and Fe contents . To minimize the contaminations of Ganga River water at Kanpur the values of correlation coefficients and their significance level will help in selecting the proper experimental methods used for treatment of water. To create increasing awareness among the people to maintain the Ganga river water at its highest quality and purity levels, the present study may prove to be useful in achieving this goal.

REFERENCES

- [1] Singh S.P., Pathak D. and Singh R. *Eco. Env. And Cons.*, 2002,8(3):289-292.
- [2] Petak W.J. *Environ. Managem.*1980, 4, 287-295.
- [3] (Sinha A.K. , Singh V. P. and Srivastava K., *Physico –chemical studies on river Ganga and its tributaries in Uttar Pradesh –the present status. Pollution and Biomonitoring of Indian Rivers.*(ed.) Dr. R.K. Trivedi.(Ed.), ABD publishers, Jaipur. 2000:1-29
- [4] Pandey P.K and Pandey ,G.N. , *J.Inst.Engr. India* 1980, 60, 27-34
- [5] Tare,V.,Yadav,A.V.S and Bose,P. *Water Research* 2003,37 :67-77.
- [6] Pahwa, D.V. and Mehrotra, S.N. *Proc. Nat. Acad. Sci., India*, 1966, Sec. 368 (2):157-189.

- [7] Sinha, U.K., Ganga pollution and health hazard. Inter-India Publication, New Delhi. 1986
- [8] Khan A.A, Haque N, Instisar A.S and Narayanan K, : J. Freshwater Biol.1984, 6(4), 295-304
- [9] Kaur S and Joshi B.D, -Him. J.Zool., 2003, 17(1) :45-55.
- [10] Zafer A and Sultana N., Seasonal Analysis in the Water Quality of River Ganga Disaster Ecology and Environment Arivnd Kumar (Ed.)Daya publishing House, India. 2007, 57- 62.
- [11] Sinha U.K. ,Ganga pollution and health hazard, Inter – India Publication, New Delhi,1986
- [12] Mehrotra M.N. J. of the Ind. Association of Sedimentologists, 1990, 9, 1-14
- [13] Sinha A.K. , Singh V. P. And Srivastava K., Physico –chemical studies on river Ganga and its tributaries in Uttar Pradesh –the present status. In pollution and Biomonitoring of Indian Rivers.(ed.) Dr. R.K. trevedi. ABD publishers, Jaipur. 2000,1-29
- [14] Bhandari N. S and Nayal K E-Journal of Chemistry, 2008, 5, No.2, 342-346
- [15] Garg D. K, Goyal R. N and Agrawal V. P, Ind. J. Envir.Prot.1990, 10(5), 355-359.
- [16] Sarkar M, Banerjee A , Pratim.P and Chakraborty S, J. Indian Chem. Soc., 2006 , 83, 1023-1027.
- [17] World Health Organization, Guidelines for drinking water quality-I, Recommendations, 2nd Ed. Geneva WHO, 1993 www.lenntech.com/drinkingwater-standards.htm.
- [18]. Standard Methods for the Examination of Water and Waste Water, 20th Ed., APHA, AWWA, WEF. Washington DC, 1998.
- [19] Vogel A.I, A text book of Quantitative Inorganic Analysis Including Elementary Instrumental Analysis 4th Edition. The English Language Book Society and Langman.Co 1978 (a) 837 (b) 328-329 (c) 504-506
- [20] Trivedi R.K and Goel P.K, Chemical and Biological Methods for Water Pollution Studies, Environmental Publication, India 1986
- [21] Priyanka Trivedi1, Amita Bajpai2 and Sukarma Thareja1.Evaluation of Water Quality: Physico – Chemical Characteristics of Ganga River at Kanpur by using Correlation Study; Nature and Science, 2009; 1(6)

Efficient Method of Detecting Data Leakage Using Misuseability Weight Measure

¹K.Sundaramoorthy, ²Dr.S.Srinivasa Rao Madhane

¹Research Scholar, St.Peter's University,Chennai ,Tamilnadu, India,

²Adhiparasakthi college of Engineering, Kalavai Tamilnadu, India

Abstract

Users within the organization's perimeter perform various actions on this data and may be exposed to sensitive information embodied within the data they access. In an effort to determine the extent of damage to an organization that a user can cause using the information she has obtained, we introduce the concept of misuseability Weight. To calculate the M-Score, A misuseability weight measure, this calculates a score that represents the sensitivity level of the data exposed to the user and by that predicts the ability of the user to maliciously exploit the data. By assigning a score that represents the sensitivity level of the data that a user is exposed to, the misuseability weight can determine the extent of damage to the organization if the data is misused. Using this information, the organization can then take appropriate steps to prevent or minimize the damage.

Index Terms: Data leakage, data misuse, security measures, misuseability weight.

I. INTRODUCTION

Sensitive information such as customer or patient data and business secrets constitute the main assets of an organization. Such information is essential for the organization's employees, subcontractors, or partners to perform their tasks. Conversely, limiting access to the information in the interests of preserving secrecy might damage their ability to implement the actions that can best serve the organization. Thus, data leakage and data misuse detection mechanisms are essential in identifying malicious insiders. The focus of this paper is on mitigating leakage or misuse incidents of data stored in databases (i.e., tabular data) by an insider having legitimate privileges to access the data. There have been numerous attempts to deal with the malicious insider scenario. The methods that have been devised are generally based on user behavioral profiles that define normal user behavior and issue an alert whenever a user's behavior significantly deviates from the normal profile. The most common approach for representing user behavioral profiles is by analyzing the SQL statement submitted by an application server to the database (as a result of user requests), and extracting various features from these SQL statements. Another approach focuses on analyzing the actual data exposed to the user, i.e., the result-sets. However, none of the proposed methods consider the different sensitivity levels of the data to which an insider is exposed. This factor has a great impact in estimating the damage that can be caused to an organization when data is leaked or misused. Security-related data measures including k-Anonymity, I-Diversity, and (k, l)-Anonymity is mainly used for privacy-preserving and is not relevant when the user has free access to the data. Therefore, we present a new concept, Misuseability Weight, which assigns a sensitivity score to data sets, thereby estimating the level of harm that might be inflicted upon the organization when the data is leaked. Four optional usages of the misuseability weight are proposed.

- [1] Applying anomaly detection by learning the normal behavior of an insider in terms of the sensitivity level of the data she is usually exposed to.
- [2] Improving the process of handling leakage incidents identified by other misuse detection systems by enabling the security officer to focus on incidents involving more sensitive data.
- [3] Implementing a Dynamic Misuseability-Based Access Control (DMBAC), designed to regulate user access to sensitive data stored in relational databases;.
- [4] Reducing the misuseability of the data.

II. MISUSEABILITY WEIGHT CONCEPTS

Data stored in an organization's computers is extremely important and embodies the core of the organization's power. An organization undoubtedly wants to preserve and retain this power. On the other hand, this data is necessary for daily work processes. Users within the organization's perimeter (e.g., employees, subcontractors, or partners) perform various actions on this data (e.g., query, report, and search) and may be

exposed to sensitive information embodied within the data they access. In an effort to determine the extent of damage to an organization that a user can cause using the information she has obtained, we introduce the concept of Misuseability Weight. By assigning a score that represents the sensitivity level of the data that a user is exposed to, the misuseability weight can determine the extent of damage to the organization if the data is misused. Using this information, the organization can then take appropriate steps to prevent or minimize the damage.

2.1 Dimensions of Misuseability

Assigning a misuseability weight to a given data set is strongly related to the way the data is presented (e.g., tabular data, structured or free text) and is domain specific. Therefore, one measure of misuseability weight cannot fit all types of data in every domain. In this section, we describe four general dimensions of misuseability. These dimensions, which may have different levels of importance for various domains, can serve as guidelines when defining a misuseability weight measure. While the first two dimensions are related to entities (e.g., customers, patients, or projects) that appear in the data, the last two dimensions are related to the information (or properties) that are exposed about these entities. The four dimensions are: Number of entities. This is the data size with respect to the different entities that appear in the data. Having data about more entities obviously increase the potential damage as a result of a misuse of this data. Anonymity level. While the number of different entities in the data can increase the misuseability weight, the anonymity level of the data can decrease it. The anonymity level is regarded as the effort that is required in order to fully identify a specific entity in the data. Number of properties. Data can include a variety of details, or properties, on each entity (e.g., employee salary or patient disease). Since each additional property can increase the damage as a result of a misuse, the number of different properties (i.e., amount of information on each entity) should affect the misuseability weight. Values of properties. The property value of an entity can greatly affect the misuseability level of the data. For example, a patient record with disease property equals to HIV should probably be more sensitive than a record concerning patient with a simple flu. In the context of these four dimensions, we claim that PPDP measures are only effective in a limited way through their capability of measuring the anonymity level dimension of the data. These measures, however, lack any reference to the other important dimensions that are necessary for weighting misuseability. For example, consider a table that shows employee names and salaries. Even if we double all the salaries that appear in the table, there may not be any change in neither of these measures' scores, and therefore no reference to the values of properties dimension. As a result of this lack, as well as others, we conclude that PPDP measures are not sufficiently expressive to serve as a misuseability weight measure and that a new measure is needed. In the following section, we introduce our proposal for addressing this need.

Fig. 1. An example of quasi-identifier and sensitive attributes.

First Name	Last Name	Job	City	Sex	Area code	Phone number
<ul style="list-style-type: none"> • Quasi-identifier attributes 						
<ul style="list-style-type: none"> • Sensitive attributes 						
Customer type						
Description: The group that the customer is associated with.						
Optional values: <i>Business; Private</i>						
Average monthly bill						
Description: The average bill per month for the account.						
Optional values: <i>(any real number)</i>						
Account type						
Description: The level of importance of the account.						
Optional values: <i>Gold; Silver; Bronze; White</i>						
Days to contract expiration						
Description: The time left until the current account contract is ended.						
Optional values: <i>(any positive integer)</i>						
Main usage						
Description: The usage that the customer spends most of her payments on: phone calls, SMS, data (like surfing the internet) or paid services (buying ringtones, downloading music or movies etc.)						
Optional values: <i>Phonecalls; SMS; Data; Paid services</i>						

III. THE M-SCORE MEASURE

To measure the misuseability weight, we propose a new algorithm—the M-score. This algorithm considers and measures different aspects related to the misuseability of the data in order to indicate the true level of damage that can result if an organization's data falls into wrong hands. The M-score measure is tailored for tabular data sets (e.g., result sets of relational database queries) and cannot be applied to non-tabular data such as intellectual property, business plans, etc. It is a domain independent measure that assigns a score, which represents the misuseability weight of each table exposed to the user, by using a sensitivity score function acquired from the domain expert.

3.1 Formal Definition

In this section, we provide the formal definitions for the M-score. Without loss of generality, we assume that only a single database exists. Nevertheless, the measure can be easily extended to cope with multiple databases. The first definition discusses the building blocks of our measure—table and attributes.

Definition 1 (Table and Attribute). A table $T(A_1; \dots; A_n)$ is a set of r records. Each record is a tuple of n values. The value i of a record, is a value from a closed set of values defined by A_i , the i 's Attribute of T . Therefore, we can define A_i either as the name of the column i of T , or as a domain of values. We define three, nonintersecting types of attributes: quasi-identifier attributes; sensitive attributes; and other attributes, which are of no importance to our discussion. To exemplify the computation of the M-score, we use throughout this paper the database structure of a cellular company as represented in Fig. 1.

Source and Published Tables

(A) THE SOURCE TABLE					(B) THE PUBLISHED TABLE				
Job	City	Sex	Account Type	Average Monthly Bill	Job	City	Sex	Account Type	Average Monthly Bill
Lawyer	NY	Female	Gold	\$350	Lawyer	NY	Female	Gold	\$350
Gardener	LA	Male	White	\$160	Lawyer	NY	Female	Bronze	\$600
Gardener	LA	Female	Silver	\$200	Teacher	DC	Female	Silver	\$300
Lawyer	NY	Female	Bronze	\$600	Gardener	LA	Male	Bronze	\$200
Teacher	DC	Female	Silver	\$300	Programmer	DC	Male	White	\$20
Gardener	LA	Male	Bronze	\$200	Teacher	DC	Female	White	\$160
Teacher	DC	Female	Gold	\$875					
Programmer	DC	Male	White	\$20					
Teacher	DC	Female	White	\$160					

Definition 2 (Quasi-Identifier Attributes). Quasi-identifier attributes are $Q = \{q_{i1}, \dots, q_{ik}\} \subseteq \{A_1, \dots, A_n\}$ attributes that can be linked, possibly using an external data source, to reveal a specific entity that the specific information is about. In addition, any subset of the quasi-identifiers (consisting of one or more attributes of Q) is a quasi-identifier itself. $q_1 = \text{First Name}$; $q_2 = \text{Last Name}$; $q_3 = \text{Job}$; $q_4 = \text{City}$;

$q_5 = \text{Sex}$; $q_6 = \text{Area Code}$; and $q_7 = \text{Phone Number}$.

Definition 3 (Sensitive Attributes). Sensitive attributes

$S_j = \{s_{j1}, \dots, s_{jk}\} \subseteq \{A_1, \dots, A_n\}$ are attributes that are used to evaluate the risk derived from exposing the data. The sensitive attributes are mutually excluded from the quasi-identifier attributes (i.e., $\forall j S_j \cap Q = \emptyset$). In our example; we have five different sensitive attributes— $s_1 = \text{Customer Group}$ to $s_5 = \text{Main Usage}$.

Definition 4 (Sensitivity Score Function). The sensitivity score function $f: [0,1]$ assigns a sensitivity score to each possible value x of S_j , according to the specific context $c \in C$ in which the table was exposed. For each record r , we denote the value x_r of S_j as $S_j[x_r]$. The sensitivity score function should be defined by the data owner (e.g., the organization) and it reflects the data owner's perception of the data's importance in different contexts. When defining this function, the data owner might take into consideration factors such as privacy and legislation, and assign a higher score to information that eventually can harm others (for example, customer data that can be used for identity theft and might result in compensatory costs). In addition, the data owner should define the exact context attributes.

3.2 Calculating the M- Score

The M-score incorporates three main factors.

- [1] Quality of data—the importance of the information.
- [2] Quantity of data—how much information is exposed.
- [3] The Distinguishing Factor (DF)—given the quasi-identifiers, the amount of efforts required in order to discover the specific entities that the table refers to. In order to demonstrate the process of calculating the M-score, we use the example presented in Table 1. Table 1 a represents our source table (i.e., our “database”) while Table 1b is a published table that was selected from the source table and for which we calculate the M- score. In the following sections, we explain each step in the proposed measure calculation.

3.3 Calculating Raw Record Score

The calculation of the raw record score of record i (or RRS_i), is based on the sensitive attributes of the table, their value in this record, and the table context. This score determines the quality factor of the final M-score, using the sensitivity score function f , defined in Definition 4.

Definition 5 (Raw Record Score).

$$RRS_i = \min \left(1, \sum_{S_j \in T} f(c, S_j[x_i]) \right)$$

S_{j2T} For a record i , RRS_i will be the sum of all the sensitive values score in that record, with a maximum of 1. When comparing two tables with different number of attributes, the table with the larger number of sensitive attributes will tend to have a higher sensitivity value for each individual record. In order to be able to compare the sensitivity of tables having different number of attributes, we need to eliminate this factor. Therefore, we have set an upper bound on the RRS_i by taking the minimum between 1 and the sum of sensitivity scores of the sensitive attributes.

3.4 Calculating Record Distinguishing Factor

Using the distinguishing factor, the M-score incorporates the uniqueness of the quasi-identifier's value in the table when weighting its misuseability. The DF measures to what extent a quasi-identifier reveals the specific entity it represents (e.g., a customer). It assigns a score in the range of [0,1], when the lower the score is, the harder it is to distinguish one entity from another, given this quasi-identifier. In other words, the DF of record indicates the effort a user will have to invest in order to find the exact entity she is looking for.

Usually, the DF is not easily acquired, and therefore we use the record distinguishing factor (D_i) as an approximation. The record distinguishing factor (D_i) is a kanonymity-like measure, with a different reference table from which to calculate k . While k -anonymity calculates, for each quasi-identifier, how many identical values are in the published table, the distinguishing factor's reference is "Yellow Pages." This means that an unknown data source, denoted by R_0 , contains the same quasi-identifier attributes that exist in the organization's source table, denoted by R_1 (for example, Table 1a). In addition, the quasi-identifier values of R_1 are a subset of the quasi-identifier values in R_0 , or more formally—quasi-identifier R_1 quasi-identifier R_0 .

In the example presented in Table 1b, the distinguishing factor of the first record is equal to two (i.e., $D_1 = 2$) since the tuple {Lawyer, NY, Female} appears twice in Table 1a. Similarly, $D_3 = 3$, ({Teacher, DC, Female} appears three times in Table 1a); $D_4 = 2$; and $D_5 = 1$. If there are no quasi-identifier attributes in the published table, we define that for each record i , D_i equals to the published table size.

As previously mentioned, the k -anonymity may suffer from the common sensitive attribute problem in which an adversary may not be able to match a record with its true entity, but she can still know the sensitive values. We opt to use the variation of the k -anonymity measure since it is well known and widely used in various tasks and implementations. However, other PPDP measures such as l -Diversity and (l, k)-Anonymity can be used as well.

3.5 Calculating the Final Record Score (RS)

The Final Record Score uses the records' RRS_i and D_i , in order to assign a final score to all records in the table. Definition 6 (Final Record Score). Given a table with r records, RS is calculated as follows:

$$RS = \max_{0 \leq i \leq r} (RS_i) = \max_{0 \leq i \leq r} \left(\frac{RRS_i}{D_i} \right).$$

For each record i , RS calculate the weighted sensitivity score RS_i by dividing the Record's Sensitivity Score (RRS_i) by its distinguishing factor (D_i). This ensures that as the record's distinguishing factor increases (i.e., it is harder to identify the record in the reference table) the weighted sensitivity score decreases. The RS of the table is the maximal weighted sensitivity score.

3.6 Calculating the M-Score

Finally, the M-score measure of a table combines the sensitivity level of the records defined by RS and the quantity factor (the number of records in the published table, denoted by r). In the final step of calculating the M-score, we use a settable parameter x ($x > 1$). This parameter sets the importance of the quantity factor within the table's final M-score. The higher we set x , the lower the effect of the quantity factor on the final M-score.

Definition 7 (M-Score). Given a table with r records, the table's M-score is calculated as follow:

$$MScore = r^{1/x} \times RS = r^{1/x} \times \max_{0 \leq i \leq r} \left(\frac{RRS_i}{D_i} \right),$$

Where r is the number of records in the table, x is a given parameter and RS is the final Record Score presented in Definition 6. The derived M-score value is not bounded. Thus, it is difficult to understand the meaning of the derived value and in particular the level of threat that is reflected by the M-score value. Therefore, we propose the following procedure for normalizing the M-score to the range [0,1]. Assume that T is the published table which is derived by applying the selection operator on the source table S , given a set of conditions, and then the projection operator: $T = \Pi_{a_1, a_2, \dots, a_n}(\sigma_{condition}(S))$. Let T be the projection of a_1, a_2, \dots, a_n on the source table: $T^* = \Pi_{a_1, a_2, \dots, a_n}(S)$.

The M-score of table T can be normalized by dividing the M-score of T by the M-score of T :
 $NormM-Score(T) = M-Score(T)/M-Score(T^*)$.

IV. EXTENDING THE M-SCORE

Until now, we were describing how the M-score can measure the misuseability weight of a single publication, without considering the information the user already has; i.e., “prior knowledge.” Prior knowledge can be: 1) previous publications (previous data tables the user was already exposed to); and 2) knowledge on the definition of the publication (e.g., the user can see the WHERE clause of the SQL query). In this section, we extend the M-score basic definition and address these issues.

4.1 Multiple Publications

A malicious insider can gain valuable information from accumulated publications by executing a series of requests. The result of each request possibly revealing information about new entities, or enriching the details of entities already known to her. Here, we focus on the case where the user can uniquely identify each entity (e.g., customer) in the result-set, i.e., the distinguishing factor is equal to 1 ($D_i=1$) Fig. 3 depicts nine optional cases resulting from two fully identifiable sequential publications. Each

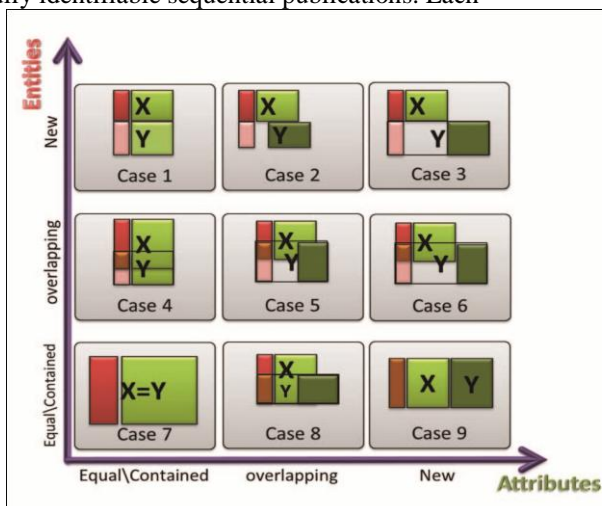


Fig. 3. Nine cases resulting from two fully identifiable publications.

Case is determined by the relation (equal, overlapping, or distinct) between the two publications with respect to the publications' sensitive attributes (marked in shades of green) and the exposed entities which are the distinct identifier values (marked in red). For example, in Case 1 on Fig. 3, the publications share the same schema (i.e., include the same attributes in all tuples), but have no common entities; Case 6 presents two publications that share some of the entities, but each publication holds different attributes on them.

Based on these nine possible cases, we introduce the Construct Publication Ensemble procedure. The Construct Publication Ensemble procedure is recursive. For each new publication, the procedure first creates an ensemble set X of all the previous publications that are within the time frame F. Then, the procedure checks which case in Fig. 3 fits the current publications and acts according. Finally, on the resulting ensemble set is returned

4.2 Multirelational Schema

In this section, we address the scenario of multirelational schema in which more than one table is released. In particular, following Nergiz et al. [18], we assume that we are given a multirelational schema that consists of a set of tables $T_1; \dots; T_n$, and one main table PT, where each tuple corresponds to a single entity (for example in Table 1 the main entity is the customer). The joined table JT is defined as $JT = PT \bowtie T_1 \bowtie \dots \bowtie T_n$. Note that the quasi-identifier set can span across various tables, namely the “quasi-identifier set for a schema is the set of attributes in JT that can be used to externally link or identify a given tuple in PT”. The various ingredients of the M-score can be calculated on an individually basis by using JT. For each entity i in PT we calculate the RRS_i by summing the scores of all sensitive values that appear in all her records in JT after eliminating duplicate values (for example if there are two records in JT that correspond to the same customer and each one of these records redundantly indicate that the customer is living in NY, then the sensitive score for the city NY will be counted only once). The D_i for an entity should be calculated by first calculating the D_i for each record in J. Then, the entity's D_i is set to the minimum among all her records' D_i in JT. Finally, the M-score is calculated.

4.3 Knowledge on Request Definition

A user may have additional knowledge on the data she receives emanating from knowing the structure of the request created this data, such as the request's constraints. In such cases, the basic M-score does not consider such knowledge. For example, a user might submit the following request: "Select "Name" of customers with "Account type" \neq "Gold". In this case, the user knows that all customers are "gold" customers. However, since the result-set of this request will only include the names, the M-score cannot correctly compute its misuseability weight. In order to extend the M-score to consider this type of prior knowledge, RES(R) and COND(R) operators are defined.

V. CONCLUSIONS AND FUTURE WORK

We introduced a new concept of misuseability weight and discussed the importance of measuring the sensitivity level of the data that an insider is exposed to. We defined four dimensions that a misuseability weight measure must consider. To the best of our knowledge and based on the literature survey we conducted, there is no previously proposed method for estimating the potential harm that might be caused by leaked or misused data while considering important dimensions of the nature of the exposed data. Consequently, a new misuseability measure, the M-score, was proposed. We extended the M-score basic definition to consider prior knowledge the user might have and presented four applications using the extended definition. Finally, we explored different approaches for efficiently acquiring the knowledge required for computing the M-score, and showed that the M-score is both feasible and can fulfill its main goals.

Two important issues, which relate to the knowledge elicitation and representation, should be further investigated: the temporal aspect of the M-score and the validity of the knowledge, acquired from the experts, over time; and the knowledge acquisition that might be subjective and not consistent among different experts which, in turn, may lead to an inaccurate sensitivity function.

In regards to the time factor, we assumed that the sensitivity level of an attribute's value will change in rare cases and especially the order of the values with respect to their sensitivity level. However, we are aware of the need to validate and reacquire the knowledge from timeto-time, and although we showed in the experiments that the knowledge can be acquired accurately with relatively minimal effort (in terms of experts time) using the pairwise comparison approach, we plan to explore methods for incremental learning, or postlearning fine tuning of the elicited sensitivity score function in future work.

With respect to the subjectivity of the elicited scoring function, our experiments indicate that the methods used ensure that the acquired knowledge is not biased. In fact, we showed that using knowledge acquired from one expert is sufficient in order to calculate sound M-scores for the entire domain. We plan to further investigate this important issue and check the effect of combining knowledge from several experts (e.g., ensemble of knowledge models) on the quality of the acquired knowledge and the accuracy of the M-score. In addition, in some cases the value of customers can be calculated by using known knowledge on the customer (e.g., how much she spends) and by predicting future revenue from the customer. In such cases, the sensitivity level of sensitive attributes can be objectively obtained by using machine learning techniques; in particular by fitting the sensitive parameter values to the customer value.

REFERENCES

- [1] 2010 Cyber Security Watch Survey, <http://www.cert.org/archive/pdf/ecrimesummary10.pdf>, 2012.
- [2] A. Kamra, E. Terzi, and E. Bertino, "Detecting Anomalous Access Patterns in Relational Databases," *Int'l J. Very Large Databases*, vol. 17, no. 5, pp. 1063-1077, 2008.
- [3] S. Mathew, M. Petropoulos, H.Q. Ngo, and S. Upadhyaya, "DataCentric Approach to Insider Attack Detection in Database Systems," *Proc. 13th Conf. Recent Advances in Intrusion Detection*, 2010.
- [4] L. Sweeney, "k-Anonymity: A Model for Protecting Privacy," *Int'l J. Uncertainty, Fuzziness and Knowledge Based Systems*, vol. 10, no. 5, pp. 571-588, 2002.
- [5] A. Machanavajjhala et al., "L-Diversity: Privacy beyond K-Anonymity," *ACM Trans. Knowledge Discovery from Data*, vol. 1, no.1, article 1, 2007.
- [6] R.C. Wong, L. Jiuyong, A.W. Fu, and W. Ke, "(, k)-Anonymity: An Enhanced k-Anonymity Model for Privacy-Preserving Data Publishing," *Proc. 12th ACM SIGKDD Int'l Conf. Knowledge Discovery and Data Mining*, 2006.
- [7] E. Celikel et al., "A Risk Management Approach to RBAC," *Risk and Decision Analysis*, vol. 1, no. 2, pp. 21-33, 2009.
- [8] B. Carminati, E. Ferrari, J. Cao, and K. Lee Tan, "A Framework to Enforce Access Control over Data Streams," *ACM Trans. Information Systems Security*, vol. 13, no. 3, pp. 1-31, 2010.
- [9] Q. Yaseen and B. Panda, "Knowledge Acquisition and Insider Threat Prediction in Relational Database Systems," *Proc. Int'l Conf. Computational Science and Eng.*, pp. 450-455, 2009.
- [10] G.B. Magklaras and S.M. Furnell, "Insider Threat Prediction Tool: Evaluating the Probability of IT Misuse," *Computers and Security*, vol. 21, no. 1, pp. 62-73, 2002.
- [11] M. Bishop and C. Gates, "Defining the Insider Threat," *Proc. Ann. Workshop Cyber Security and Information Intelligence Research*, pp. 13, 2008.

- [12] C.M. Fung, K. Wang, R. Chen, and P.S. Yu, "Privacy-Preserving Data Publishing: A Survey on Recent Developments," *ACM Computing Surveys*, vol. 42, no. 4, pp. 1-53, 2010.
- [13] A. Friedman and A. Schuster, "Data Mining with Differential Privacy," *Proc. 16th ACM SIGKDD Int'l Conf. Knowledge Discovery and Data Mining*, pp. 493-502, 2010.
- [14] C. Dwork, "Differential Privacy: A Survey of Results," *Proc. Fifth Int'l Conf. Theory and Applications of Models of Computation*, pp. 1-19, 2008.
- [15] T. Dalenius, "Finding a Needle in a Haystack or Identifying Anonymous Census Records," *J. Official Statistics*, vol. 2, no. 3, pp. 329-336, 1986.
- [16] B. Berendt, O. Günther, and S. Spiekermann, "Privacy in e-Commerce: Stated Preferences vs. Actual Behavior," *Comm. ACM*, vol. 48, no. 4, pp. 101-106, 2005.
- [17] A. Barth, A. Datta, J.C. Mitchell, and H. Nissenbaum, "Privacy and Contextual Integrity: Framework and Applications," *Proc. IEEE Symp. Security and Privacy*, pp. 184-198, 2006.
- [18] M.E. Nergiz et al., "Multirelational k-Anonymity," *IEEE Trans. Knowledge and Data Eng.*, vol. 21, no. 8, pp. 1104-1117, Aug. 2009.

Design of Contact Stress Analysis in Straight Bevel Gear

¹N.Mohan Raj , ²M.Jayaraj

¹PG Scholar, Dept.of Mech.Engg., Sri Krishna college of Technology, Kovaipudur, Tamilnadu, India-641042

²Assistant Professor, Dept.of Mech.Engg, Sri Krishna college of Technology, Kovaipudur, Tamilnadu, India-42

Abstract

Our present work concentrates on the three dimensional fillet stress analysis of bevel gear tooth using finite element method using APDL (Ansys Parametric Design Language). The stress distribution of bevel gear at the root of the tooth is evaluated under various load conditions such as uniformly varying load and a concentrated load at pitch point load. This paper also discusses load distribution on the pitch line and the stress distributions at the root fillet.

Keywords: bevel gear; root fillet; finite element method.

I. INTRODUCTION

Gears are used to transmit the power from one shaft to another shaft. For bevel gear is used to transmit the motion and power between to intersecting shaft and non-intersecting shaft. In recent years many approaches have done for stress analysis in straight bevel gear. Nalluveetil and Muthuveerappan [1] evaluate the bending stress of bevel gear by using FE method by changing pressure angle, torque, shaft angle, rim thickness and face width in gear model. Ramamurti, Nayak, Vijayendra and Sujatha [2] using finite element method, studied the three dimensional stress analysis of bevel gear teeth using cyclic symmetry concept. In this concept the displacement of a tooth is computed for each Fourier harmonic component of the contact line load and its reduced the computational effort. Nour, Djedid, Chevalier, Si-Chaib, Bouamrene [3] using FE method the contact analysis of spiral bevel gear has is done to evaluate the stress at root fillet of gear tooth. Vijayarangan and Ganesan [4] using three dimensional FE methods to analysis the behavior of composite bevel gear and it's compared to the carbon steel and they concluded that boron/epoxy composite material is very much thought of as material for transmit the power. Faydor, Litvin and Alfonso Fuentes [5] is evaluate the stress analysis for low-noise spiral bevel gear drives with adjusted bearing contact using FE method.

As, the stress value of gear is depends upon the parameters of the gear and loading conditions on it. In our, work, the influence of stress at root of bevel gear under different loading conditions are discussed.

II. MODELING OF GEAR TOOTH

The bevel gear geometrical model is developed in finite element software package ANSYS through APDL (ANSYS Parametric Design Language) program using analytical equations given by Buckingham [1]. The gear specifications considered for analysis in this work are given in Table 1. The sequence of operations done to generate the geometrical model of the bevel gear is given in Fig. 1. 20 noded iso-parametric 3 dimensional element having 3 Degrees of freedom per node (solid 95) is used to discretize the geometric model. In this model 54000 element are used for the present study. Single tooth is considered for finite element analysis. The single tooth sector finite element model is shown in fig.2

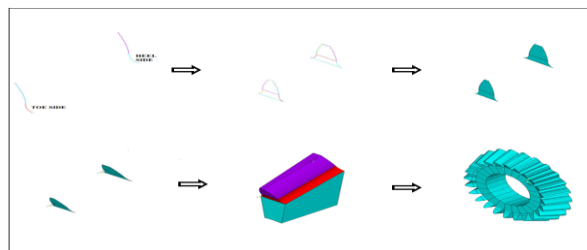


Fig 1 Bevel gear tooth model

III. Bevel gear specification [4]

Table 1

S.NO	PARAMETERS	VALUE
1	Pressure angle, α	20°
2	Shaft angle, β	90
3	Module(mm)	4
4	Addendum(mm)	5.38
5	Dedendum(mm)	3.37
6	Rim thickness(mm)	18.8
7	Number of teeth	24
8	Face width(mm)	20
9	Cone distance(mm)	107.33
10	Pitch radius (mm)	48
11	Semi cone angle, δ	26 °.34'
12	Root fillet	Trochoid
13	Material	C45Steel
14	Poisson ratio	0.3
15	Young's Modulus	2.01e5N/mm ²

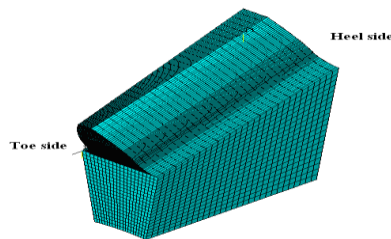


Fig 2 Meshed tooth model (Number of elements: 54000)

III. BOUNDARY CONDITIONS FOR APPLYING LOAD

The nodes at the inner radius of the rim are constrained in all directions and nodes in the side face of rim are constrained in the direction perpendicular to the surface area. A study has been made for two different loading conditions. They are uniform linear distributed load, and pitch point load at pitch point. The face width of the bevel gear tooth has divided into 31 nodes for applying load and to evaluate. In our work, the total resultant force for applying load in gear is 1651N from [4]. In bevel gear, resultant tooth force F_n is applied in tangentially (torque producing), radially (separating), and axially (thrust) components to the pitch point of gear, is designated F_t , F_r and F_a , respectively shown in figure-3.

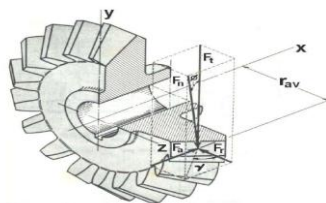


Fig 3 Gear tooth forces

IV. PITCH POINT LOAD

In this loading conditions F_n is resolved in to F_t , F_r and F_a and they are applied to the pitch point. The pitch point load in bevel gear tooth shown in figure-4. The loads are calculated using the expressions,

$$F_n = F_t / \cos \alpha, F_r = F_t \tan \alpha \cos \delta, F_a = F_t \tan \alpha \sin \delta$$

Where,

F_t = Tangential force

α = Pressure angle

δ = Semi cone angle

V. UNIFORMLY DISTRIBUTED LINEAR LOAD

The load uniformly distributed along the face width on pitch line and it is shown in figure.5

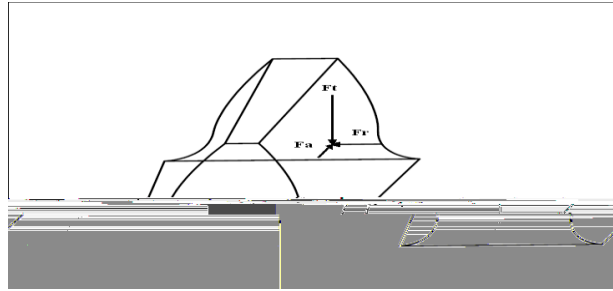
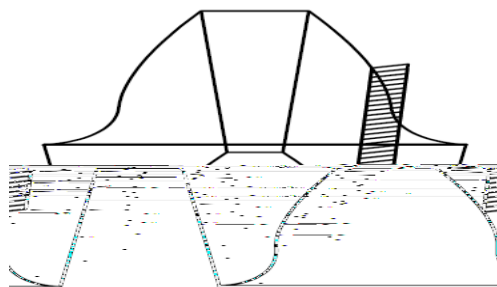


Fig 4 Pitch point load

Fig 5 Uniform distributed Linear load



VI. EVALUATION OF STRESS AT THE ROOT FILLET

The tooth behavior is studied for the given load and the maximum principle stress is illustrated in Fig 6,7, for various loading conditions. The maximum fillet stress calculated as per AGMA standard for the given load is only 52.43N/mm².

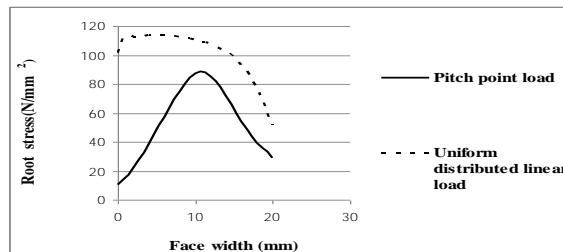


Figure 6 Root stress's at drive side along face width

It is observed from the graph that for the pitch point load the fillet stress at the drive side is gradually increasing from toe side to mid section and similar manner from the mid section to heel side it is gradually reducing. When the load is uniformly distributed along the entire pitch line, the stress value is more nearer to toe side when compare to that of heel side.

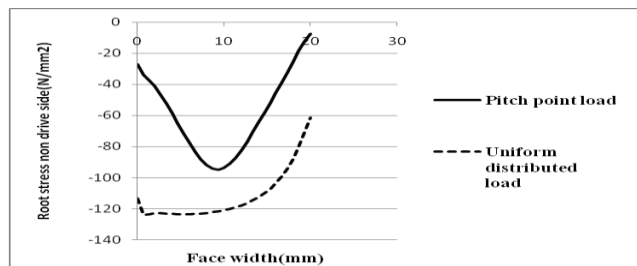


Figure 7 Root stress's at non drive side along face width

It is observed from the graph that for the pitch point load the fillet stress at the non-drive side is gradually decreasing from toe side to mid section and similar manner from the mid section to heel side it is gradually increasing. When the load is uniformly distributed along the entire pitch line, the stress value is more nearer to toe side when compare to that of heel side

VII. CONCLUSION

3D bevel gear model at finite element model using ANSYS has been generated and analyzed in this work. The influence load on the root stress in straight bevel gear is evaluated for two different conditions. The stress in gear tooth is high at toe side and comparatively low at heel side.

REFERENCE

- [1] Buckingham .E, Analytical mechanics of gears, Dover pubns, 1988.
- [2] S. J. Nalluveetil and G. Muthuveerappan, "Finite element modeling and analysis of a straight bevel gear tooth", computers & structures, vol. 48, no.4, pp.739-744, 1993.
- [3] V. Ramamurti, Nayak h. Vijayendra and c. Sujatha. "Static and dynamic analysis of spur and bevel gears using fem," Mech mach. Theory vol.33, no.8, pp.1177-1193, 1998.
- [4] SS.Vijayarangan and N.Ganesan, " Static stress analysis of a composite bevel gear using a three dimensional finite element method", computers & Structures, vol. 51, No. 6, pp, 771-783, 1994.
- [5] A. Nour, T. Djedid, Y. Chevalier, M.O. Si-Chaïb, and M.S.Bouamrene, " Stress analysis of spiral bevel gears using finite element method"
- [6] Faydor L. Litvin and Alfonso fuentes, "design and stress analysis of low-noise adjusted bearing contact spiral bevel gears", Nasa/Cr, 2002

Web Mining: Summary

¹Sonia Gupta , ²Neha Singh
¹Computer Science Department Ifim University
Moradabad(India)

Abstract

World Wide Web is a very fertile area for data mining research, with huge amount of information available on it. From its very beginning, the potential of extracting valuable knowledge from the Web has been quite evident. The term Web mining has been used in two different ways. The first, called Web content mining and the second, called Web usage mining. The web content mining is the process of information discovery from sources across the World Wide Web. Web usage mining is the process of mining for user browsing and access patterns. Interest in Web mining has grown rapidly in its short existence, both in the research and practitioner communities.

Keywords: Web mining, information retrieval, information extraction

I. INTRODUCTION

Web mining is the application of data mining techniques to extract knowledge from Web data - including Web documents, hyperlinks between documents, usage logs of web sites, etc. With more than two billion pages created by millions of Web page authors and organizations, the World Wide Web is a tremendously rich knowledge base. The knowledge comes not only from the content of the pages themselves, but also from the unique characteristics of the Web, such as its hyperlink structure and its diversity of content and languages.

Web mining research overlaps substantially with other areas, including data mining, text mining, information retrieval, and Web retrieval. The classification is based on two aspects: the purpose and the data sources. **Retrieval** research focuses on retrieving relevant, existing data or documents from a large database or document repository, while **mining** research focuses on discovering new information or knowledge in the data. Web retrieval and Web mining share many similarities. Web document clustering has been studied both in the context of Web retrieval and of Web mining. Web mining is not simply the application of information retrieval and text mining techniques to Web pages; it also involves non textual data such as Web server logs and other transaction-based data.

Table 1.1 A classification of retrieval and mining techniques and applications

Purpose/Data information sources	Any data	Textual data	Web-based data
Retrieving known data or documents efficiently and effectively	Data Retrieval	Information Retrieval	Web Retrieval
Finding new patterns or knowledge previously Unknown	Data Mining	Text Mining	Web Mining

It is also interesting to note that, although Web mining relies heavily on data mining and text mining techniques, not all techniques applied to Web mining are based on data mining or text mining.

Web mining is the application of data mining techniques to extract knowledge from Web data, where **at least one of structure (hyperlink) or usage (Web log) data is used in the mining process** (with or without other types of Web data).

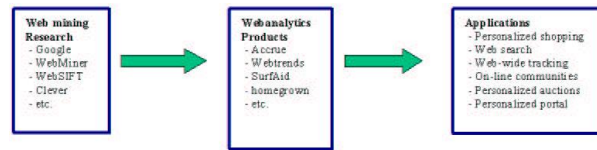


Figure 1.1: Web mining research & applications

Web mining technique could be used to solve the information overload problems above directly or indirectly. However, we could not claim that Web mining techniques are only tools to solve these problem. Other techniques and works from different research areas such as database(DB), information retrieval(IR), natural language processing(NLP), and the web document community, could also be used.

II. WEB MINING TAXONOMY

Web Mining can be broadly divided into three distinct categories, according to the kinds of data to be mined:

- [1] **Web Content Mining:** Web Content Mining is the process of extracting useful information from the contents of Web documents. Content data corresponds to the collection of facts a Web page was designed to convey to the users. It may consist of text, images, audio, video, or structured records such as lists and tables. While there exists a significant body of work in extracting knowledge from images - in the fields of image processing and computer vision - the application of these techniques to Web content mining has not been very rapid.
- [2] **Web Structure Mining:** The structure of a typical Web graph consists of Web pages as nodes, and hyperlinks as edges connecting between two related pages. Web Structure Mining can be regarded as the process of discovering structure information from the Web. This type of mining can be further divided into two kinds based on the kind of structural data used.
 - **Hyperlinks:** A Hyperlink is a structural unit that connects a Web page to different location, either within the same Web page or to a different Web page. A hyperlink that connects to a different part of the same page is called an *Intra-Document Hyperlink*, and a hyperlink that connects two different pages is called an *Inter-Document Hyperlink*.
 - **Document Structure:** In addition, the content within a Web page can also be organized in a tree-structured format, based on the various HTML and XML tags within the page.

Web Usage Mining: Web Usage Mining is the application of data mining techniques to discover interesting usage patterns from Web data, in order to understand and better serve the needs of Web-based applications.

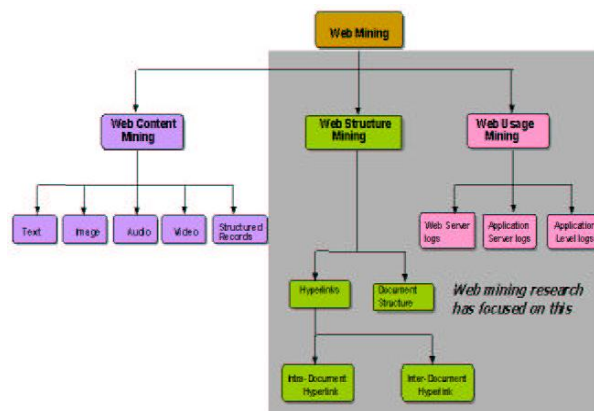


Figure 2.1: Web mining Taxonomy

III. WEB MINING

3.1 OVERVIEW

Web mining is the use of data mining technique to automatically discover and extract information from Web documents and services. Web mining is decomposed into subtasks such as:

- [1] **Resource finding:** the task of retrieving intended Web document.
- [2] **Information selection and pre-processing:** automatically selecting and pre-processing specific information from retrieved Web resources.
- [3] **Generalization:** automatically discovers general patterns at individual Web sites as well as across multiple sites,
- [4] **Analysis:** validation and/or interpretation of the mined patterns.

By resource finding we mean retrieving the data that is either online or offline from the text sources that is available on the Web such as electronic newsletter, electronic newswires, newsgroups, the text content of HTML document obtained by removing HTML tags and also manual selection of Web resources. The information selection and pre-processing step is any kind of transformation process of any kind of original data retrieving in IR process. Thus, Web mining refers to overall process of discovering potentially useful and previously unknown information or knowledge from the Web data.

3.2 WEB MINING AND INFORMATION RETREIVAL

Information Retrieval is automatic retrieval of all relevant documents while at same time retrieving as few of the non-relevant as possible. Information retrieval has the primary goals of indexing the text and searching for useful documents in a collection and nowadays in research. Information retrieval includes modeling, document classification and categorization, user interfaces, data visualization, filtering etc. Web mining is the part of Information Retrieval process.

3.3 WEB MINING AND INFORMATION EXTRACTION

Information Extraction has the goal of transforming a collection of documents, usually with the help of Information Retrieval system into information that is more readily digested and analyzed. Building Information Extraction system manually is not feasible and salable for such a dynamic and diverse medium such as Web contents. Due to this nature of Web, most information Extraction system focuses on the specific Websites to extract. Others use machine learning or data mining techniques to learn extraction patterns or rules for Web document semi-automatically or automatically. Web mining is the part of Information Extraction. There are basically two types of Information Extraction: Information Extraction from unstructured text and Information Extraction from semi-structured data.

3.4 Web Mining and Machine Learning Applied on the Web

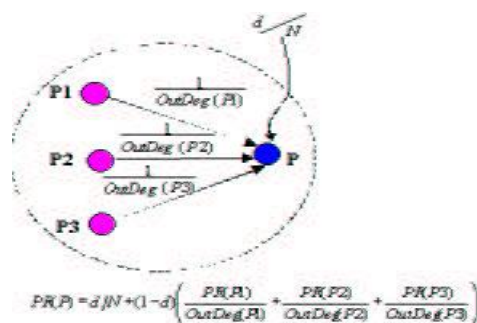
Web mining is not the same as learning from the Web or machine learning techniques applied from the Web.

IV. KEY ACCOMPLISHMENTS

We briefly describe the key new concepts introduced by the Web mining research community.

4.1 Page ranking metrics - Google's Page Rank function

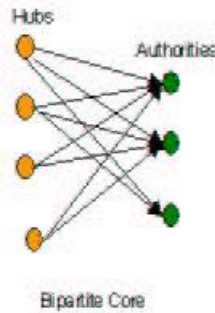
Page Rank is a metric for ranking hypertext documents that determines the quality of these documents. The key idea is that a page has high rank if it is pointed to by many highly ranked pages.



Page rank

4.2 Hubs and Authorities - Identifying significant pages in the Web

Hubs and Authorities can be viewed as ‘fans’ and ‘centers’ in a bipartite core of a Web graph. A Core (i, j) is a complete directed bipartite sub-graph with at least i nodes from F and at least j nodes from C. With reference to the Web graph, i pages that contain the links are referred to as ‘fans’ and the j pages that are referenced are the ‘centers’. From a conceptual point of view ‘fans’ and ‘centers’ in a Bipartite Core are basically the Hubs and Authorities. The hub and authority scores computed for each Web page indicate the extent to which the Web page serves as a “hub” pointing to good “authority” pages or as an “authority” on a topic pointed to by good hubs. First a query is submitted to a search engine and a set of relevant documents is retrieved. This set, called the ‘root set’, is then expanded by including Web pages that point to those in the ‘root set’ and are pointed by those in the ‘root set’.



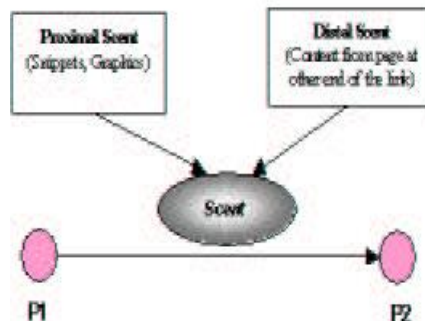
Hubs and authorities

4.3 Robot Detection and Filtering - Separating human and non human Web behavior

Web robots are software programs that automatically traverse the hyperlink structure of the World Wide Web in order to locate and retrieve information. The importance of separating robot behavior from human behavior prior to extracting user behavior knowledge from usage data. First of all, e-commerce retailers are particularly concerned about the unauthorized deployment of robots for gathering business intelligence at their Web sites. In addition, Web robots tend to consume considerable network bandwidth at the expense of other users. Sessions due to Web robots also make it more difficult to perform click-stream analysis effectively on the Web data. Conventional techniques for detecting Web robots are often based on identifying the IP address and user agent of the Web clients. While these techniques are applicable to many well-known robots, they may not be sufficient to detect camouflaging and previously unknown robots.

4.4 Information scent - Applying foraging theory to browsing behavior

Information scent is a concept that uses the snippets and information presented around the links in a page as a “scent” to evaluate the quality of content of the page it points to and the cost to access such a page. The key idea is a user at a given page “foraging” for information would follow a link with a stronger “scent”. The “scent” of the pages will decrease along a path and is determined by network flow algorithm called spreading activation.



Information scent

4.5 User profiles - Understanding how users behave

The Web has taken user profiling to completely new levels. For example, in a 'brick-and-mortar' store, data collection happens only at the checkout counter, usually called the 'point-of-sale'. This provides information only about the final outcome of a complex human decision making process, with no direct information about the process itself. In an on-line store, the complete click-stream is recorded, which provides a detailed record of every single action taken by the user - which can provide much more detailed insight into the decision making process.

4.6 Interestingness measures

When multiple sources provide conflicting evidence One of the significant impacts of publishing on the Web has been the close interaction now possible between authors and their readers. In the pre-Web era, a reader's level of interest in published material had to be inferred from indirect measures such as buying/borrowing, library checkout/ renewal, opinion surveys, and in rare cases feedback on the content. For material published on the Web it is possible to track the precise click-stream of a reader to observe the exact path taken through on-line published material, with exact times spent on each page, the specific link taken to arrive at a page and to leave it, etc. Much more accurate inferences about readers' interest about published content can be drawn from these observations. Mining the user click-stream for user behavior, and use it to adapt the 'look-and-feel' of a site to a reader's needs.

V. FUTURE DIRECTIONS

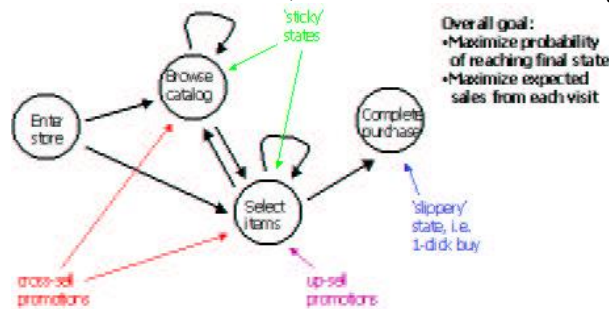
As the Web and its usage grows, it will continue to generate evermore content, structure, and usage data, and the value of Web mining will keep increasing. Outlined here are some research directions that must be pursued to ensure that we continue to develop Web mining technologies that will enable this value to be realized.

5.1 Process mining

Mining of 'market basket' data, collected at the point-of-sale in any store, has been one of the visible successes of data mining. However, this data provides only the end result of the process, and that too decisions that ended up in product purchase. Research needs to be carried out in (i) extracting process models from usage data, (ii) understanding how different parts of the process model impact various Web metrics of interest, and (iii) how the process models change in response to various changes that are made - changing stimuli to the user.

5.2 Temporal evolution of the Web

While storing the history of all of this interaction in one place is clearly too staggering a task, at least the changes to the Web are being recorded by the pioneering. Research needs to be carried out in extracting temporal models of how Web content, Web structures, Web communities, authorities, hubs, etc. are evolving. Large organizations generally archive (at least portions of) usage data from their Web sites. The temporal behavior of the three kinds of Web data: Web Content, Web Structure and Web Usage.



Shopping Pipeline modeled as State Transition Diagram

5.3 Fraud and threat analysis

The anonymity provided by the Web has led to a significant increase in attempted fraud, from unauthorized use of individual credit cards to hacking into credit card databases for blackmail purposes. Since all these frauds are being perpetrated through the Internet, Web mining is the perfect analysis technique for detecting and preventing them. Research issues include developing techniques to recognize known frauds, and characterize and then recognize unknown or novel frauds, etc. The issues in cyber threat analysis and intrusion detection are quite similar in nature.



(a) Change in Web Content of a document over time.



(b) Change in Web Structure of a document over time



(c) Change in Web Usage of a document over time

VI. CONCLUSION

As the Web and its usage continues to grow, so grows the opportunity to analyze Web data and extract all manner of useful knowledge from it. The past five years have seen the emergence of Web mining as a rapidly growing area, due to the efforts of the research community as well as various organizations that are practicing it. In this paper we have briefly described the key computer science contributions made by the field, the prominent successful applications, and outlined some promising areas of future research. Our hope is that this overview provides a starting point for fruitful discussion.

REFERENCES

- [1] J. Borges and M. Levene. Mining Association Rules in Hypertext Databases. In *Knowledge Discovery and Data Mining*, pages 149–153, 1998.
- [2] K. Bollacker, S. Lawrence, and C.L. Giles. CiteSeer: An autonomous webagent for automatic retrieval and identification of interesting publications. In *Katia P. Sycara and Michael Wooldridge, editors, Proceedings of the Second International Conference on Autonomous Agents*, pages 116–123, New York, 1998. ACM Press.
- [3] E.H. Chi, P. Pirolli, K. Chen, and J.E. Pitkow. Using Information Scent to model user information needs and actions and the Web. In *Proceedings of CHI 2001*, pages 490–497, 2001.
- [4] S. Abiteboul. Querying semi-structured data. In *F. N. Afrati and P. Kolaitis, editors database theory-ICDT '97, 6th International Conference, Delphi Greece, January 8-10, 1997, proceedings, volume 1186 of lecture note in computer science*, pages 1-18. Springer, 1997.
- [5] S. Abiteboul, D. Quass, J. Mchugh, J. Widom and J. L. Wiener. The lorel Query language for semi-structured data. *Int. J. on Digital Libraries* 1(1):68-88, 1997.
- [6] E.H. Chi, J. Pitkow, J. Mackinlay, P. Pirolli, R. Gossweiler, and S.K. Card. Visualizing the evolution of web ecologies. In *Proceedings of the Conference on Human Factors in Computing Systems CHI'98*, 1998.
- [7] E. Colet. *Using Data Mining to Detect Fraud in Auctions*, 2002.
- [8] R. Cooley. *Web Usage Mining: Discovery and Application of Interesting Patterns from Web Data*. PhD thesis, University of Minnesota, 2000.
- [9] K.L. Ong and W. Keong. *Mining Relationship Graphs for Eective Business Objectives*.
- [10] B. Prasetyo, I. Pramudiono, K. Takahashi, M. Toyoda, and M. Kitsuregawa. *Naviz user behavior visualization of dynamic page*.

A Study on User Future Request Prediction Methods Using Web Usage Mining

Dilpreet kaur¹, Sukhpreet Kaur²

¹Master of Technology in Computer Science & Engineering, Sri Guru Granth Sahib World University, Fatehgarh Sahib, Punjab, India.

²Assistant Professor, Department Of Computer Science & Engineering, Sri Guru Granth Sahib World University, Fatehgarh Sahib, Punjab, India.

Abstract

Web usage mining is an important type of web mining which deals with log files for extracting the information about users how to use website. It is the process of finding out what users are looking for on internet. Some users are looking at only textual data, where others might be interested multimedia data. Web log file is a log file automatically created and manipulated by the web server. The lots of research has done in this field but this paper deals with user future request prediction using web log record or user information. The main aim of this paper is to provide an overview of past and current evaluation in user future request prediction using web usage mining.

Keywords: Future request prediction, log file, Web usage mining

I. INTRODUCTION

The web is an important source of information retrieval now-a days, and the users accessing the web are from different backgrounds. The usage information about users are recorded in web logs. Analyzing web log files to extract useful patterns is called web usage mining. Web usage mining approaches include clustering, association rule mining, sequential pattern mining etc., To facilitate web page access by users, web recommendation model is needed.[10]

Web usage mining is valuable in many applications like online marketing, E- businesses etc. The use of this type of web mining helps to gather the important information from customers visiting the site. This enables an in-depth log to complete analysis of a company's productivity flow. E-businesses depend on this information to direct the company to the most effective Web server for promotion of their product or service.[12]In this paper we did literature survey on user future request prediction in web usage mining. The paper gives the overview of various methods of user future request prediction. The advantages and disadvantages of these methods have also been discussed. The rest of the paper is organized as below. Section 2 presents the motivation of paper, Section 3 presents Literature Survey on users next request prediction, and Section 4 gives the conclusion and Future Work.

II. MOTIVATION

With the growing popularity of the World Wide Web, A large number of users access web sites in all over the world. When user access a websites, a large volumes of data such as addresses of users or URLs requested are gathered automatically by Web servers and collected in access log which is very important because many times user repeatedly access the same type of web pages and the record is maintained in log files. These series of accessed web pages can be considered as a web access pattern which is helpful to find out the user behavior. Through this behavior information, we can find out the accurate user next request prediction that can reduce the browsing time of web page thus save the time of the user and decrease the server load. In recent years, there has been a lot of research work done in the field of web usage mining „ Future request prediction“. The main motivation of this study is to know the what research has been done on Web usage mining in future request prediction.

III. LITERATURE SURVEY

The focus of the literature survey is to study or collecting information about web usage mining which is used to find out web navigation behavior of user and collecting the information about “User Future Request Prediction” approach which is used to predict the next request of the user. Alexandras Nanopoulos, Dimitris Katsaros and Yannis Manolopoulos[1] focused on „web pre-fetching“ because of its importance in reducing user perceived latency present in every web based application. From the web popularity, there is heavy traffic in the internet and the result is that there is delay in response.

The reasons of delay are the web servers under heavy load, Network congestion, Low bandwidth, Bandwidth underutilization and propagation delay. The solution is to increase the bandwidth but this is not proper solution because of economic cost. For that propose, this technique proposed in which reducing the delay of client future requests for web objects and getting that objects into the cache in the background before an explicit request is made for them. Architecture shows how web server could cooperate with a pre-fetch engine to disseminate hints every time a client request to a document of the server. In this paper author presented important factors which affects on web pre-fetching algorithm like order to dependencies between web document accesses and the interleaving of requests belonging to patterns with random ones within user transactions and the ordering of requests. WMO (Ordered Web Mining) algorithm it compares with previously proposed algorithm like PPM, DG and existing approaches from the application of web log mining to web pre-fetching and the author got a result WMO achieved large accuracy in prediction with quite low overhead in network traffic.[1]

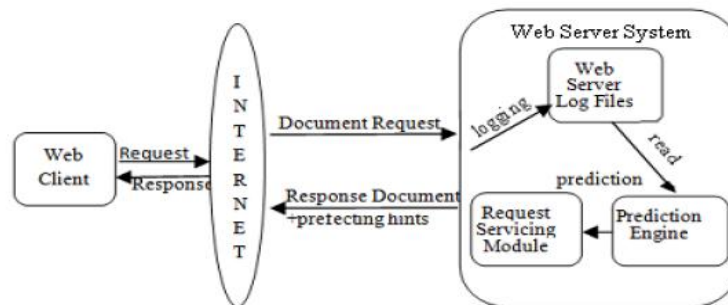


Figure 1 Proposed architecture of a prediction enabled Web server[1]

Yi-Hung Wu and Arbee L. P. Chen,[2] proposed user behaviors by sequences of consecutive web page accesses, derived from the access log of a proxy server. Moreover, the frequent sequences are discovered and organized as an index. Based on the index, they propose a scheme for predicting user requests and a proxy based framework for prefetching web pages. They perform experiments on real data. The results show that their approach makes the predictions with a high degree of accuracy with little overhead. In the experiments, the best hit ratio of the prediction achieves 75.69%, while the longest time to make a prediction only requires 1.9ms. The disadvantage of this experiment is that the average service rate is very low. The other problem is the setting of the three thresholds used in the mining stage. These thresholds have great impacts on the construction of the pattern trees. The use of minimum support and minimum confidence is to prune the useless paths. Obviously, some information may be lost if the pruning effects are overestimated. On the other hand, the grouping confidence is only useful for the strongly related web pages due to some editorial techniques, such as the embedded images and the frames.

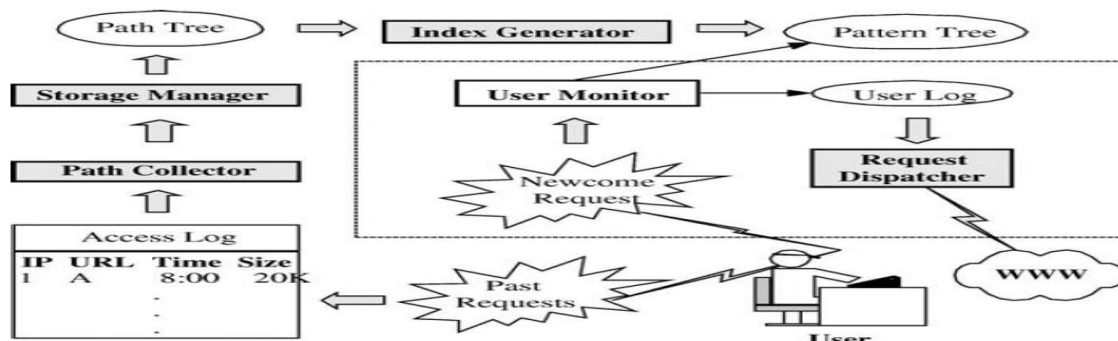


Figure 2 The flowchart of prediction system using proxy server log.[2]

According to Mathis Gery & Hatem Huddad,[3] Author distinguished three web mining approaches that exploit web logs: Association Rules (AR), Frequent Sequences (FS) and Frequent Generalized Sequences (FGS). Algorithm for three approaches were developed and experiments have been done with real web log data. Association Rule: In data mining, association rule learning is a popular and well researched method for discovering interesting relations between variables in large database. Describes analyze and present strong rules discovered in database using different measures of interestingness.

In [3] The problem of finding web pages visited together is similar to finding associations among item sets in transaction databases. Once transaction have been identified each of them could represent a basket and each research an item. Frequent Sequences: The attempt of this technique is to discover time ordered sequences of URLs that have been followed by past users. Frequent Generalized Sequences (FGS): a generalized sequence is a sequence allowing wildcards in order to reflect the users navigation in a flexible way. In order to extract frequent generalized subsequences they have used the generalized algorithm proposed by Gaul.

Author performed some experiments for this purpose they used three collections of web log datasets. One weblog dataset for small web site, another for large website and the third weblog dataset for intranet website. By using above three web mining approaches they evaluate the three different types of real web log data and they found Frequent Sequence (FS) gives better accuracy than AR and FGS.[3]Siriporn Chimphee, Naomie Salim, Mohd Salihin, Bin Ngadiman , Witcha Chimphee [4] proposed a method for constructing first-order and second-order Markov models of Web site access prediction based on past visitor behavior and compare it association rules technique. In these approaches, sequences of user requests are collected by the session identification technique, which distinguishes the requests for the same web page in different browses. In this experiment, the three algorithms first-order Markov model, second-order Markov and Association rules are used. These algorithms are not successful in correctly predicting the next request to be generated. The first-order Markov Model is best than other because it can extracted the sequence rules and choose the best rule for prediction and at the same time second-order decrease the coverage too. This is due to the fact that these models do not look far into the past to discriminate correctly the difference modes of the generative process.

Christos Makris, Yannis Panagis, Evangelos Theodoridis, and Athanasios Tsakalidis in [5] Proposed a technique for predicting web page usage patterns by modeling users' navigation history using string processing techniques, and validated experimentally the superiority of proposed technique. In this paper weighted suffix tree is used for modeling user navigation history. The method proposed has the advantage that it demands a constant amount of computational effort per user action and consumes a relatively small amount of extra memory space.

Vincent S. Tseng, Kawuu Weicheng Lin, Jeng-Chuan Chang in [6] Propose a novel data mining algorithm named *Temporal N-Gram (TNGram)* for constructing prediction models of Web user navigation by considering the temporality property in Web usage evolution. In this three kinds of new measures Support-based Fundamental Rule Changes, Confidence-based Fundamental Rule Changes, and Changes of Prediction Rules are proposed for evaluating the temporal evolution of navigation patterns under different time periods. Through experimental evaluation on both of real-life and simulated datasets, the proposed *TN-Gram* model is shown to outperform other approaches like N-gram modeling in terms of prediction precision, in particular when the web user's navigating behavior changes significantly with temporal evolution.

Mehrdad Jalali, Norwati Mustapha, Md. Nasir Sulaiman, Ali Mamat in [7] Proposed a recommendation system called WebPUM, an online prediction using Web usage mining system for effectively provide online prediction and propose a novel approach for classifying user navigation patterns to predict users' future intentions. The approach is based on the new graph partitioning algorithm to model user navigation patterns for the navigation patterns mining phase. LCS algorithm is used for classifying current user activities to predict user next movement. The architecture of WEBPUM is divided into two parts:-

- [1] Offline phase This phase consists two main modules, which are data pretreatment and navigation pattern mining. Data pretreatment module is designed to extract user navigation sessions from the original Web user log files. A new clustering algorithm based on graph partitioning is introduced for navigation patterns mining.
- [2] Online phase The main objective of this phase is to Classifying the user current activities based on navigation patterns in a particular Web site, creating a list of recommended Web pages as prediction of user future movement. The main online component is the prediction engine.

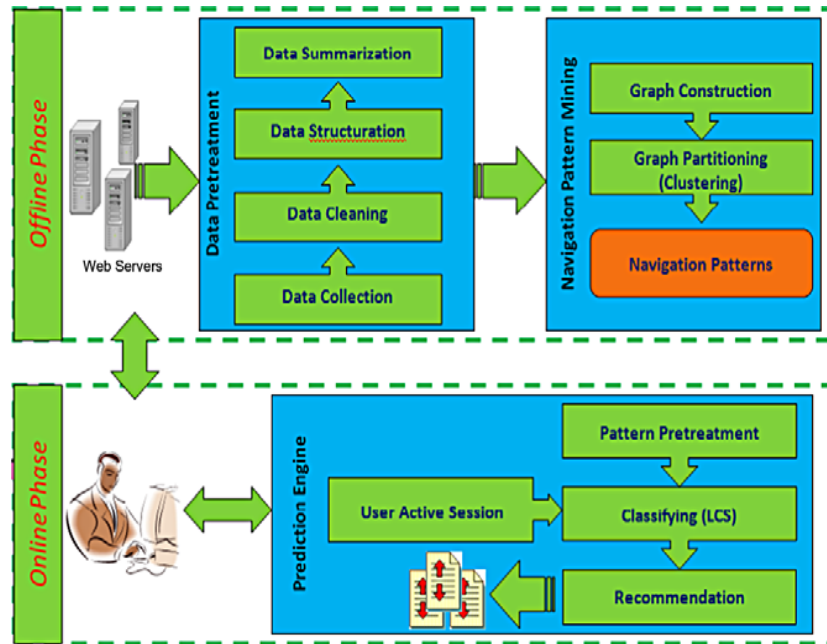


Figure 3 Architecture of WebPUM.[7]

Chu-HuiLee , Yu-lung Lo, Yu-Hsiang Fu [8] propose an efficient prediction model, two-level prediction model (TLPM), using a novel aspect of natural hierarchical property from web log data. TLPM can decrease the size of candidate set of web pages and increase the speed of predicting with adequate accuracy. The experiment results prove that TLPM can highly enhance the performance of prediction when the number of web pages is increasing.

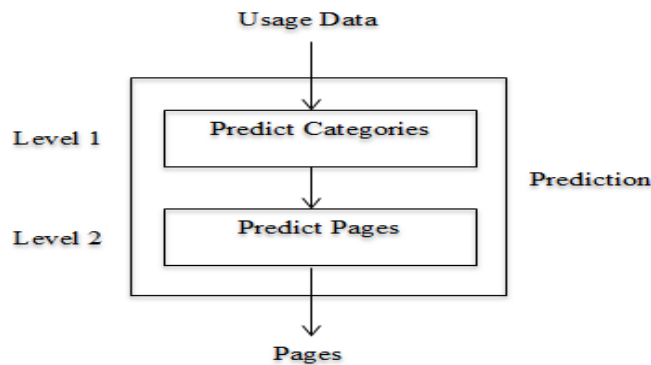


Figure 4 Two level prediction model(TLPM).[8]

In the TLPM [8] , in level one, Markov model is used to predict the next possible category which will be browsed by the user . Inlevel two, Bayesian theorem is used to predict the next possible page which belongs to the predicted category of level one to archive the goal ofreducing prediction scope more efficiently through the two-level framework. The experiment result proves that TLPM can archive the purpose and improve the efficiency of prediction by the way of finding out the important category in level one and decreasing the candidate page set in level two. Finally, the prediction result of TLPM can be applied in pre-fetching and caching on web site, personalization, target sales, improving web site design,etc.

V. Sujatha, Punithavalli [9] proposed the Prediction of User navigation patterns using Clustering and Classification (PUCC) from web log data. In the first stage PUCC focuses on separating the potential users in web log data, and in the second t stage clustering process is used to group the potential users with similar interest and in the third stage the results of classification and clustering is used to predict the user future requests.

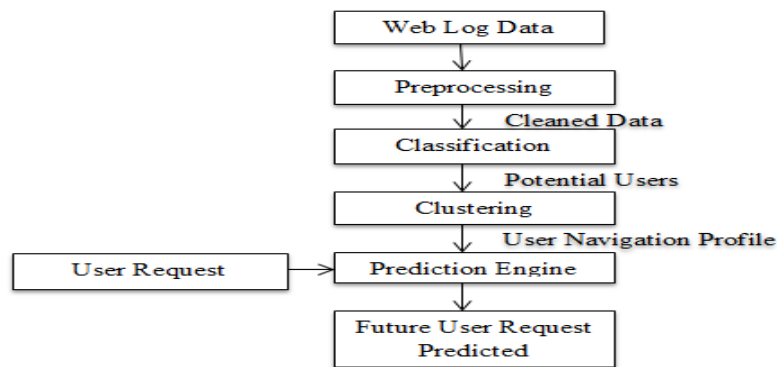


Figure 5 PUCC Model.[9]

The first stage is the cleaning stage, where unwanted log entries were removed. In the second stage, cookies were identified and removed. The result was then segmented to identify potential users. From the potential user, a graph partitioned clustering algorithm was used to discover the navigation pattern. An LCS classification algorithm was then used to predict future requests.[9]

Trilok Nath Pandey, Ranjita Kumari Dash , Alaka Nanda Tripathy ,Barnali Sahu [11] proposed IMC(Integrating Markov Model with Clustering) approach for user future request prediction. In this paper author presented the improvement of markov model accuracy by grouping web sessions into clusters. The web pages in the user sessions are first allocated into categories according to web services that are functionally meaning full. Then k-means clustering algorithm is implemented using the most appropriate number of clusters and distance measure. Markov model techniques are applied to each cluster as well as to the whole data set. The advantage of this approach is that it improves the accuracy of lower order markov model and disadvantage of this method is that it reduce the state space complexity of higher order markov model.

IV. CONCLUSION AND FUTURE WORK

The conclusion based on the literature survey is that Various research had done on future request prediction approach. In existing research various algorithms of pattern discovery techniques like graph partition techniques of clustering, LCS and Naive Bayesian techniques of classification etc are used for user future request prediction and many types of models are developed for prediction. In future prediction can be improved by using different techniques of data mining pattern discovery like classification, clustering, association rule mining etc.

REFERENCES

- [1] Alexandros Nanopoulos, Dimitris Katsaros and Yannis Manolopoulos “Effective prediction of web-user accesses: A data mining approach,” in Proc. Of the Workshop WEBKDD, 2001.
- [2] Yi-Hung Wu and Arbee L. P. Chen, “Prediction of Web Page Accesses by Proxy Server Log” World Wide Web: Internet and Web Information Systems, 5, 67–88, 2002.
- [3] Mathias Gery, Hatem Haddad “Evaluation of Web Usage Mining Approaches for User’s Next Request Prediction” WIDM’03 Proceedings of the 5th ACM international workshop on web information and data management p.74-81, November 7-8,2003.
- [4] Siriporn Chimphee, Naomie Salim, Mohd Salihin, Bin Ngadiman , Witcha Chimphee “Using Association Rules and Markov Model for Predict Next Access on Web Usage Mining” © 2006 Springer.
- [5] Christos Makris, Yannis Panagis, Evangelos Theodoridis, and Athanasios Tsakalidis “A Web-Page Usage Prediction Scheme Using Weighted Suffix Trees” © Springer-Verlag Berlin Heidelberg 2007.
- [6] Vincent S. Tseng, Kawuu Weicheng Lin, Jeng-Chuan Chang “Prediction of user navigation patterns by mining the temporal web usage evolution” © Springer-Verlag 2007.
- [7] Mehrdad Jalali, Norwati Mustapha, Md. Nasir Sulaiman, Ali Mamat, “WebPUM: A Web-based recommendation system to predict user future movements” Expert Systems with Applications 37 , 2010.
- [8] Chu-Hui Lee , Yu-lung Lo, Yu-Hsiang Fu, “A novel prediction model based on hierarchical characteristic of web site”, Expert Systems with Applications 38 , 2011.
- [9] V. Sujatha, Punithavalli, “Improved User Navigation Pattern Prediction Technique From Web Log Data”, Procedia Engineering 30 ,2012.
- [10] A. Anitha, “A New Web Usage Mining Approach for Next Page Access Prediction”, International Journal of Computer Applications, Volume 8– No.11, October 2010
- [11] TrilokNathPandey, Ranjita Kumari Dash , Alaka Nanda Tripathy ,Barnali Sahu, “Merging Data Mining Techniques for Web Page Access Prediction: Integrating Markov Model with Clustering”, IJCSI International Journal of Computer Science Issues, Vol. 9, Issue 6, No 1, November 2012.
- [12] <http://www.webdatamining.net/usage/>

A Study on Image Indexing and Its Features

Rajni Rani¹, Kamaljeet Kaur²

¹Master of Technology in Computer Science & Engineering, Sri Guru Granth Sahib World University, Fatehgarh Sahib, Punjab, India.

²Assistant Professor, Department Of Computer Science & Engineering, Sri Guru Granth Sahib World University, Fatehgarh Sahib, Punjab, India.

Abstract

The visual information available in the form of images, effective management of image archives and storage systems is of great significance and an extremely challenging task indeed. Indexing such a huge amount of data by its contents, is a very challenging task. data representation and feature based content modeling are two basic components required by the management of any multimedia database. As far as the image database is concerned, the former is concerned with image storage while the latter is related to image indexing. And it is also used to the different features like color, shape and textures of images. The color and texture features are obtained by computing the mean and standard deviation on each color band of image and sub-band of different wavelets.

Keywords: Feature Of Image Indexing, Image Indexing , Texture Extraction Of Image.

I. INTRODUCTION

A database indexing is a data structure that improves the speed of data retrieval operations on a database table at the cost of slower writes and increased storage space and content modeling are two basic components required by the management of any multimedia database. [9] the image database is concerned, the former is concerned with image storage while the latter is related to image indexing. The image indexing is to retrieve similar images from an image database for a given query image . Each image has its unique feature. Hence image indexing can be implemented by comparing their features, which are extracted from the images. The criterion of similarity among images may be based texture, and above mentioned other image attributes. n the features such as color, intensity, shape, location and and texture, and above mentioned other image attribute.

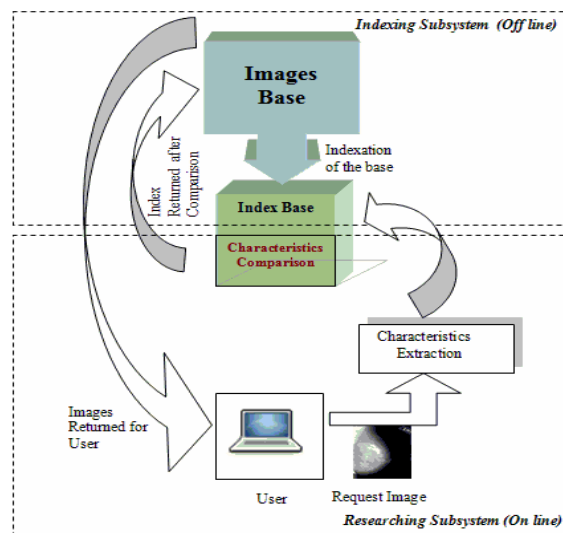


Figure1. Typical architecture of images indexing system [6]

In this paper we did literature survey of image indexing in database. The paper gives the overview of various features of image indexig. The various methods have also been discussed. The rest of the paper is organized as below. Section 2 presents the features , Section 3 represent the texture feature extraction .and Section 4 gives the conclusion.

II. FEATURES OF IMAGE INDEXING

2.1 Color

Color is one of the most widely used low-level features in the context of indexing. It is relatively robust to background complication and independent of image size and orientation. The color of an image is represented through some color model. A color model is specified in terms of 3-D coordinate system and a subspace within that system where each color is represented by a single point. The more commonly used color models are RGB, HSV and YIQ (luminance and chrominance). [8] A method of compressing an image that enables 8 bits per pixel to look almost as good as 24 bits per pixel. The technique determines the 256 most frequently used colors in the image and creates a color lookup table, also called a "color map" that is stored with the image. Rather than each pixel in the image having all three RGB colors, the Major Problem When early computer screens were commonly limited to 256 colors, indexed color methods were essential. Two indexed photos on screen at the same time with vastly different color schemes would overload the hardware's color capacity and display improperly. Today, computer hardware easily renders full 24-bit color, but 8-bit indexed images are still widely used to save bandwidth and storage space.[7]

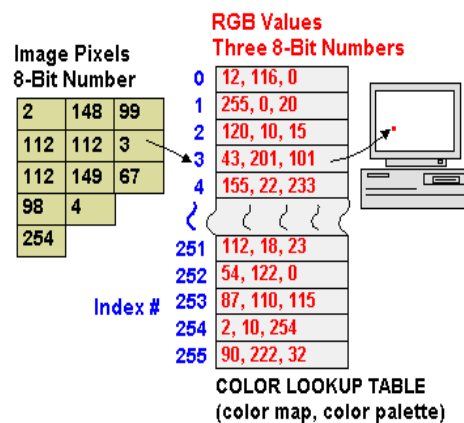


Figure 2:-RGBlookup table [7]

(i) RGB Color

It can be partially reliable even in presence of changes in lighting, view angle, and scale. In image retrieval, the color histogram is the most commonly used global color feature. It denotes the probability of the intensities of the three color channels. Color composition is done by color histograms, which identifies the object using color histogram indexing. The color histogram is obtained by counting the number of times each color occurs in the image array. Histogram is invariant to translation and rotation of the image plane, and change only slowly under change of angle of view. RGB color space is used i.e. histogram for each color channel is used as feature for image database.[4]

(ii) HSV Color

The alternative to the RGB color space is the Hue-Saturation-Value (HSV) color space. Instead of looking at each value of red, green and blue individually, a metric is defined which creates a different continuum of colors, in terms of the different hues each color possesses. The hues are then differentiated based on the amount of saturation they have, that is, in terms of how little white they have mixed in, as well as on the magnitude, or value, of the hue. In the value range, large numbers denote bright colorations, and low numbers denote dim colorations.[4]

(iii) Color Histogram

Color histograms contain highly correlated information and so they can be effectively compressed. They can be represented by a few numbers. As such, color histogram comparison is no slower than any other color-based indexing method. Color histograms are created by partitioning color space into equi-area regions and counting the number of pixels falling in each region, then allocating that total to the related histogram bin (each histogram has the same number of bins as there are equi-area regions). The RGBs falling in the i th region of color space. The smaller the distance, the closer the similarity of the images. In considering how color histograms might be most efficiently encoded.[5]

2.2 Shape

Shape is an important criterion for matching objects based on their profile and physical structure. All shapes are assumed to be non occluded planar shape allowing for each shape to be represented as a binary image. shape representation is boundary-based and region-based. The former uses only outer boundary of the shape while the latter uses entire shape of the region. Fourier Descriptors and Moment invariants are the most widely used shape representation schemes. The main idea of Fourier Descriptor is to use the Fourier transformed boundary as the shape feature. Moment invariant technique uses region-based moments, which are invariant to transformations, as the shape feature. This set of moments is invariant to translation, rotation and scale changes. Finite Element Method (FEM) has also been used as shape representation tool. In shape can be classified into global and local features.[8]

(i) **Global** :- Global features are the properties derived from the entire shape such as roundness, circularity, central moments, and eccentricity.[8]

(ii) **Local** :- it is derived by partial processing of a shape including size and orientation consecutive boundary segments, points of curvature, corners and turning angle.[8]

2.3 Texture

In the case of low level texture feature, we apply Gabor filters on the image with scales and orientations and we obtain an array of magnitudes[1]. the image features associated with these regions can be used for search and retrieval. Although no formal definition of texture exists, intuitively this descriptor provides measures of properties such as smoothness, coarseness, and regularity. These properties can generally not be attributed to the presence of any particular color or intensity. Texture corresponds to repetition of basic texture elements called texels. A texel consists of several pixels and can be periodic, or random in nature. Texture is an innate property of virtually all surfaces, including clouds, trees, bricks, hair, fabric, etc. It contains important information about the structural arrangement of surfaces and their relationship to the surrounding environment.[8] And texture feature are extract with the help of entropy, local range, standard deviation. [3]

The three principal approaches used in practice to describe the texture. Statistical approaches yield characterization of textures as smooth, coarse, grainy and so on. Structural techniques deal with the arrangement of image primitives, such as description of texture based on regularly spaced parallel lines. Spectral techniques are based on properties of Fourier spectrum and are used primarily to detect global periodicity in an image by identifying high-energy, narrow peaks in the spectrum.[8]

(i) Standard Wavelet

The wavelet transform provides a multi-resolution approach to texture analysis and classification. Studies of human visual system support a multi-scale texture analysis approach, since researchers have found that the visual cortex can be modelled as a set of independent channels, each tuned to a particular orientation and spatial frequency band. That is why wavelet transforms are found to be useful for texture feature extraction.[4]

(ii) Gabor Wavelet

A Gabor function is a Gaussian modulated by a complex sinusoid. It can be specified by the frequency of the sinusoid and the standard deviations and the Gaussian. It has been demonstrated that the 2D Gabor functions are local spatial band pass filters that achieve the theoretical limit for conjoint resolution on information in the 2D spatial and 2D Fourier domains. The Gabor wavelets are obtained by dilation and rotation of the generating function.[4]

III. TEXTURE FEATURE EXTRACTION

3.1 Gabor Function

Gabor functions do not result in an orthogonal decomposition. Expanding a signal using this basis provides a localized frequency description. A class of self-similar functions, which means that a wavelet transform based upon the Gabor wavelet is redundant. It proposed a design strategy to project the filters so as to ensure that the half-peak magnitude supports of the filter responses in the frequency spectrum touch one another. It can be ensured that the filters will capture the maximum information with minimum redundancy. [1]

3.2 Gabor Filter Design

The nonorthogonality of the Gabor wavelets implies that there is redundant information in the filtered images, and the strategy is used to reduce this redundancy. Then the design strategy is to ensure that the half-peak magnitude support of the filter responses in the frequency spectrum touch each other. In order to eliminate sensitivity of the filter response to absolute intensity values, the real (even) components of the 2D Gabor filters are biased by adding a constant to make them zero mean.[1]

3.3 Gabor Wavelet Transform

After applying Gabor filters on the image with different orientation at different scale. The main purpose of texture-based retrieval is to find images or regions with similar texture. It is assumed that we are interested in images or regions that have homogenous texture, therefore the following mean and standard deviation of the magnitude of the transformed coefficients are used to represent the homogenous texture feature of the region and it is used for remove the noise of different images.[4]

IV. CONCLUSION AND FUTURE WORK

In this paper proposed a various feature for image indexing using color histogram and texture analysis of image. The color image in gray level images to check the color histogram values after extract the color feature. And texture feature are also used to the Gabor wavelet transform and HSV color histogram presented. Simulation the higher performance of the proposed method compared to the RGB Color Histogram + Standard Wavelet Transform in terms of average precision and recall. In future work the performance of the proposed method can be improved by applying the same low level features on texture based image indexing.

REFERENCES

- [1] B.S. Manjunathi And W.Y. Ma, "Texture Features For Browsing And Retrieval Of Image Data" VOL. 18, NO. 8, AUGUST 1996.
- [2] J.Berens, G.D.Finlayson and G.Qiu, "Image indexing using compressed colour histograms" IEE Proc.-Vis. Image Signal Process., Vol. 147, No. 4, August 2000.
- [3] Wasim Khan, Shiv Kumar, Neetesh Gupta, Nilofar Khan, "A Proposed Method for Image Retrieval using Histogram values and Texture Descriptor Analysis" ISSN: 2231-2307, Volume-I Issue-II, May 2011
- [4] Narendra Gali, B.Venkateshwar Rao, Abdul Subhani Shaik, "Color and Texture Features for Image Indexing and Retrieval. Volume 3, Issue (1) NCRTCST, ISSN 2249-071X (2012).
- [5] S. Mangijao Singh, K. Hemachandran, "Content-Based Image Retrieval using Color Moment and Gabor Texture Feature" Issues, Vol. 9, Issue 5, No 1, September 2012.
- [6] N. Bourkache, M. Laghrouche and F.oulebsir boumghar, "Images Indexing based on the texture parameters and medical information content retrieval".
- [7] <http://www.pcmag.com/encyclopedia/term/44894/indexed-color>
- [8] Faisal Bashir, Shashank Khanvilkar, Ashfaq Khokhar, and Dan Schonfeld, "Multimedia Systems: Content Based Indexing and Retrieval" University of Illinois at Chicago.
- [9] http://en.wikipedia.org/wiki/Database_index

Reactive Power Reserve Management by Using Improved Particle Swarm Optimization Algorithm

¹S. Sakthivel, ²A. Subramanian ³S. Gajendran ⁴P. Viduthalai Selvan

¹Associate Professor Department of Electrical and Electronics Engineering, V.R.S. College of Engineering and Technology, Villupuram, Tamil Nadu, India.

²Professor, Department of Electrical and Electronics Engineering, V.R.S. College of Engineering and Technology, Villupuram, Tamil Nadu, India.

³UG Scholar, Department of Electrical and Electronics Engineering, V.R.S. College of Engineering and Technology, Villupuram, Tamil Nadu, India.

⁴UG Scholar, Department of Electrical and Electronics Engineering, V.R.S. College of Engineering and Technology, Villupuram, Tamil Nadu, India.

Abstract

A power system needs to be with sufficient reactive power capability to maintain system voltage stability and system reliability. Reactive power reserve can be ensured by installing var sources or optimizing the reactive power generation from the existing var sources. This work aims to optimize the total reactive power generation by adjusting the power flow pattern in a system. Generator bus voltage magnitudes, transformer tap positions and static var compensator(SVC) settings are taken as control parameters. Total reactive power generation is taken as the objective function value. An enhanced version of PSO algorithm, the improved PSO (IPSO) is suggested for the optimization task. The likelihood for trapping into local minima by PSO is overcome in this enhanced version. The effectiveness of the proposed algorithm is tested on the standard IEEE-30 bus system. The performance is compared with the basic version of PSO and improved results are seen.

Key Words: Reactive power reserve, PSO, IPSO, Voltage stability, SVC, var sources.

I. INTRODUCTION

Voltage instability is generally associated with power systems which are heavily stressed or loaded. The stressed condition is usually caused by disturbances and characterized by shortage of fast-acting adequate reactive reserves. Voltage instability is related to reactive power demands not being met because of limitations on the production and transmission of reactive power [1]. Reactive power demand generally increases with a load increase. The fast reactive sources are generators, synchronous condensers and power electronics-based flexible ac transmission systems (FACTS) devices.

During disturbances, reactive power resources should supply power to compensate for load bus voltage levels. This action reduces reactive losses of transmission lines and transformers, and increases line charging and shunt capacitor outputs. Generally, one or two critical resources reaching their limits can lead to cascading limiting effects at neighboring units. Hence it is wise to keep enough reserves in order to improve the voltage stability margin. Reactive power margins have always been linked with voltage stability.

The minimum reactive power margin is determined by the voltage-var (V-Q) curve method. The V-Q method has been well studied [2]–[3]. Reference [4] discusses a reactive management program for a practical power system. The authors discuss a planning goal of supplying system reactive demands by installation of properly sized and properly located capacitor banks which will allow generating units to operate at or near unity power factor. However, it is a cost-intensive proposition. Besides, this strategy is not always very effective since not all the shunt capacitors are fully utilized.

In [5], reactive power margins are used to evaluate voltage instability problems for coherent bus groups. These margins are based on the reactive reserves of generators and SVCs that exhaust reserves in the process of computing a V-Q curve at any bus in a coherent group or voltage control area. In [6], the authors introduce a methodology to reschedule the reactive injection from generators and synchronous condensers with the aim of improving the voltage stability margin. Their method is formulated based on modal participations factors and an optimal power flow (OPF) wherein the voltage stability margin, as computed from eigenvectors of a reduced Jacobian, is maximized by reactive rescheduling.

However, the authors avoid using a security-constrained OPF formulation and thus the computed voltage stability margin from the Jacobian would not truly represent the situation under a stressed condition. In [7], the authors employ a security-constrained OPF for optimal var expansion planning design.

For optimal reactive power reserve management, an effective optimization algorithm is necessary for proper settings of the control variables. A number of conventional optimization methods have been exploited for engineering optimization. Techniques such as non linear programming technique [8] and gradient based optimization algorithm [9] are some of them. But they have several disadvantages like large numerical iteration and insufficient convergence properties which leads to large computation and more execution time. The recently developed meta-heuristics based algorithms are proving better performance than the conventional methods. They find global best or nearly global best solutions for engineering problems. These algorithms are better utilised for power system optimization. Some of them are Tabu Search (TS) [10], Simulated Annealing (SA) [11], Genetic Algorithm (GA) [12], Evolutionary Programming (EP) [13], Hybrid Evolutionary Programming (HEP) [14], Particle Swarm Optimization PSO [15], Chaotic Ant Swarm Optimization (CASO) [16] and Differential Evolution (DE) [17] are developed which provides fast and optimal solution for reactive power optimization.

In this work, a reactive reserve management program based on IPSO algorithm is proposed to manage reactive power generation from its sources. The IPSO overcomes the problem of trapping into local minima by updating the velocity some crazy particles by a random manner. A balance between velocity updating by the standard equation and random manner is maintained. The proposed method is tested on the IEEE-30 bus test system.

II. REACTIVE POWER RESERVES

The reactive power sources of a power system include synchronous generators and static var compensators. During disturbances, the real power component of line loadings does not change significantly, whereas the reactive power flow can change dramatically. This is due to the fact that the voltage drops resulting from the contingency decreases the reactive power generation from line charging and shunts capacitors, thereby increasing reactive power losses. Sufficient reactive reserves should be made available to meet additional var demand. Simply speaking, the reactive power reserve is the ability of the generators to support bus voltages under increased load condition or system disturbances. How much more reactive power the system can deliver depends on the operating condition and the location of the reserves, as well as the nature of the impending change. The reserves of reactive sources can be considered a measure of the degree of voltage stability. The available reactive power reserve of a generator is determined by its capability curves [9]. It is worth noting that for a given real power output, the reactive power generation is limited by both armature and field heating limits.

$$Q_g^{max} = -\frac{V_g^2}{x_d} + \sqrt{\left(\frac{V_g^2 I_{fd}^{max}}{x_d^2}\right) - P_g^2} \quad (1)$$

The maximum reactive power of the generator is determined by the maximum field current. The relationship (1) also shows that the maximum reactive generation is a function of the terminal voltage.

The maximum reactive power output should also satisfy the armature current limitation as follows:

$$Q_g^{max} = \sqrt{(V_g^2 I_a^2{}_{max} - P_g^2)} \quad (2)$$

The reactive power reserve of the i^{th} generator can be written as

$$Q_{g\text{res}}^{max} = Q_g^{max} - Q_g \quad (3)$$

In this work, the reactive power reserve is maximized by minimizing the reactive power generation from the generators and var sources.

III. FORMULATION

The objective function of this optimization problem is to minimize the reactive power generation. Therefore, the following objective function is used.

$$F(X, U) = \min \sum_{i=1}^{N_{PV}} Q_{gi} \quad (4)$$

Where X stands for the system state variables or dependent variables, which are usually bus voltages and angles; U represents the system control variables or independent variables like generator bus voltage or tap or SVC var outputs. Q_{gi} is the reactive power generation of the i^{th} generator, $i=1, \dots, N_{PV}$.

The constraints to the problem are as follows:

3.1 Equality constraints:

Real power balance equation at all buses

$$P_i = P_g - P_d = V_i \sum_{j=1}^{NB} V_j (G_{ij} \cos \theta_{ij} + B_{ij} \sin \theta_{ij}) \quad (5)$$

Reactive power balance equation at all buses

$$Q_i = Q_g - Q_d = V_i \sum_{j=1}^{NB} V_j (G_{ij} \sin \theta_{ij} - B_{ij} \cos \theta_{ij}) \quad (6)$$

3.2 Inequality constraints:

Reactive power generation limit

$$Q_g^{\min} \leq Q_g \leq Q_g^{\max} \quad (7)$$

Voltage magnitude limit

$$V_i^{\min} \leq V_i \leq V_i^{\max} \quad i \in N_{PV} \quad (8)$$

Tap changer limit

$$t_i^{\min} \leq t_i \leq t_i^{\max} \quad i \in N_T \quad (9)$$

SVC MVAR output limit

$$Q_{svc}^{\min} \leq Q_{svc} \leq Q_{svc}^{\max} \quad (10)$$

Line MVA flow limit

$$MVA_{ij} \leq MVA_{ij}^{\max} \quad (11)$$

Where:

V_i : Voltage magnitude at load bus; θ_{ij} : Voltage angle difference between bus i and bus j ;

G_{ij}, B_{ij} : Elements of the admittance matrix;

P_i, Q_i : Active/reactive power injected into the network at bus i ;

N_T, N_{PV}, N_{PQ} : Number of transformers, generators, and loads, respectively;

Q_g^{\min}, Q_g^{\max} : Reactive power capacity limits at generator bus.

V_i^{\min}, V_i^{\max} : Limits of voltage at i^{th} load bus;

t_i^{\min}, t_i^{\max} : Limits of tap setting of transformer i ;

MVA_{ij}^{\max} : MVA capacity limit of transmission line between buses i and j .

Equation (4) is the objective function, which minimizes the sum of the reactive power generation. Equations (5) and (6), show the bus injections in terms of flows in the lines and the static power flow equations at sending and receiving ends in terms of steady state values of bus voltage magnitudes and bus angles.

IV. PARTICLE SWARM OPTIMIZATION (PSO)

PSO is a recently developed bio inspired optimization algorithm based on the food foraging behavior of swarm of fish or birds [18]. The particle swarm optimization method has become quite popular for solving complex problems during the last decade. Its excellent random parallel search capability and constraint handling mechanism make it very efficient for locating good solution in the complex search domain.

4.1 Basic Particle swarm optimization (BPSO): The PSO is a simple and powerful optimization tool which scatters random particles i.e. solutions into the problem space. These particles, called swarms collect information from each other through an array constructed by their respective positions. The particles update their positions using the velocity of particles.

Position and velocity are both updated in a heuristic manner using guidance from a particle's own experience and the experience of its neighbors. The position and velocity vectors of the i^{th} particle of a D-dimensional search space can be $X_i = (x_{i1}, x_{i2}, \dots, x_{iD})$ and $V_i = (v_{i1}, v_{i2}, \dots, v_{iD})$. Each particle keeps track of the solutions visited and remembers the best one as the P_{best} . The particle best may be represented as $P_{besti} = (p_{besti1}, p_{besti2}, \dots, p_{bestiD})$. The best among the particle bests is called global best, the G_{best} .

The particle tries to modify its position using the current velocity and the distance from P_{best} and G_{best} . The modified velocity and position of each particle for fitness evaluation in the next iteration are calculated using the following equations.

$$v_{id}^{k+1} = wv_{id}^k + c_1 rand_1 (P_{best\ id} - x_{id}) + c_2 rand_2 (G_{best\ id} - x_{id}) \quad (12)$$

$$x_{id}^{k+1} = x_{id}^k + v_{id}^{k+1} \quad (13)$$

Here w is the inertia weight parameter which controls the global and local exploration capabilities of the particle. c_1 and c_2 are cognitive and social coefficients, and $rand_1$, $rand_2$ are random numbers between 0 and 1. A larger inertia weight factor is used during initial exploration and its value is gradually reduced as the search proceeds. The time varying inertial weight is given by:

$$w = (w_{max} - w_{min}) \times \frac{(iter_{max} - iter_{min})}{iter_{max}} \quad (14)$$

where $max\ iter$ is the maximum number of iterations. Constant c_1 pulls the particles towards local best position whereas c_2 pulls it towards the global best position.

4.2 Improved PSO: The basic PSO searches in the solution space by the guidelines of the P_{best} and G_{best} . as the new particles take new positions that are based on the P_{best} and G_{best} , there may be solutions that are not visited. This increases the probability of PSO to trap into local minima. Instead of adjusting the velocities of all particles by the standard equation of PSO, some particles are given randomly generated velocities [19]. These particles are called crazy particles. The particles that are to be given random velocity are selected randomly. A proper balance is maintained between exploration (global search) and exploitation (local search) and random search.

Then velocities of particles are randomized as per the following logic:

$$V_j^k = \begin{cases} rand(0, V_{max}); & \text{if } p_{cr} \geq rand(0,1) \\ V_j^k, & \text{otherwise} \end{cases} \quad (15)$$

4.3 IPSO applied to reactive reserve management: IPSO algorithm involves the steps shown below in reactive power generation control.

Step 1: Form an initial generation of NP particles in a random manner respecting the limits of search space. Each candidate is a vector of all control variables, i.e. $[V_g, T_k, Q_{svc}]$. There are 6 V_g 's, 4 T_k 's and 2 Q_{svc} in the IEEE-30 system and hence a candidate is a vector of size 1×12 .

Step 2: Calculate the fitness function (objective function) values of all candidate solutions by running the NR load flow. The control variable values taken by different candidates are incorporated in the system data and load flow is run. The total reactive power generation corresponding to different candidates are calculated.

Step 3: Identify P_{best} of all particles. Compare the fitness values of a particle in all the iterations until the current iteration. P_{best} of a particle is the best solution the particle ever visited. Determine the G_{best} by comparing the P_{best} 's of all particles in the current iteration.

Step 4: Update the velocity and position of each particle by the standard equations. Select some particles for assigning random velocities.

Step 5: Repeat steps 2-4 until stopping criteria has not been achieved.

V. NUMERICAL RESULTS AND DISCUSSIONS

The proposed IPSO algorithm based method for reactive power reserve management is tested on the standard IEEE-30 bus test system [20]. The algorithm is coded in MATLAB 7.6 language tool. The test system has the following parameters.

Table 1. System parameters

Sl.No	Variable	Quantity
1	Buses	30
2	Branches	41
3	Generators	6
4	Shunt capacitors	2
5	Tap-Changing transformers	4

There are six generator buses, four tap changer transformers and two SVCs in the test system. These 12 control variables are found to be suitable for reactive power reserve management. The upper and lower limits of these parameters are given in table 2.

Table 2. Range of control parameters

Parameters	Quantity	Range
Generator bus voltage(V_g)	6	0.9-1.1(p.u.)
Transformer tap setting(T_{ij})	4	0.9-1.1(p.u.)
SVC setting	2	2-30 (MVAR)
Total control variables		12

The IPSO algorithm based optimization approach is with few parameters. In most of the population based algorithms their performance is greatly affected by the parameter values. Therefore tuning of the parameters is necessary and it is not very easy. IPSO being with only one parameter is easy for implementation

and produces better results. The algorithm converges when number of individuals is taken as 30 and run for 200 iterations. The optimal parameter values of the algorithm are shown in table 3.

Table 3. IPSO parameter values

Sl. No	Parameter	Optimal value
1	No of individuals (NP)	30
2	Self accelerating constant (c_1)	1.2
3	Global accelerating constant (c_2)	1.2
4	Inertia constant (w)	Linearly decreasing

The optimal values of control parameters that minimizes the total reactive power generation are as shown in table 4. The proposed algorithm adjusted the control parameter values within the limits. PSO algorithm suggests additional 44.4416 MVAR of reactive power support from SVCs. The IPSO recommends a reduced level of reactive power support by SVCs and it is 42.7959 MVAR. This alone reserves 1.6457 MVAR of reactive power.

Table 4. Optimal values for control parameters

Sl. no	Parameter	Initial value	PSO	IPSO
1	V_{g1}	1.05	1.0369	1.0478
2	V_{g2}	1.04	1.0282	1.0479
3	V_{g5}	1.01	1.0062	1.0170
4	V_{g8}	1.01	1.0221	1.0400
5	V_{g11}	1.05	1.0356	0.9755
6	V_{g13}	1.05	1.0299	1.0341
7	T_{6-9}	0.978	0.9918	1.0352
8	T_{6-10}	0.969	1.0078	0.9789
9	T_{4-12}	0.932	0.9855	0.9862
10	T_{28-27}	0.968	1.0197	1.0716
11	Q_{SVC10}	19	23.6268	26.1354
12	Q_{SVC24}	4.3	20.8148	16.6605

Reactive power generation minimization offers other benefits like real power loss minimization. Table 5 compares the performance of IPSO with that of basic PSO. IPSO performs better than PSO in reactive power generation and loss minimization.

Table 5. Benefits of reactive power generation optimization

Reactive power generation		Real power losses	
PSO	IPSO	PSO	IPSO
102.711	102.075	5.468	5.454

Voltage magnitudes of generator buses are varied for achieving the goal without violating its limits. Voltage profile of the system buses are maintained at about 1.0 p.u. Figure 1 depicts the voltage profile of the test system that most of the bus voltages are in the acceptable range of 0.95 p.u. to 1.05 p.u.

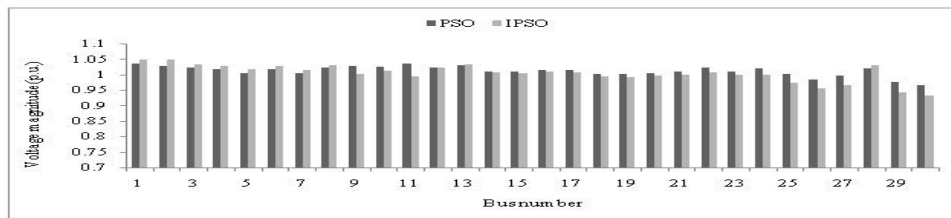


Figure 1. Voltage profile of the IEEE-30 bus system

VI. CONCLUSIONS

This work proposes an efficient method to improve stability and reliability of a power system. Optimized reactive power generation ensures better utilization of the available var sources and reactive power reserve. This delays the need for the installation of additional var sources in the near future. The numerical results show that this method minimizes the total reactive power generation considerably and leaves the system

with sufficient reactive capability. The improved version of PSO algorithm overcomes the drawback of trapping into local minima and produces improved results. This enhanced version of PSO can be an optimization tool for many other power system optimization tasks as well. When a power system has sufficient reactive power capability, the increased reactive power demand during faults can be easily met and voltage instability can be avoided. Optimization of reactive power also minimizes the real power loss and hence increases the economy of power system operation.

REFERENCES

- [1] D. Faraji, A. Rabiei, B. Mohammadi, M. Hoseynpoor, "Reactive Power Generation Management to Improve Voltage Stability Margin of Power Systems" *Australian Journal of Basic and Applied Sciences*, Vol. 5, No. 6, pp. 957-963, 2011.
- [2] Z. Feng, W. Xu, C. Oakley, and S. Mcgoldrich, "Experiences on assessing alberta power system voltage stability with respect to the WSCC reactive power criteria," in *IEEE Power Engineering Society Summer Meeting*, Vol. 2, Edmonton, AB, Canada, pp. 1297-1302 Jul. 1999.
- [3] B. H. Chowdhury and C. W. Taylor, "Voltage stability analysis: V-Q power flow simulation versus dynamic simulation," *IEEE Trans. Power Syst.*, vol. 15, no. 4, pp. 1354-1359, Nov. 2000.
- [4] P. Nedwick, A. F. Mistr Jr., and E. B. Croasdale, "Reactive management a key to survival in the 1990s," *IEEE Trans. Power Syst.*, vol. 10, no. 2, pp. 1036-1043, May 1995.
- [5] R. A. Schlueter, "A voltage stability security assessment method," *IEEE Trans. Power Syst.*, vol. 13, no. 4, pp. 1423-1438, Nov. 1998.
- [6] T. Menezes, L. C. da Silva, and V. F. da Costa, "Dynamic VAR sources scheduling for improving voltage stability margin," *IEEE Trans. Power Syst.*, vol. 18, no. 2, pp. 969-971, May 2003.
- [7] E. Vaahedi, J. Tamby, Y. Mansour, L. Wenyuan, and D. Sun, "Large scale voltage stability constrained optimal VAR planning and voltage stability applications using existing OPF/optimal VAR planning tools," *IEEE Trans. Power Syst.*, Vol. 14, No. 1, pp. 65-74, Feb. 1999.
- [8] C. W. Taylor and R. Ramanathan, "BPA reactive power monitoring and control following the august 10, 1996 power failure," in *Proc. VI Symp. Specialists in Electric Operational and Expansion Planning*, Salvador, Brazil, May 1998.
- [9] C. W. Taylor, *Power System Voltage Stability*. New York: McGraw-Hill, 1994.
- [10] Gan D, Qu Z, Cai H, "Large-Scale VAR Optimization and Planning by Tabu Search", *Electric Power Systems Research*, Vol. 39, No. 3, pp. 195-204, December 1996.
- [11] Hsiao YT, Chiang HD, "Applying Network Window Scheme and a Simulated Annealing Technique to Optimal VAR Planning in Large-Scale Power Systems", *Electric Power Systems Research*, Vol. 22, No. 1, pp.1-8, January 2000.
- [12] Iba K. "Reactive Power Optimization by Genetic Algorithm", *IEEE Transactions on Power Systems*, Vol.9, No. 2, pp. 685-692, May 1994.
- [13] Abido M.A., Bakhshwain JM, "Optimal VAR Dispatch Using a Multi Objective Evolutionary Algorithm, *Electric Power & Energy Systems*, Vol.27, No. 1, pp.13-20, January 2005.
- [14] Swain AK, Morris AK, "A Novel Hybrid Evolutionary Programming Method for Function Optimization", *Proc. 2000 Congress on Evolutionary Computation*, Vol. 1, pp. 699-705, 2000.
- [15] Esmin AAA, Lambert-Torres G, de Souza ACZ, "A Hybrid Particle Swarm Optimization Applied to Power Loss Minimization", *IEEE Transactions on Power Systems*, Vol. 20, No. 2, pp. 859-866, May 2005.
- [16] Cai J, Mab X, Li Q, Li L, Peng H, "A Multi-Objective Chaotic Ant Swarm Optimization for Environmental/Economic Dispatch", *Electric Power & Energy Systems*, Vol.32, No.5, pp. 337-344, June 2010.
- [17] Shaheen HI, Rashed GI, Cheng SJ, "Optimal Location and Parameter Setting of UPFC for Enhancing Power System Security based on Differential Evolution Algorithm", *Electric Power & Energy Systems*, Vol. 33, No.1, pp. 94-105, Jan 2011.
- [18] J. Kennedy and R. Eberhart, "Particle Swarm Optimization", *Proceedings of IEEE International Conference on Neural Networks*, Vol. IV, pp.1942-1948, Perth, Australia, 1995.
- [19] Rajkumari Batham, Kalpana Jain, Manjaree Pandit, "Improved particle swarm optimization approach for nonconvex static and dynamic economic power dispatch", *International Journal of Engineering, Science and Technology*, Vol. 3, No. 4, pp. 130-146, 2011.
- [20] A. Abou El Ela, M.A. Abido, S. R. Spea "Optimal Power Flow using Differential Evolution Algorithm", *Electric Power Systems Research*, Vol. 80, No. 7, pp. 878-885, July 2010.

AUTHOR BIOGRAPHIES



S. Sakthivel received the Degree in Electrical and Electronics Engineering in 1999 from Madras University and Master Degree in Power Systems Engineering in 2002 from Annamalai University. He is pursuing the Ph.D., Degree in Electrical Engineering faculty from Anna University, Chennai, India. He is presently working as an Associate Professor in Electrical and Electronics Engineering Department at V.R.S. College of Engineering and Technology, Villupuram, Tamil Nadu, India. His research areas of interest are Power System control, Optimization techniques, FACTS, Economic load dispatch, Power system deregulation and Voltage stability improvement. He has published 35 research papers in various internationally reputed journals.



A. Subramanian received B.E. Degree in Electrical and Electronics Engineering from Annamalai University in 1995, M.Tech., Degree from Pondicherry Engineering College in 2004 and now pursuing Ph.D (Engg) at Anna University, Chennai. At present he is working as a professor in Electrical and Electronics Engineering Department at V.R.S. College of Engineering and Technology Arasur, Tamil Nadu. His field of interest are power system reactive power reserve management, voltage stability and optimization techniques.



S. Gajendran is an undergraduate student in the Department of Electrical and Electronics Engineering at VRS College of Engineering and Technology, Villupuram, Tamil Nadu, India. He is interested in power system operation optimization by using intelligent techniques.



P. Viduthalaiselvan is an undergraduate student with the Department of Electrical and Electronics Engineering at VRS College of Engineering and Technology, Villupuram, Tamil Nadu, India. Optimal power flow using evolutionary algorithms is his important area of interest.

On The Zeros of Polynomials and Analytic Functions

M. H. Gulzar

Department of Mathematics University of Kashmir, Srinagar 190006

Abstract

In this paper we obtain some results on the zeros of polynomials and related analytic functions, which generalize and improve upon the earlier well-known results.

Mathematics Subject Classification: 30C10, 30C15

Key-words and phrases: Polynomial, Analytic Function, Zero.

I. INTRODUCTION AND STATEMENT OF RESULTS

Regarding the zeros of a polynomial, Jain [2] proved the following results:

Theorem A: Let $P(z) = a_0 + a_1z + \dots + a_{p-1}z^{p-1} + a_pz^p + \dots + a_nz^n$ be a polynomial of degree n such that $a_{p-1} \neq a_p$ for some $p \in \{1, 2, \dots, n\}$,

$$M = M_p = \sum_{j=p+1}^n |a_j - a_{j-1}| + |a_n|, \quad (1 \leq p \leq n), M_n = |a_n|$$

$$m = m_p = \sum_{j=1}^{p-1} |a_j - a_{j-1}|, \quad (2 \leq p \leq n), m_1 = 0.$$

Then $P(z)$ has at least p zeros in

$$|z| < \frac{p}{M} \frac{(a_p - a_{p-1})}{p+1},$$

provided

$$\frac{p}{M} \frac{(a_p - a_{p-1})}{p+1} < 1$$

and

$$|a_0| + m \frac{p}{M} \left(\frac{a_p - a_{p-1}}{p+1} \right) < \left(\frac{p}{M} \right)^p \left(\frac{a_p - a_{p-1}}{p+1} \right).$$

Theorem B: Let $P(z) = a_0 + a_1z + \dots + a_{p-1}z^{p-1} + a_pz^p + \dots + a_nz^n$ be a polynomial of degree n such that $a_{p-1} \neq a_p$ for some $p \in \{1, 2, \dots, n\}$,

$$|\arg a_j - \beta| \leq \alpha \leq \frac{\pi}{2}, \quad j = 0, 1, \dots, n,$$

for some real β and α and

$$|a_n| \geq |a_{n-1}| \geq \dots \geq |a_1| \geq |a_0|.$$

Then $P(z)$ has at least p zeros in

$$|z| < \frac{p}{L} \frac{|a_p - a_{p-1}|}{p+1},$$

where

$$L = L_p = |a_n| + (|a_n| - |a_p|) \cos \alpha + \sum_{j=p+1}^n (|a_j| + |a_{j-1}|) \sin \alpha$$

and

$$l = l_p = (|a_{p-1}| - |a_0|) \cos \alpha + \sum_{j=1}^{p-1} (|a_j| + |a_{j-1}|) \sin \alpha \quad (2 \leq p \leq n-1), l_1 = 0,$$

provided

$$|a_0| + l \frac{p}{L} \frac{|a_p - a_{p-1}|}{p+1} < \left(\frac{p}{L}\right)^p \left(\frac{|a_p - a_{p-1}|}{p+1}\right)^{p+1}.$$

In this paper, we prove the following results:

Theorem 1: Let $P(z) = a_0 + a_1z + \dots + a_{p-1}z^{p-1} + a_pz^p + \dots + a_nz^n$ be a polynomial of degree n such that $a_{p-1} \neq a_p$ for some $p \in \{1, 2, \dots, n-1\}$ and $\rho \geq 0$,

$$\rho + a_n \geq a_{n-1} \geq \dots \geq a_p > a_{p-1} \geq \dots \geq a_1 \geq a_0.$$

Then $P(z)$ has at least p zeros in

$$\frac{|a_0|}{K(2\rho + a_n - a_0 + K^n|a_n|)} \leq |z| \leq K = \frac{p}{M} \frac{(a_p - a_{p-1})}{p+1},$$

where

$$M = 2\rho + |a_n| + a_n - a_p,$$

provided

$$|a_0| + \frac{p}{M} \left(\frac{a_p - a_{p-1}}{p+1}\right) (a_{p-1} - a_0) < \left(\frac{p}{M}\right)^p \left(\frac{a_p - a_{p-1}}{p+1}\right)^{p+1}$$

and $K < 1$.

Remark 1: Taking $\rho = 0$ in Theorem 1, we get the following result:

Corollary 1: Let $P(z) = a_0 + a_1z + \dots + a_{p-1}z^{p-1} + a_pz^p + \dots + a_nz^n$ be a polynomial of degree n such that $a_{p-1} \neq a_p$ for some $p \in \{1, 2, \dots, n-1\}$

$$a_n \geq a_{n-1} \geq \dots \geq a_p > a_{p-1} \geq \dots \geq a_1 \geq a_0.$$

Then $P(z)$ has at least p zeros in

$$\frac{|a_0|}{2\rho + a_n - a_0 + K_1^n|a_n|} \leq |z| \leq K_1 = \frac{p}{M_1} \frac{(a_p - a_{p-1})}{p+1},$$

where

$$M_1 = |a_n| + a_n - a_p,$$

provided

$$|a_0| + \frac{p}{M_1} \left(\frac{a_p - a_{p-1}}{p+1}\right) (a_{p-1} - a_0) < \left(\frac{p}{M_1}\right)^p \left(\frac{a_p - a_{p-1}}{p+1}\right)^{p+1}$$

and $K_1 < 1$.

This result was earlier proved by Roshan Lal et al [4].

If the coefficients are positive in Theorem 1, we have the following result:

Corollary 2: Let $P(z) = a_0 + a_1z + \dots + a_{p-1}z^{p-1} + a_pz^p + \dots + a_nz^n$ be a polynomial of degree n such that $a_{p-1} \neq a_p$ for some $p \in \{1, 2, \dots, n-1\}$ and $\rho \geq 0$,

$$\rho + a_n \geq a_{n-1} \geq \dots \geq a_p > a_{p-1} \geq \dots \geq a_1 \geq a_0 > 0.$$

Then $P(z)$ has at least p zeros in

$$\frac{a_0}{K_2\{2\rho - a_0 + (K_2^n + 1)a_n\}} \leq |z| \leq K_2 = \frac{p}{M_2} \frac{(a_p - a_{p-1})}{p+1},$$

where

$$M_2 = 2(\rho + a_n) - a_p,$$

provided

$$|a_0| + \frac{p}{M_2} \left(\frac{a_p - a_{p-1}}{p+1} \right) (a_{p-1} - a_0) < \left(\frac{p}{M_2} \right)^p \left(\frac{a_p - a_{p-1}}{p+1} \right)^{p+1}$$

and $K_2 < 1$.

If the coefficients of the polynomial $P(z)$ are complex, we prove the following result:

Theorem 2: Let $P(z) = a_0 + a_1 z + \dots + a_{p-1} z^{p-1} + a_p z^p + \dots + a_n z^n$ be a polynomial of degree n such that $a_{p-1} \neq a_p$ for some $p \in \{1, 2, \dots, n-1\}$ and $\rho \geq 0$,

$$|\rho + a_n| \geq |a_{n-1}| \geq \dots \geq |a_p| > |a_{p-1}| \geq \dots \geq |a_1| \geq |a_0|$$

and for some real β and α ,

$$|\arg a_j - \beta| \leq \alpha \leq \frac{\pi}{2}, j = 0, 1, \dots, n.$$

Then $P(z)$ has at least p zeros in

$$|z| < K_3 = \frac{p}{M_3} \left(\frac{|a_p - a_{p-1}|}{p+1} \right),$$

where

$$M_3 = (\rho + |a_n|)(\cos \alpha + \sin \alpha + 1) - |a_p| \cos \alpha + \sum_{j=p+1}^{n-1} (|a_j| + |a_{j-1}|) \sin \alpha,$$

provided

$$|a_0| + \frac{p}{M_3} \left(\frac{|a_p - a_{p-1}|}{p+1} \right) m' < \left(\frac{p}{M_3} \right)^p \left(\frac{|a_p - a_{p-1}|}{p+1} \right)^{p+1}$$

Remark 2: Taking $\rho = 0$ in Theorem 2, it reduces to Theorem B.

Remark 3: It is easy to see that $K_3 < 1$.

Next, we prove the following result on the zeros of analytic functions :

Theorem 3: Let $f(z) = \sum_{j=0}^{\infty} a_j z^j \neq 0$ be analytic in $|z| \leq K_4$ and for some natural number p with

$$\frac{a_{p-1}}{a_p} < 2 + \frac{1}{p},$$

$$\rho + a_0 \geq a_1 \geq a_2 \geq \dots \geq a_{p-1} > a_p \geq a_{p+1} \geq \dots,$$

for some $\rho \geq 0$, and

$$|a_0| + \frac{p}{a_p} \left(\frac{a_{p-1} - a_p}{p+1} \right) (2\rho + a_0 - a_{p-1}) < \left(\frac{p}{a_p} \right)^p \left(\frac{a_p - a_{p-1}}{p+1} \right)^{p+1}.$$

Then $f(z)$ has at least p zeros in

$$|z| < K_4 = \frac{p}{p+1} \left(\frac{a_{p-1} - a_p}{a_p} \right).$$

Remark 4: Taking $\rho = 0$, Theorem 3 reduces to the following result:

Corollary 3: Let $f(z) = \sum_{j=0}^{\infty} a_j z^j \neq 0$ be analytic in $|z| \leq K_4$ and for some natural number p with

$$\frac{a_{p-1}}{a_p} < 2 + \frac{1}{p},$$

$$\rho + a_0 \geq a_1 \geq a_2 \geq \dots \geq a_{p-1} > a_p \geq a_{p+1} \geq \dots ,$$

for some $\rho \geq 0$, and

$$|a_0| + \frac{p}{a_p} \left(\frac{a_{p-1} - a_p}{p+1} \right) (a_0 - a_{p-1}) < \left(\frac{p}{a_p} \right)^p \left(\frac{a_p - a_{p-1}}{p+1} \right)^{p+1} .$$

Then $f(z)$ has at least p zeros in

$$|z| < K_4 = \frac{p}{p+1} \left(\frac{a_{p-1} - a_p}{a_p} \right) .$$

Cor.3 was earlier proved by Roshan Lal et al [4].

II. LEMMA

For the proofs of the above results, we need the following lemma due to Govil and Rahman [1]:

Lemma : If a_1 and a_2 are complex numbers such that

$$|\arg a_j - \beta| \leq \alpha \leq \frac{\pi}{2}, j = 1, 2, \text{ for some real numbers } \beta \text{ and } \alpha ,$$

then

$$|a_1 - a_2| \leq (|a_1| - |a_2|) \cos \alpha + (|a_1| + |a_2|) \sin \alpha .$$

III. PROOFS OF THE THEOREMS

3.1 Proof of Theorem 1: Consider the polynomial

$$\begin{aligned} F(z) &= (1-z)P(z) \\ &= (1-z)(a_0 + a_1z + \dots + a_{p-1}z^{p-1} + a_pz^p + \dots + a_nz^n) \\ &= a_0 + \sum_{j=1}^{p-1} (a_j - a_{j-1})z^j + (a_p - a_{p-1})z^p + \sum_{j=p+1}^n (a_j - a_{j-1})z^j \\ &\quad - a_nz^{n+1} \\ &= \phi(z) + \psi(z), \end{aligned}$$

where

$$\phi(z) = a_0 + \sum_{j=1}^{p-1} (a_j - a_{j-1})z^j$$

and

$$\psi(z) = (a_p - a_{p-1})z^p + \sum_{j=p+1}^n (a_j - a_{j-1}) - a_nz^{n+1} .$$

For $|z| = K (<1)$, we have, by using the hypothesis,

$$\begin{aligned} |\psi(z)| &\geq |a_p - a_{p-1}|K^p - \left(\sum_{j=p+1}^n |a_j - a_{j-1}|K^j + |a_n|K^{n+1} \right) \\ &\geq (a_p - a_{p-1})K^p - K^{p+1} \left(|a_n|K^{n-p} + |a_n - a_{n-1}|K^{n-p-1} + \sum_{j=p+1}^{n-1} |a_j - a_{j-1}|K^{n-(p+1)} \right) \\ &\geq (a_p - a_{p-1})K^p - K^{p+1} (|a_n| + |\rho + a_n - a_{n-1} - \rho| + a_{n-1} - a_p) \\ &\geq (a_p - a_{p-1})K^p - K^{p+1} (|a_n| + \nu + a_n - a_{n-1} + \rho + a_{n-1} - a_p) \\ &\geq (a_p - a_{p-1})K^p - K^{p+1} (2\rho + |a_n| + a_n - a_p) \end{aligned}$$

$$\begin{aligned}
 &= (a_p - a_{p-1}) \left[\frac{p(a_p - a_{p-1})}{2\rho + |a_n| + a_n - a_p} \right]^p \\
 &\quad - \left[\frac{p(a_p - a_{p-1})}{2\rho + |a_n| + a_n - a_p} \right]^{p+1} (2\rho + |a_n| + a_n - a_p) \\
 &= \left[\frac{p}{2\rho + |a_n| + a_n - a_p} \right]^p \left[\frac{a_p - a_{p-1}}{p+1} \right]^{p+1} \\
 &= \left[\frac{p}{M} \right]^p \left[\frac{a_p - a_{p-1}}{p+1} \right]^{p+1} \tag{1}
 \end{aligned}$$

Also for $|z| = K (<1)$,

$$\begin{aligned}
 |\phi(z)| &\leq |a_0| + \sum_{j=1}^{p-1} |a_j - a_{j-1}| K^j \\
 &\leq |a_0| + K \sum_{j=1}^{p-1} (a_j - a_{j-1}) \\
 &\leq |a_0| + K(a_{p-1} - a_0) \\
 &= |a_0| + \left(\frac{p(a_p - a_{p-1})}{2\rho + |a_n| + a_n - a_p} \right) \left(\frac{a_{p-1} - a_0}{p+1} \right) \\
 &= |a_0| + \frac{p}{M} \left(\frac{a_p - a_{p-1}}{p+1} \right) (a_{p-1} - a_0) \tag{2}
 \end{aligned}$$

Since, by hypothesis

$$|a_0| + \frac{p}{M} \left(\frac{a_p - a_{p-1}}{p+1} \right) (a_{p-1} - a_0) < \left(\frac{p}{M} \right)^p \left(\frac{a_p - a_{p-1}}{p+1} \right)^{p+1},$$

it follows from (1) and (2) that

$$|\psi(z)| < |\phi(z)| \text{ for } |z| = K.$$

Hence, by Rouché's theorem, $\phi(z)$ and $\phi(z) + \psi(z)$ i.e. $F(z)$ have the same number of zeros in $|z| < K$

Since the zeros of $P(z)$ are also the zeros of $F(z)$ and since $\psi(z)$ has at least p zeros in $|z| < K$, it follows that $P(z)$ has at least p zeros in $|z| < K$. That prove the first part of Theorem 1.

To prove the second part, we show that $P(z)$ has no zero in

$$|z| < \frac{|a_0|}{2\rho + a_n - a_0 + |a_n|K^n}.$$

Let $F(z) = (1-z)P(z)$

$$\begin{aligned}
 &= (1-z)(a_0 + a_1z + \dots + a_{p-1}z^{p-1} + a_pz^p + \dots + a_nz^n) \\
 &= a_0 + \sum_{j=1}^n (a_j - a_{j-1})z^j - a_nz^{n+1} \\
 &= a_0 + g(z),
 \end{aligned}$$

where

$$g(z) = \sum_{j=1}^{n-1} (a_j - a_{j-1})z^j - a_n z^{n+1}.$$

For $|z| = K (<1)$, we have, by using the hypothesis,

$$\begin{aligned} |g(z)| &\leq \sum_{j=1}^n |a_j - a_{j-1}| |z|^j + |a_n| |z|^{n+1} \\ &= \sum_{j=1}^n |a_j - a_{j-1}| K^j + |a_n| K^{n+1} \\ &\leq K \left[|a_n - a_{n-1}| + \sum_{j=1}^{n-1} (a_j - a_{j-1}) + |a_n| K^n \right] \\ &= K \left[\rho + a_n - a_{n-1} - \rho + a_{n-1} - a_0 + |a_n| K^n \right] \\ &\leq K \left[\rho + a_n - a_{n-1} + \rho + a_{n-1} - a_0 + |a_n| K^n \right] \\ &\leq K \left[2\rho + a_n - a_0 + |a_n| K^n \right]. \end{aligned}$$

Since $g(z)$ is analytic for $|z| \leq K$, $g(0)=0$, we have, by Schwarz's lemma,

$$|g(z)| \leq K \left[2\rho + a_n - a_0 + |a_n| K^n \right] |z| \text{ for } |z| \leq K.$$

Hence, for $|z| \leq K$,

$$\begin{aligned} |F(z)| &= |a_0 + g(z)| \\ &\geq |a_0| - |g(z)| \\ &\geq |a_0| - K \left[2\rho + a_n - a_0 + |a_n| K^n \right] |z| \\ &> 0 \end{aligned}$$

if

$$|z| < \frac{|a_0|}{K(2\rho + a_n - a_0 + |a_n| K^n)}.$$

This shows that $F(z)$ and therefore $P(z)$ has no zero in

$$|z| < \frac{|a_0|}{K(2\rho + a_n - a_0 + |a_n| K^n)}.$$

That proves Theorem 1 completely.

Proof of Theorem 2: Consider the polynomial

$$\begin{aligned} F(z) &= (1-z)P(z) \\ &= (1-z)(a_0 + a_1 z + \dots + a_{p-1} z^{p-1} + a_p z^p + \dots + a_n z^n) \\ &= a_0 + \sum_{j=1}^{p-1} (a_j - a_{j-1}) z^j + (a_p - a_{p-1}) z^p + \sum_{j=p+1}^n (a_j - a_{j-1}) z^j \\ &\quad - a_n z^{n+1} \\ &= \phi(z) + \psi(z), \end{aligned}$$

where

$$\phi(z) = a_0 + \sum_{j=1}^{p-1} (a_j - a_{j-1}) z^j$$

and

$$\psi(z) = (a_p - a_{p-1})z^p + \sum_{j=p+1}^n (a_j - a_{j-1}) - a_n z^{n+1} ..$$

For $|z| = K_3 (<1)$, we have, by using the hypothesis,

$$\begin{aligned} |\psi(z)| &\geq |a_p - a_{p-1}|K_3^p - \left(\sum_{j=p+1}^n |a_j - a_{j-1}|K_3^j + |a_n|K_3^{n+1} \right) \\ &\geq |a_p - a_{p-1}|K_3^p - K_3^{p+1} \left(|a_n|K_3^{n-p} + |a_n - a_{n-1}|K_3^{n-p-1} + \sum_{j=p+1}^{n-1} |a_j - a_{j-1}|K_3^{n-(p+1)} \right) \\ &> |a_p - a_{p-1}|K_3^p - K_3^{p+1} \left(|a_n| + |\rho + a_n - a_{n-1} - \rho| + \sum_{j=p+1}^{n-1} |a_j - a_{j-1}| \right) \\ &\geq |a_p - a_{p-1}|K_3^p - K_3^{p+1} \left(|a_n| + |\rho + a_n - a_{n-1}| + \rho + \sum_{j=p+1}^{n-1} |a_j - a_{j-1}| \right) \\ &\geq |a_p - a_{p-1}|K_3^p - K_3^{p+1} [\rho + |a_n| + \{(\rho + |a_n|) - |a_{n-1}|\} \cos \alpha + \\ &\quad \{(\rho + |a_n|) + |a_{n-1}|\} \sin \alpha + (|a_{p+1}| - |a_p|) \cos \alpha + (|a_{p+1}| + |a_p|) \sin \alpha \\ &\quad + + (|a_{n-1}| - |a_{n-2}|) \cos \alpha + (|a_{n-1}| + |a_{n-2}|) \sin \alpha] \\ &= |a_p - a_{p-1}|K_3^p - K_3^{p+1} [(\rho + |a_n|)(\cos \alpha + \sin \alpha + 1) - |a_p| \cos \alpha \\ &\quad + \sum_{j=p+1}^{n-1} (|a_j| + |a_{j-1}|) \sin \alpha] \\ &= |a_p - a_{p-1}|K_3^p - K_3^{p+1} M_3 \\ &= |a_p - a_{p-1}| \left(\frac{p}{M_3} \frac{|a_p - a_{p-1}|}{p+1} \right)^p - \left(\frac{p}{M_3} \frac{|a_p - a_{p-1}|}{p+1} \right)^{p+1} M_3 \\ &= \left(\frac{p}{M_3} \right)^p \left(\frac{|a_p - a_{p-1}|}{p+1} \right)^{p+1} \\ &> |a_0| + \frac{p}{M_3} \left(\frac{|a_p - a_{p-1}|}{p+1} \right) m' \\ &= |a_0| + K_3 m' \end{aligned} \tag{3}$$

Also, for $|z| = K_3$, we have, by using the lemma and the hypothesis,

$$\begin{aligned} |\phi(z)| &\leq |a_0| + \sum_{j=1}^{p-1} |a_j - a_{j-1}| |z|^j \\ &= |a_0| + \sum_{j=1}^{p-1} |a_j - a_{j-1}| K_3^j \\ &< |a_0| + K_3 \sum_{j=1}^{p-1} |a_j - a_{j-1}| \end{aligned}$$

$$\begin{aligned} &\leq |a_0| + K_3 [(|a_1| - |a_0|) \cos \alpha + (|a_1| + |a_0|) \sin \alpha + \dots] \\ &\quad + (|a_{p-1}| - |a_{p-2}|) \cos \alpha + (|a_{p-1}| + |a_{p-2}|) \sin \alpha] \\ &= |a_0| + K_3 [(|a_{p-1}| - |a_0|) \cos \alpha + \sum (|a_j| + |a_{j-1}|) \sin \alpha] \\ &= |a_0| + K_3 m' \tag{4} \end{aligned}$$

Thus, for $|z| = K_3$, we have from (3) and (4), $|\psi(z)| < |\phi(z)|$.

Since $\phi(z)$ and $\psi(z)$ are analytic for $|z| \leq K_3$, it follows by Rouché's theorem that $\phi(z)$ and $\phi(z) + \psi(z)$ i.e. $F(z)$ have the same number of zeros in $|z| < K_3$. But the zeros of $P(z)$ are also the zeros of $F(z)$. Therefore, we conclude that $P(z)$ has at least p zeros in $|z| < K$, as the same is true of $\psi(z)$. That proves Theorem 2.

Proof of Theorem 3: Consider the function

$$\begin{aligned} F(z) &= (z-1)f(z) \\ &= (z-1)(a_0 + a_1z + a_2z^2 + \dots) \\ &= -a_0 + \sum_{j=1}^{p-1} (a_{j-1} - a_j)z^j + (a_{p-1} - a_p)z^p + \sum_{j=p+1}^{\infty} (a_{j-1} - a_j)z^j \\ &= \phi(z) + \psi(z), \end{aligned}$$

where

$$\begin{aligned} \phi(z) &= -a_0 + \sum_{j=1}^{p-1} (a_{j-1} - a_j)z^j, \\ \psi(z) &= (a_{p-1} - a_p)z^p + \sum_{j=p+1}^{\infty} (a_{j-1} - a_j)z^j. \end{aligned}$$

For $|z| = K_4$ ($K_4 < 1$, by hypothesis for $\frac{a_{p-1}}{a_p} < 2 + \frac{1}{p}$), we have

$$\begin{aligned} |\psi(z)| &\geq |a_{p-1} - a_p| K_4^p - K_4^{p+1} \left(\sum_{j=p+1}^{\infty} |a_{j-1} - a_j| K_4^{j-(p+1)} \right) \\ &\geq |a_{p-1} - a_p| K_4^p - K_4^{p+1} \left(\sum_{j=p+1}^{\infty} |a_{j-1} - a_j| \right) \\ &= |a_{p-1} - a_p| K_4^p - K_4^{p+1} a_p \\ &= |a_{p-1} - a_p| \left[\left(\frac{p}{p+1} \right) \left(\frac{a_{p-1} - a_p}{a_p} \right) \right] - \left[\left(\frac{p}{p+1} \right) \left(\frac{a_{p-1} - a_p}{a_p} \right) \right] a_p \\ &= \left(\frac{p}{a_p} \right)^p \left(\frac{a_{p-1} - a_p}{p+1} \right)^{p+1}. \tag{5} \end{aligned}$$

and

$$\begin{aligned} |\phi(z)| &\leq |a_0| + \sum_{j=1}^{p-1} |a_{j-1} - a_j| K_4^j \\ &< |a_0| + [|a_0 - a_1| + |a_1 - a_2| + \dots + |a_{p-2} - a_{p-1}|] K_4 \end{aligned}$$

$$\begin{aligned}
 &= |a_0| + [|\rho + a_0 - a_1 - \rho| + |a_1 - a_2| + \dots + |a_{p-2} - a_{p-1}|] K_4 \\
 &\leq |a_0| + [|\rho + a_0 - a_1| + \rho + |a_1 - a_2| + \dots + |a_{p-2} - a_{p-1}|] K_4 \\
 &= |a_0| + [\rho + a_0 - a_1 + \rho + a_1 - a_2 + \dots + a_{p-2} - a_{p-1}] K_4 \\
 &= |a_0| + [2\rho + a_0 - a_{p-1}] K_4 \\
 &= |a_0| + \frac{p}{a_p} \left(\frac{a_{p-1} - a_p}{p+1} \right) (2\rho + a_0 - a_{p-1}) \tag{6}
 \end{aligned}$$

Since, by hypothesis,

$$|a_0| + \frac{p}{a_p} \left(\frac{a_{p-1} - a_p}{p+1} \right) (2\rho + a_0 - a_{p-1}) < \left(\frac{p}{a_p} \right)^p \left(\frac{a_p - a_{p-1}}{p+1} \right)^{p+1},$$

it follows from (5) and (6) that $|\psi(z)| < |\phi(z)|$ for $|z| = K_4$.

Since $\phi(z)$ and $\psi(z)$ are analytic for $|z| \leq K_3$, it follows, by Rouché's theorem, that $\phi(z)$ and

$\phi(z) + \psi(z)$ i.e. $F(z)$ have the same number of zeros in $|z| < K_3$. But the zeros of $P(z)$ are also the zeros of

$F(z)$. Therefore, we conclude that $P(z)$ has at least p zeros in $|z| < K$, as the same is true of $\psi(z)$. That proves Theorem 3.

REFERENCES

- [1] N. K. Govil and Q. I. Rahman, On the Enestrom-Kakeya Theorem, Tohoku Math. J.20 (1968), 126-136.
- [2] V.K. Jain, On the zeros of a polynomial, Proc.Indian Acad. Sci. Math. Sci.119 (1) ,2009, 37-43.
- [3] M. Marden, Geometry of Polynomials, Math. Surveys No. 3, Amer. Math. Soc. Providence, RI, 1966.
- [4] Roshan Lal, Susheel Kumar and Sunil Hans, On the zeros of polynomials and analytic functions, Annales Universitatis Mariae Curie –Skłodowska Lublin Polonia, Vol.LXV, No. 1, 2011, Sectio A, 97-108.

Using Novel, Flexible Benchmarking Tool for Robustness Evaluation of Image Watermarking Techniques.

¹, Sweta .S. Palewar , ²Ranjana Shende

¹ Mtech IV Semester Student, GHRIETW, Nagpur.

² Lecturer, GHRIETW, Nagpur.

Abstract

The main idea of this paper is to propose an innovative ,benchmarking tool based on genetic algorithm to evaluate robustness of visible and invisible watermarking techniques. Image fidelity metrics such as mean square error(MSE), signal to noise ratio(SNR),peak signal to noise ratio(PSNR), weighted peak signal to noise ratio(WPSNR) are being used. However, when large quantities of data are to be assessed, subjective metrics such as mean opinion score(MOS),signal to noise ratio(SNR),peak signal to noise ratio(PSNR) are not pragmatic since it needs experts and inordinate amount of time.PSNR and WPSNR are independent of human visual system(HVS) parameters and hence they are inappropriate scales to measure potential research results. This brings out a new image fidelity metric called Enhanced Weighted peak signal to noise ratio(EWPSNR) which is experimentally proven to be better than PSNR and WPSNR.

Keywords: Genetic algorithm, perceptual quality, digital image watermarking, robustness ,benchmark,image fidelity metric.

I. INTRODUCTION

In the age of information technology, it has become easier and easier to access and redistribute digital multimedia data. Digital Watermarking techniques have been widely developed as an effective instrument against piracy, improper use or illegal alteration of contents.Two main problems seriously darken the future of this technology though.Firstly, the large number of attacks performed against watermarking systems and weaknesses which appear in existing systems have shown that far more research is required to improve the quality of existing watermarking methods. Secondly, the requirements, tools and methodologies to assess the current technologies are almost non existent.Consequently,the role of performance evaluation tools has become far more important[2]. A novel and flexible benchmarking tool based on genetic algorithms has been proposed to assess the robustness of digital watermarking system.The main idea is to evaluate robustness of watermarking scheme in terms of perceptual quality, measured by metrics Signal to noise ratio (SNR),Peak signal to noise ratio(PSNR),Weighted peak signal to noise ratio(WPSNR). The goal is to remove the watermark from a content while maximizing perceptual quality[1]. Here additional enhanced fidelity metric is introduced called Enhanced Weighted peak signal to noise ratio (EWPSNR) considering the limitations of PSNR and WPSNR which are independent of human visual system parameters and hence are inappropriate scales to measure potential research results.

II. LITERATURE REVIEW:

In the literature, there are several benchmarking tools, which standardize the process of evaluating a watermarking system on a large set of single attacks.Fabien A. P. Petitcolas ,Ross J.Anderson,Markus G.Kuhn proposed a system called StirMark[3] in the year 1997,which is a generic tool for basic robustness testing of image watermarking algorithms. The first proposed benchmarking tool StirMark , applies a number of attacks (one at each time) to the given watermarked content and performs the detection process to check the presence of the mark.

The drawbacks of the system are that it does not take into account the method's false alarm probability(probability to detect watermark in a non watermarked image),embedding and detection time are not evaluated. Jan C. Vorbruggen,Franois Cayre proposed a system called Certimark[5] in the year 2000. In the system, an image source delivering the multimedia data to be watermarked, is taken. The attack module simulates all sorts of attacks on the watermark (intentional and non-intentional) resulting in possible loss of watermark readability.

There is System Under Test(SUT) watermark encoder and System Under Test watermark decoder, performs detection of the watermark and extraction of the payload for monitoring purposes. A comparator module is used to compare payload to the original values. Then all results are taken into account to write a benchmark report, with tables and graphics to ease analysis. At the end, if required, a certificate of compliance is generated[5]. This design approach provides several crucial advantages: modules can be exchanged easily; given well-defined interfaces, they can be developed separately; and they can be upgraded when needed. However, the certimark benchmark supports only still images and a limited set of professional quality video clips.

V. Solachidis, A. Tefas, N. Nikolaidis, S. Tsekeridou, A. Nikolaidis, I. Pitas, proposed a system called Optimark[6] in the year 2002. In the benchmarking system, the embedding module embeds a watermark W_j and a message M_k to an image I_i . The watermarked image should satisfy the quality specification Q_i . The above procedure is repeated for the sets of images, keys, messages, attacks and a set of watermarked images is generated. Then attacks are performed to distort the watermarked images that have been generated in the watermark embedding stage. First, the detection algorithm detects the watermark W_i that has been indeed embedded in the image I_a in the embedding procedure and the message M is decoded. The same procedure is repeated for erroneous watermark W_i ($i \neq j$). Thus, for each attacked image two pairs of detector and decoder outputs are extracted. Then detector and decoder outputs are collected for correct key and for erroneous key. During the watermark detection-decoding procedure the execution times are also measured and stored. The relative performance of the algorithm under test or its suitability for a certain application scenario is then checked[6]. The time needed for watermark and message embedding in each image is evaluated. The main drawback of optimark is the lack of possibility to expand the number of attacks.

III. PROPOSED ALGORITHM

Visual quality degradation due to the watermark embedding and the removing process is an important but often neglected issue to consider in order to design a fair watermarking benchmark. Given a pattern of possible attacks, the aim of this work is to find a near-optimal combination of them, which removes the mark minimizing the degradation perceived by the Human vision system (HVS). Hence, we need to define a proper quality metric. In general, several metrics can be used to evaluate the artifacts but the most popular one is the peak signal-to-noise ratio (PSNR) metric. The success of this measure is due to its simplicity but several tests show that such a metric is not suitable to measure the quality perceived by HVS. A modified version of PSNR, the so-called WPSNR, is introduced: it takes into account that HVS is less sensitive to changes in highly textured areas and introduces an additional parameter, called the noise visibility function (NVF), which is a texture masking function:

$$WPSNR(dB) = 10 \log_{10} \frac{I_{peak}^2}{MSE \times NVF^2} \quad (1)$$

Where I_{peak} is the peak value of the input image.

The value of NVF ranges from:

$$NVF = \text{norm} \left\{ \frac{1}{1 + \sigma_{block}^2} \right\} \in (0,1) \quad (2)$$

Where norm is the normalization function and σ_{block}^2 is the luminance variance of $8 * 8$ block. The main idea of this contribution is to evaluate the robustness of a watermarking system in terms of perceptual quality measured by WPSNR. Namely, fixed a set of admissible image processing operators, the robustness of a method is qualified as:

$$R(q) = \frac{Q}{M(q)} \quad (3)$$

Where Q is fixed quality threshold, q is perceptual quality of watermarked image I_w , and $M(q)$ is the maximal perceptual quality of the unmarked image obtained from I_w by applying any combination of the selected attacks. If $R(q)$ is greater than 1, then it is possible to remove the mark from the given image only degrading its maximal perceptual quality $M(q)$ under q . As a consequence, the watermarking algorithm can be declared robust since a large degradation needs to be introduced in the image to remove the mark. On the other hand, the embedded watermark is not robust if $M(q)$ assumes values higher than the threshold Q (i.e., $R(q)$ is less than 1).

3.1 Robustness Evaluation Metric

$Q \geq M(q) \quad R(q) \geq 1 \quad \text{Robust}$
 $Q < M(q) \quad R(q) < 1 \quad \text{Non Robust}$

3.2 Tool Description

In the proposed tool, Genetic algorithm(GA) is applied in the detection procedure of the watermarking scheme. An image previously watermarked by the algorithm to be tested and with perceived quality q is attacked with different combinations of selected image processing operators(attacks such as Rotation, Gray effect, Fixed Resolution) in order to remove the embedded mark. The aim is to find a near-optimal combination of attacks to apply in order to remove the watermark, while granting a perceptual quality of the resulting image as high as possible. The algorithm robustness is then measured via $R(q)$ i.e optimization process is performed by GA and WPSNR is the fitness value to be maximized.

Step 1 : Randomly generate combinations of parameters to be applied to processing operators and convert them into chromosomes . This way, an initial population is created.

Step 2: Apply each generated attack to the input image and evaluate the WPSNR of each chromosome in the current population which removes the watermark, i.e. which generates an unmarked image, and then create a new population by repeating the following steps: 1) pick as parents the chromosomes with the higher WPSNR, according to the selection rule; 2) form new children (new patterns of attacks) by applying to parents the stochastic operator of crossover with probability P_c 3) mutate the position in the chromosome with probability P_m . Among all individuals of the current population which allow removing the watermark, the one that provides an image with the higher WPSNR will survive to the next generation. We set to zero the fitness value of those chromosomes which do not succeed in removing the mark.

If in Step 2 no solutions for the problem are found, i.e., none of the individuals of the population succeeds in removing the watermark, another population is re-initialized and the process is repeated until a termination criterion is met (number of generation exceeded). Consequently, the result of the test is that the analyzed watermarking technique is robust to the selected attacks.

Step 3: A new iteration with the just generated population is processed. This new population provides new attacks

parameters, their corresponding fitness values are evaluated, and at every generation the individual with the highest fitness value is kept.

Step 4: The process ends when a given number of generation is exceeded (termination criteria). At that point a near-optimal combination of attacks removing the watermark from the image has been discovered. In particular, given the quality threshold Q , $M(q) < Q$ means that it is hard to remove the watermark while keeping a high perceptual quality, hence, the watermarking technique is declared to be robust. On the other hand, if $M(q) > Q$, our robustness measure indicates a serious weakness corresponding to high quality of the unmarked image.

3.3 Why Modify WPSNR?

- [1] WPSNR does not consider the ROI(Region of interest) of the image. Therefore, the noise on ROI and ROB regions are given equal weightage.
- [2] Consider a situation where there are two distorted images having same MSE(Mean Square error). In one, distortion is concentrated at one part of the image and hence it is visible. In other, distortion is not visible because the distortion is spread on the whole image with low intensity. If error distortion is localized on an image it will be annoying to the viewer while if it is spreaded on whole image it will be less annoying even though the total MSE is the same.

3.4 Algorithm for EWPSNR

- [1] Read reference image $H(i; j)$ and distorted image $H'(i; j)$. Obtain the NVF of the image.
- [2] Create a binary image $B(i; j)$ corresponding to Region of Interest (ROI) of the image such that binary is assigned at ROI area and binary '0' is assigned at Region of Background (ROB) area.
- [3] Fix the Just Noticeable Difference(JND) value according to the subjective assessment.
- [4] Initialize $i = j = 1$.
- [5] If $B(i; j) = 1$, $R = 9$. Otherwise, $R = 1$ where R is an index corresponding to ROI. The minimum value is selected as 1 because the Mean Square Error(MSE) will remain same as in the original expression for WPSNR. $R = 9$ corresponds to maximum penalty to noise in ROI part.
- [6] Find difference between the images. If $\text{Difference} < \text{JND}$; then $Th = 1$. Otherwise, $Th = 9$. Th is the threshold value corresponding to JND value. Minimum value of Th is selected as unity due to the reason stated in step 5.
- [7] A new variable is defined: $\lambda = R \times \sigma^2 \times Th$

[8] If $\delta! = 0$, then $H(i; j) = 2^B - 1$, else $H(i; j) = 0$, where B is the resolution of the image.

[9] If not last pixel, increment i and j and go to step 5.

[10] Obtain denominator D of the expression:

$$D = \sum_{i,j} \sum_{i,j} \frac{(N \times F^2 \times L)}{M \times N}$$

11) Calculate EWPSNR in db as:

$$EWPSNR = 10 \log_{10} \left(\frac{B^2 - 1}{n \times D} \right)$$

IV. SIMULATION RESULTS:

Modules implemented are described below: An image to be watermarked with text is considered (lena image). The Text is watermarked on the image (case of visible watermarking).

Figure1: Lena image to be watermarked.

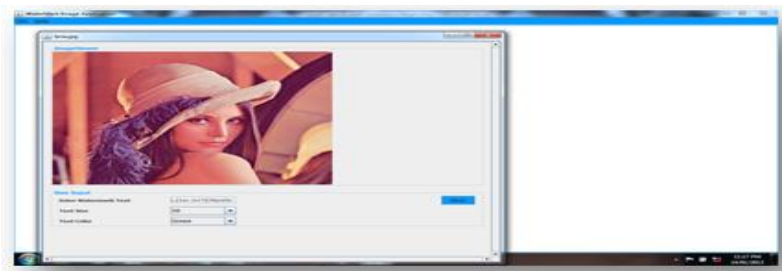


Figure2: Text watermarked (in green colour) on lena image.

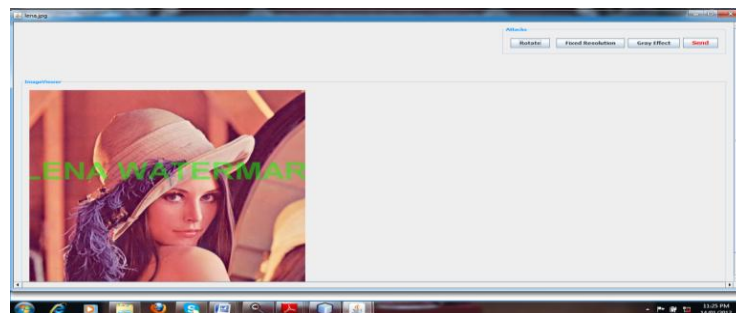


Figure 3: Lena image after applying rotation.

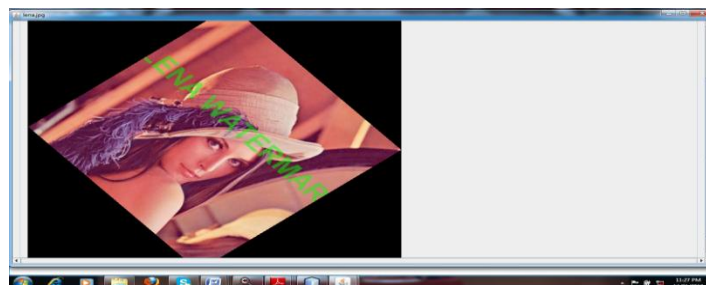


Figure 4: Lena Image after applying gray effect



V. CONCLUSION

An innovative benchmarking tool have been presented to evaluate the robustness of any digital watermarking technique considering the quality of the unmarked images in terms of perceived quality. Therefore, a new metric based on WPSNR is introduced. The goal is to remove the watermark from a content while maximizing perceptual quality. So, given a set of attacks,we look for a parameterization able to remove the watermark, optimizing the WPSNR of the unmarked image.The poor correlation of PSNR and WPSNR with HVS, was explored and experimentally proved the superiority of the proposed metric EWPSNR. The new fidelity metric can be used for the evaluation of the fidelity of images in the areas of compression, filtering, denoising,data embedding etc.

REFERENCES

- [1] Giulia Boato, Valentina Conotter, Francesco G. B. De Natale , and Claudio Fontanari:” Watermarking Robustness Evaluation Based on Perceptual Quality via Genetic Algorithms”, IEEE Transaction on information forensics and security,vol 4,No 2,June 2009.
- [2] Fabien A. P. Petitcolas,”Watermarking schemes evaluation”, in IEEE Signal Processing, vol. 17, no. 5, 2000, pp. 58–64.
- [3] Fabien A. P. Petitcolas, Ross J. Anderson, Markus G. Kuhn: “Information Hiding:A Survey”,Proceedings of IEEE, vol. 87, No. 7, July 1999.
- [4] Fabien A. P. Petitcolas, Ross J. Anderson, Markus G. Kuhn: “Attacks on copyright marking systems”, in Proc. Of David Aucsmith (Ed), Information Hiding, U.S.A., 1998.
- [5] Jan C. Vorbruggen,Franois Cayre:”The Certimark Benchmark:Architecture and future perspectives”, 2002 IEEE.
- [6] V. Solachidis, A. Tefas, N. Nikolaidis, S. Tsekeridou, A. Nikolaidis,I.Pitas, ``A benchmarking protocol for watermarking methods”, in IEEE Int. Conf. on Image Processing (ICIP'01), 2001, pp. 1023-1026.
- [7] Zhou Wang, and A-C Bovik, Mean Squared Error: Love It or Leave It?,IEEE Signal Processing Magazine, 98-117, January 2009.
- [8] Wen Lu, and Xinbo Gao, and Xuelong Li, and Dacheng Tao, An image quality assessment metric based contourlet, University of London, 2008.
- [9] K. A. Navas and M. Sasikumar Image Fidelity Metrics: Future Directions,IETE Technical review, Vol 28, Issue 1, Jan-Feb 2011.

Performance Comparison of Uncoded & Coded Adaptive OFDM System over AWGN Channel

Swati M. Kshirsagar¹, A. N. Jadhav²

^{1,2}Department of E & TC, D.Y. Patil College of Engg. & Tech., Kolhapur, Maharashtra, India.

Abstract

Adaptive OFDM (AOFDM) is the important approach to fourth generation of mobile communication. Adaptive modulating scheme is employed according to channel fading condition for improving the performance of OFDM. This gives improved data rate, spectral efficiency & throughput. OFDM is flexible to adapt modulation schemes on subcarriers according instantaneous signal-to-noise ratio (SNR). In this paper, we compare Bit Error Rate (BER), Mean Square Error (MSE), Spectral Efficiency, Throughput performance of uncoded & coded adaptive OFDM with BPSK, QPSK & QAM modulation over AWGN channel.

Keywords: AOFDM, BER, FFT, MSE, OFDM, SNR, Spectral Efficiency, Throughput

I. INTRODUCTION

Orthogonal Frequency Division Multiplexing (OFDM) is the most popular modulation technique for wireless communications. OFDM is a digital multicarrier modulation scheme which uses a large number of closely spaced orthogonal subcarriers [2]. OFDM signals are generated using the Fast Fourier transform. Each individual carrier, commonly called as subcarrier. Each subcarrier is modulated with a conventional modulation scheme at a low symbol rate, maintaining data rates similar to conventional single carrier modulation schemes in the same bandwidth. OFDM is a logical next step in broadband radio evolution. It is applied in IEEE standards like IEEE 802.11 (Wi-Fi) and 802.16 (WiMAX). OFDM is flexible to adapt modulation schemes on subcarriers according to instantaneous SNR. Adaptive OFDM (AOFDM) is the important approach to fourth generation of mobile communication. Adaptive modulation scheme is employed according to channel fading condition to improve OFDM performance. This improves data rate, spectral efficiency & throughput.

In this paper, we analyze Bit Error Rate (BER), Mean Square Error (MSE), Spectral Efficiency, Throughput performance of coded adaptive OFDM with BPSK, QPSK & QAM modulation over AWGN channel.

II. SYSTEM MODEL :

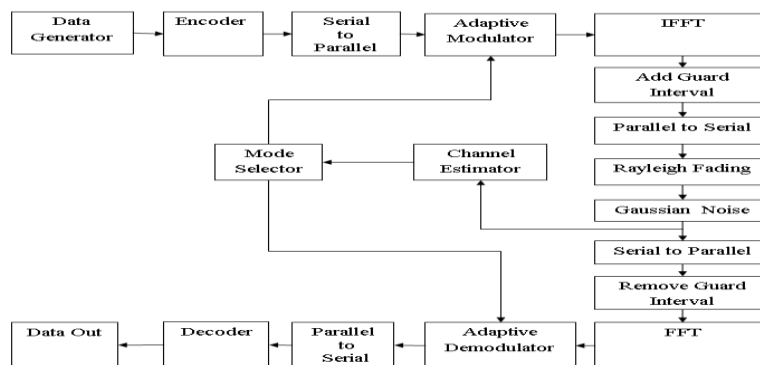


Figure 1. Adaptive OFDM system

The system model for Adaptive OFDM system is as shown in "Fig.1". The data is generated with the help of data generator. It is represented by a code word that consists of prescribed number code elements. The transmitter first converts this data from serial stream to parallel sets. Each set of data contains one symbol, S_i , for each subcarrier. For example, a set of four data would be $[S_0 S_1 S_2 S_3]$. The flexibility to rigorous channel conditions can be further improved if information about the channel is sent over a return channel. Based on this feedback information adaptive modulation & channel coding may be applied across all subcarriers or individually to each subcarrier.

An inverse Fourier transform (IFFT) converts the frequency domain data set into samples of the corresponding time domain representation. Specifically IFFT is useful for OFDM because it maintains orthogonality between subcarriers. Since the duration of each symbol is long it is feasible to insert a guard interval between the OFDM symbols. Thus eliminating intersymbol interference. Parallel to serial block creates the OFDM signal by sequentially outputting the time domain samples. At receiver guard interval is removed. FFT is applied to have frequency domain signals. Adaptive demodulator does the reverse of modulator.

The channel estimator is used to estimate the instantaneous SNR of the received signal. Based on the instantaneous SNR the best mode will be selected for next transmission frame. This task is done by the mode selector block [1]. The channel estimation and mode selection are done at the receiver side and the information is sent to the transmitter using a feedback channel [4]. In this model the adaptation is done frame by frame. At the transmitter the adaptive modulator block consists of different modulators which are used to provide different modulation modes. The switching between these modulators will depend on the instantaneous SNR. This system model is used to describe three types of modulation schemes as BPSK, QPSK & QAM.

III. SYSTEM PARAMETERS:

Table1. System Parameters

Parameter	Value
IFFT size	512
Number of subchannels N	512
Number of subband	32
Number of subcarriers per subband	16
SNR	0-30dB
Guard interval N/4	128
Pilot interval	8
Modulation scheme	BPSK, QPSK, QAM
Channel length L	16
Number of pilots(P= N/8)	64

OFDM system parameters considered here to analyze the Bit Error Rate (BER), Mean Square Error, Spectral Efficiency, Throughput performance of uncoded & coded adaptive OFDM with BPSK, QPSK & QAM modulation over AWGN channel are mentioned in Table1.

IV. RESULTS & DISCUSSIONS:

Here we analyzed the the Bit Error Rate (BER), Mean Square Error, Spectral Efficiency, Throughput performance of uncoded & coded adaptive OFDM with BPSK, QPSK & QAM modulation over AWGN channel. Here we used Cyclic coding. "Fig.2" & "Fig.3" shows BER performance of uncoded & coded adaptive OFDM respectively. It is observed from "Fig.2" that for SNR is in between 0 dB - 3dB, highest modulation scheme i.e. 64QAM is used. For SNR is between 3dB - 6dB, 32QAM is used. When SNR is in between 6dB - 9dB modulation scheme 16 QAM is used. For SNR in between 9dB - 12dB, 8QAM is used. For SNR is between 12dB- 15dB lower modulation scheme i.e. QPSK is used & for SNR is from 12dB-18dB lowest modulation scheme i.e. BPSK is used. For value of SNR above 18dB signal is not transmitted. Thus adaptation is achieved on the basis of instantaneous SNR. BER performance of coded AOFDM is similar to uncoded for SNR upto 9dB, for higher SNR value it degrades.

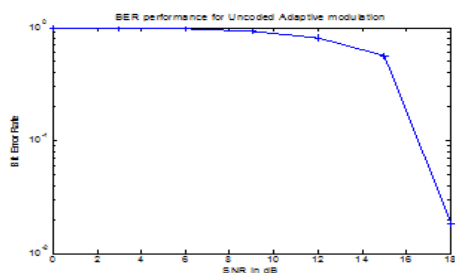


Figure 2. BER Performance of Uncoded AOFDM with BPSK, QPSK, QAM

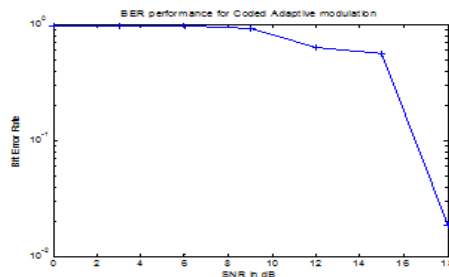


Figure 3. BER Performance of Coded AOFDM with BPSK, QPSK, QAM

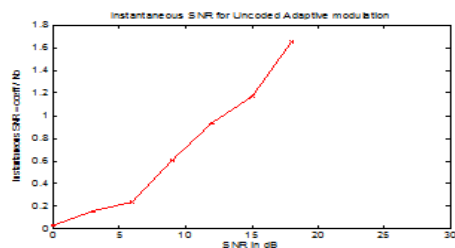


Figure 4. Instantaneous SNR of Uncoded AOFDM with BPSK, QPSK, QAM

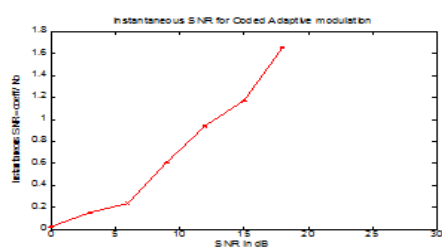


Figure 5. Instantaneous SNR of Coded AOFDM with BPSK, QPSK, QAM

Instantaneous SNR of uncoded & coded adaptive OFDM is shown in “Fig. 4” & “Fig. 5”. It increases with SNR value.

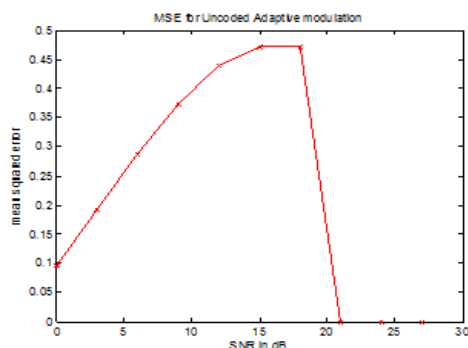


Figure 6. Mean Square Error of Uncoded AOFDM with BPSK, QPSK, QAM

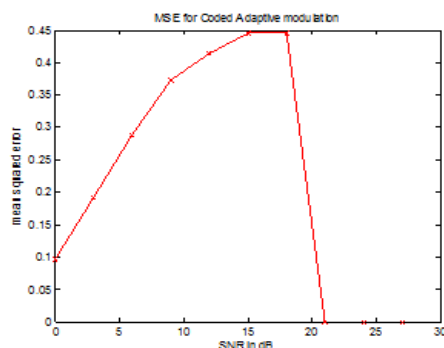


Figure 7. Mean Square Error of Coded AOFDM with BPSK, QPSK, QAM

It is observed from “Fig.6” & “Fig.7” that Mean Square Error (MSE) of uncoded & coded adaptive OFDM with BPSK, QPSK, QAM increases from 0.1 to 0.47 & 0.1 to 0.45 respectively for SNR value from 0dB to 18dB. After that it decreases & becomes 0 at & above SNR 21dB due to no transmission.

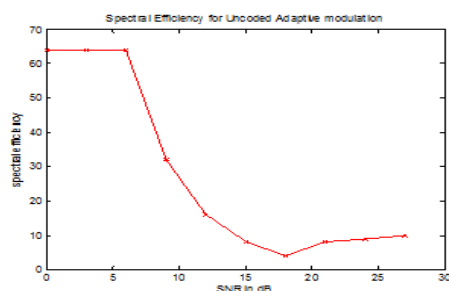


Figure 8. Spectral efficiency of Uncoded AOFDM with BPSK, QPSK, QAM

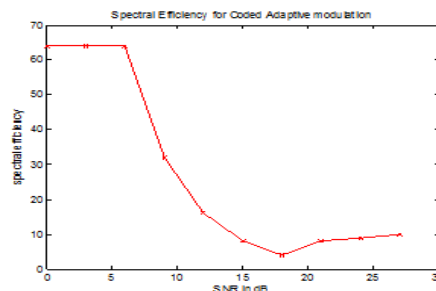


Figure 9. Spectral efficiency of Coded AOFDM with BPSK, QPSK, QAM

Spectral efficiency of uncoded & coded adaptive OFDM with BPSK, QPSK, QAM is shown in “Fig.8” & “Fig.9” respectively. It is same for the both. For SNR 0dB to 6 dB both shows better Spectral efficiency as about 64%. As SNR is still increasing accordingly Spectral efficiency decreases.

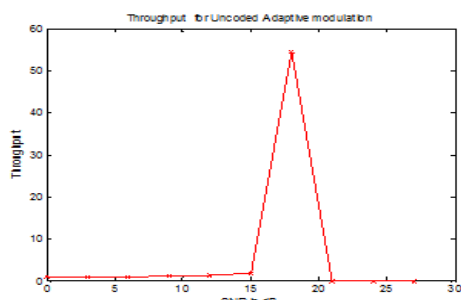


Figure 10. Throughput of Uncoded AOFDM with BPSK, QPSK, QAM

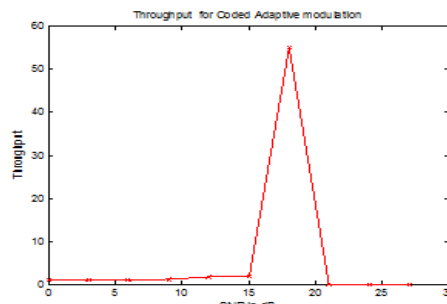


Figure 11. Throughput of Coded AOFDM with BPSK, QPSK, QAM

“Fig.10” & “Fig.11” shows Throughput of uncoded & coded adaptive OFDM with BPSK, QPSK, QAM respectively. Throughput of coded AOFDM is the same as that of uncoded for SNR up to 9dB. Above 9 dB it gradually increases & becomes maximum as 54.97 in comparison with 54.47 at SNR 18 dB. So for SNR up to 12 dB Throughput of both is less due to higher modulation schemes. As SNR increases above 12dB lower level modulation schemes as QPSK & BPSK are employed so Throughput increases. Throughput is maximum for SNR values 18 dB. After SNR above 18 dB it decreases. For SNR values in between 21dB to 27 dB Throughput is minimum i.e. 0 due to no transmission.

V. Conclusion:

In this paper, we have evaluated Bit Error Rate (BER), Mean Square Error (MSE), Spectral Efficiency, Throughput performance of uncoded & coded adaptive OFDM with BPSK, QPSK & QAM modulation over AWGN channel. It is observed that according to instantaneous SNR suitable modulation scheme is employed. If SNR is from 0dB to 3dB & 3dB to 6dB spectrally efficient modulation schemes such as 64 QAM & 32 QAM are used respectively. BER performance of coded AOFDM is similar to uncoded for SNR upto 9dB, for higher SNR value it degrades. MSE of uncoded & coded adaptive OFDM increases from 0.1 to 0.47 & 0.1 to 0.45 respectively for SNR value from 0dB to 18dB. After that it decreases & becomes 0 at & above SNR 21dB due to no transmission. Spectral efficiency is same for the both. For SNR 0dB to 6 dB both shows better Spectral efficiency as about 64%. As SNR is still increasing accordingly Spectral efficiency decreases. Throughput of coded AOFDM is the same as that of uncoded for SNR up to 9dB. Above 9 dB it gradually increases & becomes maximum as 54.97 in comparison with 54.47 at SNR 18 dB i.e. for SNR up to 12 dB Throughput of both is less & becomes maximum at 18dB. Thus coded AOFDM gives better Throughput than uncoded one. Also Adaptive modulation achieves a good tradeoff between spectral efficiency and overall BER.

REFERENCES

- [1] A.Sohail and M.N.Jafri, “Adaptive OFDM over Frequency Selective and Fast Fading Channel Using Blockwise Bit Loading Algorithm”, IEEE International Conference on Wireless and Optical Communication Networks, pp. 1-4, July 2007.
- [2] A. Cyzlwik, “Adaptive OFDM for wideband radio channels”, Global Telecommunications Conference, vol 1, pp713-718, Nov 1996.
- [3] X She, Z.Zhang, S.Zhou, Yan Yao, “Adaptive Turbo Coded Modulation for OFDM Transmissions”, Proceedings of ICCT, pp.1491-1495, 2003.
- [4] K.M. Hadi, R.Tripathi and K.Kant, “Performance of Adaptive Modulation in Multipath Fading Channel”, The 8th International Conference on Advanced Communication Technology, ICACT, vol. 2, pp.1277- 1282, 20-22 February 2006.
- [5] L. Khalid and A. Anpalagan, “Threshold-Based Adaptive Modulation with Adaptive Subcarrier Allocation in OFCDM-Based 4G Wireless Systems,” IEEE Vehicular Technology Conference, pp.1-6, Sept. 2006.
- [6] S.Sampegi and H. Harada, “System Design Issues and Performance Evaluations for Adaptive Modulation in New Wireless Access Systems”, Proceedings of the IEEE, Vol.95, no.12, pp. 2456-2471, Dec 2007.
- [7] B. Le Flock, M. Alard, and C. Berrou, “Coded orthogonal frequency division multiplex,” Proceedings of the IEEE, Vol. 83, no. 6, June 1995.
- [8] T.S.Rappaport, Wireless Communications Principles & Practice (II nd Edition, Pentice-Hall, January 2002).
- [9] J.G.Prokis, Digital Communications (Mc-Graw Hill, New York NY, IVth Edition, 2000).

Mathematical Model By Using Mixture Weibull Distribution For Finding The Combination Of Gad65 And Gaba For Modulation Of Spasticity

¹,S.Lakshmi , ²P.Gomathi Sundari

¹Head and Associate Professor of Mathematics, K.N.Govt.Arts College for Women,Thanjavur -613005, TamilNadu, India.

²Assistant Professor of Mathematics, Rajah Serfoji Government College, Thanjavur-613005, TamilNadu, India.

Abstract

Loss of GABA-mediated pre-synaptic inhibition after spinal injury plays a key role in the progressive increase in spinal reflexes and the appearance of spasticity. Clinical studies show that the use of baclofen (GABAB receptor agonist), while effective in modulating spasticity is associated with major side effects such as general sedation and progressive tolerance development. The present study was to assess if a combined therapy composed of spinal segmentspecific upregulation of GAD65 (glutamate decarboxylase) gene once combined with systemic treatment with tiagabine (GABA uptake inhibitor) will lead to an antispasticity effect and whether such an effect will only be present in GAD65 gene over-expressing spinal segments. Here we use the mixture distribution produced from the combination of two or more Weibull distributions which has a number of parameters. A mixture distribution is even more useful because multiple causes of failure can be simultaneously modeled. Also these functions were represented by graphs that showed this variation. The estimation of parameters were effected by the different values of the mixing parameter and the results have been discussed from the corresponding mathematical figures.

Keywords: Weibull distribution, Mixture Weibull distribution, Mixing parameter, GABA, GAD65, Tiagabine

AMS Classification: 60 G_{xx}, 62 H_{xx}, 62P_{xx}

I. MATHEMATICAL MODELS

The mixture Weibull distribution produced from the combination has five or more parameters. These are; the shape parameters, scale parameters, location parameters, in addition to the mixing parameter (w). This type of distribution is even more useful because multiple causes of failure can be simultaneously modelled. Different values of the mixing parameter were used to obtain the estimation of the parameters and to find the probability density function of the mixture Weibull distribution.

1.1 MIXTURE MODELS

When we have n-fold mixture model that involves n sub-populations, then

$$F(x) = \sum_{i=1}^n w_i F_i(x_i) \quad \text{with } w_i > 0, \text{ and } \sum_{i=1}^n w_i = 1$$

where w_i is a mixing parameter and $F_i(x)$, $i=1,2,\dots,n$ are distribution functions either with two or three parameter Weibull distributions. The models involve two or more distributions with one or more being Weibull distribution. The distributions involved are called sub-populations or components, and the model is called finite Weibull mixture model. In the literature the Weibull mixture model has been referred by many other names [5,6], such as additive-mixed Weibull distributions, bimodal-mixed Weibull (for a two fold mixture), mixed-mode Weibull distribution, Weibull distribution of the mixed type, multi modal Weibull distribution, and so forth.

II. MIXTURE WEIBULL DISTRIBUTION

The probability density function (pdf) of a 2-parameter Weibull distribution is,

$$f(x : \alpha, \beta) = \frac{\alpha(x)^{\alpha-1}}{\beta^\alpha} \exp\left(-\left(\frac{x}{\beta}\right)^\alpha\right) \quad \text{for } 0 \leq x < \infty \quad (1)$$

and for a 3-parameter Weibull distribution is

$$f(x : \alpha, \beta, \gamma) = \frac{\alpha(x - \gamma)^{\alpha-1}}{\beta^\alpha} \exp\left(-\left(\frac{x - \gamma}{\beta}\right)^\alpha\right) \quad \text{for } \gamma \leq x < \infty \quad (2)$$

where α , β , and γ are the shape, scale and location parameters respectively.

A mixture distribution is a distribution made of combining two or more component distributions. The probability density function of this mixture distribution can be shown as;

$$f(x) = w_1 f_1(x) + \dots + w_n f_n(x) \quad w_i > 0, \text{ and } \sum_{i=1}^n w_i = 1$$

where w_i is the mixing parameter which represents the proportion of mixing of the component distributions. The function $f_i(x)$ is the probability density function of the component distribution i . While n is the number of component distributions being mixed [7]. In this paper we will consider a simple case of only two component distributions, and the mixing parameter for each component will be defined simply as w and $(1-w)$.

The probability density function of the mixture Weibull distribution of the two distributions in (1) and (2) is as follows;

$$f(x) = \frac{\alpha_1(x)^{\alpha_1-1}}{\beta_1^{\alpha_1}} \exp\left(-\left(\frac{x}{\beta_1}\right)^{\alpha_1}\right) + (1-w) \frac{\alpha_2(x - \gamma_2)^{\alpha_2-1}}{\beta_2^{\alpha_2}} \exp\left(-\left(\frac{x - \gamma_2}{\beta_2}\right)^{\alpha_2}\right) \quad (3)$$

where, $\alpha_1, \alpha_2, \beta_1, \beta_2 > 0 \leq \gamma \leq x$ and $0 < w < 1$

Here w is the mixing parameter.

As a result, when the two sub-populations are given by equation (1), the model is characterized by five parameters, the shape and scale parameters for the two sub-populations and the mixing parameter w ; with $0 < w < 1$

The probability density function and failure rate of the two-fold Weibull mixture are given by;

$$f(x) = wf_1(x) + (1-w)f_2(x)$$

and

$$h(x) = \sum_{i=1}^n w_i(x)h_i(x)$$

where

$$w_i(x) = \frac{w_i R_i(x)}{\sum_{i=1}^n w_i R_i(x)} \quad \text{and} \quad \sum_{i=1}^n w_i(x) = 1$$

and

$$R_i(x) = 1 - F_i(x)$$

$R_i(x)$ is the reliability function, Hence

$$h(x) = \frac{wR_1(x)}{wR_1(x) + (1-w)R_2(x)} h_1(x) + \frac{(1-w)R_2(x)}{wR_1(x) + (1-w)R_2(x)} h_2(x)$$

[7] who assumed that only the mixing proportions are unknown for the two component case;

$$f(x) = wf_1(x) + (1-w)f_2(x)$$

By integrating a family of equations of the form;

$$F(x) = wF_1(x) + (1-w)F_2(x)$$

which leads to the following

$$w = \frac{F(x) - F_2(x)}{F_1(x) - F_2(x)}$$

This gives necessary and sufficient conditions on F_1 and F_2 for the uniform attainment of the Cramer-Rao bound on the variance of w .

III. APPLICATIONS

We first quantified the loss of GABA-ergic neurons and boutonlike terminals in laminae VII and IX of lumbar spinal cord sections taken from spastic and sham-operated control animals. In comparison with control animals spastic animals had 50% less GABA-ergic neurons (average 39.0 ± 13.4 vs. 19.5 ± 4.2 per section; $p < 0.01$; Fig. 1A, B) in lamina VII. In those same sections, GABA-ergic contact with a-motoneurons was also assessed, revealing a significant reduction in spastic animals (Fig. 1D-white arrows): 19.4 ± 0.9 GABA/Syn-immunoreactive (IR) boutons contacting each motoneuron soma in control tissue compared to 10.1 ± 0.8 in animals with spasticity ($p < 0.01$; Fig. 1C, D). We next examined the number of GAD65 or GAD67 bouton-like structures that contacted VGLuT1-IR primary afferent terminals in lamina IX (i.e. the site of GABAergic presynaptic Ia afferent inhibition). In control animals $26.7 \pm 4.2\%$ of primary afferent terminals had clear GAD65 contact, compared to only $5.3\% \pm 1.2\%$ in ischemia-injured tissue ($p < 0.001$; Fig. 1E, F).

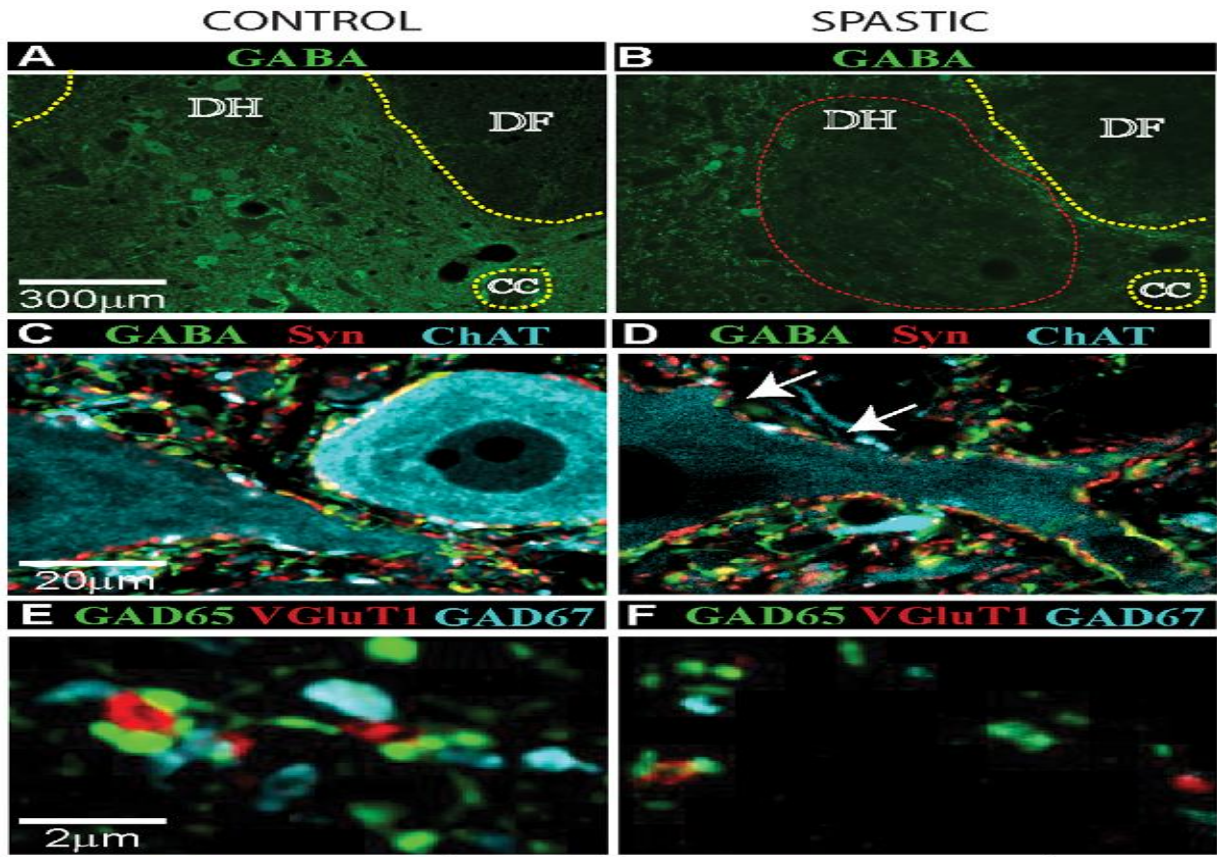


Figure 1. Loss of segmental inhibitory GABA-ergic interneurons and increased expression of GABA B R1+R2 receptor in motoneurons after transient spinal cord ischemia is associated with the development of chronic muscle spasticity. (A, B) Transverse spinal cord sections taken from L2–L5 segments in control (A) or spinal ischemia-induced-spastic rat (B) at 24 h after intrathecal colchicine injection and stained for GABA. Note an apparent loss of GABA-ergic interneurons in the intermediate zone in spastic rat (B; red circle). (C–F) Loss of GABAergic interneurons corresponds with loss of GABA-IR

We tested if spinal GAD65 overexpression will lead to increased local GABA release and if such a release will have a similar anti-spastic effect once combined with systemic tiagabine (1, 4, 10, 20 or 40 mg/kg) treatment. Spastic animals received a total of 20 bilateral injections of HIV1-CMV-GAD65-GFP ($n=6$) or HIV1-CMV-GFP ($n=6$; control) lentivirus targeted into ischemia-injured L2–L5 spinal segments and underwent spasticity assessments 7–21 days after virus delivery. In control HIV1-CMV-GFP-injected spastic animals, systemic administration of tiagabine (40 mg/kg.i.p.) was without effect (Fig. 2A). In contrast, in HIV1-CMV-GAD65-GFP-injected rats, treatment with tiagabine led to a potent and significant anti-spasticity effect. The peak effect was seen at 25 min after tiagabine administration and returned back to baseline by 60 min (Fig. 2A; $p > 0.01$). Dose response analysis for tiagabine showed that doses ≥ 4 mg/kg provided significant ($p > 0.01$) anti-spasticity effect at 15–25 min after tiagabine injection. No detectable effect on upper limb motor

function was seen after tiagabine treatment and all animals showed continuing ability to move their upper limbs and grab food pellets if offered.

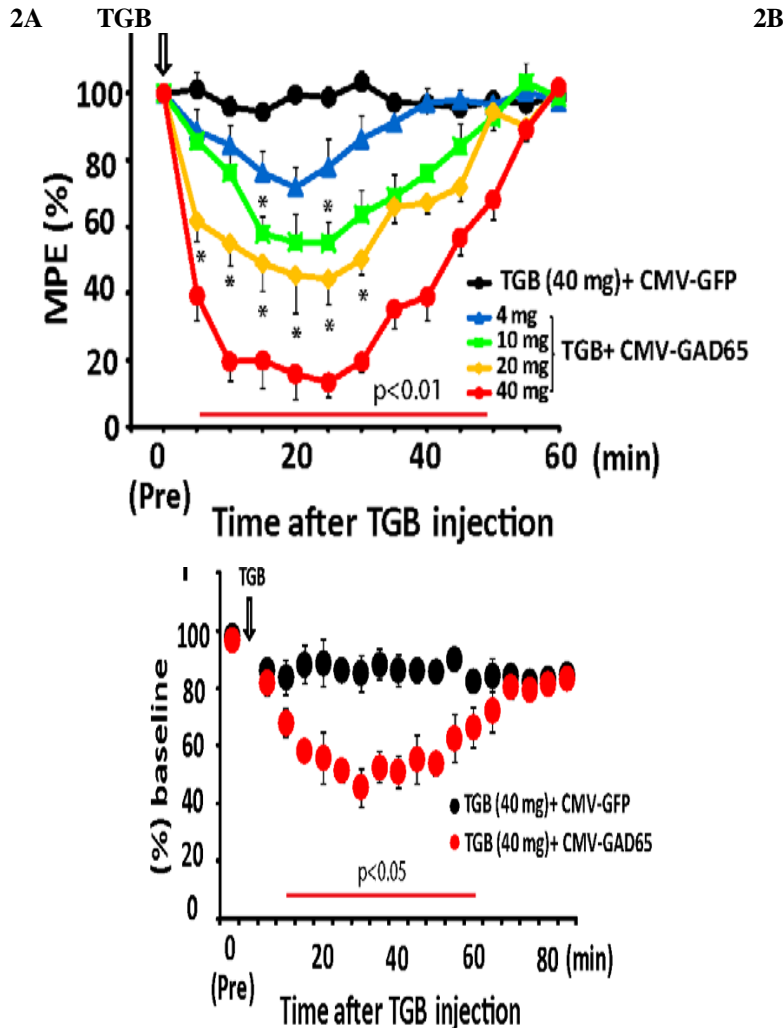


Figure 2A. Effective suppression of spasticity after combined therapy with systemic tiagabine and intrathecal injection of GABA or spinal parenchymal GAD65 gene delivery.

Time-course of anti-spastic effect after tiagabine treatment expressed as % of maximum possible effect in measured ankle resistance in HIV1-CMV-GFP or HIV1-CMV-GAD65-GFP lentivirus-injected animals (* P< 0.01; one-way analysis of variance-ANOVA, Bonferroni's posthoc test; MPE-maximum positive effect). **Figure 2B** Time-course of changes in H-wave amplitudes before and up to 90 min after tiagabine administration (red line-P,0.05; unpaired t test).

In separate experimental sessions, changes in H-reflex amplitudes evoked by high frequency stimulation was tested in ketamine-sedated animals. In spastic animals previously injected spinally with control lentivirus (HIV1-CMV-GFP; n = 6) no change in H-reflex amplitudes were seen up to 90 min after tiagabine injections (Fig. 2B). In animals receiving spinal injections of HIV1-CMV-GAD65-GFP lentivirus (n= 6) a significant (p,0.05) reduction of the H-wave amplitude was measured between 20–45 min after tiagabine injection and returned back to baseline by 65 min (Fig. 2B). Similar significant suppression of H-reflex activity in spastic patients after intrathecal baclofen treatment was reported [2].

The professionals believe, that the ability of such combined therapy in which systemically administered drugs (such as tiagabine) is effective in regulating the activity of the therapeutic product (GABA) in remote GAD65 gene-overexpressing sites can potentially have a significant clinical implications. **First**, the identity of specific spinal segments innervating the affected spastic muscle groups can be neurologically mapped, lateralized and selected for the segment/site-specific GAD65 gene delivery.

Second, extensive clinical data show a potent anti-spastic effect after intrathecal baclofen delivery and this effect is independent on the spinal or supraspinal origin of spasticity [1]. Thus, it is likely that spinal segmental GAD65 upregulation once combined with systemic GABA uptake inhibitor treatment will have a similar therapeutic effect in spasticity of supraspinal and spinal origin.

Third, comparable site-specific delivery of GAD65-encoding vectors targeting functionally/electrophysiologically-defined brain epileptic foci can be performed. Previous data from other laboratories have confirmed an improvement in the parkinsonian behavioural phenotype and neuronal rescue after AAV-CBAGAD65 delivery into the subthalamic nucleus in 6-OHDA-lesioned rats [2]. We speculate that proposed combination treatments can lead to a more pronounced anti-epileptic effect with less side effects such as general sedation.

Fourth, the serum half-life of tiagabine in human patients is between 5–8 hrs and therefore comparable duration of the antispasticity effect can be expected in human patients once combined with spinal parenchymal GAD65 gene delivery [3,4].

MATHEMATICAL RESULTS

Figure 2A :

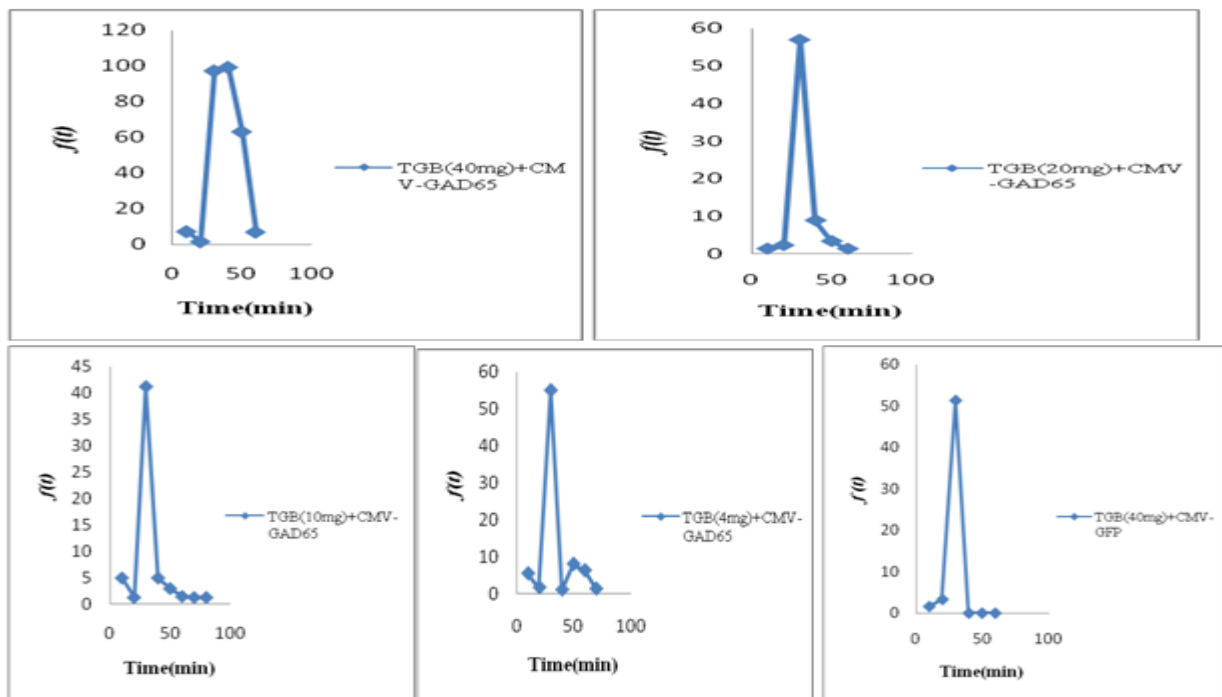
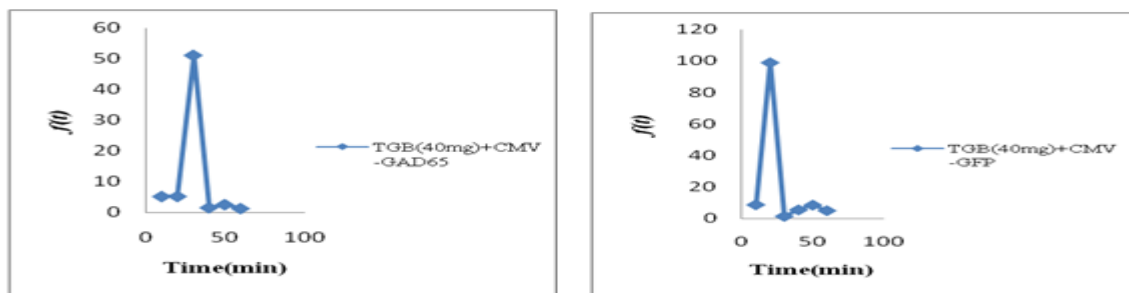


Figure 2B :



The function $f(t)$ reaches the peak in the time interval (20, 30) and sudden decrease in the interval (30, 40). When the 10 mg Tiagabine injection given mixture probability density function $f(t)$ reaches the peak at time $t=30$ minutes and sudden decrease to time axis at $t=40$ minutes. Similarly for the 3 case when 20 gm Tiagabine injection is given. The last case when the Tiagabine injection 40 mg is given mixture probability density function $f(t)$ reaches the peak at time $t=30$ and is constant over there till $t=40$ and suddenly decreases to the baseline level when time $t=60$.

IV. CONCLUSION

These data show that treatment with orally bioavailable GABA-mimetic drugs if combined with spinal-segment-specific GAD65 gene over expression can represent a novel and highly effective anti-spasticity treatment which is associated with minimal side effects and is restricted to GAD65-gene over-expressing spinal segments. We also found the mixture probability density function. We graphed these functions and saw the variation on the curves when different values are given for the mixture probability density function. The function $f(t)$ reaches the peak in the time interval (20, 30) and sudden decrease in the interval (30, 40). When the 10 mg Tiagabine injection given mixture probability density function $f(t)$ reaches the peak at time $t=30$ minutes and sudden decrease to time axis at $t=40$ minutes. Similarly for the 3 case when 20 gm Tiagabine injection is given. The last case when the Tiagabine injection 40 mg is given mixture probability density function $f(t)$ reaches the peak at time $t=30$ and is constant over there till $t=40$ and suddenly decreases to the baseline level when time $t=60$.

REFERENCES

- [1] Remy-Neris O, Barbeau H, Daniel O, Boiteau F, Bussel B (1999) Effects of intrathecal clonidine injection on spinal reflexes and human locomotion in incomplete paraplegic subjects. *Exp Brain Res* 129: 433–440.
- [2] Lazorthes Y, Sallerin-Caute B, Verdie JC, Bastide R, Carillo JP (1990) Chronic intrathecal baclofen administration for control of severe spasticity. *J Neurosurg* 72: 393–402.
- [3] Gustavson LE, Mengel HB (1995) Pharmacokinetics of tiagabine, a gammaaminobutyric acid-uptake inhibitor, in healthy subjects after single and multiple doses. *Epilepsia* 36: 605–611.
- [4] Dalby NO (2000) GABA-level increasing and anticonvulsant effects of three different GABA uptake inhibitors. *Neuropharmacology* 39: 2399–2407.
- [5] Ahmad, K.E. and AbdulRahman, A.M. (1994) Upgrading a Nonlinear Discriminate Function Estimated from a Mixture of two Weibull Distributions, *Mathematics and Computer Modelling*, 18, 41-51.
- [6] Murthy, D.N.P, Xie, M. and Jiag, R. (2004), *Weibull Models*, John Wiley & Sons, Inc. Hoboken, New Jersey.
- [7] Talis, G.M. and Light, R. (1968). The Use of Fractional Moments for Estimating the
- [8] Parameters of Mixed Exponential Distribution. *Technometrics*, 10, 161-75.

Mobile Phone Radiation Effects on Human Health

¹, Bhargavi K, ², KE Balachandrudu, ³, Nageswar P

¹Assistant Professor, Palamur University, Mahabubnagar

²Professor & HOD-CSE, PRRMEC, SHABAD.

³Professor & CSE Department, MVS Govt. Degree College, Mahabubnagar

Abstract

A boon for better communication, cell phone usage nonetheless has many health hazards. Various studies indicate that the emissions from a cell phone can be extremely harmful, causing genetic damage, tumors, memory loss, increased blood pressure and weakening of the immune system. The fact that this radiation is invisible, intangible, and enters and leaves our bodies without our knowledge makes it even more intimidating. Global System for Mobile Communications (GSM) and Code Division Multiple Access (CDMA) are the two most prevalent second generation (2G) mobile communication technologies. This paper discusses on the analysis conducted to study the effect of electromagnetic radiation of two mobile phone technologies with different frequencies and power level via experimental works. The experiment was conducted in a laboratory using 10 human volunteers. The period of operation is 10 minutes as the talking time on the phone. Electroencephalogram is used to monitor and capture the brain signals during the experimental analysis for 10 minutes interval. The result shows that mobile phone serving GSM has the larger effect on brain compared to mobile phone serving CDMA.

The effect of mobile phone radiation on human health is the subject of recent interest and study, as a result of the enormous increase in mobile phone usage throughout the world (as of June 2009, there were more than 4.3 billion users worldwide). Mobile phones use electromagnetic in the microwave range. Other digital wireless systems, such as data communication networks, The WHO have classified mobile phone radiation on the IARC scale into Group 2B - possibly carcinogenic. That means that there "could be some risk" of carcinogenicity, so additional research into the long-term, heavy use of mobile phones needs to be conducted. Some national radiation advisory authorities have recommended measures to minimize exposure to their citizens as a precautionary approach. The rapidly evolving mobile phone technology raised public concern about the possibility of associated adverse health effects. The current body of evidence is summarized addressing epidemiological studies, studies investigating adverse biological effects, other biological effects, basic mechanisms and indirect effects. Currently, the balance of evidence from epidemiological studies suggests that there is no association between mobile phone radiation and cancer. This finding is consistent with experimental results. There is some evidence for biological effects, which, however, are not necessarily hazardous for humans. No basic mechanisms of biological effects have been consistently identified yet.

Using a mobile phone while driving a car is significantly associated with a higher risk of vehicle collisions, independently of the use of hands-free kits. Medical equipment or implanted pacemakers may be affected by mobile phone radiation under very specific conditions. Current studies, however are affected by several limitations and do not generally exclude any increased health risk. Further high-quality research is therefore necessary. Furthermore, it is important that the results of scientific research are communicated to the public in a transparent and differentiated way.

Keywords: GSM, CDMA, 2G, Electromagnetic Radiation, EEG, Mobile phone, hand-held Cellular telephone, Microwaves, non-ionizing radiation, radiation risk.

I. INTRODUCTION

Safety is a legitimate concern of the users of wireless equipment, particularly, in regard to possible hazards caused by electromagnetic (EM) fields. There has been growing concern about the possible adverse health effects resulting from exposure to radiofrequency radiations (RFR), such as those from mobile communication devices. Mobile communication is where signal is transferred via electromagnetic wave through radio frequency and microwave signals. This signal produces electromagnetic radiation in the form of thermal radiation that consists of harmful ionizing radiation and harmless non-ionizing radiation. When using mobile phone, electromagnetic wave is transferred to the body which causes health problems especially at the place near ear skull region where they are known to affect the neurons. The radiations interfere with the electrical impulses that two neurons connect each other with.

This can lead to deafness and migraines. People using cell phones are prone to high blood pressure and other symptoms such as hot ears, burning skin, headaches and fatigue. There have been various studies into the connection between mobile phones and memory loss. Because of their smaller heads, thinner skulls and higher tissue conductivity, children may absorb more energy from a given phone than adults. International guidelines on exposure levels to microwave frequency limit the power levels of wireless devices and it is uncommon for wireless devices to exceed the guidelines. But these guidelines only take into account thermal effects, as non-thermal effects have not yet been conclusively demonstrated. This paper shows that the non-thermal radiation affects the human brain. Global System for Mobile Communications or GSM is the world's most popular standard for mobile telephone systems. GSM is a cellular network, which means that mobile phones connect to it by searching for cells in the immediate vicinity.

GSM networks operate in a number of different carrier frequency ranges. GSM networks operate in the 900 MHz or 1800 MHz bands. Where these bands were already allocated, the 850 MHz and 1900 MHz bands are used instead. Regardless of the frequency selected by an operator; it is divided into timeslots for individual phones to use. This allows eight full-rate or sixteen half-rate speech channels per radio frequency. These eight radio timeslots (or eight burst periods) are grouped into a TDMA frame. Half rate channels use alternate frames in the same timeslot. The transmission power in the handset is limited to a maximum of 2 watts in GSM850/900 and 1 watt in GSM1800/1900. Code division multiple access (CDMA) is a channel access method used by various radio communication technologies. One of the basic concepts in data communication is the idea that it allows several transmitters to send information simultaneously over a single communication channel. This allows several users to share a band of frequencies. This concept is called Multiple Access. CDMA employs spread-spectrum technology and a special coding scheme where each transmitter is assigned a code to allow multiple users to be multiplexed over the same physical channel. The transmission power in the handset is limited to a maximum of 6 to 7 mille Watts. Table 1.1 shows the specifications of GSM and CDMA mobile phone technologies, their power level and mode of transmission.

Table 1.1: Specifications of GSM and CDMA [1] [2].

MOBILE TECHNOLOGY	POWER LEVEL	MODE OF TRANSMISSION
GSM	1-2 watt	Burst
CDMA	6-7 mW	Continuous

II. EFFECTS

Many scientific studies have investigated possible health symptoms of mobile phone radiation. These studies are occasionally reviewed by some scientific committees to assess overall risks. A recent assessment was published in 2007 by the European Commission Scientific Committee on Emerging and Newly Identified Health Risks (SCENIHR). It concludes that the three lines of evidence, viz. animal, in vitro, and epidemiological studies, indicate that "exposure to RF fields is unlikely to lead to an increase in cancer in humans". With the way technology has grown, especially in the field of genetic engineering, has led scientists to figure out a way to alter how food is made. This raises concerns and lot of questions regarding the methods they are using. From what possible side effects can occur to the risks it poses to everyone and everything. Unfortunately, there has been limited research and testing done. With that in mind there is not enough information available about the hazards of genetically modified foods. But, what we do know is alarming. Most of the debate surrounding GM foods are focus on the following three issues: 1. Human and environmental safety, 2. Labeling, and 3. Consumer choice. In this section of the paper I will be discussing how genetically modified food can be dangerous on the health of humans. First we will start with the definition of Genetically Modified (GM) is "a special set of technologies that alter the genetic makeup of such living organisms as animals, plants, or bacteria. Bacteria is general term, refers to using living organisms or their components, such as enzymes, to make products that include medicines and vaccines, foods and food ingredients, feeds, and fiber

The unique structure of GM food creates risk to humans which can affect them in the following ways: allergic reactions, toxicity, antibiotic resistance, adverse health side effects and death. It is impossible to foresee the damage inflicted by genetic food; it is a matter of wait and sees what consequences occur because of it. During the genetic modification process, proteins from organisms that have never before been a part of the human food chain are being used and so, GM food may cause allergic reactions. Allergens could be transferred from foods people are allergic to into foods that they think are safe. For example in 1996, Pioneer Hi-Bred International Inc.

III. RADIATION ABSORPTION

Part of the radio waves emitted by a mobile telephone handset is absorbed by the human head. The radio waves emitted by a GSM handset can have a peak power of 2 watts, and a US analogue phone had a maximum transmit power of 3.6 watts. Other digital mobile technologies, such as CDMA2000 and D-AMPS, use lower output power, typically below 1 watt. The maximum power output from a mobile phone is regulated by the mobile phone standard and by the regulatory agencies in each country. In most systems the cell phone and the base station check reception quality and signal strength and the power level is increased or decreased.

IV. ELECTROMAGNETIC RADIATION

Electromagnetic radiation is a form of energy exhibiting wave-like behavior as it travels through space. Electromagnetic radiation has both electric and magnetic field components, which oscillate in phase perpendicular to each other and perpendicular to the direction of energy propagation. Electromagnetic radiation can be classified into ionizing radiation and non-ionizing radiation, based on whether it is capable of ionizing atoms and breaking chemical bonds Non-ionizing radiation is associated with two major potential hazards: electrical and biological. Extremely high power electromagnetic radiation can cause electric currents strong enough to create sparks (electrical arcs) when an induced voltage exceeds the breakdown voltage of the surrounding medium. These sparks can then ignite flammable materials or gases, possibly leading to an explosion.

The biological effect of electromagnetic fields is to cause dielectric heating. Complex biological effects of weaker non-thermal electromagnetic fields also exists, including weak Extremely Low Frequency magnetic fields and modulated Radio Frequency and microwave fields. Magnetic fields induce circulating currents within the human body and strength of these magnetic fields depends directly on the intensity of the impinging magnetic field. These currents cause nerves and muscles to stimulate which in turn affects biological processes. The influence of the weak EM radiations on human can be realized as sequence of events which includes exposure to EM radiations which when absorbed modulates the biological field patterns, accumulation of energy and information into the body fluid, change in the functional activities of cell which finally results into some disease. The number of mobile phone users has increased exponentially recently and it has become an important device in human daily life. Estimates suggest there are around 1.6 billion mobile phone users throughout the world and the numbers are increasing and hence the level of background electromagnetic radiation. Figure 1 shows the effect of electromagnetic radiation on human head.

Figure 1 shows the level of electrical activities generated in brain. The voltage level ranges from blue to red and represents electrical activities ranging from minimum to maximum.

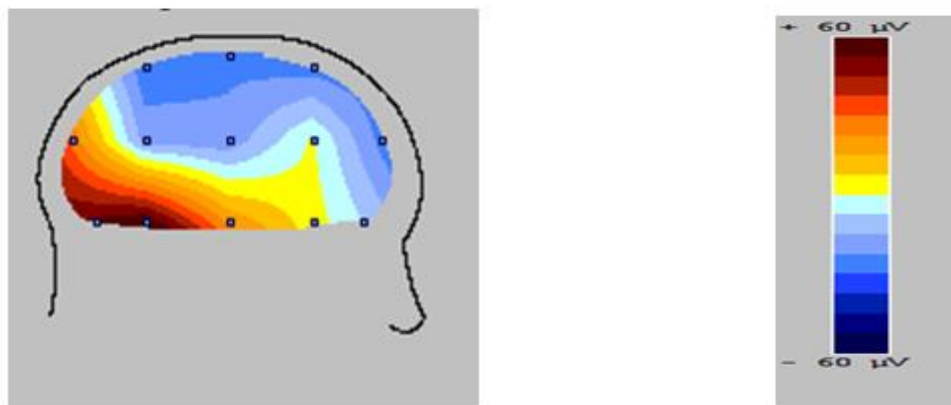


Figure 1: Effect of electromagnetic radiation on human brain

4.1 Harmful Effects of Nuclear Energy on Human Health and the Environment

Over the past decades, scientists, conservationists and environmentalists alike have been searching for clean, renewable sources of energy. As we enter move further into the Common Era, the human population will continue to grow exponentially; therefore, the demand for resources will grow as well. Energy is the primary resource needed to sustain a human population; however, commonly used energy resources, such as coal and oil, have either become scarce, or have caused harmful effects to the human environment. In recent years, scientists have discovered other sources of renewable energy. Wind, sunlight, water, and nuclear chemicals have been deemed the cost effective and harmless to the environment. Extensive research has led to the development of new technologies that utilize sources of renewable energy. However, it has been argued that salvaging nuclear energy has produced unnecessary radioactive waste, and has caused detrimental effects on human health the environment.

Scientists from the National Institutes of Health claim that nuclear energy is produced “when an atom’s nucleus is split into smaller nuclei by a process called fission.” These fissions create a large quantity of energy that can be collected to produce electricity and provide suitable power for advanced technologies such as the atomic bomb and the space craft. The use of nuclear energy has been growing significantly; unfortunately, there are some drawbacks to the use of nuclear energy. The use of nuclear energy has been in debate for a long time. Nuclear waste can be detrimental to human health as well as the environment. Scientists commonly refer nuclear energy with the creation of nuclear weapons. If nuclear elements react in a manner that produces too much energy, the result could be tremendous.

V. ELECTROENCEPHALOGRAM

Electroencephalography (EEG) is the recording of the brain's spontaneous electrical activity produced by the firing of neurons within the brain over a short period of time, usually 20–40 minutes, as recorded from multiple electrodes placed on the scalp. Spontaneous activity is measured on the scalp or on the brain and is called the electroencephalogram. The amplitude of the EEG is about 100 μ V when measured on the scalp, and about 1-2 mV when measured on the surface of the brain. The bandwidth of this signal is from under 1 Hz to about 50 Hz. Spontaneous activity implies that activity goes on continuously in the living individual. Evoked potentials are those components of the EEG that arise in response to a stimulus (which may be electric, auditory, visual, etc.). The information transmitted by nerve is called an action potential. A stimulus must be thousand levels above a threshold level to set an Action potential. Very weak stimuli cause a small local electrical disturbance, but do not produce a transmitted Action potential. As soon as the stimulus strength goes above the threshold, an action potential appears and travels down the nerve. For a human being the amplitude of the Action potential ranges between approximately -60 mV and 10 mV.

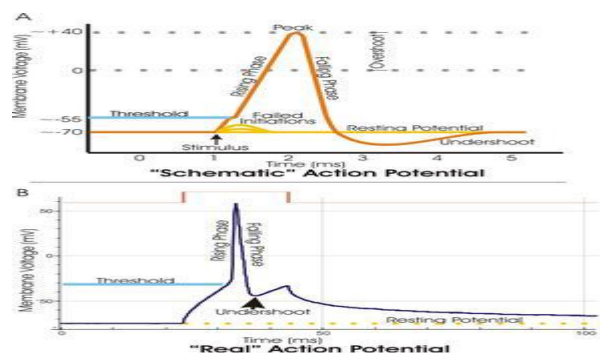
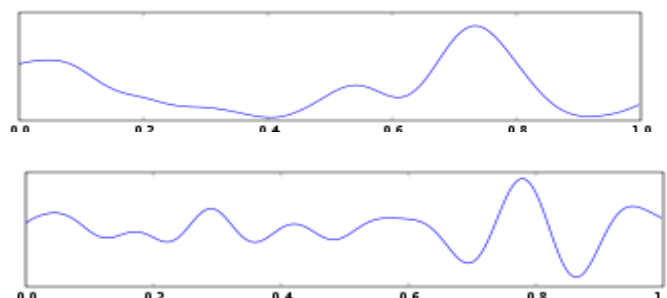


Figure 2.: Action potential generated in brain in response to a stimulus



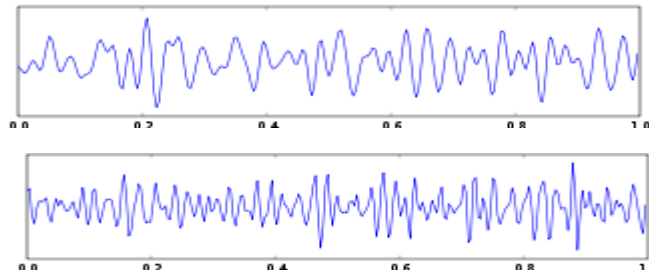


Figure 3: EEG Spectrum (δ , θ , α , β , γ)

Electroencephalogram (EEG) system consists of a number of delicate electrodes, a set of differential amplifiers (one for each channel) followed by filters. The computerized systems allow variable settings, stimulations, and sampling frequency, and some are equipped with simple or advanced signal processing tools for processing the signals. Correct EEG electrode placement is important to ensure proper location of electrodes in relation to cortical areas so that they can be reliably and precisely maintained from individual to individual. Figure 2.4 shows international 10-20 system for placement of electrodes on scalp for recording of electrical activities originating from the brain.

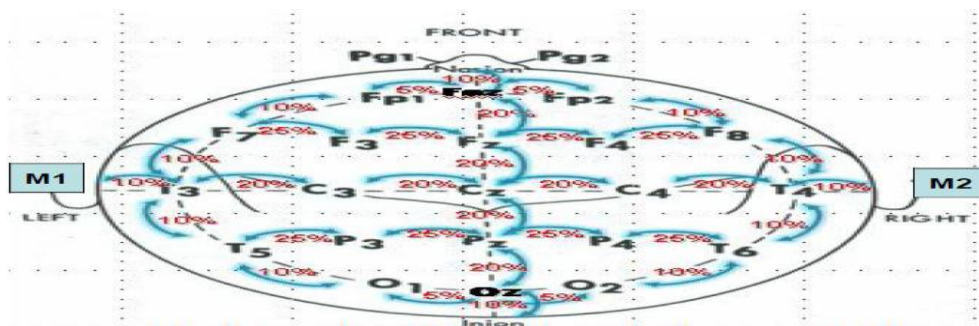


Figure 4 International 10-20 Electrode Placement Systems

VI. METHODOLOGY

In this project electroencephalogram machine is used to capture the brain activity under three conditions, which are, without any radiations in the vicinity of volunteer, while using a GSM operated mobile phone and with a CDMA operated mobile phone as shown in figure 3.1. Data is recorded for duration of 10 minutes and the same experiment is performed with five different volunteers under same conditions.

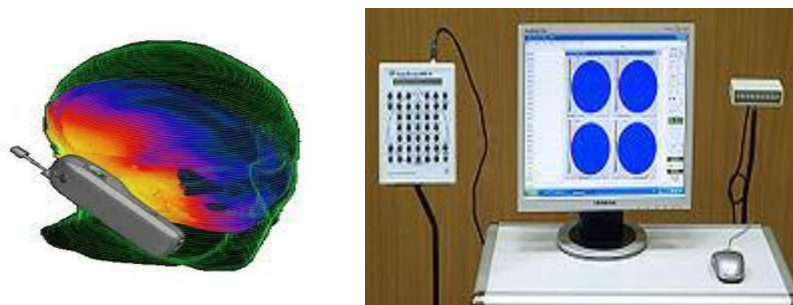


Figure 5: Setup for the Analysis of Electromagnetic Radiations of Mobile Phone

To examine the effect of electromagnetic radiations on human brain digital signal processing techniques are applied. Fast Fourier transform is calculated to obtain the power spectrum density of the acquired electrical signals originated in the brain in response to the stimuli impinged in the form of radiations emitted by the mobile phone. A fast Fourier transform (FFT) is an efficient algorithm to compute the discrete Fourier transform (DFT). An FFT computes the DFT and produces exactly the same result as evaluating the DFT definition directly; the only difference is that an FFT is much faster.

VII. ADVANTAGES AND BARRIERS OF MOBILE PHONE

Vast technology in communication world has made mobile phone important gadgets for 21st century. Now a day it is very rare to see people not having a mobile phone and it shows mobile phone playing an important role in everyday life.

Through mobile phone, communication between people become fast, easier and cheaper especially people in different countries. For business purpose, important event such as meeting and discussion can be held through mobile phone that is much more efficient and cost effective. While in emergency situation, we can easily reach emergency help line or the loved ones through mobile phone. In the past, we need map for travelling but nowadays mobile phone can be use as navigator or to check the weather forecast. Despite all the above, mobile phone still cannot eliminate its disadvantages. Communicate with mobile phone behind steering wheel can cause a serious crime because it's not only dangerous to the driver itself but also people surrounding. In 2009, a report stated that more than 45 countries already banned using mobile phone while driving. Other than that enhanced technology allows the transmission of pictures and videos through mobile phone that is offensive and inappropriate that can create unhealthy atmosphere among youngster. This can lead to immoral ethic and can cause social problem in our society. Mobile phone can also give impact to human health such as cancer, hearing capability, sleeping disorder and blurring vision. Even though all the above matter still not proven scientifically from medical perspective but we cannot ignore the possible consequences. It is crucial that in every aspect mobile phone makes our life easier. However we still cannot ignore the negative impact in our society. Today, mobile phone has become popular with everybody as it is very convenient to use. The advantage of having a mobile phone is you can communicate with your family and your friends no matter where you are. For instance, you can contact your friends easily by calling or sending messages everywhere. It is the main reason why almost all people today choose to own a mobile phone.

Students need the phone for safety and security reasons. From the customer's point of view, it is obvious that mobile phones assist you in business a lot, such as, make schedule of working, surf the internet, and keep in touch with their companies. Moreover, you can relax with mobile phone's applications, for example, play games, listen to music, or chat with your friends. On the other hand, there are certain disadvantages. Using a lot mobile phone can harm your brain, particularly teenager and children who are under 16yearsold. If you constantly use mobile phones, it might may you feel dizzy, or cause blood-brain barrier, or ears problems. In addition, when you use mobile phones while you are driving, can cause a fatal accident. Moreover, "radiations emitted from the phone are dead harmful for the eardrum", and it has been proved by many scientist. It has irritating effect on other people in restaurants, cinema halls, and buses etc. from users shouting down their phone. Owning a mobile phone in your hand can solve many issues and hold most of information around the world. Mobile phone is a good technology which has added quality to our lives. It's up to us how we can maximize its advantages over disadvantages.

Using mobile phones has lots of advantages and disadvantages and most you will be aware of that. Earlier days, when we are out of home or office, we need to search for a public telephone booth to make a phone call, but now, just pick up your mobile phone and dial. I am trying to list the Pros and cons of using a mobile phone in this post. Advantage of using a mobile phone. You are always connected; anybody who knows your mobile number can contact you. If you are travelling out of your territory or to another country, you can use the roaming facility to be connected anywhere and all the time.

You can use features like Text messaging to send messages, receive messages, and send greetings, MMS for sending pictures, get information like news, flight timings and many more features. Now most of the mobile phone service providers has GPRS or EDGE or 3G enabled network. You can using internet anytime and anywhere. If you need to check your mail, you can do that when you are travelling or out of your office. You can reply to important messages or emails from your mobile phone itself. Features like Microsoft Exchange and Blackberry are really great. When you receive an email at your server, you get it pushed to your mobile phone. Latest PDA's, or iPhone are not just mobile phones, you even term it as Mobile Office. I get all my mails pushed to my HTC TyTN II. Even if I am travelling, I am always aware of the important messages and I can respond quickly without entering my office. I use remote desktop with my Pocket PC using wi-fi connections, through which I can access all my office desktop computers from anywhere in the World. There is an excellent service called Legmen, which is something I have been using for long time. Other excellent feature of mobile internet is that you can use internet sharing to using internet on your laptop while you are travelling. Just connect your PDA or pocket pc or your mobile phone with GPRS or EDGE or 3G internet.

7.1 Advantages and Disadvantages of Mobile Phone Effect

As time passes by technology are growing faster and move faster. The most important and common part of technology in our life is mobile phone technology. We bring mobile phone with us in everywhere that we go and use it on a daily basis. It is being the part and parcel of our daily life. Mobile phones have been around for quite some time, but as time goes on, mobile phones continue to gain many features. A mobile phone started out as a simple device that had only numbers, and most people used them for emergencies only. Nowadays, cell phones have many features such as phone calls, text messaging, taking pictures, accessing the web, using calculator etc as many accessories. People become addicted to cell phones because they are getting many facilities by using it. For example whenever they go outside they can take the phone with them because of its size, networking range, a full charge battery, easy connection etc. There is no doubt about the benefits of mobile phones. Mobile phones have so many advantages but there are some disadvantages too. It has become a vital element for every person but nowadays it has also become an addiction to the young generation. If we talk about Bangladesh, nine out of ten young people in the town area, have their own mobile phone. They use it for various purposes. Their attraction to mobile phones is increasing day by day. Medical science says that the radiation of mobile phones is too bad for human health.

In 1995 mobile phones were introduced to Bangladeshi people. The first mobile service provider company was City Cell. Then Grameenphone, Aktel, Banglalink, Teletalk, and Warid which is being named as Airtel an Indian telecom company who has also started their business in Bangladesh. In the arena of communication mobile has become the latest fashion and also the most essential means of communication. These mobile phones let us enjoy all the comforts within a single device.

VIII. RESULTS AND DISCUSSION

The result is shown in Table 2 and Figure 4. It shows that GSM operated phones have the highest effect on brain activity as compared to a CDMA operated mobile phone.

Table 2: Average PSD Values of Four Channels (CH1, CH2, CH3, and CH4) of Montage For Three Conditions Of Recording.

	CH1	CH2	CH3	CH4
GSM	13655	13914	20291	94619
CDMA	6482	3119	4361	4711
IDLE	3009	626	2512	3399

The result shows power spectral density values for the three conditions of experiment that includes, idle with no radiation in vicinity, with GSM phone and with a CDMA phone. It can be seen from the table that PSD values with phone serving GSM technology has the highest values whereas when no phone is present that is when there is no radiation in the vicinity of the subject, has the least values and values for the phone serving CDMA lies between GSM and Idle condition.

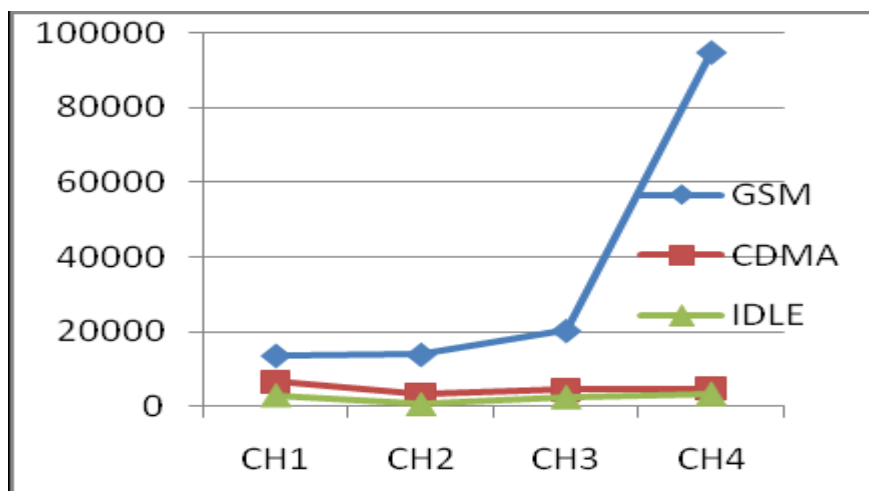


Figure 6: Plot of Average Psd Values of Four Channels of Montage

Analyses shows that mobile radiations effect human brain and GSM operated mobile phones has the higher effect on brain activity as compared to CDMA operated mobile phones. Globalization is the new mantra. In this age, it is very difficult not to have technology. But as shown in this study, with every technology invented to facilitate human beings, there come certain hazards. The only way to beat these negative aspects of new technologies is again, a new but better technology. Electromagnetic radiation is everywhere. More and more wireless communication services are expected, so is the artificial electromagnetic radiation. It seems that there is no way to reverse this trend. Scientists and engineers must develop better and safer wireless systems and devices. Smaller cell size, better base station antennas and other more advanced technologies will allow future cell phones to radiate much lower power and make technology a real boon.

REFERENCES

- [1] Vijay Kr Garg, IS-95 CDMA and cdma2000: Cellular/pcs system implementation.
- [2] Wikipedia. [Online] available at: en.wikipedia.org/wiki/Electromagnetic_radiation
- [3] Binhi, Vladimir N; Repiev, A & Edelev, (2002). *Magneto biology: underlying physical problems*. San Diego: Academic Press. pp. 1–16. [4] Delgado JM, Leal J, Monteagudo JL, Gracia MG (1982). "Embryological changes induced by Weak, extremely low frequency electromagnetic fields". *Journal of Anatomy* 134.pg: 533–51.
- [5] Harland JD, Liburdy RP (1997). "Environmental magnetic fields inhibit the ant proliferative action of tamoxifen and melatonin in a human breast cancer cell line". *Bioelectromagnetics* 18, pg: 555– 62.
- [6] Aalto S, Haarala C, Brück A, Sipilä H, Hämäläinen H, Rinne JO (July 2006). "Mobile phone affects cerebral blood flow in humans". *Journal of Cerebral Blood Flow and Metabolism*.pg: 885–90.
- [7] 18th Int. Crimean Conference "Microwave Telecommunication Technology" (2008). 8-12 September, Sevastopol, Crimea, Ukraine.
- [8] Wikipedia. Mobile Phone [Online]. Available at: http://en.wikipedia.org/wiki/Mobile_phone.
- [9] Saeid Sanei, J.A. Chambers, Centre of Digital Signal Processing, Cardiff Uuniversity,UK
- [10] [Online]. Available: mildpdf.com/result-standard-international-10-20-electrode-placement-pdf.html

Gsm Based Controlled Switching Circuit Between Supply Mains and Captive Power Plant

¹Mr.S.Vimalraj, ²Gausalya.R.B, ³Samyuktha.V, ⁴Shanmuga Priya, ⁵M,Minuramya.B

¹Assistant Professor, ^{2,3,4}UG Final Year
^{1,2,3,4}Sri Krishna College of Technology

Abstract

In the present scenario, the requirement of surplus electrical energy in case of power failure is met by generators. In this paper, the remote management of the generator done by a specific SMS with an authenticated mobile phone is elucidated. This system is extremely handy at places where we have to control the switching of the machine but no wired connection to that place is available. To implement this, a GSM modem is connected to a programmed microcontroller. Commands were used for controlling the functionality of GSM modem in both transmitter and receiver design, operating at 900 or 1800MHZ band. The GSM technology also enables the user to know about the various parameters like temperature of the coolant, pressure of lubricant, fuel level, speed of the generator and to control the machine. This system is low cost, secure, ubiquitously accessible, remotely controlled solution for automation of power plant. The extensive capabilities of this system are what make it so interesting.

Index Terms - Short Message Service (SMS), Global Systems for Mobile Communication (GSM), Radio frequency (RF), Cranking, diesel plant.

FIELD OF CONTRIVE: This conception relates to a communication system and to a method for remotely regulating and switching of the captive diesel plant.

I. INTRODUCTION

Real-time point-to-point data reporting architecture is useful for remote surveillance and control, if communication network can be convenient to access. In the new age of technology, mobile phone redefines communication. The worldwide trend for wireless communication has elevated into wide band data instead of voice only. Sending written text messages is very popular among mobile phone users. We have used the very concept to control the captive diesel plant from a remote area. Remotely the user can establish effective monitor and control via the mobile phone set by sending commands in the form of SMS. This system provides ideal solution to the problems caused in situations when a wired connection between a remote appliance/device and the control unit might not be feasible.

II. SYSTEM DESCRIPTION

The system has two parts, namely; hardware and software. The hardware architecture consists of a stand-alone embedded system that is based on PIC microcontroller, a GSM handset with GSM Modem and a driver circuit. The GSM modem provides the communication by means of SMS messages. The SMS message consists of commands to be executed. The format of the message is predefined. The SMS message is sent to the GSM modem via the GSM public networks as a text message with a definite predefined format. Once the GSM modem receives negative signal from the EB supply, it sends the SMS to the user consisting of non-availability of power supply, fuel level, temperature of the coolant, etc..

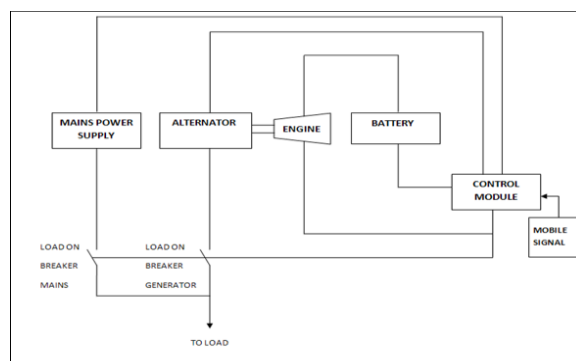


Fig:1. Block Diagram of the System

The user can decide whether to switch the generator on/off and issue the command. Based on the message, the commands sent will be extracted and executed by the microcontroller. In this case, if the EB power supply resumes, again the user is made to know the status of on-site. Even then the user can decide about the switching. If the command is successfully executed, an intimation will be sent to the user. Thus, the communication is made bi-directional. The detailed description of individual modules in the system are as follows.

2.1. CIRCUIT CHANGE-OVER UNIT

This unit adjudicates the take over of the load during switching conditions. The functionality of this unit relies upon the command/control signal received over the SMS via GSM.

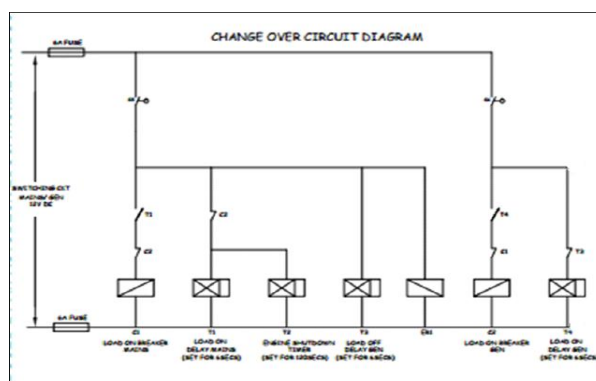


Fig:2. Change over circuit Diagram

To ensure safer switching between the plant and mains supply, the electrical inter-locking amidst the two circuit breakers is needed. It is also to be noted that some time delay will be there as soon as the plant gets switched on for voltage build-up, which is known as a dark time.

2.2. ENGINE CRANKING CONTROL

Whenever the plant has to be initiated, the engine needs to be cranked. i.e., the fuel (diesel) has to be supplied to the generator and the dc supply is to be given to the auxillary contactor resulting in the take over of the load by generator.

2.3. FAULT ISOLATION UNIT

This block is concerned for the safety operation of the system. This unit enables the monitoring of various parameters like fuel level, Lubricant oil pressure, High coolant temperature, Engine over speed, Engine belt failure and Momentary fault. The input from different sensors are feed to micro-controller and processed to operate respective task autonomously. The above mentioned conditions can also be received in the authenticated mobile.



Fig:3.Part of the Control Module

2.4.GSM IMPLEMENTATION

2.5 AUTHENTICATED MOBILE

Cellular phone containing SIM (Subscriber’s Identifying Module) card has a specific number through which communication takes place. The mode of communication is wireless and mechanism works on the GSM (Global System for Mobile communication) technology. Here, the communication is made bi- directional where the user transmits and also receives instructions to and from the system in the form of SMS.

2.6 GSM TRANSMITTER

This GSM transmitter handset is used to send the status signal regarding the availability of supply, status of the generator, fuel and temperature details to the authenticated end user. While considering the remote area, this transmitter is used to send the control signal to the on-site plant whether to on/off.

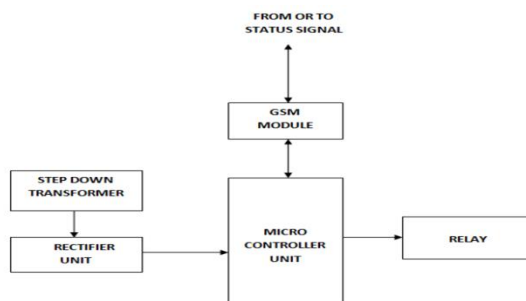


Fig:4. GSM Block Diagram

2.7 GSM RECEIVER

This GSM receiver handset is used to receive the SMS sent by the user and then to transmit an acknowledgement or status to the user’s mobile. The receiver handset has to be equipped with a Modem and a valid SIM card. This is the main module of the system. On receipt of the SMS message, text words are checked with predetermined format which includes desired device ON/OFF commands. The microcontroller then processes the command and sends the appropriate controlling signal to the switching module.



Fig:5.Gsm Technology

III. TECHNOLOGY CONSIDERATIONS

The considerations for this system are:

- [1] Cellular Networks: The widely available networks are based on GSM. This network provides wide area coverage and can be utilized more cost-effective. In addition the power of the GSM mobiles is closely controlled so that the battery of the mobile is conserved, and also the levels of interference are reduced and performance of the base station is not compromised by high power local mobiles.
- [2] Communication Protocols: The available communication protocol that we have used is SMS. The SMS is the most efficient because this project requires a cellular communication and limited data to be sent. SMS Messages can be sent and read at any time. SMS Message can be sent to an offline Mobile Phone.
- [3] I/O interfaces between microcontroller and devices: Serial I/O is considered as options for connection between the GSM receiver and the microcontroller. Using the microcontroller, a control circuit will be implemented to control the electrical appliances.
- [4] Choice of controllers: The PIC micro controller is being used because it is popular with both industrial developers and educationalists due to their low cost, wide availability, large user base, extensive collection of application notes, availability of low cost or free development tools, and serial programming (and re-programming with flash memory) capability. The Harvard architecture of PIC in which instructions and data come from separate sources—simplifies timing and microcircuit design greatly, and this benefits clock speed, price, and power consumption.

IV. ALGORITHM

Once the GSM modem is initiated, the status signal of the EB mains supply is continuously monitored by sensing unit present in the control module. If the EB supply is found to be healthy, then the load is being supplied by the mains supply. In case of weaker EB supply, the status signal is sent to the user that there is no power supply from Electricity Board. If the necessity for the user regarding power requirement arises, then, at that instant, the authenticated user sends message to switch on the generator set

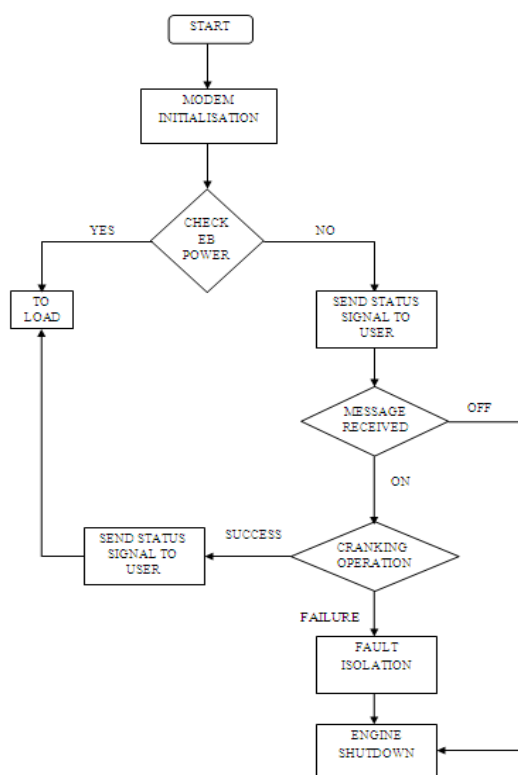


Fig:6. System Operation Flow Diagram

. After the reception of the required message, control goes to the cranking unit initiating the cranking operation. The cranking process enables the engine to start so as the generator starts generating the power. The success of the cranking operation results in sending message regarding the status signal to the user and hence the load is taken-over by the generator.

If the cranking process fails, the control goes to the fault isolation circuit. In this circuit, based upon the various types of faults the corresponding relays are closed. Once the faults are resolved the fuel pump of the generator is opened and cranking process initiates, as a result of which the load is undertaken by the generator. In case of not clearing the faults in the respective unit, the engine gets shutdown. If the mains supply resumes, the user receives the status signal accordingly and hence the user sends message to the control module to switch-off the generator. As the control module receives the off signal, the generator breaker is switched to mains breaker. Hence the load is taken over by the EB supply.

V. ASSUMPTIONS

Certain assumptions have to be made in order to implement our project. The list of assumptions for our project is:

- The user and control unit will establish communication via GSM
- The cell phone and service provider chosen will support text messaging service.
- The user is familiar with the text messaging program on their cell phone.
- All service charges (standard messaging rates) from the service provider apply.
- The controlled appliances can and will have to have an electrical interface in order to be controlled by the microcontroller.

VI. EXPECTED OUTPUT

The outcome of the system would be bidirectional reception of signals to the authenticated mobile and control module to control the generator in switching. Also monitoring of the diesel generator can be done by notifications sent to the user about the various parameters like temperature of the coolant, pressure of lubricant, fuel level, speed of the generator through GSM technology. Such monitoring ensures the proper functioning of generator

VII. ENHANCEMENT

- This system is a small implication of our concept in automating and monitoring a system.
- The future implications of the project are very great considering the amount of time and resources it saves.
- The project we have undertaken can be used as a reference or as a base for realizing a scheme to be implemented in other projects.
- Our project is been made with an idea, which gives the first level of approach for the automation.

VIII. LIMITATIONS

The proposed idea has certain limitations and a list of such is mentioned below:

- The receiver must reside in a location where a signal with sufficient strength can be received from a cellular phone network.
- Operation of the controlling unit is only possible through a cell phone with SMS messaging capabilities.
- The Controlling unit must be able to receive and decode SMS messages.

IX. CONCLUSION

The hunch delineated in this paper is immense in the ever changing technological world. It allows a greater degree of freedom to an individual to sway via GSM. In particular the suggested system will be a powerful, flexible and secure tool that will offer this service at any time, and from anywhere with the constraints of the technologies being applied. However, the GSM system pose some potential threats. But the suggested system can be used as a reference or as a base for realizing a scheme to be implemented in other projects of greater level. Further it is hoped that it will serve as a basis for further study of industrial power management strategies. The end product will have a simplistic design making it easier for the users to interact with.

REFERENCES

- [1] GSM Based Device ON-OFF Control Especially Designed For Agricultural Needs http://www.iecehtn.org/htn/index.php/GSM_Based_Device_Control. International Journal of Computer Trends and Technology- March to April Issue 2011 ISSN:2231-2803 - 1 – IJCTT
- [2] Telephone Operated Remote Control By Sayed Taher Zewari, Ahmed Alnajadah, Hamed Alsaleh- George Mason University Fairfax, Virginia ,May 2003.
- [3] Data signaling functions for a cellular mobile telephone system", V.Hachenburg, B. Holm and J. Smith, IEEE Trans Vehicular Technology, volume 26, #1 p. 82 (1977).
- [4] Multiple Unit GSM Controlled Devices. <http://www.ijctjournal.org/volume-1/issue-1/ijctjournal-v1i1p17.pdf>
- [5] A Cellular Phone Based Home / Office Controller & Alarm System H.Haldun GÖKTAŞ, Nihat DALDAL Gazi University Technical Education Faculty, 06500, Besevler, Ankara, TURKEY.
- [6] Control of Remote Domestic System Using DTMF by Tuljappa M Ladwa, Sanjay M Ladwa, R Sudharshan Kaarthik, Alok Ranjan Dhara, Nayan Rourkela.

Review: Soft Computing Techniques (Data-Mining) On Intrusion Detection

¹Shilpa Batra , ²Pankaj Kumar, ³Sapna Sinha

^{1,2,3} Amity School of Engineering and Technology, Amity University, Noida, U.P.

Abstract:

With the tremendous growth of various web applications and network based services, network security has become an alarming issue in the vicinity of IT engineers. As the numerous amazing services come to the clients, so does the extensive growth of hackers on the backend. Intrusion poses a serious security risk in the networking environment. Too often, intrusion arises havoc in LANs and heavy loss of time and cost of repairing them. It is said that “prevention is better than cure”, so intrusion prevention systems (IPS) and the intrusion detection system (IDS) are used. In addition to the well established intrusion prevention schemes like encryption, client authorization and authentication, IDS can be viewed as a safety belt or fence for network framework. As, the use of interconnected networks have become common, so to have world-wide reports of vulnerabilities and intrusive attacks on systems have increased. CERT noted that between 2000 and 2006 over 26,000 distinct vulnerabilities were reported. An intrusion, which is the set of actions that compromise the integrity, confidentiality, or availability of any resource, and generally exploits one or more bottlenecks of the network. In this paper, we describe various data mining approaches applied on IDS that can be used to handle various network attacks and their comparative analysis.

Keywords: IDS (intrusion detection system), DOS (denial of service), U2R (user to root), R2L (remote to local), ANN (artificial neural network), MLP (multi-layer perception), GA (genetic

I. INTRODUCTION

In the recent study, it is being explored that the size of the data has increased worldwide. The need for the larger and larger database has increased. Numerous social networking sites namely Facebook, Twitter etc. use server and databases which stores information of users that are confidential. The latest trend has evoked the use of net banking in which highly confidential data of user is transacted[2]. As the confidential data has grown on network, network security has become more vital. Despite of using prevention techniques like firewalls and secure architecture screening, IDS plays a pivotal role. IDS acts as a burglar or theft alarm which rings whenever a thief tries to steal or hack any data over network. It is used to inform the SSO (Site Security Officer) to defend and take appropriate action in response to the attack; .IDS strengthens the perimeter of the laid network. There are various kinds of attackers but generally can be classified as two:- one who tries to hack the password and steal the user information and the other who exploits its privileges at user level and want to play with the system resources like files, directories and configuration etc.

Network attacks could be:-

- [1] DOS (Denial of service):- It aims at limiting the server to provide a particular service to its clients by flooding approach. The general method to do this is ping of death, SYN flags, overloading the target machine.
- [2] Probing: - It aims to achieve the computer configuration over network. This can be done by port scanning and port sweeping.
- [3] User to Root (U2R) attack: - Its motto is to access the administrator or super user privileges from a given user on which the attacker has previously been given the user level access.
- [4] Remote to Local (R2L) attack: - It aims to access the machine by a user which he cannot access by sending message packets to it in order to expose its vulnerabilities. Example guest passwords send mail etc. ADAM (AUDIT DATA ANALYSIS AND MINING) is an intrusion detection built to detect attacks on network level. It uses training and actions mechanism. It classifies the cluster of attacks and alarms on abnormal behaviour of the network.

There are basically two major principles of intrusion detection namely anomaly detection and signature based detection. The former method focuses on analysing the unexpected or abnormal behaviour of the system attributes like deviated CPU cycles, abnormal output to a service requested by a client etc. The issue with using this approach is that, it is difficult to compute the granular attribute characteristics; which are actually time consuming and high rate of false alarm as it is difficult to built tools for such typical and to the depth analysis[6].The latter focuses on determining some predefined signatures or footprints of the attackers who have previously attempt to hack the system. These signatures are stored in KDD (knowledge databases). It is used by expert systems to analyse the previously experienced attacks; but the problem is that it is difficult to keep the records of the type of attacks, the attackers and the issue of storing and maintaining such a huge database of footprints up to date.

Now, we come to the issue of how to implement IDS[5], .the pivotal issue is what to observe while detecting the intrusion and that the source that gives rise to the attack. For this purpose, we take traces to analyse through network log files or also called audits.Moving on to the nature of the source or stimulus of attack, we come to how to observe the stimulus. For observing the point of view, we will use the security log audits, but it is actually a cumbersome and frustrating task. As understanding logs that we need to observe are not actually getting all the necessary traffic that we need, but a flood of network traffic that might be unusable to us. Furthermore, it is not yet concluded that what type of traffic is useful in what kind of circumstances[8][10].This brings us to the results of security logging-what can we observe or what we suspect to observe. Precisely committing the log files is the aim. Henceforth, we need to govern or built rules to classify the data packets in the routes to make IDS successful and effective. As the detector is used to sense the attack occurring in IDS, we need to make an effective decision making IDS. The detector uses various approaches to react to an attack and in the light of this, the main motivation for taking in depth approach to different kinds of detectors that has been deployed on different networking environments.In this paper, we will cover various data mining approaches that underlie the detector principles and mechanisms to react to the different kind of attacks and network layouts.

II. SYSTEM ATTRIBUTES AFFECTING IDS

These are the features that do not affect the detecting principles directly[13]. This divides the cluster of systems based on their approaches to detecting the intrusion in audit data. Following are the vital points:-

- [1] Detection time: - It covers two main genres, first: those attackers who try to attack in real time and these need online data analysis and mining them. Second: It processes data with some delay that is non-real time or offline. Although the online analysis can be time delaying to some extent but its computation is much faster than offline.
- [2] Stimulus of attack: - The source of attack is considered here. The data for analysis can be taken form two resources: network logs and host logs. The network logs are implemented in NIDS (Network intrusion detection systems) and host logs are used in HIDS (host based intrusion detection).The host log contains kernel logs, application program logs etc. The network log contains the filtered traffic form equipments like routers and firewalls.
- [3] Depth of data processing: - The mechanism of data processing could be either continuous data processing or batch processing. In continuous processing all the data traffic running is processed together. While in batch processing, the data is taken in lumps to process. But these terms could be used interchangeably in real time or online data analysis in IDS.
- [4] Reaction to the detected attack: - There are two main types of responses to the detected attacks by IDS namely passive and active reactions or response. The passive system responds by notifying on the attack and do not come to remove the affected area of intrusion directly. While the active system comes to eradicate the effect to attack and can be further classified into two categories: firstly, that modifies the state of the attacked system in order to fight back example: terminating the network sessions. Secondly, in response to a detected attack, it attacks back the hacker in order to remove him from his platform.

III. A CLOSER VIEW TO THE DATA MINING APPROACHES IN IDS

3.1 Fuzzy Logic:

It is a form of many valued logic or probabilistic logic that deals with reasoning that is either in true or false form. They range in the degree of 0 or 1. Fuzzy logic is applicable to fuzzy set theory which defines operator on fuzzy set. IF-THEN rules are constructed

The syntax is: IF variable IS event THEN respond The AND, OR & NOT are the Boolean logical operations used. When combined with minimum maximum and compliment, they are called Zadeh operators. Fuzzy relations are stored in the form of relational database. The first fuzzy relation was shown in Maria Zemankoras dissertation. By combining fuzzy logic with data mining the problem of sharp boundary and false positive errors is overcome. This approach can be used with both anomaly as well as signature based IDS. It can be implemented in real time environment. Classification of parameters like SYN flags, FIN flags and RST Flags in TCP headers can be done using fuzzy logic. AN intelligent intrusion detection model integrates fuzzy logic with data mining in two ways; that is fuzzy association rule and fuzzy frequency episode. It integrates both the network level and machine level information. The fuzzy logic represents the commonly found patterns and trends in association rules[1]. For instance occurrence of event X in Y. A variable S (support) tells how often X comes in Y and C (confidence) tells how often Y is associated with X. For example, say sample fuzzy is:

$$\{RN=LOW, SN=LOW\} \rightarrow \{FN=LOW\}$$

C=0.67 & S=0.45, this can be interpreted as SN, FN & RN occurred in 45% of the training sets and the probability of FN occurring at the same time as SN and RN is 67%. In order to implement data mining in anomaly detection approach, mine a set of fuzzy association rules from data set with no anomalies, then given a new data, mine fuzzy association rules on this and compare the similarities of the set of rules mined from new data and normal data. Given a fuzzy episode R: $\{e_1, e_2, \dots, e_{k-1}\} \rightarrow \{e_k\}$, C, S, w; If $\{e_1, e_2, \dots, e_{k-1}\}$ has occurred in the given sequence, then $\{e_k\}$ could be predicted as next to occur event. If the next event does not match any prediction from the rule set then the IDS will alarm it as anomaly. Percentage of anomaly detected can be calculated by the number of anomalies and the number of events occurring. It can be written as: Percentage anomaly = number of anomalies / number of events. Features selected for IP spoofing and port scanning attacks can be source IP FYN, data size and port number and source IP destination IP, source port and data size respectively.

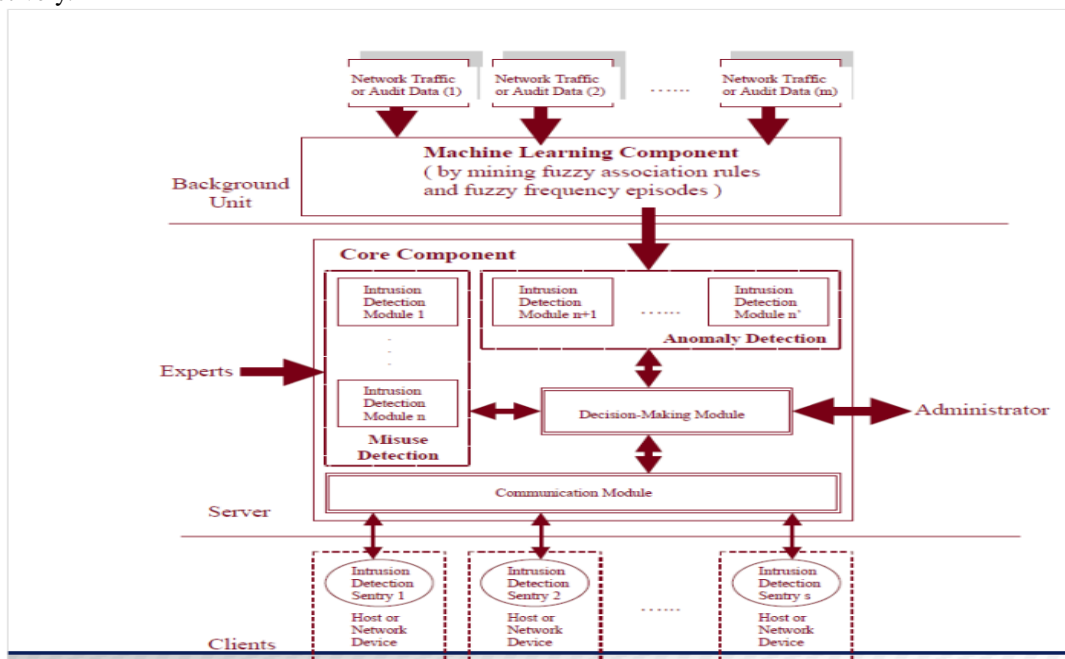


Fig: 1 depicts the implementation of fuzzy rule set and episodes over IDS[1]

3.2 Graph based approach (GrA) :

The graph based approach was developed at UC Davis computer lab that collects data about host and network traffic. Then it aggregates information into activity graphs; that deals with the causal relationship of network activities. The analysis could be done using dedicated hardware like RMON/RMONII. This machine is quick enough to cope up with the speed of network. For the implementation of the graphical data mining approach, we need a supervised network in which modules like packet sniffing, traffic matrix construction, graph clustering, event generation and visualisation are set up. In the graph, the computers in the network layout are represented by node and communication among them is represented by subsequent edges weighted by the amount of data exchanged. Various graph clustering algorithm are then implemented.

Assume we have a graph G with V vertices and E edges then[3]:

G= {V, E} having C_n clusters can be considered as

$$C_1 = (V_1, V_2, V_3)$$

$$C_2 = (V_4, V_5)$$

$$\vdots$$

$$\vdots$$

$$\vdots$$

$$C_n = (V_{n-1}, V_n)$$

Then, $G = C_1 \cup C_2 \cup C_3 \cup C_4 \dots C_n$
 Such that $C_i \cap C_j = \Phi$

There are various algorithms applied for graph computation namely: hierarchal and non-hierarchal algorithms. The former creates the hierarchy of clusters by subdivision of clusters or combining them. In an agglomerative algorithm, the entire graph forms initially a single cluster which is then subdivided. The latter divides the graph into clusters within one step. Graph visualisation of network traffic is a vital task for planning and managing large network. The network layout is done generally in a geographical way. We cluster the nodes in a structure and this helps to analyse the modification of the network behaviour. A special benefit of visualisation is it is capable of diagnosing modifications in the network structure by building traffic matrices. Changes in network topology, network devices are the reasons for the modifications. Font and colour of nodes indicate changes in their membership to different clusters. It is easy to detect the changes in computer behaviour and information on nodes. The problem with IDS is the rate of false positive and false negative alarms. Therefore, visualization helps in discovering false positive efficiently and reducing the number of false negative. Graph drawing is the task of drawing a given graph on the platform. The tool first places the clusters on the plane. The clusters added form a new graph; this visualisation helps the security manager to build his own opinion on messages from event generation. For event generation, our system collects online network traffic and implements clustering algorithms. Attributes like number of communicating nodes, found clusters, minima, maxima, out degree and in degree of graph; sink and source node in a cluster; the internal nodes in a cluster and external edges in a cluster are collected. Modifications in a graph could be due to addition of new nodes, lost nodes, splitting of clusters and merging of clusters. CLIQUE and PROCLUS are the methods applied for dimension growth sub-space clustering and dimension reduction, sub space method respectively.

3.3 Neural Networks :

With the rapid expansion of computer networks security has become a very critical issue for computer networks. Various soft computing based methods are being implemented for the development of IDS. A multi-layer training technique is used to evolve a new data domain and offline analysis. Different neural network structure are analysed with regards to the hidden layers. Soft computing is a general term used in context of uncertainty and includes fuzzy logic, AI, Neural networks and genetic algorithms. The idea behind this is to evolve a new and hidden connection records and generalise them. The neural network approach is appropriate for offline data analysis. The training procedure of neural networks is done using validation methods. A non-real time IDS is implemented using multilayer perception (MLP) model. ANN (Artificial Neural Network) is based upon human nervous system processing. It comprises of large number of inter connected processing units called neurons co-ordinating with each other to solve a particular problem. Each processing unit acts upon an activation function. The output of each subsequent layer acts as an input to the next layer. The mechanism of working in ANN is; feed the uppermost layer with input domain and check how closely the actual output for a specific input matches the desired output. Change the weights attached to each layer accordingly. If an unknown input is given to the ANN it presents the output as irrelevant that time but corresponds to that input set.

In IDS, the ANN is implemented by training neurons with the sequence of log audit files and sequence of commands. For the first time when the ANN is fed with current commands it is compared with past W commands (W is the size of window command under examination). Once the ANN is trained with user profile and put into action, it can discover the user behaviour deviation. The next time it is logged in. It is suitable to analyse a small network of computers ranging from 10-15 and analyse a single user command for the whole day. There are numerous commands which describe the user behaviour. Neural networks in the past study were implemented in the UNIX lab for detecting attack specific keywords for host based attacks. A neural network produces two kinds of output in multilayer perception namely normal & abnormal. The output generated is in the form of binary digits 0&1. However, neural network is not capable of identifying attack type. During training phase the neural networks are fed and forward with inputs that are class of network connections and audit logs. The neural network accepts the input processes it through its layered architecture and tries to output the corresponding result. If the output is deviated the neural network gains the knowledge of abnormality and alarms about the attack. In a recent study, data sets contain each event combined with 41 features which were grouped as connection sets, properties of connections etc.

For example, cluster 1 contains the commands used in the connections like file creation, number of root access; cluster 2 includes connection specifications like protocol type service type, duration, number of bytes etc. During investigation it turned out that features like urgent, number of failed logins, is_host_login etc. where playing no role in ID. However, making the data set time consuming and complicated. Therefore, these were removed later. The different possible values were allotted to the rest of the features like TCP=1, UDP=2 etc. The ranges of attributes were different and incompatible and therefore their values were normalised by binary mapping. ANN is efficient to solve a multiclass problem. A binary set approach is used to denote the attack type to feed the neural networks. For example, if an attack is given a value of [0 1 1] and the output generated is [1 1 0]. It is considered as irrelevant. A three layer Neural Network means it has two hidden layers. The uppermost layer is considered as input or buffer layer because no processing task takes place. The cost of neural networks increases as the number of hidden layer increases. But by increasing the number of layers the efficient approximation and accuracy of anomaly detection increases. If we use the neural network of two layers the training cost and time are less. Various tools are used in MATLAB that allows the user to specify the number of layers and activation functions to the layers of ANN[4].

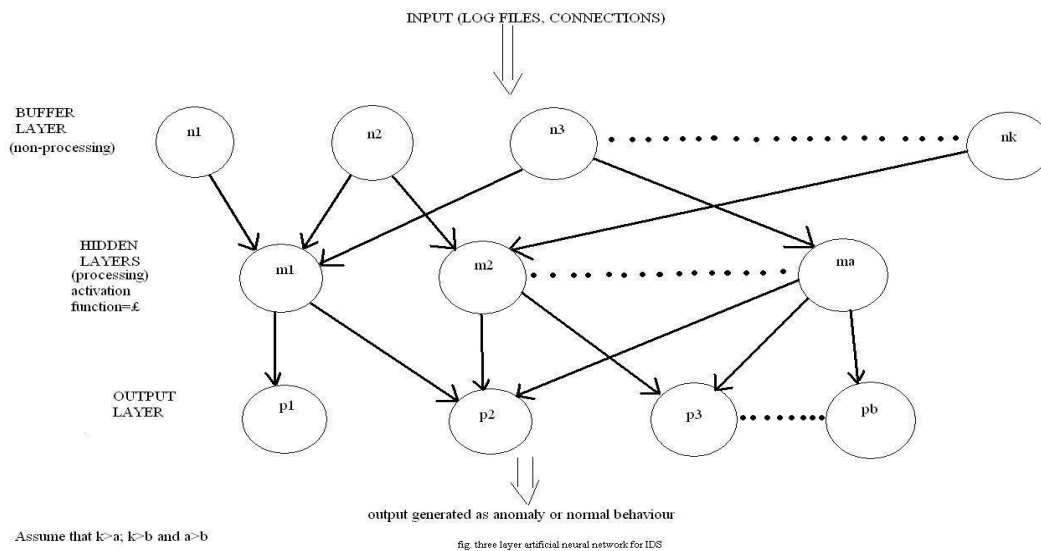


Fig: 2. Working of Neural Network

3.4 Genetic algorithm (GA):

Genetic algorithm is one of the soft computing skills based on the mechanism of evolution and natural selection. The input data set is a set of chromosomes and evolves the next generation of chromosomes using selection, crossover and mutation. The input data set is randomly selected. The problem to be solved is divided into desired input domain. The chromosomes selected are converted into bits, characters or numbers. They are positioned as genes. The set of chromosomes are considered as population. An evaluation function is used to calculate fitness or goodness of each chromosome[7]. Two basic operators are used for reproduction that is crossover and mutation. The best individual chromosome is finally selected for optimization criteria.

The rules used in GA are represented by:

IF {condition} THEN {action};

The conditions to detect the intrusion is generally the current network traffic or connection details like source IP address, destination IP address, port numbers (like TCP, UDP), duration of the connection, protocols used. The action taken in accordance to the security policies are followed by the organisation like alerting the admin by alarm or terminating a connection.

Example IF (the connection having the properties)

Source IP=125.168.90.01;

Destination IP=145.165.10.90;

Destination port=21;

Time=0.2;

THEN (alert by alarming)

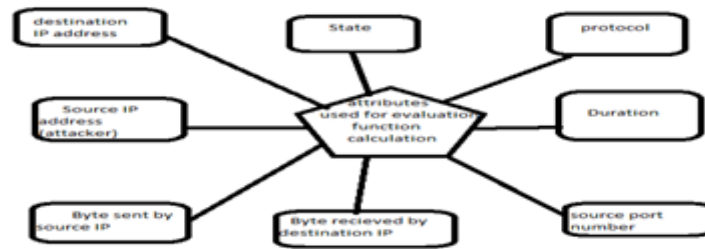


Fig.3. Attribute of Genetic Algorithm

The parameters in GA are the evaluation functions which determine whether the connection matches the pre-defined data set and multiply the weights of the field. The matched value ranges from 0 to 1.

Outcome=summation (matched values*weights attached);

Destination IP address is the target of the attack while the source IP is the originator (stimulus) of intrusion. The destination port number indicates the application of the target system to be attacked like FTP, DNS etc.

The suspicious level is the threshold that indicates the extent to which two network connections are considered “matched”.

Ω = (outcome-suspicious level);

If a mismatch occurs, the penalty value is computed. The ranking in the equation determines the level of ease of identifying an intrusion represented as:

Penalty= (Ω * ranking / 100);

The fitness of a chromosome is computed as:

Fitness=1 – penalty

The Fitness value ranges from 0 to 1.

The mechanism for GA can be followed as:-

Pass 1: Gather the input set and initialise the population in any order (arbitrarily)

Pass 2: Do the summation of the records

Pass 3: the new population of chromosomes are produced.

Pass 4: Calculate the result by implementing Crossover operator to the Chromosome

Pass 5: Apply Mutation operator to the chromosome

Pass 6: Evaluate Fitness $f(x) = f(x) / f(\text{sum})$

Where, $f(x)$ is the fitness of individual x

and f is the sum of fitness of all individuals in a pop

Pass 7: Rank Selection $P_s(i) = r(i) / r_{\text{sum}}$

Where, $P_s(i)$ is probability of selection Individual $r(i)$ is rank of Individuals r_{sum} is sum of all fitness values.

Pass 8: Choose the top best 60% of Chromosomes Into new population

Pass 9: if the number of generations is not reached, go to Pass 3[7][11][12].

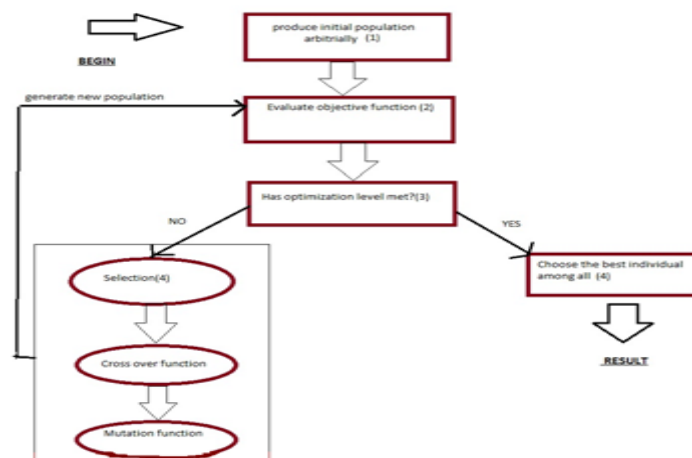


Fig: 4 Working of Genetic Algorithm

As there are various types of attacks which can be listed as:

- DOS attack: Smurf, Neptune, Pod
- U2R:buffer overflow, Perl
- R2L:guest password, ftp write, phf, spy
- Probe: satan, IP sweep, portsweep

There are various samples Rule sets used to determine the types of attacks by using GA approach. For instance:

- [1] IF (duration=0 and protocol=ICMP) THEN (smurf)
- [2] IF (duration=0 and protocol=TCP and host_srv_count is greater than 1 and less than 128) THEN (Perl (u2R attack))
- [3] IF (duration=0 to 289, protocol=UDP and src_bytes=0) THEN (guess password)

There is numerous work done related to GA like: Lu developed a method to determine a set of rule classification with the help of past data of networks; Xiao detected abnormal behaviour of networks by using mutual information and complexity reduction; Li implemented GA by using quantitative features.

IV. CONCLUSION

Fuzzy logic is one of the soft computing technique efficient in implementation of rule based data mining on intrusion over non fuzzy data sets. Although much of the success has been achieved by using this technique yet it is needed to be applied on high speed workstations and misuse rule base is still in progress by using fuzzy association rules. The fuzzy is now days optimised by the integration of genetic algorithm with it[1]. In graph based approach, The visualization helps the security manager to get insight to the current usage of the computer network[3]. He has the possibility to learn more about the reasons for events or warnings from his intrusion detection system. This form of presentation helps detecting false positives. The event generating system has to be improved. The concepts are interesting, but additional work is needed to optimize the process. It is possible to automatically detect anomalies in the communication structure of a surveyed network, but the goal of detecting a large number of different attacks is not yet reached. Integration in the existing intrusion detection system is planned for the near future. Additional graph algorithms, especially clustering algorithms will be tested and compared with the used ones. More features shall be extracted from the clustered traffic graphs and different learning methods will be tested. The visualization will be optimized to the needs of the permanent usage of the system. An approach for a neural network based intrusion detection system, intended to classify the normal and attack patterns and the type of attacks. It should be mentioned that the long training time of the neural network was mostly due to the huge number of training vectors of computation facilities. However, when the neural network parameters were determined by training, classification of a single record was done in a negligible time[4].

Therefore, the neural network based IDS can operate as an online classifier for the attack types that it has been trained for. The only factor that makes the neural network off-line is the time used for gathering information necessary to compute the features. The basic problem with ANN is the over fitting, it is alright to use a small data set but becomes cumbersome as the size of the data increases. The paper presents the Genetic Algorithm for the Intrusion detection system for detecting DoS, R2L, U2R, Probe. The time to get thorough with the features to describe the data will be reduced with a combination of Genetic Algorithm based IDSs. This provides a high rate of the rule set for detecting different types of attacks. The results of the experiments are good with an 83.65% of average success rate and got satisfied. Presently, systems are more flexible for usage in different application areas with proper attack taxonomy. As the intrusions are becoming complex and alter rapidly an IDS should be capable to compete with the thread space. Genetic Algorithm detects the intrusion while correlation techniques identify the features of the network connections. Optimizing the parameters present in the algorithm reduces the training time. More reduction techniques may be referred to get valuable features in future

REFERENCES

- [1] Susan M. Bridges, Rayford B. Vaughn 'FUZZY DATA MINING AND GENETIC ALGORITHMS APPLIED TO INTRUSION DETECTION' 23rd National Information Systems Security Conference October 16-19, 2000.
- [2] Bertrand Portier, Froment-Curtil Data Mining Techniques for Intrusion Detection.
- [3] Jens Tölle, Oliver Niggemann 'Supporting Intrusion Detection by Graph Clustering and Graph Drawing'.
- [4] Mehdi Moradi, Mohammad Zulkernine 'A Neural Network Based System for Intrusion Detection and Classification of Attacks' Natural Sciences and Engineering Research Council of Canada (NSERC).
- [5] Jungwon Kim, Peter J. Bentley, UWE Aikckelin, Julie Greensmith, Gianni Tedesco, Jamie Twycross 'Immune system approaches to intrusion detection –a review' Natural Computing (2007) 6:413–466 _ Springer 2007DOI 10.1007/s11047-006-9026-4, Springer 200

- [6] Wenke Lee, Salvatore J. Stolfo, Kui W. Mok 'Adaptive Intrusion Detection: A Data Mining Approach' Artificial Intelligence Review 14: 533-567, 2000. issues on the Application of Data Mining. © 2001 Kluwer Academic Publishers. Printed in the Netherlands.
- [7] Wei Li 'Using Genetic Algorithm for Network Intrusion Detection'.
- [8] Justin Lee, Stuart Moskovich, Lucas Silacci 'A Survey of Intrusion Detection Analysis Methods' CSE 221 spring 1999.
- [9] Mikhail Gordeev 'Intrusion Detection Techniques and Approaches'.
- [10] Wenke Lee, Salvatore J. Stolfo 'Data Mining Approaches for Intrusion Detection' 7th USENIX Security Symposium, 1998
- [11] A.A. Ojugo, A.O. Eboka, O.E. Okonta, R.E Yoro (Mrs), F.O. Aghware 'Genetic Algorithm Rule-Based Intrusion Detection System (GAIDS)' Journal of Emerging Trends in Computing and Information Sciences VOL. 3, NO. 8 Aug, 2012
- [12] Detection System (GAIDS)" Journal of Emerging Trends in Computing and Information Sciences ©2009-2012 CIS Journal.
- [13] B. Uppalaiah, K. Anand, B. Narsimha, S. Swaraj, T. Bharat 'Genetic Algorithm Approach to Intrusion Detection System' IJCST Vol. 3, Issue 1, Jan. - March 2012 .
- [14] Stefan Axelsson 'Intrusion Detection Systems:-A Survey and Taxonomy' 14 March 2000

Dielectric Properties of Irradiated and Non Irradiated Muga (Antheraea Assama) Silk Fibre in Presence of Oxygen at Elevated Temperature

¹Manoranjan Talukdar

Dept. of Physics, Bajali College, Pathsala-781325, Assam, India.

Abstract.

In presence of oxygen the dielectric properties such as dielectric constant (ϵ'), dielectric loss factor and dielectric loss tangent of Muga fibre are studied in audio frequency range at different temperature. The range of the temperature is 303K to 573K. It has been seen that in presence of oxygen an additional peak is arises for the curve of dielectric constant and temperature, which is not seen when the experiment is carried out in vacuum and in air medium. The values of dielectric constant, dielectric loss factor and dielectric loss tangent at 323K & at 473K for irradiated Muga fibre in presence of oxygen are 2.31, 0.231, 0.1 & 5.03, 2.012, 0.4 accordingly. These values for non irradiated sample are 4.96, 0.496, 0.1 & 67.49, 128.23, 1.9 respectively.

Keywords. Audio frequency, dielectric constant, dielectric loss factor, Dielectric loss tangent, irradiation, Oxygen, Silk fibre.

I. INTRODUCTION

The natural silk fibre muga (Antheraea assama) are organic polymers¹. The common character and properties such as thermal, chemical and physical of organic textile fibre depends on the high polymeric compounds that constitute the fibre. One of the main objectives of polymer physics is the elucidation of interconnection between the structure and the physical properties of polymers. A profound knowledge of the interconnection between the structure and properties makes it possible to control the production and quality of textile fibre and regulate their specific consumption depending upon the condition for their use or process. The silk fibre muga are semicrystalline and hygroscopic in nature². The study of the thermal behaviour of these fibres has great importance in textile and other industrial field. The importance of study of degradation of polymer under the action of high energy such as γ -radiation has been attached^{3,4}. The most important kind of chemical degradation are oxydative degradation. Heat intensify the oxydative degradation. Amongst the physical properties of textile fibre the dielectric properties is one of the most important property of the fibres. Dielectric properties of polymeric and cellulosic yarn and fabric have been studied by some investigators⁵⁻⁹. In present investigation attempt have been made to study the dielectric properties of raw and irradiated muga fibre in presence of oxygen.

II. MATERIALS AND METHODS

2.1 Sample collection.

The muga silk fibres were extracted from it.

2.2 Sample preparation.

The fibres were divided into two parts. One part is used as raw sample and other part is irradiated and used as irradiated sample.

2.3 Irradiation.

One part of the raw muga fibres have been exposed to γ - radiation of dose 2.4×10^3 rad. The fibres were irradiated by ^{60}Co source. The samples are irradiated at low energy γ - dose rate ranging from 0.34×10^6 to 0.44×10^6

roentgens per hour. Calibrations are done at BARC, Bombay. For irradiated the samples, the raw fibres are packed into saperate paper envelops. The surface area of the envelop is $10.2 \times 10.2 \text{ cm.}^2$. They are placed at 45.7 cm. distance from the γ - emitter. The samples are irradiated in 298 K and 65 % r.h.

2.4 Methods

The experimental arrangement for dielectric measurements consisted a frequency osciullator (Agronic), an insulating transformer of type TM7120 (Marconi) and universal bridge of type TF2700 (Marconi).The experimental arrangement and measurement were taken by the method describe elsewhere^{10,11}. Here an additional part for oxygen supply has attached. For this a glass tube with stop cock is joined with the main tube. The other end of the tube is connected with an oxygen cylinder.

III. RESULTS AND DISCUSSION.

The colour of raw muga fibres are golden yellow. When raw muga fibres are irradiated by γ - radiation of dose 2.4×10^3 rad it has noticed that the lustre of the fibre is increased. The observed values of dielectric constant (ϵ') at different temperature (T) for raw and irradiated samples in presence of air and in presence of oxygen at the frequency 1 KHz are displayed in table 1.

Table 1. Dielectric constant (ϵ') of raw and irradiated muga fibres at different temperature ($^{\circ}\text{K}$)

$^{\circ}\text{K}$	Ra	Ro	Ia	Io
303	8.58	8.54	10.87	2.72
323	8.36	4.96	8.40	2.41
373	4.40	11.12	4.94	2.31
423	4.40	15.28	4.94	9.05
473	5.50	51.61	4.94	5.03
525	7.92	3970.00	7.41	20.00
543	6.56	3570.00	8.40	98.59

Samples : Ra -raw in air , Ro - Raw in oxygen,

From the table 1 it is observed that the values of dielectric constant are very high in presence of oxygen at elevated temperature. The values of dielectric constant for the fibres in air medium are gradually increased. This variation may be based on the agreement that due to increase of temperature the rotations of sides groups and also by the segmental mobility of the fibre constituents occur.

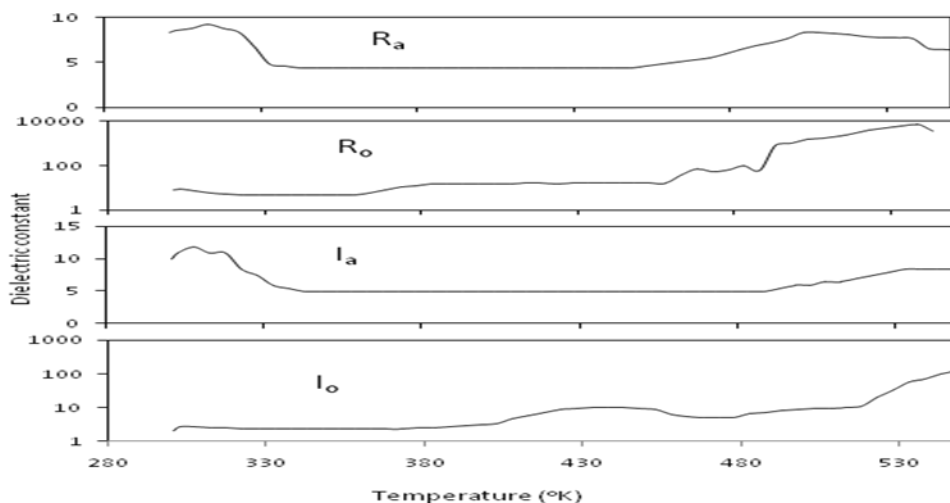


Figure1. Dielectric constant (ϵ') of raw and irradiated fibres at different temperature in presence of air and oxygen (Samples : Ra -raw in air , Ro - Raw in oxygen, Ia-irradiated in air, Io-irradiated in oxygen)

The variations of (ϵ') and temperature for the fibre at air and oxygen at the frequency 1 KHz are shown in fig 1. From the figure it has also been seen that the degradation temperature has decreased and decomposition peak arises in the temperature range 300 to 500 K in presence of oxygen. This may be due to increase of the rate of thermal degradation in presence of oxygen¹². From figure 1 it has also seen that the glass transition temperature has decreased in oxygen medium. The observed values of dielectric loss tangent with temperature for the raw and irradiated fibres in the medium of air and oxygen. are displayed in table 2. From table2 it has found that at low temperature the values of dielectric loss for the fibre in the air medium are less than those of the fibres in oxygen medium. But at high temperature the dielectric loss is greater for the fibres in air medium than those of the fibres in oxygen medium. This indicates that the dielectric loss has decreased in presence of oxygen at higher temperature. Figure 2 represent the variation of dielectric loss tangent with temperature for the raw and irradiated fibres in the medium of air and oxygen.

Table 2. Dielectric loss tangent of raw and irradiated muga fibres at different temperature (°K) in presence of air and oxygen at the frequency 1 KHz.

°K	Ua	Uo	Ia	Io
303	0.08	0.40	0.08	0.10
323	0.90	0.10	0.90	0.10
373	2.98	0.60	2.98	0.09
423	5.01	0.90	5.01	0.70
473	7.01	3.50	7.01	0.40
525	9.04	3.80	9.04	1.70
543	9.86	3.80	9.86	2.20

Samples : Ra -raw in air , Ro - Raw in oxygen, Ia-irradiated in air, Io-irradiated in oxygen.

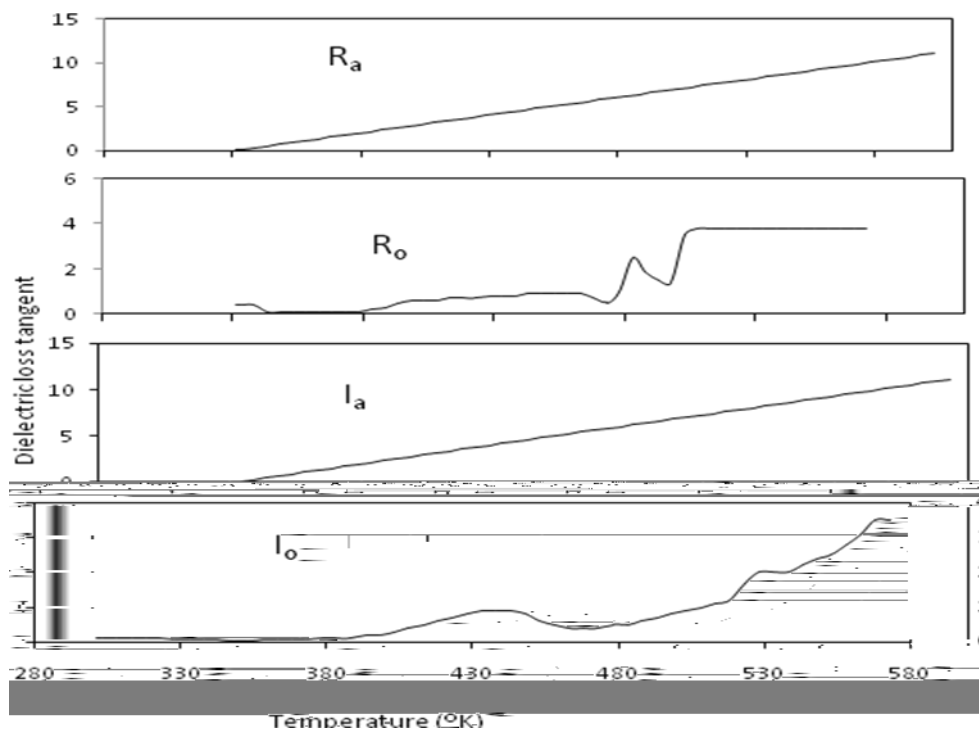


Figure 2. Dielectric loss tangent of raw and irradiated fibres at different temperature (°K) in presence of air and oxygen at the frequency 1 KHz. (Samples : Ra -raw in air , Ro - Raw in oxygen, Ia-irradiated in air, Io-irradiated in oxygen.)

From figure2 it has been seen that the dielectric losses of raw and irradiated fibres in air are linearly increased with the increased of temperature. The simillar result had been obtained for some non irradiated cellulosic fibres¹³.

From the figure it is seen that some peaks are arises for the dielectric loss tangent in presence of oxygen. This may occur due to the change of physical state of the fibres in presence of oxygen , because the dipolar contribution to the polarisation take time to its static position vary between days and 10^{-12} second depending on temperature, chemical constitution of the material and physical state¹⁴.

IV. CONCLUSION.

The degradation and decomposition temperature has decreased in presence of oxygen. The polarisation effect also change in presence of oxygen.

REFERENCES.

- [1] Baruah G C, Talukdar C & Bora M N, Indian J Physics, 65B(6) (1991) 651
- [2] Bora M N, Saikia D, Saikia R & Talukdar C , High temp High press 29 (1997) 683.
- [3] Gilgg R E , Radiation research 6 (1957) 469-473.
- [4] Florine A Blouin & Jett C Aurther, The effect of gamma radiation on cotton , Part V : Post irradiation reactions, Southern regional laboratory, New orleans, Louistad.
- [5] McCubbin W L , J Polym. Sci. , 30 (1970) 181.
- [6] Lews T J & Bowen P J, IEEE Trans, Electr. Insul. El. 19(3) (1984) 254.
- [7] Abdel Moteleb N M, Naoumn M M, Shirouda H G & Rizk H A , J Polym. Sci. 20(3) (1982) 765.
- [8] Bora M N , Baruah G C, Saikia D, Talukdar M & Talukdar C , 5th ATP conference Proceedings, Seoul, Korea, (1998) 73.
- [9] Bora M N , Baruah G C, & Talukdar C , Thermochemica acta (1993) 218.
- [10] Bora M N & Talukdar M , Indian J Physics, 74 A (3) (2000) 263-265.
- [11] Studies on the thermophysical properties of some organic complexases(Fibres) by X-ray diffraction and other physical methods, Ph.D. thesis, G C Baruah, (Gauhati University) 1991,pp 92
- [12] Physical Chemistry of Polymers, A Tager, (Mir Publication, Moscow) 1978, pp.71.
- [13] Talukdar M & Bora M N, Proceedings of 6th ATP Conference, India, (2001) 688-692.
- [14] Solid State Physics, A J Dekker, (Mcmillan India Limited) 2000, pp.150.

Dynamic Topology Control In To Mitigate Spam Attacks Using Secure Communication Protocols.

¹, N.NIMITHA , ²V.NIRMALA

¹M.E (P.G Student)-ECE, M.Kumarasamy college of Engineering
Karur, Tamilnadu, India

²Lecturer-ECE, M.Kumarasamy college of Engineering
Karur, Tamilnadu, India

Abstract

Security is the main concern and bottleneck for widely deployed wireless applications due to the fact that wireless channels are vulnerable to attacks and that wireless bandwidth is a constrained resource. In this sense, it is desirable to adaptively achieve security according to the available resource. In particular, mobile ad hoc networks (MANETs) based on cooperative communication (CC) present significant challenges to security issues, as well as issues of network performance and management. This paper presents a secure decentralized clustering algorithm for mobile ad-hoc networks (SADTCA). The algorithm operates without a centralized controller, operates asynchronously, and does not require that the location of the nodes be known a priori. Based on the cluster-based topology, secure hierarchical communication protocols and dynamic quarantine strategies are introduced to defend against spam attacks, since this type of attacks can exhaust the energy of mobile nodes and will shorten the lifetime of a mobile network drastically. By adjusting the threshold of infected percentage of the cluster coverage, our scheme can dynamically coordinate the proportion of the quarantine region and adaptively achieve the cluster control and the neighborhood control of attacks. Elliptic Curve Digital Signature Algorithm (ECDSA) which is one of the variants of Elliptic Curve Cryptography (ECC) proposed as an alternative to established public key systems such as Digital Signature Algorithm (DSA) has recently gained a lot of attention in industry and academia. The key generated by the implementation is highly secured and it consumes lesser bandwidth because of small key size used by the elliptic curves. ,QH[LVWLQJ VVWHP -RLQW WRSRORJFRQWURO DQG DXWKHQWLFDWI with cooperative communication scheme the spam attacks are not avoided, hence the throughput is minimized. Simulation results show that the proposed approach is feasible and cost effective for mobile ad-hoc networks.

Keywords:Secure communication protocols; adaptive topology control, MANETs, Cooperative communication, JATC topology control, quarantine region.

I. INTRODUCTION

Mobile networks are typically characterized by limited power supplies, low bandwidth, small memory sizes and limited energy [1, 2]. Thus the resource-starved nature of Mobile networks poses great challenges for security, since wireless networks are vulnerable to security attacks due to the broadcast nature of the transmission medium [2–15]. In most Mobile network applications, the lifetime of Mobile nodes is an important concern, which can shorten rapidly under spam attacks. Moreover, maintaining network connectivity is crucial to provide reliable communication in wireless ad-hoc networks. In order not to rely on a central controller, clustering is carried out by adaptive distributed control techniques. To this end, the Secure Adaptive Distributed Topology Control Algorithm (SADTCA) aims at topology control and performs secure self-organization in four phases: (I) Anti-node Detection, (II) Cluster Formation, (III) Key Distribution; and (IV) Key Renewal, to protect against spam attacks. In Phase I, in order to strengthen the network against spam attacks, the secure control is embedded into the SADTCA. A challenge is made for all Mobiles in the field such that normal nodes and anti-nodes can be differentiated. In Phase II, based on the operation in Phase I, the normal Mobiles may apply the adaptive distributed topology control algorithm (ADTCA) from [16] to partition the Mobiles into clusters. In Phase III, a simple and efficient key distribution scheme is used in the network. Two symmetric shared keys, a cluster key and a gateway key, are encrypted by the pre-distributed key and are distributed locally.

A cluster key is a key shared by a clusterhead and all its cluster members, which is mainly used for securing locally broadcast messages. Moreover, in order to form a secure inter-cluster communication channel, a symmetric shared key may be used to encrypt the sending messages between the gateways of adjacent clusters. Since using the same encryption key for extended periods may incur a cryptanalysis risk, in Phase IV, key renewing may be necessary for protecting the Mobile network and guarding against the adversary getting the keys. Built upon the cluster-based network topology, three quarantine methods, Method 1: quarantine for clusters, Method 2: quarantine for nodes, and Method 3: quarantine for infected areas, are proposed for dynamically determining the quarantine region. In order to explore the fundamental performance of the SADTCA scheme, an analytical discussion and experiments are presented to investigate the energy consumption, communication complexity, the increase of communication overheads for data dissemination, and the percentage of the quarantine region in the sensing field when facing the spam attack. The organization of this paper is as follows: In Section 2., we briefly introduce the related work and summary of security issues for wireless Mobile network environment. Section 3. describes the system model and algorithm for secure self-organization in a cluster-based network topology. Section 4. presents dynamic approaches for determining the quarantine region. In Section 5., we analyze the SADTCA and make comparisons with protocols in the flat-based topology. In Section 6., the simulation results are shown and discussed. Finally, Section 7. draws conclusions and shows future research directions.

II. LITERATURE REVIEW

There are many vulnerabilities and threats to wireless Mobile networks. The broadcast nature of the transmission medium incurs various types of security attacks. Different schemes to detect and defend against the attacks are proposed in [2–15]. A number of anti-nodes deployed inside the sensing field can originate several attacks to interfere with message transmission and even paralyze the whole Mobile network. Most network layer attacks against Mobile networks fall into one of the following categories:

- Acknowledgement Spoofing.
- Selective Forwarding.
- Sybil attacks.
- Wormholes attacks.
- Sinkhole attacks.
- Hello flood attacks.

The spam attack, which is a kind of flooding Denial of Service (DoS) attack, can be carried out by the anti-node inside the Mobile network. Such attack can retard the message transmission and exhaust the energy of a Mobile node by generating spam messages frequently.

2.1 SECURE ADAPTIVE DISTRIBUTED TOPOLOGY CONTROL ALGORITHM

In this section we present a secure adaptive distributed topology control algorithm (SADTCA) for wireless Mobile networks. The proposed algorithm organizes the Mobiles in four phases: Anti-node Detection, Cluster Formation, Key Distribution, and Key Renewal. The main keys used in the network are (a) Pre-distributed Key, (b) Cluster Key, and (c) Gateway Key. Each Mobile is pre-distributed with three initial symmetric keys, an identification message, and a key pool. Pre-distributed key is established with key management schemes [6, 7], and is used for anti-node detection and cluster formation in Phases I and II. The Cluster Key and Gateway Key are used for key distribution in Phase III. The key pool is used for key renewing in Phase IV. Note that since our research aims at network topology control, the pre-distributed key establishment is beyond the scope of this paper.

2.2 Phase I: Anti-Node detection:

In order to strengthen the network against spam attacks, the secure control is embedded into the SADTCA. An authenticated broadcasting mechanism, such as the μ TESLA in SPINS [20], may be applied in this phase. In the authenticated broadcasting mechanism, a challenge is made for all Mobiles in the field such that normal nodes and anti-nodes can be differentiated. The challenge is that when a Mobile broadcasts a Hello message to identify its neighbors, it encrypts the plaintext and then broadcasts; when receiving the Hello message, the Mobile decrypts it. If the Mobile decrypts the received message successfully, the sender is considered normal. Otherwise, the sender is said to be an anti-node. Therefore, we keep on the network topology without anti-nodes in order to make the network safe. If an anti-node is presented in the first deployment of a Mobile network, its neighboring normal nodes will notice the existence of the anti-node, since the anti-node will fail in authentication. Thus, referring to the cluster-based topology formed in Phase II, the spam attacks can be handled by adaptively forming the quarantine region as detailed in Section 4. Notice that an external attack can be prevented by the operation of Phase I. In this work, we do not have a lightweight countermeasure to defend against authenticated malicious nodes. If the authenticated node is compromised and performs malicious activities, a mechanism for evicting the compromised nodes is required [7].

2.3 Phase II: Cluster Formation

When Mobiles are first deployed, the adaptive distributed topology control algorithm (ADTCA) from [16] may be used to partition the Mobiles into clusters. The following subsections overview the mechanisms of the ADTCA scheme for cluster formation.

2.4 Cluster head Selection:

Each Mobile sets a random waiting timer, broadcasts its presence via a „Hello“ signal, and listens for its neighbors „Hello“. The Mobiles that hear many neighbors are good candidates for initiating new clusters; those with few neighbors should choose to wait. By adjusting randomized waiting timers, the Mobiles can coordinate themselves into sensible clusters, which can then be used as a basis for further communication and data processing. Mobiles update their neighbor information (i.e., a counter specifying how many neighbors it has detected) and decrease the random waiting time based on each „new Hello message received“. This encourages those Mobiles with many neighbors to become clusterheads. Therefore, if the timer expires, then the Mobile declares itself to be a clusterhead, a focal point of a new cluster. However, events may intervene that cause a Mobile to shorten or cancel its timer. For example, whenever the Mobile detects a new neighbor, it shortens the timer. On the other hand, if a neighbor declares itself to be a clusterhead, the Mobile cancels its own timer and joins the neighbor's new cluster. After applying the ADTCA, there are three different kinds of Mobiles: (1) the clusterheads (2) Mobiles with an assigned cluster ID (3) Mobiles without an assigned cluster ID, which will join any nearby cluster after seconds and become 2-hop Mobiles, where T is a constant chosen to be larger than all of the waiting times. In this phase, each Mobile initiates 2 rounds of local flooding to its 1-hop neighboring Mobiles, one for broadcasting Mobile ID and the other for broadcasting cluster ID, to select clusterheads and form 2-hop clusters. Hence, the time complexity is $O(2)$ rounds. Thus, the topology of the ad-hoc network is now represented by a hierarchical collection of clusters.

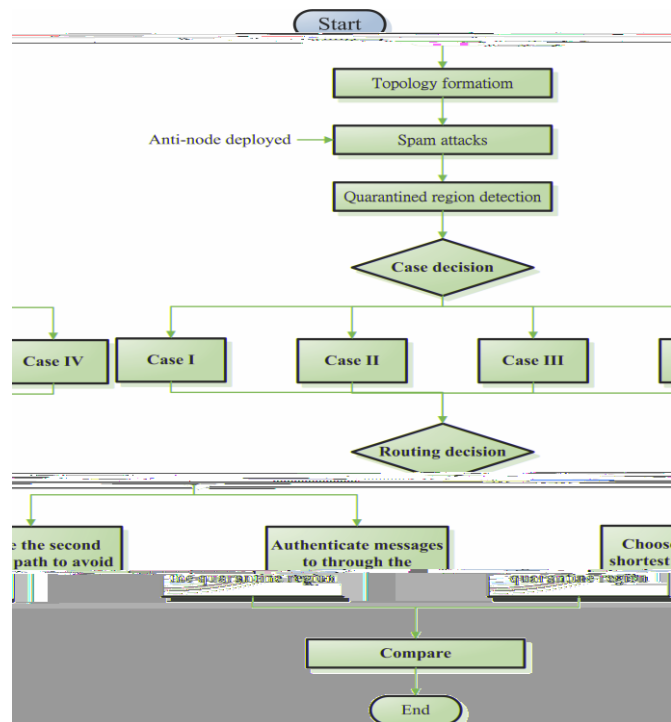


Figure 1. Simulation flowchart of a SADTCA



Figure 2a. The Mobile network without secure topology control

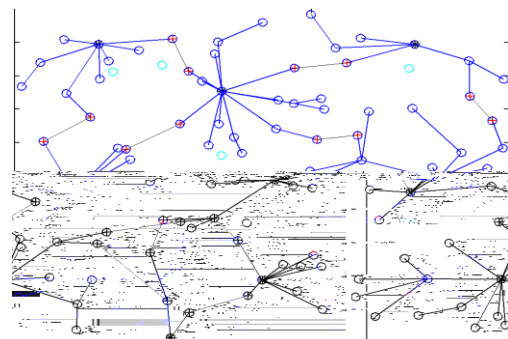


Figure 2b. The Mobile network with secure topology control

2.5 Phase III: Key Distribution:

According to the cluster construction in Phase II, a simple and efficient key distribution scheme is applied in the network. In this phase, two symmetric shared keys, a cluster key and a gateway key, are encrypted by the pre-distributed key and are distributed locally. A cluster key is a key shared by a clusterhead and all its cluster members, which is mainly used for securing locally broadcast messages, e.g., routing control information, or securing Mobile messages. Moreover, in order to form a secure communication channel between the gateways of adjacent clusters, a symmetric shared key may be used to encrypt the sending message. The process of key distribution is shown in Figure 3. In this phase, another challenge may be made to guard against anti-nodes that have not been found out in Phase I. The challenge is that if any Mobile cannot decrypt ciphertext encrypted by a cluster key or a gateway key, the node will be removed from the member or neighbor list. Therefore, the security of intra-cluster communication and inter-cluster communication are established upon a cluster key and a shared gateway key, respectively.

2.6 Phase IV: Key Renewal:

Using the same encryption key for extended periods may incur a cryptanalysis risk. To protect the Mobile network and prevent the the adversary from getting the keys, key renewing may be necessary. In the case of the revocation, in order to accomplish the renewal of the keys, the originator node generates a renewal index, and forwards the index to the gateways. The procedures of key renewal are detailed as follows. Initially all clusterheads (CHs) choose an originator to start the “key renewals”, and then it will send the index to all clusterheads in the network. There are many possible approaches for determining the originator. For instance, the clusterhead with the highest energy level or the clusterhead with the lowest cluster ID. After selecting the originator, it initializes the “Key renewal” process and sends the index to its neighboring clusters by gateways. Then the clusterhead refreshes the two keys from the key pool and broadcasts the two new keys to their cluster members locally. The operation repeats the way through to all clusters in the network. The key renewing process is depicted in Figure 3. A period of time (T_r) is set in order to avoid that the originator does not start the “key renewal” process. If the other clusters do not receive the index after T_r , they will choose a new originator from themselves. The method helps to rescue when the previous originator is broken off.

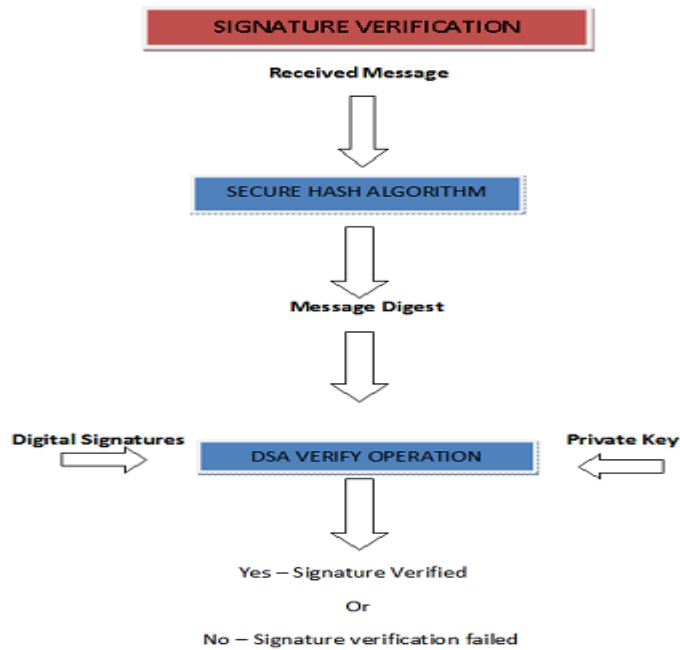
-
- [1] Select a random integer d in the interval $[1, n-1]$.
 - [2] Compute $Q = dP$.
 - [3] A 's public key is Q , A 's private key is d .

3.2 ECDSA Signature Generation:

To sign a message m , an entity A with domain parameters $D = (q, FR, a, b, G, n, h)$ does the following:

- [1] Select a random or pseudorandom integer k in the interval $[1, n-1]$.
- [2] Compute $kP = (x_1, y_1)$ and $r = x_1 \bmod n$ (where x_1 is regarded as an integer between 0 and $q-1$). If $r = 0$ then go back to step 1.

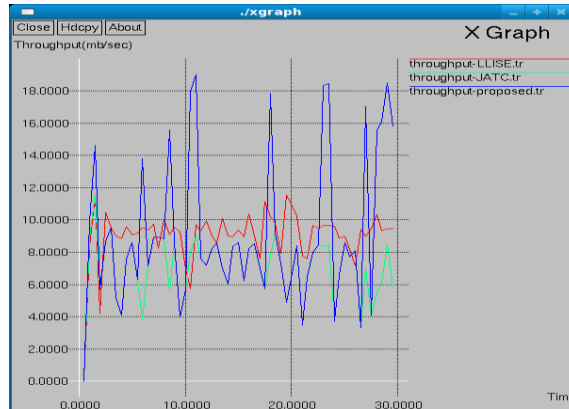
- [5] Accept the signature if and only if $v = r$
- [6] Comparison of ECDSA with DSA
- [1] Both algorithms are based on the ElGamal signature scheme and use the same signing equation: $s = k^{-1}\{h(m) + dr\} \pmod n$.
- [2] In both algorithms, the values that are relatively difficult to generate are the system parameters (p, q and g for the DSA; E, P and n for the ECDSA).
- [3] In their current version, both DSA and ECDSA use the SHA-1 as the sole cryptographic hash function.
- [4] The private key d and the per-signature value k in ECDSA are defined to be statistically unique and unpredictable rather than merely random as in DSA [11].



Symmetric	RSA/DSA/DH	ECC	Time to break in MIPS
80	1024	160	10^{12}
112	2048	224	10^{24}
128	3072	256	10^{28}
192	7680	384	10^{47}
256	15360	512	10^{66}

Table 1 Key comparison of Symmetric, RSA/DSA/DH, ECC





Aggregate throughput and digital signature in the Aggregate throughput using elliptic curve algorithm with respect to authentication protocol versus different numbers of nodes time

IV. CONCLUSION

We describe a secure protocol for topology management in wireless Mobile networks. By adaptively forming quarantine regions, the proposed secure protocol is demonstrated to reach a network security agreement and can effectively protect the network from energy-exhaustion attacks. Therefore, in a hierarchical network topology, the SADTCA scheme can adapt cluster control and neighborhood control in order to achieve dynamic topology management of the spam attacks. Compare to the JATC scheme, the spam attacks are avoided and the throughput is increased. The main reason for the attractiveness of ECDSA is the fact that there is no sub exponential algorithm known to solve the elliptic curve discrete logarithm problem on a properly chosen elliptic curve. Hence, it takes full exponential time to solve while the best algorithm known for solving the underlying integer factorization for RSA and discrete logarithm problem in DSA both take sub exponential time. The key generated by the implementation is highly secured and it consumes lesser bandwidth because of small key size used by the elliptic curves. Significantly smaller parameters can be used in ECDSA than in other competitive systems such as RSA and DSA but with equivalent levels of security. Some benefit

-
- [12] Newsome, J.; Shi, E.; Song, D.; Perrig, A. The sybil attack in sensor networks: Analysis & defenses. In Proceedings of the third international symposium on Information processing in sensor networks, Berkeley, CA, USA, April 26-27, 2004; pp. 259-268.
- [13] Hu, Y.C.; Perrig, A.; Johnson, D.B. Wormhole detection in wireless ad hoc networks. In Rice University Department of Computer Science Technical Report TR01-384, Rice University, Houston, TX, USA, 2002.
- [14] Anderson, R.; Kuhn, M. Tamper resistance - a cautionary note. In Proceedings of the Second Usenix Workshop on Electronic Commerce, Oakland, California, November 18-21, 1996; pp. 1-11.
- [15] Roosta, T.; Shieh, S.; Sastry, S. Taxonomy of security attacks in sensor networks and countermeasures. In Proceedings of The First IEEE International Conference on System Integration and Reliability Improvements, Hanoi, Vietnam, December, 2006; pp. 13-15.
- [16] Shaikh, R.A.; Jameel, H.; d Auriol, B.J.; Lee, H.; Lee, S.; Song, Y.-J. Group-based trust management scheme for clustered wireless sensor networks. *IEEE Trans. Parall. Distrib. Sys.* 2009, 20, 1698–1712.
- [17] Chu, K.-T.; Wen, C.-Y.; Ouyang, Y.-C.; Sethares, W. A. Adaptive distributed topology control for wireless ad-hoc sensor networks. In Proceedings of 2007 International Conference on Sensor Technologies and Applications (SENSORCOMM 2007), Valencia, Spain, October 14-20, 2007; pp. 378-386.
- [18] Sancak, S.; Cayirci, E.; Coskun, V.; Levi, A. Sensor wars: detecting and defending against spam attacks in wireless sensor networks. In Proceedings of IEEE International Conference on Communications, Paris, France, June 20-24, 2004; pp. 3668-3672.
- [19] Coskun, V.; Cayirci, E.; Levi, A.; Sancak, S. Quarantine region scheme to mitigate spam attacks in wireless sensor networks. *IEEE Trans. Mobil. Comput.* 2006, 5, 1074–1086.
- [20] Wen, C.-Y.; Sethares, W. A. Automatic decentralized clustering for wireless sensor networks. *EURASIP J. Wirel. Commun. Netw.* 2005, 5, 686–697.
- [21] Perrig, A.; Szewczyk, R.; Tygar, J. D.; Wen, V.; Culler, D. E. SPINS: Security protocols for sensor networks. *Wirel. Netw.* 2002, 8, 521–534.
- [22] Santi, P. *Topology Control in Wireless Ad Hoc and Sensor Networks*; John-Wiley & Sons: Chichester, UK, 2005.
- [23] Quansheng Guan, Member, IEEE, F. Richard Yu, Senior Member, IEEE, Shengming Jiang, Senior Member, IEEE, and Victor C. M. Leung, Fellow, IEEE. Joint Topology Control and Authentication Design in Mobile Ad Hoc Networks With Cooperative Communications, *IEEE transactions on vehicular technology*, vol. 61, no. 6, July 2012

Graphical Password Authentication System with Integrated Sound Signature

¹, Anu Singh , ²,Kiran Kshirsagar, ³,Lipti Pradhan

¹(Department of Computer Engineering, Pune University, India

Abstract

We are proposing a system for graphical password authentication with the integration of sound signature. In this work, Cued Click Point scheme is used. Here a password is formed by a sequence of some images in which user can select one click-point per image. Also for further security user selects a sound signature corresponding to each click point, this sound signature will help the user in recalling the click points. The system showed better performance in terms of usability, accuracy and speed. Many users preferred this system over other authentication systems saying that selecting and remembering only one point per image was aided by sound signature recall.

Keywords: Sound signature, Authentication, Cued Click points

I. INTRODUCTION

Basically passwords are used for

- [1] Authentication (verifying an imposter from actual user).
- [2] Authorization (process to decide if the valid person is allowed to access the data)
- [3] Access Control (Restricting the user to access the secured data).

Usually passwords are selected by the users are predictable. This happens with both graphical and text based passwords. Users tend to choose password which are easy to remember, unfortunately it means that the passwords tend to follow predictable patterns that are easier for attackers to hack. While the predictability problem can be solved by disallowing user choice and assigning passwords to the users, this usually leads to usability problems since it's difficult for the user to remember such passwords. Many graphical password systems have been developed; research shows that a text-based password suffers with both usability and security problems. According to a recently published article, a security team at a company ran a network password cracker and within 30 seconds and they identified about 80% of the passwords. According to the practical research, it is well known that the human brain is better at recognizing and recalling the pictorial content, graphical passwords exploit this human characteristic.

II. RELATED WORK

Considerable work has been done in this field, the best known of these systems are Pass faces ^{[1][4]}. Brostoff and Sasse (2000) carried out an empirical study of Pass faces, which demonstrate well how a graphical password recognition system typically works. Blonder-style passwords are based on cued click recalls. A user clicks on several previously chosen locations in a single image for logging in. As implemented by Passlogix Corporation (Boroditsky, 2002), the user chooses some predefined regions in an image as a password. To log in the user has to click on the same regions selected at the time of creation of the password. The problem with this system is that the number of predefined regions is small for selecting, perhaps around 10-12 regions in a picture. The password may have to be up to 12 clicks for adequate security, which again tedious for the user to operate. Another problem of this system is the need for the predefined regions to be readily recognizable. In effect, this requires artificial, cartoon-like images rather than complex, real-world scenes ^{[2][3]}. Cued Click Points (CCP) is a proposed alternative to previous graphical authentication system. In the proposed system, users click one point on each of 5 images rather than on five points on one image.

III. PROPOSED WORK

In the proposed work along with the cued click point we have integrated sound signature to help in recalling the password easily. No system has been designed so far which uses sound signature in graphical password authentication. As per the research it has been said that sound effect or tone can be used to recall facts like images, text etc ^[3]. Our idea is inspired by this novel human ability. Using this sound signature and click points the user can be intimidated if he or she is going in a write direction. It also makes the task of the hackers

more challenging. As shown in Figure 1, each click is directing the user to the next image, in effect leading users down a “path” as they click on their sequence of points. A wrong click leads down an incorrect path, with an explicit indication of authentication failure only after the final click. In the proposed system, users click one point on each of 5 images rather than clicking on five points on one image. A wrong click leads down an incorrect path, with an explicit indication of authentication failure only after the final click. Users can choose their images only to the extent that their click-point dictates the next image. If they dislike the resulting images, they could create a new password involving different click-points to get different images.



Fig 1.Click Point per image

Two vectors are created for in this system:

3.1. Profile Vectors

The proposed system creates user profile as follows-

3.2 Master vector

(User ID, Sound Signature frequency, Tolerance)

3.3 Detailed Vector (Image, Click Points)

As an example of vectors – Master vector (Smith, 2689, 50)

Detailed Vector

Image	Click points
I ₁	(123,678)
I ₂	(176,134)
I ₃	(450,297)
I ₄	(761,164)

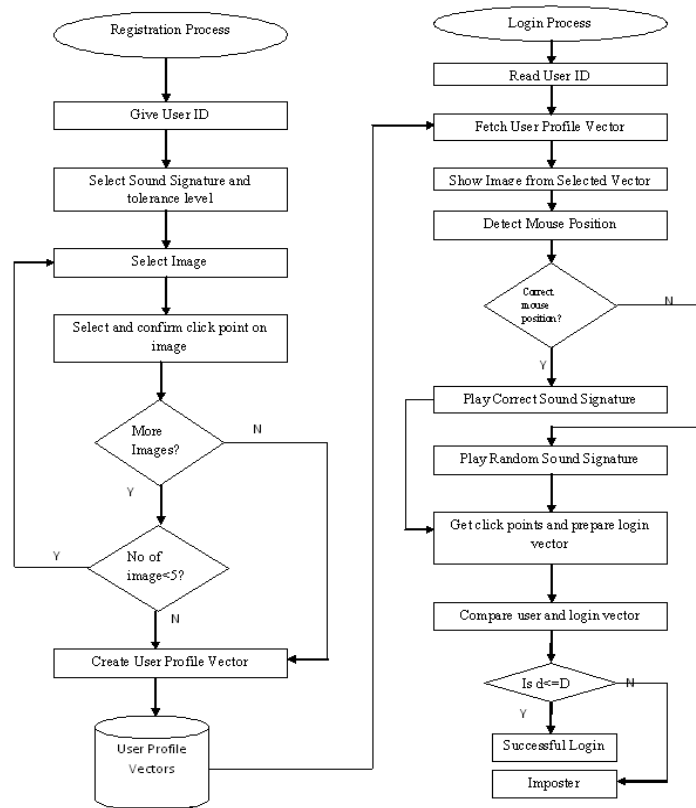


Fig.2 System Flow

3.4 System Tolerance

After creation of the login vector, system calculates the Euclidian distance between login vector and profile vectors stored. Euclidian distance between two vectors **p** and **q** is given by-

$$d(p, q) = \sqrt{(p_1 - q_1)^2 + (p_2 - q_2)^2 + \dots + (p_n - q_n)^2} = \sqrt{\sum_{i=1 \text{ to } n} (p_i - q_i)^2}$$

Above **distance is calculated for each image** if this distance comes out less than a tolerance value D. The value of D is decided according to the application. In our system this value is selected by the user.

This is the registration form which shows that the userID is given by the system itself.

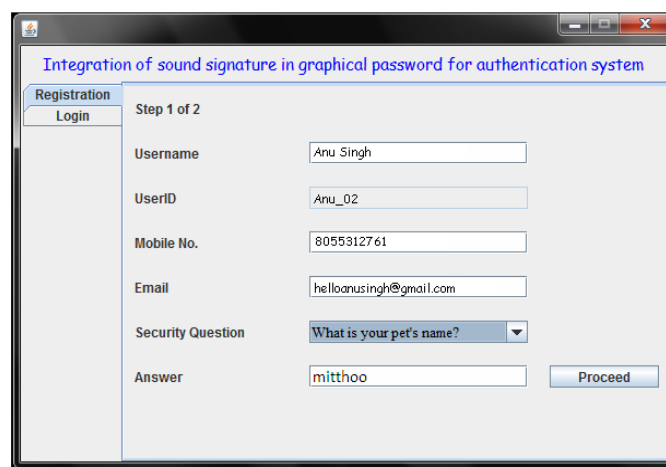


Fig 3.Registration Step 1

This is the selection of sound signature and the click points for creating the password.



Fig 3.Registration Step 2

IV. PROJECT SCOPE

In proposed work a click-based graphical password scheme called Cued Click Points (CCP) is presented. In this system a password consists of sequence of some images in which user can select one click-point per image. Cued Click Points (CCP) is a proposed alternative to Pass Points. In CCP, users click one point hotspot analysis more challenging. Each click results in showing a next-image, in effect leading users down on each of 5 images rather than on five points on one image. It offers cued-recall and introduces visual cues that instantly alert valid users if they have made a mistake when entering their latest click-point (at which point they can cancel their attempt and retry from the beginning). It also makes attacks based on a “path” as they click on their sequence of points. A wrong click leads down an incorrect path, with an explicit indication of authentication failure only after the final click. Users can choose their images only to the extent that their click-point dictates the next image. If they dislike the resulting images, they could create a new password involving different click-points to get different images. In addition user is asked to select a sound signature corresponding to each click point this sound signature will be used to help the user in recalling the click point on an image.

System showed very good Performance in terms of speed, accuracy, and ease of use. Users preferred CCP to Pass Points, saying that selecting and remembering only one point per image was easier and sound signature helps considerably in recalling the click points. In the proposed work we have integrated sound signature to help in recalling the password. No system has been devolved so far which uses sound signature in graphical password authentication.

4.1 Authentication:

The only significant user study on the security of graphical passwords for authentication was performed by Davis^[2] and the present authors^[3] in that work; we studied the security of two schemes based on image recognition, denoted “Face” and “Story,” which are described shortly. This study focused specifically on the impact of user selection of passwords in these schemes, and the security of the passwords that resulted. We recount some of the notable results from this study, and the methodologies used to reach them, as an illustration of some of the challenges that graphical passwords can face. In particular, this study demonstrated that graphical password schemes can be far weaker than textual passwords when users are permitted to choose their password.

V. CONCLUSION AND FUTURE WORK

We have proposed a novel approach which uses sound signature to recall graphical password click points. No previously developed system used this approach this system is helpful when user is logging after a long time. In future systems other patterns may be used for recalling purpose like touch of smells, study shows that these patterns are very useful in recalling the associated objects like images or text.

REFERENCES

- [1] Cranor, L.F., S. Garfinkel. Security and Usability. O’Reilly Media, 2005.
- [2] Davis, D., F. Monrose, and M.K. Reiter. On User Choice in Graphical Password Schemes. 13th USENIX Security Symposium, 2004.
- [3] R. N. Shepard, "Recognition memory for words, sentences, and pictures," Journal of Verbal Learning and Verbal Behavior, vol. 6, pp. 156-163, 1967.
- [4] A. Perrig and D. Song, "Hash Visualization: A New Technique to Improve Real-World Security," in Proceedings of the 1999 International Workshop on Cryptographic Techniques and E-Commerce, 1999.

AUTHOR PROFILES

- [1] **Anu Singh** pursuing the bachelor degree in computer science from Pune University, in 2013.
- [2] **Kiran Kshirsagar** pursuing the bachelor degree in computer science from Pune University, in 2013.
- [3] **Lipti Pradhan** pursuing the bachelor degree in computer science from Pune University, in 2013.

Managing Order Batching Issue of Supply Chain Management with Multi-Agent System

¹Manoj Kumar , ²Dr. S Srinivasan , ³Dr. Gundeep Tanwar

¹Research Scholar, Suresh GyanVihar University Jaipur, Rajasthan (India),

²Professor & Head, PDM College of Engineering, Bahadurgarh, Haryana (India),

³Associate Professor, BRCM College of Engineering & Technology, Bahal, Haryana (India),

Abstract

Recently, agent-based technology has been taken as a promising approach for developing advanced manufacturing systems. Such an approach provides rapid responsive and dynamic reconfigurable structures to facilitate flexible and efficient use of manufacturing resources in a rapidly changing environment. A multi-agent system (MAS) is a loosely coupled network of software agents that interact to solve problems that are beyond the individual capacities or knowledge of each problem solver. In this paper we will apply the concept of Multi-agent system for handling the order batching issue faced in the supply chain management. The order batching is major cause of generating the bullwhip effect. The bullwhip effect produces the worst impact on the performance of the supply chain system. With this aim, we have used the JADE for developing the supply chain management system in which the intelligent agents maintain the information related the order batching issues and the decisions regarding managing the order batching.

Keywords: Supply chain management, Bullwhip effect, Multi-agent system, Ordering Batching, Coordination, JADE.

I. INTRODUCTION

For most application tasks, it is extremely difficult or even impossible to correctly determinate the behavioral repertoire and concrete activities of a multi-agent system a priori, that is, at the time of its design and prior to its use. This would require, for instance, that it is known a priori which environmental requirements will emerge in the future, which agents will be available at the time of emergence, and how the available agents will have to interact in response to these requirements. Such problems resulting from the complexity of multi-agent systems can be avoided or at least reduced by endowing the agents with the ability to learn, that is, with the ability to improve the future performance of the total system, or a part of the system.

Over the past decade, there has been an increased industry interest in the application of multi-agent systems. With the advent of distributed software applications, traditional approaches to programming the interaction between sub-systems has proven to be time consuming and error prone. Typically, distributed systems are embedded in, and must interact with, a changing environment. The interaction with the environment is particularly problematic where there are many external entities that must be controlled, serviced or modeled. In the past, implementing such systems has entailed explicit programming of the interaction with each external entity. If this is more than a simple client/server interaction, then the application can become hard to manage, that is, difficult to implement, maintain or change. Furthermore, the application may not have the required flexibility or responsiveness to its environment.

Agent-based approaches have proven to be well suited where complex interaction with an ever-changing environment is required. Arguably, the most significant attribute of agent-based systems is that each agent is an autonomous computational entity. Autonomy, coupled with an ability to perceive the environment, act upon it and communicate with other agents, provides system builders with a very powerful form of encapsulation. A given agent can be defined in terms of its goals, knowledge and social capability, and then left to perform its function autonomously within the environment it was designed to function in. This is a very effective way of building distributed systems—each agent in the system is responsible for pursuing its own goals, reacting to events and communicating with other agents in the system. There is no need to explicitly program the interactions of the whole system; rather, the interactions *emerge* as a by-product of the individual goals and capabilities of the constituent agents. In the next section, we will further expand our discussion of the motivation for adopting agent-oriented design and programming in industry.

II. MULTI-AGENT SYSTEM

Multi-agent systems (MAS) consist of intelligent agents that are autonomous, dynamic, cooperative or self-interested by nature. Each agent in a multi-agent system is characterized by a degree of autonomy. On basis of its autonomy feature, the agents have ability to decide on their own behaviour. Given the autonomous nature of each agent, agents need to coordinate among themselves, or else, the group quickly changes to a number of individuals with chaotic behaviour. The intelligent agent can update on its knowledge base regarding the environment. They are dynamic by the nature. Cooperative agents coordinate among themselves towards achieving a common goal, where self-interested agents have individual interacting goals. An effective way to achieve coordination is via imposing a specific group organization. An organization comprises roles and their interrelations.



Figure 1: Intelligent Agent

The basic features of MAS are that (1) each agent has partial information or capabilities for solving the problem; (2) the data are decentralized; and (3) working out is not synchronous (4) there does not exist any system global control. The multiagent systems have various capabilities & abilities to implement various types of real time applications. The Multi-agent systems have aptitude to solve problems that are too large for a centralized agent to solve because of resource limitations or the sheer risk of having one centralized system that could be a performance bottleneck or could fail at critical times. The Multi-agent systems can resolve the problems efficiently in which information sources that are spatially distributed. They can also provide the solutions in situations where capability is distributed. Examples of such problems include concurrent engineering. The Multi-agent systems have potential to allow for the interconnection and interoperation of multiple existing inheritance systems. The MAS can provide solutions to problems that can naturally be regarded as a society of autonomous interacting components agents.

There are some major concerns or issues that have to resolve in implementing the real time applications. For example task allocation, communication & decision-making are some of the main issues. Task allocation is the problem of assigning duties and problem-solving resources to an agent. KQML is a protocol for communications among both agents and application programs. Agents need to deliberate effectively by evaluating their options and opportunities towards achieving their shared goals without considering low-level details of their plans. To plan and act robustly in a dynamically and unpredictably changing environment, agents must reason about their intended behavior in an abstract way. An MAS has the following advantages over a single agent or centralized approach:

- The MAS distributes computational resources and capabilities across a network of interconnected agents. Whereas a centralized system may be plagued by resource limitations, performance bottlenecks, or critical failures, an MAS is decentralized and thus does not suffer from the "single point of failure" problem associated with centralized systems.
- The MAS allows for the interconnection and interoperation of multiple existing legacy systems. By building an agent wrapper around such systems, they can be incorporated into an agent society.
- The MAS models problems in terms of autonomous interacting component-agents, which is proving to be a more natural way of representing task allocation, team planning, user preferences, open environments, and so on.
- The MAS efficiently retrieves, filters, and globally coordinates information from sources that are spatially distributed.
- The MAS provides solutions in situations where expertise is spatially and temporally distributed.
- The MAS enhances overall system performance, specifically along the dimensions of computational efficiency, reliability, extensibility, robustness, maintainability, responsiveness, flexibility, and reuse.

III. RELATED WORK

Hsu et al. 2005 developed an order batching approach based on genetic algorithms (GAs) to deal with order batching problems with any kind of batch structure and any kind of warehouse layout. Unlike to previous batching methods, the proposed approach, additionally, did not require the computation of order/batch proximity and the estimation of travel distance. The proposed GAbased order batching method, namely GABM, directly minimized the total travel distance. The potential of applying GABM for solving medium- and large-scale order batching problems was also investigated by using several examples. From the batching results, the proposed GABM approach appeared to obtain quality solutions in terms of travel distance and facility utilization.

Potter et al. 2006 derived a closed form expression for bullwhip when demand is deterministic. This was validated through a simple model of a production control system. An expression for bullwhip in a “pass on orders” scenario with stochastic demand was also derived and validated. Using simulation, they showed the impact of changing batch size on bullwhip in a production control system. Their results showed that a manager may achieve economies through batching while minimizing the impact on bullwhip through the careful selection of the batch size. Zunino et al. 2009 described Chronos, a multi-agent system for helping users in organizing their meetings. The system assigned an intelligent Organizer Agent to each user. These agents were able to schedule events negotiating time, place, day, etc. according to users’ habits and preferences. Chronos agents did not reveal users’ habits or calendars to other users in order to maintain privacy. In addition, each Organizer Agent learnt from its user’s preferences and from negotiations with other agents, to provide better and more accurate assistance. The paper reported encouraging experimental results and comparisons with related approaches. Herrero et al. 2009 focused the development of network-based IDSs from an architectural point of view, in which multiagent systems were applied for the development of IDSs, presenting an up-to-date revision of the state of the art. Intrusion Detection Systems (IDSs) are seen as an important component in comprehensive security solutions. Thus, IDSs are common elements in modern infrastructures to enforce network policies. So far, plenty of techniques have been applied for the detection of intrusions, which has been reported in many surveys.

Henn et al. 2010 dealt with the question of how a given set of customer orders should be combined such that the total length of all tours is minimized which are necessary to collect all items. The authors introduced two metaheuristic approaches for the solution of this problem: the first one is based on Iterated Local Search; the second on Ant Colony Optimization. In a series of extensive numerical experiments, the newly developed approaches are benchmarked against classic solution methods. It demonstrated that the proposed methods are not only superior to existing methods but provide solutions which may allow distribution warehouses to be operated significantly more efficiently. Kocsis et al. 2010 gave firstly a classification scheme of scheduling problems and their solving methods. The main aspects under examination were the following: machine and secondary resources, constraints, objective functions, uncertainty, mathematical models and adapted solution methods. In a second part, based on this scheme, they examined a corpus of 60 main articles in scheduling literature from 1977 to 2009. The main purpose was to discover the underlying themes within the literature and to examine how they had evolved. To identify documents likely to be closely related, they were going to use the cocitation-based method. Their aim is to build a base of articles in order to extract the much developed research themes and find the less examined ones as well, and then try to discuss the reasons of the poorly investigation of some areas.

IV. ORDER BATCHING PROBLEM IN SUPPLY CHAIN MANAGEMENT

Order batching is one of the methods used in warehouses to minimize the travel distance of pickers. In this paper, we focus on developing order-batching methods for an order-picking warehouse with two cross aisles and an I/O point at one of its corners. Each of these methods is made up of one seed-order selection rule and one accompanying-order selection rule. Eleven seed-order selection rules and 14 accompanying-order selection rules are studied here. These rules include those newly proposed by us and those by others. Rules proposed by others have been shown to perform well in minimizing the travel distance of pickers. They are included here for the comparison purpose. Unlike previous studies that only focus on developing aisle or location-based rules, this study also develops rules that are distance- or area-based.

Order picking, or order selection, is the process of retrieving individual items (from storage locations) for the purpose of fulfilling an order for a customer. Schemes by which to achieve efficient order picking will vary widely. However, in all cases it involves locating the items in storage; creating a plan for retrieving the items; physically picking the items (either automatically or manually); sorting and/or assembling them into discrete orders; and in the end even packaging the orders for delivery.



Although defined as a process, order picking cannot be achieved without the appropriate computer software and mechanical equipment, including the storage medium, such as pallet racks, shelving, AS/RS(including carousels) and flow delivery racks, and a means for transporting items from receiving to storage and from storage to packaging and shipment. A variety of industrial trucks and conveyors will be found in most order picking applications. Order picking may also involve robotic like devices for physically picking discrete items from their storage location. When performing his/her tasks, an order picker is guided by a so-called pick list.

This list specifies the sequence according to which the requested articles should be collected, as well as the quantities in which they are to be picked. A pick list may contain the articles of a single customer order (pick-by- order) or of a combination of customer orders (pick-by-batch). In practice, the sequence in which the articles are to be picked and the corresponding route of the order picker (which starts at the depot, proceeds to the respective storage locations, and returns to the depot) is usually determined by means of a so-called routing strategy, e.g., by the S-Shape Heuristic or by the Largest-Gap Heuristic. Despite the fact that an optimal polynomial time algorithm for the picker routing problem exists, it is hardly ever used in practice. Order pickers seem not to accept the optimal routes provided by the algorithm, because of their not-always-straightforward or sometimes even confusing routing schemes. The heuristic routing schemes on the other hand, are fast to memorize and quite easy to follow. This helps to reduce the risk of missing an article to be picked -- an aspect that might be more important than a small reduction of the tour length.

Batching determines which orders are released together. With batch picking, multiple orders are picked together in one pick tour and need to be sorted by order later. By sharing a pick tour, the average travel time per order is reduced. Basically, two criteria for batching exist: proximity of pick locations batching and time-window batching. Proximity batching refers to the clustering of a given number of orders based on retrieval locations. Time-window batching studies the order batching problem in a stochastic context. The number of orders per batch can be fixed or variable. Variable time-window batching groups all orders that arrive during the same time interval or window. With fixed number of orders time-window batching, the time window is the variable length until a batch has a predetermined number of orders. Zoning is closely related to batching; it divides the pick area into sub-divisions (or zones), each with one or few pickers dedicated to it.

The major advantages of zoning are: reduction of the travel time (because of the smaller traversed area and also the familiarity of the picker with the zone) and of the traffic congestion. Depending on the pick process sequence, zoning can be further classified as progressive zoning or synchronized zoning. With progressive zoning, orders are sequentially picked zone by zone (this system is also called 'pick-and-pass'); a batch is finished when all (order) lines of the orders in the batch are picked. In contrast, in synchronized (or parallel) zoning, pickers in all zones can work on the same batch at the same time. In synchronized zoning, the picking process must be followed by a sorting (and often also a packing) process, to group the items of the same order picked by the multiple pickers. Zoning has received little attention in the literature despite its important impact on the performance of the order picking system. Choe et al. (1993) study the effects of three order picking strategies in an aisle-based system: single order pick, sort-while-pick, and pick-and-sort. They propose analytical tools for the planner to quickly evaluate various alternatives without using simulation.

V. INFORMATION MAINTAINED BY MAS

In this proposed work , the system concentrate on the order processing D Bng



- Timeliness of shipment windows - when shipments need to be completed based on carriers can create processing variations
- Availability of capital expenditure dollars - influence on manual verses automated process decisions and longer term benefits
- Value of product shipped - the ratio of the value of the shipped product and the order fulfillment cost
- Seasonality variations in outbound volume - amount and duration of seasonal peaks and valleys of outbound volume
- Predictability of future volume, product and order profiles -
- Predictability of distribution network - whether or not the network itself is going to change

This list is only a small sample of factors that influence the choice of a distribution centers operational procedures are being managed by multi-agent system. Because each factor has varying importance in each organization the net effect is that each organization has unique processing requirements.

VI. MULTI-AGENT SYSTEM ARCHITECTURE FOR HANDING ORDER BATCHING ISSUE

In this system, there are multiple intelligent agents having the information about the order scheduling. These intelligent agents communicate with each other to shared the information regarding scheduling. Lets us discuss how multi-agent system can be applied to solve timetable-scheduling problem very efficiently. In supply chain management system at big organization, whole operational responsibilities are divided on various coordinators. Each coordinator has responsibility of own departments. Each coordinator has maintained own knowledge base. It also follows the soft & hard constraints. They share the information regarding the product scheduling. Consider there are multiple departments in the organization. In proposed multi-agent system, the various intelligent agents are communicating with each other.

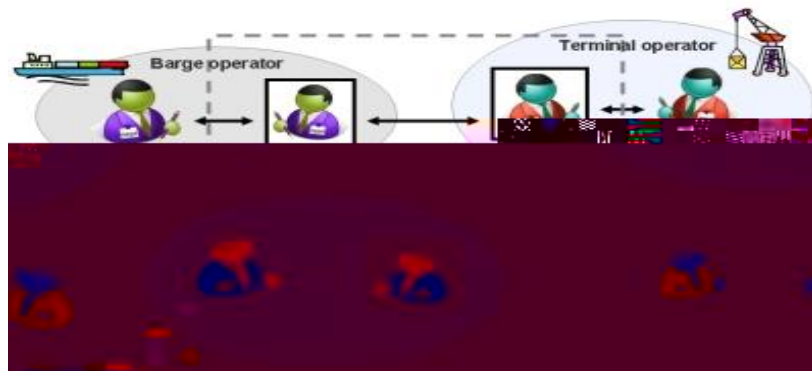


Figure 2: Multi-agent Based SCM

VII. IMPLEMENTATION

For this work we use the JADE soft for designed the multi-agent based supply chain for resolving the order batching issues. The Java Agent Development Environment is a software framework fully implemented in Java language. It simplifies the implementation of multi-agent systems through a middleware that complies with the Foundation for Intelligent Physical Agents specifications and through a set of graphical tools that supports the debugging and deployment phases. The agent platform can be distributed across machines that not even need to share the same OS and the configuration can be controlled via a remote graphical user interface (GUI). The configuration can be even changed at run-time by moving agents from one machine to another one, as and when required. First we create the JADE agent is as simple as defining a class extending the jade.core.Agent class and implementing the setup() method as shown in the code below.

```
import jade.core.Agent;
public class SCMAgent extends Agent {
protected void setup() {
// The logic of the agent will be written here
```

The setup() method is intended to include agent initializations. The actual job an agent has to do is typically carried out within “behaviours”. JADE is relatively suitable for simple agent applications and developers, that require FIPA compliance. JADE’s debugging and monitoring tools and its support for FIPA ACL message format are a sound foundation for systems interactions that require cross-platform interoperability. JADE can be distributed over several hosts, resulting in a distributed system that seems like a

single platform from the outside. For running the jade, the following command is being executed `java jade.Boot -gui` then we get following screen

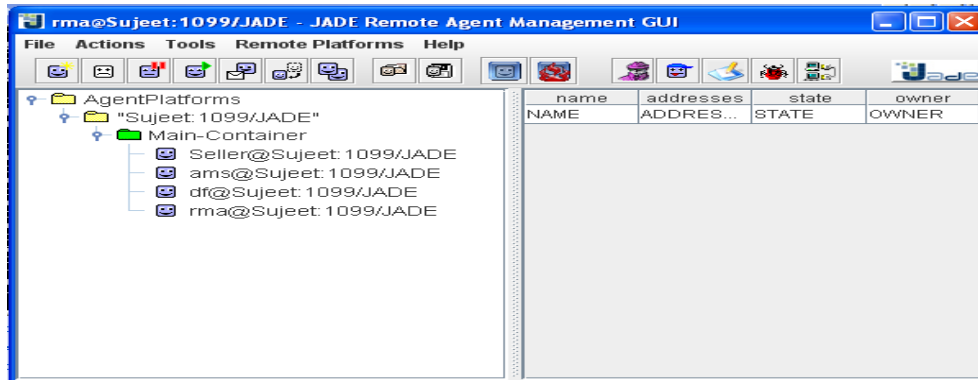


Figure 3: JADE Screen

Now we can create various intelligent agent in the main containers deployed in the tool.

VIII. CONCLUSION

In this paper, we have applied the Multi-agent system in the supply chain management system. This approach is more efficient in comparison of other techniques such like genetic algorithm, machine learning & searching algorithms. Due to autonomous & distributed nature of Multi-agent system, it is more efficient in term of time space. Other techniques are time consuming. It provides more flexibility. It means there is scope of flexibility. Whole system is not dependent on set of predefined rules.. Further research will mainly focus on the improvement of the Multi-agent case base reasoning system. For the RETRIEVE phase, it should be done in distributed mode. The case should be retrieved from all other individual intelligent agent case base.

REFERENCES

- [1] Weiss, G. "Multiagent systems", The MIT Press, Cambridge,Massachusetts, 1999.
- [2] Wooldridge, M., and Jennings, N.R. "Intelligent agents: theory and practice". The Knowledge Engineering Review, 10, 2, 115-152. 2002.
- [3] FIPA. "The foundation for intelligent physical agents". URL: <http://www.fipa.org>, 2003.
- [4] Same, D., and Grosz, B. "Estimating Information Value in Collaborative Multi-Agent Planning Systems" In AAMAS. Forthcoming., 2007
- [5] M. M. Veloso, "Planning and Learning by Analogical Reasoning", Lecture Notes in Artificial Intelligence 886, Springer, Berlin, 1994.
- [6] E. Crawford and M. Veloso "Opportunities for learning in multi-agent meeting scheduling" In Proceedings of the Fall AAAI Symposium on Artificial Multiagent Learning, Wash- ington, DC, October 2004.
- [7] A. B. Hassine and T. B. Ho. "An agent-based approach to solve dynamic meeting scheduling problems with preferences" Eng. Appl. Artif. Intell., 20(6):857-873, 2007.
- [8] Sahay, B. S. & Gupta, A. K, Supply Chain Modeling and Solutions, (1sted.). New Delhi: Macmillan India Ltd.,2007
- [9] Schnetzler, M., "Supply Chain Strategies for Business Success", Proceedings of the International IMS Forum 2004 Global Challenges in Manufacturing, (pp. 691-698.) Cernobbio, Italy., 2004
- [10] Sebestyénová, "Case-Based Reasoning in Agent-Based Decision Support System", ActaPolytechnicaHungarica, 4(1), pp. 127 – 138, 2007.
- [11] Z. Udin, "Collaborative Supply Chain Management:The Hybrid Knowledge-Based Development Approach of Suppliers-Customers Perspective", Operations and Supply Chain, Vol. 3 Issue 2, pp. 130-147, 2008

Study of the Effect of Substrate Materials on the Performance of UWB Antenna

¹D.Ujwala, ²D.S.Ramkiran, ³N.Brahmani, ³D.Sandhyarani, ³K.Nagendrababu

¹ Assistant Professor, Department of ECE, K L University

² Associate Professor, Department of ECE, K L University

³ Students, B.Tech, Department of ECE, K L University

Abstract:

In this paper, a compact Ultra Wide Band antenna prototyped on FR4 Substrate is proposed and analyzed. The antenna is fed by linearly tapered Co-planar waveguide (CPW) transmission line. The parametric study is first performed on the feed of different substrate materials. The simulated results of proposed antenna has an advantages of low power consumptions, security systems, tracking applications, low data rate and low complexity. The simulation results for the voltage standing wave ratio (VSWR), Return loss, Radiation pattern and Impedance matching are in good agreement with the measurements. Moreover the Ultra wide band antennas enable the user to achieve a lower visual profile, lower radar cross sections (RCS) and a lower space. The model is analyzed for different substrate thicknesses using Finite Element Method based Ansoft High Frequency Structure Simulator v.13.

Index Terms: CPW, FCC, VSWR, UWB.

I. INTRODUCTION

Over the years, several studies used various antenna structures in Ultra wideband antenna design. The UWB antenna, which is an essential part of the UWB system. UWB also refers to a broad frequency range encompassing many narrow band frequencies, requires UWB antennas to transmit and receive throughout all narrow band frequencies in the range. However, the allocated frequency band for the UWB is 3.1-12.6 GHz [1] in between there exists a several wireless frequency bands such as WIMAX operates at 3.3-3.7 GHz and 5.8 GHz, IEEE 802.11a, WLAN operates at 5.15-5.35 and 5.725-5.825 GHz, downlink of X band satellite communication operates at 7.25-7.75 GHz and ITU services operates at 8.025-8.4 GHz.

The conventional method is to cutting a slot on the patch, inserting a slit on patch. The typical shapes of the patch antenna are circular, ellipse [2],[3] and rectangular [4],[5]. The main objective of this paper is to design UWB with different substrate materials. Here, we are going to use fr4 as a best substrate material as it gave best results regarding utilization of band width, resonating frequency and return loss. FR4 have good fabrication process, good electrical insulator as its features. Fr4 is also used in relays, switches, washers and transformers. Here we are going to use CPW feed. CPW is a transmission line system consisting of a central current carrying trace on top of substrate. Coplanar with side grounds extending beyond a symmetric gap to either side of the trace. Here we are going to use finite ground transmission line [6]. CPW has the same advantage as micro strip, in that the signal is carried on an exposed surface trace, on which surface-mount components can be attached and has little parasitic losses between surface mounted components and an underlying ground plane. Both the radiating patch and the ground plane are beveled to cover the entire UWB band from 3.1 to 12.6 GHz with VSWR less than 2. Characteristics of the proposed antenna are simulated using HFSS.

II. ANTENNA DESIGN

The proposed antenna has dimensions of 26mm x 31.8 x 1.6mm. It is prototyped on FR4 substrate of with dielectric constant, $\epsilon_r = 4.4$ and fed by Coplanar Waveguide transmission line. The Geometrical parameters are shown in Figure 1. The model consists of a circular patch of radius 10mm. The gap between ground plane and patch is 0.4mm. To increase the performance of antenna two identical trapezoidal ground planes are designed. The antenna parameters are as follows: $L_{sub}=31.8\text{mm}$, $W_{sub}=26\text{mm}$, $R_1=10\text{mm}$, $L_1=8\text{mm}$, $L_2=10\text{mm}$, $L_3=10.8\text{mm}$, $W_1=4.3\text{mm}$, $g=0.4\text{mm}$, $W_f=2.6\text{mm}$.

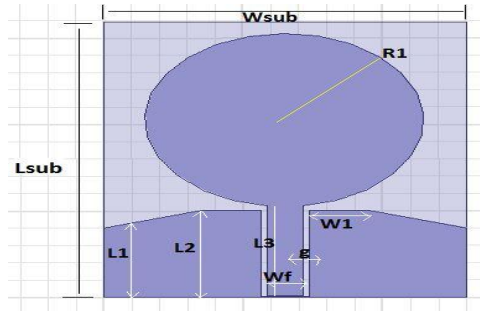


Figure 1: Proposed UWB Antenna Model

The antenna with the proposed geometry is analyzed using High Frequency Structure Simulator. It exhibits a Voltage Standing Wave Ratio (VSWR) of less than 2 in the operating frequency range with less Return Loss and acceptable Gain quasi omni-directional and bi-directional radiation patterns. A comparative analysis is made by varying the substrate materials and its effect on Return Loss is observed.

III. RESULTS ANALYSIS

A CPW fed Ultra Wide Band antenna with a Circular shaped patch is simulated using HFSS. By varying the substrate materials, the variations in Return Loss are observed and shown in Figure 2. Among the substrate materials FR4, Teflon, Rogers RT/Duroid, Quartz, Polystyrene and Neltec, wide operating bandwidth is obtained for FR4 substrate.

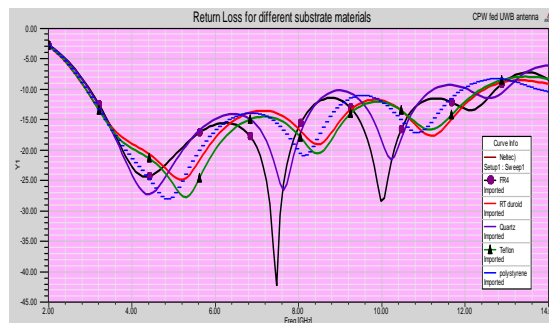


Figure 2: Return Loss curves for different substrate materials

For different substrate materials, the corresponding bandwidth, resonant frequencies and their Return Losses are shown in Table 1. The operating bandwidth of UWB antenna with FR4 Substrate is 9.745GHz from 2.9980GHz – 12.7350GHz and resonated at frequencies 4.3356GHz, 7.4765GHz, 9.9732GHz, 12.1477GHz with a corresponding Return Loss of -24.3854dB, -42.2670dB, -28.4086dB, -13.4235dB. The Frequency versus Return Loss is shown in figure 3.

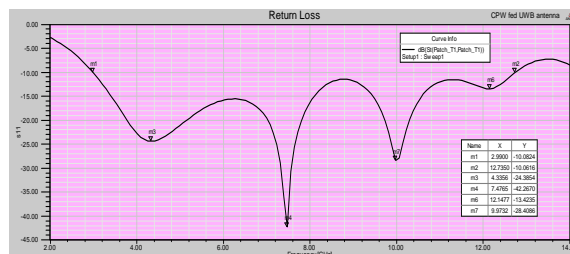


Figure 3: Frequency vs. Reflection Coefficient

Figure 4 shows the Voltage Standing Wave Ratio plot and desirable VSWR is less than 2 and the proposed design has VSWR<2 in the entire operating range. VSWR is a function of Reflection Coefficient and it describes the power reflected from the antenna. The VSWR values at the resonant frequencies are 1.13, 1.02, 1.08 and 1.54 respectively.

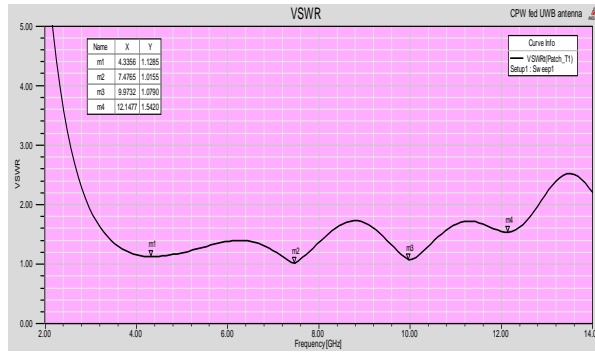


Figure 4: VSWR vs. Frequency

The impedance of an antenna relates voltage to the current at the input to the antenna and hence called as Input Impedance. The input impedance in smith chart is shown in Figure 5. The proposed model achieved an impedance bandwidth of 21%.

Material	Dielectric Constant	Band Width (GHZ)	Resonant Frequency (GHZ)	Return loss (dB)
FR4	4.4	9.745 (2.9980-12.7350)	4.3356	-24.3854
			7.4765	-42.2670
			9.9732	-28.4086
			12.1477	-13.4235
TEFLON	2.1	9.4893 (2.9000-12.3893)	5.3020	-27.7461
			8.4430	-20.5721
			11.1812	-16.6554
ROGERS RT DUROID	2.2	9.552 (2.8980-12.4500)	5.2215	-24.8585
			8.4430	-19.0736
			11.1812	-17.6819
QUARTZ	3.78	8.28 (2.9700-12.1200)	4.4161	-27.2814
			7.6376	-26.6020
			10.2148	-21.5166
POLYSTYRENE	2.6	9 (2.9350-13.8230)	4.8993	-28.0574
			8.2013	-20.8018
			10.8591	-17.1622
NELTECH	3	8.91 (2.9400-12.8000)	4.5772	-28.2154
			7.9597	-24.1389
			10.6174	-21.4509

Table 1: Bandwidth, Resonant Frequencies and Return Loss for different substrate materials

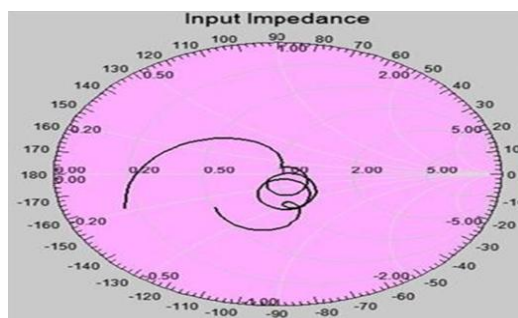


Figure 5: Input Impedance Smith Chart

Antenna gain is often related to the gain of an isotropic radiator, resulting in units dBi. Antenna gain at all the Resonant Frequencies is observed and shown in Figure 6. Maximum Gain is of 4.5 dBi is obtained at 9.9732 GHz.

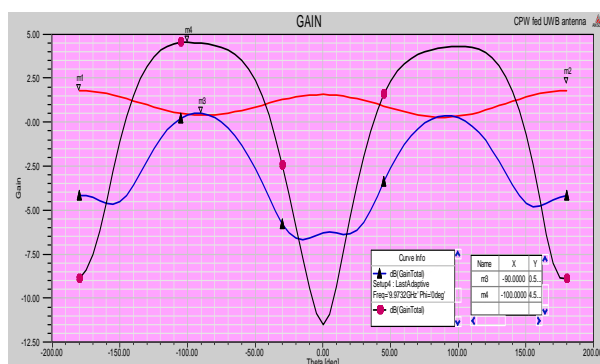
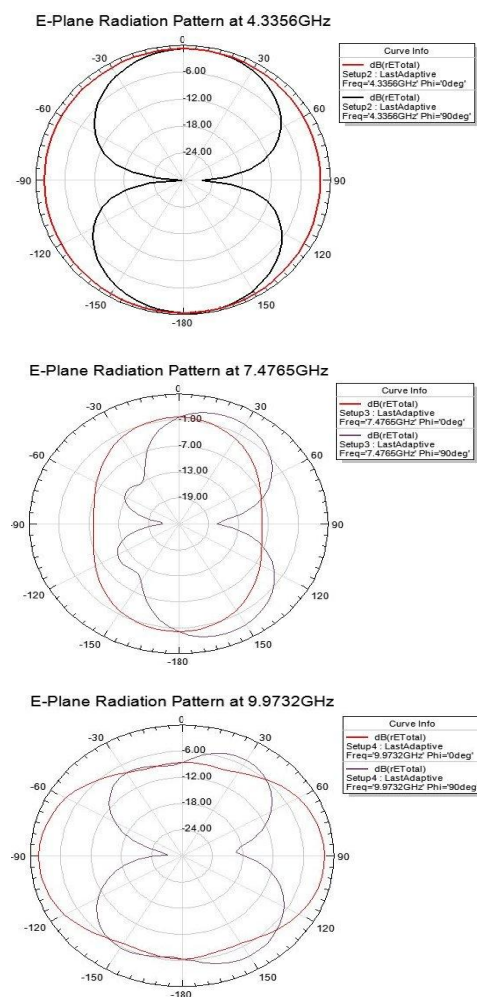


Figure 6: Gain vs. Frequency

E-Plane and H-Plane Radiation Patterns at the Resonant Frequencies 4.3356GHz, 7.4765GHz, 9.9732GHz, 12.1477GHz are shown in Figures 7 and 8 respectively. The far-zone electric field lies in the E-plane and far-zone magnetic field lies in the H-plane. The patterns in these planes are referred to as the E and H plane patterns respectively. Figure 7 shows the radiation pattern in E-plane for Phi=0 degrees and Phi=90 degrees for all the four resonant frequencies. Figure 8 shows the radiation pattern in H-plane for Theta=0 degrees and Theta=90 degrees for all the four resonant frequencies.



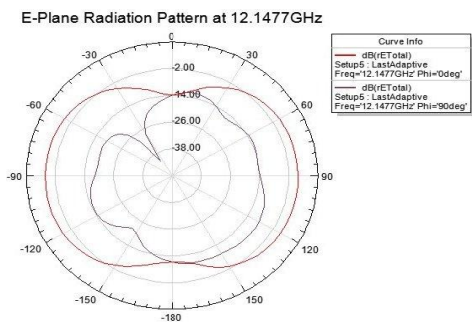


Figure 7: E-Plane Radiation Patterns at Resonant Frequencies

A Quasi Omni Directional Radiation pattern is observed from the simulated patterns.

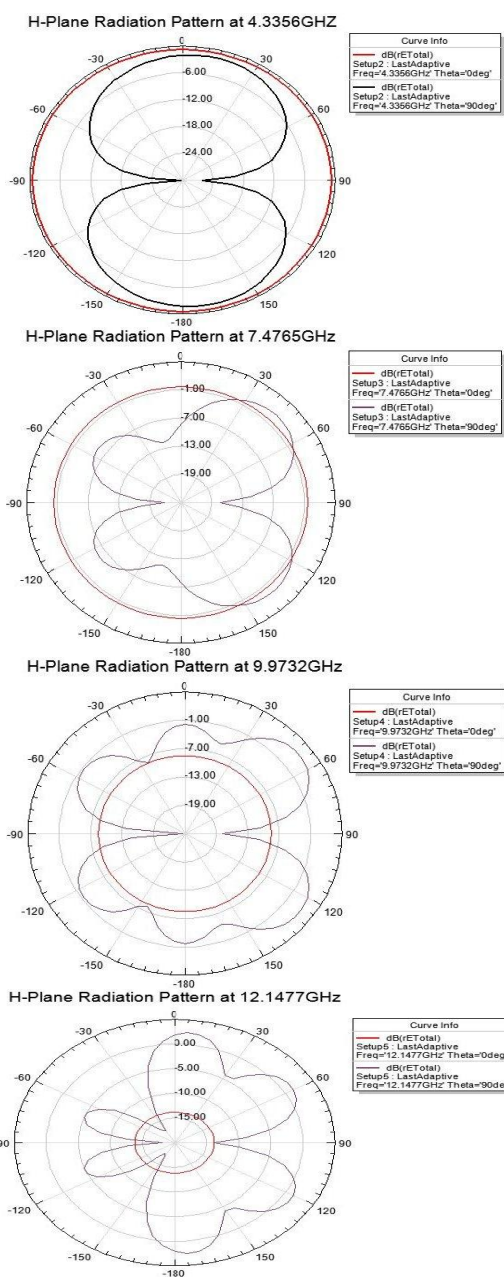


Figure 8: H-Plane Radiation Patterns at Resonant Frequencies

IV. CONCLUSION

A CPW fed Circular shaped patch with compact size is proposed and simulated. It can be used for number of wireless applications like WLAN, Wi-Fi, Wi-Max, Bluetooth etc. A comparative study is done on antenna by varying the substrate materials which are used in popular. Finally, it is observed that wide operating bandwidth of 9.745 GHz is obtained for FR4 substrate material. Hence, other parameters like Return Loss, VSWR etc. are analyzed for antenna prototyped on FR4 Substrate. The operating band is below -10dB and resonated at four frequencies. VSWR is less than 2. Peak Gain is 4.5 dBi. Quasi Omni-directional Radiation Pattern is observed.

V. ACKNOWLEDGMENT

The authors would like to express their gratitude towards the faculty of Department of ECE, K L University, for excellent encouragement during the tenure of work.

REFERENCES

- [1] Federal Communications Commission (FCC), Washington, DC, "First report and order in the matter of revision of Part 15 of the commission's rules regarding ultra-wideband transmission systems," ET-Docket 98-153, 2002.
- [2] N. P. Agrawal, G. Kumar, and K. P. Ray, "Wide-band planar monopole antennas," *IEEE Trans. Antennas Propag.*, vol. 46, no. 2, pp. 294–295, Feb. 1998.
- [3] L. Jianxin, C. C. Chiau, X. Chen, and C. G. Parini, "Study of a printed circular disc monopole antenna for UWB systems," *IEEE Trans. Antennas Propag.*, vol. 53, no. 11, pp. 3500–3504, Nov. 2005.
- [4] M. J. Ammann and Z.-N. Chen, "Wideband monopole antennas for multi-band wireless systems," *IEEE Antennas Propag. Mag.*, vol. 45, no. 2, pp. 146–150, Apr. 2003.
- [5] M. J. Ammann and Z. N. Chen, "A wide-band shorted planar monopole with bevel," *IEEE Trans. Antennas Propag.*, vol. 51, no. 4, pp. 901–903, Apr. 2003.
- [6] K. P. Ray and S. Tiwari, "Ultra wideband printed hexagonal monopole antennas," *Microwave, Antennas Propag.*, vol. 4, no. 4, pp. 437–445, 2010.

AUTHORS BIOGRAPHY



D. Ujwala, born in A.P, India in 1987. Completed B.Tech in 2008 from Koneru Lakshmaiah College of Engineering affiliated to Acharya Nagarjuna University, Guntur. Worked as Associate Software Engineer for KLU University from 2009-2010. Pursued M.Tech (Communication and Radar) from KLU. Presently working as Assistant Professor in KLU.

A Phased Approach to Solve the University Course Scheduling System

Rohini V,

Department of Computer Science, Christ University, Bangalore

Abstract:

Scheduling is an important activity of our life. Course scheduling is a complicated task faced by every university. This paper presents a phased approach to solve the constraint satisfaction problem of scheduling the resources. Here the idea is to use a genetic algorithm which is a good solution for the NP hard problems like scheduling. The paper starts by defining the problem of scheduling the courses in Christ University, Department of computer science and defining the various complicated constraints available. Then the problem model is explained with the set of resources like professors, rooms, labs, student etc. Finally the paper describes the different phases used to get the final well defined schedule[1].

Keywords: Constraints, Course scheduling, Genetic algorithm, NP hard problem, Phased, Hard constraints, Soft constraints

I. INTRODUCTION

Course scheduling in a university is a complex manual work done twice in a year. The problem involves fixing the time slots for the subjects, allocating the resources (lab, class rooms, projectors), allocating the staff satisfying the hard constraints and minimize the cost of a set of soft constraints. The constraints will not be common for all universities. It will be practised according to the constraints of the departments.

II. GENETIC ALGORITHM

In 1975, Holland developed the idea of genetic algorithm idea in his book “Adaptation in natural and artificial systems”[2]. He described how to apply the principles of natural evolution to optimization problems and built the first Genetic Algorithms. Holland’s theory has been further developed and now Genetic Algorithms (GAs) stand up as a powerful tool for solving search and optimization. An algorithm is a series of steps for solving a problem. A genetic algorithm is a problem solving method that uses genetics as its model of problem solving. It’s a search technique to find approximate solutions to optimization and search problems[4]. Basically, an optimization problem looks really simple. One knows the form of all possible solutions corresponding to a specific question. The set of all the solutions that meet this form constitute the search space. The problem consists in finding out the solution that fits the best, i.e. the one with the most payoffs, from all the possible solutions. If it’s possible to quickly enumerate all the solutions, the problem does not raise much difficulty. Genetic Algorithms work in a similar way, adapting the simple genetics to algorithmic mechanisms. GA handles a population of possible solutions. Each solution is represented through a chromosome, which is just an abstract representation. Coding all the possible solutions into a chromosome is the first part, but certainly not the most straightforward one of a Genetic Algorithm. A set of reproduction operators has to be determined, too. Reproduction operators are applied directly on the chromosomes and are used to perform mutations and recombinations over solutions of the problem. Appropriate representation and reproduction operators are really something determinant, as the behavior of the GA is extremely dependant on it.

Frequently, it can be extremely difficult to find a representation, which respects the structure of the search space and reproduction operators, which are coherent and relevant according to the properties of the problems. Selection is supposed to be able to compare each individual in the population. Selection is done by using a fitness function. Each chromosome has an associated value corresponding to the fitness of the solution it represents. The fitness should correspond to an evaluation of how good the candidate solution is. The optimal solution is the one, which maximizes the fitness function. Genetic Algorithms deal with the problems that maximize the fitness function. But, if the problem consists in minimizing a cost function, the adaptation is quite easy. Either the cost function can be transformed into a fitness function, for example by inverting it; or the selection can be adapted in such way that they consider individuals with low evaluation functions as better.

Once the reproduction and the fitness function have been properly defined, a Genetic Algorithm is evolved according to the same basic structure. It starts by generating an initial population of chromosomes. This first population must offer a wide diversity of genetic materials. The gene pool should be as large as possible so that any solution of the search space can be engendered. Generally, the initial population is generated randomly.

Then, the genetic algorithm loops over an iteration process to make the population evolve. Each iteration consists of the following steps:

- **SELECTION:** The first step consists in selecting individuals for reproduction.
- This selection is done randomly with a probability depending on the relative fitness of the individuals so that best ones are often chosen for reproduction than poor ones.
- **REPRODUCTION:** In the second step, offspring are bred by the selected individuals.
- For generating new chromosomes, the algorithm can use both recombination and mutation.
- **EVALUATION:** Then the fitness of the new chromosomes is evaluated.
- **REPLACEMENT:** During the last step, individuals from the old population are killed and replaced by the new ones.
- The algorithm is stopped when the population converges toward the optimal solution.
- The basic genetic algorithm is as follows:
- [start] Genetic random population of n chromosomes (suitable solutions for the problem)
- [Fitness] Evaluate the fitness $f(x)$ of each chromosome x in the population
- New population] Create a new population by repeating following steps until the New population is complete
- [selection] select two parent chromosomes from a population according to their fitness (the better fitness, the bigger chance to get selected).
- [crossover] With a crossover probability, cross over the parents to form new offspring (children). If no crossover was performed, offspring is the exact copy of parents.
- [Mutation] With a mutation probability, mutate new offspring at each locus (position in chromosome)
- [Accepting] Place new offspring in the new population.

2.1 A Simple Genetic Algorithm

- [Replace] Use new generated population for a further sum of the algorithm.
- [Test] If the end condition is satisfied, stop, and return the best solution in current population.
- [Loop] Go to step2 for fitness evaluation.

The Genetic algorithm process is discussed through the GA cycle in Fig. 1.

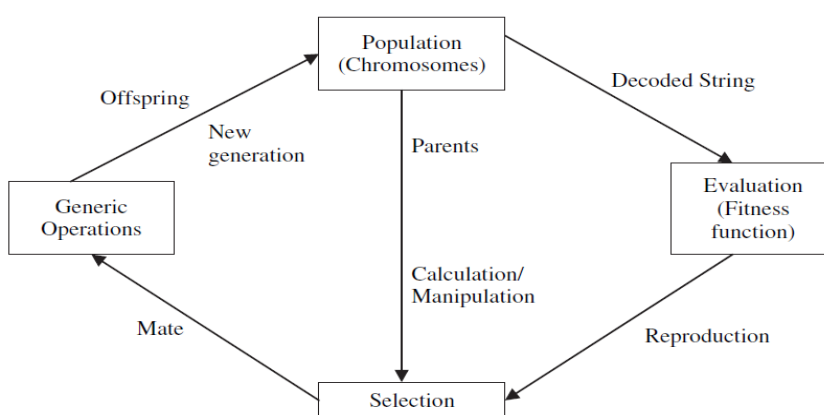


Fig.1 Genetic algorithm cycle

Reproduction is the process by which the genetic material in two or more parent is combined to obtain one or more offspring. In fitness evaluation step, the individual's quality is assessed. Mutation is performed to one individual to produce a new version of it where some of the original genetic material has been randomly changed. Selection process helps to decide which individuals are to be used for reproduction and mutation in order to produce new search points.

The flowchart showing the process of GA is as shown in Fig. 2.

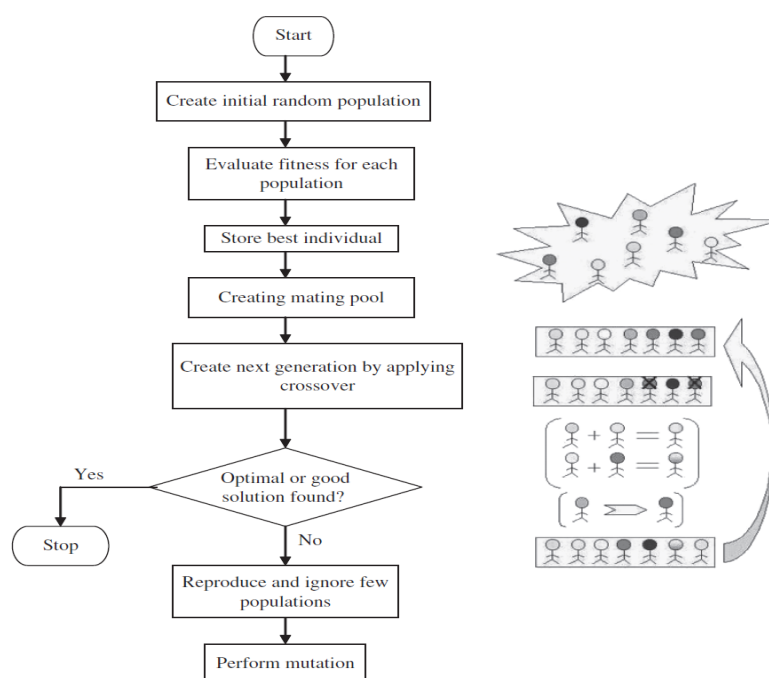


Fig.2 Genetic algorithm flowchart

Before implementing GA, it is important to understand few guidelines for designing a general search algorithm i.e. a global optimization algorithm based on the properties of the fitness landscape and the most common optimization method types:

- [1] **determinism:** A purely deterministic search may have an extremely high variance in solution quality because it may soon get stuck in worst case situations from which it is incapable to escape because of its determinism. This can be avoided, but it is a well-known fact that the observation of the worst-case situation is not guaranteed to be possible in general.
- [2] **nondeterminism:** A stochastic search method usually does not suffer from the above potential worst case "wolf trap" phenomenon. It is therefore likely that a search method should be stochastic, but it may well contain a substantial portion of determinism, however. In principle it is enough to have as much nondeterminism as to be able to avoid the worst-case wolf traps.

III. EMPIRICAL STUDY

In this section, a real world university course scheduling system is represented and is solved by the genetic algorithm described above. The Department of Computer Science, Christ University, Bangalore is a big department consisting of various courses in computer science as BCA, B.Sc., MCA, M.Sc. and consists of thirty professors. Scheduling the subjects to the various course in the allotted time slot and resources is a complex hard problem. The job involves of scheduling the various subjects to the course, various staff and resources adhering to the constraints stated below. The problem consists of the following entities:

Days, Timeslots, and Periods.: We are given a number of teaching days in the week (typically 6). Each day is split in a fixed number of timeslots of 6 (9 am to 4 pm, except 1 – 2 pm for lunch) and Saturdays only 4 hours (9 am – 1 pm). A period is a pair composed by a day and a timeslot. The total number of scheduling periods is the product of the days times the day timeslots.

Courses and professors: Each course consists of a fixed number of lectures to be scheduled in distinct periods; it is attended by given number of students, and is taught by a teacher. For each course there is a minimum number of days that the lectures of the course should be spread in, moreover there are some periods in which the course cannot be scheduled.

Rooms.: Each room has a capacity, expressed in terms of number of available seats. All rooms are equally suitable for all courses (if large enough). Rooms will have the resources like board(white / black), Projector etc. The timetables are feasible if and only if the following hard constraints are satisfied:

No instructor teaches more than one course at a given time.
Number of courses taught during any time slot should not exceed the maximum number of classrooms and labs available at that specified time.
Restrictions on the starting time, ending time, lunch time.
Lectures, seminars and labs of each group of students should not overlap.
Practical courses should run on two continuous time slots.
Class timings is 9 -4 with a break of lunch from 1-2 pm.
Subjects of other department should be accommodated in their possible time slot.
While two Elective of one course is happening, one more class should be in the lab.
The following soft constraints should be satisfied if possible:
There should be a gap of at least one hour in the schedule between courses taught by the same instructor.
Course should be spread over evenly throughout the week (Monday to Saturday).
All lectures of a particular course should be assigned to the same room.
Students can attend only one lecture at a time.
All first hour (9-10 am) should be allocated to different subject/faculty.
The problem is solved in a phased approach as follows :[5]
Phase I: Allot the subjects to the professors.
Phase II : Allot the labs to the courses..
Phase III: Assign lectures to time slots.
Phase IV: Assigns labs and tutorials to days and available time slots in the days.
The flow of data as allocation of subjects of the various courses to the professors are done and given to the committee. The scheduling committee is responsible for allotting the time slots, resources to the various courses satisfying the above mentioned constraints. According to the genetic algorithm method described in the paper and the relationship of those events and resources, a course scheduling system is developed. Finally, a solution which has the best fitness is obtained. Through analysis of the time table prepared, the constraints are satisfied and some soft constraints are not able to satisfy. It is demonstrated that the method in this problem is feasible and widely accepted.

IV. CONCLUSION

University course scheduling system is a NP hard problem[1].In this paper, we have discussed about the real life case study of how the timetabling is done with the constraints and the goal of optimization etc. Genetic algorithm, which is a commonly used evolutionary algorithm is applied to solve the problem described. During the process, genetic representation and a fitness function are defined according to the problem.

REFERENCES

- [1] Bratković, Z., Herman, T., Omrčen, V., Čupić, M., Jakobović, D.: University course timetabling with genetic algorithm: A laboratory exercises case study. In: Cotta, C., Cowling, P. (eds.) *EvoCOP 2009*. LNCS, vol. 5482, pp. 240–251. Springer, Heidelberg (2009)
- [2] J.H. Holland , *Adaptation in Natural and Artificial systems*, Cambridge, The MIT press, 1992
- [3] D.Goldberg, *Genetic Algorithm in Search, Optimization and Machine Learning*, Addison Wesley, 1989
- [4] S.N.Sivanandam and S.N.Deepa , *Introduction to Genetic Algorithms*, Springer, 2007
- [5] Minhaz Fahim Zibran, *A Multi-phase Approach to University Course Timetabling*, University of Lethbridge (Canada), 2007

Dynamic Neighbor Positioning In Manet with Protection against Adversarial Attacks

¹K. Priyadharshini , ² V. Kathiravan , ³S.Karthiga, ⁴A.Christopher Paul,

¹UG Scholar,SNS College Of Technology, INDIA

⁴Assistant Professor, Department Of Computer Science And Engineering,,SNS College Of Technology, INDIA

Abstract

In Mobile Ad-Hoc Networks, Routes May Be Disconnected Due To Dynamic Movement Of Nodes. Such Networks Are More Vulnerable To Both Internal And External Attacks Due To Presence Of Adversarial Nodes. These Nodes Affect The Performance Of Routing Protocol In Ad-Hoc Networks. So, It Is Essential To Identify The Neighbours In A MANET. The Proposed Scheme Identifies A Neighbour And Verifies Its Position Effectively.

I. INTRODUCTION

A MANET is an autonomous collection of mobile users that communicate over relatively bandwidth constrained wireless links. Since the nodes are mobile, the network topology may change rapidly and unpredictably over time. The network is decentralized; where all network activity including discovering the topology and delivering messages must be executed by the nodes themselves. The verification of node locations is an important issue in mobile networks, and it becomes particularly challenging in the presence of adversaries aiming at harming the system. In order to find the neighbour nodes and verify them various techniques are proposed.

1.1 Finding the position of a neighbour

Neighbour discovery deals with the identification of nodes with which a communication link can be established or that are within a given distance. An adversarial node could be securely discovered as neighbour and be indeed a neighbour (within some range), but it could still cheat about its position within the same range. In other words, SND lets a node assess whether another node is an actual neighbour but it does not verify the location it claims to be at .this is most often employed to counter wormhole attacks.

1.2 confirmation of claimed position

Neighbour verification schemes often rely on fixed or mobile trustworthy nodes, which are assumed to be always available for the verification of the positions announced by third parties. In ad hoc environments, however, the pervasive presence of either infrastructure or neighbour nodes that can be aprioristically trusted is quite unrealistic. Thus, a protocol is devised that is autonomous and does not require trustworthy neighbours.

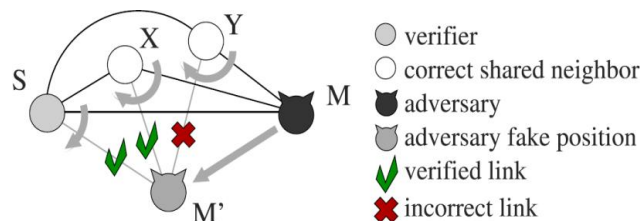


Figure1: Neighbour discovery in adversarial environment

1.3 Importance of Neighbour position update

An ad hoc network is a collection of wireless mobile hosts forming a temporary network without the aid of any established infrastructure or centralized administration. In such an environment, it is necessary for one mobile host to enlist the aid of other hosts in forwarding a packet to its destination, due to the limited range of each mobile host's wireless transmissions. In order to procure the position of other nodes while moving, an approach is proposed such a way that it helps in obtaining the position of a dynamic mobile node. This paper presents a protocol for updating the position of a node in dynamic ad hoc networks. The protocol adapts quickly to position changes when host movement is frequent, yet requires little or no overhead during periods in which hosts move less frequently

II. PROPOSED WORK

Nodes carry a unique identity and can authenticate messages of other nodes through public key cryptography. In particular, it is assumed that each node X owns a private key, k_x , and a public key, K_x , as well as a set of one-time use keys $\{k_{0X}; K_{0X}\}$. Nodes are correct if they comply with the NPV protocol, and adversarial if they deviate from it.

2.1 Distributed cooperative NPV scheme

A node S is called as a verifier, which discovers and verifies the position of its communicating neighbours. A verifier, S , can initiate the protocol at any time instant, by triggering the 4-step message exchange. The aim of the message exchange is to let S collect information it can use to compute distances between any pair of its communication neighbours. After the distances are calculated the nodes are classified as:

- Verified:* Node is in the claimed position.
- Faulty:* Node has announced an incorrect position.
- Unverifiable:* Insufficient information.

The verification tests aim at avoiding false negatives (i.e., adversaries announcing fake positions that are deemed verified) and false positives (i.e., correct nodes whose positions are deemed faulty), as well as at minimizing the number of unverifiable nodes. It also allows the verifier to independently classify its neighbours.

2.2 NPV Protocol

This protocol exchanges messages and verify the position of communicating nodes. Here four set of messages are exchanged they are:

- POLL message
- REPLY message
- REVEAL message
- REPORT message

POLL message

A verifier S initiates this message. This message is anonymous. The identity of the verifier is kept hidden. Here software generated MAC address is used. This carries a public key K'_S chosen from a pool of onetime use keys of S' .

REPLY message

A communication neighbour X receiving the POLL message will broadcast REPLY message after a time interval with a freshly generated MAC address. This also internally saves the transmission time. This also contains some encrypted message with S public key (K'_S). This message is called as commitment of X C_X .

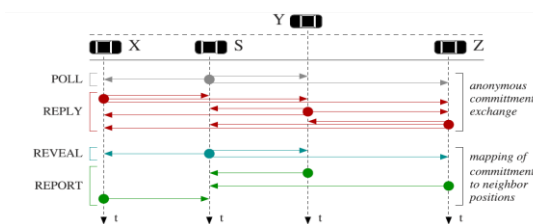


Figure 2: Message exchange

REVEAL message

The REVEAL message is broadcasted using Verifier’s real MAC address. It contains A map M_S , a proof that S is the author of the original POLL and the verifier identity, i.e., its certified public key and signature.

REPORT message

The REPORT carries X ’s position, the transmission time of X ’s REPLY, and the list of pairs of reception times and temporary identifiers referring to the REPLY broadcasts X received. The identifiers are obtained from the map M_S included in the REVEAL message. Also, X discloses its own identity by including in the message its digital signature and certified public key.

2.3 Position verification

To verify the position of a node following three tests is done, they are:

- Direct symmetry test
- Cross symmetry test
- The Multilateration Test

In the Direct Symmetry Test, S verifies the direct links with its communication neighbours. To this end, it checks whether reciprocal Time of Flight-derived distances are consistent with each other, with the position advertised by the neighbour, and with a proximity range R. In cross symmetry test information mutually gathered by each pair of communication neighbours are checked. This ignores nodes already declared as faulty by the DST and only considers nodes that proved to be communication neighbours between each other, i.e., for which ToF-derived mutual distances are available. In multilateration test, the unnotified links are tested. For each neighbour X that did not notify about a link reported by another node Y, with $X, Y \in W_S$ range. Once all couples of nodes have been checked, each node X for which two or more unnotified links exist is considered as suspect.

2.4 Dynamically updating neighbour position

The neighbour discovery protocol is based on nodes sending notification messages tagged with ID and their current region whenever they enter or leave a region. In particular, there are three types of messages:

- Leave
- Join
- Join_reply.

Table 1
Summary of notations

Notation	Description
F_{rcv}^+	Upper bound on a specific message being delivered
F_{ack}^+	Upper bound on an acknowledgment being received
k	Maximum size of the queue
t	Initial time

When a node is about to move into a new region, it broadcasts a leave message some time before leaving. This message indicates to its neighbouring nodes that they should begin tearing down the corresponding link if appropriate.

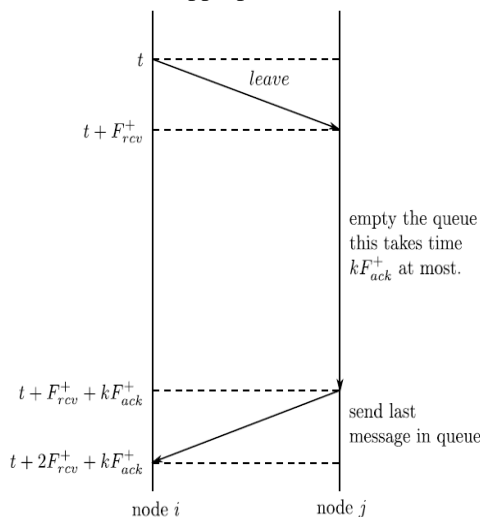


Figure 3: Leave message exchange

When a node enters a new region and determines that it is going to remain there for sufficiently long, it broadcasts a join message. This message indicates to the neighbours that they should start position verification for the corresponding link. It also serves as a request to learn the ids of neighbours.

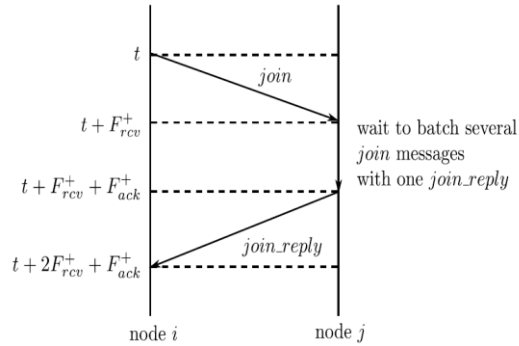


Figure 4: Join and join_reply message exchange

Nodes that receive a join message send a join_reply message in response so that the original node can learn their ids. The timing of these messages ensures that the proper semantics of the corresponding links are maintained. This means that the overhead for setting up and tearing down links is taken into account, and reliable message delivery is guaranteed.

III. SYSTEM MODEL

From the figure 5, the overall flow of the system can be understood. The positioning of neighbours is done and the nodes are classified. Later these positions that are claimed are verified. When a new node enters or leave the range they are updated .while updating also the same verification processes are done.

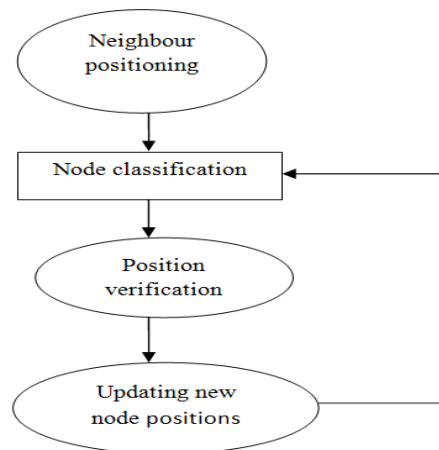


Figure 5: System flow

IV. ROBUSTNESS ANALYSIS OF THE PROPOSED SYSTEM

A single independent adversary cannot perform any successful attack against the NPV scheme. When the shared neighbourhood increases in size, the probability that the adversary is tagged as faulty rapidly grows to 1. Multiple independent adversaries can only harm each other, thus reducing their probability of successfully announcing a fake position. In coordinated attacks, it is the nature of the neighbourhood that determines the performance of the NPV scheme in presence of colluders. However, in realistic environments, our solution is very robust even to attacks launched by large groups of knowledgeable colluders. This system yields small advantage to the adversaries in terms of displacement. Finally, the overhead introduced by the NPV protocol is reasonable, as it does not exceed a few tens of Kbytes even in the most critical conditions.

V. CONCLUSION

Techniques for finding neighbours effectively in a non priori trusted environment are identified. The proposed techniques will eventually provide security from malicious nodes. The protocol is robust to adversarial attacks. This protocol will also update the position of the nodes in an active environment. The performance of the proposed scheme will be effective one.

REFERENCES

- [1] J.H. Song, V.Wong, and V.Leung, "Secure Location verification for Vehicular Ad-Hoc Networks," Proc.IEEE Globecom, Dec.2008 (adversarial environment).
- [2] M.Poturalski, P.Papadimitratos, and J- P.Hubaux, "Secure Neighbor Discovery in Wireless Networks: Formal Investigation of Possibility," proc.ACM Symp.Information, Computer and comm Security (ASIACCS), Mar.2008 (time based verification).
- [3] P.Papadimitratos, M.Poturalski, P.Lafourcade, D.Basin, S.Capkun, and J-P,Hubaux, "Secure Neighborhood Discovery: A Fundamental Element for Mobile Ad-Hoc Networks," IEEE comm.Magazine, vol.46, no.2, pp.132-139, Feb.2008 (neighbor discovery based on distance).
- [4] R.Shoki, M.Poturalski, G.Ravot, P.Papadimitratos, and J-P.Hubaux, "A Partial Secure Neighbor Verification Protocol for wireless Sensor Networks," Proc. Second ACM Conf.Wireless Network Security (Wisec), Mar.2009 (secure neighbor discovery).
- [5] S.Capkun and J-P.Hubaux, "Secure Positioning in Wireless Networks," IEEE J.Selected Areas in Comm., Vol.24, pp.221-232, Feb.2009 (triplet node verification).
- [6] Marco Fiore, Claudio Ettore Casetti, Carla-Fabiana Chiasserini, Panagiotis Papadimitratos. "Discovery and Verification of Neighbor Positions in Mobile Ad Hoc Networks". ieee transactions on mobile computing, vol. 12, no. 2, february 2013.
- [7] Alejandro Cornejo, Nancy Lynch, Saira Viqar, Jennifer L. Welch "Neighbor Discovery in Mobile Ad Hoc Networks Using an Abstract MAC Layer" November 20, 2009.

Solving Optimal Linear Time-Variant Systems via Chebyshev Wavelet

¹Hatem Elaydi , ²Atya A. Abu Haya
Faculty of Engineering, Islamic University, Gaza, Palestine

Abstract

Over the last four decades, optimal control problem are solved using direct and indirect methods. Direct methods are based on using polynomials to represent the optimal problem. Direct methods can be implemented using either discretization or parameterization. The proposed method here is considered as a direct method in which the optimal control problem is directly converted into a mathematical programming problem. A wavelet-based method is presented to solve the linear quadratic optimal control problem. The Chebyshev wavelets functions are used as the basis functions. Numerical examples are presented to show the effectiveness of the method, several optimal control problems were solved, and the simulation results show that the proposed method gives good and comparable results with some other methods.

Keywords: Chebyshev wavelet, optimal control problem, time-variant systems

I. INTRODUCTION

The goal of an optimal controller is the determination of the control signal such that a specified performance index is optimized, while at the same time keeping the system equations, initial condition, and any other constraints are satisfied. Many different methods have been introduced to solve optimal control problem for a system with given state equations. Examples of optimal control applications include environment, engineering, economics etc. The most popular method to solve the optimal control problem is the Riccati method for quadratic cost functions however this method results in a set of usually complicated differential equations [1]. In the last few decades orthogonal functions have been extensively used in obtaining an approximate solution of problems described by differential equations [2], which is based on converting the differential equations into an integral equation through integration. The state and/or control involved in the equation are approximated by finite terms of orthogonal series and using an operational matrix of integration to eliminate the integral operations. The form of the operational matrix of integration depends on the choice of the orthogonal functions like Walsh functions, block pulse functions, Laguerre series, Jacobi series, Fourier series, Bessel series, Taylor series, shifted Legendry, Chebyshev polynomials, Hermit polynomials and Wavelet functions [3].

This paper proposes a solution to solve the general optimal control problem using the parameterization direct method. The Chebyshev wavelets are used as new orthogonal polynomials to parameterize the states and control of the time-varying linear problem. Then, the cost function can be casted using the parameterized states and control. This paper is organized as follow: section 2 talks about the wavelets and scaling functions, section 3 discusses using Chebyshev wavelets to approximate functions, section 4 presents the formulation of problems, section 5 gives numerical examples, and section 6 conclude this study.

II. SCALING FUNCTIONS AND WAVELETS

Wavelets constitute a family of functions constructed from dilation and translation of a single function called the mother wavelet. When the dilation parameter a and the translation parameter b vary continuously [4], the following family of continuous

$$\Psi_{a,b}(t) = |a|^{-\frac{1}{2}} \Psi\left(\frac{t-b}{a}\right), \quad a, b \in \mathbb{R}, a \neq 0 \quad (1)$$

Chebyshev wavelets $\psi_{nm}(t) = \psi(k, m, n, t)$ have four arguments; $k = 1, 2, 3, \dots$, $n = 1, 2, 3, \dots, 2^k$, m is the order for Chebyshev polynomials and t is the normalized time. They are defined on the interval $[0, 1)$ by:

$$\Psi_{nm}(t) = \begin{cases} \frac{\alpha_m 2^{\frac{k}{2}}}{\sqrt{\pi}} T_m(2^{k+1}t - 2n + 1), & \frac{n-1}{2^k} \leq t \leq \frac{n}{2^k} \\ 0 & \text{elsewhere} \end{cases} \quad (2)$$

where

$$\alpha_m = \begin{cases} \sqrt{2} & m = 0 \\ 2 & m = 1, 2, \dots \end{cases}$$

Here, $T_m(t)$ are the well-known Chebyshev polynomials of order m , which are orthogonal with respect to the weight function $w(t) = \frac{1}{\sqrt{1-t^2}}$ and satisfy the following recursive formula [5]:

$$\begin{aligned} T_0(t) &= 1, \quad T_1(t) = t, \\ T_{m+1}(t) &= 2tT_m(t) - T_{m-1}(t), \quad m = 1, 2, 3, \dots \end{aligned} \quad (3)$$

The set of Chebyshev wavelets are an orthogonal set with respect to the weight function

$$\omega_n(t) = \omega(2^{k+1}t - 2n + 1) \quad (4)$$

3. Statement of the optimal control of linear time-varying systems

Find the optimal control that minimizes the quadratic performance index

$$J = \int_0^{t_f} (x^T Q x + u^T R u) dt \quad (5)$$

subject to the time-varying system given by

$$\dot{x}(t) = A(t)x(t) + B(t)u(t), \quad x(0) = x_0 \quad (6)$$

where

$x \in R^s$ is the state variables vector, $u \in R^r$ is the control vector, $x_0 \in R^s$ is the vector of initial conditions, $A(t)$ and $B(t)$ are time-varying matrices, Q is a positive semidefinite matrix, and R is a positive definite matrix.

III. OPTIMAL CONTROL PROBLEM

3.1 Control state parameterization

Approximating the state variables and the control variables by Chebyshev scaling functions, we get [5]

$$x_i(t) = \sum_{n=1}^{2^k} \sum_{m=0}^{M-1} \alpha^i_{nm} \phi_{nm}(t) \quad i = 1, 2, \dots, s \quad (7)$$

$$u_i(t) = \sum_{n=1}^{2^k} \sum_{m=0}^{M-1} b^i_{nm} \phi_{nm}(t) \quad i = 1, 2, \dots, r \quad (8)$$

We can write these two equations in compact form as :

$$x(t) = (\Phi^T(t) \otimes I_s) a$$

$$u(t) = (\Phi^T(t) \otimes I_r) b \quad (10)$$

Where I_s, I_r are $s \times s$ and $r \times r$ identity matrices respectively, $\Phi^T(t)$ is $N \times 1$, ($N = 2^k(M)$), vector of Chebyshev scaling function given by :

$$\Phi(t) = [\Phi_{1m-1}(t), \Phi_{2m-1}(t), \Phi_{3m-1}(t), \dots, \Phi_{2^k m-1}(t)]^T \quad (11)$$

$$\Phi_{im-1}(t) = [\phi_{i0}(t), \phi_{i1}(t), \dots, \phi_{iM-1}(t)] \quad (12)$$

and

$$a = [\alpha^1 \ \alpha^2 \ \dots \ \alpha^s]^T \quad (13)$$

$$\alpha^i = [a^i_{10} \ a^i_{11} \ \dots \ a^i_{1M-1} \ a^i_{20} \ \dots \ a^i_{2M-1} \ \dots \ a^i_{2^k 0} \ \dots \ a^i_{2^k M-1}] \quad i = 1, 2, \dots, s \quad (14)$$

$$b = [\beta^1 \ \beta^2 \ \dots \ \beta^r]^T \quad (15)$$

$$\beta^i = [b^i_{10} \ b^i_{11} \ \dots \ b^i_{1M-1} \ b^i_{20} \ \dots \ b^i_{2M-1} \ \dots \ b^i_{2^k 0} \ \dots \ b^i_{2^k M-1}] \quad i = 1, 2, \dots, r \quad (16)$$

a and b are vectors of unknown parameters have dimensions $sN \times 1$ and $rN \times 1$ respectively.

3.2 The product operational matrix of chebyshev wavelets

The following property of the product of two Chebyshev wavelets vectors [5] will also be used. Let

$$\Psi(t)\Psi^T(t)F = \tilde{F}\Psi(t), \quad (17)$$

Where \tilde{F} is $(2^k M) \times (2^k M)$ matrix. To illustrate the calculation procedure we choose

$M = 3$ and $k = 2$.

Thus we have: $F = [f_{10}, f_{11}, f_{12}, \dots, f_{40}, f_{41}, f_{42}]^T$
 $\Psi(t) = [\psi_{10}(t), \psi_{11}(t), \psi_{12}(t), \dots, \psi_{4,0}(t), \psi_{41}(t), \psi_{42}(t)]^T$

Then

$$\tilde{F} = \begin{bmatrix} \tilde{F}_1 & 0 & 0 & 0 \\ 0 & \tilde{F}_2 & 0 & 0 \\ 0 & 0 & \tilde{F}_3 & 0 \\ 0 & 0 & 0 & \tilde{F}_4 \end{bmatrix}$$

In general case \tilde{F} is a $(2^k M) \times (2^k M)$

$$\tilde{F} = \begin{bmatrix} \tilde{F}_1 & 0 & \dots & 0 \\ 0 & \tilde{F}_2 & \dots & 0 \\ \vdots & \vdots & \ddots & \vdots \\ 0 & 0 & \dots & \tilde{F}_{2^k} \end{bmatrix} \quad (18)$$

Where

$$\tilde{F}_i = \frac{2^{\frac{k}{2}}}{\sqrt{\pi}} \begin{bmatrix} f_{i0} & f_{i1} & f_{i2} & f_{i3} & \dots & f_{i,M-2} & f_{i,M-1} \\ f_{i1} & f_{i0} + \frac{1}{\sqrt{2}}f_{i2} & \frac{1}{\sqrt{2}}(f_{i1} + f_{i3}) & \frac{1}{\sqrt{2}}(f_{i2} + f_{i4}) & \dots & \frac{1}{\sqrt{2}}(f_{i,M-3} + f_{i,M-1}) & \frac{1}{\sqrt{2}}f_{i,M-2} \\ f_{i2} & \frac{1}{\sqrt{2}}(f_{i1} + f_{i3}) & f_{i0} + \frac{1}{\sqrt{2}}f_{i4} & \frac{1}{\sqrt{2}}(f_{i1} + f_{i5}) & \dots & \frac{1}{\sqrt{2}}f_{i,M-4} & \frac{1}{\sqrt{2}}f_{i,M-3} \\ \vdots & \vdots & \vdots & \ddots & \dots & \vdots & \vdots \\ \dots & \dots & \dots & f_{i0} + \frac{1}{\sqrt{2}}f_{i,\mu} & f_{i1} + \frac{1}{\sqrt{2}}f_{i,\mu+1} & \dots & \frac{1}{\sqrt{2}}f_{i,\nu} \\ \dots & \dots & \dots & f_{i1} + \frac{1}{\sqrt{2}}f_{i,\mu+1} & f_{i0} & \vdots & \vdots \\ \dots & \dots & \dots & \dots & \dots & \dots & \dots \\ \dots & \dots & \dots & \dots & \dots & f_{i0} & \frac{1}{\sqrt{2}}f_{i1} \\ f_{i,M-1} & \frac{1}{\sqrt{2}}f_{i,M-2} & \dots & \dots & \dots & \frac{1}{\sqrt{2}}f_{i1} & f_{i0} \end{bmatrix}$$

$$\mu = \begin{cases} M - 2 & M \text{ even} \\ M - 1 & M \text{ odd} \end{cases}$$

$$\nu = \begin{cases} M/2 & M \text{ even} \\ \frac{M - 1}{2} & M \text{ odd} \end{cases} \quad (19)$$

3.3 Performance index approximation

To approximate the performance index, we substitute Eq. (9) and (10) into (5) to get [6]

$$J = \int_0^1 (a^T (\Phi(t) \otimes I_s) Q (\Phi^T(t) \otimes I_s) a + b^T (\Phi(t) \otimes I_r) R (\Phi^T(t) \otimes I_r) b) dt \quad (20)$$

It can be simplified as

$$J = \int_0^1 (a^T (\Phi(t) \Phi^T(t) \otimes Q) a + b^T (\Phi(t) \Phi^T(t) \otimes R) b) dt \quad (21)$$

Because of orthogonality of Chebyshev scaling function and using Lemma1 in chapter three

$$\int_0^1 \Phi(t) \Phi^T(t) dt = RR \quad (22)$$

$$\text{Then } J = a^T (RR \otimes Q) a + b^T (RR \otimes R) b \quad (23)$$

It can be wrote as

$$J = [a^T \quad b^T] \begin{bmatrix} RR \otimes Q & 0_{N_s \times N_r} \\ 0_{N_r \times N_s} & RR \otimes R \end{bmatrix} \begin{bmatrix} a \\ b \end{bmatrix} \quad (24)$$

To approximate the state equations we write equation (9) as

$$x = \sum_{i=1}^{2^k} \sum_{j=0}^{M-1} \phi_{ij}(t) \alpha_{ij} \quad (25)$$

Or

$$x = \Phi^T(t) [\alpha_{10} \alpha_{11} \dots \alpha_{1M-1} \alpha_{20} \dots \alpha_{2M-1} \alpha_{2^k 0} \dots \alpha_{2^k M-1}]^T \\ = \Phi^T(t) \alpha \quad (26)$$

Where $\alpha_{ij} = [a_{ij}^1 a_{ij}^2 \dots a_{ij}^s]$

The control variables (10) can be rewritten as

$$u = \sum_{i=1}^{2^k} \sum_{j=0}^{M-1} \phi_{ij}(t) \beta_{ij} \quad (27)$$

Or

$$u = \Phi^T(t) [\beta_{10} \beta_{11} \dots \beta_{1M-1} \beta_{20} \dots \beta_{2M-1} \beta_{2^k 0} \dots \beta_{2^k M-1}]^T \\ = \Phi^T(t) \beta \quad (28)$$

Where $\beta_{ij} = [b_{ij}^1 b_{ij}^2 \dots b_{ij}^r]$

3.4 Time varying elements approximation

Then we need to express $A(t)$ and $B(t)$ in terms of Chebyshev scaling functions. The approximation of $A(t)$ can be given by [6]:

$$A(t) = \sum_{i=1}^{2^k} \sum_{j=0}^{M-1} A_{ij} \phi_{ij}(t) \quad (29)$$

$$A(t) = [A_{10} \ A_{11} \dots A_{1M-1} \ A_{20} \dots A_{2M-1} \dots A_{2^k 0} \dots A_{2^k M-1}] \Phi(t) \quad (30)$$

Where A_{ij} is an $s \times s$ constant matrix of the coefficients of Chebyshev scaling function $\phi_{ij}(t)$. These constant matrices can be obtained as

$$A_{ij} = \int_{\frac{i-1}{2^k}}^{\frac{i}{2^k}} A(t) \phi_{ij}(t) dt \quad (31)$$

Similarly, $B(t)$ can be expanded via Chebyshev scaling functions as follows

$$B(t) = [B_{10} \ B_{11} \dots B_{1M-1} \ B_{20} \dots B_{2M-1} \dots B_{2^k 0} \dots B_{2^k M-1}] \Phi(t) \quad (32)$$

Where B_{ij} is an $s \times r$ constant matrix

3.5 Initial condition

The initial condition vector x_0 can be expressed via Chebyshev scaling function as

$$x_0 = \frac{\sqrt{\pi/2}}{2^{k/2}} (\Phi^T(t)) [\alpha_0^1 \ \alpha_0^2 \ \dots \ \alpha_0^s] \\ = \frac{\sqrt{\pi/2}}{2^{k/2}} (\Phi^T(t)) g_0 \quad (33)$$

where $g_0 = [\alpha_{10}^0 \ 0 \ \dots \ 0 \ \alpha_{20}^0 \ 0 \ \dots \ 0 \ \dots \ \alpha_{2^k 0}^0 \ 0 \ \dots \ 0]^T$

and $\alpha_{i0}^0 = [x_1(0) \ x_2(0) \ \dots \ x_s(0)]$

We multiply Eq. (33) by factor,

$$\delta = \frac{\sqrt{\pi}}{2^{\frac{k}{2}}}$$

because from Eq. (2) we can obtain

$$\Phi_{n0} = \frac{2^{k/2}}{\sqrt{\pi/2}}$$

To express the state equations in terms of the unknown parameters of the state variables and the control variables, Eq. (2) can be integrated as

$$x(t) - x_0 = \int_0^t A(\tau) x(\tau) d\tau + \int_0^t B(\tau) u(\tau) d\tau \quad (34)$$

By substituting (26), (28), (30), (32) and (33) into (34), we get

$$\begin{aligned} &\Phi^T(t)\alpha - \Phi^T(t)\delta g_0 \\ &= \int_0^t [A_{10} \dots A_{2^k M-1}] \Phi(t)\Phi^T(t)\alpha dt \\ &+ \int_0^t [B_{10} \dots B_{2^k M-1}] \Phi(t)\Phi^T(t)\beta dt \end{aligned} \tag{35}$$

But from (17) we have

$$[A_{10} \dots A_{2^k M-1}] \Phi(t)\Phi^T = \Phi^T \tilde{A} \tag{36}$$

$$[B_{10} \dots B_{2^k M-1}] \Phi(t)\Phi^T = \Phi^T \tilde{B} \tag{37}$$

where \tilde{A} and \tilde{B} are $sN \times sN$ and $sN \times rN$ constant matrices respectively. Substituting (36) and (37) into equation (35) gives

$$\Phi^T(t)\alpha - \Phi^T(t)\delta g_0 = \int_0^t \Phi^T \tilde{A}(t)\alpha dt + \int_0^t \Phi^T(t)\tilde{B}\beta dt \tag{38}$$

Using the integration operational matrix P of Chebyshev scaling function , we get

$$\Phi^T(t)\alpha - \Phi^T(t)\delta g_0 = \Phi^T(t)P^T \tilde{A}\alpha + \Phi^T(t)P^T \tilde{B}\beta \tag{39}$$

$$(\Phi^T(t) \otimes I_s)\alpha - (\Phi^T(t) \otimes I_s)\delta g_0 = (\Phi^T(t)P^T \otimes I_s)\tilde{A}\alpha + (\Phi^T(t)P^T \otimes I_s)\tilde{B}\beta \tag{40}$$

$$I_{Ns}\alpha - \delta g_0 = (P^T \otimes I_s)\tilde{A}\alpha + (P^T \otimes I_s)\tilde{B}\beta \tag{41}$$

3.6 Continuity of the state variables

To insure the continuity of the state variables between the different sections we must add constraints.

There are $2^k - 1$ points at which the continuity of the state variables have to ensured [8].

Theses points are :

$$t_i = \frac{i}{2^k} \quad i = 1, 2, \dots, 2^k - 1 \tag{42}$$

So there are $(2^k - 1)s$ equality constraints given by :

$$(I_s \otimes \Phi'(t))\alpha = 0_{(2^k-1)s \times 1} \tag{43}$$

Where

$$\Phi' = \begin{bmatrix} \phi_{1m-1}(t_1) & -\phi_{2m-1}(t_1) & 0 & 0 & 0 & \dots & 0 \\ 0 & \phi_{2m-1}(t_2) & -\phi_{3m-1}(t_2) & 0 & 0 & \dots & 0 \\ 0 & 0 & \phi_{3m-1}(t_3) & -\phi_{4m-1}(t_3) & 0 & \dots & 0 \\ \vdots & \vdots & \vdots & \vdots & \vdots & \dots & \vdots \\ 0 & 0 & 0 & \dots & 0 & \phi_{(2^k-1)m}(t_{2^k-1}) & -\phi_{(2^k-1)m}(t_{2^k-1}) \end{bmatrix} \tag{44}$$

Φ' is $(2^k - 1) \times (2^k M)$ matrix

IV. QUADRATIC PROGRAMMING PROBLEM TRANSFORMATION

Finally by combining the equality constraints (41) with (43) we get

$$\begin{bmatrix} (P^T \otimes I_s)\tilde{A} - I_{Ns} & (P^T \otimes I_s)\tilde{B} \\ (\Phi' \otimes I_s) & 0_{(2^k-1)s \times Nr} \end{bmatrix} \begin{bmatrix} \alpha \\ b \end{bmatrix} = \begin{bmatrix} -g_0 \delta \\ 0_{(2^k-1)s \times 1} \end{bmatrix} \tag{45}$$

We saw that the optimal control problem is converted into a quadratic programming problem of minimizing the quadratic function (24) subject to the linear constraints (45) and solved it using MATLAB program.

4.1 Numerical Example

Find the optimal control $u(t)$ which minimizes

$$J = \frac{1}{2} \int_0^1 (x^2 + u^2) dt$$

subject to $\dot{x} = tx + u$ $x(0) = 1$

We solved this problem for

$k = 2$ and $M = 3,4,5$, the optimal value we get as in Table (1) as shown

Table (1)

	$K = 2,$ $M = 3$	$K = 2,$ $M = 4$	$K = 2,$ $M = 5$
J	0.4848235986044	0.4842684350618	0.4842678105389

The optimal state and control variables are shown in Figures (1-3), we noticed from Figures (1 – 3) and from Table (1) that when we increase M we obtained at a good trajectories plots and at good results of performance index (J).

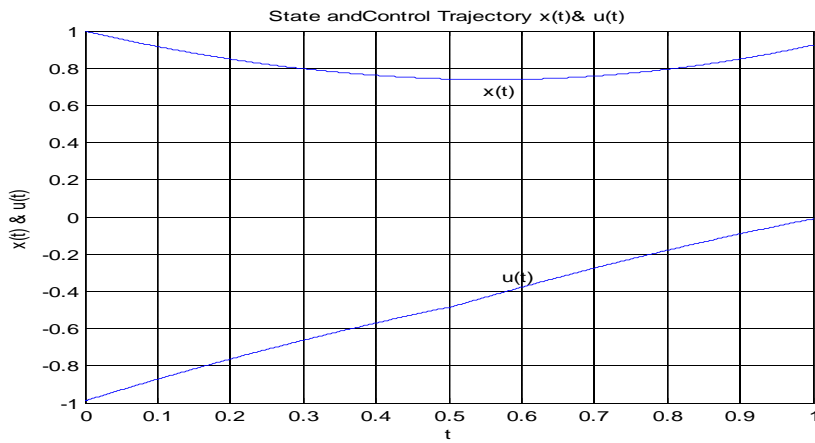


Figure (1) Optimal state and control $K=2$ $M=3$

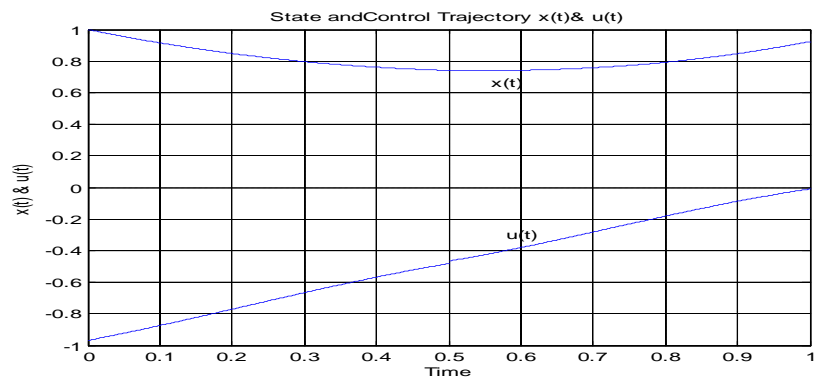


Figure (2) Optimal state and control $K=2$ $M=4$

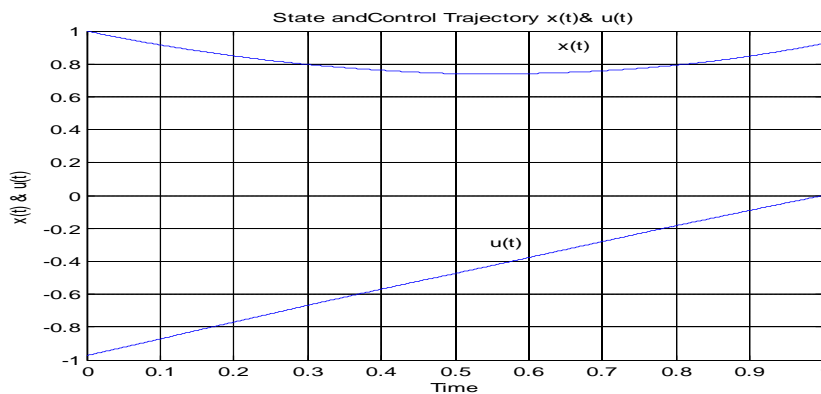


Figure (3) Optimal state and control $K=2$ $M=5$

Table (2)

Research name	Jaddu[6]	[7]	This research
<i>J</i>	0.48426760037684	0.48427022	0.484267810538982

Table (2) shows the comparison between our research and other researches to solve the previous problem , from the table we notice that our method is good compared with other methods. In this chapter we proposed a method to solve the optimal control problem time-varying systems using Chebyshev wavelet scaling function, we applied this method at a numerical example to see the effectiveness of the method and compared with other methods. We need to solve the optimal control problem time-varying systems because we must need it to solve the nonlinear optimal control problem in the next chapter.

V. CONCLUSION

In this paper, a numerical methods to solve optimal control problems for linear time-variant systems was proposed. This method was based on parameterizing the system state and control variables using a finite length Chebyshev wavelet. The aim of the proposed method is the determination of the optimal control and state vector by a direct method of solution based upon Chebyshev wavelet. An explicit formula for the performance index was presented. In addition, Chebyshev wavelet operational matrix of integration was presented and used to approximate the solution. A product operational matrix of Chebyshev wavelets was also presented and used to solve linear time-varying systems. Thus, the solution of the linear optimal control problem is reduced to a simple matrix-vector multiplication that can be solved easily using MATLAB. Numerical examples were solved to show the effectiveness and efficiency of the proposed method. The proposed method gave better or comparable results compared to other research. Future work can deal with using Chebyshev wavelet to solve nonlinear optimal control problems.

VI. REFERENCES

- [1] Kirk, D. Optimal Control Theory: An Introduction. Prentice-Hall, Englewood Cliffs, NJ. 1970.
- [2] Jaddu, H. Numerical methods for solving optimal control problems using Chebyshev polynomials. PHD Thesis. JAIST, Japan. 1998.
- [3] Mohammad Ali Tavallaei and Behrouz Tousi. Closed form solution to an optimal control problem by orthogonal polynomial expansion. American J. of Engineering and Applied Sciences. 2008.
- [4] E. Babolian, F. Fatahadeh. Numerical solution of differential equations by using Chebyshev wavelet operational matrix of integration. Applied Mathematics and Computation. 188. 417–426. 2007.
- [5] M. Ghasemi , M. Tavassoli Kajani. Numerical solution of time-varying delay systems by Chebyshev wavelets. Applied Mathematical Modelling. 35 5235–5244. 2011.
- [6] H. Jaddu. Optimal control of time-varying linear systems using wavelets. School of Information Science, Japan Advanced Institute of Science and technology. 1998.
- [7] G. Elnagar. State-control spectral Chebyshev parameterization for linearly constrained quadratic optimal control problems. Journal of Computational and Applied Mathematics. Vol. 79. 19-40. 1997.
- [8] Hatem Elaydi, Atya A. Abu Haya. Solving Optimal Control Problem for Linear Time-invariant Systems via Chebyshev Wavelet. International Journal of Electrical Engineering, 5:7.541-556. 2012.

Effect of Process Parameters on Performance Measures of Wire EDM for AISI A2 Tool Steel

¹S. B. Prajapati , ²N. S. Patel
¹P.G Student , , M.E (CAD/CAM) GEC Dahod, Gujarat
²Associate Professor, GEC Dahod, Gujarat

Abstract

Wire EDM is most progressive non-conventional machining process in mechanical industries. There are so many parameter affect the performance of Wire EDM. Few of them are investigated in this research paper. The effect of process parameter like Pulse ON time, Pulse OFF time, Voltage, Wire Feed and Wire Tension on MRR, SR, Kerf and Gap current is studied by conducting an experiment. Response surface methodology is used to analyze the data for optimization and performance. The AISI A2 tool steel is used as work piece material in the form of square bar.

Keyword: Wire Electrical Discharge Machining (WEDM), Taguchi Method, RSM and AISI A2.

I. INTRODUCTION

In mechanical industry, the demands for alloy materials having high hardness, toughness and impact resistance are increasing. Nevertheless, such materials are difficult to be machined by traditional machining methods. Hence, non-traditional machining methods including electrochemical machining, ultrasonic machining, electrical discharging machine (EDM) etc. are applied to machine such difficult to machine materials. WEDM is popular in all conventional EDM process, which used a wire electrode to initialize the sparking process. WEDM process with a thin wire as an electrode transforms electrical energy to thermal energy for cutting materials. With this process, alloy steel, conductive ceramics and aerospace materials can be machined irrespective to their hardness and toughness. Furthermore, WEDM is capable of producing a fine, precise, corrosion and wear resistant surface. A continuously travelling wire electrode made of thin copper, brass or tungsten of diameter 0.05-0.30 mm, which is capable of achieving very small corner radii. There is no direct contact between the work piece and the wire, eliminating the mechanical stresses during machining. The WEDM is a well-established machining option for manufacturing geometrically complex or hard material parts that are extremely difficult-to-machine by conventional machining processes. The non-contact machining techniques have been continuously evolving in a mere tool and die making process to a micro-scale application.

II. WORKING PRINCIPLE OF WEDM

The Wire EDM machine tool has one main worktable for work piece mounting an auxiliary table and wire feed mechanism. The movements of main table call axis X and Y. The wire feed mechanism consist of wire feeder which continuously fed wire along work table. The wire tension mechanism provides tension in wire and let it in straight position. The wire is fed in few possible speeds as meter per minute. Two wire guides located at the opposite sides of the work piece. The lower wire guide is stationary where as the upper wire guide, supported by the auxiliary table. The wire is connected to negative charge and work piece is connected to positive charge. Now series of electrical pulses generated by the pulse generator unit is applied between the work piece and the wire electrode so the spark is occurs. The material is removed from work piece by electro-erosion. The feed is given to the work table by servo motor but the wire guide remains stationary. Generally CNC controller is used here. To let out the removed material from work area, during the cutting operation continuous flashing water is applied. It is called dielectric fluid and continuously filtered to maintain its conductivity. To achieve taper cutting, the upper table is tilted in U-V direction. With combination of X-Y movement and U-V movement desire taper is produced.

III. LITERATURE RIVIEW

So many research papers and articles are survey on Wire EDM those are related to know the effect of process parameter on performance of process. The materials investigated on WEDM are most of HSS, other Tool material, Hot Die material, Cold Die material, Nickel alloys and Titanium alloys which are hard compare to other material. These materials are AISI M2, AISI D2, AISI D3, AISI D5, AISI H11, AISI 4140, SKD 11, En 16, En 19, En 31, En 32, 1040, 2379, 2738, Inconel, Ti alloys, Al alloys, 7131 cemented, Tungsten Carbide (WC) etc. Different author use different combination of process parameter. They analyze the experimental data by plotting Interaction graphs, Residual plots for accuracy and Response curves. Some other methods used by different author

for analysis of Taguchi’s DOE data regarding to EDM and WEDM are Regression analysis, Response Surface Methodology, Central Composite Design (CCD), Feasible-Direction Algorithm, SA algorithm, Pareto, Artificial Bee Colony (ABC), Grey Relational Analysis, Genetic Algorithm, Fuzzy clustering, Artificial Neural Network, Tabu-Search Algorithm, Principle component method etc. Most of the author used L_{27} Orthogonal Array. Generally the effect of Pulse ON time, Pulse OFF time, Spark gap set Voltage, Peak current, Flushing Pressure, Work piece height, wire tension and wire feed on the material removal rate, surface roughness, kerf and gap current is investigated.

IV. DESIGN OF EXPERIMENTS

4.1 SELECTION OF ORTHOGONAL ARRAY

Taguchi method is used as Design of Experiment. Taguchi Method. Genichi Taguchi, a Japanese scientist developed a technique based on Orthogonal Array of experiments. This technique has been widely used in different fields of engineering experimental works. The control factors considered for the study are Pulse-on, Pulse- off, Bed speed and Current. Four levels for each control factor will be used. Based on number of control factors and their levels, L_{27} orthogonal array (OA) was selected. Table-1 represents various levels of control factors and Table-2 experimental plan with assigned values. The values of constant parameters are as under.

Pulse Peak Current (IP)	210 A
Pulse Peak Voltage (VP)	2 volts
Flushing Pressure	12 kgf/cm ²
Work piece Material	Work piece Material

Table-1&2 Levels of various control factors

	Level 1	Level 2	Level 3
Pulse ON time – (A)	115	120	125
Pulse OFF time – (B)	45	50	55
Voltage – (C)	21	23	25
Wire Feed - (D)	4	6	8
Wire Tension - (E)	2	7	10

Table-2 Taguchi L_{27} OA

	(A)	(B)	(C)	(D)	(E)
1	115	45	21	4	2
2	115	45	21	4	7
3	115	45	21	4	10
4	115	50	23	6	2
5	115	50	23	6	7
6	115	50	23	6	10
7	115	55	25	8	2
8	115	55	25	8	7
9	115	55	25	8	10
10	120	45	23	8	2
11	120	45	23	8	7
12	120	45	23	8	10
13	120	50	25	4	2
14	120	50	25	4	7
15	120	50	25	4	10
16	120	55	21	6	2
17	120	55	21	6	7
18	120	55	21	6	10
19	125	45	25	6	2
20	125	45	25	6	7
21	125	45	25	6	10
22	125	50	21	8	2
23	125	50	21	8	7
24	125	50	21	8	10
25	125	55	23	4	2
26	125	55	23	4	7
27	125	55	23	4	10

4.2 SELECTION OF MATERIAL

An **AISI A2** is Air-Hardening tool steel which containing five percent chromium. They Replaces the oil hardening (O1 type) when safer hardening, less distortion and increased wear-resistance are required. They Provides an intermediate grade between the oil hardening and the high carbon, high chromium (D2) types. The Designations in other countries are as AFNOR Z 100 CDV 5 in France, DIN 1.2363 in Germany, JIS SKD 12 in Japan.

Table-3: Chemical Composition of AISI A2 Tool Steel

element	C	Mn	Si	Mo	Cr	V	Ni
%	0.95-1.05	0.95-1.05	0.95-1.05	0.95-1.05	0.95-1.05	0.95-1.05	0.95-1.05

4.3 EXPERIMENTAL WORK

The experiments were carried out on a wire-cut EDM machine (ELEKTRA SUPERCUT 734) of HI-TECH ENGINEERS installed at Gayatri CNC Wire cut, CTM, Ahmedabad, Gujarat, India shown in figure-1

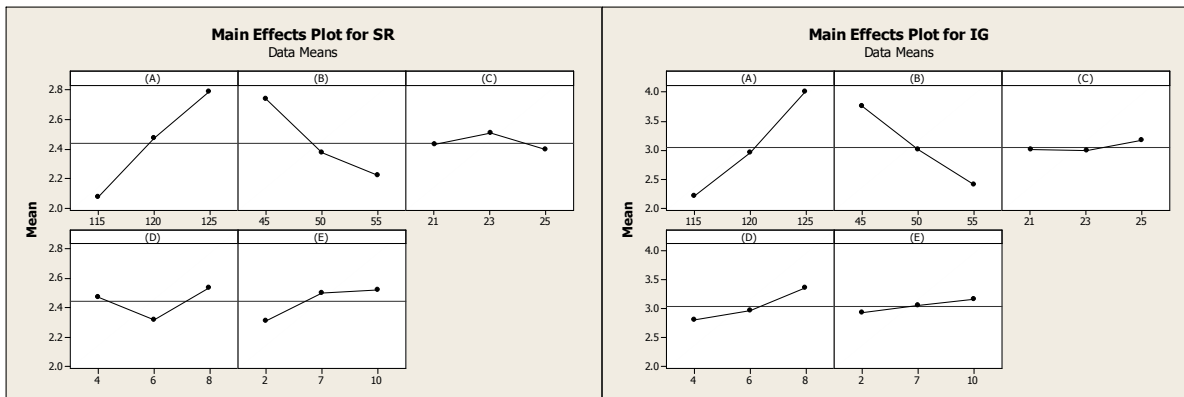
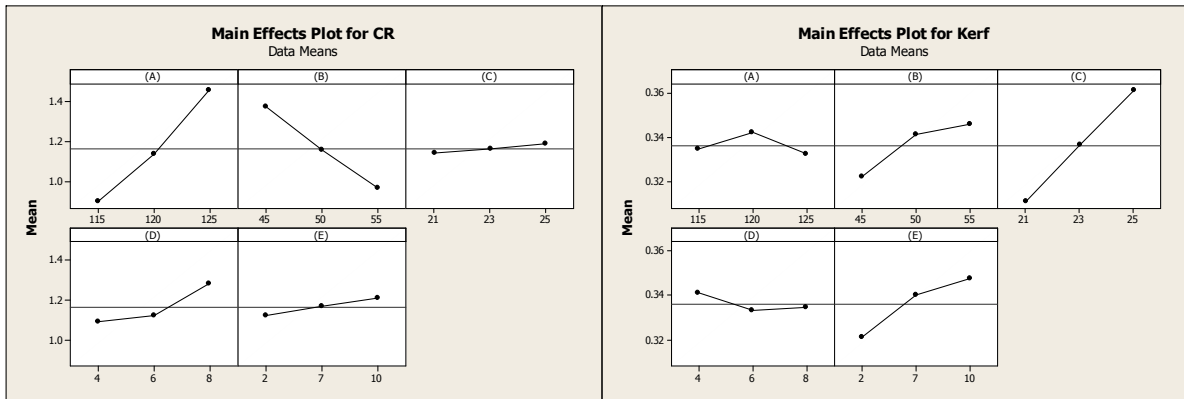
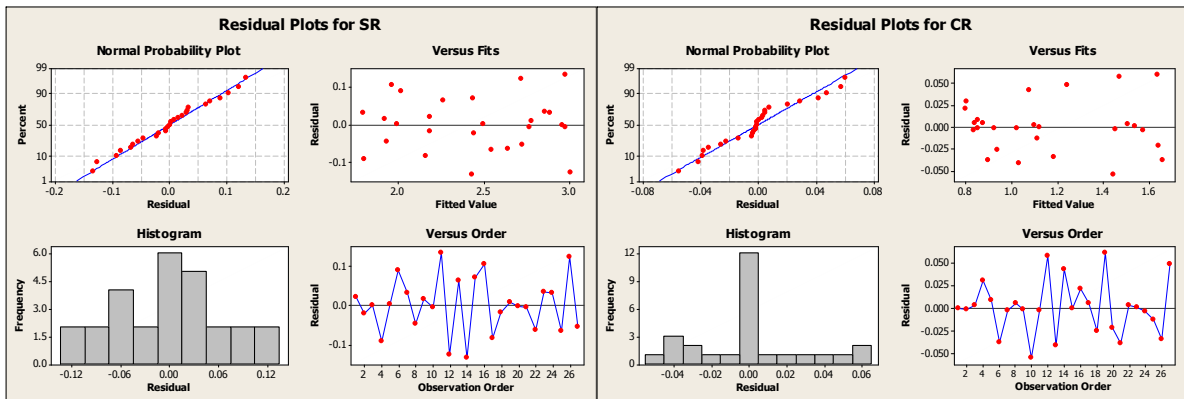
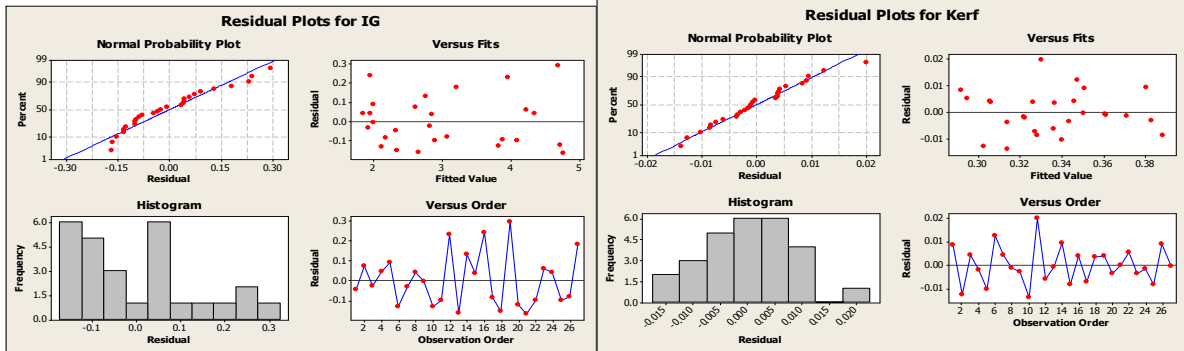


Figure- 1 Wire cut EDM Machine

SR NO	CR	SR	KERF	IG
1	0.92	2.21	0.30	2.3
2	1.02	2.42	0.29	2.7
3	1.10	2.50	0.31	2.8
4	0.83	1.71	0.32	1.9
5	0.86	2.00	0.33	2.1
6	0.86	2.11	0.36	2.0
7	0.83	1.83	0.35	1.9
8	0.84	1.89	0.37	2.0
9	0.85	1.94	0.38	2.0
10	1.39	2.76	0.30	3.7
11	1.45	3.11	0.35	3.8
12	1.53	2.88	0.33	4.2
13	0.99	2.33	0.36	2.5
14	1.12	2.30	0.39	2.9
15	1.12	2.51	0.38	2.9
16	0.82	2.07	0.31	2.2
17	0.88	2.08	0.32	2.1
18	0.91	2.17	0.34	2.2
19	1.70	2.79	0.33	5.0
20	1.62	2.96	0.34	4.6
21	1.62	2.97	0.35	4.6
22	1.51	2.58	0.30	4.0
23	1.54	2.89	0.31	4.3
24	1.57	2.92	0.32	4.4
25	1.10	2.48	0.32	2.8
26	1.15	2.84	0.36	3.0
27	1.29	2.67	0.36	3.4

V. ANALYSIS BY RESPONSE SURFACE METHODOLOGY (RSM)

The following graph developed by RSM in MINITAB software.



VI. CONCLUSION

It is clear from above graph that for cutting rate and surface roughness, the pulse ON and pulse OFF time is most significant. The spark gap set voltage is significant for kerf. The normal probability distribution for all measurement indicates high confidence.

REFERANCES

- [1] Anand Pandey and Shankar singh "review on Current research trends in variants of Electrical Discharge Machining" International Journal of Engineering Science and Technology Vol. 2(6), 2010, 2172-2191
- [2] K.H. Ho and S.T. Newman , "A State of the art electrical discharge machining (EDM)" International Journal of Machine Tools & Manufacture 43 (2003) 1287-1300
- [3] Michael F.W. Festing "Guidelines for the Design and Statistical Analysis of Experiments" ATLA 29, 427.446, 2001
- [4] J.L. Lin and C.L. Lin "grey-fuzzy logic for the optimization of the manufacturing process" Journal of Materials Processing Technology 160 (2005) 9-14
- [5] J. T. Huang and Y. S. Liao "Optimization of machining parameters of Wire-EDM based on Grey relational and statistical analyses" int. j. prod. res., 2003, vol. 41, no. 8, 1707-1720
- [6] Scott F. Millera, Chen-C. Koa, Albert J. Shiha and Jun Qub "investigation the wire electrical discharge machining of thin cross-sections" International Journal of Machine Tools & Manufacture 45 (2005) 1717-1725
- [7] Saurav Datta and Siba Sankar Mahapatra "Modeling, simulation and parametric optimization of wire EDM process using response surface methodology coupled with grey-Taguchi technique" International Journal of Engineering, Science and Technology, Vol. 2, No. 5, 2010, pp. 166-183
- [8] M Sadeghi, H Razavi, A Esmailzadeh, and F Kolahan, "Optimization of cutting conditions in WEDM process using regression modelling and Tabu-search algorithm" Proc. IMechE Vol. 225 Part B: J. Engineering Manufacture
- [9] A. Klinka, Y.B. Guoa,b*, F. Klockea, "Surface integrity evolution of powder metallurgical tool steel by main cut and finishing trim cuts in wire-EDM" Procedia Engineering 19 (2011) 178 - 183
- [10] V. Muthuraman, R. Ramakrishnan and L. Karthikeyan, "Influences of Process Variables during Wire Electric Discharge Machining of O1 Steel" 2012 published in European Journal of Scientific Research.
- [11] Miss Swati D. Lahane, Prof. Manik K. Rodge and Dr.Sunil.B. Sharma, "Multi-response optimization of Wire-EDM process using principal component analysis" IOSR Journal of Engineering (IOSRJEN) ISSN: 2250-3021 Volume 2, Issue 8 (August 2012), PP 38-47
- [12] Samar Singh and Mukesh Verma "Parametric Optimization of Electric Discharge Drill Machine Using Taguchi Approach" Journal of Engineering, Computers & Applied Sciences (JEC&AS) ISSN No: 2319-5606 Volume 1, No.3, December 2012
- [13] S Sivakiran, C. Bhaskar Reddy and C. Eswara reddy "Effect of Process Parameters on MRR in Wire Electrical Discharge Machining of En31 Steel" International Journal of Engineering Research and Applications (IJERA) ISSN: 2248-9622 www.ijera.com Vol. 2, Issue 6, November-December 2012, pp.1221-1226

Design Evaluation of a Two Wheeler Suspension System for Variable Load Conditions

¹Kommalapati. Rameshbabu , ²Tippa Bhimasankara Rao

¹PG Student, Department of Mechanical Engineering, Nimra Institute of Science and Technology

² HOD, Department of Mechanical Engineering, Nimra Institute of Science and Technology, Vijayawada, AP, INDIA

Abstract

A suspension system or shock absorber is a mechanical device designed to smooth out or damp shock impulse, and dissipate kinetic energy. The shock absorbers duty is to absorb or dissipate energy. In a vehicle, it reduces the effect of travelling over rough ground, leading to improved ride quality, and increase in comfort due to substantially reduced amplitude of disturbances. The design of spring in suspension system is very important. In this project a shock absorber is designed and a 3D model is created using Pro/Engineer. The model is also changed by changing the thickness of the spring. Structural analysis and modal analysis are done on the shock absorber by varying material for spring, Spring Steel and Beryllium Copper. The analysis is done by considering loads, bike weight, single person and 2 persons. Structural analysis is done to validate the strength and modal analysis is done to determine the displacements for different frequencies for number of modes. Comparison is done for two materials to verify best material for spring in Shock absorber.

Keywords: ANSYS. Damp Stock. Kinetic Energy. Ride Ouality. Pro-E.

I. INTRODUCTION

A shock absorber or damper is a mechanical device designed to smooth out or damp shock impulse, and dissipate kinetic energy.

1.1 Description

Pneumatic and hydraulic shock absorbers commonly take the form of a cylinder with a sliding piston inside. The cylinder is filled with a fluid (such as hydraulic fluid) or air. This fluid-filled piston/cylinder combination is a dashpot.

1.2 Explanation

The shock absorbers duty is to absorb or dissipate energy. One design consideration, when designing or choosing a shock absorber, is where that energy will go. In most dashpots, energy is converted to heat inside the viscous fluid. In hydraulic cylinders, the hydraulic fluid will heat up, while in air cylinders, the hot air is usually exhausted to the atmosphere. In other types of dashpots, such as electromagnetic ones, the dissipated energy can be stored and used later. In general terms, shock absorbers help cushion cars on uneven roads.

1.3 Applications

Shock absorbers are an important part of automobile and motorcycle suspensions, aircraft landing gear, and the supports for many industrial machines. Large shock absorbers have also been used in structural engineering to reduce the susceptibility of structures to earthquake damage and resonance. A transverse mounted shock absorber,

called a yaw damper, helps keep railcars from swaying excessively from side to side and are important in passenger railroads, commuter rail and rapid transit systems because they prevent railcars from damaging station platforms. The success of passive damping technologies in suppressing vibration amplitudes could be ascertained with the fact that it has a market size of around \$ 4.5 billion.



Fig.1: Rear shock absorber and spring of a BMW R75/5 motorcycle

II. Vehicle suspension

In a vehicle, it reduces the effect of traveling over rough ground, leading to improved ride quality, and increase in comfort due to substantially reduced amplitude of disturbances. Without shock absorbers, the vehicle would have a bouncing ride, as energy is stored in the spring and then released to the vehicle, possibly exceeding the allowed range of suspension movement. Control of excessive suspension movement without shock absorption requires stiffer (higher rate) springs, which would in turn give a harsh ride. Shock absorbers allow the use of soft (lower rate) springs while controlling the rate of suspension movement in response to bumps. They also, along with hysteresis in the tire itself, damp the motion of the unsprung weight up and down on the springiness of the tire. Since the tire is not as soft as the springs, effective wheel bounce damping may require stiffer shocks than would be ideal for the vehicle motion alone. Spring-based shock absorbers commonly use coil springs or leaf springs, though torsion bars can be used in torsional shocks as well. Ideal springs alone, however, are not shock absorbers as springs only store and do not dissipate or absorb energy. Vehicles typically employ springs or torsion bars as well as hydraulic shock absorbers. In this combination, "shock absorber" is reserved specifically for the hydraulic piston that absorbs and dissipates vibration.

2.1 Shock Absorber types

There are a number of different methods of converting an impact /collision into relatively smooth cushioned contact.

- Metal Spring
- Rubber Buffer
- Hydraulic Dashpot
- Collapsing safety Shock Absorbers
- Pneumatic Cylinders
- Self compensating Hydraulic

2.2 Model of shock absorber

- parts of shock absorber

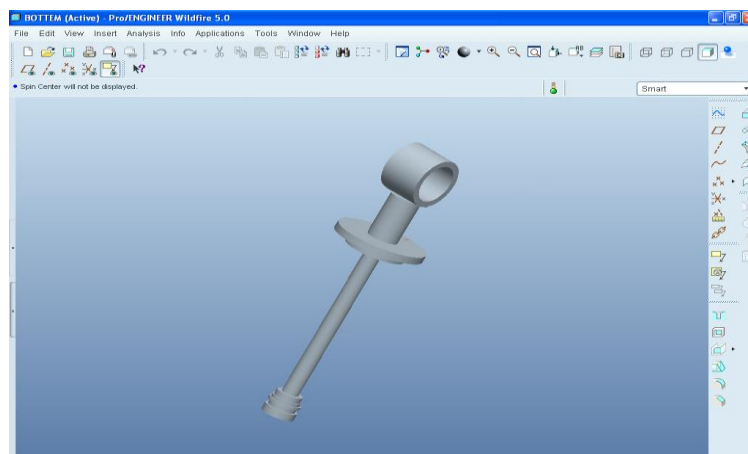


Fig.2: Bottom

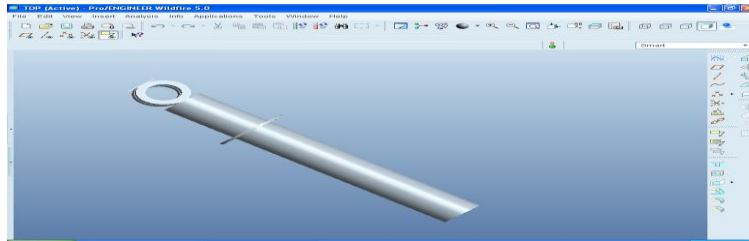


Fig.3: Top

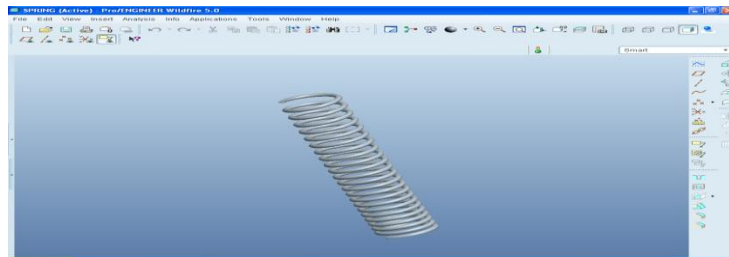


Fig.4: Spring

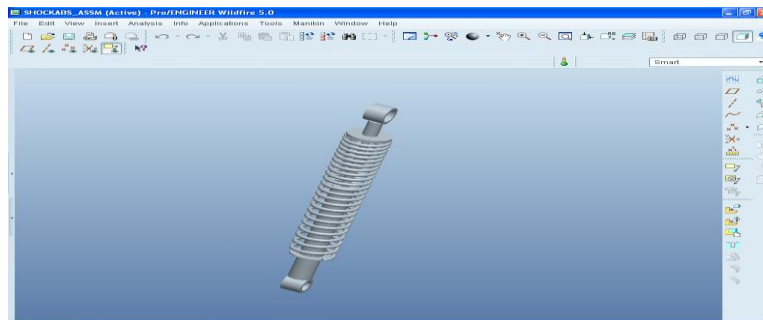


Fig.5: Total assembly

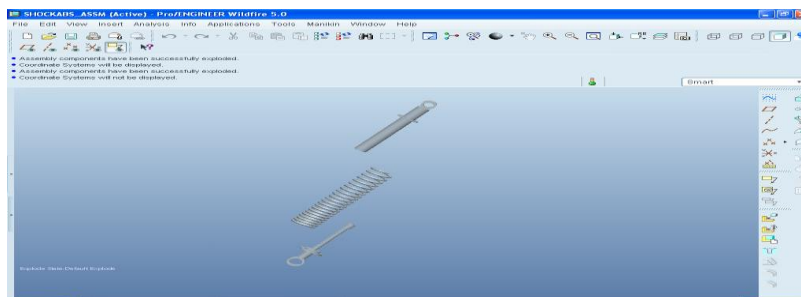


Fig.6: Explode view

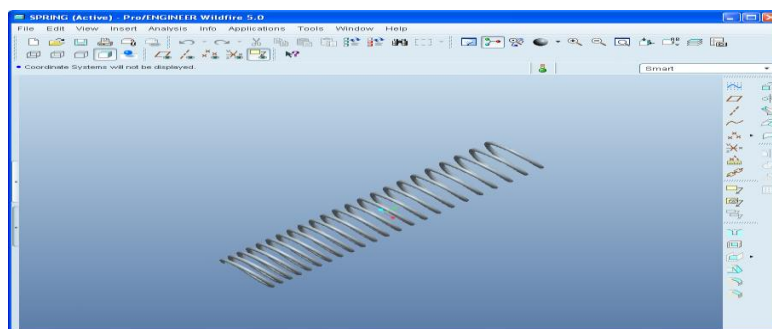


Fig.7: Modified spring of shock absorber

III. ANALYSIS OF SHOCK ABSORBER

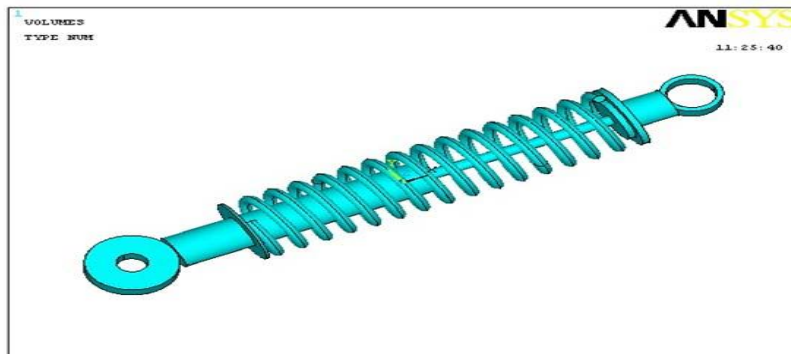


Fig.8: Imported Model from Pro/Engineer



Fig.9: Meshed Model

IV. RESULTS & DISCUSSION

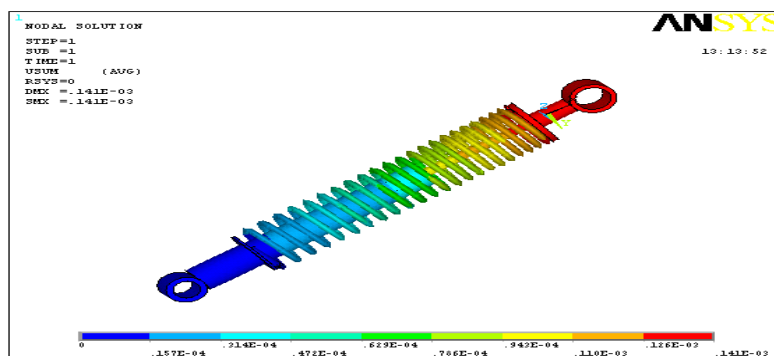
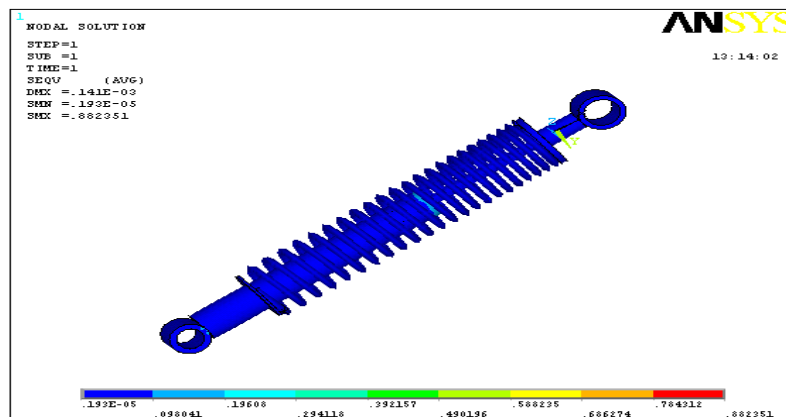


Fig.10: DOF Solution



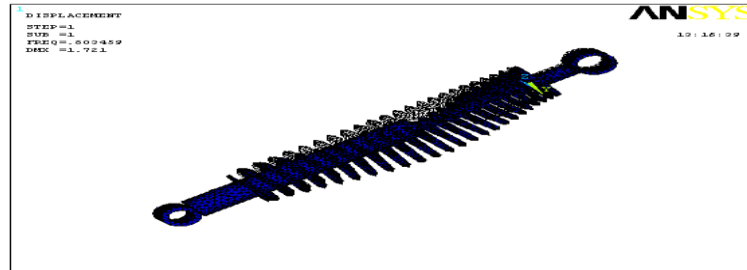


Fig.12: Deformed Shape

V. CONCLUSION

In our project we have designed a shock absorber used in a 150cc bike. We have modeled the shock absorber by using 3D parametric software Pro/Engineer. To validate the strength of our design, we have done structural analysis and modal analysis on the shock absorber. We have done analysis by varying spring material Spring Steel and Beryllium Copper. By observing the analysis results, the analyzed stress values are less than their respective yield stress values. So our design is safe. By comparing the results for both materials, the stress value is less for Spring Steel than Beryllium Copper. Also the shock absorber design is modified by reducing the diameter of spring by 2mm and structural, modal analysis is done on the shock absorber. By reducing the diameter, the weight of the spring reduces. By comparing the results for both materials, the stress value is less for Spring Steel than Beryllium Copper. By comparing the results for present design and modified design, the stress and displacement values are less for modified design. So we can conclude that as per our analysis using material Spring steel for spring is best and also our modified design is safe.

REFERENCES

- [1]. Machine design by r.s. khurmi
- [2]. Psg, 2008."design data," kalaikathir achchagam publishers, coimbatore, india
- [3]. Intelligent Systems": A Comparative Study Hindawi Publishing Corporation Applied Computational Intelligence and Soft Computing Volume 2011, Article ID 183764, 18 pages.
- [4]. Abbas Fadhel Ibraheem, Saad Kareem Shather & Kasim A. Khalaf, "Prediction of Cutting Forces by using Machine Parameters in end Milling Process", Eng.&Tech. Vol.26.No.11, 2008.
- [5]. S. Abainia, M. Bey, N. Moussaoui and S. Gouasmia." Prediction of Milling Forces by Integrating a Geometric and a Mechanistic Model", Proceedings of the World Congress on Engineering 2012 Vol III WCE 2012, July 4 - 6, 2012, London, U.K.
- [6]. Md. Anayet u patwari, a.k.m. nurul amin, waleed f. Faris, 'prediction of tangential cutting force in end milling of Medium carbon steel by coupling design of experiment and Response surface methodology'. Journal of mechanical engineering, vol. Me 40, no. 2, December 2009 Transaction of the mech. Eng. Div., the institution of engineers, Bangladesh.
- [7]. Smaoui, M.; Bouaziz,z. &Zghal,A., 'Simulation of cutting forces for complex surfaces in Ball-End milling', Int j simul model 7(2008) 2,93-105.

Analysis of Image Registration Using RANSAC Method

¹Riddhi J Ramani, ²Kanan P Patel

¹ Assistant prof. in Department of Electronics and communication Engineering, SITG

²Assistant prof. in Department of Electronics and communication Engineering, SITG

Abstract

Image registration is a prerequisite step prior to image fusion or image mosaic. It is a fundamental image processing technique and is very useful in integrating information from different sensors, finding changes in images taken at different times, inferring three- dimensional information from stereo images, and recognizing model-based objects. RANSAC is applied for removal the wrong matching points.

Keywords: Image Registration, RANSAC

I. INTRODUCTION

Image registration is multi spectral. Satellite image is a crucial problem for remote sensing applications, and remains challenging because of the inherent nonlinearity in intensity changes [1].Image registration is the process of overlaying two or more images of the same scene taken at different times, from different viewpoints, and by different sensors. It geometrically aligns two images - the reference and sensed images [2].Image processing which are possibly able to visualize objects inside the human body, are of special interest. Advances in computer science have led to reliable and efficient image processing methods useful in medical diagnosis, treatment planning and medical research. In clinical diagnosis using medical images, integration of useful data obtained from separate images is often desired. The images need to be geometrically aligned for better observation. This procedure of mapping points from one image to corresponding points in another image is called Image Registration. It is a spatial transform. The reference and the referred image could be different because were taken [3].

- At different times
- Using different devices like MRI, CT, PET, SPECT etc (multi modal).
- From different angles in order to have 2D or 3D perspective (multi temporal).

II. IMAGE REGISTRATION ALGORITHM

2.1 RANSAC

RANSAC (RANDOM SAMPLE CONSENSUS) is an iterative method to estimate parameters of a mathematical model from a set of observed data which contains outliers. It is a non-deterministic algorithm in the sense that it produces a reasonable result only with a certain probability, with this probability increasing as more iteration are allowed. The algorithm was first published by Fischler and Bolles in 1981.RANSAC is a re sampling technique that generates candidate solutions by using the minimum number observations (data points) required to estimate the underlying model parameters. As pointed out by Fischler and Bolles unlike conventional sampling techniques that use as much of the data as possible to obtain an initial solution and then proceed to prune outliers, RANSAC uses the smallest set possible and proceeds to enlarge this set with consistent data points [4].

The Algorithm Steps

- (1) Select the randomly the no of points required to determine the images.
- (2) Determine the how many points from the set of all points fit with a images.
- (3) Select the optimum parameters according to the final parameters output.



(a)



(b)



(c)

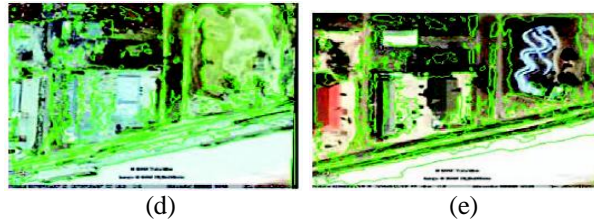


Figure 1 - Sample of results (a) Matched points after RANSAC, (b) The two images after registration, (c) The change mask, (d) Changes in first image, (e) Changes in second Image [5].

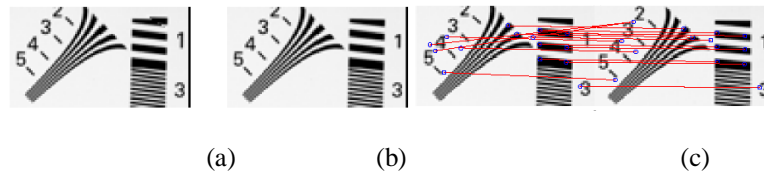


Figure 2 – (a) Input Image, (b) Reference Image, (c) RANSAC Point Matching [6].

Simulation Result More than 2 Input Images

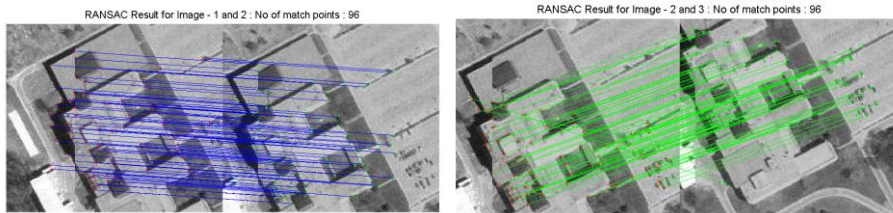


Figure 3 – Input image and reference image with output

Figure 4–Reference image and reference image with output

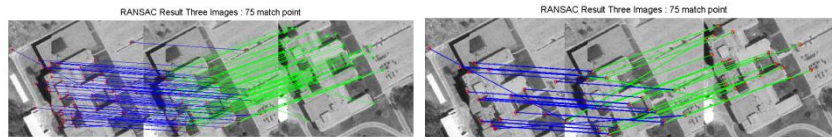


Figure 5– Input image and reference output and reference images with output

Figure 6 – Input image and reference and reference images with output

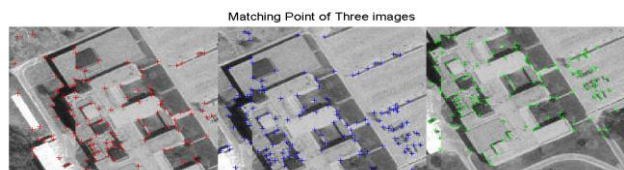


Figure 7 – Input image and reference and reference images with output

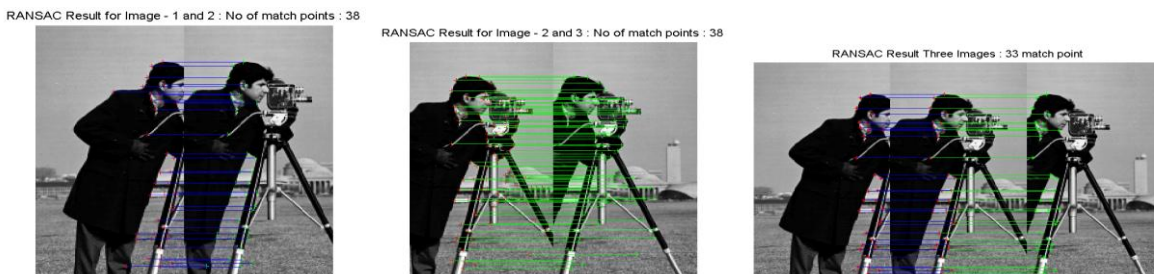


Figure 8 – Input image and reference output

Figure 9 – reference and reference and reference images with output

Figure 10– Input image and reference output

2.2 RANSAC Methods

RANSAC (RANDOM SAMPLE CONSENSUS)
This method checks the number of elements of the input feature point data set which are consistent with the model just chosen.
RANSAC repeats the two steps within a specified threshold until it finds the maximum number of elements within a model. It then selects this model and rejects mismatches.
In the transform fits a certain number of matches, it is considered a 'good' transform. Any points that do not match are discarded and then the transformation is recalculated using these new points.
In RANSAC when reinserted window it gives much better result with very short process.
RANSAC is much more efficient than the Hough transform when SIFT Features are used.
Nevertheless, for symmetric environments or when there is a lack of features, global localization with the current frame may be uncertain and the robot should rotate or move around.

III. CONCLUSION

These Algorithms recover good registered images for more than two input images using RANSAC methods. This algorithm is applicable when there is matching point between two images. Image registration algorithm using RANSAC method take few minutes to register images. So the delay execution is time is very less comparatively to other methods i.e. one minute This algorithms are applicable to stereo images to find feature points.

REFERENCES

- [1] Sang Rok Lee, "A Coarse-to-Fine Approach for Remote-Sensing Image Registration Based on a Local Method" International journal on smart sensing and intelligent system, vol.3, no.4, December 2010.
- [2] Barbara Zitova, Jan Flusser, "Image registration methods: a survey" Received 9 November 2001; received in revised form 20 June 2003; accepted 26 June 2003.
- [3] Medhav V. Wyawahare, Dr. Pradeep M. Patil, and Hemant K. Abhyanka "Image Registration Techniques: An overview", Vishwakarm Institute of Technology, Pune, Maharashtra state, India. Vol.2, No3, September 2009.
- [4] Konstantinos G. Derpanis, "Overview of the RANSAC Algorithm" May 13, 2010.
- [5] Mostafa Abdelrahman, Asem Ali, Aly A. Farag "Precise Change Detection In Multi-Spectral Remote Sensing Imagery Using SIFT-based Registration" Computer Vision & Image Processing Laboratory (CVIP), Univ. of Louisville, Louisville, KY, 40292.
- [6] Haidawati Nasir, Vladimir Stankovic, and Stephen Marshall, "IMAGE REGISTRATION FOR SUPER RESOLUTION USING SCALE INVARIANT FEATURE TRANSFORM, BELIEF PROPAGATION AND RANDOM SAMPLING CONSENSUS", 18th European Signal Processing Conference (EUSIPCO-2010) Aalborg, Denmark, August 23-27, 2010.

ANFIS Based Terminal Sliding Mode Control Design for Nonlinear Systems

Yi-Jen Mon

Department of Computer Science and Information Engineering, Taoyuan Innovation Institute of Technology, Chung-Li, Taoyuan, 320, Taiwan, R. O. C.

Abstract

In this paper, an adaptive network based fuzzy inference system (ANFIS) terminal sliding (TS) mode (ANFISTS) controller is developed to deal with the disturbed nonlinear system. This ANFISTS control system is composed of an ANFIS controller and a TS controller. The ANFIS controller is designed to do as a main controller and the TS controller is designed to cope with disturbances and uncertainties. In simulations, the nonlinear inverted pendulum system is illustrated to verify this proposed ANFISTS control methodology. The results possess better performances and robustness by comparisons with fuzzy control.

Keywords: Nonlinear system; adaptive network based fuzzy inference system (ANFIS) control; terminal sliding mode control

I. INTRODUCTION

The neural network control scheme has already been proposed as a design method for control of dynamic systems in recent years. The most useful property of neural networks is their ability to approximate linear or nonlinear mapping through learning. With this property, the neural network-based controllers have been developed to compensate the effects of nonlinearities and system uncertainties, so that the stability, convergence and robustness of the control system can be improved. The concept of fuzzy-neural control incorporating fuzzy logic into a neural network has recently grown into popular research topics [1]. The fuzzy neural network possesses advantages both of fuzzy systems and neural networks since it combines the fuzzy reasoning capability and the neural network on-line learning capability. Since the adaptive network based fuzzy inference system (ANFIS) [2] has been embedded in Matlab™ software to become a tool of more easily using and implementations. Meanwhile, there are many applications of ANFIS have been developed which can be searched in web site such as Google Scholar. The ANFIS is a hybrid learning algorithm which is to construct a set of input-output pairs of fuzzy if-then rules with appropriate membership functions. The outputs of ANFIS can be generated as a fuzzy associated memory (FAM).

Sliding mode (SM) controls or switching controls have been proposed by many researchers, recently [3]. This control scheme is based on the variable structure system (VSS) methodology and its goal is to drive the trajectories of the system's states onto a specified sliding surface and maintain the trajectories on this sliding surface continuously to guarantee the stability of system. In recent years, there have been some new mechanisms developed for improving SM control performance, such as the terminal sliding (TS) control [4]. The TS scheme has ability to eliminate the singularity problems of conventional sliding mode control [4]. In this paper, an intelligent method called ANFIS based terminal sliding mode (ANFISTS) control is developed for the design of the pendulum system. This ANFISTS control system comprises an ANFIS controller and a TS controller. The ANFIS controller is used to approach an ideal controller, and the TS controller is designed to compensate for the approximation error between the ANFIS controller and the ideal controller. Finally, a simulation is demonstrated to compare the performances and effectiveness for inverted pendulum system design between the proposed ANFISTS control and the traditional fuzzy control.

II. ANFIS BASED TERMINAL SLIDING MODE CONTROLLER DESIGN

Consider a nonlinear system includes disturbances:

$$\dot{\mathbf{x}} = \mathbf{f} + \mathbf{g}u + \mathbf{d} \quad (1)$$

where \mathbf{x} denotes the state vector, u denote the control input, \mathbf{d} denotes the unknown disturbances with a known upper bound and functions of \mathbf{f} and \mathbf{g} depend on \mathbf{x} .

Since the system parameters may be unknown or perturbed, the ideal controller u_{id} cannot be implemented. To overcome this, an ANFIS controller will be designed to approximate this ideal controller. In addition, a terminal sliding (TS) controller is designed to compensate for the approximation error between the ANFIS controller and the ideal controller of TS and to overcome the disturbances. Suppose that a first order terminal sliding function is defined as [4]

$$s = \dot{\mathbf{x}} + k\mathbf{x}^p \quad (2)$$

where $k > 0$ and $p > q$, all are positive constants. Then

$$\dot{s} = \ddot{\mathbf{x}} + kx^{p-1} \dot{\mathbf{x}} \quad (3)$$

The control law of ANFISTS control is defined as

$$u_i = u_{anfists} = u_{anfis} + u_{ts} \quad (4)$$

where u_{anfis} is the ANFIS controller and u_{ts} is the TS controller.

The inputs of the ANFIS controller are s and its derivative value of \dot{s} . u_{ts} is designed as $h \operatorname{sgn}(s)$, where h is a positive constant; and 'sgn' implies a sign function which can be replaced by a saturation function to avoid chattering effect.

The ANFIS is a hybrid learning algorithm which can generate Takagi-Sugeno (T-S) type fuzzy inference systems (FIS) to model a given training data. The principle of ANFIS is briefly described as follows [2].

$$\begin{aligned} R_i: & \text{If } x_1 \text{ is } A_{i1} \dots \text{and } x_n \text{ is } A_{in} \\ & \text{then } u_i = p_{i1}x_1 + \dots + p_{in}x_n + r_i \end{aligned} \quad (5)$$

where R_i denotes the i th fuzzy rules, $i=1, 2, \dots, j$; A_{ik} is the fuzzy set in the antecedent associated with the k th input variable at the i th fuzzy rule; and $p_{i1}, \dots, p_{in}, r_i$ are the fuzzy consequent parameters.

Based on the ANFIS, the output u can be got as

$$\begin{aligned} u &= \frac{w_1}{w_1 + \dots + w_j} u_1 + \dots + \frac{w_j}{w_1 + \dots + w_j} u_j \\ &= \bar{w}_1 u_1 + \dots + \bar{w}_j u_j \end{aligned} \quad (6)$$

where $\bar{w}_1 = \frac{w_1}{w_1 + \dots + w_j}, \dots, \bar{w}_j = \frac{w_j}{w_1 + \dots + w_j}$.

Because the fuzzy inference system is a T-S type, i.e. $u_i = p_{i1}x_1 + \dots + p_{in}x_n + r_i$, equation (6) can be expressed as

$$\begin{aligned} u &= \bar{w}_1 u_1 + \dots + \bar{w}_j u_j \\ &= (\bar{w}_1 x_1) p_{11} + \dots + (\bar{w}_1 x_n) p_{1n} + (\bar{w}_1) r_1 \\ &\quad + \\ &\quad \vdots \\ &\quad + (\bar{w}_j x_1) p_{j1} + \dots + (\bar{w}_j x_n) p_{jn} + (\bar{w}_j) r_j. \end{aligned} \quad (7)$$

The neural network learning algorithm developed in [2] can be applied to (7) directly. A neural network structure of ANFIS is shown in Fig. 1.

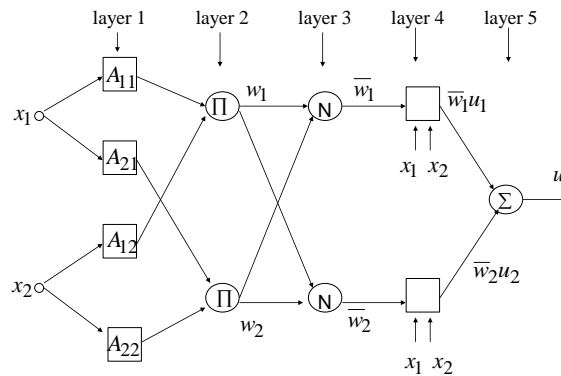


Fig. 1. Diagram of ANFIS architecture [2]

III. SIMULATION RESULTS

For nonlinear system, the equation as following famous pendulum system is considered: [5]

$$\begin{aligned}\dot{x}_1 &= x_2 + w_1 \\ \dot{x}_2 &= \frac{g \sin(x_1) - amlx_2^2 \sin(2x_1)/2 - a \cos(x_1)u}{4l/3 - aml \cos^2(x_1)} + w_2\end{aligned}\quad (8)$$

where parameters are $\mathbf{w} = [w_1 \ w_2]^T = [0.05 \cos(0.05t) \ 0.05 \sin(0.05t)]^T$, the initial states are $\pi/6, 0$. The x_1 denotes the angle of the pendulum from the vertical and x_2 is the angular velocity and $g = 9.8 \text{ m/sec}^2$ is the gravity constant, m is the mass of the pendulum, M is the mass of the cart, $2l$ is the length of the pendulum, and u is the forced applied to the cart. $A = 1/(m + M)$. The $m = 2.0 \text{ kg}$, $M = 8.0 \text{ kg}$ and $2l = 1 \text{ m}$. In these initial fuzzy rules, membership functions of x_1 and x_2 are given as $\pm \pi/4$. The learning rate is set as 0.1, $p = 3$ and $q = 1$. The designed FAM of ANFIS is shown in Fig. 2. By using this designed FAM of ANFIS controller and TS controller, the inverted pendulum can be controlled to be stable and robust. The simulation results are shown in Fig. 3 which is compared with fuzzy control. These simulation results demonstrate better performances and robustness of ANFISTS.

IV. CONCLUSION

An adaptive networks based fuzzy inference system (ANFIS) terminal sliding (TS) mode control denoted as ANFISTS controller for inverted pendulum system is developed in this paper; and is compared with fuzzy control system. In the simulations, the better performances and effectiveness of ANFISTS is possessed by comparison with that of the traditional fuzzy control.

V. ACKNOWLEDGMENT

This research is partially funded by the teachers' research project of the Taoyuan Innovation Institute of Technology, Taiwan, R. O. C.

REFERENCES

- [1] C. T. Lin, C. S. G. Lee, *Neural Fuzzy Systems: A Neural-Fuzzy Synergism to Intelligent Systems*, Prentice-Hall, Englewood Cliffs, NJ, 1996.
- [2] J. S. R. Jang, "ANFIS: adaptive-network-based fuzzy inference system," *IEEE Transactions on Systems, Man and Cybernetics*, Vol. 23, 1993, pp. 665-685.
- [3] Y. J. Mon, "H-infinity Fuzzy Sliding Parallel Distributed Compensation Control Design for Pendulum System," *Advanced Science, Engineering and Medicine*, Vol. 5, No. 7, pp. 752-755, 2013.
- [4] Y. Fenga, X. Yub and Z. Man, "Non-singular terminal sliding mode control of rigid manipulators," *Automatica*, Vol. 38, pp. 2159-2167, 2002.
- [5] J-J. E. Slotine and W. Li, *Applied Nonlinear Control*, Englewood Cliffs, NJ: Prentice-Hall, 1991.

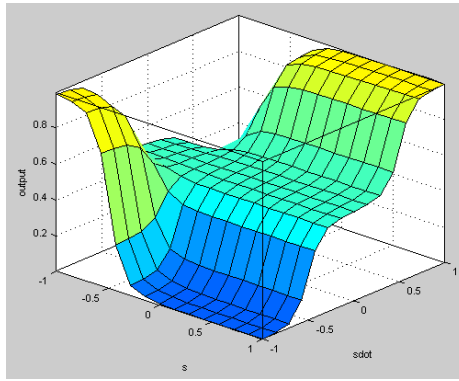


Fig. 2. Diagram of ANFIS FAM surface

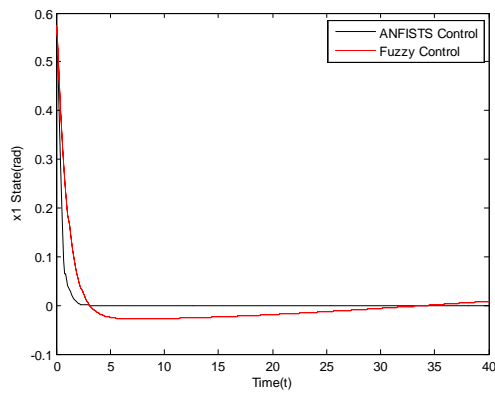


Fig. 3 (a). States of x1 trajectories

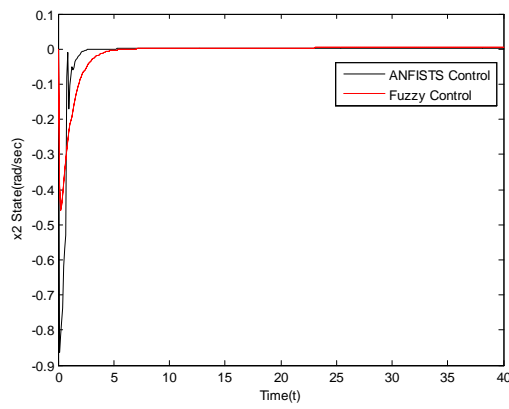


Fig. 3 (b). States of x2 trajectories

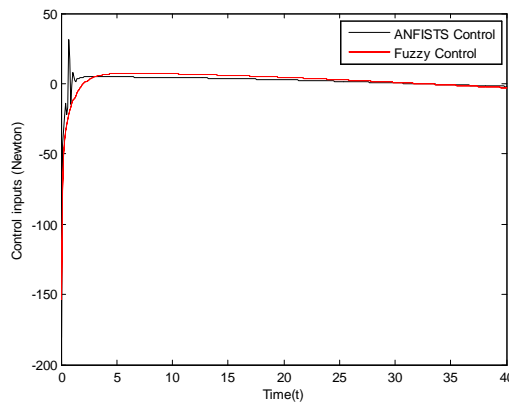


Fig. 3 (c). Control inputs

Energy Conservation in Wireless Sensor Networks Using Data Reduction Approaches: A Survey

¹Ms.Pallavi R , ²Shreya Animesh , ³Preetesh Shivam , ⁴Raghunandana Alse Airody , ⁵Niraj Kumar Jha

^{1,2,3,4,5}Sir M Visvesvaraya Institute of Technology, Bangalore – 562157

Abstract

Wireless Sensor Networks (WSN) which are battery powered, present a challenge of long term sustainability. So power management is an import concern which can be done at two levels such as sensor subsystems and network subsystem. This paper mainly concentrates on the network subsystem aspect of the power management touching the energy conservation schemes like duty cycling, data driven approaches and mobility. This in turn deals with the data driven approaches such as data reduction and energy efficient data acquisition. An in depth study of data reduction techniques is done in this paper which includes in network processing, data compression and data prediction. A proper comparison has been tabulated between the fore mentioned techniques based on certain parameters.

Keywords: Wireless Sensor Networks (WSN's), Power Management, Data Driven approaches, Data Reduction, In Network processing, Data Compression, Data Prediction

I. INTRODUCTION

A Wireless Sensor Network (WSN) can be defined as a [1] network of devices denoted as nodes that can sense the environment and communicate the information gathered from the sensor field through wireless links. The data is transmitted via multiple hops relaying to a sink that can use it locally, or is connected to other networks or cloud through a gateway. The nodes can be:

- [1] stationary or moving
- [2] aware of their location or not
- [3] homogeneous or heterogeneous

A scheme of a WSN connected to the Internet is presented in Fig. 1. WSNs are implemented in a wide range of distributed, remote and wireless sensing applications in environmental monitoring, agriculture, production and delivery, military, structural health monitoring, ambient intelligence, medical applications, etc.

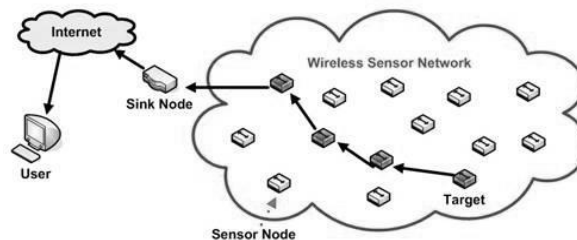


Fig 1: A wireless sensor network

Deployment of WSNs avoids installation costs due to wire depositions, introducing at the same time power efficiency as a main challenge. Wireless sensor nodes are mainly battery powered, thus having restricted amounts of energy. Even if they are equipped with power harvesting units (retrieving e.g. solar, vibrational or wind energy), energy is a critical point and should be tackled wisely. A WSN should be autonomous and self-sustainable, able to function for several years with a battery power supply. A node's lifetime is defined as the node's operating time without the need for any external intervention, like battery replacement. A WSN lifetime[2] can be defined as the lifetime of the shortest living node in the network. But, depending on the application, density of the network and possibilities of reconfiguration, it can also be defined as the lifetime of some other (main or critical) node. Anyway, in order to enhance a WSN lifetime, it is required to reduce the energy consumption of the nodes as much as possible and form an energy aware system.

The rest of the paper is organized as follows. Section II discusses the general approaches to energy conservation in sensor nodes, and introduces the three main approaches (*duty-cycling*, *data reduction*, and *mobility*). In Section III we break down this high-level classification, and highlight the *data driven approaches* that will be then described in detail in the following sections. Specifically, Section IV deals with schemes related to the *data reduction* approach. Finally, conclusions and open issues are discussed in Section V.

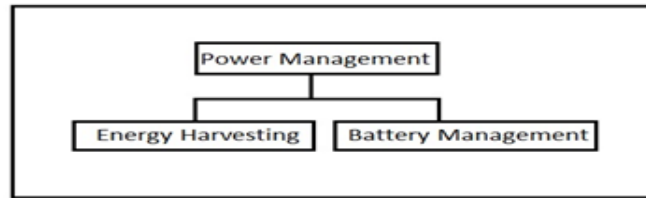


Fig 2: Ways of Power Management

II. POWER MANAGEMENT

As mentioned in the previous section and Fig. 2, power management in sensor networks can be done in two ways:

- [1] Energy Harvesting
- [2] Battery Management

Power management is an important concern in sensor networks, because a tethered energy infrastructure is not available and an obvious concern is to use the available battery energy efficiently. However, in some of the sensor networking applications, an additional facility is available to overcome the energy problem: *harvesting energy* [3] from the environment. Certain considerations in using an energy harvesting source are fundamentally different from that in using a battery because, rather than a limit on the maximum energy, it has a limit on the maximum rate at which the energy can be used. Further, the harvested energy availability typically varies with time in a nondeterministic manner. Thus energy harvesting is not an optimal solution where the sensor nodes are placed remotely.

So in order to prolong a WSN lifetime, it is required to reduce the energy consumption of the nodes as much as possible and, form an energy aware system which reduces the consumption of battery power i.e. *Battery Management*. It can be done at two levels:

- [1] Sensor Subsystems
- [2] Network Subsystems

From a sensor network standpoint, we mainly consider the model depicted in Fig. 1, which is the most widely adopted model in the literature.

2.1 Sensor Subsystems and Network Subsystems

Fig.3 shows the architecture of [4] a typical wireless sensor node. It consists of four main components: (i) a sensing subsystem including one or more sensors (with associated analog-to-digital converters) for data acquisition; (ii) a processing subsystem including a micro-controller and memory for local data processing; (iii) a radio subsystem for wireless data communication; and (iv) a power supply unit.

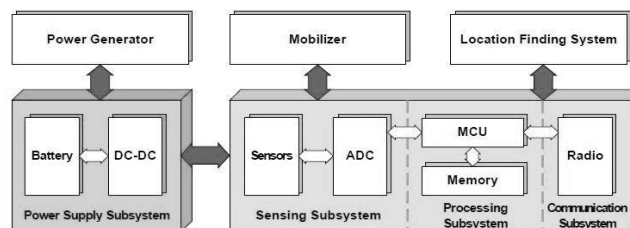


Fig 3: Architecture of sensor node

However, the *network subsystem* has much higher energy consumption than the sensor subsystem. It has been shown that transmitting one bit may consume as much as executing a few thousands instructions [5]. Therefore, communication should be traded for computation. The radio energy consumption is of the same order in the reception, transmission, and idle states, while the power consumption drops of at least one order of magnitude in the sleep state. Therefore, the radio should be put to sleep (or turned off) whenever possible. Depending on the specific application, the sensing subsystem might be another significant source of energy consumption, so its power consumption has to be reduced as well.

Based on the above architecture and power breakdown, several approaches have to be exploited, to reduce power consumption in wireless sensor networks. At a very general level, we identify three main enabling techniques namely, *duty cycling*, *data-driven approaches*, and *mobility*.

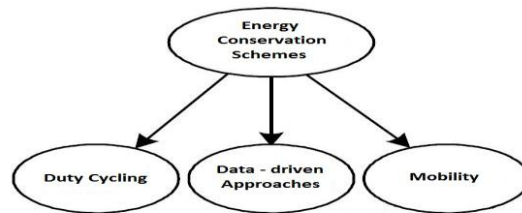


Fig 4: Energy conservation schemes in network subsystem

Duty cycling focuses on the networking subsystem. The most effective energy-conserving operation is to put the radio transceiver in the sleep mode whenever communication is not required. Ideally, the radio should be switched off as soon as there is no more data to send/receive, and should be resumed as soon as a new data packet becomes ready. In this way nodes alternate between active and sleep state depending on network activity. This behaviour is usually referred to as duty cycling, and duty cycle is defined as the fraction of time nodes are active during their lifetime. As sensor nodes perform a cooperative task, they need to coordinate their sleep/wakeup times. A sleep/wakeup scheduling algorithm thus accompanies any duty cycling scheme. It is typically a distributed algorithm based on which sensor nodes decide when to transition from active to sleep, and back. It allows neighbouring nodes to be active at the same time, thus making packet exchange feasible even when nodes operate with a low duty cycle (i.e., they sleep for most of the time) Duty-cycling schemes are typically oblivious to data that are sampled by sensor nodes. Hence, *data-driven approaches* can be used to improve the energy efficiency even more. In fact, data sensing impacts on sensor nodes' energy consumption in two ways:

- Unneeded samples: Sampled data generally has strong spatial and/or temporal correlation [6], so there is no need to communicate the redundant information to the sink.
- Power consumption of the sensing subsystem: Reducing communication is not enough when the sensor itself is power hungry.

In the first case unwanted samples result in useless energy consumption, even if the cost of sampling is negligible, because they result in unneeded communications. The second issue arises whenever the consumption of the sensing subsystem is not negligible. Data driven techniques presented in the following are designed to reduce the amount of sampled data by keeping the sensing accuracy within an acceptable level for the application.

In case some of the sensor nodes are mobile, *mobility* can finally be used as a tool for reducing energy consumption (beyond duty cycling and data-driven techniques). In a static sensor network, packets coming from sensor nodes follow a multi-hop path towards the sink(s). Thus, a few paths can be more loaded than others, and nodes closer to the sink have to relay more packets so that they are more subject to premature energy depletion (funnelling effect) [7]. If some of the nodes (including, possibly, the sink) are mobile, the traffic flow can be altered if mobile devices are responsible for data collection directly from static nodes. Ordinary nodes wait for the passage of the mobile device and route messages towards it, so that the communications take place in proximity (directly or at most with a limited multi-hop traversal). As a consequence, ordinary nodes can save energy because path length, contention and forwarding overheads are reduced as well. In addition, the mobile device can visit the network in order to spread more uniformly the energy consumption due to communications. When the cost of mobilizing sensor nodes is prohibitive, the usual approach is to "attach" sensor nodes to entities that will be roaming in the sensing field anyway, such as buses or animals.

III. DATA DRIVEN APPROACHES

As mentioned in the previous section, data driven approaches can be mainly classified as:

- Data Reduction
- Energy Efficient Data Acquisition

Data reduction mainly focuses on the data which is already present in the nodes, whereas energy efficient data acquisition mainly focuses on retrieving the data from the environment or surroundings efficiently using sophisticated algorithms.

3.1 Data Reduction

Data reduction is the process in which the large entity of the collected data is converted to the smaller useful entity so that at a later stage the same data can be retrieved without any loss. This concept is very much important in power management as transmission of data by nodes uses up lot of power, thus by reducing the size of the data, power consumption can be reduced. At the same time, data reduction approach also concentrates on preventing the nodes from transmitting data to the sink, thus reducing the transmission load on the node as well as, reducing the communication and processing overhead at the sink side.

The above mentioned approach can be achieved in the following three ways as shown in Fig 5:

- In Network processing
- Data compression
- Data prediction

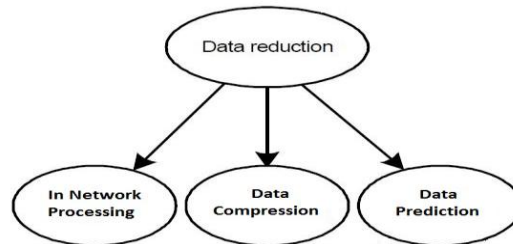


Fig 5: Data reduction techniques

In network processing is a technique wherein sensors are grouped into smaller clusters which in turn will have a special node called aggregator [8] that collects data from all the nearby nodes, processes it and broadcast it to the sink if needed.

In data compression, sensor nodes transmit data to neighboring nodes which has some correlated data, thus compressing the aggregated data with its own data reducing redundancy. Alternatively every node can compress the data on its own and transmit.

Data Prediction is an approach where, instead of transmitting data every now and then, the data is compared with the sampled model (based on previously sensed records). If the data lies within the expected range of the model, the model is considered valid. If not, the updated model is sent to the sink. Thus, reducing overall number of transmissions.

3.2 Energy Efficient Data Acquisition

Energy efficient data acquisition is an approach where there is reduced data acquisition based on energy efficient algorithms. However this is not exclusive to reduce energy consumption through sensing. It also reduces the number of communication along with reduced sensed data.

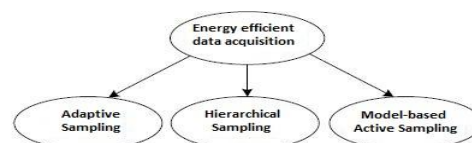


Fig 6: Taxonomy of energy efficient acquisition

Energy efficient data acquisition can be classified as follows:

- Adaptive sampling
- Hierarchical sampling
- Model based Active sampling

Adaptive sampling takes advantage of correlated and gradually changing data, thus reducing the number of data sensing. Hierarchical sampling looks into the dynamics of the nodes such as accuracy and energy consumption, thus ensuring a balance between afore mentioned attributes. Model based active sampling exploits the pre-sensed data by building upon the sampled models. Thus, reducing the number of acquisitions and also the number of communications between the nodes.

IV. DATA REDUCTION

As mentioned in the previous sections data reduction is an efficient approach to reduce power consumption. This section explains in detail the various approaches to data reduction and also compares them. A common way to facilitate data reduction is to follow predict and adapt models. These models can be applied at both the source and destination for the nodes. As this mechanism relies upon the data prediction and adaptation to the changing pattern of data, utilization of communication resources is drastically reduced, hence reducing the power usage. This is also a challenging approach as data exists in the form of continuous bits. Therefore, the predict and adapt models have to process the sensed data in real time with utmost accuracy. The spatial and temporal [9] characteristics of WSN's help the nodes to adapt to the environment and also predicting it, which aids to the data reduction. As mentioned in section 3.1 data reduction is subdivided as in network processing, data compression and data prediction.

4.1 In network processing

In network processing in large scale WSN's improves scalability, reduces data redundancy and also enhances the life time of the WSN. Sensor nodes are placed in an environment where usually the sensing regions of the nodes overlap. This leads to the data redundancy. The technique which can help to overcome this is *in network processing*. Here, as mentioned earlier, *aggregators* come into picture. These aggregators collect the data from the neighboring nodes, process them and combine correlated data into a single packet and send it to the sink. This is known as *data amalgamation*. The reverse process is known as *data dissemination* wherein the control message from the sink is transmitted to the *aggregators* and eventually to other sensor nodes. Fig.7 demonstrates the above scenario.

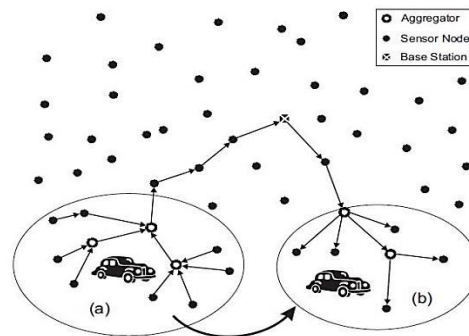


Fig 7: A tracking application using both (a) aggregation and (b) dissemination.

4.2 Data compression

This method basically compresses the received data and then transmits it when needed. Time sensitive phenomena like change in temperature needs to be constantly monitored and recorded. This results in large accumulation of redundant data. As there is redundant data, the transmission of such data to the base station or the sink requires tremendous amount of energy which could be reduced if there is less transmission load. This is where data compression is useful as it compresses the data at the nodes or *aggregators* and thus transmits only the required data. Some of the algorithms that are used for data compressions are:

- Lossless compression[10]
- Deterministic compression techniques[11]
- KEN[12]
- PREMON[13]
- Adaptive Model Selection (AMS)[14, 15]
- Dual Kalman filter[16]

4.3 Data prediction

As mentioned in section 3.1, this approach mainly depends on the previously sampled models. The efficiency of this approach is governed by the way the model is built. These models are sampled through any of the following techniques shown in Fig.8:

- Stochastic Approaches
- Time series forecasting
- Algorithmic approaches

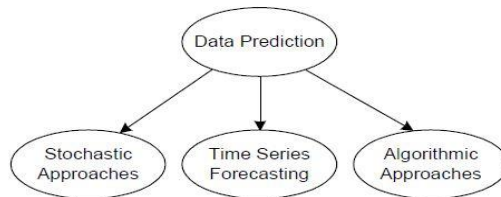


Fig 8: Data prediction approaches

Stochastic Approach mainly deals with the probability and statistical properties of the data. On one hand, the data is sampled as probability density functions (p.d.f) and data prediction can be done by combining these p.d.f's. Or on the other hand, data can be mapped as state space representations wherein the unpredicted sample can be discarded as noise.

Time series forecasting uses historical values for predicting future data in the series. It can be represented as a pattern which is characterized by long term variation and seasonality. Once this pattern is full-fledged it can be used to predict future values in the time series,

Algorithmic approaches rely on heuristics and state-transition model which derives methods and procedures to derive a model and update it based on the characterization.

4.4 Discussion

Specs	In network processing	Data compression	Data prediction
Accuracy	Very high	High	Moderate
Communication overload on node	Very high	Less compared to in network	Dependent on the input to the node
Communication overload on sink	Low	Slightly more than in network	Dependent on the input to the node
Processing overload	High	High	Dependent on the input to the node

Table 1: Comparison of the three data reduction approaches

In network processing is an accurate method as the data processing is done based on the inputs of all the nodes by a special node. This results in less overload of communication for the sink. However, the overhead on nodes is high due to the constant transmission of data from the nodes to the aggregator.

Data compression on other hand has high accuracy of the data but slightly less compared to that of the in network processing due to the fact that not all data is processed and there are chances of key data to be missed. As less data needs to be transmitted from the node, communication overload on the node is slightly less compared to that of in network processing. Whereas the load at the sink side is higher compared to that of in network processing as every node communicates with the sink. As lot of data compression is involved high processing is required.

As data prediction involves statistics and probability, data accuracy is compromised a bit. However the communication load on the node and sink mainly depends on the data sensed by the node. As it has the predefined range, any offset in the sensed data from the range results in communication or transmission of data to update the model.

V. CONCLUSION

In this paper we have surveyed the power management techniques in a wireless sensor network. Specifically we studied the various data driven approaches and went in deep with the data reduction. In data reduction we studied the three techniques such as: in network processing, data compression and data prediction. We also did a comparison of the three approaches based on certain parameters such as communication overhead, processing overhead and accuracy of the data. From the comparison we inferred that fusing the data compression and in network processing approaches at the nodes we can drastically reduce the communication overhead on them resulting in reduced power consumption. As WSN's have a wide variety of applications such as smart video surveillance, smart gas detection, health monitoring, natural hazard predictions as well as weather forecast, power management is a very important concern for a long lasting and sustainable network. Thus data reduction approaches have a huge impact on energy conservation.

VI. ACKNOWLEDGMENT

It gives us immense pleasure to express our sincere gratitude to the management of Sir M Visvesvaraya Institute of Technology, Bangalore for providing the opportunity and resources to accomplish our survey in their premises. Our sincere thanks to Dr. M S Indira, Principal, Sir MVIT for her encouragement throughout the course. Words are not enough to convey our gratitude to Prof. Dilip K Sen, HOD, Computer Science and Engineering for his constant support and motivation.

REFERENCES

- [1] Wireless Sensor Networks, Salvatore La Malfa
- [2] Power Management in Wireless Sensor Networks with High-Consuming Sensors, Vana Jelić
- [3] Power Management in Energy Harvesting Sensor Networks, Aman Kansal, Jason Hsu, Sadaf Zahedi and Mani B Srivastava
- [4] Energy Conservation in Wireless Sensor Networks: a Survey, Giuseppe Anastasi, Marco Conti, Mario Di Francesco, Andrea Passarella
- [5] G. Pottie, W. Kaiser, Wireless Integrated Network Sensors, Communication of ACM, Vol. 43, N. 5, pp. 51-58, May 2000
- [6] M. C. Vuran, O. B. Akan, and I. F. Akyildiz, "Spatio-Temporal Correlation: Theory and Applications for Wireless Sensor Networks", Computer Networks Journal, Vol. 45, No. 3, pp. 245-261, June 2004
- [7] J. Li, P. Mohapatra, "Analytical Modeling and Mitigation Techniques for the Energy Hole Problem in Sensor Networks", Pervasive Mobile Computing, 3(3):233-254, June 2007
- [8] Secure and Efficient In-Network Processing for Sensor Networks, Tassos Dimitriou, Dimitris Foteinakis
- [9] Data Reduction in Low Powered Wireless Sensor Networks, Qutub Ali Bakhtiar, Kia Makki and Niki Pissinou
- [10] A Simple Algorithm for Data Compression in Wireless Sensor Networks, Francesco Marcelloni, Member, IEEE, and Massimo Vecchio, Member, IEEE
- [11] Deterministic Data Reduction in Sensor Networks, Hervé Brönnimann, Hüseyin Akcan
- [12] Chu, D., Deshpande, A., Hellerstein, J. M. & Hong, W. [2006]. Approximate data collection in sensor networks using probabilistic models, p. 48
- [13] Goel, S. & Imielinski, T. [1994]. Prediction based monitoring in sensor networks taking lessons from mpeg, ACM Computer Communication Review pp. 510-514
- [14] Santini, S. [2006]. Poster abstract: Towards adaptive wireless sensor networks, 3rd European Workshop on Wireless Sensor Networks (EWSN 2006) pp. 13-15
- [15] Santini, S. & Romer, K. [2006]. An adaptive strategy for quality-based data reduction in wireless sensor networks, Proceedings of 3rd International Conference on Networked Sensing Systems (INSS 2006), Chicago
- [16] Jain, A., Chang, E. & Wang, Y. [2004]. Adaptive stream resource management using kalman filters., ACM SIGMOD/PODS Conference (SIGMOD '04), Paris, France
- [17]

Ethnomedicinal Investigation of Medicinal Plants Used By the Tribes of Pedabayalu Mandalam, Visakhapatnam District, Andhra Pradesh, India.

¹S. B. Padal, ²Chandrasekhar P. , ³K. Satyavathi

^{1,3},Department of Botany, Mrs. A.V.N. College, Visakhapatnam District-530001.

²Department of Botany, Govt. Degree College, Yelamanchili, Visakhapatnam District.

Abstract:

The present study documents the traditional knowledge of medicinal plants that are in use in Pedabayalu Mandalam, Visakhapatnam District, Andhra Pradesh, India. Ethnomedicinal uses of 80 plant species along with botanical name, vernacular name, family, plant parts, life forms and disease are presented. They belong to 70 genera and 21 families. These plants used to cure 30 types of ailments. Most remedies were taken orally, accounting for 60% of medicinal use. Most of the remedies were reported to have been from trees and herb species. High number of medicinal plant species available for the treatment of dysentery, skin disease and fever.

KeyWords: Ethnomedicinal plants, Investigation, Tribal people, Pedabayalu Mandalam, Visakhapatnam District,

I. INTRODUCTION

Ethnobotany came into being when the earliest man observed the animals mostly the apes and monkeys eating certain plant often to satisfy his hunger and at other times to heal his wound and to get rid from pains and sufferings. The observations on apes and monkeys (which were very close to human beings in morphology and also in anatomy and physiology) eating certain plant parts-roots, stems, leaves, flowers, fruits and seeds and the beneficial effects on their body gave a food for thought to these early men and it started the genesis of basic thoughts in human brain. An analysis of such observations provoked them to use plants for maintenance of life and alleviation of diseases. In this way, it helped them in formulating the basic concepts of sciences of life which were evaluated rationally, later on over a period of time. Thus, on the basis of the uses of plants first by animals and later by human beings the concept of ethno zoology and Ethnobotany emerged which merged to give birth to ethno biology.

In India it was Dr. S.K. Jain (1986) from NBRI, Lucknow, affectionately known as 'Father of Indian Ethnobotany' who made pioneering investigations. Ethnobotany has assumed new significance and a new dimension today when the modern civilization realized that all those plant products they are using today either as a food or as a medicine are the gift of those early men who used those plants to satisfy their hunger and heal their wounds and to know and evaluate the utility of those plants often experimented on their own body, sometimes also accidentally suffering due to their use, such as in case of some poisonous plants.

II. STUDY AREA

Generally the Pedabayalu Mandalam of Visakhapatnam district is with full of tribal population (Fig.1). The tribal communities live in forests, hilly tracts and naturally isolated areas from the civilized urban society. That's why in nature they developed their cultures of their own. They depend up on the nature for their food, shelter, and livelihood, thus the vegetation has much influence on the tribal life. The total population of scheduled tribes in India is 683.81 lakhs and constitutes 8.08% of the total population as per 1991 census report. The tribal population of Andhra Pradesh is 41.99 lakhs which is 6.3% of the total population. 13 tribal groups who inhabit this Mandalam are, Bagata, Gadaba, Kammara, Konda Doras, Khondu, Kotia, Kulia, Malis, Manne Dora, Mukha Dora, Porja, Reddi Doras, Nooka Dora and Valmiki.

In Pedabayalu Mandalam the tribals Konda Dora, Kotias, Kondus are lived in group of houses called huts. Generally, the houses are constructed with Bamboo (*Bambusa arundinacea*), Palmyra culms and other timber yielding plants. Palmyra culms are used for thatching the roofs of the houses. The walls are constructed with mud mixed with ash of burn grass and are smeared with cow dung.

The tribal communities which live in forest area collect minor forest produce or non timber forest produce like tamarind, amla, adda leaves, bamboo, beedi leaves, roots, tubers, wild fruits and honey. They generally sell them in the weekly markets or Shandys known as "Santha". The main occupation of tribal people in Pedabayalu Mandalam is agriculture. Podu cultivation is one of the old methods of cultivation particularly in mountain tracts and hill slopes.

III. MATERIAL AND METHODS:

The approaches and methodologies for ethnobotanical work, suggested by Jones (1941), Schultes (1960, 1962), Croom (1983), Jain (1987, 1989), Bellany (1993), Chadwick and Marsh (1994) and Cotton (1996) were followed. Emphasis was given mainly on intensive field work in selected tribal habitations. The focus of the present study is to record the ethnobotanical knowledge with special reference to medicinal plants possessed by the tribal people. They represent the pockets of human gene pool and have distinct habitats and habits with ample knowledge on the medicinal properties of their surrounding plants. Plants employed in materiel culture and plants associated with folk songs, folk tales, worship, mythology, taboos, magico-religious beliefs, ceremonies etc. were studied in addition to vernacular names. Plant identifications were made with the help of Flora of the Presidency of Madras (Gamble, 1915-1935) using the field observations. The identifications were later confirmed with the help of Flora of Visakhapatnam District (Rao and Kumari, 2002) and by comparison with authentic specimens in the Andhra University Herbarium.

Table. 1. Ethnomedicinal plants used by tribal people of Pedabayalu Mandalam.

F	G/sp.	Botanical name	Local name	Habit	Life form	Plant parts	Disease
1		ANNONACEAE					
	1	<i>Annona squamosa</i> Linn.	Sitaphalam	Tree	Ph-meso	Seeds	wounds
	2	<i>Polyalthia longifolia</i> Benth.	Naramamidi	Tree	Ph-mega	Bark	Rheumatism
2		MENISPERMACEAE					
	3	<i>Cissampelos pareira</i> Linn	Bankatheega	Climber	Ph-micro	Root	Stomachic
	4	<i>Cocculus hirsutus</i> (Linn.) Diels	Dussarateega	Climber	Ph-nano	Root	Eczema
	5	<i>Tinospora cordifolia</i> Miers	Tippatheega	Climber	Ph-micro	Stem	Jaundice
3		NYMPHAECACEAE					
	6	<i>Nelumbo nucifera</i> Gaertn.	Tamara	Herb	C-hydro	Rhizome	Dysentery
	7	<i>Nymphaea pubescens</i> Willd.	Kaluva	Herb	C-hydro	Root	Dysentery
4		BRASSICACEAE					
	8	<i>Brassica juncea</i> (Linn.) Czernajew	Telle avalu	Herb	Th	Seed	Diarrhoea
	9	<i>Raphanus sativus</i> Linn.	Mullangi	Herb	C-geo	Root	Urinary trouble
5		CAPPARACEAE					
	10	<i>Cadaba fruticosa</i> (Linn.) Druce	Chedonda	Shrub	Ph-micro	Leaf	Eczema
	11	<i>Capparis sepiaria</i> Linn.	Nallauppi	Straggler	Ph-micro	Plant	Skin trouble
	12	<i>Cleome gynandra</i> Linn.	Vominta	Herb	Th	Leaf	Headache
	13	<i>Cleome viscosa</i> Linn.	Kukkavominta	Herb	Th	Seed	Pain
	14	<i>Maerua oblongifolia</i> (Forsk.)A.Rich.	Dholo Katkiyo	Shrub	Ph-micro	Root	Headache
6		MALVACEAE					
	15	<i>Abelmoschus esculentus</i> Moench.	Benda	Shrub	Ph-micro	Leaf	Dysentery
	16	<i>Abutilon indicum</i> (Linn.) Sw.	Thuthurubenda	Shrub	Ph-micro	Leaf	Piles
	17	<i>Hibiscus rosa-sinensis</i> Linn.	Mandhara	Shrub	Ph-nano	Flower	Mennorrhagia
	18	<i>Sida cordifolia</i> Linn.	Bala	Herb	Th	Root	Leucorrhoea
	19	<i>Thespesia populnea</i> Corr.	Gangaravi	Tree	Ph-meso	Root	Diabetes
7		BOMBACACEAE					
	20	<i>Adansonia digitata</i> Linn.	Bandaru	Tree	Ph-mega	Leaves	Dysentery
	21	<i>Bombax ceiba</i> Linn.	Buruga	Tree	Ph-mega	Root	Diabetes
	22	<i>Cieba Pentandra</i> (Linn.)Gaertn.	Tellaburuga	Tree	Ph-mega	Leaf	Boils
8		TILIACEAE					
	23	<i>Corchorus capsularis</i> Linn.	Tellanara	Herb	Th	Seed	Stomachic
	24	<i>Triumfetta rhomboidea</i> Jacq.	Chiruchitrica	Herb	Ph-nano	Root	Ulcers
9		ZYGOPHYLLACEAE					
	25	<i>Tribulus terrestris</i> Linn.	Palleru	Herb	Th	Root	Diabetes
10		RUTACEAE					
	26	<i>Aegle marmelos</i> (Linn). Corr.	Maredu	Tree	Ph-meso	Bark	Dysentery
	27	<i>Citrus limon</i> (Linn). Burm.	Nimmakaya	Shrub	Ph-meso	Fruit	Stomachic
	28	<i>Citrus medica</i> Linn	Madeepalamu	Shrub	Ph-meso	Fruit	Dysentery
	29	<i>Murraya koenigii</i> Spreng.	Karivepaku	Tree	Ph-meso	Leaf	Vomiting
11		MELIACEAE					
	30	<i>Azadirachta indica</i> A. Juss.	Vepa	Tree	Ph-mega	Bark	Skin trouble

	31	<i>Melia azedarach</i> Linn.	Turakavepa	Tree	Ph-mega	Leaf	Fever
	32	<i>Soymida febrifuga</i> A. Juss.	Chavachettu	Tree	Ph-mega	Bark	Fever
12		RHAMNACEAE					
	33	<i>Zizyphus mauritiana</i> Lamk	Rgichettu	Tree	Ph-meso	Seed	Diarrhoea
	34	<i>Zizyphus nummularia</i> (Burm.f.) Wt. & Arn.	Nelaregu	Shrub	Ph-micro	Leaf	Scabies
	35	<i>Zizyphus xylopyra</i> Willd.	Gotti	Tree	Ph-meso	Bark	Asthma
13		FABACEAE					
	36	<i>Abrus precatorius</i> Linn.	Guruvinda	Climber	Ph-micro	Seed	Paralysis
	37	<i>Butea monosperma</i> (Lam.) Kuntze	Moduga	Tree	Ph-mega	Bark	Piles
	38	<i>Clitoria ternatea</i> Linn.	Sankupulu	Herb	Th	Root	Eye disease
	39	<i>Dalbergia sissoo</i> Roxb.	Sissoo	Tree	Ph-mega	Bark	Urinary infection
	40	<i>Derris indica</i> (Lam.) Bennet	Nalla theega	Tree	Ph-mega	Root	Snake bite
	41	<i>Mucuna pruriens</i> Bak	Durada Gondi	Climber	Th	Seed	Eczema
	42	<i>Petrocarpus marsupium</i> Prain.	Yegisa	Tree	Ph-mega	Bark	Cough
	43	<i>Sesbania grandiflora</i> Pers.	Avisachettu	Tree	Ph-mega	Bark	Diarrhoea
	44	<i>Vigna aconitifolia</i> (Jacq.) Marechal	Pillipesara	Climber	Th	Seed	Fever
	45	<i>Teramnus labialis</i> Spr.	Masaparni	Climber	Th	Root	Fever
14		CAESALPINIACEAE					
	46	<i>Bauhinia racemosa</i> Lam.	Arichettu	Tree	Ph-mega	Bark	Dysentery
	47	<i>Caesalpinia bonduc</i> (Linn.) Roxb.	Gachapodha	Shrub	Ph-micro	Seed	Vomiting
	48	<i>Caesalpinia pulcherrima</i> (Linn.) Swartz.	Phydi thangedu	Shrub	Ph-micro	Flower	Fever
	49	<i>Cassia absus</i> Linn.	Chanupalavittu	Shrub	Th	Leaf	Cough
	50	<i>Cassia auriculata</i> Linn.	Thangedu	Shrub	Ph-micro	Root	Skin disease
	51	<i>Cassia fistula</i> Linn.	Rela	Tree	Ph-mega	Bark	Skin disease
	52	<i>Cassia occidentalis</i> Linn.	Kasinta	Shrub	Ph-micro	Leaf	Eczema
	53	<i>Delonix elata</i> (Linn.) Gamble	Chittikesaram	Tree	Ph-mega	Leaf	Rheumatism
15		MIMOSACEAE					
	54	<i>Acacia farnesiana</i> (Linn.) Willd	Murikithuma	Tree	Ph-meso	Stem	Cough
	55	<i>Acacia leucophloea</i> (Roxb.) Willd	Tella thumma	Tree	Ph-meso	Stem	Arthritis
	56	<i>Acacia nilotica</i> (Linn.) Del.	Nalla thumma	Tree	Ph-mega	Bark	Dysentery
	57	<i>Dichrostachys cinerea</i> (Linn.) Wt. & Arn.	Veluthuruchett	Tree	Ph-meso	Root	Rheumatism
	58	<i>Pithecolobium dulce</i> (Roxb.) Benth.	Cheemachinta	Tree	Ph-mega	Seed	Diabetes
	59	<i>Prosopis cineraria</i> (Linn.) Druce	Jammi	Tree	Ph-mega	Bark	Skin disease
16		CUCURBITACEAE					
	60	<i>Citrullus colocynthis</i> (Linn.) schar.	Verri pucha	Herb	Ch	Fruit	Jaundice
	61	<i>Cucumis sativus</i> Linn	Dosakaya	Climber	Th	Fruit	Urinary disease
	62	<i>Lagenaria siceraria</i> (Molina) Standl.	Sorakaya	Climber	Th	Root	Jaundice
	63	<i>Momordica charantia</i> Linn	Kakara	Climber	Th	Leaf	Ulcers
17		APIACEAE					
	64	<i>Ammi majus</i> Linn.	Pitchikothimer	Herb	Th	Leaf	Fever
	65	<i>Centella asiatica</i> (Linn.) Urban	Saraswatiaku	Herb	Th	Leaf	Diabetes
18		RUBIACEAE					
	66	<i>Adina cordifolia</i> Hook. f. ex Brandis.	Bandaru	Tree	Ph-mega	Bark	Dysentery
	67	<i>Mitragyna parvifolia</i> (Roxb.) Korth.	Battaganapa	Tree	Ph-mega	Fruit	Eye disease
	68	<i>Morinda tomentosa</i> Heyne ex Roth.	Togaru	Tree	Ph-mega	Root	Eczema
19		ASTERACEAE					
	69	<i>Ageratum conyzoides</i> Linn	Pumpulla	Herb	Th	Leaf	Wounds
	70	<i>Eclipta alba</i> Linn	Guntagalaga	Herb	Th	Leaf	Jaundice
	71	<i>Tridax procumbens</i> Linn	Gadichamanti	Herb	Ch	Leaf	Dysentery
	72	<i>Xanthium strumarium</i> Linn.	Marulamatang	Herb	Th	Seed	Small pox
20		APOCYNACEAE					
	73	<i>Alstonia scholaris</i> R. Br.	Edakula pala	Tree	Ph-meso	Bark	Asthma
	74	<i>Nerium indicum</i> Mill	Erraganneru	Shrub	Ph-micro	Root	Skin disease
	75	<i>Thevetia peruviana</i> (Pers.) Merr.	Patchaganneru	Shrub	Ph-meso	Leaf	Cancer
	76	<i>Wrightia tinctoria</i> Br.	Ankudu	Tree	Ph-meso	Bark	Psoriasis
21		CONVOLVULACEAE					
	77	<i>Argyrea nervosa</i> (Burm f.) Boj.	Samudrapala	Shrub	Ph-micro	Root	Wounds

78	<i>Evolvulus alsinoides</i> Linn.	Vishnukrantha	Herb	Ch	Leaf	Asthma
79	<i>Ipomoea batatas</i> (Linn.) Lam.Tab.	Theepigadda	Herb	Th	Leaf	Scorpion sting
80	<i>Merremia gangetica</i> (Linn.) Cufod.	Nallakula tiga	Herb	Th	Root	Eye disease

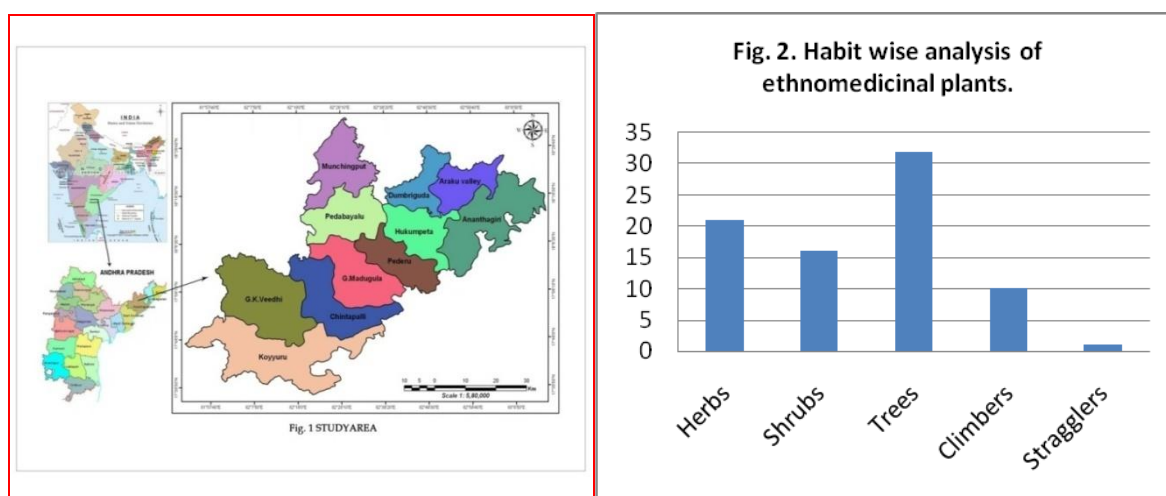
F=Family, sp=species,

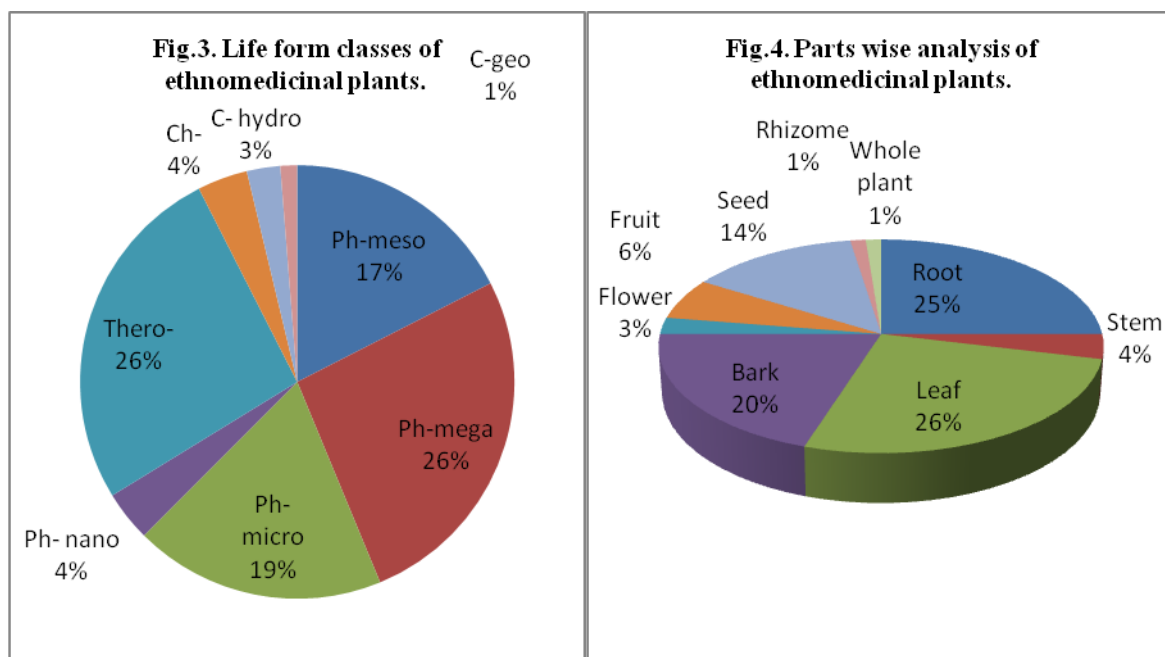
IV. RESULT AND DISCUSSIONS:

Conservation of biological resources and of the indigenous traditional knowledge is essential for sustainable development and managing of natural resources the world over. The history of indigenous knowledge as old as the human race. This knowledge has always been very important for the people who generate it. It is a matter of survival for them. Many scientists, researchers and environmentalists all over the world are now striving to explore, know, Document and use the resource base knowledge for the welfare of the wider human race. Documentation of ethnic groups' knowledge related to plant resources is known as 'Ethnobotany'. The study deals with the relationships of man to the plant he used or uses. Analysis of information presented in appendix-I indicates that Pedabayalu Mandalam tribes inhabitant of Visakhapatnam district possess rich knowledge about plant resource around them. This is evident form the following fact. A total of 80 angiosperm plant species belonging to 70 genera of 21 families have been identified and recorded for ethnobotanical uses. Out of the 21 families Fabaceae is the dominated family. Out of the total 80 flowering species, 32 are trees, 16 shrubs, 21 herbs, 10 are climber and stragglers. (Table. 1, Fig. 2). This study shows that Trees are dominating the forest. This is probably owing to the semi-arid conditions and erratic rainfall. Further, the scrubby plant species (small trees and shrubs) can be observed as the dominant perennial vegetation of the area.

The various life form classes (Rauchier, 1934) as phanerophytes (nano, micro, meso, mega, epi) are represented by 53 species while chamaephytes account for 3 species, cryptophytes (geo, helo, hydro) by 3 and therophytes are represented by 21 of the total number of species. The phanerophytes and therophytes dominate in all the parts (Table –I, Fig. 3). The biological spectrum reflects the adaptation of plants to environment and primary climate (Smith 1980). Geographically widely separated plant communities can be very usefully compared with one another on the basis of biological spectrum. Since life forms are related to the environment, biological spectrum is also an indicator of prevailing environment. In the Padabayalu Mandalam, Visakhapatnam district the tribes has been using the indigenous plant species in a crude form. The present study accounts for 80 plant species, which are of medicinal value. As there is no medical pharmacy the medicinal plants are an instantly available form of medication for the indigenous/aboriginal people. These plants are presently receiving an enormous amount of attention. They utilize singly or in combination for the treatment of 30 ailments (Table. 1). The frequent health problems are Dysentery and Skin disorders 16 species are used. The maximum number of plants used for a particular ailment can possibly show the prevalence of the ailment in the area. Various plant parts, such as roots (20 spp), stem (3 spp) leaves (21 spp), flowers (2 spp), seeds (11 spp), stem bark (16 spp), rhizome (1 spp) entire plant (1 spp) and fruits (5) are used for the treatment of the above ailments generally through oral administration (Fig.4).

fig.1. Study area-Pedabayalu Mandalam.





V. CONCLUSIONS:

However, we feel that the indigenous knowledge and practices of the Padabayalu Mandalam tribes on utilization of plant resources as medicine should be reported and preserved before they get lost due to increasing integration. In the information obtained, there were many details about the appropriate indication of each plant. There are plants that are traditionally employed for specific symptoms or conditions that often accompany itching, allergy and other skin disorders. This vast array of rare medicinal plants can be used for further research only if we ensure proper conservation of these endangered species. Thus researchers should observe ethnomedicinal information before deciding which kind of screening should be used in the search of drugs for skin diseases which may also be a potential source of modern drug industries.

VI. ACKNOWLEDGEMENT:

The authors are thankful to the notified and denotified adivasis groups, their vairs, ojhas, bhops etc. and forest officials who provided valuable information on this subject. We are also thankful to the authorities of various herbaria and, museums for their help and co-operation extended in several ways.

REFERENCE:

- [1] Chadwick, D. J. and J. Marsh (ed.), (1994), Ethnobotany and the search for new Drugs. John Wiley & Sons, Chichester, U.K
- [2] Gamble, J. S. and C. E. C. Fischer, (1915-1935), Flora of Presidency of Madras, (3 vols.) (repr. Ed. 1957) Botanical Survey of India, Howrah.
- [3] Jain, S. K., (Ed.) (1989), Methods and approaches in Ethnobotany, Society of Ethnobotanists, Lucknow.
- [4] John, S., Groeger, D. & Hesse. (1971), Alkaloids. 142. New alkaloids from *Adhatoda Vasica*. *Helv. Chem. Acta.* 54:826
- [5] Rama Rao Naidu, B. V. A, (2002), Ethno Medicine from Srikakulam District, Andhra Pradesh, India. Ph.D Thesis, Andhra University, Visakhapatnam.
- [6] Rao, B. T., B. B. Lakhmi, L. M. Rao, K. Rameswari and V. Hymavathi, (2000), Medicinal plants of Paderu forest division in the Eastern Ghats of Visakhapatnam. *Asian J. Micr. Biotech. Environ. 1 Sci.* 5: 67-80.
- [7] Rao, V. L. N., B. R. Busi, B. Dharma Rao, Ch. Seshagiri Rao, K. Bharathi and M. Vekaiah (2005), Ethnomedicinal practices among Khonds of Visakhapatnam District, Andhra Pradesh. *Indian Journal of Traditional Knowledge* Vol. 5(2) P.P. 217-219.
- [8] Rajendran, A. N. Rama Rao and A. N. Henry, (1997), Rare and noteworthy plants of Eastern Ghats in Andhra Pradesh with their ethnic uses. *Ethnobotany*, 9: 39-43.
- [9] Sudarsanam, G. and G. Siva Prasad, (1995), Medical Ethnobotany of plants. Used as antidotes by Yanadi tribes in South India., *Jour. Herbs Spices and Medical Plants*, 3(1): 57-66.
- [10] Sudhakar, S., (1980), Studies on medicinal plants of Upper East Godavari district, A.P. *J. Indian Bot. Soc.* 59(Suppl.): 168 (abstract).
- [11] Sudhakar, S. and R. S. Rao (1985), Medicinal plants of Upper East Godavari District, Andhra Pradesh, India *J. Econ. Taxon. Bot.* 7(2): 399 - 406.
- [12] Sudhakar, A. and S. Vedavathy, (1999), Wild edible plants used by the tribals of Chittoor District (Andhra Pradesh), India. *J. Econ. Tax. Bot.*, 23(2): 321-329.
- [13] Schultes, R. E., (1960), Tapping our heritage of Ethnobotanical lore. *Econ. Bot.*, 14: 257-262.
- [14] Schultes, R. E., (1962), The role of Ethnobotanist in the search of new medicinal plants. *Lloydia*, 25: 257-266.
- [15] Venkaiah, M., 1998. Ethnobotany of some plants from Vizianagaram District, Andhra Pradesh. *Flora and Fauna*. 4: 90-92.
- [16] Venkaiah, M., (2002), Report of Northern districts of Andhra Pradesh in NATP Biodiversity Project work. (C.S.R. Project).

- [17] Venkanna, P., (1990), Medicinal plant wealth of Krishna district (A.P.) - A preliminary survey. *Anci. Sci. Life*, 102: 137-140.
- [18] Venkataram, P., .S. S. N. Yoganasimhan and V. S. Togunashi, (1975), Sanjeevnee: its identity and therapeutic claims. *Jour. Res. Ind. Med.*, 10:92-95.
- [19] Venkata Ratnam K. and Venkata Raju R.R. (2008), Traditional Medicine used by the Adivasis of Eastern Ghats, Andhra Pradesh, for Bone fractures. *Univ. of Sri Krishnadevaraya, Anantapur*.
- [20] Venkateswarlu, J., Murthy, P. V. B. & Rao, P. N. (1972). *The Flora of Visakhapatnam*, Andhra Pradesh Academy of Sciences, Hyderabad.

Enhancing Productivity by Using Adjustable Multi-Spindle Attachment

¹M. Narasimha , ²M. Hailu Shimels , ³R. Reji Kumar , ⁴Achamyeleh Aemro
Kassie

^{1,2,3,4}, Lecturer, School of Mechanical and Industrial Engineering, Bahir Dar University, Bahir Dar, Ethiopia,

Abstract

Productivity improvement has become an important almost in all mass manufacturing industries, who really implement various methods in the manufacturing process. Productivity improvement techniques can be applied effectively in enterprises of any size, from one-person companies to corporations with thousands of staff. The majority of the techniques were first seen in mass – production operations but the benefits they can yield in SME are not to be underestimated. Indeed, the absence in SME of many of the rigidities commonly found in large companies make it easier for them to reap the benefits of productivity improvement techniques. Lean thinking and enterprise resource planning systems, it zooms in on productivity improvement techniques. Productivity also applies to service sector and many organizations of these sectors are also implementing various methods to improve their productivity.

Manufacturing is becoming the provision of complete service over the whole product life cycle. This new service provision requires manufacturers to get closer to their customer and to operate far more responsively than past. Many mass manufacturing industries like machine building, automobile and electronics industries are serious about their productivity improvements.

The time study, method study engineers of production engineering in collaboration with process planning engineering staff trying to reduce the time of manufacturing process, by clubbing more operations at a time or going for an accessories which can reduce the cycle time of operation. This paper is related to one of time reducing operation process by using the adjustable multi spindle attachment, for machining the three T-slots at a time to increase the output rate. By using this attachment three T- slots can be machined at a time reducing the operation time of the component to 1/3 of original time. That means the time saving is 2/3 of total machining time. The output of component from the operation is three instead of one by conventional machining process. Hence it enhances the productivity time saving of the operation and the quality remains the same.

Key Words: Machining time, Side and Face Cutter carbide inserted type, T-slot cutter, Table, Bolster and Accessory

I. INTRODUCTION

Manufacturing is becoming the provision of complete service over the whole product lifecycle. This new service provision requires manufacturers to get much closer to their customers and to operate far more responsively than they have in the past. [9] The second report, Emerging Global Manufacturing Trends - Output from the working sessions at Inform an 2000, prepared by the Institute for Manufacturing at the University of Cambridge, contains the following list of issues that organisations should consider in response to the main trends in global manufacturing:

- Human resources issues
- Using regulations as a positive force
- Intellectual capital/knowledge management
- Agility and dynamic supply chain network

- Innovation
- Migration to higher/value-added service
- Clear core competencies that will create a barrier to new entrants

One of the primary responsibilities of the operations manager is to achieve productive use of an organization's resources (labor, equipment, facilities, money, etc.) In very general terms productivity is a measure of output based on input. This is usually calculated as a productivity ratio.[10]

$$\text{Productivity} = \text{Output/Input}$$

A single factor productivity measure is Machine Productivity, Labor Productivity, capital Productivity and Energy Productivity. In this paper Machining Productivity is considered and units of output per machine hour, dollar value of output per machine hour are considered as the main criteria. [1]

To improve Productivity

- Develop Productivity measures for each operational development.
- Determine critical operations by looking at the systems as whole to see how interrelationships or bottlenecks affect productivity.
- Develop methods for soliciting improvement ideas.
- Establish reasonable goals for improvement.
- Make it clear that management supports improvement ideas and consider incentives for contributors. [3]

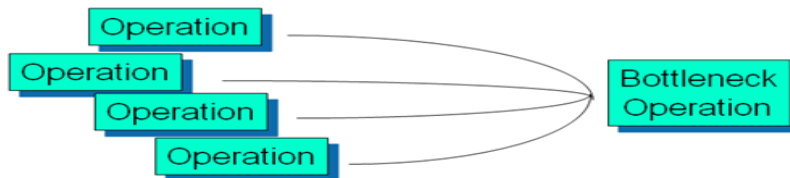


Fig. 1. Productivity development

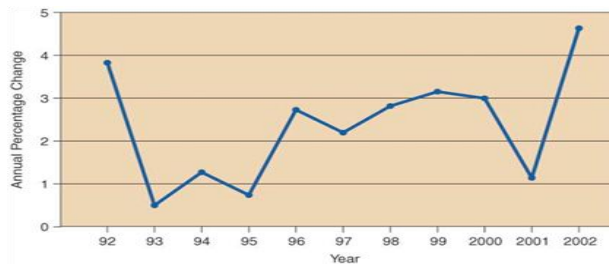


Fig. 2. Productivity development [2]

Productivity improvements are necessary to remain competitive. One of the production managers responsibilities is to seek out productivity improvements on a routine basis. Productivity improvements can result when organizations

- . Become more efficient
- . Downsize
- . Expand
- . Retrench
- . Achieve breakthroughs



Fig. 3. Productivity improvement[3]

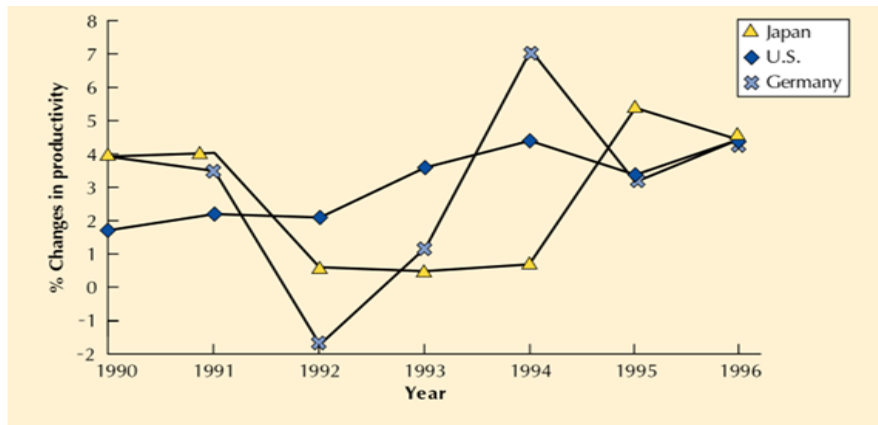


Fig. 4. Change in Productivity [3]

Productivity is scorecard on effective resource use

- A nations productivity effects its standard of living
- US productivity growth averaged 2.8% from 1948-1973
- Productivity growth slowed for the next 25 years to 1.1%
- Productivity growth in service industries has been less than in manufacturing.

1.1. The Role of SME in supporting large Manufacturing Firms

Of the entire 1999 business population of 3.7 million enterprises, only 24,000 were medium sized (having 50-249 employees and fewer than 7,000 were large(having 250 or more employees) Small business, including those without employees, accounted for over 99% of business, 45% of non – governmental employment and (excluding the finance sector) 38% turnover. [3]In contrast, the 7,000 largest businesses accounted for 45% of non-government employment and 49% of non-government and 49% of turn over as shown in Fig.5

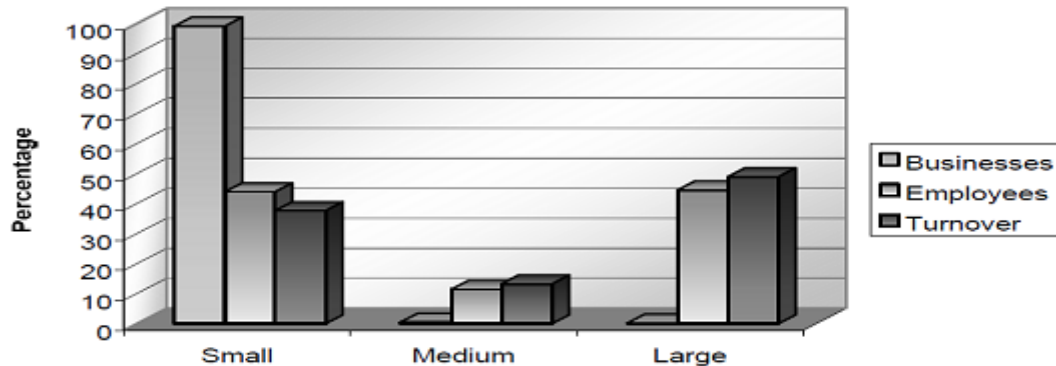
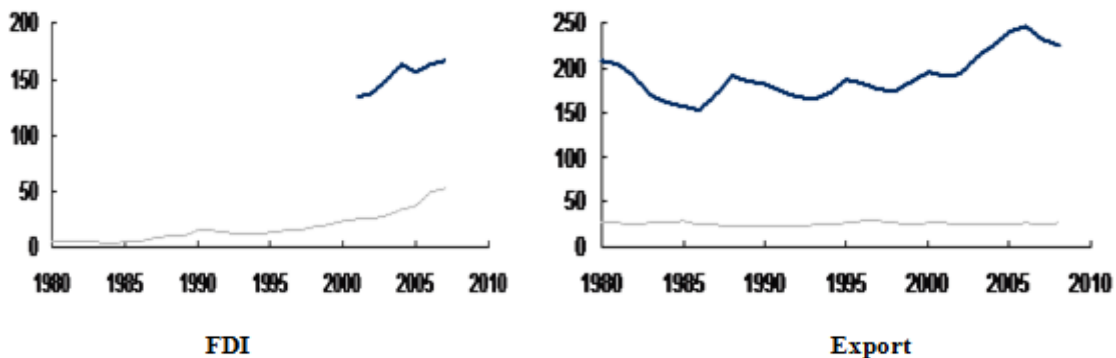


Figure 5: Proportion of businesses, employment and turnover firms at start of 1999 [4]

1.2. Singapore’s Productivity growth was associated with FDI, export and R&D [5]



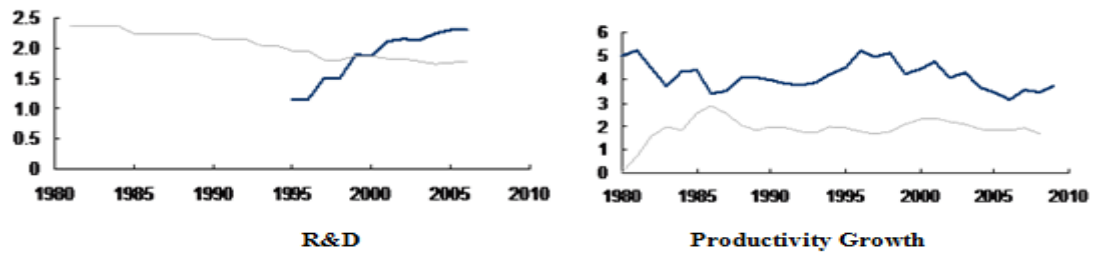


Fig.6. Singapore's Productivity growth

1.3. KEY ACHIEVEMENTS OF SWEDEN

- [1] Productivity grew by 2.8% p.a. between 1990 and 2000 – almost twice the OECD average
- [2] Private sector productivity growth of 3.3% p.a. was even greater
- [3] R&D expenditure of 4.25% of GDP in 2001 second highest in OECD
- [4] Exports doubled from 1978 to 2008

- Following the crisis of 1990-93, there was broad acceptance that product market reforms to increase competition were required to restore economic competitiveness. (5) In the retail sector, this was largely achieved through an easing of municipality planning restrictions. Prior to 1992, planning applications from aspirational market entrants were considered by a committee including representatives of incumbent firms, and were seldom successful
- In 1992, the government changed the municipality guidelines, requiring them to “consider the competitive landscape” when deciding whether or not to award planning permission to new retailers
- This led to a significant increase in competition in retail, and a large increase in large, high-productivity out-of-town stores (see chart to right), which resulted in sectoral productivity growth of 4.5% p.a. (OECD 1.5%)

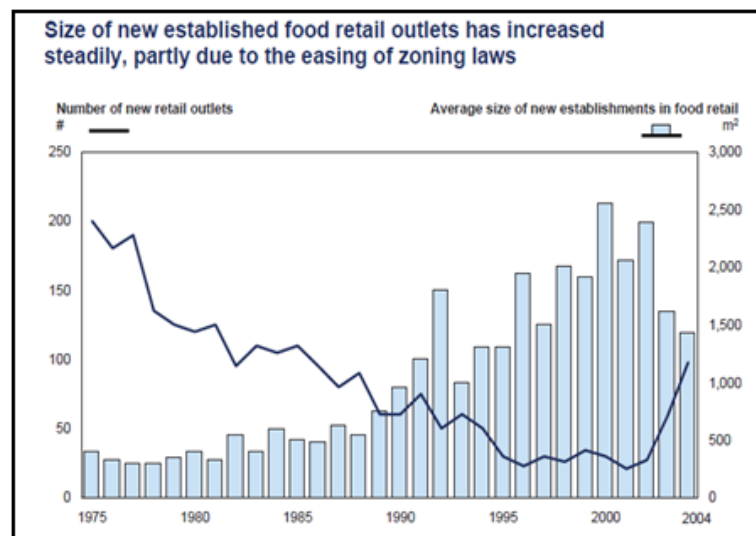


Fig.7. Productivity growth

- The financial sector also experienced significant reforms, including the creation of a government-backed mortgage lender to drive competition. (11)As a result, the market share of the “Big 4” banks fell from 82% to 69%. This resulted in 4.6% p.a. productivity growth in retail banking, as opposed to the OECD average of 3.0%
- These developments contributed to Sweden's high private sector productivity growth of 3.3%, as opposed to OECD average of 2.2% between 1992 and 2004
- Sweden was particularly successful at using the economic crisis of the early 1990s to align the country around a clear vision of change, and driving through reforms by citing national interest

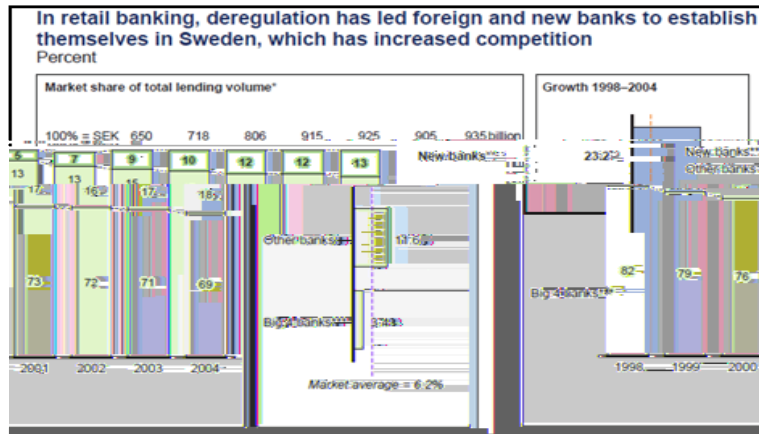


Fig.8. Productivity growth in finance

II. ADJUSTABLE MULTI-SPINDLE ATTACHMENT

Design of this accessory is very simple Fig. 9 and can be manufactured easily in any workshop by using conventional machines and weight is also not heavy. The accessory can be easily mounted on heavy duty vertical milling machines and horizontal boring machines [6]. Its gear box is very simple, changing oil is easy and will not leak even it is mounted horizontally on horizontal boring machine. This is designed particularly for machining three T- slots of either milling machine table or bolster plate of press machine see fig.10 in the machine tool manufacturing industry. It is well balanced by statically and dynamically.

As mentioned, this accessory is designed to perform the machining operation of all the three T-slots at a time for the components of milling tables and bolster plates of press machines in machine building units in mass manufacturing process. There are various methods to perform this operation by using conventional machines like milling, planing and Plano milling machines with standard cutting tools. But there is no possibility of machining all the three T-slots at a time in milling machine, since it has only one spindle possible to mount only one T-slot cutter and same thing in planing machine only one single point tool can be mounted on the cross rail/on clapper box. The operation process in planing machine is first machining the plane slots and using single point T-slot tool left hand at a time and after finishing that, machine right side by using single point T-slot tool right side. This takes three operations and process time will be more. This time can be minimised by performing two cuts of left hand and right T-slots at a time with this adjustable multi spindle attachment

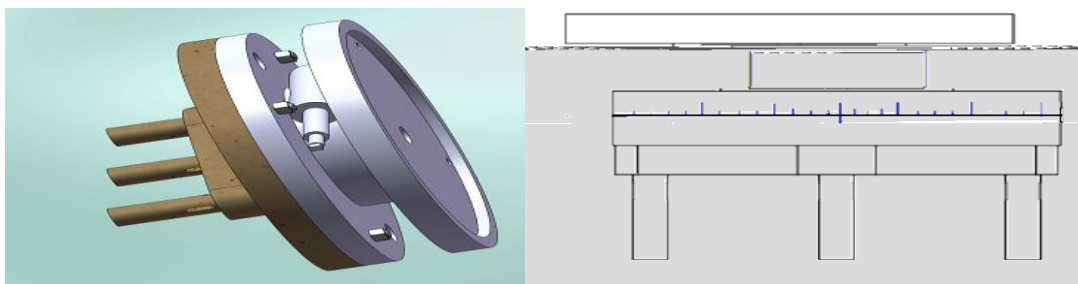


Fig.9. Adjustable multi spindle attachment

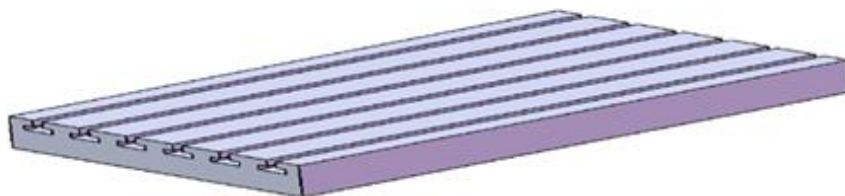


Fig.10. Bolster plate

2.1. Mechanism of adjusting centre distance of T-slots

As shown in the fig.14 the pitch circle of 160MM is selected to have max. distance between the T-slots as 160MM if the central spindle will run without cutter. That means with this arrangement only two T-slots can be machined. If the distance between T- slots is 80MM, all the three T-slots will be machined and this will be the max. distance and min. will be up to 25MM centre distance. To change the distance a Worm shaft and Helical Gear drive is used. Ref. fig. 15 to index in degree which is graduated on the fixed body housing and a vernier line is marked on the rotating spindle of the attachment. The body is provided with four holes on particularly PCD to facilitate to have four numbers of circular T- bolts of suitable size, and the rotating spindle housing is provided with circular T-slot on the same PCD of hole on the fixed body. After indexing to the required angle to obtain the centre distance of T-slot to be machined, tighten all the nuts on the fixed body.



Fig. 15 Worm shaft & Helical gear

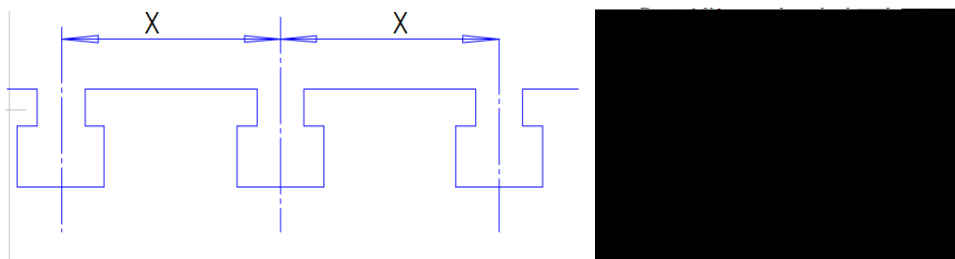


Fig. 14 Centre distance of T- slots

Indexing degree to obtain required centre distance between two T- slots will be $\Theta = \sin^{-1} x/80$

III. CONCLUSION

The productivity improvement tools highlighted in this report are all low-cost; indeed some incur no direct cost at all. They are about working smarter rather than harder. In particular the 5S principles are easy to apply and do not require major capital investment other than training, and they should quickly identify possible areas for further productivity-improvement drives.

A gradual implementation of selected tools and techniques should lead to reduction in production waste and improve the morale of employees involved as they see the immediate visual impact of their productivity improvement ideas.

An agency of the UK Government companies can get advice and information from their contact centre and from their network of local providers, which includes many of the Business Links. These organisations have Innovation and Technology Counsellors, Design Counsellors and other specialist staff, available to provide local advice. As we have seen all the process of T-slots milling, the first one in milling simply plane slot by end mill, and next T-slot milling using the T-slot cutter one by one it takes more and more time than milling all the three plain slots by using side and face cutters three slots at a time and then milling individually each T-slot at a time reduces the operation while compared to the earlier process. Next using planning machine planning single plane slot at a time for all the three T-slots and then using left hand T-slot cutter planning one slot at a time machining individually each T- slot at a time for all the three T-slots and then planning by repeating the same process for right side will take more time. This process of machining will not improve any amount of productivity and will not contribute to save time of machining for that operation. Hence the productivity is zero in this case.

The other case of milling all the three T-slots at a time after all the three plain slots are being machined using side and face milling cutters three at a time arranged on the arbor and then in similar way arrange all the three special T-slot cutters in place of side and face cutters milling three T-slots at a time may save time but there is the cost of cutter involvements and its maintenance cost, with all these it is not economic to go for this method, since this is not conventional way of machining. The productivity also improves by using carbide inserted side and face cutters instead of standard HSS cutters to some extent.

In order to reduce the time of machining for cutting all the T-slot it is suggested to go for multiple milling operations at a time, since it will save the time of operation and save the cost of operation thereby the productivity will be increasing considerably for the whole batch of mass production. The lean manufacturing process also suggest for this process and encourage such type of process to minimize the time and cost of operation. In fact this accessory has been designed manufactured and successfully utilised by one of the reputed machine building industry in India. It is proved that the rate of production is enhanced to more than 60% by using this accessory.

Finally to say by using accessory of adjustable multi spindle attachment the machining time will be reduced considerably. It has to be used exclusively to machine all the three slots in one pass. Milling plain slots is time consuming process and it is not economical process. Also it will not contribute to productivity. Hence for milling multiple T-slots at a time, first start with milling plain slots as gang milling operation, mounting all the three side and faces cutters on arbor and after that machine three T-slots using the accessory. This will give better results in machining operation and reduce machining time considerably. This accessory can be further improved with simplifying other mechanisms and can be designed for wide distance between T-slots for heavy duty machines.

REFERENCES

- [1] William J. Stevenson 8th edition
- [2] Bureau of Labor Statistics
- [3] Prime Faraday Technology Watch – May 2001
- [4] Office of National statics 2001
- [5] Global insight(GDP, export, productivity),OECD(R&D expenditure),IMF
- [6] PSG Design data, PSG College of Technology (COIMBATORE), 1968
- [7] Sandvik Asia milling cutters catalogue
- [8] ITM cutting tools catalogue
- [9] Pine, Joseph B. (1993) Mass Customization - The New Frontier in BusinessCompetition, Harvard Business School Press, Boston, MA
- [10] Willis, T. Hillman (1998) Operational competitive requirements for the twenty-first century, Industrial Management & Data Systems, Vol. 98, No. 2, 83-86
- [11] Literature review, press search, expert interview

AUTHORS BIBLIOGRAPHY:



Mr. M. Narasimha received his B.Tech. Degree in Mechanical Engineering from JNTU, Hyderabad, India. He received M.E. Degree from VMU, TAMILNADU; currently working as Lecturer in the School of Mechanical and Industrial Engineering, Institute of Technology, Bahir Dar University, Bahir Dar, Ethiopia.



Mr. Hailu Shimels received his B.Sc. Degree in Mechanical Engineering from Jimma University, Ethiopia. He received M.Sc. Degree in Mechanical Design from Addis Ababa University; currently working as Lecturer in the School of Mechanical and Industrial Engineering, Institute of Technology, Bahir Dar University, Bahir Dar, Ethiopia.



R.Rejikumar received his B.E., Degree in Mechanical Engineering from Anna University, Chennai. He received M.E. Degree from ANNA University, Thiruchirapalli. Currently working as Teaching Faculty in the School of Mechanical and Industrial Engineering, Institute of Technology, Bahir Dar, University, Bahir Dar, Ethiopia



Achamyeleh Aemro Kassie received his B.Sc. Degree in Mechanical Engineering from Addis Ababa University, Ethiopia. He received M.Tech. Degree from NIT, Warangal, India. Currently working as Lecture in the School of Mechanical and Industrial Engineering, Institute of Technology, Bahir Dar University, Bahir Dar, Ethiopia.

Analysis of Rivets Using Finite Element Analysis

¹Arumulla. Suresh, ²Tippa Bhimasankara Rao

¹pg Student, Department Of Mechanical Engineering, Nimra Institute Of Science And Technology

² Hod, Department Of Mechanical Engineering, Nimra Institute Of Science And Technology, Vijayawada, Ap, India

Abstract:

A rivet is a cylindrical body called a shank with a head. A hot rivet is inserted into a hole passing through two clamped plates to be attached and the heads supported whilst a head is formed on the other end of the shank using a hammer or a special shaped tool. The plates are thus permanently attached. Cold rivets can be used for smaller sizes the - forming processes being dependent on the ductility of the rivet material. When a hot rivet cools it contracts imposing a compressive (clamping) stress on the plates. The rivet itself is then in tension the tensile stress is approximately equal to the yield stress of the rivet material. Design of joints is as important as that of machine components because a weak joint may spoil the utility of a carefully designed machine part. Here in this project we are modeling the rivet using proe and analysing the rivet forces by Ansys which will give results by using finite element analysis.

Keywords: ANSYS. Cold rivet. Hot rivet. Pro-E.

I. INTRODUCTION

Rivets are considered to be permanent fasteners. Riveted joints are therefore similar to welded and adhesive joints. When considering the strength of riveted joints similar calculations are used as for bolted joints. Rivets have been used in many large scale applications including shipbuilding, boilers, pressure vessels, bridges and buildings etc. In recent years there has been a progressive move from riveted joints to welded, bonded and even bolted joints. A riveted joint, in larger quantities is sometimes cheaper than the other options but it requires higher skill levels and more access to both sides of the joint. There are strict standards and codes for riveted joints used for structural/pressure vessels engineering but the standards are less rigorous for using riveted joints in general mechanical engineering. Mechanical joints are broadly classified into two categories viz., non-permanent joints and permanent joints. Non-permanent joints can be assembled and disassembled without damaging the components. Examples of such joints are threaded fasteners (like screw-joints), keys and couplings etc.

Permanent joints cannot be disassembled without damaging the components. These joints can be of two kinds depending upon the nature of force that holds the two parts. The force can be of mechanical origin, for example, riveted joints, joints formed by press or interference fit etc, where two components are joined by applying mechanical force. The components can also be joined by molecular force, for example, welded joints, brazed joints, joints with adhesives etc.

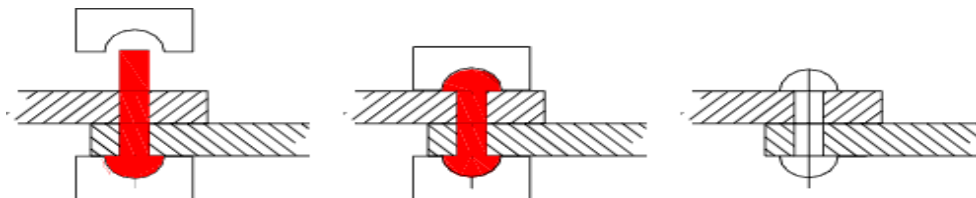


Fig.1.0 rivets

II. RIVET

A Rivet is a short cylindrical rod having a head and a tapered tail. The main body of the rivet is called shank (see figure 1.1). According to Indian standard specifications rivet heads are of various types. Rivets heads for general purposes are specified by Indian standards IS: 2155-1982 (below 12 mm diameter) and IS: 1929-1982 (from 12 mm to 48 mm diameter). Rivet heads used for boiler works are specified by IS: 1928-1978.

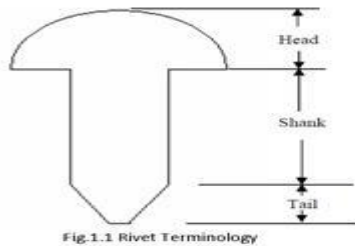


Fig.1.1 Rivet Terminology

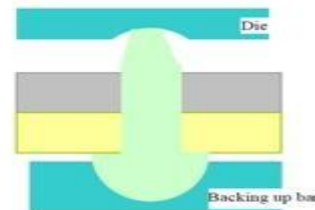


Figure 1.2: Riveting operation

Riveting is an operation whereby two plates are joined with the help of a rivet. Adequate mechanical force is applied to make the joint strong and leak proof. Smooth holes are drilled (or punched and reamed) in two plates to be joined and the rivet is inserted. Holding, then, the head by means of a backing up bar as shown in fig 1.2, necessary force is applied at the tail end with a die until the tail deforms plastically to the required shape.

III. RIVET MATERIAL

Rivets are manufactured for the materials conforming to IS: 1148-1982 and IS: 1149-1982 for structural work and to IS: 1990-1973 for pressure vessels. Rivets are usually made from the tough and ductile material namely low carbon steel (C15), nickel alloy steel, and wrought iron. Rivets are also made from non-ferrous material such as copper, aluminum alloys and brass for anti corrosive properties where strength is not major requirement. According to BIS, the rivet material should have tensile strength more than 350 N/mm² and elongations not more than 20%.

3.1 Manufacturing of rivet

Solid rivets which is of commonly used in mechanical system are generally manufactured in large numbers starting with a wire, rod or bar of material of substantially the same diameter as the desired shank of the finished rivet. In fabrication, the rod is cut off; the end of the rod is inserted into the die defining the rivet, and then typically given an initial upset followed by a final blow to form the head and tapered region between the head and shank of the rivet.

- Selecting of rod of same dia as of rivet
- Cutting of rod
- Cold heading of rivet into dies

IV. RIVETING TECHNIQUES

There are several common methods or techniques for performing riveting operations. There is the standard hand riveting with a bucking bar or a blind rivet. Three basic alternative methods of riveting are cold riveting, hot riveting, and automated riveting. Each method is used to achieve different characteristics. In the standard riveting process and in cold or hot riveting a bucking bar is used at the bottom end of the rivet to cause it to form a head when the rivet is driven through the hole. Bucking bars are of different weights depending on the size of the rivet being used. In the cold riveting process the rivets are kept in a refrigerator until they are ready to be used. The rivet is driven while it is still cold. While it is cold the rivet remains soft and is more malleable. The rivet will cure at room temperature and become hardened. This process is necessary for rivets produced from certain aluminum alloys. The hot riveting process is done for the same reasons. The difference is the rivet will be at room temperature before its use. When the rivet is needed it will be heated and then driven while it is still hot. When it cools again it will return to its hardened state. Automated riveting processes are cheaper, but do to lengthy setup time they are usually limited to one rivet type. Automated riveting can include the hot or cold riveting methods. The most common types of riveting other than the standard methods are cold riveting, hot riveting, and automated riveting. Each of the riveting methods have advantages, whether it is strength, ease of production, or cost.

V. DESIGN STRESSES

For rivets used for structures and vessels etc the relevant design stresses are provided in the applicable codes. For rivets used in mechanical engineering, values are available in mechanical equipment standards which can be used with judgment. BS 2573 Pt 1 Rules for the design of cranes includes design stress values based on the Yield stress (0.2% proofstress) $Y_{R0.2}$ as follows Hand driven rivets tensile stress (40% $Y_{R0.2}$), Shear (36.6% $Y_{R0.2}$), Bearing (80% $Y_{R0.2}$) Machinery's handbook includes some values for steel rivets. I have interpreted these values and include them below as rough approximate values for first estimate. These are typical values for ductile steel. Tensile (76MPa), Shear (61MPa), Bearing (131MPa)

VI. ANALYSIS OF RIVET

The material properties which are used for analysis of rivet

Table Material properties of adherents and adhesive used			
Material	Young's modulus (N/mm ²)	Poisson's ratio	Shear modulus (Gpa)
Adhesive	2.5×10^3	0.38	0.905
Steel	2.0×10^5	0.30	78.1

Table.1.0 Material properties

6.1 Results and discussions

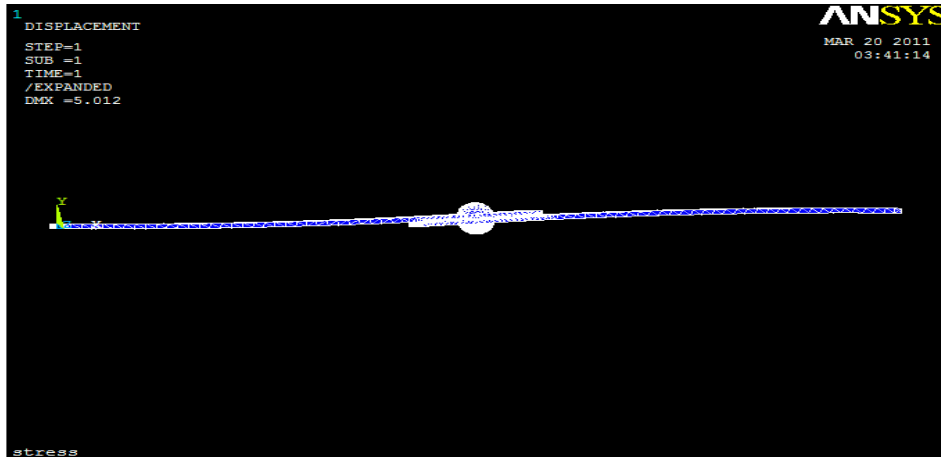


Fig.1.3 The Deformation of a single lap riveted joint without adhesive

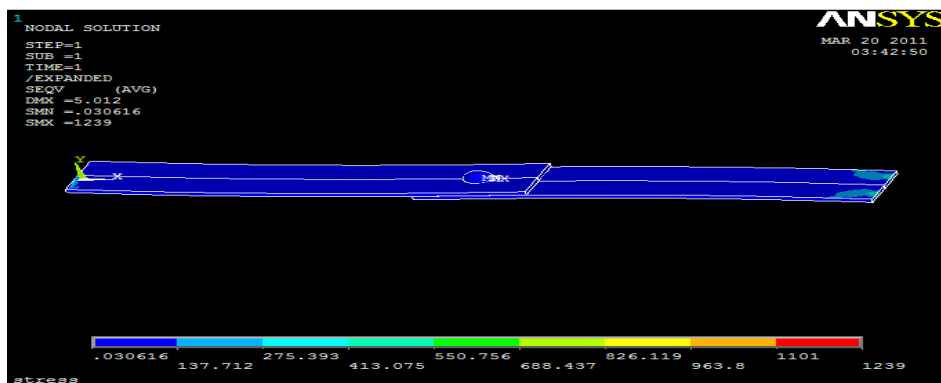


Fig.1.4 The stress distribution of a single lap riveted joint without adhesive

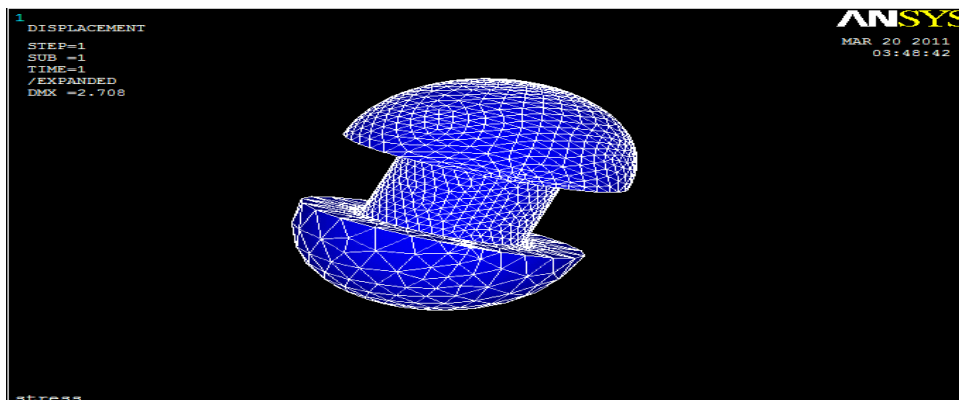


Fig.1.5 the Deformation of a rivet without adhesive

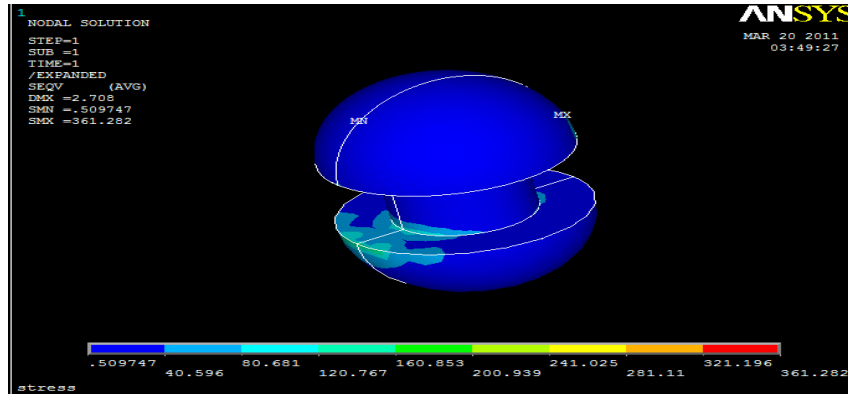


Fig.1.6 The stress distribution of a rivet without adhesive

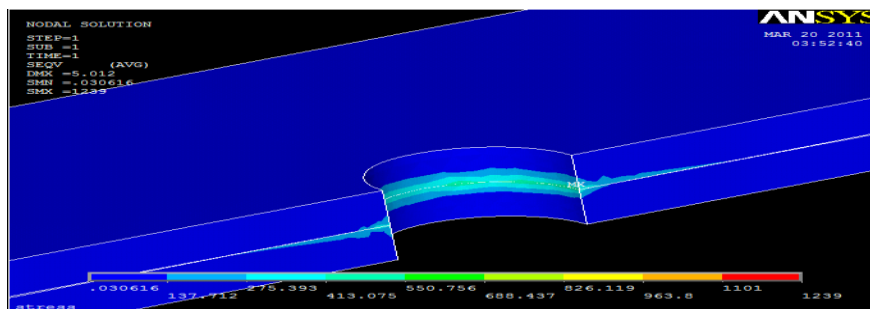


Fig.1.7 The stress distribution of a single lap riveted joint without adhesive and shows at the contact of plates and rivet.

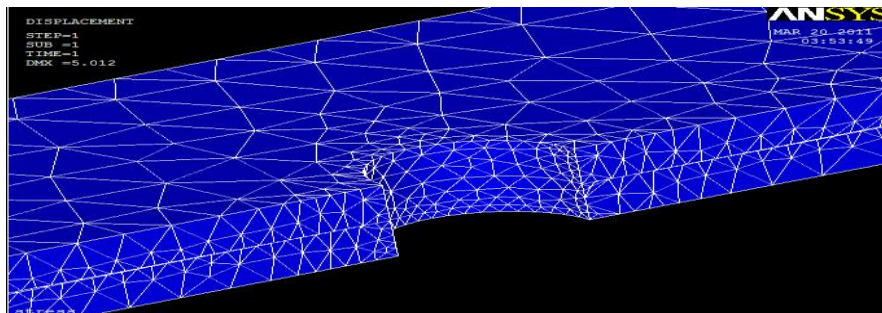


Fig.1.8 The stress distribution of a single lap riveted joint without adhesive and shows at the contact of plates and rivet with meshing elements.

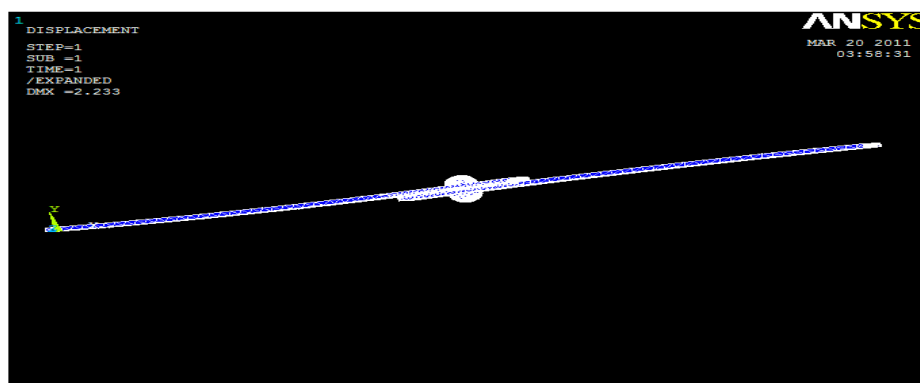


Fig.1.9 The deformation of a single lap riveted joint with adhesive b/w the plates only.

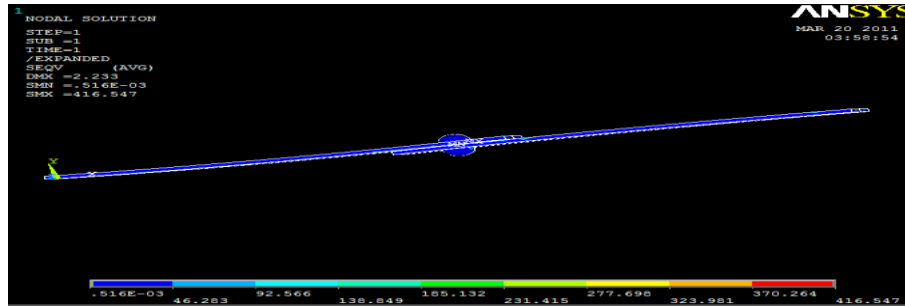


Fig.2.0The stress distribution of a single lap riveted joint with adhesive b/w the plates only.

VII. CONCLUSION

- Finite Element Method is found to be most effective tool for designing mechanical components like single lap riveted joints.
- ANSYS can be used for analysis of complex and simple models of different type without any effect on practical and economical issues.
- The results obtained from ANSYS software for the Adhesively Bonded Single lap riveted joints are compared with each other at different conditions of using adhesives at described locations leads to decreasing the stresses, uniform distribution of load gives more efficient and life to the joints.

REFERENCES

- [1]. Ali M. Ai-Samhan presented the paper on "Analysis of adhesively bonded riveted joints" he considered a model for sample Analysis.
- [2]. Gonzalez Murillo, C.Fagan, M.Ansell, M.P.Meo, Presented A Methods of Analysis and Failure Predictions for Adhesively Bonded Joints of Uniform and Variable Bond line Thickness.
- [3]. Methods of Analysis and Failure Predictions for Adhesively Bonded Joints of Uniform and Variable Bond line Thickness By Yuqiao Zhu and Keith Ked ward.
- [4]. Engineering Chemistry by Jain.Jain 15th edition Dhanpat Rai publishing company P-491-498
- [5]. A Text Book Of Strength of Materials (SI units) by Dr.R.K.Bansal P-881-910
- [6]. A Text Book Of Machine Design by R.S.kurmi, J.K.Gupta P-281-340
- [7]. Introduction to Finite Element s in Engineering Tirupathi R.Chandrupatla.

Modeling and Analysis of Hydrant Clutch

¹Gudavalli. Baby Theresa, ²Tippa Bhimasankara Rao

¹pg Student, Department Of Mechanical Engineering, Nimra Institute Of Science And Technology

² Hod, Department Of Mechanical Engineering, Nimra Institute Of Science And Technology, Vijayawada, Ap, India

Abstract:

Underground hydrant is a component used in underground piping's for an Australian based company. This hydrant is used in outdoor firefighting system, which enables firefighters to tap into the municipal water supply assist in extinguishing a fire. This is also used in many conventional daily user like fertilizer pumps, gas pipelines etc..., where the pressure is to be released or outlet is to be provided without any leak. The actual use is that it acts as a stopper at the outlet provided, and the two hooks on the top help in locking the device tapped into it. As this hydrant is subjected to huge pressure, the chances of failure are more on this, if not designed properly. This hydrant is subjected to strength analysis using 2Tr of loads with two different materials, one is the conventional material, i.e. ductile cast iron, and other is Kevlar - 29. In this project we are modeling the hydrant by using Pro-E and analysis is done by using Ansys while doing the analysis we are comparing the results with the actual cast iron material with the kevlar material which is used mostly in clutch plates as a friction material.

Keywords: ANSYS, Clutch, Hydrant, Pressure, Pro-E.

I. INTRODUCTION

A hydrant is an outlet from a fluid main often consisting of an upright pipe with a valve attached from which fluid (e.g. water or fuel) can be tapped. A fire hydrant (also known colloquially as a fire plug in the United States or as a Johnny pump in New York City),^[1] is an active fire protection measure, and a source of water provided in most urban, suburban and rural areas with municipal water service to enable firefighters to tap into the municipal water supply to assist in extinguishing a fire. Buildings near a hydrant may qualify for an insurance discount since fire-fighters should be a concept of fire plugs dates to at least the 17th century. This was a time when firefighters responding to a call would dig down to the wooden water mains and hastily bore a hole to secure water to fight fires. The water would fill the hole creating a temporary well, and be transported from the well to the fire by bucket brigades or, later, by hand-pumped fire engines. The holes were then plugged with stoppers, normally redwood, which over time came to be known as fire plugs. The location of the plug would often be recorded or marked so that it could be reused in future fires. This is the source of the colloquial term fire plug still used for fire hydrants today. After the Great Fire of London in 1666, the city installed water mains with holes drilled at intervals, equipped with risers, allowing an access point to the wooden fire plugs from street level.

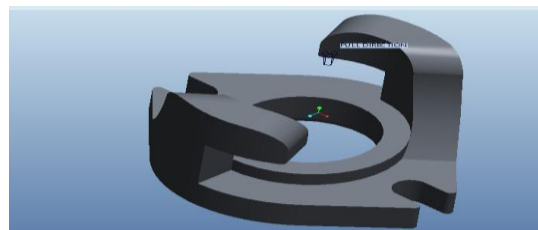


Fig.1 basic hydrant model

1.1 Making procedure of hydrant using Die casting

Die casting is a versatile process for producing engineered metal parts by forcing molten metal under high pressure into reusable steel molds. These molds, called dies, can be designed to produce complex shapes with a high degree of accuracy and repeatability. Parts can be sharply defined, with smooth or textured surfaces, and are suitable for a wide variety of attractive and serviceable finishes. Die castings are among the highest volume, mass-produced items manufactured by the metalworking industry, and they can be found in thousands of consumer, commercial and industrial products. Die cast parts are important components of products ranging

from automobiles to toys. Parts can be as simple as a sink faucet or as complex as a connector housing. Die casting is a method of producing alloy castings by injecting molten metal into metallic mold under pressure. Die casting process can be classified into

- a) Hot Chamber Process
- b) Cold Chamber Process

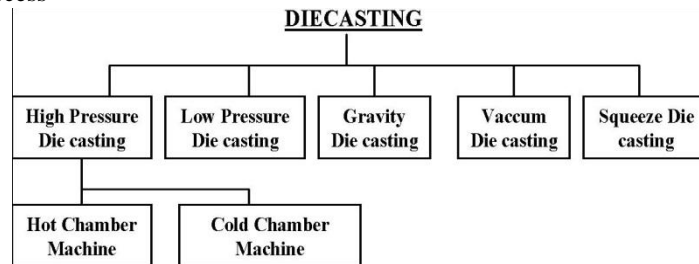


Fig.2 die-casting procedure for making hydrant

II. MODELING OF HYDRANT USING PRO-E

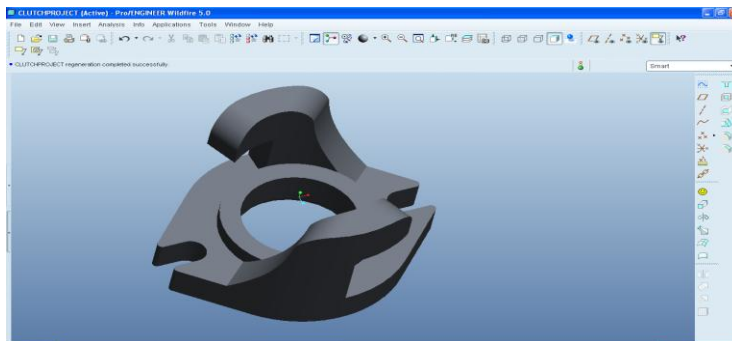


Fig.3 the generated model using pro-e

2.1 Analysis of hydrant

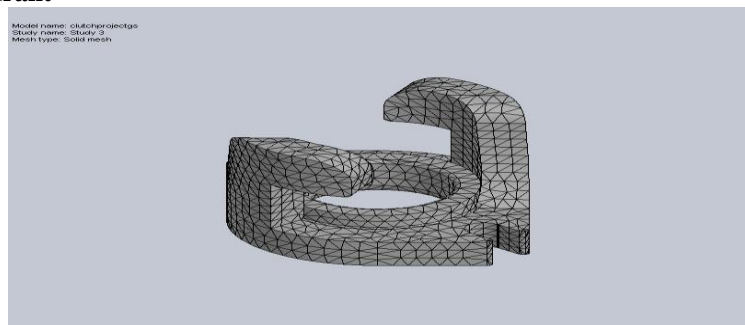


Fig.4 meshed model of hydrant

III. RESULTS & DISCUSSION

3.1 Cast-iron hydrant

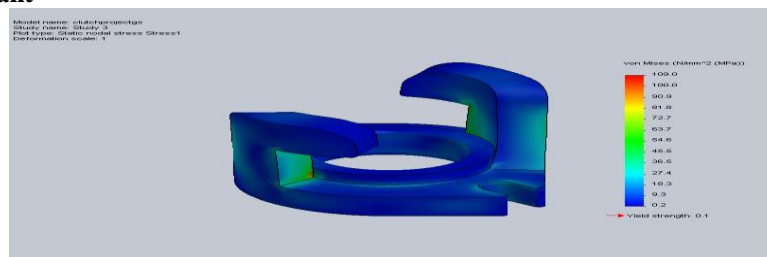


Fig.5 stress intensity of cast-iron hydrant

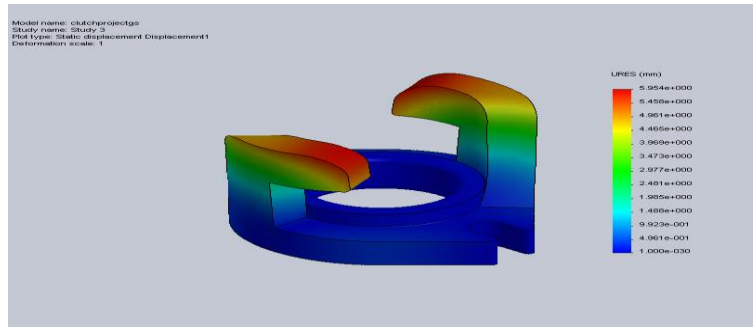


Fig.6 displaced shape of cast-iron hydrant

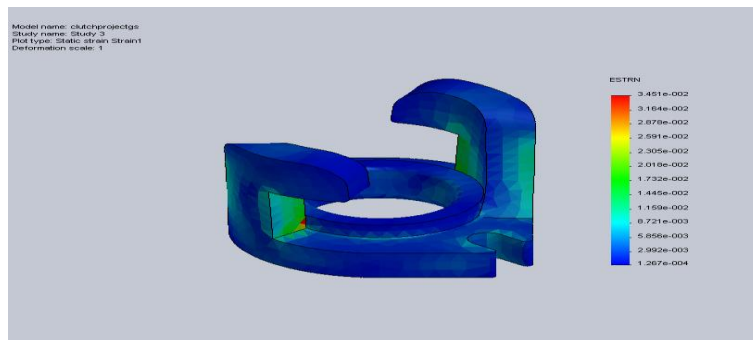


Fig.7 stain intensity of cast-iron hydrant

3.2 Kevlar hydrant

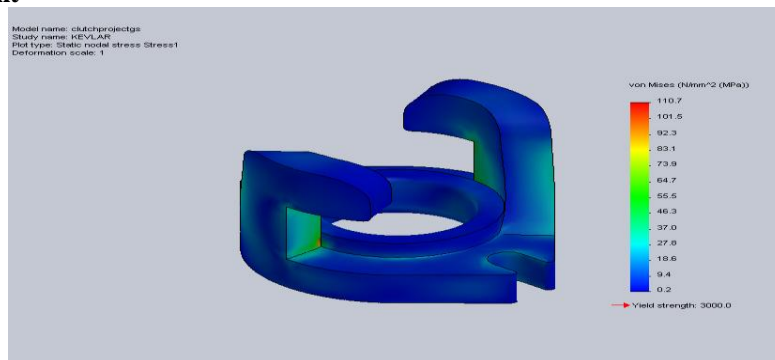


Fig.8 stress intensity of Kevlar hydrant

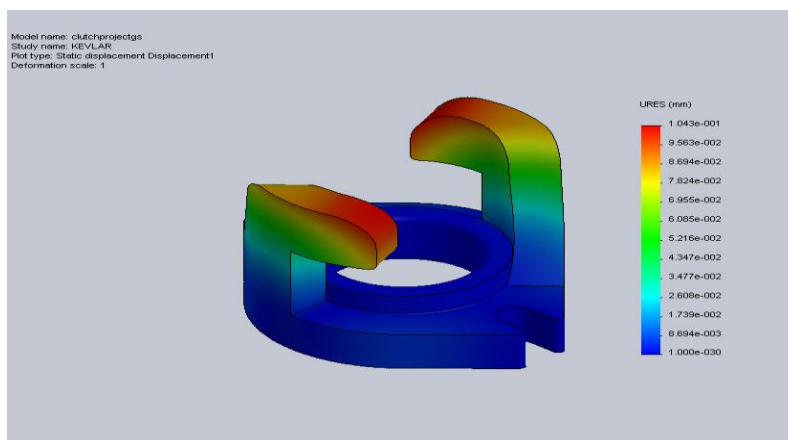


Fig.9 displaced shape of Kevlar hydrant

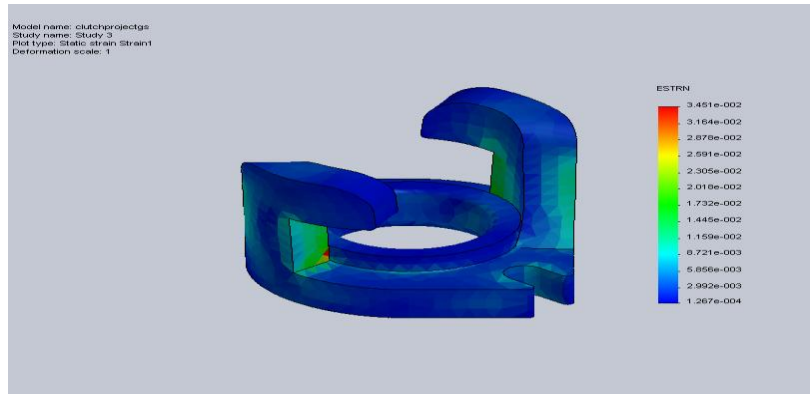


Fig.10 stain intensity of Kevlar hydrant

	STRESS(N/mm ²)	DISPLACEMENT(mm)	STRAIN
CAST IRON	109.028	5.953	0.0345
KEVLAR FIBER	110.747	0.104	6.198e ⁻⁴

Table.1 results comparison of cast-iron and Kevlar

IV. CONCLUSION

In my thesis, We have Modeled a hydrant clutch which is used in underground water supplying pipelines for industries. The modeling is done in Pro/Engineer. Presently we are using cast iron material to produce hydrant clutch. In this project we have analyzed hydrant clutch using “COSMOS” FEM based software by applying CAST IRON and KEVLAR material properties. We have replacing material with Kevlar Fiber since its density is less than that of Cast Iron, thereby reducing the weight of the component. By observing the displacement, stress and strain we are concluding that KEVLAR is better option to manufacturing of hydrant clutch. By observing the results, using Kevlar for Hydrant clutch is safe. And we have designed mould tool for the same and generated CNC codes for the core and cavity.

REFERENCES

- [1]. Machine design by r.s. khurmi
- [2]. Psg, 2008. "design data," kalaikathir achchagam publishers, coimbatore, india
- [3]. Intelligent Systems": A Comparative Study Hindawi Publishing Corporation Applied Computational Intelligence and Soft Computing Volume 2011, Article ID 183764, 18 pages.
- [4]. Abbas Fadhel Ibraheem, Saad Kareem Shather & Kasim A. Khalaf, "Prediction of Cutting Forces by using Machine Parameters in end Milling Process", Eng.&Tech. Vol.26.No.11, 2008.
- [5]. S. Abainia, M. Bey, N. Moussaoui and S. Gouasmia. " Prediction of Milling Forces by Integrating a Geometric and a Mechanistic Model", Proceedings of the World Congress on Engineering 2012 Vol III WCE 2012, July 4 - 6, 2012, London, U.K.
- [6]. Md. Anayet u patwari, a.k.m. nurul amin, waleed f. Faris, 'prediction of tangential cutting force in end milling of Medium carbon steel by coupling design of experiment and Response surface methodology'. Journal of mechanical engineering, vol. Me 40, no. 2, December 2009 Transaction of the mech. Eng. Div., the institution of engineers, Bangladesh.
- [7]. Smaoui, M.; Bouaziz, z. & Zghal, A., 'Simulation of cutting forces for complex surfaces in Ball-End milling', Int j simul model 7(2008) 2,93-105.
- [8]. Pro/Engineer Wildfire 2.0 by Steven G. Smith
- [9]. Handbook of Die design by By Ivana Suchy
- [10]. Product Design and Manufacturing by R.C. Gupta and A.K. Chaitle
- [11]. Fundamentals of Die Casting Design Genick Bar-Meir, Ph. D.

Comparative Study of Image Enhancement and Analysis of Thermal Images Using Image Processing and Wavelet Techniques

¹Ms. Shweta Tyagi , ²Mr. Hemant Amhia. ³Mr Shivdutt Tyagi³

¹(M.E. Student, Deptt. Of Electrical Engineering, JEC Jabalpur)

²(Asstt.Professor, Deptt. Of Electrical Engineering, JEC Jabalpur)

³(DRDO (ADRDE), Scientist-C,Agra)

Abstract

Principle objective of Image enhancement is to process an image so that result is more suitable than original image for specific application. Thermal image enhancement used in Quality Control ,Problem Diagnostics,Research and Development,Risk Management Programme,Digital infrared thermal imaging in health care, Surveillance in security, law enforcement and defence. Various enhancement schemes are used for enhancing an image which includes gray scale manipulation, Histogram Equalization (HE), fast Fourier transform, Image fusion and denoising. Image enhancement is the process of making images more useful. The reasons for doing this include, Highlighting interesting detail in images, removing noise from images, making images more visually appealing, edge enhancement and increase the contrast of the image.

Keywords: Adaptive filtering, Denoising, fast Fourier transform, histogram equalisation, Image enhancement. Image fusion. linear filtering. morphology. opening and closing.

I. INTRODUCTION

The aim of image enhancement is to improve the interpretability or perception of information in images for human viewers, or to provide 'better' input for other automated image processing techniques. Digital image processing is used in various applications in medicines medicine, space exploration, authentication, automated industry inspection and many more areas.

II. IMAGE ENHANCEMENT AND ANALYSIS TECHNIQUES OF IMAGE PROCESSING

Image enhancement is actually the class of image processing operations whose goal is to produce an output digital image that is visually more suitable as appearance for its visual examination by a human observer

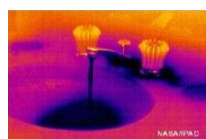
- ⇔ The relevant features for the examination task are enhanced
- ⇔ The irrelevant features for the examination task are removed/reduced

- Specific to image enhancement:

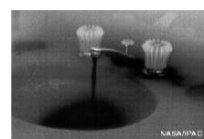
- Input = digital image (grey scale or color)
- Output = digital image (grey scale or color)

2.1. Conversion of the RGB image into GRAYSCALE image:

In RGB images each pixel has a particular colour; that colour is described by the amount of red, green and blue in it. If each of these components has a range 0–255, this gives a total of 256^3 different possible colours. Such an image is a “stack” of three matrices; representing the red, green and blue values for each pixel. This means that for every pixel there correspond 3 values. Whereas in greyscale each pixel is a shade of gray, normally from 0 (black) to 255 (white). This range means that each pixel can be represented by eight bits, or exactly one byte. Other greyscale ranges are used, but generally they are a power of 2.so, we can say gray image takes less space in memory in comparison to RGB images



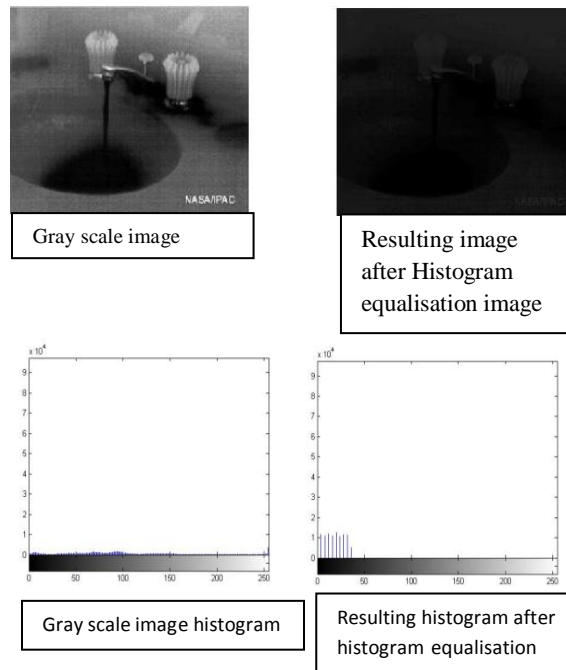
Original image (RGB image)



Gray scale image

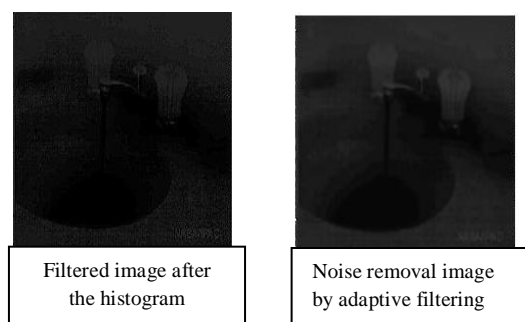
2.2 HISTOGRAM, HISTOGRAM EQUALISATION AND CONTRAST ENHANCEMENT

The histogram of an image shows us the distribution of grey levels in the image massively useful in image processing, especially in segmentation. The shape of the histogram of an image gives us useful information about the possibility for contrast enhancement. A histogram of a narrow shape indicates little dynamic range and thus corresponds to an image having low contrast. Histogram equalization is used to enhance the contrast of the image it spreads the intensity values over full range. Histogram equalization involves finding a grey scale transformation function that creates an output image with a uniform histogram. Under Contrast adjustment, overall lightness or darkness of the image is changed. Contrast enhancements improve the perceptibility of objects in the scene by enhancing the brightness difference between objects and their backgrounds. A contrast stretch improves the brightness differences uniformly across the dynamic range of the image,



2.3 Linear filtering and noise removal image

Filtering is a technique for modifying or enhancing an image. For example, you can filter an image to emphasize certain features or remove other features. Image processing operations implemented with filtering include smoothing, sharpening, and edge enhancement. Linear filtering is filtering in which the value of an output pixel is a linear combination of the values of the pixels in the input pixel's neighbourhood. The noise is removed by adaptive filtering approach, often produces better results than linear filtering. The adaptive filter is more selective than a comparable linear filter, preserving edges and other high-frequency parts of an image

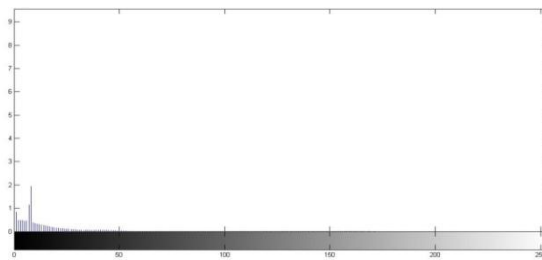


2.4 Morphology:

Morphological techniques typically probe an image with a small shape or template known as a **structuring element**. The structuring element is positioned at all possible locations in the image and it is compared with the corresponding neighborhood of pixels. Morphological operations differ in how they carry out this comparison. Mathematical morphology is based on geometry. The theoretical foundations of morphological image processing lies in set theory and the mathematical theory of order. The basic idea is to probe an image with a template shape, which is called structuring element, to quantify the manner in which the structuring element fits within a given image.



output = I – B, where output is the image obtained after the removal of non-uniform background (B) from greyscale image (I) uniform background throughout the image



Output histogram of the above image

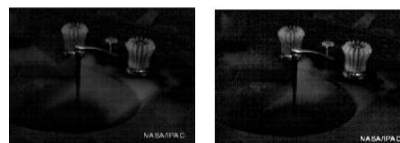
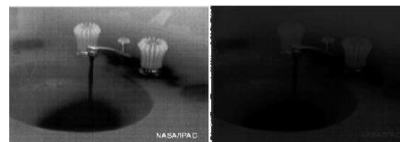
2.4. FFT transforms:

FFT function is an effective tool for computing the discrete Fourier transform of a signal. In Fourier transform it actually changes the domain of the image. In this we get the restored image after taking the inverse FFT. The FFT contains information between 0 and f_s ; however, we know that the sampling frequency must be at least twice the highest frequency component. Therefore, the signal's spectrum should be entirely below $f_s/2$, the Nyquist frequency.



FFT image

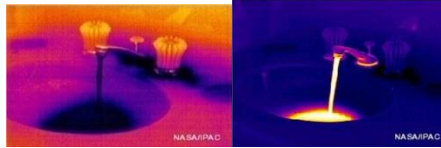
III. RESULTS FROM IMAGE PROCESSING TECHNIQUES:



(a) Gray scale image (b) resulting image after histogram equalisation (c) image after morphological operation (d) restored image after the fft transform

IV. VARIOUS TECHNIQUES OF WAVELET:

Wavelet analysis is capable of revealing aspects of data that other signal analysis techniques miss aspects like trends, breakdown points, discontinuities in higher derivatives, and self-similarity. Furthermore, because it affords a different view of data than those presented by traditional techniques, wavelet analysis can often compress or de-noise a signal without appreciable degradation. There are so many techniques to enhance an image that I have used in this to enhancement. There are two thermal images on that I have applied enhancement methods:



4.1 IMAGE FUSION:

In general, the problem that image fusion tries to solve is to combine information from several images (sensors) taken from the same scene in order to achieve a new fused image, which contains the best information original images The wavelets-based approach is appropriate for performing fusion tasks for the following reasons:

- [1] It is a multiscale (multiresolution) approach well suited to manage the different image resolutions. In recent
- [2] Years, some researchers have studied multiscale representation (pyramid decomposition) of a signal and
- [3] Have established that multiscale information can be useful in a number of image processing applications including the image fusion.
- [4] The discrete wavelets transform (DWT) allows the image decomposition in different kinds of coefficients preserving the image information.
- [5] Such coefficients coming from different images can be appropriately combined to obtain new coefficients, so that the information in the original images is collected appropriately.
- [6] Once the coefficients are merged, the final fused image is achieved through the inverse discrete wavelets transform (IDWT), where the information in the merged coefficients is also preserved.
- [7] Hence, the fused image has better quality than any of the original images

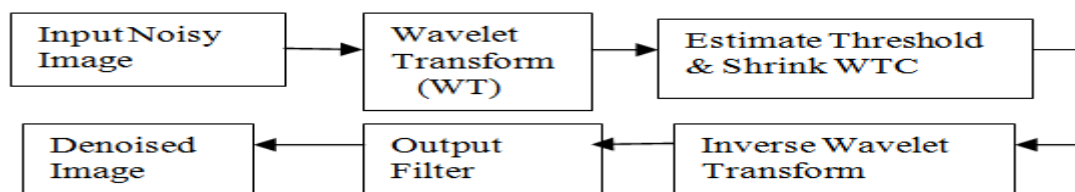


4.2 DENOISING IMAGE:

The image usually has noise which is not easily eliminated in image processing. According to actual image characteristic, noise statistical property and frequency spectrum distribution rule, people have developed many methods of eliminating noises, which approximately are divided into space and transformation fields The space field is data operation carried on the original image, and processes the image grey value, like neighbourhood average method, wiener filter, centre value filter and so on. The transformation field is management in the transformation field of images, and the coefficients after transformation are processed. Then the aim of eliminating noise is achieved by inverse transformation, like wavelet transform. Successful exploitation of wavelet transform might lessen the noise effect or even overcome it completely.

The general wavelet denoising procedure is as follows:

- Apply wavelet transform to the noisy signal to produce the noisy wavelet coefficients to the level which we can properly distinguish the PD occurrence.
- Select appropriate threshold limit at each level and threshold method (hard or soft thresholding) to best remove the noises.
- Inverse wavelet transforms of the threshold wavelet coefficients to obtain a denoised signal



Block diagram of Image denoising using wavelet transform.



4.3 COMPRESSED IMAGE:

Images require much storage space, large transmission bandwidth and long transmission time. The only way currently to improve on these resource requirements is to compress images, such that they can be transmitted quicker and then decompressed by the receiver. In image processing there are 256 intensity levels (scales) of grey. 0 is black and 255 are white. Each level is represented by an 8-bit binary number so black is 00000000 and white is 11111111. An image can therefore be thought of as a grid of pixels, where each pixel can be represented by the 8-bit binary value for grey-scale. "Image compression algorithms aim to remove redundancy in data in a way which makes image reconstruction possible." This basically means that image compression algorithms try to exploit redundancies in the data; they calculate which data needs to be kept in order to reconstruct the original image and therefore which data can be 'thrown away'. By removing the redundant data, the image can be represented in a smaller number of bits, and hence can be compressed

Two fundamental components of compression are redundancy and irrelevancy reduction.

- Redundancy reduction aims at removing duplication from the signal source (image/video).
- Irrelevancy reduction omits parts of the signal that will not be noticed by the signal receiver, namely the Human Visual System (HVS).



(A) By global Thresh holding method: balance Sparsity norm
Retained energy=99.90, No. of zeros=93.64



(B) By global Thresh holding method: remove near zero
Retained energy=100 No. of

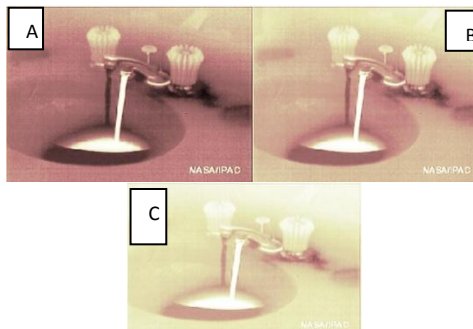


(c) By global Thresh holding method: balance Sparsity norm (sqrt)
Retained Energy=99.99
No. Of zeros=91.91



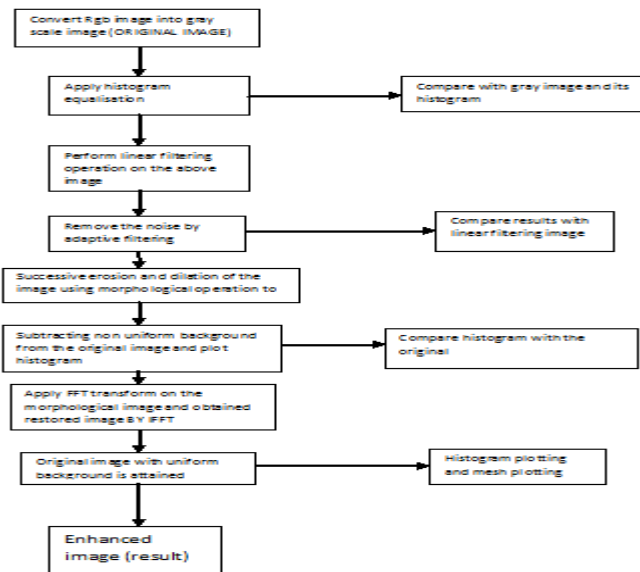
(d) By level thresh holding:
scarce low
Retained energy=100%
No. of zeros= 61.51%

V. RESULTS FROM WAVELET TECHNIQUES:



(a) Fusion image (b) denoised image(c) Compressed image

VI. PROPOSED FLOW CHART OF IMAGE PROCESSING:



VII. COMPARATIVE RESULTS

The result obtained from the wavelet techniques is better than the image processing techniques. The image gets enhanced using wavelet techniques in comparison to image processing. The enhancement of an image is easy through wavelet as in comparison to the image processing. The denoised image and compressed image is also better and is easy to obtain result through wavelet by using graphical user interface.

VIII. CONCLUSION

This work highlights the successful application of wavelet based methods for analysis of thermal images. Although in wavelet, global thresholding can be used successfully to compress images it is difficult to find a global threshold that will give near optimal results because of how the different detail sub signals differ. Global Thresholding leads to unnecessary energy losses in order to obtain a certain compression rate.

Therefore it is more logical to use local thresholds. The image processing work indicates that histogram equalization technique can't be used for images suffering from non-uniform illumination in their backgrounds specifically for particle analysis purposes as this process only adds extra pixels to the light regions of the image and removes extra pixels from dark regions of the image resulting in a high dynamic range in the output image.

REFERENCES:

- [1] Komal Vij, et al. "Enhancement of Images Using Histogram Processing Techniques Vol 2", pp309-313, 2009.
- [2] Kevin Loquin, et al. "Convolution Filtering And Mathematical Morphology On An Image: A Unified View", pp1-4, 2010.
- [3] M. Kowalczyk, et al. "Application of mathematical morphology operations for simplification and improvement of correlation of images in close-range photogrammetry", pp153-158, 2008.
- [4] J. Zimmerman, S. Pizer, E. Staab, E. Perry, W. McCartney. Brenton, "Evaluation of the effectiveness of adaptive histogram equalization for contrast enhancement," IEEE Transactions on Medical Imaging, pp. 304-312, 1988.
- [5] M. Abdullah-Al-Wadud, Md. Hasanul Kabir, M. Ali Akber Dewan, Oksam Chae, "A dynamic histogram equalization for image contrast enhancement", IEEE Transactions. Consumer Electron. vol. 53, no. 2, pp. 593- 600, May 2007.
- [6] Rafael C. Gonzalez, Richard E. Woods, "Digital Image Processing", 2nd edition, Prentice Hall, 2002
- [7] A. K. Jain, "Fundamentals of Digital Image Processing". Englewood Cliffs, NJ: Prentice-Hall, 1991.
- [8] J. Alex Stark "Adaptive Image Contrast Enhancement Using Generalizations of Histogram Equalization", IEEE Transactions on Image Processing, Vol. 9, No. 5, May 2000.
- [9] Mulcahy, Colm. "Image compression using the Haar wavelet transforms. Spelman Science and Math Journal
- [10] S. G. Chang, B Yu and M Vetterli. "Adaptive Wavelet Thresholding for image Denoising and Compression.. IEEE Transactions on Image Processing, Vol. 9, No. 9, September 2000
- [11] Walker, J.S. A Primer on Wavelets and Their Scientific Applications .Boca Raton, Fla. : Chapman & Hall/CRC, 1999
- [12] C.S. Burrus, R.A. Gopinath, H. Guo, Introduction to Wavelets and Wavelet Transforms: a Primer, Prentice-Hall, Upper Saddle River, NJ, 1998.
- [13] Chang, S. G., Yu, B., and Vetterli, M. (2000). Adaptive wavelet thresholding for image denoising and compression. IEEE Trans. On Image Proc., 9, 1532-1546.
- [14] 14. Kekre, H. B. (2011). Sectorization of Full Kekre ' s Wavelet Transform for Feature extraction of Color Images. International Journal of Advanced Computer Science and Ap plications - IJACSA, 2(2), 69-74.

Survey Paper Based On Hand Gesture Hex Color Matrix Vector

¹Sukrit Mehra, ²Prashant Verma, ³Harshit Bung, ⁴Deepak Bairagee
¹²³⁴Swami Vivekanad College Of Engineering, Indore

Abstract

In order to enable a more natural communication with reality systems, automatic hand gesture recognition appears as a suitable means. Hand gesture recognition making use of digital images has been a research topic for many years. The aim of this paper is the proposal of real time vision system for its application within visual interaction environments through hand gesture recognition, using general purpose low cost software, so any user could make use of it in his office or home. The basis of our approach is a fast segmentation process to obtain the moving hand from the whole image, which is able to deal with a large number of hand shapes against different background and lighting conditions. The most important part of the recognition process is robust shape comparison carried out through Hidden Markov Model approach, which operates on edge maps. The visual memory use allows the system to handle variation within the gestures.

Keyword: Man-Machine Interaction, Image Processing, Segmentation, Hand gesture recognition, Hidden Markov Model, Visual Memory, Range camera.

I. INTRODUCTION

Hand gesture recognition is an important research issue in the field of Human Interaction with Computer, because of its extensive applications in virtual reality, sign language recognition, and computer games. Despite lots of previous work, building a robust hand gesture recognition system that is applicable for real-life applications. Body language is an important way of communication among humans. Gesture recognition is the mathematical interpretation of a human motion by a computing device. Gesture recognition, along with facial recognition, voice recognition, eye tracking and lip movement recognition are components of what developers refer to as a perceptual user interface (PUI)[1]. The goal of PUI is to enhance the efficiency and ease of use for the underlying logical design of a stored program, a design discipline known as usability. In personal computing, gestures are most often used for input commands. Recognizing gestures as input allows

computers to be more accessible for the physically-impaired and makes interaction more natural in a gaming or 3-D virtual environment. Body language is an important way of communication among humans, adding emphasis to voice messages or even being a complete message by itself. Thus, automatic posture recognition systems could be used for improving human-machine interaction. This kind of human-machine interfaces would allow a human user to control remotely through hand postures a wide variety of devices. Different applications have been suggested. Interactions between human and computer are currently[2] performed using keyboards, mice or different hectic devices. In addition to being different from our natural way of interacting. In gesture recognition technology, a camera reads the movements of the human body and communicates the data to a computer that uses the gestures as input to control devices or applications.

II. PROBLEM DOMAIN

The main obstacle in achieving a natural interaction between man and machine based on gestures is the lack of appropriate methods of recognition and interpretation of the gestures by the computer. Different methods can be divided into two main classes:

2.1 Vision Based

a) CAMSHIFT Algorithm Limitation

There are quite a few parameters: the number of histogram bins, the minimum saturation, minimum and maximum intensity, and the width-to-height ratio for faces [3]. There's also a parameter for enlarging the face region while doing Mean Shift to increase the chances of finding the maximum for skin-probability density.

b) Time Flight Camera Limitation

Background light

Although most of the background light coming from artificial lighting or the sun is suppressed, the pixel still has to provide a high dynamic range. The background light also generates electrons, which have to be stored. For example, the illumination units in today's TOF cameras [4] [5] can provide an illumination level of about 1 watt. The Sun has an illumination power of about 50 watts per square meter after the optical bandpass filter. Therefore, if the illuminated scene has a size of 1 square meter, the light from the sun is 50 times stronger than the modulated signal.

Interference

If several time-of-flight cameras are running at the same time, the cameras may disturb each others' measurements. There exist several possibilities for dealing with this problem:

- Time multiplexing: A control system starts the measurement of the individual cameras consecutively, so that only one illumination unit is active at a time.
- Different modulation frequencies: If the cameras modulate their light with different modulation frequencies, their light is collected in the other systems only as background illumination but does not disturb the distance measurement.

Multiple reflections

In contrast to laser scanning systems, where only a single point is illuminated at once, the time-of-flight cameras illuminate a whole scene. Due to multiple reflections, the light may reach the objects along several paths and therefore, the measured distance may be greater than the true distance.

c) Naïve Bayes' Classifier Limitation

Assumption of class conditional independence usually does not hold Dependencies among these cannot be modeled by Naïve Bayesian Classifier [6].

2.2 Data Glove Based Limitation

[1] **Cost:** Even though glove-based technology has come down in price (under \$500 for the 5DT Glove), the cost of robust and complex posture and gesture recognition is going to be high if a glove-based solution is used. The cost of a tracking device and a robust glove is in the thousands of dollars. On the other hand, a vision-based solution is relatively inexpensive, especially since modern-day workstations are equipped with cameras.

[2] **User Comfort:** With a glove-based solution, the user must wear a tracking device and glove that are connected to a computer. Putting these devices on takes time, can be quite cumbersome, and can limit one's range of motion. With a vision-based solution, the user may have to wear a glove, but the glove will be extremely lightweight, easy to put on, and not connected to the computer. Applications, in which no gloves are used, give the user complete freedom of motion and provides a cleaner way to interact and perform posture and gesture recognition.

[3] **Hand Size:** Human hands vary in shape and size. This is a significant problem with glove-based solutions: some users cannot wear these input devices because their hands are too big or too small.

[4] **Hand Anatomy:** Glove-based input devices may not always fit well enough to prevent their position sensors from moving relative to the joints the sensors are trying to measure. This problem reduces recognition accuracy after extended periods of use and forces users to recalibrate the devices which can be a nuisance.

[5] **Accuracy:** In both vision- and glove-based solutions for hand posture and gesture recognition, accuracy is one of the most critical components to providing robust recognition. Both these solutions provide the potential for high levels of accuracy depending on the technology and recognition algorithms used. Accuracy also depends on the complexity and quantity of the postures and gestures to be recognized. Obviously, the quantity of possible postures and gestures and their complexity greatly affect accuracy no matter what raw data collection system is used.

[6] **Calibration:** Calibration is important in both vision- and glove-based solutions but, due to the anatomy of the hand, it is more critical with glove-based solutions. In general, a calibration procedure or step is required for every user and, in some cases, every time a user wants to run the system.

- [7] **Portability:** In many applications, especially gesture to speech systems, freedom from being tied down to a workstation is important. With glove-based solutions, this freedom is generally available as long as hand tracking is not involved, since these input devices can be plugged right into a laptop computer. Vision-based solutions were originally quite difficult to use in a mobile environment due to camera placement issues and computing power requirements.
- [8] **Noise:** In glove-based solutions where hand tracking is required, some type of noise is bound to be associated with the data (it can come from a variety of sources depending on the tracking technology used). Filtering algorithms are therefore necessary to reduce noise and jitter. In some cases this can get computationally expensive when predictive techniques such as Kalman filtering are used.

III. PROPOSED SOLUTION

A low cost computer vision system that can be executed in a common PC equipped with USB web cam is one of the main objectives of our approach. The system should be able to work under different degrees of scene background complexity and illumination conditions.

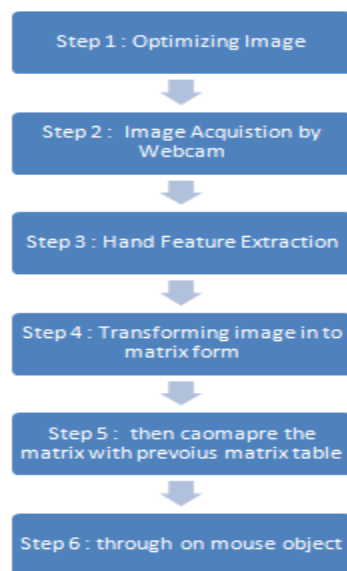


Figure 1: Proposed System Framework

The proposed technique is depending on the following approach:

- A pre image of hand is stored in the template.
- Capture the hand at initial point through frame.
- Match the captured hand with the pre hand stored in the template and marked or set the captured image as a reference image.
- Take the video frame of hand through webcam and convert the YUV color format to RGB color format.
- The RGB formatted image is saved in the form of matrix.
- Taking continues frame and match with the RGB matrix, the number of changes in the matrix is know and the movement of hand can be recognized.

3.1 Method Used: The Hidden Markov model is a stochastic process built on the top of another stochastic process, the Markov process. A time domain process exhibits first-order Markov property if the conditional probability density of the current event, given all past and present events, depends only on the most recent events. In a HMM [7], the

3.2 Using YUV Colorspace: YUV colorspace is a bit unusual. The Y component determines the brightness of the color (referred to as luminance or luma), while the U and V components determine the color itself (the chroma) [9]. Y ranges from 0 to 1 (or 0 to 255 in digital formats), while U and V range from -0.5 to 0.5 (or -128 to 127 in signed digital form, or 0 to 255 in unsigned form). Some standards further limit the ranges so the out-of-bounds values indicate special information like synchronization.

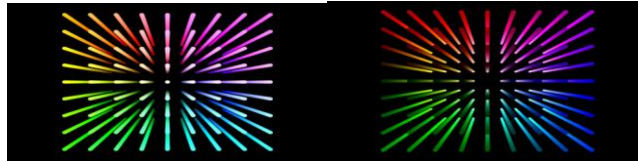


Figure2: YUV Image on Y-axis

These images show us rods at various points on the UV plane, extending through Y. This allows us to see how each UV point's color is changed as the Y value is increased or decreased.

3.3 YUV – RGB Conversion:

There are many slightly different formulas to convert between YUV and RGB. The only major difference is a few decimal places. The CCIR 601 Standard [10] specifies the correct coefficients. Since I'm lazy and haven't looked up this spec, I don't know if the following coefficients are correct or not. In any event, I've used them for many conversions with no obvious discoloration.

These formulas assume U and V are unsigned bytes.

$$R = Y + 1.4075 * (V - 128)$$

$$G = Y - 0.3455 * (U - 128) - (0.7169 * (V - 128))$$

$$B = Y + 1.7790 * (U - 128)$$

$$Y = R * .299000 + G * .587000 + B * .114000$$

$$U = R * -.168736 + G * -.331264 + B * .500000 + 128$$

$$V = R * .500000 + G * -.418688 + B * -.081312 + 128$$

JPEG/JFIF - RGB Conversion:

JPEG/JFIF files store compressed images in a YUV-like colorspace [11][12] that uses slightly different coefficients to convert to RGB. These formulas are:

$$R = Y + 1.40200 * (U - 128)$$

$$G = Y - 0.34414 * (V - 128) - 0.71414 * (U - 128)$$

$$B = Y + 1.77200 * (V - 128)$$

IV. CONCLUSION

The mouse works on 120dpi and the frame captured through webcam is 30-25 fps. Using HMM with color hex method we would increase the accuracy mouse movement interface and the process of the image in the form of vector i.e. in the form of matrix would give an 60% optimum result.

REFERENCES

- [1] Zhou Ren, Junsong Yuan, Zhengyou Zhang, "Robust Hand Gesture With Kinetic Sensor", Proceeding Of The 19th ACM International Conference On Multimedia, November 28-December 01, 2011 Scottsdale, Arizona USA, Pp. 759-760. [2] Fukunaga, Keinosuke; Larry D. Hostetler (January 1975). "The Estimation Of The Gradient Of A Density Function, With Applications In Pattern Recognition". IEEE Transactions On Information Theory(IEEE) 21 (1): 32-40. Doi:10.1109/TIT.1975.1055330. Retrieved 2008-02-29.
- [3] VADAKKAPAT, P ET.AL, "MULTIMODAL APPROACH TO HUMAN-FACE DETECTION AND TRACKING", INDUSTRIAL ELECTRONICS, IEEE TRANSACTIONS ON ISSUE DATE: MARCH 2008, VOLUME: 55 ISSUE:3, PP.1385 - 1393
- [4] E. KOLLORZ, J. HORNEGGER AND A. BARKE, "GESTURE RECOGNITION WITH A TIME-OF-FLIGHT CAMERA, DYNAMIC 3D IMAGING", INTERNATIONAL JOURNAL OF INTELLIGENT SYSTEMS TECHNOLOGIES AND APPLICATIONS ISSUE: VOLUME 5, NUMBER 3-4 2008, PP.334 - 343.
- [5] B'OHME, M., HAKER, M., MARTINETZ, T., AND BARTH, E. (2007) "A FACIAL FEATURE TRACKER FOR HUMAN-COMPUTER INTERACTION BASED ON 3D TOF CAMERAS", DYNAMIC 3D IMAGING (WORKSHOP IN CONJUNCTION WITH DAGM 2007).
- [6] PUJAN ZIAIE ET.AL, "USING A NAÏVE BAYES CLASSIFIER BASED ON K-NEAREST NEIGHBORS WITH DISTANCE WEIGHTING FOR STATIC HAND-GESTURE RECOGNITION IN A HUMAN-ROBOT DIALOG SYSTEM" ADVANCES IN COMPUTER SCIENCE AND ENGINEERING COMMUNICATIONS IN COMPUTER AND INFORMATION SCIENCE, 2009, VOLUME 6, PART 1, PART 8, PP.308-315.
- [7] A. MARKOV. AN EXAMPLE OF STATISTICAL INVESTIGATION IN THE TEXT OF EUGENE ONYEGIN, ILLUSTRATING COUPLING OF TESTS IN CHAINS. PROCEEDINGS OF THE ACADEMY OF SCIENCES OF ST. PETERSBURG, 1913
- [8] L. BAUM ET. AL. A MAXIMIZATION TECHNIQUE OCCURRING IN THE STATISTICAL ANALYSIS OF PROBABLISTIC FUNCTIONS OF MARKOV CHAINS. ANNALS OF MATHEMATICAL STATISTICS, 41:164-171, 1970.
- [9] N. SOONTRANON, S. ARAMVITH, AND T.H. CHALIDABHONGSE. FACE AND HANDS LOCALIZATION AND TRACKING FOR SIGN LANGUAGE RECOGNITION. INTERNATIONAL SYMPOSIUM ON COMMUNICATIONS AND INFORMATION TECHNOLOGIES 2004 (ISCIT 2004), SAPPORO, JAPAN, OCTOBER26-29, 2004
- [10] U. AHLVERS, U. ZÖLZER, R. RAJAGOPALAN. MODEL-FREE FACE DETECTION AND HEAD TRACKING WITH MORPHOLOGICAL HOLE MAPPING, EUSIPCO'05, ANTALYA, TURKEY.
- [11] S. ASKAR, Y. KONDRATYUK, K. ELAZOUZI, P. KAUFF, O. SCHEER. VISION-BASED SKIN-COLOUR SEGMENTATION OF MOVING HANDS FOR REAL-TIME APPLICATIONS. PROC. OF. 1ST EUROPEAN CONFERENCE ON VISUAL MEDIA PRODUCTION, CVMP, LONDON, UNITED KINGDOM, 2004.
- [12] A. HADID, M. PIETIKAINEN, B. MARTINKAUPPI. COLOR-BASED FACE DETECTION USING SKIN LO-CUS MODEL AND HIERARCHICAL FILTERING. PROC. OF 16TH INTERNATIONAL CONFERENCE ON PATTERN RECOGNITION 2002, VOL4, PP. 196-200, 2002

Token Based Contract Signing Protocol using OTPK

Bhagyashree Bodkhe¹, Ms. Pallavi Jain²,

¹Department of Computer Science and Engineering, Shri Vaishnav Institute of Technology and Science, Indore (M.P.), India

ABSTRACT:

In the Information Security field there are many of the techniques that make the application secure by exchanging data between two parties. A fair exchange is required for increasing the chances of attack. Hence a new contract signing protocol is proposed based on the OTPK (one time private key) scheme. This protocol will allow two parties to exchange their digital signature between them by signing contract. The proposed protocol ensures fairness such that either both parties receive each other's signatures or neither of them. The proposed protocol uses offline Trusted Third Party (TTP) that will be brought into play only if one party is cheating in other case, the TTP remains inactive. The idea is to use a better authentication between two parties in which a token is send to the TTP in response to that one private key is generated that is used for the authentication between two parties and after a certain amount of time that key has be destroyed. Thus with OTPK scheme the key is not stored at any place so the storage cost will be reduced.

Keywords: asymmetric, digital signature, fairness, OTPK, private key, TTP, security.

I. INTRODUCTION

In electronic transactions the involved parties do not trust each other; hence a contract signing is needed in this situation. The contract signing is simple in the paper based scenario due to the existence of simultaneity. Two hard copies of the same contract are signed by both people at the same place and at the same time. After that, each one keeps one copy as a legal document that shows both of them have committed to have the contract. Therefore the other party must provide the signed contract to a judge in court if one party does not abide. Forging a signature is a difficult matter for a false person would need to be present physically to produce it. Instead simultaneity is achieved through the notion of fairness. Contracts play an important role in many business transactions. Traditionally, paper-based contracts it is necessary that the contract is signed by both the parties at same time and at the same venue. Both the parties sign a copy of the contract for every contracting party so that every party has a copy of the signed contract. If the parties, however, are not able to meet to sign the paper-based contract, then signing an electronic contract is an alternative. The problem with signing electronic contracts, however, is exchanging the signatures of the parties, especially where there is a lack of trust between parties. One party may send the other party their signature on the contract but may not receive the signature of the other party in return. To solve the problems of exchanging digital signatures, contract signing protocols are used. Contract Signing Protocols ensure that either contracting parties receive signature or neither of them. Thus a new, efficient contract signing protocol is proposed. The proposed protocol is based on offline trusted third party (TTP) that brought into play only if one party fails to send their signature on the contract. In the normal execution of the protocol, the transaction parties will exchange their signatures directly.

1.1 One Time Private Key

In daily life there are various electronic transactions possible for the quick transfer of information from one party to other. During the exchange of information between two parties fairness between the parties is important otherwise it will give rise to various types of attacks [9]. Thus to overcome such limitation a secure technique for strong authentication is One time private key in which sender and receiver uses his/her own key for the authentication and when the encryption and decryption is performed at both the end by sender and receiver then the key will be destroyed.

Salient features of OTPK

OTPK is only for One-time use. The certificate is short-lived.

Each time a signature is needed; the key is generated, certified, used to sign the transaction, and then deleted.

Key always remains in client possession throughout the short lifetime, and never stored on a permanent basis.

Main security lies in the online certification process where the user would use strong (2-factor) authentication to the CA.

II. BACKGROUND

A Contract Signing protocol is a new way of securing the exchange of data information over the internet, since the chance of cheating over the network has been increased, hence the solution is implement a new and efficient protocols for the prevention from various attacks in the network as well as different online applications such as E-commerce can be done securely. Also during the exchange of information between two parties fairness is maintained and no party can cheat the other in an optimistic manner.

III. RELATED WORK

The contract signing protocol will allow two parties to sign the same contract and then exchange the digital signature between them. The proposed protocol ensures fairness in such a way that it offers parties greater security: either both parties receive each other's signatures or neither of them. But the fair exchange always needs a trusted third party.

In 2011 Alfin Abraham[1] has proposed a Abuse-Free Optimistic Contract Signing Protocol which allow the two parties to sign the contract using digital signature. This protocol is based on RSA technique. In this protocol the contract is signed using multiple TTP's thus there is no single point of failure will cause and with multiple TTP's the chances of attack will be less.

In 2011 Alfin Abraham, Vinodh Edwards, Harlay Maria Mathew [2] has implemented optimistic fair digital exchange protocol. Here in this paper he made a survey of optimistic and fair exchange protocol. Optimistic, means the third trusted party (TTP) is involved only in the situations where one party is cheating or the communication channel is interrupted.

In Park et al.'s RSA-Based Multisignature Protocol [5] Here in this protocol he use RSA signature and multisignature model for an efficient fair exchange protocol and for zero knowledge proof.

In Verifiable Escrows Based Protocol [2] that allows two parties to exchange digital signatures so that either each party gets the other's signature, or neither party does. Here the trusted third party is used as an "escrow service". The basic idea is that Alice, the initiator, encrypts her signature under the public key of the trusted third party. So Bob, the responder, can have it decrypted by the trusted third party. Together with this escrow scheme a standard "cut-and-choose" interactive proof is used which make it verifiable. In the sense that the player who receives this escrow can verify that it is indeed the escrow of a signature of the desired form with a correct condition attached. This protocol makes use of three sub-protocols: an abort protocol for the initiator, a resolve protocol for the receiver, and a resolve protocol for the initiator. The protocol can also be used to encrypt data for maintaining data integrity while it is exchanged through the internet.

In 2004 F. Bao, G. Wang, J. Zhou, and H. Zhu proposed Fair Contract Signing Protocol [6]. In this protocol, two mutually distrusted parties exchange their commitments to a contract in such that either each of them can obtain the other's commitment, or neither of them does. A efficient approach for fair contract signing is using an invisible trusted third party. TTP comes into play when one party is cheating. The protocol is a generic scheme since any secure digital signature scheme and most of secure encryption algorithms can be used to implement it. In 2006 Generic Fair Non-Repudiation Protocols with Transparent Off-Line TTP [8] was proposed. In this non-repudiation service irrefutable evidences need to be generated, exchanged, and validated via computer networks. After the completion of such a transaction, each involved party should obtain the expected items. If any dishonest party denies his/her participation in a specific transaction, others can refute such a claim by providing electronic evidences to a judge. This non-repudiation protocol [8] is a generic fair protocol with transparent off-line TTP. This protocol is exchanges a digital message and an irrefutable receipt between two mistrusting parties over the Internet. At the end of this protocol execution, either both parties obtain their expected items or neither party does.

IV. PROBLEM SPECIFICATION

Although there are many authentication techniques implemented for the contract signing between two clients but here the digital signature is based on RSA digital signature scheme and the trust in a single TTP is divided into multiple TTP. Thus this proposed protocol avoids single point of failure but doesn't provide an authentication between two parties and where the chances of cheating are more. The trapdoor commitment scheme explained in makes this protocol an abuse free one where the abuse freeness is a necessary property in contract signing but is not very efficient as per the authentication is concerned.

4.1 Objectives

- To determine mutual authentication between sender and the receiver.
- To determine simulation of data transmission between sender and receiver and multiple TTP's.
- To determine separate generation of one time private key.
- To determine simulation of contract signing.

V. PROPOSED SCHEME

As shown in the figure 1 is the architecture proposed for the contract signing protocol using OTPK, here in this technique the authentication or the digital signatures generated is one time and as soon as the transmission is successful the key is destroyed.

1. First of all one party needs to register on the TTP and make request for signing to TTP .Both the parties are issued an OTP token that can be sending over a secure channel.
2. The OTP token will be used for the authentication between two parties.
3. During the generation of digital signatures an OTPK module is used which consists of:
 - First of all generating public-private key pair for authentication of user.
 - Each user need to provide the OTP token to the CA.
 - So that the CA will verifies the authentication of user if the authentication get succeed the key pair will destroyed.
4. Thus the contract is signed between two parties in a secure way using TTP.
5. When the communication is over between parties then TTP destroys the secret key generated.

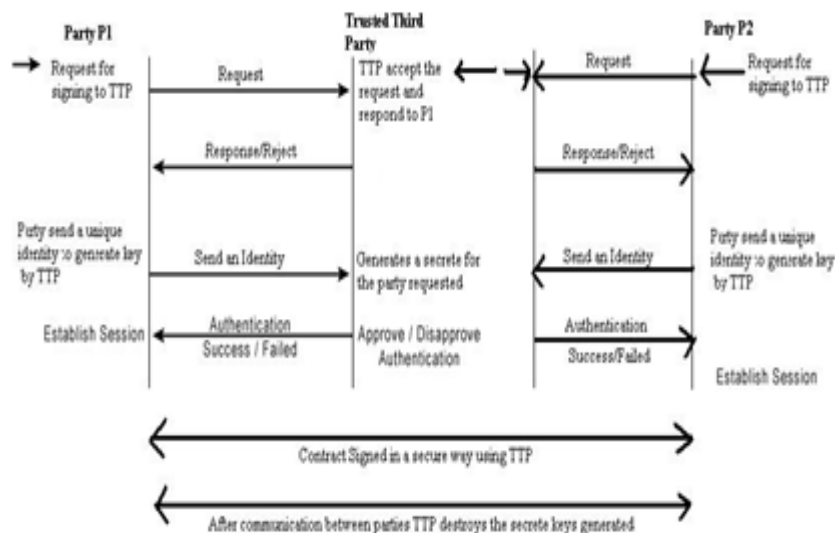


Figure 1. Architecture of OTPK scheme

VI. CONCLUSION

The aim of this paper is construct a new and efficient token based contract signing protocol with Multiple TTP's using One time private key (OTPK). Thus this protocol not only solve the problem of single point of failure by using multiple TTP's but allow the Key to always remains in client possession throughout the short lifetime, and never stored on a permanent basis so help in reducing the storage cost and thus providing security against various attacks.

REFERENCES

- [1] Alfin Abraham, "An Abuse-Free Optimistic Contract Signing Protocol with Multiple TTPs", IJCA Special Issue on "Computational Science – New Dimensions & Perspectives" NCCSE, 2011.
- [2] Alfin Abraham, Vinodh Edwards, Harlay Maria Mathew", A Survey on Optimistic Fair Digital Signature Exchange Protocols", Alfin Abraham et al. / International Journal on Computer Science and Engineering (IJCSE).
- [3] N. Asokan, V. Shoup, and M. Waidner, "Optimistic fair exchange of digital signatures," IEEE J. Sel. Areas Commun., vol. 18, no. 4, pp.591–606, Apr.2000.
- [4] Giuseppe Ateniese, "Efficient Verifiable Encryption (and Fair Exchange) of Digital Signatures", ACM 1999.
- [5] Jung Min Park, Edwin K.P. Chong, Howard Jay Siegel," Constructing Fair-Exchange Protocols for E-commerce Via Distributed Computation of RSA Signatures", ACM 2003.
- [6] F. Bao, G. Wang, J. Zhou, and H. Zhu, "Analysis and improvement of Micali's fair contract signing protocol," in Proc. ACISP'04, 2004, vol. 3108, LNCS, pp. 176–187, Springer-Verlag.
- [7] S. Micali, "Simple and fast optimistic protocols for fair electronic exchange," in Proc. PODC'03, 2003, pp. 12–19, ACM Press.
- [8] G. Wang, "Generic non-repudiation protocols supporting transparent off-line TTP," J. Comput. Security, vol. 14, no. 5, pp.441–467,Nov.2006.
- [9] Vinod Moreshwar Vaze," Digital Signature on-line, One Time Private Key [OTPK]", International Journal of Scientific& Engineering Research Volume 3, Issue 3, March -2012 I ISSN22295518".
- [10] O. Markowitch and S. Kremer. An optimistic non-repudiation protocol with transparent trusted third party. In: Information Security Conference (ISC'01), LNCS 2200, pp. 363-378. Springer-Verlag, 2001.
- [11] Y. Dodis and L. Reyzin, "Breaking and repairing optimistic fair exchange from PODC 2003," in Proc. ACM Workshop on DigitalRights Management (DRM'03), 2003, pp. 47–54, ACM Press.

State of Art on Yarn Manufacturing Process & its defects in Textile Industry

Neha Gupta, Prof. Dr. P. K. Bharti

Department of Mechanical Engineering Integral University, Lucknow, India

Abstract:

This paper is related to textile industry especially to Yarn manufacturing process. Textile is one of the biggest manufacturing industries in India. Defects rate of product plays a very important role for the improvement of yield and financial conditions of any company. Actually defects rate causes a direct effect on the profit margin of the product and decrease the quality cost during the manufacturing of product. Companies strive to decrease the defects rate of the product during the manufacturing process as much as possible. By checking and inspection of defects of product at different point in a production cycle and management implement some changes specifically at those points in production where more defects are likely to happen. The paper of defects rate of textile product in the yarn manufacturing process is so important in industry point of view. This process has large departments where the cotton passes in different process and may be effects the quality of yarn when it reaches the package form. A thousand defects opportunities create in the final package of yarn. In winding department where the final package of yarn is make. Final package of yarn is the end product and from it is direct send to the customers and if any final product passes with some defects and may chance the customer complaint.

Keywords: Defects, Yarn Manufacturing Departments, Textile Industry.

I. INTRODUCTION

This paper is related to textile industry especially to Yarn manufacturing process. In this paper identifies the different problems occurring during manufacturing of yarn in different processes, it also highlights the critical success factors which are most important in quality point of view. It also describes the preventive action against any failure. In order to tackle the complex problems, the first thing is to construct a well-structured problem formulation “a good representation”. There are different types of problem formulation like “What” what kind of problem that occurs during the yarn manufacturing process and its effects on quality “Why” why the problems create during process “How” how to solve the problems from different actions and implementation some rules in the process. In this paper describes different problems in quality perspective in different departments and identifies the reason for these problems due to carelessness of employees during manufacturing. Training of employees and preventive action against any failures in the department is necessary for any organization. [1, 2] Yarn consists of several strands of material twisted together. Each strand is, in turn, made of fibers, all shorter than the piece of yarn that they form. [3] These short fibers are spun into longer filaments to make the yarn. Long continuous strands may only require additional twisting to make them into yarns. Sometimes they are put through an additional process called texturing. The characteristics of spun yarn depend, in part, on the amount of twist given to the fibers during spinning. A fairly high degree of twist produces strong yarn; a low twist produces softer, more lustrous yarn; and a very tight twist produces crepe yarn. [5] Yarns are also classified by their number of parts. A single yarn is made from a group of filament or staple fibers twisted together. Ply yarns are made by twisting two or more single yarns. Cord yarns are made by twisting together two or more ply yarns.

Almost eight billion pounds (3.6 billion kg) of spun yarn was produced in the United States during 1995, with 40% being produced in North Carolina alone. Over 50% of spun yarn is made from cotton. Textured, crimped, or bulked yarn comprised one half of the total spun. [6, 7] Textured yarn has higher volume due to physical, chemical, or heat treatments. Crimped yarn is made of thermoplastic fibers of deformed shape. Bulked yarn is formed from fibers that are inherently bulky and cannot be closely packed.

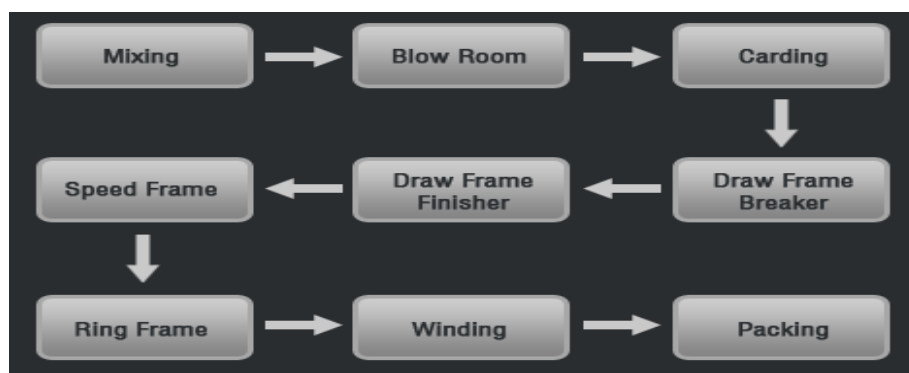


Fig. 1 Diagram of yarn manufacturing process

Yarn is used to make textiles using a variety of processes, including weaving, knitting, and felting. Nearly four billion pounds (1.8 billion kg) of weaving yarn, three billion pounds (1.4 kg) of machine knitting yarn, and one billion pounds (450 million kg) of carpet and rug yarn was produced in the United States during in 1995. [7,9,10] The U.S. textile industry employs over 600,000 workers and consumes around 16 billion pounds (7 billion kg) of mill fiber per year, with industry profits estimated at \$2.1 billion in 1996. Exports represent more than 11% of industry sales, approaching \$7 billion. The apparel industry employs another one million workers. [23]

II. HISTORY

Natural fibers—cotton, flax, silk, and wool—represent the major fibers available to ancient civilizations. The earliest known samples of yarn and fabric of any kind were found near Oberhausen, Switzerland, where bundles of flax fibers and yarns and fragments of plain-weave linen fabric, were estimated to be about 7,000 years old. Cotton has also been cultivated and used to make fabrics for at least 7,000 years. It may have existed in Egypt as early as 12,000 B.C. Fragments of cotton fabrics have been found by archeologists in Mexico (from 3500 B.C.), in India (3000 B.C.), in Peru (2500 B.C.), and in the southwestern United States (500 B.C.). Cotton did not achieve commercial importance in Europe until after the colonization of the New World. Silk culture remained a specialty of the Chinese from its beginnings (2600 B.C.) until the sixth century, when silkworms were first raised in the Byzantine Empire.[23, 24]

Synthetic fibers did not appear until much later. The first synthetic, rayon, made from cotton or wood fibers, was developed in 1891, but not commercially produced until 1911. Almost a half a century later, nylon was invented, followed by the various forms of polyester. Synthetic fibers reduced the world demand for natural fibers and expanded applications. Until about 1300, yarn was spun on the spindle and whorl. A spindle is a rounded stick with tapered ends to which the fibers are attached and twisted; a whorl is a weight attached to the spindle that acts as a flywheel to keep the spindle rotating. The fibers were pulled by hand from a bundle of carded fibers tied to a stick called a distaff. In hand carding, fibers are placed between two boards covered with leather, through which protrude fine wire hooks that catch the fibers as one board is pulled gently across the other. [26]The spindle, which hangs from the fibers, twists the fibers as it rotates downward, and spins a length of yarn as it pulls away from the fiber bundle. [23]When the spindle reaches the floor, the spinner winds the yarn around the spindle to secure it and then starts the process again. This is continued until all of the fiber is spun or until the spindle is full.

A major improvement was the spinning wheel, invented in India between 500 and 1000 A.D. and first used in Europe during the middle Ages. A horizontally mounted spindle is connected to a large, hand-driven wheel by a circular band. The distaff is mounted at one end of the spinning wheel and the fiber is fed by hand to the spindle, which turns as the wheel turns. A component called the flyer twists the thread just before it is wound on a bobbin. The spindle and bobbin are attached to the wheel by separate parts, so that the bobbin turns more slowly than does the spindle. Thus, thread can be twisted and wound at the same time. About 150 years later, the Saxon wheel was introduced. Operated by a foot pedal, the Saxon wheel allowed both hands the freedom to work the fibers. [27, 30]A number of developments during the eighteenth century further mechanized the spinning process. In 1733, the flying shuttle was invented by John Kay, followed by Hargreaves' spinning jenny in 1766. The jenny featured a series of spindles set in a row, enabling one operator to produce large quantities of yarn. Several years later Richard Arkwright patented the spinning frame, a machine that used a series of rotating rollers to draw out the fibers. A decade later Samuel Crompton's mule machine was

invented, which could spin any type of yarn in one continuous operation. [32]The ring frame was invented in 1828 by the American John Thorp and is still widely used today.

This system involves hundreds of spindles mounted vertically inside a metal ring. Many natural fibers are now spun by the open-end system, where the fibers are drawn by air into a rapidly rotating cup and pulled out on the other side as a finished yarn. [33]

III. YARN MANUFACTURING DEPARTMENT

In under the yarn manufacturing department, there are mainly seven departments:

3.1 Blow Room Process

Blow room is the initial stage in spinning process. The name blow room is given because of the “air flow” And all process is done in blow room because of air flow. Blow room is consisting of different machines to carry out the objectives of blow room. In blow room the tuft size of cotton becomes smaller and smaller. Mixing of cotton is done separately as well as in blow room. Compressed layer of bale is also open in blow room with the help of machine. [34]In blow room cotton bales are opened and cotton is transfer from different number of machines with the help of air flow. This chapter clears the main objectives of blow room such as opening, cleaning and mixing and also describes the technical point regarding to quality point of view. Here also describes the defects which affect the yarn quality and preventive action to cover these defects according to quality standard. There is lot of things in this department which is described below:



Fig. 2 Diagram of Blowroom

3.1.1 Objective of Blow Room

Following are the basic operation or objectives of blow room:

- Opening
- Cleaning
- Mixing or blending
- Micro dust removal
- To extract the contamination in the cotton such as leaf, stone, iron particles, jute, poly propylene, colour fibers, feather and other foreign material from cotton by opening and beating.
- To uniform feeding to the next stage such as carding machine.
- Recycling the waste material.

3.1.2 Technical points in Blow room

Following are the technical points in the blow room:

- Opening in blow room means opening the cotton in small pieces. The operation of opening means to increase volume of flocks while the number of fiber in the flock remains constant. That is the specific density of material is reduced.
- If the size of dirt particle is larger, it can be removed easily.
- A lot of impurities and contamination are eliminated at the start of the process.
- As much opening of cotton will be more, cleaning result will be more acceptable. But this cleaning of cotton is done on the basis of high fiber loss. High roller speed gives more better cleaning effect but also more stress on fiber. So roller speed is adjusted at a nominal speed so there should be well opening of cotton and it does not effect of quality of fiber.
- Cleaning efficiency of cotton is depending upon trash percentage. The cleaning efficiency is different for different varieties of cotton with same trash percentage.
- If the opening of cotton is done well in initial stage then cleaning becomes easier. As surface area of opened cotton is more, so therefore cleaning is more efficient.
- In traditional method more number of machine are used to open and clean natural fiber.
- If automatic bale opener machine is used, the tuft size of material should be as small as possible. In this way more efficiency of machine is achieved and machine stopping time is reduced.

- For the opening of cotton, use inclined spiked lattice (tray) at the initial stage always a better way of opening of cotton with minimum damage.
- Mechanical action on fibers creates some problems in the quality of yarn in the form of neps.
- In beating operation by using a much shorter machine sequence, fibers with better elastic properties. In this way spin ability can be produced.
- Stickiness in the cotton affects the process very badly in the way of production and quality.
- It is necessary to control the temperature inside the department, when use stickiness cotton.
- Released of dust particles into the air occurs whenever the raw material is rolled beaten or thrown about. Accordingly the air at such position is sucked away. For the removal of dust perforated drums, stationary drums are used.

3.1.3 Factors affecting on opening, cleaning and fiber loss

These are the general factors which affect the degree of opening and cleaning

- Type of opening device
- Speed of opening device
- Size of flocks in the feed
- Thickness of feed web
- Density of feed web
- Degree of penetration
- Fiber coherence
- Fiber alignment
- Distance between feed and opening device
- Through put speed of materials
- Type of grid bar. Grid bar is part of blow room machine which is used for cleaning and opening purpose.
- Air flow through the grid bar
- Condition of pre-opening
- Amount of material processed
- Ambient relative humidity percentage
- Ambient temperature

Atmospheric condition of blow room is also important to produce smooth and uniform quality yarn. It also affects the raw material that why it is very important to maintain ambient temperature and ambient relative humidity percentage in the blow room throughout the production. Low humidity and slightly higher temperature are preferred because of the cotton opening temperature. [42]

3.1.4 Defects and Causes in Blow Room

- Neps formation
- Curly cotton due to tight gauge
- Lap clicking

3.1.4.1 Causes of neps formation in blow room

Due to following points neps formation takes place. And these nep formations strongly affect the yarn quality

- Because of too high or low moisture of cotton.
- Neps formation takes place when there is extremely fine cotton with high trash content.
- Reprocessing of laps and mixing of soft waste cotton, if the reprocessing, this will create bad effect of yarn quality. During reprocessing maximum neps are create which are difficult to remove in the next stage. So it is needed to avoid reprocessing of laps and soft waste cotton.

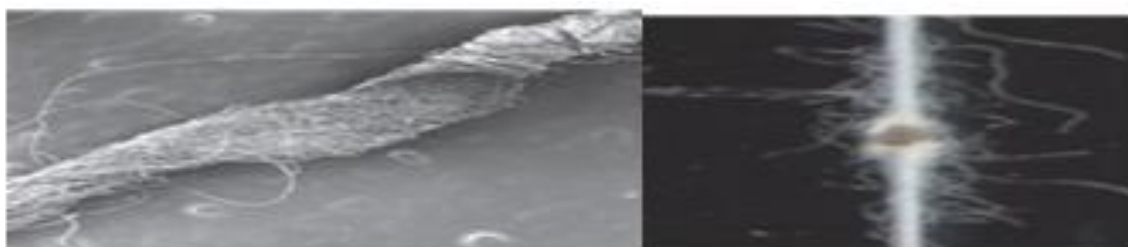


Fig. 3 A Nep Formations in Yarn

3.1.4.2 Causes of curly cotton

Due to following points of curly cotton it should be set the parts of machine in a proper way so that following causes does not happen

- Grid bar is the part of blow room machine which is used for cleaning purpose. Grid bar settings are very close to the beater.
- Causes of curly cotton are due to hooked or bent pins in beaters.

3.1.4.3 Causes of Lap Licking

Due to the following points lap clicking occurs. Lap is the output of blow room which is used for next step such as carding machine. To avoid the lap of licking we use roving ends within the lap to act as a layer separation.

- Soft waste cotton should not use in mixing because it will create problem in the next stage.
- Sticky nature of cotton, so avoid sticky cotton.

3.2 Carding Process

The second step in the yarn manufacturing process is the carding. The blow room transfers the open cotton to this section through a pipe line for further process. Carding is the heart of spinning mill and in this section maximum cleaning of cotton is done. In this stage the cotton is more opened and separates the fiber individually. In this section the material is collecting in a can in the form of rope (the technical word is silver). This section also describes the technical point, critical success factor, preventive action and also describes the defects rate which affects the yarn quality.



Fig.4 Diagram of Carding section

3.2.1 Objective of Carding Section

- To open the flocks and separate the fiber individually.
- Cleaning or elimination of impurities.
- Reduction of neps formation.
- To change the fiber into longitudinal direction or fiber alignment.
- Fiber blending.
- Removal of short fiber.
- Formation of sliver.

3.2.2 Technical points in Carding Section

Feeding of material to the card is done in a two ways:

- Feed the material in the form of lap.
- Feed the material in the form of flock feed system.
- Flocks are transported with the help of air flow.

3.2.3 Defects in Carding and Causes

- Causes of high sliver variation.
- Nep formation
- Holes or patches in card web
- High sliver variation in due to difference in draft between card
- Worn clothing and feed roller bearing also create variation in card sliver.
- If auto leveler is not working properly than this will also create high sliver variation.
- If auto leveler is off then check the wrapping of carding after every 30 minutes.

3.2.3.1 Causes for Neps Formation

- Insufficient stripping
- Dirty under casing (grid bar)

- Uneven flats setting
- Under casing chocked with fly (waste)
- High roller speed

3.2.3.2 Causes for Holes or Patches in Card web

- Poor flat stripping
- Hooked or damaged wires on flats
- Damaged cylinder
- Cluster of cotton embedded on cylinder wires

3.3 Draw Frame Section

After carding process the material is transfer to this section in the form of rope (the technical word is sliver). The carding rope (silver) is in curly form so for further process to remove this curly form, draw frame machine is used. In this section the sliver get more parallel and uniform. This chapter also describes the technical point. Critical success factor, preventive action and also describes the defects rate which affect the yarn quality.



Fig. 5 Diagram of Draw frame section

3.3.1 Objective of Draw Frame

- Parallelization of material.
- To improve evenness by doubling many card sliver.
- To produce uniformity in the material by mixing and blending different card sliver.
- Elimination of short fiber and fine dust by suction.
- To achieve sliver fineness by auto leveler
- Drafting.

3.3.2 Technical points in draw frame regarding to setting

- If back roller setting is wider then it disturbs the yarn strength. It also affects yarn evenness and increases imperfection (neps 200%, thick +50, thin -50).
- If pressure increases in back top roller then yarn strength is decreased and breakage rate is reduced.
- If front roller speed is to be keeping wider then it improves the yarn strength.
- Sliver uniformity can be reduced if draft is more but fiber parallelization is improved.[48]

3.3.3 Defects & Causes in Draw frame section

- Frame sliver variation.

3.3.3.1 Causes of draw frame sliver variation

These are the following point which affects the variation in draw frame

- Break draft.
- Improper handling of material.
- Over filling of can with material.
- Top roller overlapping.
- Thick piecing of sliver when sliver is break.
- Improper working of auto leveler.

3.4 Combing section

Combing section is used for get high quality in yarn manufacturing process. In this section the cotton is comes in the form of lap which is produce in lap former machine. In this section short fiber are removed from the cotton sheet and only that fiber which have a long length are used for getting high quality yarn. The output

of combing is also in the form of sliver which is more parallel and smooth. In this section, describes of objectives, technical point, critical success factors, preventive action and defects of section which affects the quality of yarn.



Fig.6 Diagram of Combing section

3.4.1 Objective of Combing Section

The main objectives of the comber process are given below:

- Elimination or removal of short fiber.
- Removal of impurities and fine dust from the cotton.
- To make the fiber more parallel and straightens.

3.4.2 Importance of combing process by quality point of view

Combing process is use for upgrading of the raw material. It influences the quality of yarn. Quality of yarn is affected by following main reasons:

- Yarn evenness
- Smoothness
- Cleanness
- Strength
- Visual appearance

The point which is discussed above is used for improving the strength of the yarn. Less twist is needed in this case because short fiber is removed here and fiber only having long length remains.

These are following points which are very important for quality point of view:

- As much lap weight will be more then quality according to that will be lower. It depends upon comber type and fiber fineness.
- If micronaire will be fine, lap weight can be reduced to improve combing efficiency. If micronaire will be coarse then lap weight will be increase.
- If draft will be less than fiber penalization will be less and there will be more chances of loss of fiber.
- Top comb condition should be good. If damage top comb will be used then it will badly effect of yarn quality. Top comb is very important by quality point of view.
- If cotton with low maturity is used then removal of short fiber is very necessary to avoid dying problem.

3.4.3 Defects in Combing section

- Lap licking.
- Number of piecing in comber.
- Brush cleaning problem.

3.5 Roving frame section

The input of roving frame is silver that comes from draw frame section where only parallel of comber sliver. In roving section reduce the linear density of draw frame silver by drafting. After reducing the linear density the silver is transfer into roving (a thin form of rope). This is first stage where twist is inserted for making a yarn in spinning mill. The output of this section is roving which is wind on a bobbin and this is suitable for further process. Here in this section describes a clear view of roving section objectives and technical point, critical success factor, preventive action and defects in the section. [50]



Fig. 7 Diagram of Roving frame section

3.5.1 Objectives of Roving frame section

The main objectives of roving frame are given below:

- Drafting the draw frame sliver into roving.
- To insert the twist into the roving.
- Winding the twisting roving on bobbin.



Fig. 8 Diagram of Roving Section

3.5.2 Function of Roving Frame Section

3.5.2.1 Drafting

In roving frame two drafting frame are used.

- In 4 over 4 drafting system, total draft should be 13 and in 3 over 3 drafting system the total draft should not be more than 11.
- 3 over 3 drafting system is better in that case when there is good fiber length.

3.5.2.2 Twisting

It is very important factor which produces strength in the roving and twist is inserted with the help of flyer. When flyer rotates, the twist is produce in the sliver. Twist level depends upon flyer speed and delivery speed.

3.5.2.3 Winding

For winding purpose we used builder motion. Important task of winding are:

- Shift the cone belt corresponding to increase in the bobbin diameter.
- Reverse the direction of movement of bobbin rail at the upper and lower ends of the lift stroke.



Fig. 9 Diagram of winding process

3.5.3 Defects and causes in roving

Following are the defects and causes in roving:

- Roving tension
- Improper handling of material
- Improper piecing in roving
- Roving breakage

3.6 Ring Spinning Section

The input of ring frame is roving which comes from roving section this is final stage where yarn is made. Here in this section need more drafting to reduce the liner density of roving and more twist to make a yarn. The output of ring frame is yarn which is wound on a ring bobbin which is used for next winding process. Here also describes the clear view of ring frame objective, technical points, preventive action and defects which affect the yarn quality.



Fig. 10 Diagram of Ring spinning section

3.6.1 Function of Ring Process

There is a different function of Ring Spinning process in which roving is converted into yarn through passing different zone like drafting, twisting and winding zone. There are three important zone of Ring processes below here:

- Drafting Zone
- Twisting Zone
- Winding Zone

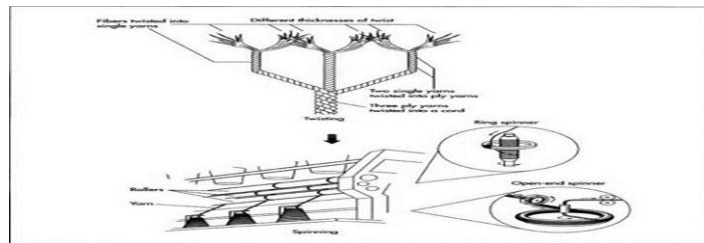


Fig. 11 Diagram of Ring spinning process

3.6.1.1 Drafting Zone

Drafting is the first zone of ring process and is very important part of machine and mostly effects on the evenness and strength of yarn. In quality point of view, there are many points which are related to the quality of drafting system.

- Type of the draft
- Selection of drafting parts like apron, rubber cots
- Range of draft
- Draft designing and setting
- Service and maintenance
- Type of perforated drum

3.6.1.2 Twisting Zone

It is the second zone and is also very important part of Ring machine in which the strands of fiber are converted into a yarn by the twist inserted. The strength of yarn is depend upon the amount of twist which are given in twisting zone and it is most important than other zone due to required strength of yarn.

There are some very important points related to twisting zone below here:

- Material and type of traveller
- Wear resistance
- Lubrication of fiber
- Smooth running
- Speed of traveler

These above points are very important in yarn quality point of view; otherwise these cause very negative effects and increase the defects in the yarn quality.

3.6.1.3 Winding Zone

This is the last section of ring machine in which yarn is wound on the plastic bobbin by the up and down movement of ring rail which is linked to a small motor. It is also very important because the setting of ring rail makes coils of yarn on bobbin in such a way that the Z-twist is not open during winding process. Some points are very important during winding process:

- Ring rail speed setting
- Bobbin material
- No. of coils per inch [48]

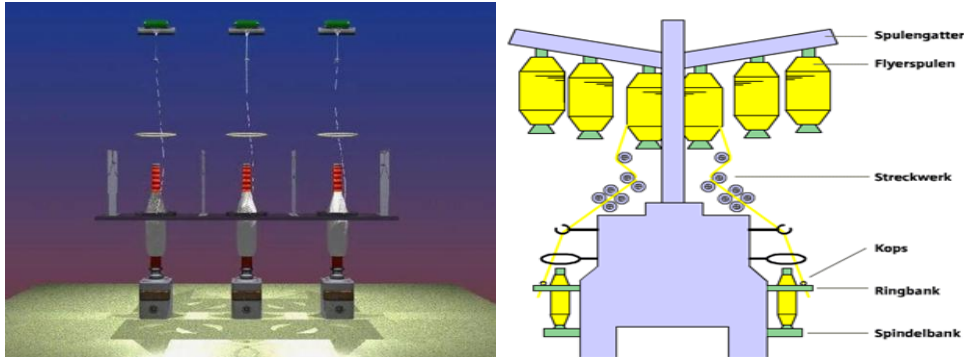


Fig.12 Diagram of Twisting System

3.6.2 Ring Spinning Effects on Quality

Ring spinning is the first stage of post spinning in which yarn produced from the roving installed on the hanger on the ring machine. Ring process is the heart of textile plant and there is lot of factors effect on the yarn quality.

- Speed of machine makes a major role on the yarn quality, as the speed increase of ring machine, the imperfection (Neps 200%, Thick +50, Thin -50) of yarn increase.
- Hairiness is also affected in ring production process and mainly produced by the movement of burnt traveler and high speed of machine.
- CV of count is also very important and ring spinning process is the last stage of process where we can reduce the CV of yarn count.
- Imperfection of yarn count in quality point of view is so important that every customer required this quality standard, that imperfection should be minimum as possible.
- Ring spinning process also effects on twist variation during manufacturing of yarn. It causes major problems during working in next process. [51]

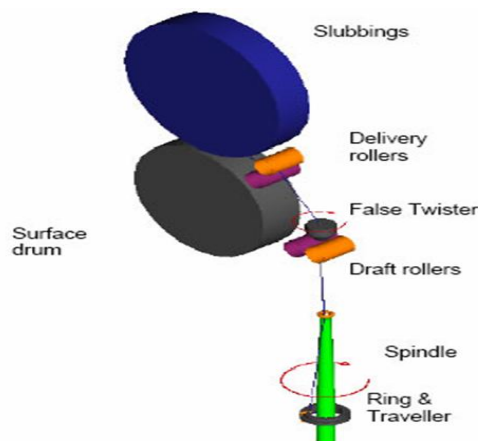


Fig. 13 Diagram of Ring spinning frame

3.6.3 Problems in Ring Process

Ring spinning process is a very critical process in the whole plant and it has also the direct relation to production of plant. It's difficult to manage it and lot of problems occurs during process. Following are some production, mechanical and electric problems here.

- Most of operators don't know about how to handle the machine.
- Due to lack of training of employees, they can create problems when they work in the department like problems of material handling, wrong traveler and bobbin colour.
- Ends down is the major problems in ring machine and it cause an efficiency and production loss.
- Due to lack of training of maintenance staff, mechanical fault is creating a problem and loss of mechanical parts, efficiency and production of plant.
- Improper maintenance is also creating problems related to maintenance and electric fault during running of machine.[52]
- Electric problems are also occurred due to lack of electric staff and they are unable to take corrective and preventive action against any fault.
- Some faults are occurred due to manufacturer of machine like software problem, communication problem and load capacity problems.

3.6.4 Defects in Ring Spinning Section

- Brush cleaning problem.
- Improper handling of material.



Fig. 14 Diagram of Ring Spinning Process

3.7 Winding Process

The cop who is prepared in the ring frame is not suitable for further process. So the yarn is converted into the shape of cone which is prepared in the winding. Practical experience shows that winding process alters the yarn structure. The factors which affect the yarn structure during winding are bobbin geometry, bobbin unwinding behavior, binding speed. This phenomenon does not affect the evenness of the yarn but it affects the properties of the yarn such as thick places, thin places, neps, and hairiness.

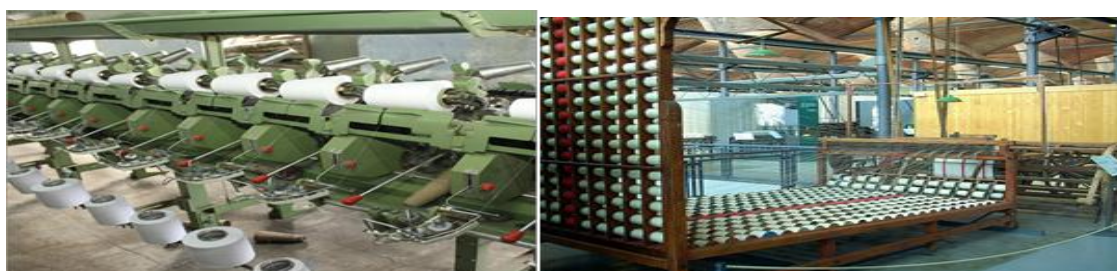


Fig.15 Diagram of Winding Department

3.7.1 Objectives of winding

- Elimination of disturbing yarn fault such as long thick places, long thin places, short thin places and short thick places.
- To get the continuous length of yarn on cones for weaving process.
- To wax the yarn during the winding process.
- To get high efficiency of machine, that is high production level.

3.7.2 How Much Importance for Quality?

Following point should be considered for quality point of view:

- Winding speed should be 1200 meter per minute for getting good quality.
- For getting good quality, yarn fault clearers device setting should be as close as possible in order to eliminate the disturbing yarn faults.
- In order to get good quality of yarn count channel setting should be less than 7%.
- Cone which we prepare for weaving purpose should have minimum fault for getting good quality, especially long thin places and long thick places.
- For getting good quality yarn, splice strength must be 75% more than of the yarn strength.
- Splice appearance should be good. Splice device should be checked twice in a week.

- To get better efficiency cone weight should be 1.8 to 2.4
- Yarn winding tension must not be high during winding. If we will keep it high then tensile properties will be affected such as elongation and tenacity.
- If waxing attachment is below the clearers, the clearers should be clean at least once in a day.
- Wax roller should rotate properly. [53]

3.7.3 Yarn faults and clearing

It is not possible that the yarn which produces is without faults because of different reasons. Stickiness of cotton can contribute to the formation of thick and thin places. Fly in the ring department is also one of the main reasons for short faults in the yarn. Because of the fly get spun into the yarn. Hence it is not possible to have fault free yarn from ring spinning. So it is necessary to have yarn monitoring system in the last production process in the spinning mill.

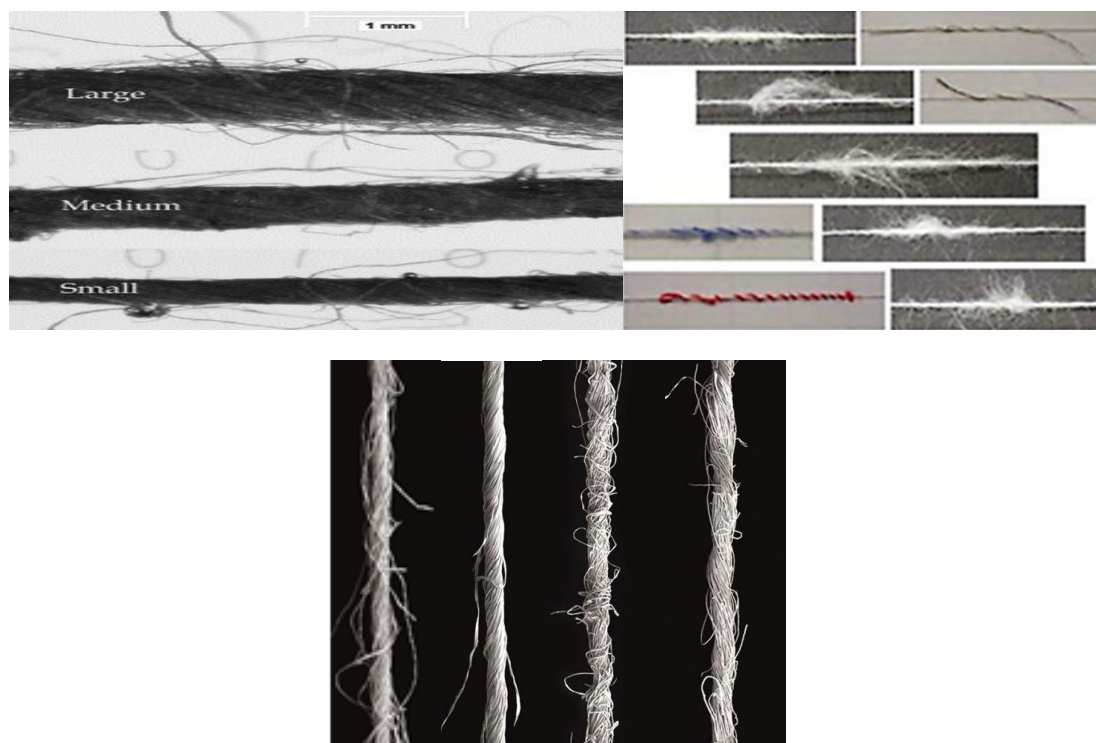


Fig. 16 Diagram of Yarn faults

3.7.4 Yarn clearing concept of Uster Quantum clearer

Yarn fault is divided into different classes according to their length and cross sectional size. The yarn fault length is measure in centimeters and cross sectional size is measured in percentage. The classes and there limits are set as below points.

- Short thick places fault contains 16 classes with the limits 0.1 to 8 cm for the length and the cross sectional size are +100% to +400%. The classes are indicating A1 to D4.
- Spinner's doubles fault lies in E class fault, whose length is over 8 cm and cross sectional size is over step to +100.
- Long thick places fault and thick ends fault have four classes. Yarn fault length is referring to be 8 cm to 38 cm and cross sectional size is -30%, -45% and -75%. The classes are designated H1, H2 and I1 and I2.

N means Neps

S means short fault

L mean long fault

CCP mean coarse count

CCM means fine count

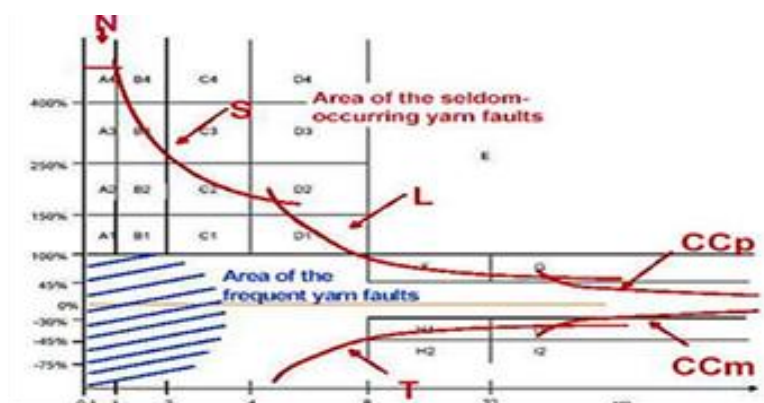


Fig. 17 Diagram of Yarn fault classes

IV. CONCLUSION

In our paper, we have achieved a lot of defects regarding to process problems during manufacturing of yarn in different departments. First we have discussed all problems that can occur in the process, then at the same time we have also gave a preventive action for those problems. We have also highlighted the critical success factors of every department that can cause more dangerous in quality point of view and improvement of process.

After the participation and share knowledge from our three applicants, the conclusion of our paper is to highlight the issues in the manufacturing process. It is a good experience for us and gained a technical knowledge from it. Actually the report which we have written is the mixture of analysis and our practical experience and in this technical and advanced world, it is necessary to work in a systemic way and try to improve financial condition of the organization. In our opinion, the paper which we have written is very useful for yarn manufacturing plant. In textile industry, especially in yarn manufacturing plant (Spinning Plant) there are seven big departments and it's difficult to achieve the objectives in every department without implement of suitable system in the process. As our practical experience in yarn manufacturing plant, it is very necessary to reduce or eliminate the defects in ever department to achieve the required specification of customers in the final yarn end product. For capture market in these days and from customer's requirements, product should have a good product of quality and service.

REFERENCES

- [1] O. Al-Araidah, A. Momani, M. Khasawneh, and M. Momani, "Lead-Time Reduction Utilizing Lean Tools Applied to Healthcare: The Inpatient Pharmacy at a Local Hospital," *Journal for Healthcare Quality*, 2010, 32(1), pp. 59-66.
- [2] M. Ali, "Six-sigma Design through Process Optimization using Robust Design Method," Master Thesis at Concordia University, Montreal, Canada, 2004.
- [3] S. Bisgaard, and R. Does, "Quality Quandaries: Health Care Quality – Reducing the Length of Stay at a Hospital, *Quality Engineering*", 2009, 21, pp. 117-131.
- [4] Y. H. Cheng, "The Improvement of Assembly Efficiency of Military Product by Six - Sigma," NCUT Thesis Archive, Taiwan, 2005.
- [5] M. E. Cournoyer, C. M. Renner, M. B. Lee, J. F. Kleinstueber, C. M. Trujillo, E. W. Krieger, C. L. Kowalczyk, "Lean Six Sigma tools, Part III: Input metrics for a Glovebox Glove Integrity Program," *Journal of Chemical Health and Safety*, Article in press, 2010, pp. 412, 1-10.
- [6] A. D. Desai, "Improving Customer Delivery Commitments the Six Sigma way: Case Study of an Indian Small Scale Industry," *International Journal of Six Sigma and Competitive Advantage*, 2006, 2(1), pp. 23-47.
- [7] E. Dickson, S. Singh, D. Cheung, C. Wyatt, and A. Nugent, "Application of Lean Manufacturing Techniques in the Emergency Department," *The Journal of Emergency Medicine*, 2009, 37, pp. 177-182.
- [8] J. Edgardo, V. Escalante, and A. Ricardo, "An application of Six Sigma methodology to the manufacture of coal products," *World Class Applications of Six Sigma*, 2006, 98-124.
- [9] M. Hook, and L. Stehn, "Lean Principles in Industrialized Housing Production: the Need for a Cultural Change," *Lean Construction Journal*, 2008, pp.20-33.
- [10] C. Huang, K. S. Chen, and T. Chang, "An application of DMADV Methodology for increasing the Yield Rate of Surveillance Cameras, *Microelectronics Reliability*," 2010, 50, pp. 266–272.
- [11] R. Jain, and A. C. Lyons, "The Implementation of Lean Manufacturing in the UK Food and Drink Industry", *International Journal of Services and Operations Management*, 2009, pp. 5(4), 548-573.
- [12] R. Krishna, G. S. Dangayach, J. Motwani and A. Y. Akbulut, "Implementation of Six Sigma in a Multinational Automotive Parts Manufacturer in India: a Case Study," *International Journal of Services and Operations Management*, 2008, 4(2), 246-276.
- [13] Q. Lee, "The mental model: Lean Manufacturing Implementation". Retrieved September 13, 2004, from http://www.strategosinc.com/lean_implementation1.htm
- [14] K. Linderman, R. Schroeder, Z. Srilata, and A. Choo, "Six Sigma: a Goal-Theoretic Perspective," *Journal of Operation Management*, 2003, 21, pp.193–203.
- [15] D. Liloyd and J. Holesback, "The Use of Six Sigma in Health Care Operations: Application and Opportunity," *Academy of Health Care Management Journal*, 2006, 2, pp. 41-49.

- [16] N. Mandahawi, O. Al-Araidah, A. Boran, and M. Khasawneh, "Application of Lean Six Sigma Tools to Minimize Length of Stay for Ophthalmology Day Case Surgery," *International Journal of Six Sigma and Competitive Advantage*, to appear, 2010.
- [17] N. Mandahawi, S. Al-Shihabi, A. A. Abdallah, and Y. M. Alfarah, "Reducing Waiting Time at an Emergency Department using Design for Six Sigma and Discreet Event Simulation," *International Journal of Six Sigma and Competitive Advantage*, 2010, 6(1/2), PP. 91-104.
- [18] J. Mari, "Using Design for Six-Sigma to Design an Equipment Depot at a Hospital," Master Thesis at Binghamton University, State University of New York, USA, 2006.
- [19] J. Miller, D. Ferrin, and J. Szymanski, "Simulating Six Sigma Improvement Ideas for a Hospital Emergency Department, Proceedings of the 2003 Winter Simulation Conference," 2003.
- [20] S. S. Raab, C. Andrew-JaJa, J. Condel, and D. Dabbs, "Improving Papanicolaou Test Quality and Reducing Medical Errors by Using Toyota Production System Methods," *American Journal of Obstetrics and Gynecology*, 2006, 194, pp.57-64.
- [21] C. M. Roberts, "Six Sigma Signals," *Credit Union Magazine* 2004, 70 (1), pp.40-43.
- [22] R. Rucker, "Citibank Increases Customer Loyalty with Defect-Free Processes, the Journal for Quality and Participation," 2000, 23 (4), pp.32-36.
- [23] M. Sampson, "Non Profit, Payload Process Improvement through Lean Management". Ph.D. Dissertation, University of Colorado.
- [24] K. Schon, "Implementing Six Sigma in a Non-American Culture," *International Journal of Six Sigma and Competitive Advantage*, 2006, 2 (4), pp.404-428.
- [25] M. Sokovic, D. Pavletic, and S. Fakin, "Application of Six Sigma Methodology for Process Design," *Journal of Materials Processing Technology*, 2005, PP. 162-163, 777-783.
- [26] C. Su and C. Chou, "A Systematic Methodology for the Creation of Six Sigma Projects: A Case Study of Semiconductor Foundry," *Expert Systems with Applications*, 2008, 34, pp. 2693-2703.
- [27] J. P. Womack, "The Right Sequence for Implementing Lean", *Lean Enterprise Institute*, Accessed on February 13, 2003.
- [28] H. Woodward, S. Scachitti, L. Mapa, C. Vanni, L. Brandford, and C. Cox, "Application of Lean Six Sigma Techniques to Optimize Hospital Laboratory Emergency Department Turnaround Time Across a Multi- hospital System," *Proceedings of the Spring, 2007, American Society for Engineering Education Illinois-Indiana Section Conference*.
- [29] Q. Yu, and K. Yang, "Hospital Registration Waiting Time Reduction through Process Redesign," *International Journal of Six Sigma and Competitive Advantage*, 2008, 4(3), pp. 240- 253.
- [30] Bourton Hall, Rugby, Warwickshire CV23 9SD, "The Six Sigma Group" 2010, Retrieved July 20.
- [31] <http://www.sixsigmagroup.co.uk/introduction/whatisixsigma.aspx>
- [32] Six Sigma. (n.d).Quality Resources for Achieving Six Sigma Results. Retrieved July 20, 2010 from [isixsigma.com](http://www.isixsigma.com/index.php?option=com)
- [33] F. M. Ahmad, & A. Khan, "Internship Report on Gull Ahmad Textile Mill Report," Retrieved July 22, 2010, from Gul Ahmad Textile Mill: <http://www.docstoc.com/docs/16936290/Spinning-report>
- [34] T. Vijykumar, "Report on experience with the Rieter C 60 CARD. Link," 2007, 19 (51), pp. 3-6.
- [35] Angelfire. (n.d.). Carding. Retrieved June 18, 2010, from Angelfire: <http://www.angelfire.com/jazz/pakspinning/CARDING.htm>
- [36] Angelfire. (n.d.). Draw Frame. Retrieved June 27, 2010, from Angelfire: <http://www.angelfire.com/jazz/pakspinning/DRAWING%20PROCESS.htm>
- [37] S. Bashir, (2010, June 6). Blow Room. Retrieved June 2010, from Angelfire: <http://www.angelfire.com/jazz/pakspinning/BLOWROOM.htm>
- [38] Yarn Spinning Technology. (n.d.) . Combed Yarn for Knitting. Retrieved June 10, 2010, from Yarn Spinning Technology: <http://textiletechnology.bravehost.com/spinning/yarnquality.htm>
- [39] Textile Spinning. (n.d.). Defects in Blow room and causes. Retrieved June 15, 2010, from Textile Spinning: http://www.textilespinning.co.cc/modernblowroom/Defects_in_Blow_Room.htm
- [40] Purushothama, B. (n.d.). MODERN AUTO LEVELLER DRAW FRAMES. Retrieved July 05, 2010, from [fibashion.com](http://fibashion.com/articles.fibashion.com/extraimage/article/document/Article_275.docx): http://fibashion.com/articles.fibashion.com/extraimage/article/document/Article_275.docx
- [41] Textile Technology Spinning. (n.d.). PROCESS PARAMETERS IN DRAW FRAME. Retrieved July 02, 2010, from Textile Technology Spinning: <http://www.textiletechnology.co.cc/spinning/processparsingdrawing.htm>
- [42] Textile spinning. (n.d.) . Defects in Card Sliver. Retrieved 2010, from Textile spinning: http://www.textilespinning.co.cc/carding/DEFECTS_IN_CARD_SLIVER.htm
- [43] Angelfire. (n.d.). Comber. Retrieved July 12, 2010, from Angelfire.com: <http://www.angelfire.com/jazz/pakspinning/COMBER%20PROCESS.htm>
- [44] Angelfire. (n.d.). Roving Frame. Retrieved July 18, 2010, from [angelfire.com](http://www.angelfire.com/jazz/pakspinning/roving_frame.htm): http://www.angelfire.com/jazz/pakspinning/roving_frame.htm
- [45] Textile Technology Spinning. (n.d.). Roving Frame. Retrieved July 18, 2010, from Textile Technology Spinning: <http://www.textiletechnology.co.cc/spinning/ROVINGFRAME.htm>
- [46] Textile Technology Spinning. (n.d.). Winding Spinning. Retrieved July 20, 2010, from Textile Technology Spinning: <http://textile-technology.blogspot.com/2008/04/winding-spinning.html>
- [47] Six Sigma. (n.d).Quality Resources for Achieving Six Sigma Results. Retrieved July 20, 2010 from [isixsigma.com](http://www.isixsigma.com/index.php?option=com)
- [48] The Six Sigma Group. Bourton Hall, Rugby, Warwickshire CV23 9SD. Retrieved July 20, 2010 <http://www.sixsigmagroup.co.uk/introduction/whatisixsigma.aspx>
- [49] Six Sigma.(n.d). Six Sigma Overview. Retrieved July 01, 2010. From [thequalityportal.com](http://www.thequalityportal.com/q_6sigma.htm)
- [50] Pyzdek Thomas, "The Six Sigma handbook; a complete guide for green belts, black belts, and managers at all levels" (Published by: New York McGraw-Hill, c2003) Chapter 1 Pages 4-5.
- [51] Tennant Geoff, "SIX SIGMA: SPC and TQM in Manufacturing and Services" Gower Publishing, Ltd. (2001) Chapter 1 "The development of quality" Pages 1-3
- [52] Educational assessment: Interpreting test scores, Reliability and validity. Retrieved 15 July, 2010 Online available: <http://course1.winona.edu/lgray/el626/MandEtext3.html>
- [53] Peter R.Loard."The Economics, Science and Technology of Yarn Production" The textile institute 10 Black friar Manchester, England 1981, Chap.12 Pages. 149-171

Analyzing Stability of a Dam using MATLAB

¹Manikanta Kotti, ²J K Chaitanya, ³Bh Vamsi Varma, ⁴K Bharat Venkat

1(B.Tech, Department of Mechanical Engineering, Swarnandhra College of Engineering & Technology, Andhra Pradesh- 534280)

2,3,4 (B.Tech, Department of Mechanical Engineering, Swarnandhra College of Engineering & Technology, Andhra Pradesh-534280)

Abstract:

Today we are living in the world of technology. Various massive constructions were being carried out every day to ensure certain purposes. Dams were one among such constructions. They were used for the purpose of irrigation, power generation or sometimes simply to store water. Number of forces act on these dams like water force, own weight etc. Considering all these forces and analyzing them manually is tedious process. In this paper, we were using MATLAB software to analyze various forces acting on the dams. The code written doesn't exist before and reduces manual calculations. The code written also offers flexibility in selecting the number of forces acting on the dams in both X and Y directions and gives final result concluding whether the structure is safe or not.

Keywords: Arch Dam, Barrages, Dam, Embankments, Stability, MATLAB, Moment

I. INTRODUCTION:

A dam is a barrier that impounds water or underground streams. Dams generally serve the primary purpose of retaining water, while other structures such as floodgates or levees (also known as dikes) are used to manage or prevent water flow into specific land regions. Hydropower and pumped-storage hydroelectricity are often used in conjunction with dams to generate electricity. A dam can also be used to collect water or for storage of water which can be evenly distributed between locations.



II. TYPES OF DAMS:

Based on the structure of the dam, dams are classified as follows:

2.1 Arch Dams:

In the arch dam, stability is obtained by a combination of arch and gravity action. If the upstream face is vertical the entire weight of the dam must be carried to the foundation by gravity, while the distribution of the normal hydrostatic pressure between vertical cantilever and arch action will depend upon the stiffness of the dam in a vertical and horizontal direction. When the upstream face is sloped the distribution is more complicated.

2.2 Gravity Dams:

In a gravity dam, the force that holds the dam in place against the push from the water is Earth's gravity pulling down on the mass of the dam. The water presses laterally (downstream) on the dam, tending to overturn the dam by rotating about its toe (a point at the bottom downstream side of the dam). The dam's weight counteracts that force, tending to rotate the dam the other way about its toe.

2.3 Arch-Gravity Dams:

A gravity dam can be combined with an arch dam into an arch-gravity dam for areas with massive amounts of water flow but less material available for a purely gravity dam. The inward compression of the dam by the water reduces the lateral (horizontal) force acting on the dam.

2.4 Barrages:

A barrage dam is a special kind of dam which consists of a line of large gates that can be opened or closed to control the amount of water passing the dam. The gates are set between flanking piers which are responsible for supporting the water load, and are often used to control and stabilize water flow for irrigation systems.

2.5 Embankment dams:

Embankment dams are made from compacted earth, and have two main types, rock-fill and earth-fill dams. Embankment dams rely on their weight to hold back the force of water, like gravity dams made from concrete.

III. FORCES ACTING ON A DAM:

In the design of a dam, the first step is the determination of various forces which acts on the structure and study their nature. Depending upon the situation, the dam is subjected to the following forces:

3.1 WATER PRESSURE:

It might be external water pressure or uplift pressure. External water pressure is the pressure of water on the upstream face of the dam. If the hydraulic gradient caused vertical uplift pressure, then the upward pressure is called uplift.

3.2 EARTHQUAKE FORCE:

The effect of earthquake is equivalent to acceleration to the foundation of the dam in the direction in which the wave is travelling at the moment. Earthquake wave may move in any direction and for design purposes, it is resolved into the vertical and horizontal directions.

3.3 SILT PRESSURE:

If h is the height of silt deposited, then the forces exerted by this silt in addition to the external water pressure is also taken into consideration.

3.4 WAVE PRESSURE:

Waves are generated on the surface of the reservoir by the blowing winds, which exert a pressure on the downstream side. Wave pressure depends upon wave height.

3.5 ICE PRESSURE:

The ice which may be formed on the water surface of the reservoir in cold countries may sometimes melt and expand. The dam face is subjected to the thrust and exerted by the expanding ice.

3.6 WEIGHT OF DAM:

The weight of dam and its foundation is a major resisting force. In two dimensional analysis of dam, unit length is considered.

IV. INTRODUCTION TO MATLAB:

MATLAB (Matrix Laboratory) Is A Numerical Computing Environment And Fourth-Generation Programming Language. Developed By Mathworks, MATLAB Allows Matrix Manipulations, Plotting Of Functions And Data, Implementation Of Algorithms, Creation Of User Interfaces, And Interfacing With Programs Written In Other Languages, Including C, C++, Java, And Fortran. MATLAB® Is A High-Level Language And Interactive Environment For Numerical Computation, Visualization, And Programming. Using MATLAB, We Can Analyze Data, Develop Algorithms, And Create Models And Applications. The Language, Tools, And Built-In Math Functions Enable Us To Explore Multiple Approaches And Reach A Solution Faster Than With Spreadsheets Or Traditional Programming Languages, Such As C/C++ Or Java. We Can Use MATLAB For A Range Of Applications, Including Signal Processing And Communications, Image And Video Processing, Control Systems, Test And Measurement, Computational Finance, And Computational Biology.

V. PROBLEM:

Consider a problem where we need to analyze stability of a dam. A number of forces, as mentioned earlier, act on the dam at different points. Force acting in X direction is taken as positive if it is towards right

while force acting in Y direction is taken as positive if it towards south direction. Consider a Dam with following forces: Force in X direction= 500 KN at a distance of 4 m from base
 Forces acting in Y direction: 1120 KN acting upwards at a distance of 2m from origin
 120KN acting downwards at a distance of 4m from origin
 420KN acting upwards at a distance of 5m from origin
 Base length of dam = 7 meters

This problem can be solved using MATLAB and the results obtained are as follows:

VI. MATLAB OUTPUT WINDOWS:

```

MATLAB 7.10.0 (R2010a)
File Edit Debug Parallel Desktop Window Help
Current Folder: C:\Users\manikanta\Documents\MATLAB
Shortcuts How to Add What's New
Workspace Current Folder
Please Provide details about Forces acting
Enter number of forces in x-direction:1
Enter force value in KN:500
Enter distance of force from base:4
Moment due to force in x direction
2000
Enter number of forces in y-direction:3
Enter force value in KN:-1120
Enter distance of force from base:2
Enter force value in KN:120
Enter distance of force from base:4
Enter force value in KN:-420
Enter distance of force from base:5
Moment due to forces in Y direction
-3860
TOTAL MOMENT DUE TO FORCES ACTING in KN-m
5860
Total force acting in Y direction in KN
-1420
Distance from origin where resultant cuts the base in m
4.1268
Enter base length of dam in meters:7
DAM IS SAFE
fx >>
Start OVR
    
```

VII. DAM UNSAFE CASES:

Similarly as done above any problem can be solved to check the stability of the dam constructed or that is to be constructed. Dam is considered to be unsafe if the resultant doesn't pass through middle third of the base. i.e. if r doesn't lie in the range (b/3, 2b/3) MATLAB code written can be checked by taking various values and one of such results is as in the fig below:

```

MATLAB 7.10.0 (R2010a)
File Edit Debug Parallel Desktop Window Help
Current Folder: C:\Users\manikanta\Documents\MATLAB
Shortcuts How to Add What's New
Workspace Current Folder
Please Provide details about Forces acting
Enter number of forces in x-direction:3
Enter force value in KN:1300
Enter distance of force from base:4
Enter force value in KN:220
Enter distance of force from base:2
Enter force value in KN:110
Enter distance of force from base:1
Moment due to force in x direction
5750
Enter number of forces in y-direction:2
Enter force value in KN:-1190
Enter distance of force from base:3
Enter force value in KN:120
Enter distance of force from base:4.5
Moment due to forces in Y direction
-6600
TOTAL MOMENT DUE TO FORCES ACTING in KN-m
7150
Total force acting in Y direction in KN
-2260
Distance from origin where resultant cuts the base in m
3.1637
Enter base length of dam in meters:4.5
DAM IS UNSAFE
fx >>
Start OVR
    
```

VIII. CONCLUSION:

The MATLAB code written for analyzing the stability of the dam was proved to be correct as the results obtained from MATLAB matched exactly with that of various problems chosen from different textbooks. The MATLAB code written was very effective, time saving and can be applied to any dam. The MATLAB code written works for any number of forces which are given as input to study the stability of the dam.

REFERENCES:

- [1.] S S Bhavikatti, ' A textbook of CLASSICAL MECHANICS', New Age International Publishers.
- [2.] E Popov, 'Engineering Mechanics of solids', Pearson Edition, 2nd Edition.
- [3.] Rudra Pratap, 'Getting started with MATLAB', Oxford University Press, updated for Version 7.8 (2009).
- [4.] Introduction to MATLAB for Engineering Students', by David Houcque, North Western University, Version 1.2, (August 2005)
- [5.] Numerical Computing with MATLAB', Cleve Moler, chairman and chief scientist at TheMathWorks.

Design and Analysis of Microstrip-Fed Band Notch Uwb Antenna

G.Karthikeyan¹, C.Nandagopal.M.E²

¹M.E: Second Year-Communication Systems M.Kumarasamy College of Engg, Karur

²LECTURER/ECE, M.Kumarasamy college of Engg,Karur

Abstract:

A compact printed microstrip-fed monopole ultra wideband antenna with multi notched bands is presented. The UWB slot antenna, covering 3.1–11 GHz A straight, open-ended quarter-wavelength slot is etched in the radiating patch to create the first notched band in 3.3–3.7 GHz for the WiMAX system. In addition, three semicircular half-wavelength slots are cut in the radiating patch to generate the second and third notched bands in 5.15–5.825 GHz for WLAN and 7.25–7.75 GHz for downlink of X-band satellite communication systems. Surface current distributions and transmission line models are used to analyze the effect of these slots.it produced broadband matched impedance and good omnidirectional radiation pattern. The designed antenna has a compact size of 25 x29 mm².

I. INTRODUCTION

In recent years, ultrawideband (UWB) systems, over the 3.1–10.6-GHz band, have attracted a lot of attention for the commercial applications. An important part of the UWB system is the antenna. For most of the applications, the antenna is required to have an omnidirectional and stable radiation pattern, high radiation efficiency, low group delay, and low profile. It is mainly used for high-data-rate wireless communication, high-accuracy radar, and imaging systems. Support low output power and high data rate (110–200 Mb/s) applications over short ranges (4–10 m). Also, lower rate intelligent applications that provide accurate location-tracking capabilities over increased link range, i.e., over 30 m, are supported. The first successful UWB application is as a wireless universal serial bus (USB) enabler, where a PC or a laptop is wirelessly connected to a printer, hard drive, or other peripherals. Antenna Design of a Planar Ultrawideband With a New Band-Notch Structure, Chong-Yu Hong, Ching-Wei Ling, I-Young Tarn, and Shyh-Jong Chung, *Senior Member, IEEE*

A novel planar ultrawideband (UWB) antenna with band-notched function. The antenna consists of a radiation patch that has an arc-shaped edge and a partially modified ground plane. The antenna that makes it different from the traditional monopole antenna is the modification in the shape of ground plane, including two bevel slots on the upper edge and two semicircle slots on the bottom edge of the ground plane. These slots improve the input impedance bandwidth and the high frequency radiation performance. With this design, the return loss is lower than 10 dB in 3.1–10.6 GHz frequency range and the radiation pattern is highly similar to the monopole antenna. By embedding a pair of T-shaped stubs inside an elliptical slot cut in the radiation patch, a notch around 5.5 GHz WLAN band is obtained. The average gain is lower than 18 dBi in the stopband, while the patterns and the gains at frequencies other than in the stopband are similar to that of the antenna without the band-notched function.

Band-Notched Design for UWB Antennas
The-Nan Chang and Min-Chi Wu

A method to form a notch band is presented. We etch complementary split-ring resonators in the T-stub region of a CPW-feed ultrawideband (UWB) antenna. Due to limited space in this region, we connect two resonators together so that they have a common slot edge. Compared with two separated CSSRs, this new design not only occupies less space but also yields high mismatch losses. It is found that high mismatch losses and deep suppression level can be obtained at the desired notch band. A Compact Ultrawideband Antenna With 3.4/5.5 GHz Dual Band-Notched Characteristics Qing-Xin Chu, *Member, IEEE*, and Ying-Ying Yang We propose a compact planar ultrawideband (UWB) antenna with 3.4/5.5 GHz dual band-notched characteristics. The antenna consists of a beveled rectangular metal patch and a 50 ohm coplanar waveguide (CPW) transmission line. By etching two nested C-shaped slots in the patch, band-rejected filtering properties in the WiMAX/WLAN bands are achieved.

The proposed antenna is successfully simulated, designed, and measured showing broadband matched impedance, stable radiation patterns and constant gain. An equivalent circuit model of the proposed antenna is presented to discuss the mechanism of the dual band-notched UWB antenna. Integrated Bluetooth and UWB Antenna-Bahadır S. Yildirim, Bedri A. Cetiner, *Member, IEEE*, Gemma Roqueta, *Student Member, IEEE*, and Luis Jofre, *Member, IEEE*

A small-sized, low-profile, and planar integrated Bluetooth and ultrawideband (UWB) antenna is presented. The antenna exhibits a dual-band operation covering 2400–2484 MHz (Bluetooth) and 3100–10600 MHz (UWB) frequency bands. It is fed by a microstrip line and built on a FR-4 substrate with 42X 46 mm² surface area. The impedance, radiation, phase linearity, and impulse response properties of the antenna are studied both theoretically and experimentally. The calculated and measured results agree well. The antenna shows acceptable gain flatness with stable omnidirectional radiation patterns across the integrated Bluetooth and UWB bands. The average group delay is approximately 0.2 ns across UWB frequencies. Bandwidth Enhancement of Novel Compact Single and Dual Band-Notched Printed Monopole Antenna With a Pair of L-Shaped Slots Reza Zaker, Changiz Ghobadi, and Javad Nourinia A dual band-notched printed ultrawideband monopole antenna is presented, with a modified ground plane. By using this modified element including a pair of variable L-shaped slots, cut in the ground plane, additional resonances are excited and hence the bandwidth is increased up to 130%. To generate single and dual band-notched characteristics, we use inverted U- and fork-shaped parasitic structures, respectively, instead of changing the patch or feedline shapes. By properly adjusting the dimensions of these capacitive-coupled elements, not only one or two controllable notch resonances are achieved, but also the lower-edge frequency of the band is decreased. The measured results show that the proposed dual band-notched monopole antenna offers a very wide bandwidth from 2.2 to 13.4 GHz (143%), defined by 10-dB return loss, with two notched bands, covering all the 5.2/5.8-GHz WLAN, 3.5/5.5-GHz WiMAX and 4-GHz C bands.

II. MICROSTRIP PATCH ANTENNAS

INTRODUCTION- In the past few years, the concept of creating microwave antennas using microstrip has gained much attention and possible designs are now emerging. Microstrip patch antennas have gained popularity in today's world of wireless technology due to its many advantages such as low profile, conformability to both planar and non-planar surfaces, low cost, ease of integration with other components, mechanically robust and simple to fabricate. However the main drawback with microstrip antennas lies in its narrow bandwidth. **INPUT IMPEDANCE STRUCTURE OF MICROSTRIP ANTENNA-** Microstrip antenna consists of a very thin metallic strip (patch) ($t \ll \lambda_0$) placed a small fraction of a wavelength above a ground plane ($h \ll \lambda_0$, usually $0.003\lambda_0 \leq h \leq 0.05\lambda_0$). The microstrip patch is designed so its pattern maximum is normal to the patch (broadside radiator). End-fire radiation can also be accomplished by proper choosing mode of excitation. For rectangular patch, the length L of the element is usually $\lambda_0/3 \leq L \leq \lambda_0/2$. The strip and the ground plane are separated by a dielectric substrate. The ones that are most desirable for antenna performance are thick substrates whose dielectric constant is low because they provide better efficiency, larger bandwidth, loosely bound fields for radiation into space, but at the expense of larger element size.

The radiating patch may be square, rectangular, thin strip (dipole), circular, elliptical, triangular or any other configuration. These and others are Square, rectangular, dipole, and circular are the most common because of ease of analysis and fabrication, and their attractive radiation characteristics. Arrays of microstrip elements, with single or multiple feeds may also be used to introduce scanning capabilities and achieve greater directivities.

III. FEEDING METHODS

There are many configurations that can be used to feed microstrip antennas. The most popular four feed methods are

MICROSTRIP FEEDING LINE- It is a conducting strip of much smaller width compared to the patch. It is easy to fabricate, simple to match by controlling the inset position and simple to model, However, as the substrate thickness increases, surface waves and spurious feed radiation increases, which for practical designs limits the bandwidth (typically 2-5%).

COAXIAL LINE FEED - The inner conductor of the coaxial line is attached to the patch while the outer conductor is connected to the ground plane. The coaxial probe feed is also easy to fabricate and match, and it has low spurious feed radiation. However, it also has narrow bandwidth and it is more difficult to model, especially for thick substrates ($h > 0.02 \lambda_0$). The previous two methods (microstrip feeding line and coaxial line

feed) generate higher order modes, which produce cross-polarized radiation. To overcome some of these problems, the following two feed may be used.

APERTURE COUPLING - It is the most difficult of all four to fabricate and it also has narrow bandwidth. However, it is easier to model and has moderate spurious radiation. It consists of two substrates separated by a ground plane. On the bottom side of the lower substrate, there is a microstrip feed line whose energy is coupled to the patch through a slot on the ground plane separating the two substrates. This arrangement, allows independent optimization of the feed mechanism and the radiating element. Typically a high dielectric material is used for the bottom substrate, and thick, low dielectric constant material for the top substrate. The ground plane between the substrates also isolates the feed from the radiating element and minimizes interference of spurious radiation for pattern formation and polarization purity. *Matching is performed by controlling the width of the feed line and the length of the slot.*

PROXIMITY COUPLING - It has the largest bandwidth (as high as 13%), it is somewhat easy to model and has low spurious radiation. However, its fabrication is somewhat more difficult. *The length of the feeding stub and the width-to-line ratio of the patch can be used to control the match.*

FEEDS WITH MODIFICATION - There are different types of feed with modification, it are mainly depend on the previous four main feed with some modifications and can be classified as follows:

PROBE FEED -Narrow slot around the probe feed- For conventional Probe-fed microstrip antennas with thick substrate, the major problem associated with impedance matching is the large probe reactance owing to the required long probe pin in the thick substrate layer. To solve this problem, a variety of designs with modified probe feed has been reported. One design method is to cut an annular slot or narrow rectangular ring slot around the feed in the radiating patch. By choosing suitable dimension of the ring slot, the large probe reactance can be compensated, and good impedance matching over a wide bandwidth can be obtained.

CAPACITIVELY PROBE FEED - Miguel et al present a single microstrip patch arrays enclosed in metallic cavities and placed on thick substrates of very low permittivity materials with the application of the capacitive probe feeding in place of the direct junction probe-radiating patch. The goal is to obtain broad-band microstrip antennas on thick substrates without the limitations due to the generation of surface waves of the conventional microstrip antennas on infinite substrates.

IV. METHODS OF ANALYSIS

The most popular models for the analysis of Microstrip patch antennas are the transmission line model, cavity model, and full wave model (which include primarily integral equations/Moment Method). The transmission line model is the simplest of all and it gives good physical insight but it is less accurate. The cavity model is more accurate and gives good physical insight but is complex in nature. The full wave models are extremely accurate, versatile and can treat single elements, finite and infinite Microstrip patch with L-probe feed arrays, stacked elements, arbitrary shaped elements and coupling. These give less insight as compared to the two models mentioned above and are far more complex in nature.

TRANSMISSION LINE MODEL- This model represents the microstrip antenna by two slots of width W and height h , separated by a transmission line of length L . The microstrip is essentially a non-homogeneous line of two dielectrics, typically the substrate and air. most of the electric field lines reside in the substrate and parts of some lines in air. As a result, this transmission line cannot support pure transverse electro- magnetic (TEM) mode of transmission, since the phase velocities would be different in the air and the substrate. Instead, the dominant mode of propagation would be the quasi-TEM mode. Hence, an effective dielectric constant (ϵ_{reff}) must be obtained in order to account for the fringing and the wave propagation in the line. The value of ϵ_{reff} is slightly less than ϵ_r because the fringing fields around the periphery of the patch are not confined in the dielectric substrate but are also spread in the air. In order to operate in the fundamental TM_{10} mode, the length of the patch must be slightly less than $\lambda/2$ where λ is the wavelength in the dielectric medium and is equal to $\lambda_0/\sqrt{\epsilon_{\text{reff}}}$ where λ is the free space wavelength. The TM_{10} mode implies that the field varies one $\lambda/2$ cycle along the length, and there is no variation along the width of the patch. In the Fig.5.4 shown below, the microstrip patch antenna is represented by two slots, separated by a transmission line of length L and open circuited at both the ends. Along the width of the patch, the voltage is maximum and current is minimum due to the open ends. The fields at the edges can be resolved into normal and tangential components with respect to the ground plane.

It is seen from that the normal components of the electric field at the two edges along the width are in opposite directions and thus out of phase since the patch is $\lambda/2$ long and hence they cancel each other in the broadside direction. The tangential components (seen in Fig.5.5), which are in phase, means that the resulting fields combine to give maximum radiated field normal to the surface of the structure. Hence the edges along the width can be represented as two radiating slots, which are $\lambda/2$ apart and excited in phase and radiating in the half space above the ground plane. The dimensions of the patch along its length have now been extended on each end by a distance ΔL .

CAVITY MODEL- Although the transmission line model discussed in the previous section is easy to use, it has some inherent disadvantages. Specifically, it is useful for patches of rectangular design and it ignores field variations along the radiating edges. These disadvantages can be overcome by using the cavity model. A brief overview of this model is given below. In this model, the interior region of the dielectric substrate is modeled as a cavity bounded by electric walls on the top and bottom. The basis for this assumption is the following observations for thin substrates ($h \ll \lambda$)

Since the substrate is thin, the fields in the interior region do not vary much in the z direction, i.e. normal to the patch. The electric field is z directed only, and the magnetic field has only the transverse components H_x and H_y in the region bounded by the patch metallization and the ground plane. This observation provides for the electric walls at the top and the bottom. When the microstrip patch is provided power, a charge distribution is seen on the upper and lower surfaces of the patch and at the bottom of the ground plane. This charge distribution is controlled by two mechanisms—an attractive mechanism and a repulsive mechanism as discussed by Richards. The attractive mechanism is between the opposite charges on the bottom side of the patch and the ground plane, which helps in keeping the charge concentration intact at the bottom of the patch. The repulsive mechanism is between the like charges on the bottom surface of the patch, which causes pushing of some charges from the bottom, to the top of the patch. As a result of this charge movement, currents flow at the top and bottom surface of the patch. The cavity model assumes that the height to width ratio (i.e. height of substrate and width of the patch) is very small and as a result of this the attractive mechanism dominates and causes most of the charge concentration and the current to be below the patch surface. Much less current would flow on the top surface of the patch and as the height to width ratio further decreases, the current on the top surface of the patch would be almost equal to zero, which would not allow the creation of any tangential magnetic field components to the patch edges. Hence, the four sidewalls could be modeled as perfectly magnetic conducting surfaces. However, in practice, a finite width to height ratio would be there and this would not make the tangential magnetic fields to be completely zero, but they being very small, the side walls could be approximated to be perfectly magnetic conducting. Hence, in order to account for radiation and a loss mechanism, one must introduce a radiation resistance R_r and a loss resistance R_L . A lossy cavity would now represent an antenna and the loss is taken into account by the effective loss tangent δ_{eff} .

V .ANTENNA DIMENSIONS

- Length of the patch = 29mm
- Width of the patch = 25mm
- Substrate thickness = 0.8mm

VI. GEOMETRY OF ANTENNA



Fig.1.Model of WiMAX rejection band

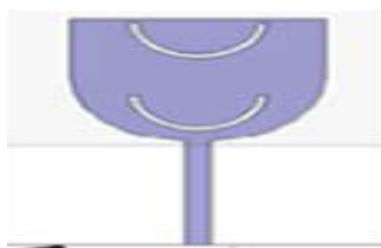


Fig.2.Model of X- band rejection

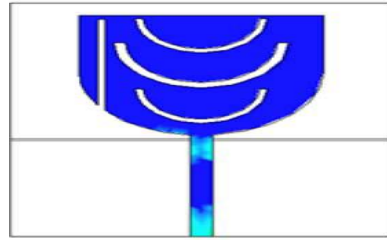


Fig.5.WiMAX,WiLAN and X-band satellite communication systems band rejection of antenna

VII.RESULTS

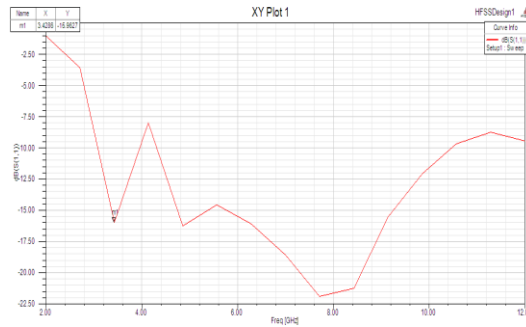


Fig.4. Output of WIMAX rejection band

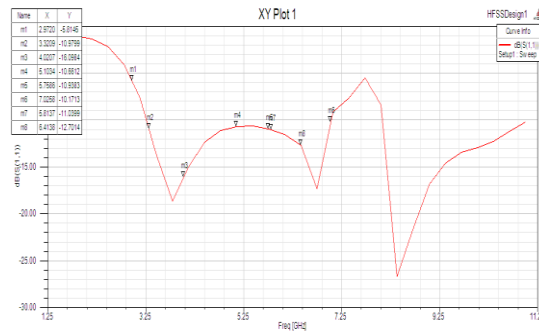


Fig.5. Output of X-band rejection

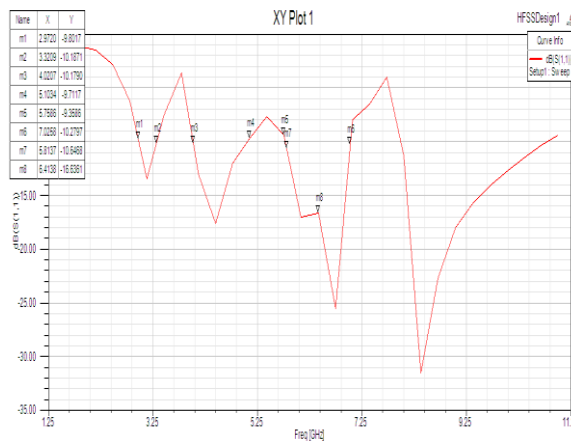


Fig.6.Output of 3 band rejection antenna

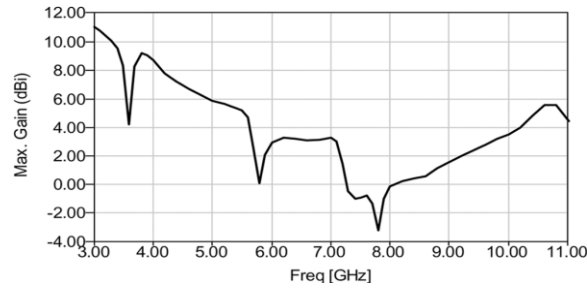


Fig.7. Calculated maximum gain of the antenna

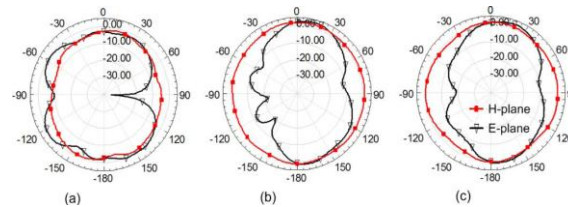


Fig. 8. Measured radiation patterns in the H- and E-planes at (a) 4.8, (b) 8.5, and (c) 10 GHz.

Simulation was performed using the commercial software Ansoft HFSS. The final design was optimized taking several aspects into consideration such as bandwidth of the antenna, bandwidth of the notched bands, and level of band rejection. The antenna has a compact volume of $25 \times 29 \times 0.8 \text{ mm}^3$ on FR4 substrate with a relative dielectric constant of 4.4 and loss tangent of 0.02. It is composed of a 50-ohm microstrip feed line, a planar radiating patch with an arc-shaped edge, a simple rectangular ground plane, and slots. Fig. 4, 5 & 6 shows simulated and measured results of the antenna with three notched bands. The measurement was performed with an Agilent 8719 A network analyzer. It is observed that the antenna notches three intended bands while maintaining broadband performance with less than 10 dB, covering the entire UWB frequency band. The discrepancy between measured and simulated results is mostly attributed to the tolerance in fabrication and loss tangent of the FR4 substrate. Measured radiation patterns in the H-plane and E-plane. The antenna displays a good omnidirectional radiation pattern in the H-plane, even at high frequencies.

VII. CONCLUSION

In this letter, a compact printed microstrip-fed dual bandnotched UWB antenna has been presented and analyzed in detail. To obtain three notched bands, two types of slots—a straight open-ended quarter-wavelength type and a semicircular half-wavelength type—were etched in the radiating patch. We introduced a new term, an effective length of a slot, and used this concept along with the surface current distributions and transmission line models to analyze the physical effects of these slots generating the band-notched characteristics. The antenna was fabricated and measured, showing broad bandwidth, three designed notched bands, and good omnidirectional radiation patterns.

REFERENCES

- [1]. "UWB Printed Slot Antenna With Bluetooth and Dual Notch Bands" Mohammad Mehdi Samadi Taheri, *Student Member, IEEE*, Hamid Reza Hassani, and Sajad Mohammad Ali Nezhad VOL. 10, 2011
- [2]. C. Y. Hong, C. W. Ling, I. Y. Tarn, and S. J. Chung, "Design of a planar ultrawideband antenna with a new band-notch structure," *IEEE Trans. Antennas Propag.*, vol. 55, no. 12, pp. 3391–3397, Dec. 2007
- [3]. "Band-Notched Design for UWB Antennas" The-Nan Chang and Min-Chi Wu VOL. 7, 2008
- [4]. Q. X. Chu and Y. Y. Yang, "3.5/5.5 GHz dual band-notch ultra-wideband antenna," *Electron. Lett.*, vol. 44, no. 3, pp. 172–174, 2008
- [5]. "Integrated Bluetooth and UWB Antenna"-Bahadir S. Yildirim, Bedri A. Cetiner, *Member, IEEE*, Gemma Roqueta, *Student Member, IEEE*, and Luis Jofre, *Member, IEEE* VOL. 8, 2009
- [6]. "Bandwidth Enhancement of Novel Compact Single and Dual Band-Notched Printed Monopole Antenna With a Pair of L-Shaped Slots" Reza Zaker, Changiz Ghobadi, and Javad Nourinia VOL. 57, NO. 12, DECEMBER 2009
- [7]. Z. N. Chen, "UWB antennas: From hype, promise to reality," in *IEEE Antennas Propag. Conf.*, 2007, pp. 19–22.
- [8]. K. Yin and J. P. Xu, "Compact ultra-wideband antenna with dual bandstop characteristic," *Electron. Lett.*, vol. 44, no. 7, pp. 453–454, 2008.
- [9]. W. S. Lee, D. Z. Kim, K. J. Kim, and J. W. Yu, "Wideband planar monopole antennas with dual band-notched characteristics," *IEEE Trans. Microw. Theory Tech.*, vol. 54, no. 6, pp. 2800–2806, Jun. 2006.
- [10]. N. D. Trang, D. H. Lee, and H. C. Park, "Compact printed ultra-wideband antenna with three subband notches," in *Proc. ICCE*, Nha Trang, Vietnam, Aug. 2010, pp. 348–351.

Strength of Binary Blended Cement Composites Containing Afikpo Rice Husk Ash

L. O. Ettu¹, I. O. Onyeyili², U. C. Anya³, C. T. G. Awodiji⁴, and A. P. C. Amanze⁵

^{1,3,4,5}Department of Civil Engineering, Federal University of Technology, Owerri, Nigeria.

²Department of Civil Engineering, Nnamdi Azikiwe University, Awka, Nigeria.

Abstract:

This work investigated the strength characteristics of binary blended cement composites made with Ordinary Portland Cement (OPC) and Afikpo Rice Husk Ash (RHA). 105 concrete cubes and 105 sandcrete cubes of 150mm x 150mm x 150mm were produced at percentage OPC replacement with Afikpo RHA of 5%, 10%, 15%, 20%, and 25% and crushed to obtain their compressive strengths at 3, 7, 14, 21, 28, 50, and 90 days of curing. The 3-14 day compressive strength values of OPC-Afikpo RHA binary blended cement concrete were found to be much lower than the control values; the 21-28 day strengths were comparable to the control values; while the 50-90 day strengths were higher than the control values especially at 5-10% replacements of OPC with Afikpo RHA, ranging from 26.80N/mm² for 10% replacement of OPC to 29.30N/mm² for 5% replacement of OPC compared with the control value of 23.60N/mm². This same trend was observed for OPC-Afikpo RHA binary blended cement sandcrete. The variation in density was not significant. Mathematical models were developed for predicting compressive strengths of OPC-Afikpo RHA binary blended cement composites using polynomial regression analysis. The model values of compressive strengths obtained from the various model equations were found to be either exactly the same as those of the equivalent laboratory values or very close to them, especially at ages 28-90 days, with percentage differences ranging from 0 to 0.05. Thus, OPC-Afikpo RHA binary blended cement composites would be good for civil engineering works and the developed model equations can be easily used to estimate their strengths for various curing ages and percentage OPC replacement with Afikpo RHA.

Key words: Binary blended cement, composites, concrete, pozzolan, rice husk ash, sandcrete.

I. INTRODUCTION

The high cost of Ordinary Portland cement in Nigeria and many other parts of Africa has resulted in extremely high cost of building thereby rendering many persons "homeless." Thus, so long as the cement industry continues to play a cardinal role in physical infrastructural development, attempts should continuously be made to (i) reduce the cost of production of Portland cement, (ii) reduce the consumption of the raw materials, (iii) protect the environment, and (iv) enhance the quality of cement. One way is to use suitable low-cost, sustainable, and environmentally friendly materials as partial replacement of Portland cement. Major materials used in this regard are industrial and agricultural by-products, otherwise regarded as wastes in technologically disadvantaged communities. Researchers have especially more recently intensified work on substitute materials for cement in making cement composites such as concrete and sandcrete (Olugbenga et al., 2007). Blended cements are currently used in many parts of the world (Bakar, Putrajaya, and Abdulaziz, 2010). During hydration of Portland cement, calcium hydroxide [Ca(OH)₂] is obtained as one of the hydration products. It is responsible for deterioration of concrete. When a pozzolanic material is blended with Portland cement it reacts with the Ca(OH)₂ to produce additional calcium-silicate-hydrate (C-S-H), which is the main cementing component. Thus the pozzolanic material reduces the quantity of Ca(OH)₂ and increases the quantity of C-S-H. Therefore, the cementing quality is enhanced if a good pozzolanic material is blended in suitable quantity with Portland cement (Padney et al., 2003; Dwivedia et al., 2006). The incorporation of agricultural by-product pozzolans calcined at high temperatures has been studied with positive results in the manufacture and application of blended cements (Malhotra and Mehta, 2004). Ezeh and Ibearugbulem (2009) found good prospect in partially replacing cement with periwinkle shell ash in river stone aggregate concrete.

Adeuyi and Ola (2005) successfully applied waterworks sludge as partial replacement for cement in concrete production. Elinwa and Awari (2001) investigated the potentials of groundnut husk ash concrete by partially replacing Ordinary Portland Cement with groundnut husk ash. Many other researchers have also confirmed rice husk ash (RHA) a pozzolanic material that can be used to partially replace OPC in making cement composites (Ikpong and Okpala, 1992; Cisse and Laquerbe, 2000; Wada et al., 2000; Rukzon and Chindaprasirt, 2006; Cordeiro, Filho, and Fairbairn, 2009; Fadzil et al., 2008; Poon, Kou, and Lam, 2006; De Sensale, 2006; Saraswathy and Song, 2007; Agbede and Obam, 2008; Habeeb and Fayyadh, 2009; Rukzon, Chindaprasirt, and Mahachai, 2009.). However, studies by Chandrasekar et al. (2003) have shown that the physical and chemical properties of RHA are dependent on a number of factors, including the soil chemistry, paddy variety, climatic and geographical conditions, and fertilizers applied during rice cultivation.

Efforts to intensify food production and local economic ventures in many Nigerian communities lead to increased agricultural wastes such as rice husk. The problem is worse in places like Afikpo district of Ebonyi State where farming in general and massive cultivation of rice in particular is the predominant business of many community dwellers, leading to the generation of some thousands of tons of rice husk annually. There is therefore a need to specifically investigate the suitability of using Afikpo rice husk ash as possible cement replacement in making cement composites. Its utilization as pozzolanic material would both reduce the problem of solid waste management (Elinwa and Ejeh, 2004) and add commercial value to the otherwise waste product. This would serve as a boost to intensive cultivation of the product and ultimately lead to increased food, more jobs for people, and more peaceful society through the elimination of various vices related to poverty and idleness.

II. METHODOLOGY

Rice husk was obtained from rice milling factories in Afikpo, Ebonyi State, Nigeria, air-dried, and calcined into ashes in a locally fabricated combustion chamber at temperatures generally below 650°C. The ash was sieved and large particles retained on the 600µm sieve were discarded while those passing the sieve were used for this work. No grinding or any special treatment to improve the ash quality and enhance its pozzolanicity was applied because the researchers wanted to utilize simple processes that can be easily replicated by local community dwellers. The resultant rice husk ash (RHA) had a bulk density of 760 Kg/m³, specific gravity of 1.81, and fineness modulus of 1.40. Other materials used for the work are Ibeto brand of Ordinary Portland Cement (OPC) with a bulk density of 1650 Kg/m³ and specific gravity of 3.13; river sand free from debris and organic materials with a bulk density of 1580 Kg/m³, specific gravity of 2.70, and fineness modulus of 2.84; Crushed granite of 20 mm nominal size free from impurities with a bulk density of 1510 Kg/m³, specific gravity of 2.94, and fineness modulus of 3.65; and water free from organic impurities.

A simple form of pozzolanicity test was carried out for the RHA. It consists of mixing a given mass of the ash with a given volume of Calcium hydroxide solution [Ca(OH)₂] of known concentration and titrating samples of the mixture against hydrochloric acid solution of known concentration at time intervals of 30, 60, 90, and 120 minutes using phenolphthalein as indicator at normal temperature. The titre value (volume of acid required to neutralize the constant volume of calcium hydroxide-ash mixture) continuously reduced with time, confirming the ash as a pozzolan that fixed more and more of the calcium hydroxide, thereby reducing the alkalinity of the mixture (The amount of lime fixed by the pozzolan could be computed.). The chemical analysis of the ash showed it satisfied the ASTM requirement that the sum of SiO₂, Al₂O₃, and Fe₂O₃ should be not less than 70% for pozzolans.

A standard mix ratio of 1:2:4 (blended cement: sand: granite) was used for concrete and 1:6 (blended cement: sand) for sandcrete. Batching was by weight and a constant water/cement ratio of 0.6 was used. Mixing was done manually on a smooth concrete pavement. The RHA was first thoroughly blended with OPC at the required proportion and the homogenous blend was then mixed with the fine aggregate-coarse aggregate mix, also at the required proportions. Water was then added gradually and the entire concrete heap was mixed thoroughly to ensure homogeneity. The workability of the fresh concrete was measured by slump test, and the wet density was also determined. One hundred and five (105) granite concrete cubes and one hundred and five (105) sandcrete cubes of 150mm x 150mm x 150mm were produced at percentage OPC replacement with RHA of 5%, 10%, 15%, 20%, and 25%. Twenty one concrete cubes and twenty one sandcrete cubes with 100% OPC were also produced to serve as controls. This gives a total of 126 concrete cubes and 126 sandcrete cubes. All the concrete cubes were cured by immersion while the sandcrete cubes were cured by water sprinkling twice daily in a shed. Three concrete cubes and three sandcrete cubes for each percentage replacement of OPC with RHA and the control were tested for saturated surface dry bulk density and crushed to obtain their compressive strengths at 3, 7, 14, 21, 28, 50, and 90 days of curing.

Average values of concrete and sandcrete compressive strengths and densities for the various curing ages and percentages of OPC replacement with RHA were obtained and presented in tables and graphs. Mathematical models were developed in form of equations through polynomial regression analysis of the data showing the variation of concrete and sandcrete compressive strengths with curing age and percentage replacement of OPC with RHA. Suitable analytical tools in Microsoft Excel were used to plot appropriate polynomial curves, generate the corresponding mathematical equations, and obtain model values of compressive strengths for comparison with corresponding laboratory values.

2.1 Results and Discussion

The particle size analysis showed that the RHA was much coarser than OPC, the reason being that it was not ground to finer particles. The implication of this is that whatever compressive strength values obtained using it can still be improved upon when the ash is ground to finer particles. The pozzolanicity test confirmed Afikpo rice husk ash as a pozzolan since it fixed some quantities of lime over time, thereby reducing the alkalinity of the mixture as reflected in the smaller titre value over time compared to the blank titre. The compressive strengths of the binary blended cement concrete and sandcrete produced with OPC and Afikpo RHA are shown in tables 1 and 2 respectively.

Table1. Compressive strength of blended OPC-RHA cement concrete

Age (days)	Compressive Strength (N/mm ²) for					
	0 % RHA	5 % RHA	10 % RHA	15 % RHA	20 % RHA	25 % RHA
3	7.90	5.20	4.70	4.20	3.50	3.30
7	14.00	9.70	9.20	8.10	7.20	7.00
14	21.50	18.00	17.70	15.50	11.70	11.00
21	22.10	22.00	21.40	18.90	16.00	14.00
28	23.00	25.30	22.50	20.80	17.90	16.00
50	23.50	28.00	24.70	23.80	21.60	20.00
90	23.60	29.30	26.80	25.90	23.20	22.00

Table2. Compressive strength of blended OPC-RHA cement sandcrete

Age (days)	Compressive Strength (N/mm ²) for					
	0 % RHA	5 % RHA	10 % RHA	15 % RHA	20 % RHA	25 % RHA
3	2.70	1.90	1.80	1.60	1.50	1.50
7	5.00	3.00	3.00	2.50	2.30	2.20
14	7.10	4.40	4.00	3.50	3.20	2.80
21	8.00	5.20	4.80	4.00	3.80	3.20
28	9.30	7.60	6.40	5.80	5.00	4.10
50	9.70	9.80	8.90	8.00	7.10	6.20
90	10.30	11.30	10.80	10.10	9.50	8.80

It can be seen from table 1 that the compressive strength values of binary blended cement concrete consistently decrease with increase in percentage replacement of OPC with Afikpo RHA. The 3-14 day compressive strength values are much lower than the control values for all percentage replacements of OPC with Afikpo RHA. The 3-day strengths range from 3.30N/mm² at 25% replacement of OPC to 5.20N/mm² at 5% replacement of OPC compared with the control value of 7.9 N/mm². The 7-day strengths range from 7.00N/mm² at 25% replacement of OPC to 9.70N/mm² at 5% replacement of OPC compared with the control value of 14N/mm². The 14-day strengths range from 11.00N/mm² at 25% replacement of OPC to 18.00N/mm² at 5% replacement of OPC compared with the control value of 21.50N/mm². However, the 90-day strength at 5-15% replacement of OPC with Afikpo RHA is higher than that of the control, ranging from 25.90 N/mm² for 15% replacement of OPC to 29.30N/mm² for 5% replacement of OPC compared with the control value of 23.60N/mm². This same trend of binary blended cement concrete strength variation with age and percentage replacement of OPC with Afikpo RHA relative to the control values is noticeable for blended cement sandcrete as shown in table 2. The 3-14 day low strength values compared to the control can be attributed to the low rate of pozzolanic reaction at those ages. The silica from the pozzolans reacts with lime produced as by-product of hydration of OPC to form additional calcium-silicate-hydrate (C-S-H) that increases the binder efficiency and the corresponding strength values at later days of curing.

The density results suggests that although the saturated surface dry bulk densities of OPC-Afikpo RHA blended cement concrete and sandcrete reduce slightly with both curing age and percentage replacement of OPC with Afikpo RHA, the variations are of no significance for engineering purposes as they all still fall within the range for normal weight composites.

As should be expected, the results show that the strength of 100% OPC concrete (the control) increases steeply with age until about 14 days. The strength still increases steadily but less steeply between 14 and 28 days, after which the strength increases much more slowly such that the strength at 90 days is not much greater than the strength at 50 days. The variation in strength with age for the binary blended OPC-Afikpo RHA cement concrete is different from the control, especially at high percentages of OPC replacement with Afikpo RHA. The results show that the variation for 5% OPC replacement with Afikpo RHA is not much different from that of the control, although, unlike the control, the binary blended cement concrete continues to attain much higher strength values up to 90 days. The variation for 10% and 15% OPC replacement with Afikpo RHA is significantly different from that of the control. The binary blended cement concrete strength picks up more slowly up to 21 days, after which it begins to increase rapidly until 90 days and beyond. At 20% and 25% OPC replacement with Afikpo RHA the strength picks up even more gradually during the early ages of up to 21 days than at 10-15% replacement levels. However the increase in strength continues more steeply at the later ages of 50 days and above.

Mathematical Models for Predicting Compressive Strength of Opc-Afikpo Rha Cement Composites

The mathematical equations for predicting compressive strength of OPC-Afikpo RHA cement concrete and sandcrete obtained from the results of polynomial regression analysis are presented in this section.

Variation of OPC-Afikpo RHA concrete strength with percentage RHA

$$Y_3 = 0.00009667X^4 - 0.00550741X^3 + 0.10786111X^2 - 0.94846561X + 7.89563492 \text{ ----- (1)}$$

Where Y_3 is the 3-day compressive strength in N/mm^2 of the binary blended OPC-Afikpo RHA concrete and X is the percentage replacement of OPC with AfikpoRHA.

$$Y_7 = -0.00001467X^5 + 0.00108000X^4 - 0.02910000X^3 + 0.35100000X^2 - 2.01333333X + 14.00000000 \text{ ----- (2)}$$

$$Y_{14} = 0.00032667X^4 - 0.01630370X^3 + 0.24972222X^2 - 1.57708995X + 21.49603175 \text{ -- (3)}$$

$$Y_{21} = 0.00009000X^4 - 0.00364815X^3 + 0.02380556X^2 - 0.04431217X + 22.08769841 \text{ --- (4)}$$

$$Y_{28} = -0.00013333X^4 + 0.00841481X^3 - 0.18322222X^2 + 1.12050265X + 23.05158730 \text{ -- (5)}$$

$$Y_{50} = 0.00005200X^5 - 0.00352667X^4 + 0.08690000X^3 - 0.93983333X^2 + 3.83500000X + 23.50000000 \text{ ----- (6)}$$

$$Y_{90} = 0.00005307X^5 - 0.00353333X^4 + 0.08590000X^3 - 0.93366667X^2 + 4.06933333X + 23.60000000 \text{ ----- (7)}$$

Model values of OPC-Afikpo RHA concrete strength from equations (1) to (7) together with their equivalent laboratory values are shown in table 3.

Variation of OPC-Afikpo RHA sandcrete strength with percentage Afikpo RHA

$$Y_3 = 0.00002667X^4 - 0.00151111X^3 + 0.03000000X^2 - 0.26984127X + 2.69523810 \text{ ----- (8)}$$

$$Y_7 = -0.00001147X^5 + 0.00079333X^4 - 0.01996667X^3 + 0.22216667X^2 - 1.10366667X + 5.00000000 \text{ ----- (9)}$$

$$Y_{14} = -0.00000880X^5 + 0.00062000X^4 - 0.01630000X^3 + 0.19850000X^2 - 1.19700000X + 7.10000000 \text{ ----- (10)}$$

$$Y_{21} = 0.00006000X^4 - 0.00381481X^3 + 0.08505556X^2 - 0.86978836X + 7.97698413 \text{ -- (11)}$$

$$Y_{28} = 0.00000480X^5 - 0.00030000X^4 + 0.00613333X^3 - 0.03850000X^2 - 0.26633333X + 9.30000000 \text{ ----- (12)}$$

$$Y_{50} = -0.00003333X^4 + 0.00203704X^3 - 0.04305556X^2 + 0.18375661X + 9.70396825 \text{ ---(13)}$$

$$Y_{90} = 0.00000133X^5 - 0.00013333X^4 + 0.00490000X^3 - 0.08266667X^2 + 0.50666667X + 10.30000000 \text{ ----- (14)}$$

Model values of OPC-Afikpo RHA sandcrete strength from equations (8) to (14) together with their equivalent laboratory values are shown in table 4.

Table 3. Model and laboratory values of OPC-Afikpo RHA concrete strength

Age (days)	Compressive Strength in N/mm ² for					
	0 % RHA	5 % RHA	10 % RHA	15 % RHA	20 % RHA	25 % RHA
L3	7.9	5.2	4.7	4.2	3.5	3.3
M3	7.9	5.2	4.7	4.2	3.5	3.3
L7	14	9.7	9.2	8.1	7.2	7
M7	14.0	9.7	9.2	8.1	7.2	7.0
L14	21.5	18	17.7	15.5	11.7	11
M14	21.5	18.0	17.7	15.5	11.7	11.0
L21	22.1	22	21.4	18.9	16	14
M 21	22.1	22.1	21.3	19.0	15.9	14.0
L28	23	25.3	22.5	20.8	17.9	16
M 28	23.1	25.0	23.0	20.3	18.2	15.9
L50	23.5	28	24.7	23.8	21.6	20
M50	23.5	28.0	24.7	23.8	21.6	20.0
L90	23.6	29.3	26.8	25.9	23.2	22
M90	23.6	29.3	26.8	25.9	23.2	22.0

L3 = Laboratory value at 3 days; M3 = Model value at 3 days.

Table 4. Model and laboratory values of OPC-Afikpo RHA sandcrete strength

Age (days)	Compressive Strength in N/mm ² for % RHA of					
	0	5	10	15	20	25
L3	2.7	1.9	1.8	1.6	1.5	1.5
M3	2.7	1.9	1.8	1.6	1.5	1.5
L7	5	3	3	2.5	2.3	2.2
M7	5.0	3.0	3.0	2.5	2.3	2.2
L14	7.1	4.4	4	3.5	3.2	2.8
M14	7.1	4.4	4	3.5	3.2	2.8
L21	8	5.2	4.8	4	3.8	3.2
M 21	8.0	5.3	4.6	4.2	3.7	3.2
L28	9.3	7.6	6.4	5.8	5	4.1
M 28	9.3	7.6	6.4	5.8	5.0	4.1
L50	9.7	9.8	8.9	8	7.1	6.2
M50	9.7	9.8	8.9	8.0	7.1	6.2
L90	10.3	11.3	10.8	10.1	9.5	8.8
M90	10.3	11.3	10.8	10.1	9.5	8.8

L3 = Laboratory value at 3 days; M3 = Model value at 3 days.

It can be seen from tables 3 and 4 that the model values of compressive strengths obtained from the various model equations 1 to 14 are either exactly the same as those of the equivalent laboratory values or very close to them, especially at ages 28-150 days, with percentage differences ranging from 0 to 0.05. Therefore, the respective model equations are all suitable for determining the compressive strength values of OPC-Afikpo RHA binary blended cement concrete and sandcrete for various curing ages and percentage replacement of OPC with Afikpo RHA.

III. CONCLUSIONS

The strength of OPC-Afikpo RHA binary blended cement concrete gets comparable to that of the control at 21 days of curing. The strength of the binary blended cement concrete at 5 to 15% replacement is higher than that of the control at 28, 50, and 90 days of curing. This clearly shows that OPC-Afikpo RHA binary blended cement concrete can be used for high strength requirements at curing ages greater than 28 days.

There is similarity in the pattern of variation of OPC-Afikpo RHA binary blended cement sandcrete strength with that of OPC-Afikpo RHA binary blended cement concrete for different percentage replacements of OPC with Afikpo RHA at 3 to 90 days of curing. Just as for concrete, OPC-Afikpo RHA binary blended cement sandcrete has very low strength compared to the control at early ages up to 14 days. The strength improves greatly thereafter and increases to become greater than that of the control at ages above 50 days. Thus OPC-Afikpo RHA binary blended cement sandcrete could also be used in civil engineering works where early strength is not a major requirement. The mathematical models/equations developed for predicting compressive strength of OPC-Afikpo RHA binary blended cement composites can be used as guide in determining appropriate percentage replacement and minimum curing age to use for required strength values since the model values of compressive strengths obtained from the equations are either exactly the same as those of the equivalent laboratory values or very close to them, especially at ages 28-150 days.

REFERENCES

- [1] Adewuyi, A. P., & Ola, B. F. (2005). Application of waterworks sludge as partial replacement for cement in concrete production. *Science Focus Journal*, 10(1): 123-130.
- [2] Agbede, I. O., & Obam, S. O. (2008). Compressive Strength of Rice Husk Ash-Cement Sandcrete Blocks. *Global Journal of Engineering Research*, Vol. 7 (1), pp. 43-46.
- [3] Bakar, B. H. A., Putrajaya, R. C., & Abdulaziz, H. (2010). Malaysian Rice Husk Ash – Improving the Durability and Corrosion Resistance of Concrete: *Pre-review. Concrete Research Letters*, 1 (1): 6-13, March 2010.
- [4] Chandrasekhar, S., Pramada, S. K. G., & Raghavan, P. N. (2003). Review Processing, Properties And Applications of Reactive Silica From Rice Husk-An Overview. *Journal Of Materials Science*, 38: 3159-3168.
- [5] Cisse, I. K., & Laquerbe, M. (2000). Mechanical characterization of sandcretes with rice husk ash additions: study applied to Senegal. *Cement and Concrete Research*, 30 (1): p.13– 18.
- [6] Cordeiro, G. C., Filho, R. D. T., & Fairbairn, E. D. R. (2009). Use of ultrafine rice husk ash with high-carbon content as pozzolan in high performance concrete. *Materials and Structures*, 42: 983–992. DOI 10.1617/s11527-008-9437-z.
- [7] De Sensale, G. R. (2006). Strength development of concrete with rice-husk ash. *Cement & Concrete Composites*, 28: 158–160.
- [8] Dwivedia, V. N., Singh, N. P., Das, S. S., & Singh, N. B. (2006). A new pozzolanic material for cement industry: Bamboo leaf ash. *International Journal of Physical Sciences*, 1 (3): 106-111.
- [9] Elinwa, A. U., & Awari, A. (2001). Groundnut husk ash concrete. *Nigerian Journal of Engineering Management*, 2 (1), 8 - 15.
- [10] Elinwa, A. U., & Ejeh, S. P. (2004). Effects of the incorporation of sawdust waste incineration fly ash in cement pastes and mortars. *Journal of Asian Architecture and Building Engineering*, 3(1): 1-7.
- [11] Ezeh, J. C., & Ibearugbulem, O. M. (2009a). Suitability of Calcined Periwinkle Shell as Partial Replacement for Cement in River stone Aggregate Concrete. *Global Journal of Engineering and Technology*, 2(4): 577-584.
- [12] Fadzil, A. M., Azmi, M. J. M., Hisyam, A. B. B., & Azizi, M. A. K. (2008). Engineering Properties of Ternary Blended Cement Containing Rice Husk Ash and Fly Ash as Partial Cement Replacement Materials. *ICCBT*, A (10): 125 – 134.
- [13] Habeeb, G. A., & Fayyadh, M. M. (2009). Rice Husk Ash Concrete: the Effect of RHA Average Particle Size on Mechanical Properties and Drying Shrinkage. *Australian Journal of Basic and Applied Sciences*, 3(3): 1616-1622.
- [14] Ikpong, A. A., & Okpala, D. C. (1992). Strength characteristics of medium workability ordinary Portland cement-rice husk ash concrete. *Building and Environment*, 27 (1): 105–111.
- [15] Malhotra, V. M., & Mehta, P. K. (2004). *Pozzolanic and Cementitious Materials*. London: Taylor & Francis.
- [16] Olugbenga, A. (2007). Effects of Varying Curing Age and Water/Cement Ratio on the Elastic Properties of Laterized Concrete. *Civil Engineering Dimension*, 9 (2): 85 – 89.
- [17] Padney, S. P., Singh, A. K., Sharma, R. L., & Tiwari, A. K. (2003). Studies on high-performance blended/multiblended cements and their durability characteristics. *Cement and Concrete Research*, 33: 1433-1436.
- [18] Poon, C. S., Kou, S. C., & Lam, L. (2006). Compressive strength, chloride diffusivity and pore structure of High Performance metakaolin and silica fume concrete. *Construction and building materials*, 20: 858 – 865.
- [19] Rukzon, S., & Chindapasirt, P. (2006). Strength of ternary blended cement mortar containing Portland cement, rice husk ash and fly ash. *J. Eng. Inst. Thailand*, 17: 33-38 (547-551).
- [20] Rukzon, S., Chindapasirt, P., & Mahachai, R. (2009). Effect of grinding on chemical and physical properties of rice husk ash. *International Journal of Minerals, Metallurgy and Materials*, 16 (2): 242-247.
- [21] Saraswathy, V., & Song, H. (2007). Corrosion performance of rice husk ash blended concrete. *Construction and Building Materials*, 21 (8): p.1779–1784.
- [22] Wada, I., Kawano, T., & Mokotomaeda, N. (2000). Strength properties of concrete incorporating highly reactive rice-husk ash. *Transaction of Japan Concrete Institute*, 21 (1): p. 57–62.

Advanced Tracking System with Automated Toll

Pritam Mhatre¹, Parag Ippar², Vinod Hingane³, Yuvraj Sase⁴, Sukhadev Kamble⁵

^{1, 2, 3, 4, 5} Sinhgad Institute of Technology and Science, Narhe, Pune

⁵ Prof. Department of Information Technology (ME I.T)

Abstract:

This paper presents a novel approach to integrate RFID (Radio Frequency Identification) in WSN (Wireless sensor network). The WSN is used to support RFID identification process by extending the reading range of an RFID system. Besides, with the WSN the environment of an object and optimize RFID reader's performance and energy can be monitored. Subsequently, methodology to integrate RFID technology, with wireless sensor network that form an intelligent vehicle tracking application is implemented. The proposed system can monitor vehicle from monitoring stations as well as toll booth stations, and can inform police whether the vehicle is arriving on particular rout with directed map also the system provides a precise way to repetitively track vehicles using SMS service. The acquired information is displayed via SMS as well as detailed report is generated of tollbooth collection and submitted to its owner via e-mail service displays inside and outside the toll booth and toll will be deducted as per type of vehicle.

Keywords: RFID, WSN, Integration, Tracking, Toll plaza, Tollbooth, Automated ,Lost.

I. INTRODUCTION:

Now a days, toll plaza and real time vehicle tracking are major component of Advanced Tracking System (ATS) with Automated Toll The automatic vehicle tracking facility delivers the flexibility, scalability, and responsiveness that today's organizations need. It provides accurate, up-to-minute information, high- speed communication, and powerful analysis features required to make better decisions faster. The major potential comes from the much acclaimed no line of sight and simultaneous reading properties of RFID. It is now widely recognized that real – time vehicle information will revolutionize the control and logistical organization with significant vehicle fleets. In a global marketplace where productivity is crucial to success, vehicle fleet operators use vehicle management systems as a formidable tool to drive down costs and increase the value of their service including the toll plaza collection as well as the hectic job of finding lost vehicles as well as real time tracking. Moreover, transport departments have no visibility over utilization of its fleet on real-time, which results in underutilization of resources. So, all these naturally results in avoidable stress, costly errors and sub cost optimal fleet utilization and finally dissatisfaction and inconvenience to millions of customers. The provision of timely and accurate transactions is so important. New technology can help the administrator to monitor the vehicles routes while increasing the satisfaction of users by reducing cost through efficient operations asset utilization at toll plaza carrying fully automated functions. At the end of work hours every day, large number of vehicles through the local vehicle-stop, forced to wait indefinitely. There are certain vehicles that ply at very low frequencies, and inevitably results in lengthy waiting times for many. When the vehicle arrives, there is an unprecedented rush. In a nutshell, returning from one's workplace/college by public vehicles is a hassled activity.

Dealing with this problem on a daily basis, we have designed and prototyped an RFID-based system that monitors vehicle activities at the monitoring hot spots as well as the toll collection booths which will help in acquiring the accurate location of the vehicles location providing an efficient way for the police department in tracking the vehicles as well as carrying out automated transactions for the related departments including toll fee collection, traffic rules following and a major factor for the RTO department for maintain a safe and efficient database on cloud. An RFID tag is mounted on each vehicle. Each of these tags holds a unique 24-bit ASCII code. For simulation purpose the low range passive tags – 125 kHz operational frequency, 5cm range is utilized. In the full-scale prototype, Gen-2 RFID tags (active) operating at 900 MHz is used.

II. SYSTEM DESIGN:

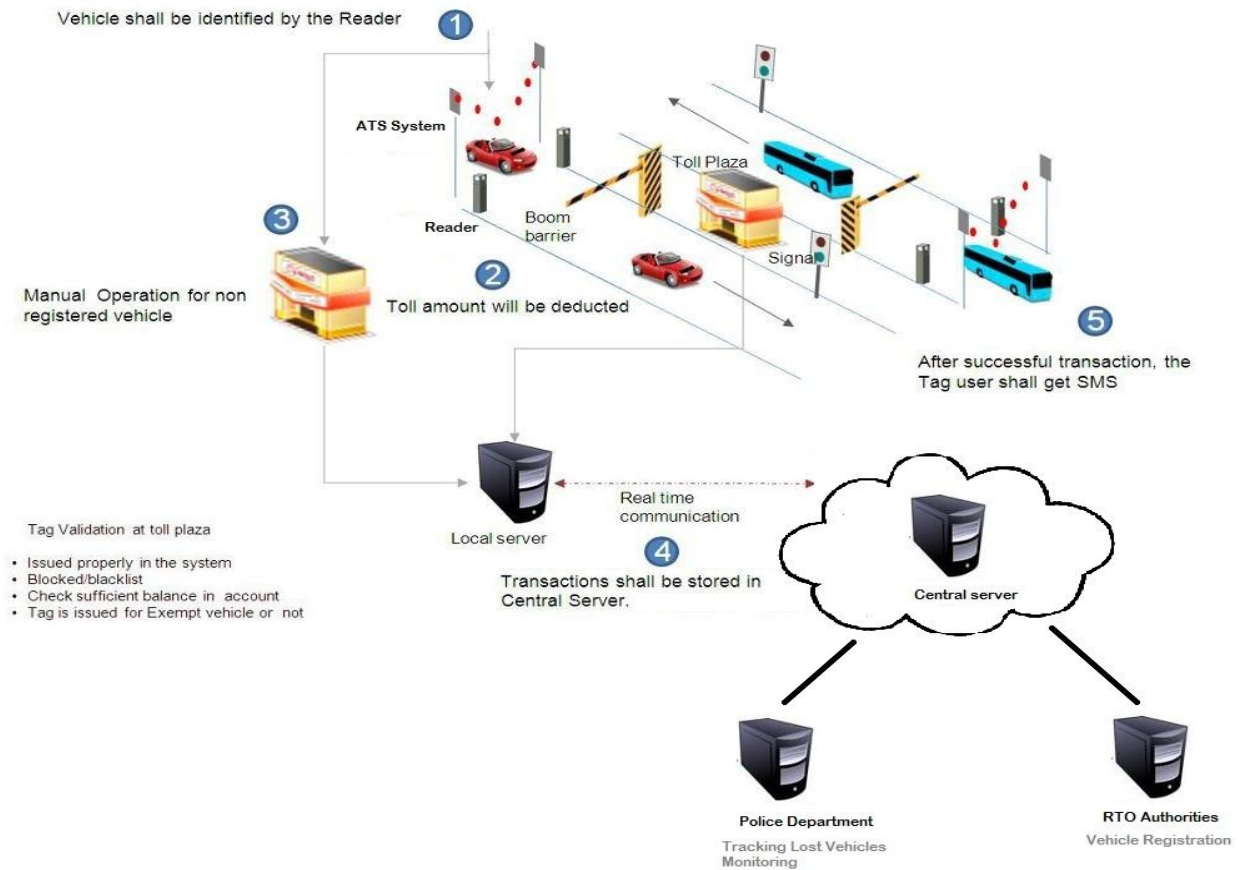


Fig 1: System Design for proposed system

2.1 Client-Server Architecture:

Every toll station shall be equipped with client machine with an RFID reader that can read the tag information once the vehicle comes in proximity. The client machines present at all toll stations shall immediately report to the central server where the database can be updated. The tracker (police) can now fetch vehicle information either using SMS service or a web based application. RFID system is extended with wireless facility to RFID readers. Each RFID tag is equipped with a wireless module which can transmit data to and from the reader. RFID reader acts as sensor node: it reads the identification of an object and performs required processing on it as designed. This provides real-time update as well as automated toll collection of every vehicle at toll station. Hence the hectic and tedious job of manual toll collection and vehicle tracking is now simplified.

2.2 Server Database:

When vehicle comes at toll station RFID Reader, reads the Tag number and processes the information such as Tag ID, vehicle ID, name of owner, etc. into the database.

The main task of server database is to fetch the information associated with the RFID tag when the vehicle arrives in proximity and update the information. This information is now synced on the database on cloud. The main server database will calculate all the credentials for toll deduction of the vehicle at its location. The calculation of credentials of the vehicle is calculated as per stored data. In case, the connection between main server and local client fails, the connection will resume whenever the connection gets re-established.

2.3 RFID Reader:

The RFID reader is to read the tag attached to the Vehicle and process that information on the server database. It sends electromagnetic waves which carries a signal to detect an RFID tag. Then, receives the information returned back to the reader. The Database is to stores and processes information collected by the reader.

2.4 Working of System:

Toll stations are equipped with an RFID reader. Each vehicle has a UHF tag, which is applied inside the windshield or integrated with any of the specified vehicle part such as the number plate. With this system, the vehicle traffic in real-time and without human intervention is monitored on toll station and monitoring hot spots. Each time, a vehicle enters or exits the toll station; the RFID reader sends its identification to the server database. Hence, the supervisor no longer needs barrier on toll station to allow entry to the vehicle. Besides, this system provides a dynamic display inside the toll station. System allows travelers to continue journey without stopping for toll collection. Each vehicle has to have sufficient balance for automatic toll deduction. System also allows authorized persons to track vehicle in case of stolen vehicle. A software application on the toll station keeps track of the entrance and the exit of vehicles and updates the database related to those vehicles with helpful information such as insurance status etc.

Displays are used to provide customer with real-time information about vehicle. Traced Maps of vehicle must be provided on each query in the case of tracking vehicle. UHF is better suited for reading tag attached to vehicles. It uses backscatter technique to communicate with the tag and provides higher read range compared to HF and LF technology. Alien circular antenna to read RFID tags regardless of orientation is utilized in this design. Also, two antennas are used in each gate, to communicate with tags. One ensures the emission of energy to the tag and the other receives energy back from the tag.

III. CONCLUSION:

RFID reader integrated with WSN will benefit from communications and sensing capabilities. The integration of the RFID and WSN will facilitate the extension of an RFID network eliminating the need of wired installation while reducing cost and saving time. The combination of these two promoting technologies has been explored in this article to provide a smart solution for managing the automatic toll deduction on toll stations & also track vehicle by authorized persons. It is believed that by the implementation of this system, problems such as high labour cost, underutilization of petrol/diesel and long waiting time at the toll station will be reduced. So, both passenger and vehicle station administrators such as police will benefit from the system as real time information are provided. It is expected that integration of RFID and WSN will provide new opportunities for applications related to the identification of object over a large area.

REFERENCES:

- [1] Ben Ammar Hatem And Hamam Habib, "Vehicle Management System Using RFID In WSN".
- [2] Aritra Paul, Nischit Bharadwaj, Jagriti R, Sameera S, "Simulation of a Real-Time Vehicle Arrival Predictor using RFID"
- [3] L. Reichardt, G. Adamiuk, G. Jereczek, and T. Zwick: "Car-to-Infrastructure Communication Using Chip-Less, Passive RFID Tags"
- [4] Klaus Finkenzeller – RFID handbook - Fundamentals and Applications in Contactless Smart cards and Identification – 2nd Edition, John Wiley and sons.
- [5] Jerry Banks, David Hanny, Manuel Panchano, Les G.Thompson – RFID Applied – 2007, John Wiley and sons.

Association Rule Mining by Using New Approach of Propositional Logic

¹Prof. M.N.Galphade, ²Pratik P. Raut, ³Sagar D. Savairam,
⁴Pravin S. Lokhande, ⁵Varsha B. Khese

¹ Prof. M.N. Galphade, Computer Engineer, Sinhgad Institute of Technology, Lonavala, Pune India.

² Pratik P. Raut, Computer Engineer, Sinhgad Institute of Technology, Lonavala, Pune India.

³ Sagar D. Savairam, Computer Engineer, Sinhgad Institute of Technology, Lonavala, Pune India.

⁴ Pravin S. Lokhande, Computer Engineer, Sinhgad Institute of Technology, Lonavala, Pune India.

⁵ Varsha B. Khese, Computer Engineer, Sinhgad Institute of Technology, Lonavala, Pune India.

Abstract :

In Data mining we collecting, searching, and analyzing a large amount of data in a database, as to discover rules and patterns. In data mining field association rules are discovered according to minimum support threshold. The accuracy in setting up this threshold directly influences the number and the quality of association rules. The algorithms which are already exist required domain experts to set up the minimum support threshold but if single lower minimum threshold is set too many association rule is generated and if threshold set high then those association rules involving rare items will not be discovered. The risks associated with incomplete rules are reduced because in proposed algorithm association rules are created without the user having to identify a minimum support threshold. . The proposed algorithm discovers the natural threshold based on observation of data set .We propose a framework to discover domain knowledge report as coherent rules. Based on the properties of propositional logic, and therefore the coherent rules are discovered.

Keywords: data mining, association rules, support, confidence a minimum support threshold, material implication, patterns.

I. INTRODUCTION

Association Rule Mining (ARM) is a unique technique. It has the advantage to discover knowledge without the need to undergo a training process. It discovers rules from a dataset, and each rule discovered has its importance measured against interesting measures such as support and confidence [2]. To describe the associations among items in a database the association rule mining technique is used. It is also useful to identify domain knowledge hidden in large volume of data efficiently. The discovery of association rules is typically based on the support and confidence framework. To start the discovery process a minimum support (min sup) must be supplied. A priori is one of the algorithm which is based on this framework. Association rules can be discovered without this threshold specified, because the procedure to discover the rules will quickly exhaust the available resources. Nonetheless, having to constrain the discovery of association rules with a preset threshold, in turn, requires in-depth domain knowledge before the discovery of rules can be automated. The use of min support generally assumes that:

- Threshold value accurately provided by the domain experts.
- The knowledge of interest must have occurred frequently at least equal to the threshold.
- To identify the knowledge sought by an analyst the single threshold is used.

In practice, there are cases where these assumptions are not appropriate and rules reported lead to erroneous actions. In this paper, we propose a novel framework to address the above issues by removing the need for a minimum support threshold. The proposed algorithm discovers the natural threshold based on observation of data set. Associations are discovered based on logical implications. The principle of the approach considers that an association rule should only be reported when there is enough logical evidence in the data. To do this, we consider both presence and absence of items during the mining. An association such as bread \Rightarrow milk will only be reported if we can also find that there are fewer occurrences of \neg bread \Rightarrow milk and bread $\Rightarrow \neg$ milk but more of \neg bread $\Rightarrow \neg$ milk. This approach will ensure that when a rule such as hair \Rightarrow milk is reported, it indeed has the strongest statistical value in the data as comparison was made on both presence and

absence of items during the mining process. In addition, the inverse case of customer not buying bread and customer not buying milk should have statistics that support the rule being discovered due to the logic properties of an equivalence.

1.1 Minimum Support Threshold-

Before association rules are mined, a user needs to determine a support threshold in order to obtain only the frequent item sets. Having users to determine a support threshold attracts a number of issues. We propose an association rule mining framework that does not require a pre-set support threshold [2].

II. ASSOCIATION RULE MINING

An association rules describes association relationships among set of data. Association rules are statements of the form $\{X_1, X_2, \dots, X_n\} \Rightarrow Y$, meaning that if we Find all of X_1, X_2, \dots, X_n in the market basket, then we have a good chance of finding Y . The probability of Finding Y for us to accept this rule is called the confidence of the rule. We normally would search only for rules that had confidence above a certain threshold. We may also ask that the confidence be significantly higher than it would be if items were placed at random into baskets. For example, we might find a rule like (milk, butter) \Rightarrow bread simply because a lot of people buy bread. However, the Beer/diapers story asserts that the rule (diapers) \Rightarrow beer holds with confidence significantly greater than the fraction of baskets that contain beer. We propose a novel association rule mining framework that can discover association rules without the need for a minimum support threshold. This enables the user, in theory, to discover knowledge from any transactional record without the background knowledge of an application domain usually necessary to establish a threshold prior to mining.

This section starts with the distinction between an association rule and the different modes of an implication as defined in propositional logic. The topic of implication from logic is raised because our proposed mining model is based on an association rule's ability to be mapped to a mode of implication. If an association can be mapped to an implication, then there is reason to report this relation as an association rule. An implication having a rule where the left-hand side is connected to the right-hand side correlates two item sets together. This implication exists because it is true according to logical grounds, follows a specific truth table value, and does not need to be judged to be true by a user. The rule is reported as an interesting association rule if its corresponding implication is true.

2.1. An Implication-

In an argument, the truth and falsity of an implication (also known as a compound proposition) (\rightarrow) necessarily rely on logic. Each implication, having met specific logical principles, can be identified each has a set of different truth values. We highlight here that an implication is formed using two propositions p and q . These propositions can be either true or false for the implication's interpretation. From these propositions, we have four implications

1. $p \rightarrow q$,
2. $p \rightarrow \neg q$,
3. $\neg p \rightarrow q$ and
4. $\neg p \rightarrow \neg q$.

Each is formed using standard symbols " \rightarrow " and " \neg ". The symbol " \rightarrow " implies that the relation is a mode of implication in logic, and " \neg " denotes a false proposition. The truth and falsity of any implication is judged by "anding" (\wedge) the truth values held by propositions p and q .

In a fruit retail business where no bread is sold, the implication that relates p and q will be false based on the operation between truth values; that is, $1 \wedge 0 = 0$. The second implication based on the operation will be true because $1 \wedge 1 = 1$. Hence, we say that the latter implication $p \rightarrow \neg q$ is true, but the first implication $p \rightarrow q$ is false. Each implication has its truth and falsity based on truth table values alone. We highlight two modes of implication and their truth table values in the next two sections.

2.1.1. Material Implication-

A material implication (\supset) meets the logical principle of a contraposition. A contrapositive (to a material implication) is written as $\neg q \rightarrow \neg p$. For example, suppose, if customers buy apples, that they then buy oranges is true as an implication. The contrapositive is that if customers do not buy oranges, then they also do not buy apples. If an implication has the truth values of its contrapositive, $\neg(p \wedge \neg q)$ it is a material implication. That is, $p \supset q$ iff $\neg(p \wedge \neg q)$. [1] The truth table for a material implication is shown in Table 1.

p	q	$P \supset q$
T	T	T
T	F	F
F	T	T
F	F	T

Table1. Truth Table for a Material Implication

2.1.2. An Equivalence-

An equivalence ($=$) is another mode of implication. In particular, it is a special case of a material implication. For any implication to qualify as an equivalence, the following condition must be met $p = q$ iff $\neg(p \text{ xor } q)$ where truth table values can be constructed in Table 2.

p	q	$p = q$
T	T	T
T	F	F
F	T	F
F	F	T

Table 2 Truth Table for an Equivalence

One of many ways to prove an equivalence is to show that the implications $p \rightarrow q$ and $\neg p \rightarrow \neg q$ hold true together. The latter is also named an inverse. Suppose, if customers buy apples, that they then buy oranges is a true implication. The inverse is that if customers do not buy apples, then they do not buy oranges.[1]

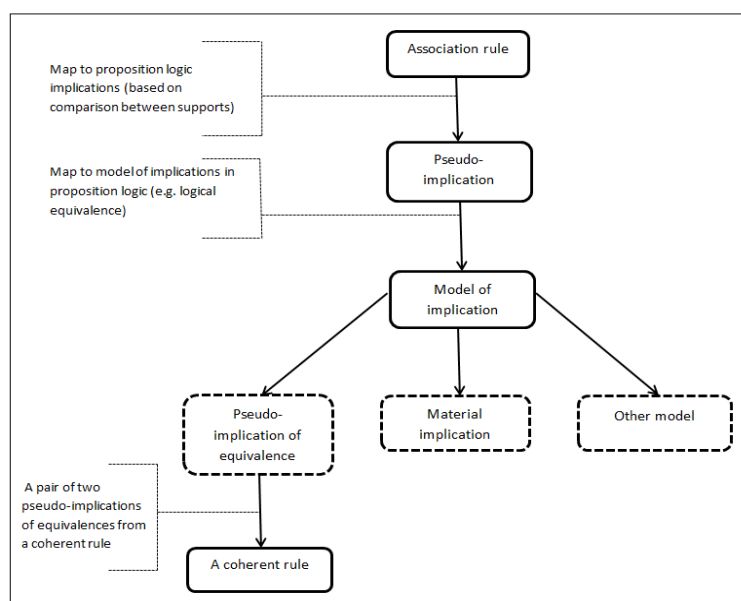


Fig 1. A generalized framework of association rules that based on pseudo implications.

We summarize in this section that a typical statement of the format “if ... then” is a conditional or a rule. If this conditional also meets specific logical principles with a truth table, they are an implication. Among many modes of implications, a material implication relates propositions together. An equivalence is a special case of the former, where propositions are necessarily related together all the time and are independent of user knowledge. In other words, equivalence is necessarily true all the time and judged purely based on logic. We are interested in finding association rules that map to this equivalence. By mapping to this equivalence, we can expect to find association rules that are necessarily related with true implication consistently based on logic. These are the association rules deemed interesting. In addition, the process of finding such association rules will be independent of user knowledge because the truth and falsity of any implication is based purely on logical grounds.

III. CH-SEARCH ALGORITHM

We propose coherent rules by using properties of positive and negative rules on the condition set (positive rule) >set (negative rule) at preselected consequence item set.

We already write a basic algorithm to generate coherent rule in Fig. 2.

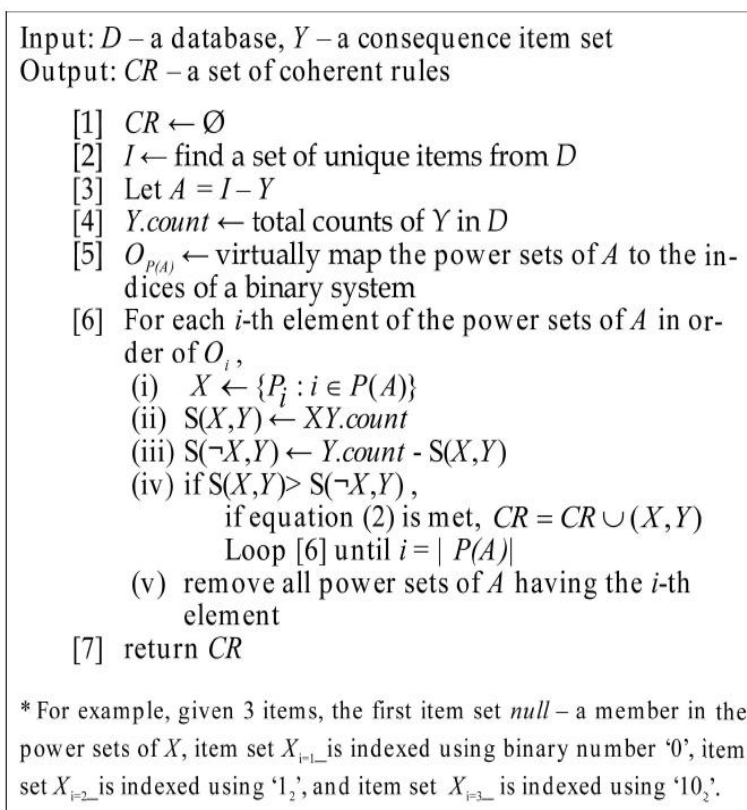


Fig 2. A simple search for coherent rules algorithm (ChSearch)

IV. FEATURES OF CH-SEARCH

- Ch-search algorithm does not require preset minimum support to find out association rules. Coherent rule found based on logical equivalence. And these rule further used as association rule.
- In ch-search, no need to generate frequent item set and also there is no need to generate association rule within each and every item set.
- In apriori algorithm, negative rules not found there. But in ch-search algorithm, we found negative rules and use them to implement both positive and negative rules found. (In apriori, database required in binary format and results are contra-dictionary.)

V. PATTERNS

We discovered pattern based on generated rule which are more efficient.

- **Positive Rules**

When we got association rules some of them consider only items enumerated in transactions, such rules are referred to as positive association rule.

Ex. bread => milk

- **Negative Rules**

Negative association rules also consider the same items, but in addition consider negated items.

Ex. \neg bread => \neg milk.

Algorithm which is presented in paper extends the support-confidence framework with a sliding correlation coefficient threshold. In addition to finding confident positive rules that have a strong correlation, the algorithm discovers negative association rules with strong negative correlation between found the strongest

correlated rules, followed by rules with moderate and small strength values. After finding the association rules we found that patterns are more efficient than the rules. In association rules only those attributes are considered which are strongly responsible to find the result.

In case of the patterns all the attributes are considered.

Ex. milk ≥ 1 and aquatic ≥ 1 and predator ≥ 1 and toothed ≥ 1 and backbone ≥ 1 and breaths ≥ 1 and fins ≥ 1 and tails ≥ 1 and cat size ≥ 1 and hair=0 and feathers=0 and eggs=0 and airborne=0 and venomous=0 and legs=0 and domestics=0 \Rightarrow MAMMAL

Patterns are more efficient than rules

Features-

- Flexible Database Compatibility
- Discovers the natural threshold.
- Expertise domain person is not required for setting min support value.
- Based on generated rule we discovered Efficient Pattern

VI. CONCLUSION

The proposed algorithm discovers the natural threshold based on observation of data set. Association rule which we get as a result include item sets that are frequently and infrequently observed in set of transaction records. There is no loss of any rule. In addition to that also we discovered pattern based on generated rule which are more efficient.

REFERENCES

- [1] Alex Tze Hiang Sim, Maria Indrawan, Samar Zutshi, Member, IEEE, and Bala Srinivasan. "Logic-Based Pattern Discovery"
- [2] Alex Tze Hiang Sim, Maria Indrawan, Bala Srinivasan. "A Threshold Free Implication Rule Mining"
- [3] Yanqing Ji, Hao Ying, Senior Member, IEEE, Peter Dews, Ayman Mansour, John Tran, Richard E. Miller, and R. Michael Massanari. "A Potential Causal Association Mining Algorithm for Screening Adverse Drug Reactions in Postmarketing Surveillance"

On a Probabilistic Approach to Rate Control for Optimal Color Image Compression and Video Transmission

Evgeny Gershikov

Department of Electrical Engineering, Braude Academic College of Engineering,
Karmiel 21982, Israel

Abstract:

Based on a recently introduced Rate-Distortion model for color image compression, optimal color coding and bit allocation are derived. We show that this Rate-Distortion model in conjunction with the probability distribution of subband coefficients can be used to develop an efficient algorithm for coding color images and video sequences. We demonstrate this approach for subband coding using the Discrete Cosine Transform (DCT) and a Laplacian distribution as the probability model. We show how the model can be used for rate-control, applicable to still images and to controlling the bit-rate or bandwidth of video transmission. Visual and quantitative results are presented and discussed to support the efficiency of our algorithms, which outperform other available compression systems.

Keywords: color image coding, subband transforms, rate-distortion model, discrete cosine transform, Laplacian distribution, rate-control, video coding

I. INTRODUCTION

Color image and video compression has become a major task in today's communication environment. Usually color images are represented by the three RGB color components, which are highly correlated [4], [7], [10], [15], [22]. Naturally, it is a naive approach to compress each color component separately. To improve the information distribution in the image data, usually a color components transform (CCT) is used. The RGB to YUV transform is employed for example in JPEG [20] and JPEG2000 [13], while the Karhunen Loeve transform (KLT) is used in [5], [8] and [21]. Nevertheless, these transforms are presently used arbitrarily since no optimization process has been proposed so far for color image compression. Part of the reason has been the lack of a model for color images and their Rate-Distortion (R-D) curve. Recently, such a model has been introduced for the analysis of color compression and its optimization [3]. The model has been proposed in the context of the widely used subband transform coders. Based on the model, a color compression algorithm has been presented, outperforming commonly used algorithms. In this work we present an improved compression algorithm based on the new Rate-Distortion theory and on a probability model for the distribution of the subband transform coefficients. We also present an application of the R-D model for rate-control of the compression. This application can be used to achieve a certain compression ratio or target rate. This approach to image compression is applicable to both still and video coding.

The structure of the work is as follows. In Subsections 1.1 and 1.2 we briefly review subband transforms and the Rate-Distortion theory of subband transform coders. In Section 2 we present the new compression algorithm for color images and compare its performance to that of presently available algorithms including [3]. In Section 3 the new rate-control algorithm is presented and its performance is measured for still images, and in Section 4 the algorithm is considered for video sequences. Finally, conclusions and a summary are given in Section 5.

1.1. Subband transforms - definitions

Subband transform coding is an efficient approach to image compression. Fig. 1 presents a filter bank interpretation of the general tree structured subband transform. The input signal $x[n]$ is decomposed by passing through a set of m analysis filters and down-sampling by a factor m . Then its low frequencies subband $y_0^{(1)}[n]$ is decomposed by the same filters and so on in an iterative fashion until depth D of the tree is reached. The signal can be reconstructed iteratively as shown in Fig. 2 by up-sampling the outputs $y_k^{(d)}[n]$ ($0 \leq k \leq m - 1$) of the analysis filters at level d by a factor of m , filtering them through a synthesis filter-

bank and summing up the results to obtain the low pass subband at level $d - 1$ ($y_0^{(d-1)}[n]$). The original signal $x[n]$ can be considered as the subband $y_0^{(0)}$ in this context, i.e., it is obtained using a reconstruction algorithm on the subbands at level **1**. Compression can be achieved by quantization of the subband components and possibly omission of the less significant subbands.

The DCT [14], the Discrete Wavelet Transform (DWT) [11] and filter-banks used for audio coding (e.g. [16]) readily fit into this typical structure.

1.2. The Rate-Distortion model

A brief presentation of the theory developed in [3] is summarized here. Given a color image in the RGB domain, we denote each pixel by a 3×1 vector $\mathbf{x} = [R \ G \ B]^T$. The RGB correlations are usually high for natural images [1], [4], [7], [10] and hence, a preprocessing stage of a color components transform (CCT) is usually performed prior to coding. Assuming that a CCT is applied to an image, denoted by a 3×3 matrix \mathbf{M} , we obtain for each pixel a new vector of 3 components $C1, C2, C3$, denoted $\tilde{\mathbf{x}} = [C1 \ C2 \ C3]^T$. Thus $\tilde{\mathbf{x}}$ is related to \mathbf{x} by:

$$\tilde{\mathbf{x}} = \mathbf{M}\mathbf{x}. \tag{1}$$

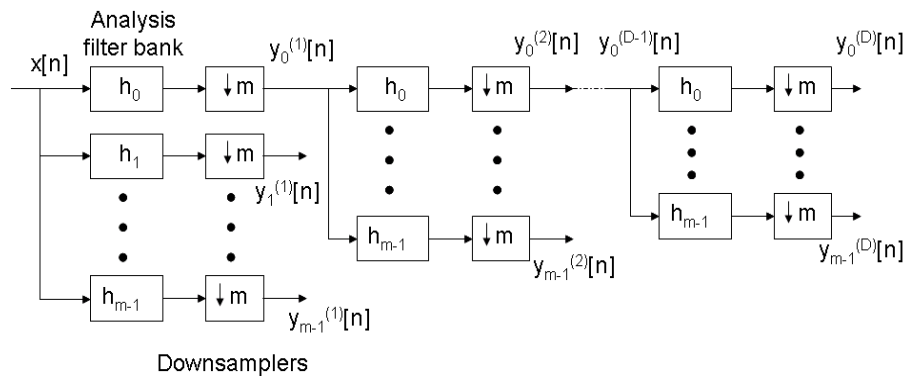


Figure 1. Tree structured subband transform: Analysis.

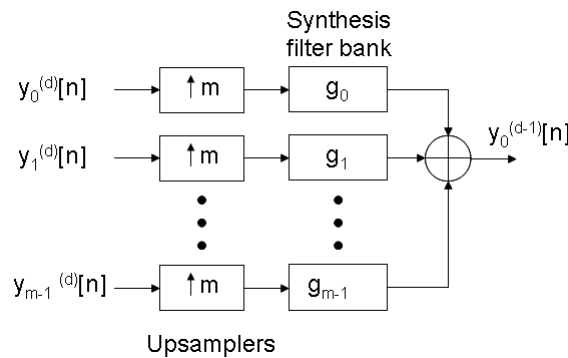


Figure 2. Tree structured subband transform: Synthesis.

Each component in the C1, C2, C3 color space is subband transformed, quantized and its samples are independently encoded (e.g., entropy coded). This description corresponds to typical image compression algorithms such as JPEG [20] and JPEG 2000 [13], when applied to a color image up to and including the quantization stage. Denote by x_{rec} the reconstructed image in the RGB domain, the error covariance matrix in the RGB domain \mathbf{Er} is given by

$$\mathbf{Er} = E[(\mathbf{x} - x_{rec})(\mathbf{x} - x_{rec})^T]. \tag{2}$$

Assume that we have B subbands in the transform for each color component, indexed by $b \in [0, B - 1]$ and $i \in \{1,2,3\}$ is the index of the color component. Then the average MSE (Mean Square Error) between the original and reconstructed images in the RGB domain is:

$$MSE = \frac{1}{3} trace(\mathbf{Er}) = \frac{1}{3} \sum_{i=1}^3 \sum_{b=0}^{B-1} \eta_b G_b \sigma_{bi}^2 \varepsilon_i^2 e^{-aR_{bi}} ((\mathbf{M}\mathbf{M}^T)^{-1})_{ii}$$

(3)

where R_{bi} stands for the rate allocated for the subband b of color component i and σ_{bi}^2 is this subband's variance. η_b is the sample rate of subband b , meaning the ratio of the number of coefficients in this subband and the total number of coefficients in each component. G_b is the energy gain of subband b equal to the squared norm of the subband's synthesis vectors [19]. ε_i^2 is a constant dependent on the distribution of the subband transform coefficients in each color component and, finally, $\alpha \triangleq 2 \ln 2$. Considering the optimization problem of minimizing (3) under the constraint $\sum_{i=1}^3 \sum_{b=0}^{B-1} \eta_b R_{bi} = R$ for some total image rate R and using Lagrange multipliers method, the Lagrangian to be minimized is:

$$L(\{R_{bi}\}, \mathbf{M}, \lambda) = \frac{1}{3} \sum_{i=1}^3 \sum_{b=0}^{B-1} \eta_b G_b \sigma_{bi}^2 \varepsilon_i^2 e^{-\alpha R_{bi}} ((\mathbf{M}\mathbf{M}^T)^{-1})_{ii} + \lambda \left(\sum_{i=1}^3 \sum_{b=0}^{B-1} \eta_b R_{bi} - R \right), \quad (4)$$

where λ is the Lagrange multiplier. By minimizing (4), one can derive the optimal subband rates R_{bi}^* and the target function for the optimal CCT. The optimal solution for this target function is image adaptive. A sub-optimal solution is the DCT as a CCT [2], as used in this work. It is of interest to note that this result (without proof, however) was also found to be most efficient in [6].

In practice, some coding systems such as JPEG perform down-sampling on part of the color components prior to coding. For such systems the down-sampling can be taken into account by introducing down-sampling factors α_i , so that the global rate constraint for the image is

$$\sum_{i=1}^3 \alpha_i \sum_{b=0}^{B-1} \eta_b R_{bi} = R, \quad (5)$$

where the down-sampling could be, for example, by a factor of 2 horizontally and vertically and then

$$\alpha_i = \begin{cases} 1 & \text{full component} \\ 0.25 & \text{down-sampled component} \end{cases}$$

We thus wish to minimize the MSE of (3) under the rate constraint of (5). Additional constraints are the non-negativity of the rates: $R_{bi} \geq 0$. Using the Lagrange multipliers method, we have to minimize:

$$L(\{R_{bi}\}, \mathbf{M}, \lambda, \{\mu_{bi}\}) = \frac{1}{3} \sum_{i=1}^3 \sum_{b=0}^{B-1} \eta_b G_b \sigma_{bi}^2 \varepsilon_i^2 e^{-\alpha R_{bi}} \cdot ((\mathbf{M}\mathbf{M}^T)^{-1})_{ii} + \lambda \left(\sum_{i=1}^3 \alpha_i \sum_{b=0}^{B-1} \eta_b R_{bi} - R \right) - \sum_{i=1}^3 \sum_{b=0}^{B-1} \mu_{bi} R_{bi}, \quad (6)$$

where λ and μ_{bi} are the Lagrange multipliers for the rate constraint and the non-negativity constraints, respectively.

Minimizing the Lagrangian $L()$ for the rates R_{bi} requires knowing the rates that are positive and those that are zero. We denote by Act_i the set of all the active subbands in the color component i , that is, those subbands with positive rates:

$$Act_i \triangleq \{b \in [0, B-1] \mid R_{bi} > 0\}. \quad (7)$$

We also define the following:

$$\xi_i \triangleq \sum_{b \in Act_i} \eta_b, \quad GMA_i \triangleq \prod_{b \in Act_i} (G_b \sigma_{bi}^2)^{\frac{\eta_b}{\xi_i}}, \quad (8)$$

i.e., the relative part of the coefficients in the active subbands from the total signal length (ξ_i) and the weighted geometric mean of their variances (corrected by the energy gains G_b) GMA_i . It can be shown that the solution for $b \in Act_i$ becomes:

$$R_{bi} = \frac{1}{a} \ln \left[\frac{\frac{\varepsilon_i^2 G_b \sigma_{b_i}^2 ((MM^T)^{-1})_{ii}}{\alpha_i}}{\prod_{k=1}^3 \left(\frac{((MM^T)^{-1})_{kk} \varepsilon_k^2 GMA_k}{\alpha_k} \right)^{\frac{\alpha_k \xi_k}{\sum_{j=1}^3 \alpha_j \xi_j}}} \right] + \frac{R}{\sum_{j=1}^3 \alpha_j \xi_j} \quad (9)$$

The determination of the active subbands can be done according to the algorithm given in [3].

II. IMPROVING THE COMPRESSION ALGORITHM

Based on the Rate-Distortion theory, a DCT-based algorithm for color image compression is proposed. This algorithm employs the DCT as the color components transform and utilizes the optimal rates expression of (9). It consists of the following stages:

1. Apply the CCT (DCT) to the RGB color components of a given image to obtain new color components $C1, C2, C3$.
2. Decimate the 2 color components with minimal energy (variance) by a factor of 2 in each direction.
3. Apply the two-dimensional block DCT to each color component Ci .
4. Quantize each subband of each color component independently using uniform scalar quantizers. The quantization step-sizes are chosen so that optimal subband rates are achieved according to Subsection 1.2. The rates are calculated using the Laplacian distribution model for the coefficients of the DCT subband transform.
5. Apply lossless coding to the quantized DCT coefficients. Coding techniques similar to JPEG [20] can be used: differential Huffman coding for the DC coefficients and zigzag scan, run-length coding and Huffman coding (combined with variable-length integer codes) for the AC coefficients.

2.1. The Laplacian distribution

We say that a stochastic variable X has Laplacian distribution if its probability distribution function is

$$p_X(x) = \frac{\mu}{2} e^{-\mu|x|} \quad (10)$$

for some positive constant μ . For such a variable, we can derive the variance σ_X^2 and entropy $h(X)$ as functions of μ :

$$\sigma_X^2 = \frac{2}{\mu^2}, \quad h(X) = \log_2 \frac{2e}{\mu} \quad (11)$$

Thus the following relationship holds:

$$2^{h(X)} = \sqrt{2} e \sigma_X \quad (12)$$

Assume that X is quantized by a uniform scalar quantizer with a step size Δ to the discrete variable \hat{X} . The probability distribution of \hat{X} is

$$\begin{aligned} P_n &\triangleq \text{Prob}(\hat{X} = n) = \text{Prob}((n - 0.5)\Delta \leq X \leq (n + 0.5)\Delta) \\ &= \int_{(n-0.5)\Delta}^{(n+0.5)\Delta} p_X(x) dx = \int_{(n-0.5)\Delta}^{(n+0.5)\Delta} \frac{\mu}{2} e^{-\mu|x|} dx. \end{aligned} \quad (13)$$

and hence:

$$P_n = \begin{cases} 1 - e^{-0.5\mu\Delta}, & n = 0 \\ \frac{1}{2} e^{-\mu n\Delta} (e^{0.5\mu\Delta} - e^{-0.5\mu\Delta}), & n > 0 \end{cases} \quad (14)$$

Defining $k \triangleq e^{0.5\mu\Delta} - e^{-0.5\mu\Delta}$ and using (9), we can derive the entropy of \hat{X} :

$$\begin{aligned} H(\hat{X}) &= - \sum_{n=-\infty}^{\infty} P_n \log_2(P_n) = -P_0 \log_2(P_0) - 2 \sum_{n=1}^{\infty} P_n \log_2(P_n) \\ &= -(1 - e^{-0.5\mu\Delta}) \log_2(1 - e^{-0.5\mu\Delta}) - e^{-0.5\mu\Delta} \left(\log_2 k - 1 \right) + \frac{\mu\Delta}{k} \log_2(e). \end{aligned} \quad (15)$$

Note that the μ parameter in (15) can be expressed by the standard deviation of X using (11) as $\mu = \frac{\sqrt{2}}{\sigma_X}$.

2.2. DCT coefficients distribution

Table 1. PSNR and PSPNR results for the DCT-based compression algorithm with estimated rates (New Alg.) and JPEG at the same compression ratio (CR).

	Image	PSNR		PSPNR		CR
		New Alg.	JPEG	New Alg.	JPEG	
	Lena	30.030	29.486	39.048	37.192	44.84
	Peppers	29.971	28.277	37.818	35.439	33.77
	Baboon	30.024	26.306	38.273	36.023	16.62
	Fruit	30.024	29.268	39.048	36.974	46.53
	Girl	29.987	28.719	38.407	36.871	52.56
	House	30.006	28.573	38.788	37.073	54.36
	Tree	29.987	28.798	39.210	38.072	14.19
	Mean	30.004	28.490	38.656	36.806	

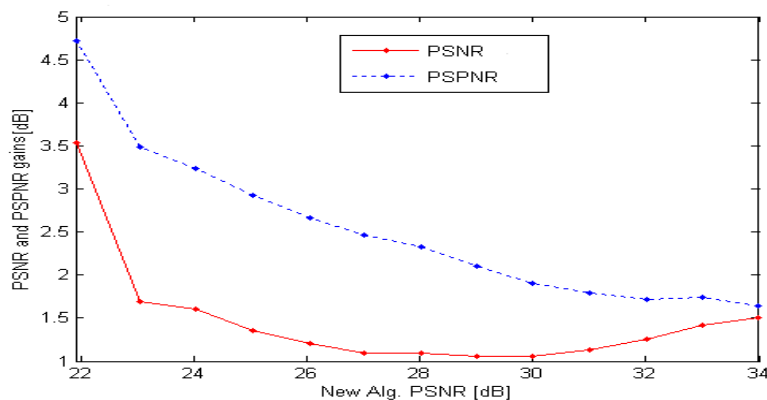


Figure 3. PSNR and PSPNR gains of the new algorithm (New Alg.) with estimated rates on JPEG for various values of PSNR.

Visual results for the House and the Tree images are shown in Fig. 4. It can be seen that JPEG introduces color artifacts in both images. These are significantly less visible in our new algorithm at the same rate. Furthermore, quantitatively, there is a gain of 1.25dB PSNR and 1.6dB PSPNR by the new algorithm for the Tree image. For the House image the gain is even larger: 1.55dB PSNR and 2.1dB PSPNR.

2.3.2. Comparison to the algorithm in [3]

Another comparison is to the algorithm in [3]. The compression results for several images are displayed in Table 2. It can be seen that the algorithm proposed in this work always outperforms the algorithm in [3] with a mean gain of 0.522dB PSNR and 0.278dB PSPNR. The gain for an individual image can be as much as 2dB PSNR as for Baboon.

The new algorithm is superior to the one in [3] also with respect to the execution times. This is elaborated in Subsection 2.4.

2.4. Run time of the algorithm

The run-times for the new algorithm, the algorithm in [3] as well as JPEG are shown in Table 3 for several image sizes. As expected, the use of estimated rates improves the run-time of the compression algorithm, especially for smaller images (15.7% improvement for 256x256 images, 3.5% improvement for 512x768 images). The new algorithm is also comparable with JPEG (14% slower for 256x256 images, 6.9% slower for 512x768 images).

III. RATE CONTROL

Having introduced a DCT-based color compression method that outperforms the baseline JPEG algorithm, it should be noted that this application does not target rate control. Since we can derive the expression for the optimal rates for some given image rate R as in Equation (9) and we can calculate the quantization tables to achieve these rates, an application for rate control can be designed. Next we describe such an application, based on the DCT block transform, aimed to achieve a given rate with performance higher or equal to JPEG. Although this algorithm employs the DCT as a CCT as well and designs the quantization tables for optimal rates, it codes the subbands differently: each subband (DC or AC) is coded independently using the size/value representation of the baseline JPEG [20]. The sizes are coded using adaptive arithmetic coding and

Table 2. PSNR and PSPNR results for the new algorithm (New Alg.) and the algorithm in [3] at the same compression ratio (CR).

	Image	PSNR		PSPNR		CR
		New Alg.	Alg. in [3]	New Alg.	Alg. in [3]	
	Lena	30.011	29.765	39.038	38.671	45.07
	Peppers	29.971	29.770	37.818	37.489	33.77
	Baboon	30.024	28.056	38.273	37.859	16.92
	Cat	30.019	29.172	40.066	39.603	21.97
	Sails	29.990	29.923	39.018	39.012	14.61
	Monarch	29.975	29.721	38.221	37.871	27.08
	Goldhill	29.999	29.928	40.519	40.499	13.23
	Mean	29.998	29.476	38.993	38.715	

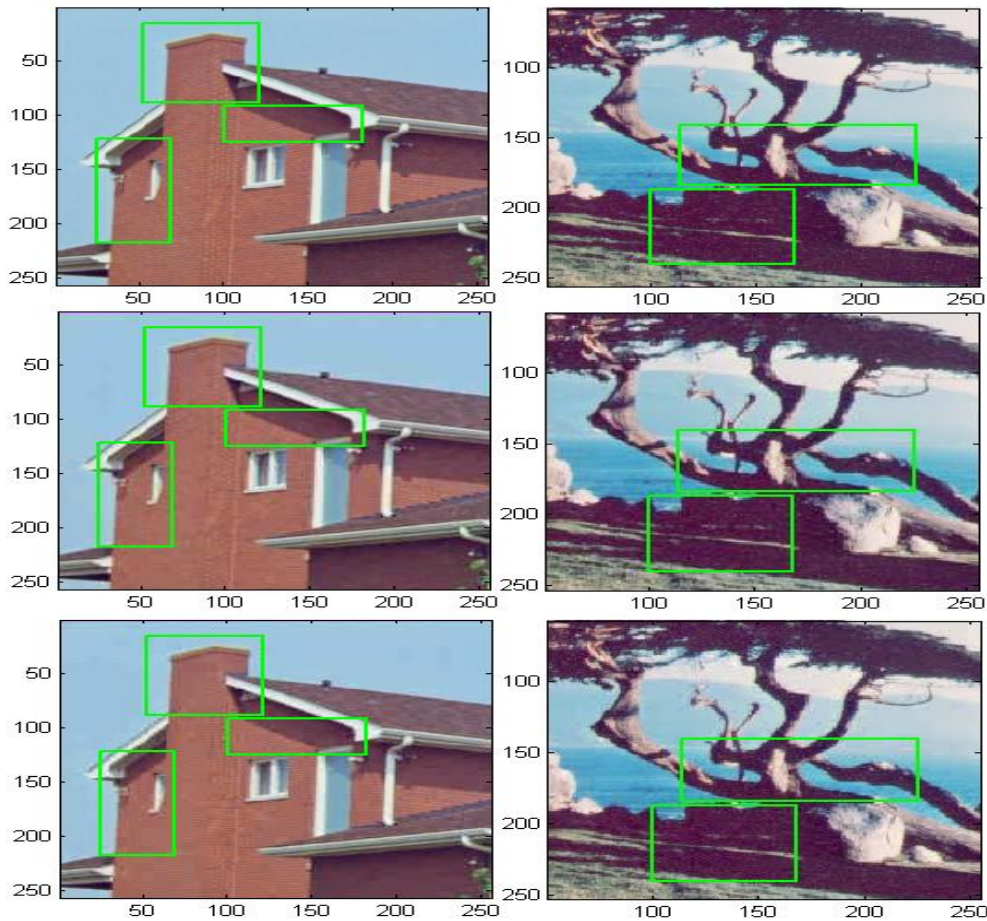


Figure 4. The House and the Tree images - from top to bottom: original, compressed by JPEG and compressed by the new algorithm.

PSNR for the House image: 29.45dB for JPEG and 30.98dB for the new algorithm. PSPNR: 38.01dB and 40.10dB, respectively, at CR=45.15.

PSNR for the Tree image: 28.73dB (JPEG) and 29.98dB (new algorithm). PSPNR: 37.99 and 39.56dB, respectively, at CR=15.36.

Table 3. Run-times in sec. for the algorithm in [3], the new algorithm and JPEG.

Image Size	The alg. in [3]	New Alg.	JPEG
256 × 256	1.53	1.29	1.13
512 × 768	7.73	7.46	6.98

the values as variable length integer (VLI) codes similar to JPEG. For the decoder to be able to reconstruct the sizes, the numbers of appearances (or counts) of each size are sent with the compressed image data to the decoder. The number of bits for these counts as well as the number of bits for the quantization tables (adaptively designed for the image) have to be taken into account. This bits overhead can be considerably reduced, especially at high compression ratios by sending the quantization steps and counts only for the active subbands (with optimal rates $R_{bi}^* > 0$) in addition to bit vectors signifying which subbands are active. This requires, however, calculating the optimal rates as described below.

The stages of the rate control algorithm are:

1. Apply the CCT (here DCT) to the RGB color components of a given image and obtain new color components $C1, C2, C3$.
2. Apply the 2D block-DCT to each color component Ci (using block size of 8×8 if comparison to JPEG is

differentially results in a greater number of bits than needed for the DC information and often in a compression ratio that is too low. If the algorithm's complexity is of lower priority than the rate-control accuracy, both options for the DC subband coding can be always tested and the more precise one chosen. Then the precision at high rates improves as demonstrated in Table 5 - it is higher in terms of (lower) mean relative absolute error and also the CRs distribution is narrower in terms of standard deviation. Note that the original algorithm usually reduces the complexity (in terms of run-time and storage capacity) by running the differential DC coding and checking the condition in (21).

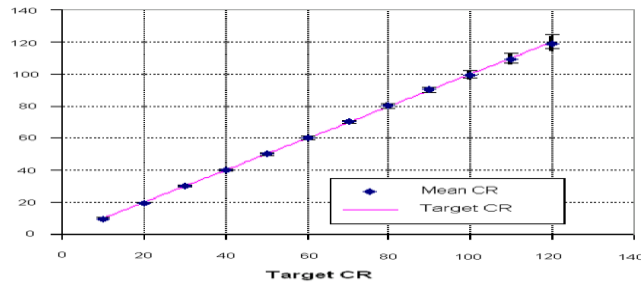


Figure 5. The mean CR for the set of images in Table 4 vs. the target CR. The solid line describes the target CR, while the points describe the achieved mean CR and the error bars are of standard deviation (STD) size.

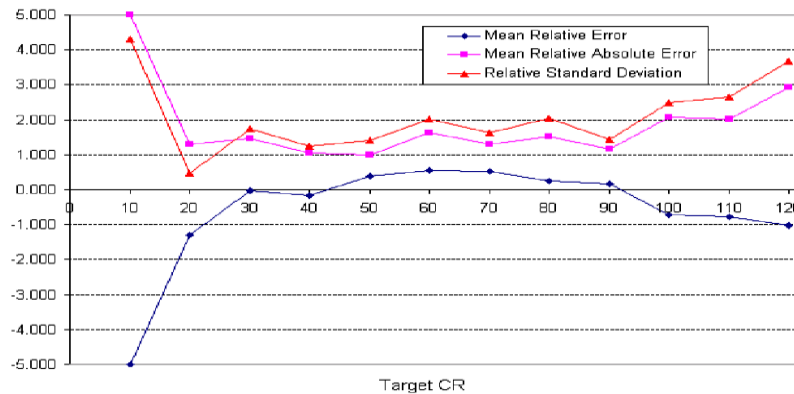


Figure 6. Accuracy measures for the rate-control algorithm: mean relative error (%), mean relative absolute error (%) and relative standard deviation (%).

Table 4. Results for the rate-control algorithm on medium size images for target CR=30. From left to right: The obtained CR, Relative Error, PSNR for the new algorithm, PSNR for JPEG at the same CR and same columns for PSPNR.

Image	CR	Rel. Err.(%)	PSNR		PSPNR		
			New Alg.	JPEG	New Alg.	JPEG	
	Lena	30.586	1.952	31.921	31.925	40.824	39.950
	Peppers	29.785	-0.718	29.982	29.271	37.696	36.515
	Baboon	30.860	2.868	24.553	24.462	35.226	33.766
	Cat	30.291	0.970	27.052	26.881	37.749	36.662
	Sails	29.500	-1.667	26.311	25.595	35.879	33.923

	Tulips	29.482	-1.727	25.826	24.987	33.784	32.431
	Monarch	29.581	-1.395	28.287	28.228	36.494	36.176
	Goldhill	29.876	-0.413	24.716	24.422	36.289	35.487
	Mean	29.995	-0.016	27.331	26.971	36.743	35.614

Table 5. Accuracy measures for the rate-control algorithm at high values of target CR: original algorithm and with both DC coding options tested.

Target CR	Original Algorithm			Both DC coding options tested		
	Mean Rel. Err. (%)	Mean Rel. Abs. Err. (%)	Rel. Std (%)	Mean Rel. Err. (%)	Mean Rel. Abs. Err. (%)	Rel. Std (%)
100	-0.713	2.085	2.483	0.401	1.679	2.149
110	-0.772	2.025	2.663	0.958	1.743	2.191
120	-1.027	2.937	3.665	0.820	2.072	2.410

We should also note that if the application requires a compression ratio not less than a given value, as perhaps can be the case in mobile applications, only differential coding should be used. In any case the algorithm’s results are comparable to [18] especially at the middle range of compression ratios.

3.1.2. Performance (PSNR and PSPNR) of the algorithm

Fig. 7 describes the performance gain of the rate-control algorithm vs. JPEG in the PSNR and PSPNR senses. Since the algorithm is based on the optimal rates, it indeed outperforms JPEG. In cases of CR = 10 the reconstructed images for both our algorithm and JPEG are visually identical to the original one (e.g. when the $PSNR > 34dB$) and thus of limited interest.

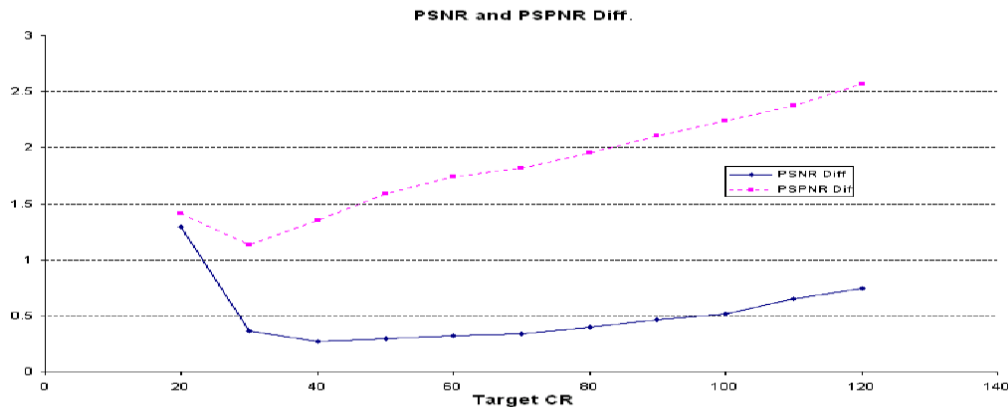


Figure 7. PSNR and PSPNR differences between the rate-control algorithm and JPEG vs. target CR. Along the whole range of values checked the new algorithm outperforms JPEG.

IV. RATE-CONTROL OF VIDEO SEQUENCES

Consider a group of frames (GOF) of a video sequence, to be encoded similarly to the MPEG standard [17]. Here, instead of applying JPEG to the frames or their prediction errors we would like to use the DCT-based compression technique of [3]. We assume for simplicity that the GOF structure is: I,P,P,P,... where I denotes an image coded using intra-frame techniques only and P stands for an image coded using the inter-frame correlation with a previous image. The correlation can be exploited using standard motion estimation. Suppose that the frames are to be coded at a given rate R in bits/sec. We consider k frames of the GOF and assume that these k images are allocated some total number of bits denoted by R_k . Denoting by MSE_j the MSE of the reconstruction of frame j , the average MSE of the frames is simply:

$$MSE = \frac{1}{k} \sum_{j=1}^k MSE_j = \frac{1}{3k} \sum_{j=1}^k \sum_{i=1}^3 \sum_{b=0}^{B-1} \eta_b G_b \varepsilon_i^2 (\sigma_{bi}^j)^2 e^{-aR_{bi}^j} ((MM^T)^{-1})_{ii}. \quad (22)$$

Here we have used (3) for MSE_j denoting by $(\sigma_{bi}^j)^2$ and R_{bi}^j the variance and rate, respectively, of subband b of color component i of frame j . If frame j is an I-frame, the variances are simply of its DCT subbands. However, if we consider a P-frame, then the variances are of the DCT subbands of the image of prediction errors. In any case what is important is that the MSE of the reconstruction of the frame is only the result of its DCT-based compression and not the prediction method used (the motion estimation). The prediction technique affects only the magnitude of the variances $(\sigma_{bi}^j)^2$. Note that \mathbf{M} stands here for the CCT as usual (for example, the RGB to YUV transform or the DCT). Substituting $\eta_b = \frac{1}{B}$ and $G_b = 1$ for the DCT subband transform and slightly rewriting (22) we have:

$$MSE = \frac{1}{3kB} \sum_{i=1}^3 \varepsilon_i^2 ((\mathbf{M}\mathbf{M}^T)^{-1})_{ii} \sum_{b=0}^{B-1} \sum_{j=1}^k (\sigma_{bi}^j)^2 e^{-\alpha R_{bi}^j}. \quad (23)$$

Similarly, the rate constraint $\frac{1}{k} \sum_{j=1}^k \sum_{i=1}^3 \sum_{b=0}^{B-1} \alpha_i \eta_b R_{bi}^j = R_k$ for the k frames can be written as:

$$\frac{1}{kB} \sum_{i=1}^3 \alpha_i \sum_{b=0}^{B-1} \sum_{j=1}^k R_{bi}^j = R_k, \quad (24)$$

where here again we have used η_b of the DCT transform. Considering (23) and (24), we conclude that the problem is similar to the case of still images. Assume for a moment that each color component has kB subbands instead of B , and that these subbands have variances $(\sigma_{bi}^j)^2$ and rates R_{bi}^j ($b \in \{0,1,\dots,B-1\}$, $j \in \{1,2,\dots,k\}$). Then finding the optimal rates allocation for these subbands will give us the subband rates allocation for our k frames. Here we can see the significance of the choice of k . If we take a higher value for k we can expect better performance of the rate-control algorithm since we will be able to allocate the bits budget more flexibly. If, for example, one frame is coded with a small number of bits, its 'spare' bits can be allocated to a greater choice of other frames. However, it leads to a more complicated optimization problem since there are $3kB$ subbands to consider. Similarly, a smaller value for k reduces the order of the optimization problem, however, it also reduces the flexibility of the bits allocation.

Using the same algorithm of Section 3 produces the results described in the next subsection.

4.1. Video rate-control results

We consider a CIF (Common Intermediate Format) color video sequence of 352×288 spatial resolution at the frame rate of 25 frames/sec. We would like to encode the video at 1.055 Mbit/sec (compression ratio of 55). Original and reconstructed frames for the video sequence "Hall Monitor" are presented in Fig. 8. We consider here a GOF starting at frame 100 of the sequence and show the first 4 frames in the GOF. The k is chosen to be 5. The rate is 1.073 MBit/sec with an error of 1.73% relative to the desired one. The motion vectors have used 4.17% of the total bits budget.

V. CONCLUSIONS

With the introduction of a Rate-Distortion model for color image compression, it has become possible to optimize subband transform coders both in the preprocessing stage and in the encoding stage itself. The optimization process leads to the use of the DCT as a color component transform in the preprocessing stage (in addition to its role in subband coding) and provides optimal rates allocation for the coding. These rates can be then used to design optimal quantization steps [12]. We have shown that the quantization stage can be further optimized by applying a Laplacian model to the distribution of the DCT coefficients. This model allows for efficient initialization and faster calculation of the optimal steps by estimating the subband entropies, thus reducing the run-time of the algorithm compared to the use of real entropies, as well as improving the compression performance in terms of PSNR and PSPNR. We have also presented an algorithm for optimized image coding with rate-control. This algorithm can be used to achieve a desired compression ratio and for controlling the bit-rate or bandwidth of video transmission. The presented simulations demonstrate that the proposed algorithms outperform JPEG, both visually and quantitatively. Our conclusion is that based on the newly introduced Rate-Distortion model, optimized compression algorithms can be designed with compression results superior to presently available methods.

ACKNOWLEDGEMENT

This research was supported in part by the HASSIP Research Program HPRN-CT-2002-00285 of the European Commission, and by the Ollendorff Minerva Center. Minerva is funded through the BMBF.

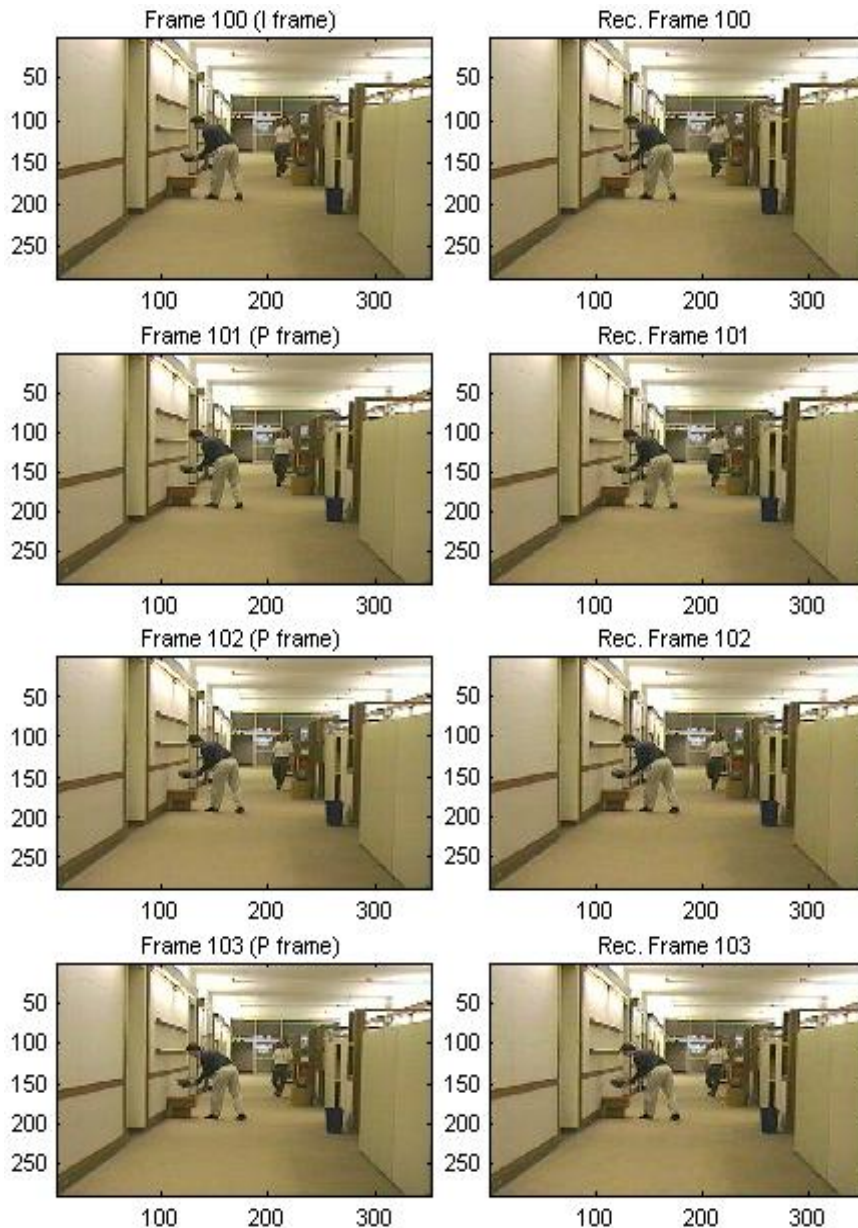


Figure 8. Original and reconstructed frames 100-103 of the Hall Monitor sequence. PSNR = 35.99dB, 34.23dB, 33.90dB and 33.41dB for frames 100, 101, 102 and 103 respectively.

REFERENCES

- [1] Gershikov E. and Porat M., "Does Decorrelation Really Improve Color Image Compression?", the International Conference on Systems Theory and Scientific Computation (ISTASC05), Malta, 2005.
- [2] Gershikov E. and Porat M., "A Rate-Distortion Approach to Optimal Color Image Compression", EUSIPCO 2006, Florence, Italy, September 2006.
- [3] Gershikov E. and Porat M., "On Color Transforms and Bit Allocation for Optimal Subband Image Compression", Signal Processing: Image Communication, 22(1), Jan. 2007, pp. 1-18.
- [4] Goffman-Vinopal L. and Porat M., "Color image compression using inter-color correlation", IEEE International Conference on Image Processing, 2, 2002, pp. II-353 - II-356.
- [5] Han S.E., Tao B., Cooper T. and Tastle L., "Comparison between Different Color Transformations for the JPEG 2000", PICS 2000, 2000, pp. 259-263.
- [6] Hao P. and Shi Q., "Comparative Study of Color Transforms for Image Coding and Derivation of Integer Reversible Color Transform", 15th International Conf. on Pattern Recognition (ICPR '00), 3, 2000, pp. 224-227.

- [7] otera H. and Kanamori K., "A Novel Coding Algorithm for Representing Full Color Images by a Single Color Image", *J. Imaging Technology*, 16, Aug. 1990, pp. 142-152.
- [8] Kouassi R.K., Devaux J.C., Gouton P. and Paindavoine M., "Application of the Karhunen-Loeve transform for natural color images analysis", *IEEE Conference on Signals, Systems & Computers*, 2, 1997, pp. 1740-1744.
- [9] Lam E. Y., Goodman J. W., "A mathematical analysis of the DCT coefficient distributions for images", *IEEE Trans. on Image Processing*, 9(10), 2000, pp. 1661-1666.
- [10] Limb J. O. and Rubinstein C.B., "Statistical Dependence Between Components of A Differentially Quantized Color Signal", *IEEE Trans. on Communications*, Com-20, Oct. 1971, pp. 890-899.
- [11] Mallat S. G., "A theory for multiresolution signal decomposition: the wavelet representation", *IEEE Trans. on Pattern Analysis and Machine Intelligence*, 11(7), July 1989, pp. 674 - 693.
- [12] Porat M. and Shachor G., "Signal Representation in the combined Phase - Spatial space: Reconstruction and Criteria for Uniqueness", *IEEE Trans. on Signal Processing*, 47(6), 1999, pp. 1701-1707.
- [13] Rabbani M. and Joshi R., "An overview of the JPEG2000 still image compression standard", *Signal Processing: Image Communication*, 17(1), 2002, pp 3-48.
- [14] Rao K. R. and Yip P., "Discrete cosine transform: algorithms, advantages, applications", Academic Press, 1990.
- [15] Y. Roterman and M. Porat, "Color Image Coding using Regional Correlation of Primary Colors", *Elsevier Image and Vision Computing*, 25, 2007, pp. 637-651.
- [16] Satt A. and Malah D., "Design of Uniform DFT Filter Banks Optimized for Subband Coding of Speech", *IEEE Trans. on Acoustics, Speech and signal Processing*, 37(11), Nov. 1989, pp. 1672-1679.
- [17] Sikora T., "MPEG digital video-coding standards", *IEEE Signal Processing*, 14(5), 1997, pp. 82-100.
- [18] Supangkat S. H. and Murakami K., "Quantity control for JPEG image data compression using fuzzy logic algorithm", *IEEE Trans. on Consumer Electronics*, 41(1), 1995, pp. 42-48.
- [19] Taubman D. S. and Marcellin M. W., "JPEG2000: image compression, fundamentals, standards and practice", Kluwer Academic Publishers, 2002.
- [20] Wallace G. K., "The JPEG Still Picture Compression Standard", *IEEE Transactions on Consumer Electronics* , 38, 1992, pp. xviii-xxxiv.
- [21] Wolf S. G., Ginosar R. and Zeevi Y. Y., "Spatio-chromatic Model for Colour Image Processing", *IEEE Proc. of the IAPR*, 1, 1994, pp. 599-601.
- [22] Yamaguchi H., "Efficient Encoding of Colored Pictures in R, G, B Components", *Trans. on Communications*, 32, Nov. 1984, pp. 1201-1209.

Fault Impact Assessment on Indirect Field Oriented Control for Induction Motor

¹R.Senthil kumar, ² R.M.Sekar, ³ L.Hubert Tony Raj, ⁴ I.Gerald Christopher Raj

¹PG scholar, Department of EEE, PSNA College of Engineering & Technology Dindigul – 624 622, Tamilnadu, India.

²Associate Professor, Department of EEE, PSNA College of Engineering & Technology Dindigul – 624 622, Tamilnadu, India.

³PG scholar, Department of EEE, PSNA College of Engineering & Technology Dindigul – 624 622, Tamilnadu, India.

⁴Associate Professor, Department of EEE, PSNA College of Engineering & Technology Dindigul – 624 622, Tamilnadu, India.

ABSTRACT:

This paper presents an induction motor drives operating under indirect field-oriented control in which rotor flux DQ axis model is used. In this model, various faults are analyzed such as voltage, current, speed and torque, stator flux. To develop the model, faults are first identified, and then, a simulation model of the setup is developed. Faults are injected into the model in sequential levels and the system performance is assessed after each fault. Here rotor flux DQ model of induction motor is developed and it's controlled by using indirect field oriented control is studied. Here IFOC with DQ model was simulated using MATLAB/ SIMULINK software. Also the waveforms of voltage, current, speed, torque, Q axis and D axis stator flux are obtained. The above faults are analyzed and rectified which results in the increase of efficiency. This analysis is shown to be simple and useful for assessing the reliability of motor drives.

Keywords : Fault impact assessment, Induction motor drive, Rotor flux DQ axis model, openloop and closedloop IFOC

I. INTRODUCTION

Reliability assessment of motor drives is essential, especially in electric transportation applications. Safety is a major concern in such applications, and it is tied directly to re-liability. Induction machines, due to their reliability and low cost, are widely used in industrial applications. However, several electro-mechanical faults may occur during their life span. In industry, most failures interrupt a process and finally reduce or even stop the production. Thus, expensive scheduled maintenance is performed in order to prevent sudden failure and avoid economic damage[1].

The computer simulation for these various modes of operation is conveniently obtained from the equations which describe the symmetrical induction machine in an arbitrary reference frame [2]. As in Fig. 1[3] shows entire block diagram of induction motor drive. To control the rotor which creates torque equation is called as rotor flux DQ model. while faults in supply voltage that is affected on stator voltage. that is not affected on rotor voltage. Because rotor voltage produced due to electromagnetic induction principle. So rotor flux DQ model is used. stator and synchronous reference frame is applicable for squirrel cage induction motor[2]. because rotor part in short circuited in squirrel cage induction motor. The rotor reference frame is applicable for slip ring or

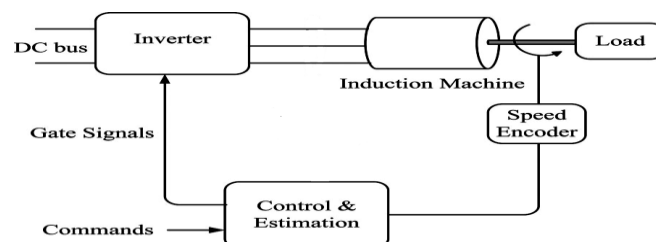


Fig. 1. Typical Induction Motor Drive

wound rotor induction motor. Here synchronous reference frame is presented. because while converting 3 phase to 2 phase which all parts considering DC quantity and control method is simple. The d-axis component is aligned with the rotor flux vector and regarded as the flux-producing current component. On the other hand, the q-axis current, which is perpendicular to the d-axis, is solely responsible for torque production. Based on the pioneering work of Blaschke, high performance induction motor drives have been developed in recent decades. The high dynamic performance is achieved using the field-orientation theory which requires controlling the stator current vector relative to the rotor flux [4]. The indirect field oriented control method is essentially the same as direct oriented control, except the unit vector signals are generated in feed forward manner [5]. Indirect field oriented control is very popular in industries IFOC being more commonly used because in closed-loop mode such drives more easily operate throughout the speed range from zero speed to high-speed field-weakening in DFOC, flux magnitude and angle feedback signals are directly calculated using so-called voltage or current models. In this paper, a complete framework for induction motor under indirect field oriented control (IFOC) is presented. Here cover the faults in voltage, current, speed, torque, Q and D axis stator flux. In this paper change the voltage and to study can be carried out to motor performance.

II. DYNAMIC MODEL OF INDUCTION MOTOR

The dynamic model model of squirrel cage induction motor [SEIM] in stationary reference frame in α - β reference frame variables [6].

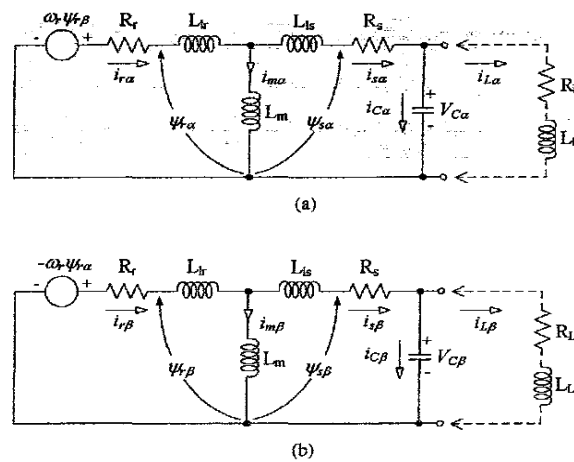


Fig. 2. Equivalent Circuit of SCIM (a) α axis (b) β axis

Components stator and rotor voltage of the induction motor can be expressed as follows:

$$V_{s\alpha} = R_s i_{s\alpha} + L_s \frac{d}{dt} i_{s\alpha} + L_m \frac{d}{dt} i_{r\alpha} \quad (1)$$

$$V_{s\beta} = R_s i_{s\beta} + L_s \frac{d}{dt} i_{s\beta} + L_m \frac{d}{dt} i_{r\beta} \quad (2)$$

$$0 = R_r i_{r\alpha} + L_r \frac{d}{dt} i_{r\alpha} + L_m \frac{d}{dt} i_{s\alpha} + \omega_r \Psi_{r\beta} \quad (3)$$

$$0 = R_r i_{r\beta} + L_r \frac{d}{dt} i_{r\beta} + L_m \frac{d}{dt} i_{s\beta} - \omega_r \Psi_{r\alpha} \quad (4)$$

The components of rotor flux linkage in the stationary reference can be written as

$$\Psi_{r\alpha} = L_m i_{s\alpha} + L_r i_{r\alpha} + \Psi_{r\alpha 0} \quad (5)$$

$$\Psi_{r\beta} = L_m i_{s\beta} + L_r i_{r\beta} + \Psi_{r\beta 0} \quad (6)$$

Where $\Psi_{r\alpha 0}$ and $\Psi_{r\beta 0}$ are the residual rotor flux linkages in α - β axis, respectively.

Then, with an electrical rotor speed of ω_r , the components of rotating voltage in the stationary reference frame are as the follows:

$$\omega_r \Psi_{r\alpha} = \omega_r L_m i_{s\alpha} + \omega_r L_r i_{r\alpha} + \omega_r \Psi_{r\alpha 0} \quad (7)$$

$$\omega_r \Psi_{r\beta} = \omega_r L_m i_{s\beta} + \omega_r L_r i_{r\beta} + \omega_r \Psi_{r\beta 0} \quad (8)$$

The expressions for capacitor voltages are,

$$V_{c\alpha} = \frac{1}{c} \int i_{c\alpha} dt + V_{c\alpha 0} \quad (9)$$

$$V_{c\beta} = \frac{1}{C} \int i_{c\beta} dt + V_{c\beta 0} \quad (10)$$

Using Fig. 2 equations (1)-(10), for the matrix equations of SCIM at no-load in the stationary reference frame are given by

$$\begin{bmatrix} 0 \\ 0 \\ 0 \\ 0 \end{bmatrix} = \begin{bmatrix} R_s + pL_s & 0 & pL_m & 0 \\ 0 & R_s + pL_s & 0 & pL_m \\ pL_m & \omega_r L_m & R_r + pL_r & \omega_r L_r \\ -\omega_r L_m & pL_m & -\omega_r L_r & R_r + pL_r \end{bmatrix} \begin{bmatrix} i_{s\alpha} \\ i_{s\beta} \\ i_{r\alpha} \\ i_{r\beta} \end{bmatrix} + \begin{bmatrix} V_{c\alpha} \\ V_{c\beta} \\ \omega_r \Psi_{r\beta 0} \\ -\omega_r \Psi_{r\alpha 0} \end{bmatrix} \quad (11)$$

From (11), can be written the state equations as follows:

$$A_p I_G + B I_G + V_G = 0 \quad (12)$$

Where,

$$A = \begin{bmatrix} L_s & 0 & L_m & 0 \\ 0 & L_s & 0 & L_m \\ L_m & 0 & L_r & 0 \\ 0 & L_m & 0 & L_r \end{bmatrix}, B = \begin{bmatrix} R_s & 0 & 0 & 0 \\ 0 & R_s & 0 & 0 \\ 0 & \omega_r L_m & R_r & \omega_r L_r \\ -\omega_r L_m & 0 & -\omega_r L_r & R_s \end{bmatrix}$$

$$I_G = \begin{bmatrix} i_{s\alpha} \\ i_{s\beta} \\ i_{r\alpha} \\ i_{r\beta} \end{bmatrix}, V_G = \begin{bmatrix} V_{c\alpha} \\ V_{c\beta} \\ \omega_r \Psi_{r\beta 0} \\ -\omega_r \Psi_{r\alpha 0} \end{bmatrix}$$

I. INDUCTION MOTOR MODEL IN DQ0 SYNCHRONOUS REFERENCE FRAMES

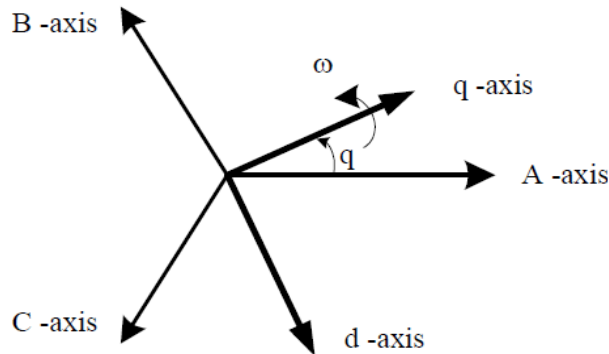


Fig. 3. Change of variables 3Φ to 2Φ conversion

Using Fig. 3[7] Synchronous frame induction motor equations are given as eqn 13 to eqn 17.

Stator $q^e d^e$ voltage equations:

$$v_{qs}^e = \frac{d\Psi_{qs}^e}{dt} + \omega_e \Psi_{ds}^e + r_s i_{qs}^e \quad (13)$$

$$v_{ds}^e = \frac{d\Psi_{ds}^e}{dt} - \omega_e \Psi_{qs}^e + r_s i_{ds}^e$$

Rotor $q^e d^e$ voltage equations:

$$v_{qr}^e = \frac{d\Psi_{qr}^e}{dt} + (\omega_e - \omega_r) \Psi_{dr}^e + r'_r i_{qr}^e \quad (14)$$

$$v_{dr}^e = \frac{d\Psi_{dr}^e}{dt} - (\omega_e - \omega_r) \Psi_{qr}^e + r'_r i_{dr}^e$$

Where,

IV. MOTOR DRIVE, FAULTS AND PERFORMANCE

A. System Overview

As in Fig. 4 faults can occur in the following six possible subsystems or components:

- [1] Faults due to voltage variations
- [2] Faults due to current variations
- [3] Faults due to speed variations
- [4] Faults due to load torque variations
- [5] Faults due to Q axis Stator Flux Variations
- [6] Faults due to D axis Stator Flux Variations

B. Voltage Variation

In this paper to change the voltage and to study can be carried out to motor performance. To control the induction motor by using indirect field oriented control method. Many problems are a result of high or low voltage, unbalanced voltage, ungrounded power systems, or voltage spikes[9].

V. SIMULATION AND EXPERIMENTS

Some of the faults could damage the experimental setup and cannot be tested directly. Also, many commercial motor drives have built-in protection circuitry and algorithms that take action after a fault by shutting down or otherwise altering operation. It is not easy (or advisable) to override protection, but fault modes used here can also integrate protection in several aspects.. Even though the simulations here do not model or cover all physical dynamics, noise, vibration, power loss, and nonlinearities of material, they provide a useful tool that can save the cost of rebuilding a motor drive, or most other systems, after severe failures.

A. Simulations

Simulations provide a safe environment to evaluate even the most extreme faults, provided a simulation has been validated in hardware. Some commercial drives have fault detection and isolation, which would not be helpful if the target is to observe drive performance under faults, Simulations of the IFOC induction motor drive shown in Fig. 4 were performed in MATLAB/SIMULINK for a 1.5-hp induction machine. The inverter involved IGBT–diode pairs from the SimPowerSystems Toolbox in SIMULINK. For the implementation of the state space equations of a system model, MATLAB/ SIMULINK. has the denominated user defined functions or s-functions [10]. In these blocks the code that defines the model in state equations can be written. In this code so much is defined the number of inputs and outputs, like the states and the state space equations of the system. This s-function will correspond to a block with the inputs, outputs and parameters shown in Fig. 5. The s-function can be called from a MATLAB/SIMULINK s-function block. In Fig. 5, one is the SIMULINK block diagram where “VSI-IM model” is the s-function that call’s the defined function. The inputs are multiplexed in a bus can be demultiplexed, and the same occurs for the outputs. Here rotor flux DQ model of induction motor is presented in programmed manner by using M-File. and fault analysis also written in the same M-File. While changing the voltage it will affect current, speed, torque and flux.

TABLE I. MACHINE PARAMETERS

Sl.no	Machine Parameters in perunit	
1	Stator resistance	$R_s = 0.01$
2	Rotor resistance	$R_r = 0.02$
3	Stator leakage inductance	$L_{sl} = 0.1$
4	Rotor leakage inductance	$L_{rl} = 0.1$
5	Magnetizing inductance	$L_m = 4.5$
6	Load torque	$T_l = 0.2375$
7	Supply voltage	$V_s = 1.0$

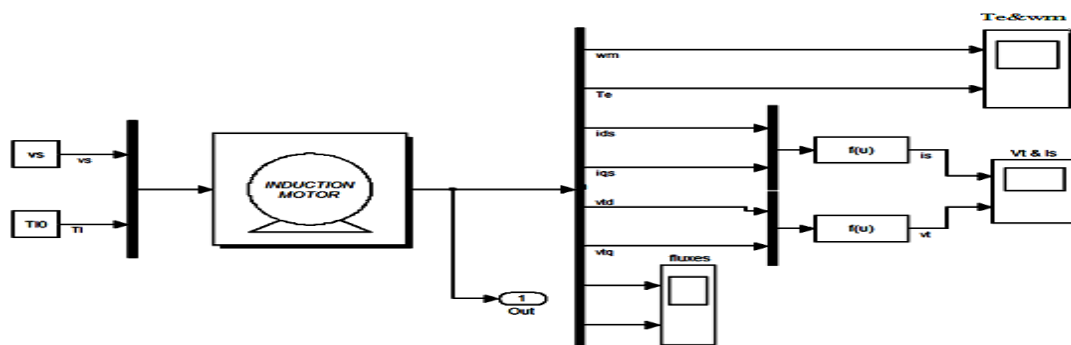


Fig. 5. Simulation Diagram of Induction Motor Under Open Circuit Condition

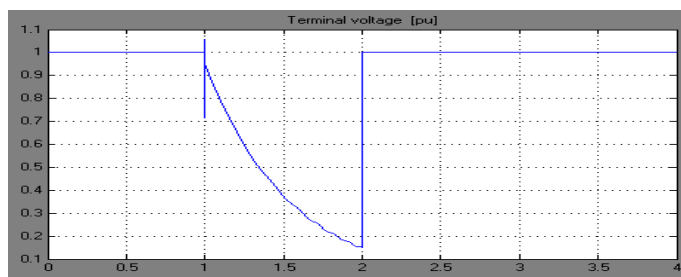


Fig 6. Voltage Response of Induction Motor Under Fault Condition

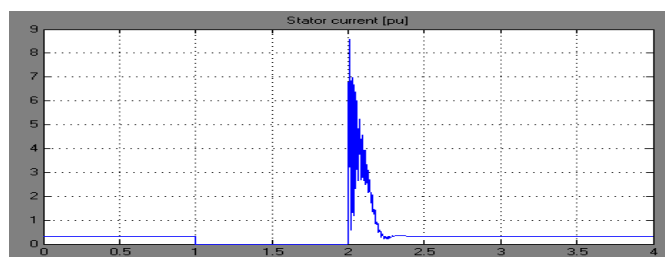


Fig. 7. Current Response of Induction Motor Under Fault Condition

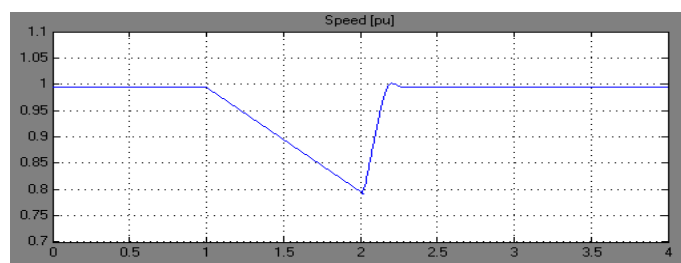


Fig. 8. Speed Response of Induction Motor Under Fault Condition

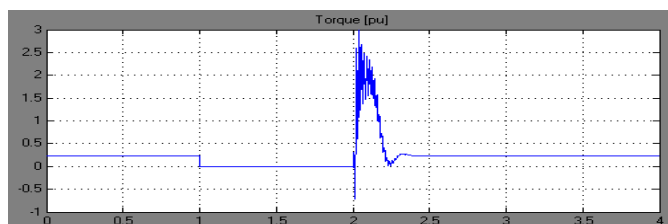


Fig 9. Load Torque Response of Induction Motor Under Fault Condition

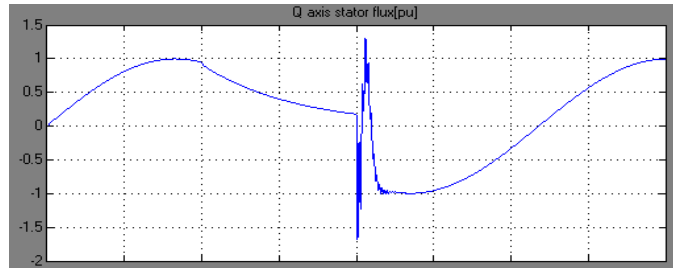


Fig. 10. Q axis Stator Flux Response of Induction Motor Under Fault Condition

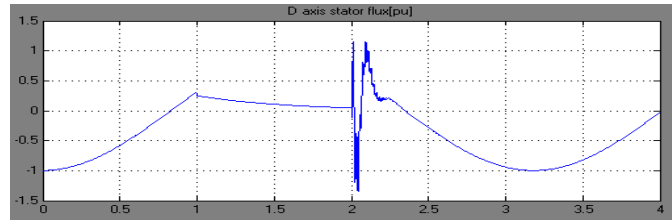


Fig. 11. D axis Stator Flux Response of Induction Motor Under Fault Condition

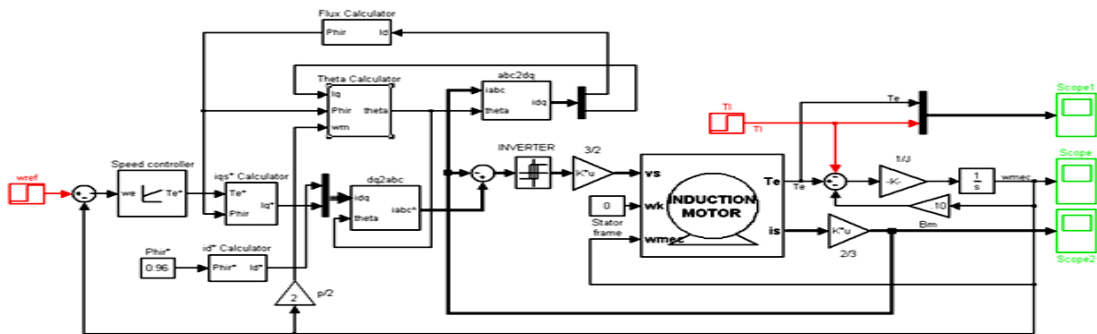


Fig. 12. Simulation Diagram of Closed loop IFOC

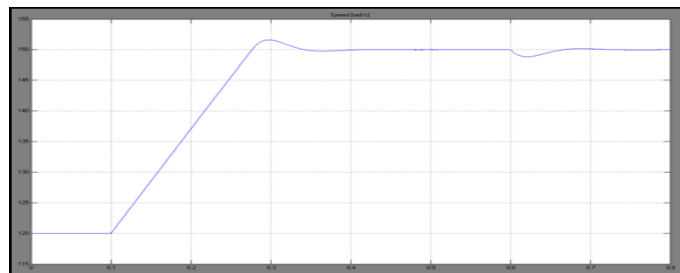


Fig. 13. Speed Response of Induction Motor Under Normal Condition

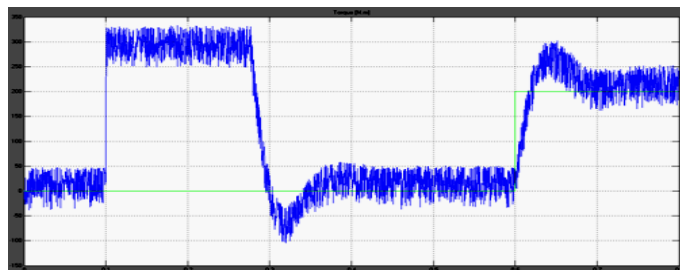


Fig. 14. Torque Response of Induction Motor Under Normal Condition

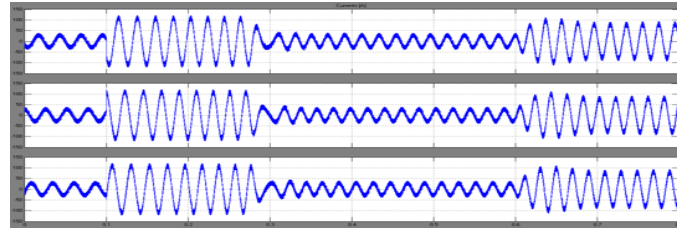


Fig. 15. Currents Response of Induction Motor Under Normal Condition

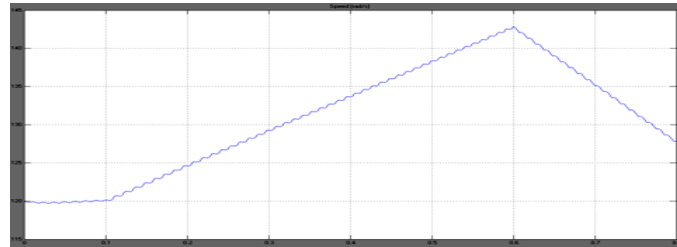


Fig. 16. Speed of Induction Motor Under Fault Condition

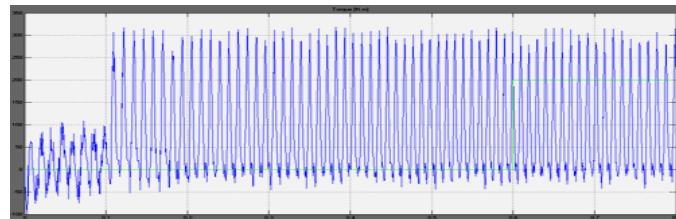


Fig. 17. Torque Response of Induction Motor Under Fault Condition

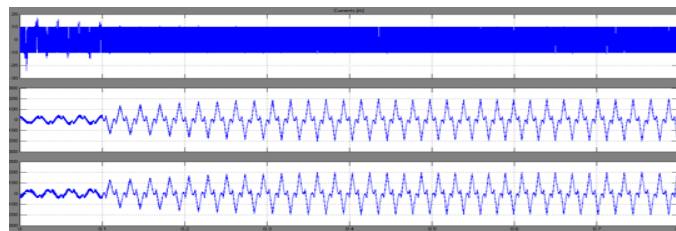


Fig. 18. Currents Response of Induction Motor Under Fault Condition

B. Simulation Results

The drive architectures of Fig.5 have been completely implemented and assessed in the , MATLAB/SIMULINK environment along with their respective control systems. The simulation is based on the parameters shown in Table I. A simulation study based on the model shown in Fig. 6 is carried out to compare open loop IFOC. The following figures shows waveforms of voltage, current, speed, torque and flux under fault conditions. As in Fig. 6, at normal condition there is no disturbance between 0 to 1. when the fault occurs at point 1, suddenly the voltage was dipped between 1 to 2. After 2, the fault was recovered so it maintain steady state condition. As in Fig. 7, at normal condition there is no disturbance between 0 to 1. when the fault occurs at point 1 suddenly the current was reached 0 between 1 to 2. After 2, the fault was recovered, in that point suddenly the current was increased more than rated current. Because current transients will occur. so it reaches steady state at 2.2. As in Fig. 8, at normal condition there is no disturbance between 0 to 1. when the fault occurs at point 1, suddenly the voltage was decreased between 1 to 2. After 2, the fault was recovered, in that point the speed not reaches steady state at point 2. It takes some time to reach steady state. So it reaches steady state at 2.2. As in Fig. 9, at normal condition there is no disturbance between 0 to 1. when the fault occurs at point 1 suddenly the torque was reached 0 between 1 to 2. After 2, the fault was recovered, in that point suddenly the torque was increased more than rated torque. so oscillations will occur. It takes some time to reach steady state. So it reaches steady state at 2.2. As in Fig. 10, at normal condition there is no disturbance between 0 to 1.

when the fault occurs at point 1 suddenly the Q axis stator flux was reached 0 between 1 to 2. After 2, the fault was recovered, in that point suddenly the flux was increased more than rated flux. so oscillations will occur. It takes some time to reach normal state. So it reaches steady state at 2.2. As in Fig. 11, at normal condition there is no disturbance between 0 to 1. when the fault occurs at point 1 suddenly the D axis stator flux was reached 0 between 1 to 2. After 2, the fault was recovered, in that point suddenly the flux was increased more than rated flux. so oscillations will occur. It takes some time to reach normal state. So it reaches steady state at 2.2.

C. Experimental Environment

The experimental setup includes all control, power electronics, motor, load, and measurements. The control and some measurements are available on an eZdspF2812 platform which is based on a Texas Instruments TMS320F2812 DSP. This control platform is integrated into the Grainger Center Modular Inverter [11] which also includes an inverter power stage rated at 400V and 100A. A dynamometer is used to set the load torque. Measurements include speed, torque, currents, voltages, and input and output power. All control and measurement devices, including the dynamometer, are controlled using MATLAB/ Simulink through the Simulink Real-Time Workshop. Communication between the software and the DSP occurs through real-time data exchange (RTDX) via a parallel port. Here fault monitoring kit is also needed to analyze various faults. There are two factors are considered. The first factor is to avoid injecting faults that could cause severe failures or trigger the protection circuitry as predicted from simulations. The second factor is to use a tight external closed-loop torque control in experiments to avoid sudden overload conditions on the dynamometer and the motor shaft. The experimental setup is shown in Fig. 13,

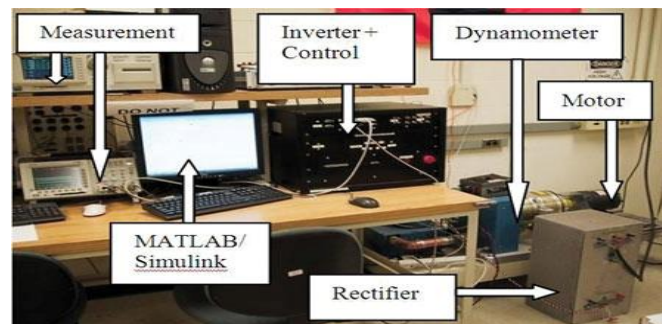


Fig. 19. Experimental setup for model validation.

VI. CONCLUSION

The Existing methodology for reliability modeling covers essential faults in a drive system, including the machine, power electronics converters, and sensors. The methodology leads to rotor flux DQ model of an induction motor drive under open loop IFOC and can be extended to other drives or to more faults in other components. A model was validated in experiments and used for the complete procedure. The survivor function of the complete system was found analytically including fault coverage. Simplifications were proposed based on dominant fault modes, which were found to be faults in the voltage, current, speed, load torque and stator flux. Further research could apply this methodology to other drive topologies, more components in any topology (e.g., link capacitors, gate drives, etc.), design of fault tolerance, and actual field failure rates. Even though DQ's model might not be accurate since faults generally vary with time, the proposed methodology serves the purpose of a comprehensive, straightforward, and versatile reliability modeling procedure. Thus the open loop and closed loop IFOC with DQ model is simulated using MATLAB/ SIMULINK.

REFERENCES

- [1] Ali. M. Bazzi, Alejandro Dominguez-Garcia, and Philip T. Krein, "Markov Reliability Modeling for Induction Motor Drives Under Field-Oriented Control," IEEE Trans. Power Electron., Vol, No. 2, feb 2012.
- [2] P. C Krause and C. H Thomas, "Simulation of Symmetrical Induction Machinery" IEEE Trans., Power Apparatus and Systems Vol. PAS-84, No. 11, 1965
- [3] A. M. Bazzi, A. D. Dominguez-Garcia, and P. T. Krein "A method for impact assessment of faults on the performance of field oriented control drives: A first step to reliability modeling" in Proc. IEEE Appl. power Electron. Conf. Expo., 2010, pp. 256-263
- [4] Zsolt Beres and Peter Vranka, "Sensor less IFOC of Induction Motor With Current Regulators in Current Reference Frame" IEEE Trans. Ind. Appl., Vol. 37, No.4, 2001.
- [5] Alfio consoli, Giuseppe Scarcella and Antonio Testa, "Slip Frequency Detection for Indirect Field Oriented Control Drives" IEEE Trans. Ind. Appl., Vol, No.1., 2004.

- [6] G. R. Slemon, "Modeling of Induction Machines for Electric Drives" IEEE Trans. Ind. Appl., Vol. 25, No.6, pp. 1126-1131, Nov/Dec 1989.
- [7] S. Green, D. J. Atkinson, A. G. Jack, B. C. Mecrow, and A. King, "Sensorless operation of a Fault Tolerant PM Drive," IEE Proc. Elect. Power Appl., Vol. 150, No.2, pp.117-125, Mar. 2003
- [8] Naceri Farid, Belkacem Sebti, Kercha Memberka and Benmokrane Tayed, "Performance Analysis of Field-Oriented Control and Direct Torque Control for Sensorless Induction Motor Drives" in Proc. 15th Mediterranean Conf., on Control & Automation, July 2007.
- [9] W. R. Finley, M. M. Hodowanec, W.G. Holter, "An Analytical Approach to Solving Motor Vibration Problems" IEEE PCIC Conf., Sep 1999.
- [10] Bin Wu, S. B. Dewan and G. R. Slemon, "PWM CSI Inverter Induction Motor Drives" IEEE Trans. Ind. Appl., Vol.28, No.1, pp 64-71, 1992
- [11] J. Kimball, M. Amerhein, A. Kwansinki, J. Mossoba, B. Nee, Z. Sorchini, W. Weaver, J. Weels and G. Zhang, "Modular Inverter for Advanced Control Applications" Technical Report CEME-TR-200-01, University of Illinois May 2006.

Brain Tumor Detection Using Clustering Method

¹Suchita Yadav, ²Sachin Meshram

^{1,2} (Department of ETC / Chouksey Engineering College, Bilaspur India)

ABSTRACT:

The segmentation of magnetic resonance images plays a very important role in medical field because it extracts the required area from the image. Generally there is no unique approach for the segmentation of image. Tumor segmentation from MRI data is an important but time consuming manual task performed by medical experts. The research which addresses the diseases of the brain in the field of the vision by computer is one of the challenge in recent times in medicine. This paper focuses on a new and very famous algorithm for brain tumor segmentation of MRI images by k means algorithm to diagnose accurately the region of cancer because of its simplicity and computational efficiency. In this an image is divided into a number of various groups or clusters. By experimental analysis various parameters such as global consistency error, variation of information, area, elapsed time and rand index have been measured

Keywords : area (A), global consistency error, K means, rand index, segmentation accuracy (SA), and variation of information.

I. INTRODUCTION

Brain cancer is one of the leading causes of death from cancer. There are two main types of brain cancer. They include primary brain cancer, in which the brain cancer originates in the brain itself. Primary brain cancer is the rare type of brain cancer. It can spread and invade healthy tissues on the brain and spinal cord but rarely spreads to other parts of the body. Secondary brain cancer is more common and is caused by a cancer that has begun in another part of the body, such as lung cancer or breast cancer that spreads to the brain. Secondary brain cancer is also called metastatic brain cancer. A diagnosis of brain cancer is generally made by a specialist called a neurologist. Imaging tests that may be performed include MRI and/or CT scan which use computer technology to create detailed pictures of the brain. There are two classifications which exist to recognize a pattern, and they are supervised classification and unsupervised classification. A commonly used unsupervised classification method is a K Means algorithm [1].

II. PROBLEM DESCRIPTION

The tumor portion of an image is exploited by using the undesired component, atmospheric interference. So, the technique which is preferred is image segmentation rather than considering the whole MRI image. Various experiments with published benchmarks are required for this research field to progress [1]. A cluster number k must be determined before cluster processing. This method cannot be used to classify data when the value of k is inadequate. If input data comes from an unknown probability distribution, it is difficult to decide a suitable value for k. Some parameters must be provided before cluster processing, and they strongly affect the results. These methods use the minimum distance clustering algorithm as a clustering system. In these methods, input data is treated as multi-dimensional vectors, the degree of similarity between input data is expressed as a distance (e.g. the Euclidean distance), and the classification of the input data is done using these distances.

III. CLUSTERING METHOD FOR SEGMENTATION OF MRI IMAGES

Clustering is a process of partitioning or grouping a given sector unlabeled pattern into a number of clusters [2] such that similar patterns are assigned to a group, which is considered as a cluster [3]. Manual segmentation of brain tumors from MR images is a challenging and time consuming task. In this study a new approach has been discussed to detect the area of tumor by applying K Means algorithm. The area of tumor is calculated and statistical parameters are evaluated.

3.1 K-Means

It is one of the clustering method and is very famous because it is simpler and easier in computation [4]. It is the simplest unsupervised learning algorithms that solve the well known clustering problems. [1] K-Means algorithm is an unsupervised clustering algorithm that classifies the input data points into multiple classes based on their intrinsic distance from each other. The algorithm assumes that the data features form a vector space and tries to find natural clustering in them. The flowchart for the k-means clustering is given below:

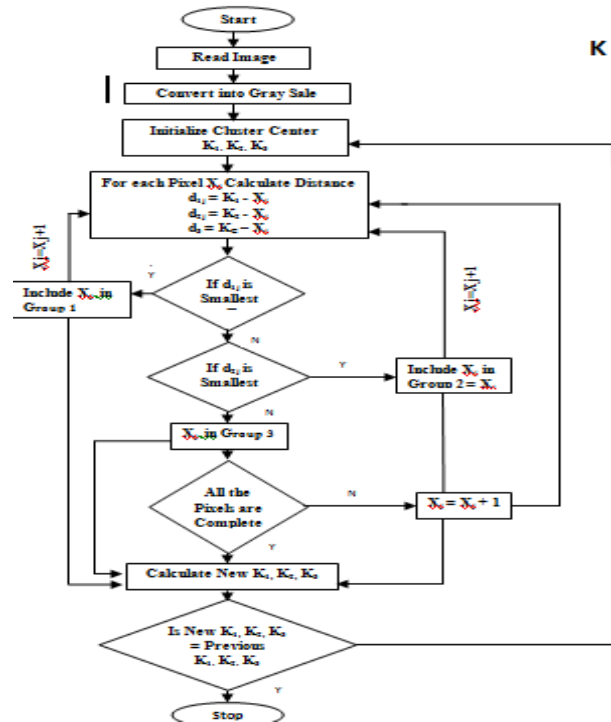


Fig3.1: Flowchart of K Means method (Proposed Method)

IV. RESULTS AND DISCUSSION

By using 6.5 version MATLAB the proposed algorithm has been implemented. The experiment is conducted over two MRI images and various statistical parameters have been evaluated such as global consistency error, variation of information, area, elapsed time and rand index.

4.1 Segmentation Accuracy

The area of the tumor extracted by Ground Truth image should be approximately same as that of the area extracted from the proposed method. Some of the segmentation accuracies are found to be more than 100% which are due to the fact that the brain tumor areas extracted by proposed method are more than the area of ground truth image

4.2 Rand Index

The Rand index counts the fraction of pairs of pixels and pixels are those whose labeling are consistent between the segmentation which was computed and the ground truth averaging across multiple ground truth segmentations [5]. The Rand index measures the similarity between two data clusters. Let there be a set of 'M' elements and two partitions of S for comparison. Now if "p" be the number of pairs of elements in 'S' that are in different sets in X and in different sets in Y "q" be the number of pairs of elements in S that are in the same set in X and in the same set in Y. "r" be the number of pairs of elements in S that are in the same set in X and in different sets in Y. "z" be the number of pairs of elements in S that are in different sets in X and in the same set in Y.

$$R = (p + q) / (p + q + r + z)$$

The number of agreements between X and Y is given by p+q the number of disagreements between X and Y is given by r+z. The values of Rand index lies between 0 & 1. Here '1' shows that the data clusters are exactly the same

4.3 Global Consistency Error

The Global consistency error measures the extent by which one segmentation can be viewed as a refinement of the other [1]. Segmentations which are related are considered to be consistent, since they could represent the same image segmented at different scales. Segmentation is simply a division of the pixels of an image into sets. The sets of pixels are K/as segments. The error is zero when pixel lies in an area of refinement, then one segment is a proper subset of the other. Suppose the manner then there is no relation of subset type. Where two segmentations S1 and S2 are considered as input to segmentation error measure. While the output which is a real valued output in the range [0 1], where no error is shown by '0'. Now the two segmentations S1 and S2 contain a given pixel "p_i".

4.4 Variation of Information

The variation of information represents the distance between two segmentations as the average conditional entropy of one segmentation given the other, and as a result measures the amount of randomness in one segmentation which cannot be explained by the other. Let there be two clustering (a division of a set into several subsets) X and Y where $X = \{X_1, X_2, \dots, X_k\}$, $p_i = |X_i| / n$,

$n = \sum_k |X_i|$. Then the variation of information between two clustering is:

$$Vi(X:Y) = H(X) + H(Y) - 2I(X,Y)$$

Where V_i is Variation of information, entropy of X is given by $H(X)$ and mutual information between X and Y is given by $I(X,Y)$. The mutual information of two clustering is the loss of uncertainty of one clustering if the other is given. Thus, mutual information is positive and bounded by

$$M.I = \{H(X), H(Y)\} - \log_2(n).$$

The tumor portion is correctly segmented if values of global consistency error and variation of information are lower as compared to the value of rand index. The area of segmented portion of ground truth image is approximately same as that of the area of segmented portion of proposed method(K Means method). In this paper values of global consistency error and variation of information are lower as compared to the value of rand index as shown in Table4.1. The segmentation accuracy is good as shown in Table4.2. Area of segmented portion of ground truth image is approximately same as that of the area of segmented portion of proposed method as shown in Table4.3. The elapsed time for the proposed method is very less as shown In Table4.4. The average value of rand index is 0.8358, average value of global consistency error is 0.2792 and average value of variation of information is 2.8596. Rand index is higher than global consistency error and variation of information, which is good approach for segmentation.

Images	Rand Index	Global Consistency Error	Variation of Information
1	0.8587	0.2763	2.3572
2	0.8129	0.2821	2.3621
3	0.7575	0.5263	4.2836

Table 4.1: Variation of Statistical Parameters for different MRI images in Proposed method (K Means method)

Images	Segmentation Accuracy
1	95.892
2	98.892
3	94.786

Table4.2: Segmentation Accuracy for different images

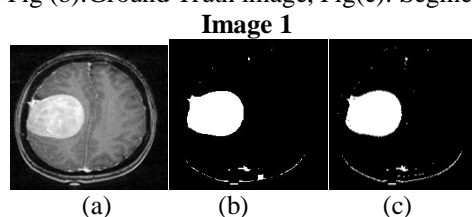
Images	Area 1 (Ground Truth Image)	Area 2 (Segmented Image of Proposed Method)
1	92.3938	92.2583
2	10.0355	10.0345
3	17.6867	17.6552

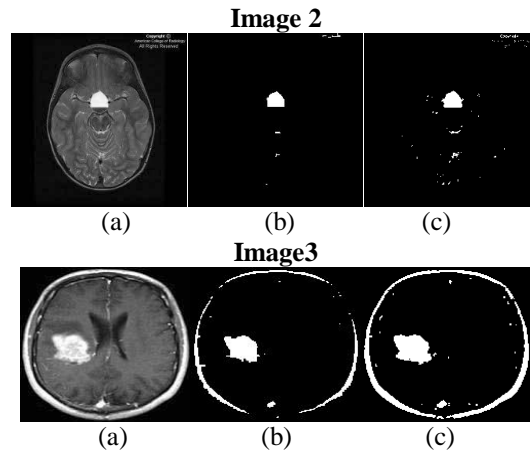
Table-4.3: Comparison of area of ground truth image and segmented image of proposed method

Images	Elapsed Time in Seconds
1	2.261788
2	3.024635
3	3.024365

Table-4.4: Elapsed Time for different images

Fig 4.1: Segmented images of Different MRI Images by applying K Means method (Proposed method)
 Fig (a): Original MRI image , Fig (b):Ground Truth image, Fig(c): Segmented image of proposed method





REFERENCES

- [1] B.Sathya and R. Manavalan ,”Image Segmentation by Clustering Methods: Performance Analysis”, IJCA vol 29- No.11,September 2011.
- [2] Siddheswar Ray and Rose H. Turi,”Determination of Number of Clusters in K-Means Clustering andApplication in Colour Image Segmentation”,School of Computer Science and Software Engineering,Monash University, Wellington Road, Clayton, Victoria, 3168, Australia
- [3] Prof.A.S.Bhide¹, Priyanka Patil²,and Shraddha Dhande³,” Brain Segmentation using Fuzzy C means clustering to detect tumor Region.”, ¹Electronics and Communication Engineering, North Maharashtra University, Jalgaon, India., ²Electronics and Communication Engineering North Maharashtra University, Jalgaon, India ,³Electronics and Communication Engineering, Vishwakarma Institute of Technology, Pune, India, *ISSN: 2277 – 9043 International Journal of Advanced Research in Computer Science and Electronics Engineering Volume 1, Issue 2, April 2012*
- [4] Khaled Alsabti ,²Sanjay Ranka ,and³Vineet Singh”An Efficient K-Means Clustering Algorithm “,Syracuse University, University of Florida, Hitachi America, Ltd.
- [5] R. UnniKrishnan, C. Pantofaru, and M. Hebert, “Toward objective evaluation of image segmentation algorithms”, IEEE Trans. Pattern Anal. Mach. Intell., vol. 29, no. 6, pp. 929-944, Jun. 2007.

Evaluation of Routing Protocols based on Performance

¹Ms. Pallavi R, ²Tanvi Aggarwal, ³Ullas Gupta
^{1,2,3}Sir M Visvesvaraya Institute of Technology, Bangalore – 562157

ABSTRACT

In a network, various routing protocols are used to forward packets. Each router maintains a routing table which stores the information of its neighbors. The extent of information stored about the network depends on the routing it follows. This information is regularly sent on the network to find the efficient path between the source and destination. Thus every protocol consumes a part of the network resources for this transmission. This paper tries to find the most efficient protocol that is best suited for a network based on its performance parameters like latency, throughput, convergence time and other factors.

Keywords: High Performance, Routing, RIP, OSPF, EIGRP, BGP

I. INTRODUCTION

A network is a group of devices connected to each other. When a process in one device is able to exchange information with a process in another device, the two devices are said to be networked. The set of rules that are required for exchanging information over a network are called *communication protocols*. Internet uses the standard internet protocol suite (TCP/IP) to serve billions of users' worldwide. Internet protocol suite TCP/IP provides end to end connectivity and also specifies how data should be formatted, addressed, transmitted, routed and received at the destination.

Efficient transmission of data between any two computer systems depends upon the overall performance of a network. Performance is of utmost importance for any network and is affected by the following four most important factors: **latency, packet loss, retransmission and throughput**. A network which has least latency, less packet loss, low retransmission and maximum throughput is ranked as a high performance network. The performance of a network is the measure of its effectiveness which can be enhanced dramatically by using proper routing techniques. As we know, the *Internet* is one of the 20th century's greatest communications developments. It is considered as a global system of interconnected networks and is thus, considered the best example of a high performance network. Routing finds a key role in such high performance networks.

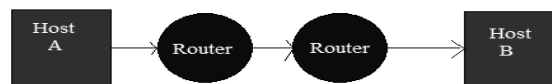


Fig. 1: Routers connecting devices

In this paper we are primarily focusing on routing which is the function of the network layer (OSI model). *Routing* is the process of moving a packet of data from source to destination. This is enabled by *router* which is a device that forwards data packets between computer networks, creating an overlay internetwork, as shown in Fig. 1. It is connected to multiple data lines (homogeneous or heterogeneous) from different networks.

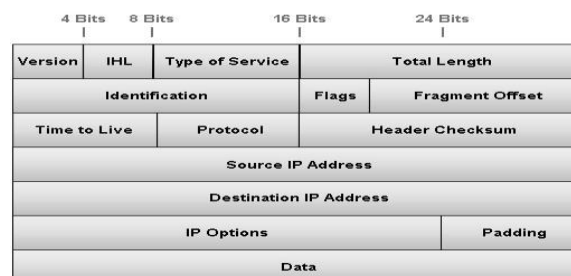


Fig. 2: IP Header Format

As shown in Fig. 2, when a data packet comes in on one of the lines, the router reads the Destination IP Address information in the packet to determine its ultimate destination. Then, using information in its routing table or routing policy, it directs the packet to the next network on its journey. The construction of routing tables is the primary goal of routing protocols.

II. ROUTING

Routing [1] is the process of moving packets across a network from one host to another. It is usually performed by dedicated devices called routers. The routing process usually directs forwarding on the basis of routing tables which is used to determine the forwarding or next hop IP address and the interface to be used. Thus, constructing routing tables, which are held in the router's memory, is very important for efficient routing.

Destination	Network mask	Gateway	Interface	Metric	Protocol
10.57.76.0	255.255.255.0	10.57.76.1	Local Area C...	1	Local
10.57.76.1	255.255.255.255	127.0.0.1	Loopback	1	Local
10.255.255.255	255.255.255.255	10.57.76.1	Local Area C...	1	Local
127.0.0.0	255.0.0.0	127.0.0.1	Loopback	1	Local
127.0.0.1	255.255.255.255	127.0.0.1	Loopback	1	Local
192.168.45.0	255.255.255.0	192.168.45.1	Local Area C...	1	Local
192.168.45.1	255.255.255.255	127.0.0.1	Loopback	1	Local
224.0.0.0	224.0.0.0	192.168.45.1	Local Area C...	1	Local
224.0.0.0	224.0.0.0	10.57.76.1	Local Area C...	1	Local
255.255.255.255	255.255.255.255	192.168.45.1	Local Area C...	1	Local
255.255.255.255	255.255.255.255	10.57.76.1	Local Area C...	1	Local

Fig. 3: Routing table

From Fig. 3, it can be seen that a routing table consists of

Network ID: The network ID or destination corresponding to the route

Network Mask: The mask is used to match a destination IP address to the network ID.

Next Hop: The IP address of the next hop.

Interface: An indication of which network interface is used to forward the IP packet.

Metric: A number used to indicate the cost of the route so the best route among possible multiple routes to the same destination can be selected.

III. ROUTING PROTOCOLS

Routing protocols are a set of rules or standards that determine how routers communicate and exchange information on a network, enabling them to select best routes to a remote network. The rest of this section discusses four different routing protocols giving a glimpse of their merits and demerits.

3.1rip - Routing Information Protocol

RIP [2][3] is a distance-vector protocol that uses hop count as its metric. This signifies the maximum distance that a routing protocols packet can travel in a network. The Routing Information Protocol provides the standard IGP protocol for local area networks, and provides great network stability, guaranteeing that if one network connection goes down the network can quickly adapt to send packets through another connection. RIP implements the splithorizon, route positioning and hold down mechanisms to prevent incorrect routing information from being propagated. RIP prevents routing loops by implementing a limit on the number of hops allowed in a path from the source to a allowed destination. The maximum number of hops for RIP is 15. This hop limit, however, also limits the size of networks that RIP can support. RIP itself evolved as an Internet routing protocol, and other protocol suites use modified versions of RIP. IP RIP is formally defined in two documents: Request for Comments (RFC) 1058 and 1723. RFC 1058 (1988) describes the first implementation of RIP, while RFC 1723 (1994) updates RFC 1058. RFC 1058 enables RIP messages to carry more information and security features.

Advantages:

- Easy Configuration.
- Minimum overload over the Processor.

Disadvantages:

- The protocol is limited to networks whose longest path involves 15 hops.
- It protocol uses fixed "metrics" to compare alternative routes.
- The protocol depends upon "counting to infinity" to resolve certain unusual situations.

3.2 Ospf - Open Shortest Path First

OSPF [4] is an interior gateway protocol which is used to distribute IP routing information throughout a single Autonomous System (AS) in an IP network. OSPF is a complex link-state routing protocol. Link-state routing protocols generate routing updates only when a change occurs in the network topology. When a link changes state, the device that detected the change creates a link-state advertisement (LSA) concerning that link and sends to all neighboring devices using a special multicast address. Each routing device takes a copy of the LSA, updates its link-state database (LSDB), and forwards the LSA to all neighboring devices.

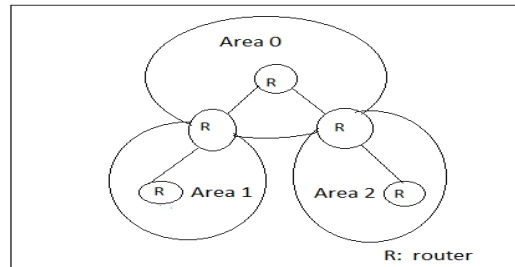


Fig. 4: Hierarchical structure of OSPF protocol

As shown in Fig. 4, OSPF provides a hierarchical structure [5] by sub-dividing large networks into AREAs and limits the multicast LSAs within routers of the same area — Area 0 is called backbone area and all other areas connect directly to it. All OSPF networks must have a backbone area.

Advantages:

- Supports VLSM and route summarization.
- Faster convergence.
- No limitation of network diameter.
- Better handling of multiple equal-cost paths.
- Divides the network into OSPF regions.
- Uses designated router[6] to reduce the number of OSPF messages that are exchanged. The designated router is elected by a hello protocol.

Disadvantages:

- It requires more memory to hold the adjacency, topology and routing tables.
- It requires extra CPU processing.

3.3 eigrp- Enhanced Interior Gateway Routing Protocol

EIGRP is a Cisco-proprietary routing protocol. It is a classless routing protocol. It is a hybrid protocol as it incorporates features of a Distance Vector routing protocol and features of a Link State routing protocol. Enhanced Interior Gateway Routing Protocol (EIGRP) is an enhanced version of IGRP used in TCP/IP and OSI internet. EIGRP and IGRP can interoperate because the metric (criteria used for selecting a route) used with one protocol can be translated into the metrics of the other protocol. EIGRP can be used not only for Internet Protocol (IP) networks but also for AppleTalk and Novell NetWare networks. A router running EIGRP stores all its neighbors' routing tables so that it can quickly adapt to alternate routes. To keep all routers aware of the state of neighbors, each router sends out a periodic "hello" packet. A router from which no "hello" packet has been received in a certain period of time is assumed to be inoperative.

Advantages:

EIGRP advantages[7] include:

- Very low usage of network resources during normal operation; only hello packets are transmitted on a stable network.
- Enhanced IGRP uses partial updates. Only changed information is sent only to the routers affected. Because of this, Enhanced IGRP is very efficient in its usage of bandwidth.
- Rapid convergence times for changes in the network EIGRP also supports VLSM, multiple network layer protocols.

Disadvantages:

- There is no area in EIGRP, so it is not good at dealing with big hierarchy network.
- EIGRP is a protocol come up with by Cisco, it is a private protocol, not a open standard.

3.4 Bgp - Border Gateway Protocol

BGP is the routing protocol that is used to span autonomous systems on the Internet. It is used for inter-domain routing. It acts as a mediator for communicating to different domains. It is a robust, sophisticated and scalable protocol that was developed by the Internet Engineering Task Force (IETF). BGP is a relatively simple protocol with a few salient features. It is used to communicate the Ad numbers across the different autonomous systems. BGP is an incremental protocol, where after a complete routing table is exchanged between neighbors, only changes to that information are exchanged. It is a distance vector protocol. It also supports VLSM(variable length subnet masking).

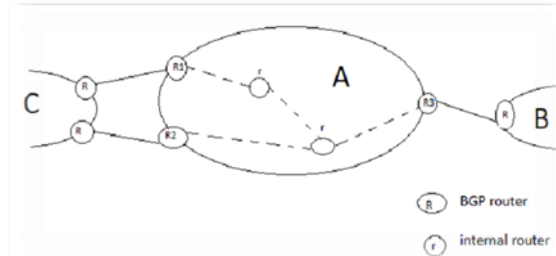


Fig.5: Example topology with 3 ISPs A, B, C

BGP sessions are established between border routers that reside at the edges of an AS and border routers in neighboring ASes. These sessions are used to exchange routes between neighboring ASes. Border routers then distribute routes learned on these sessions to non border (internal) routers as well as other border routers in the same AS using internal-BGP (iBGP). In addition, the routers in an AS usually run an Interior Gateway Protocol (IGP) to learn the internal network topology and compute paths from one router to another. Each router combines the BGP and IGP Information to construct a forwarding table that maps each destination prefix to one or more outgoing links along shortest paths through the network to the chosen border router.

Advantages:

- BGP is an incremental protocol, where after a complete routing table is exchanged between neighbors, only changes to that information are exchanged.
- It also supports VLSM (variable length subnet masking).
- It performs load balancing when there are multiple ISPs on the same router.

Disadvantage:

- Slow convergence due to the counting-to-infinity problem

IV. COMPARISON OF PROTOCOLS

Administrative distance (AD) of a protocol: Every routing protocol has an Administrative Distance (AD) [8], which is a value representing the trustworthiness of the specific routing protocol.

PROTOCOL	RIP	OSPF	EIGRP	BGP
AD	120	110	90	20

Table 1: AD values of routing protocols

A routing protocol with the lesser AD value is considered a better routing protocol in the network.

According to AD values given in the table, OSPF is considered best for networking. The other metrics for comparing the best high performed network is discussed as follows:

LINK UTILIZATION: Better link utilization [9] improves quality of service in a network. The metrics that directly affect link utilization are: required recourses, buffer size packet queues, latency and losses.

THROUGHPUT: Throughput [10] ratio of the total amount of data that reaches a receiver from a sender to the time it takes for the receiver to get the last packet.

QUEUING DELAY: The queuing delay is the time a job waits in a queue until it can be executed. It depends on both the router and the routing protocol. *This factor is responsible for the overall latency of the network.*

Table 2 gives us an overview of the comparative study made on the performance merits described above.

PROTOCOL	LATENCY	UTILIZATION	THROUGHPUT	ALGORITHM	AD
RIP	Worst	Worst	Worst	Bellman-ford Algorithm	Worst
OSPF	Average	Average	Best	SPF algorithm	Best
EIGRP	Best	Best	Average	DUAL algorithm	Average

Table 2: Comparison between different routing protocols

V. CONCLUSION

On analyzing the result of the performance of various routing protocols naming RIP, OSPF and EIGRP over a scenario for throughput, link utilization and queuing delay, we can say that OSPF has best performance overall as it has the maximum throughput amongst all routing protocol and queuing delay of it is second lowest after EIGRP and it also has second highest link utilization after EIGRP. Then EIGRP performs well in terms of throughput, queuing delay and link utilization. So for best effort service that is transmission of data packets OSPF performs better than other protocols for throughput, queuing delay, utilization.

ACKNOWLEDGEMENT

It gives us immense pleasure to express our sincere gratitude to the management of Sir M Visvesvaraya Institute of Technology, Bangalore for providing the opportunity and resources to accomplish our survey in their premises. Our sincere thanks to Dr. M S Indira, Principal, Sir MVIT for her encouragement throughout the course. Words are not enough to convey our gratitude to Prof. Dilip K Sen, HOD, Computer Science and Engineering for his constant support and motivation.

REFERENCES

- [1.] <http://www.linfo.org/routing.html>
- [2.] http://www.cisco.com/en/US/tech/tk365/tk554/tsd technology_support_sub-protocol_home.html
- [3.] <http://www.oocities.org/raja1raj/rip.htm>
- [4.] <http://searchenterprise.wan.techtargt.com/definition/OSPF>
- [5.] <http://www.9tut.com/ospf-routing-protocol-tutorial>
- [6.] Alberto Leon Garcia and IndraWidjaja, "Communication network – Fundamental Concepts and key architecture"
- [7.] http://www.cisco.com/en/US/products/ps6630/products_ios_protocol_option_home.html
- [8.] <http://itknowledgeexchange.techtargt.com/network-technologies/ccna-administrative-distance-for-the-dynamic-routing-protocols/>
- [9.] <http://dl.acm.org/citation.cfm?id=1553885>
- [10.] [10]<http://airccse.org/journal/jwmn/0211jwmn09.pdf>
- [11.] Ittiphonkrinpayorn and SuwatPattaramalai, "Link Recovery Comparison Between OSPF & EIGRP ", International Conference on Information and Computer Networks (ICIN 2012) IPCSIT vol. 27 (2012) IACSIT Press, Singapore
- [12.] <http://www.iins.co.in>

Invention of the plane geometrical formulae - Part II

Mr. Satish M. Kaple

Asst. Teacher Mahatma Phule High School, Kherda
Jalgaon (Jamod) - 443402 Dist- Buldana, Maharashtra (India)

ABSTRACT

In this paper, I have invented the formulae for finding the area of an Isosceles triangle. My finding is based on pythagoras theorem.

I. INTRODUCTION

A mathematician called Heron invented the formula for finding the area of a triangle, when all the three sides are known. Similarly, when the base and the height are given, then we can find out the area of a triangle. When one angle of a triangle is a right angle, then we can also find out the area of a right angled triangle. Hence forth, We can find out the area of an equilateral triangle by using the formula of an equilateral triangle. These some formulae for finding the areas of a triangles are not exist only but including in educational curriculum also. But, In educational curriculum. I don't appeared the formula for finding the area of an isosceles triangle with doing teaching – learning process . Hence, I have invented the new formula for finding the area of an isosceles triangle by using Pythagoras theorem. I used Pythagoras theorem with geometrical figures and algebric quations for the invention of the new formula of the area of an isosceles triangle. I Proved it by using geometrical formulae & figures, 20 examples and 20 verifications (proofs)Here myself is giving you the summary of the research of the plane geometrical formulae- Part II

II. METHOD

First taking an isosceles triangle ABC

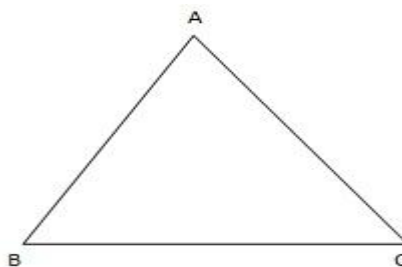


Fig. No. -1

Now taking a, a & b for the lengths of three sides of $\triangle ABC$

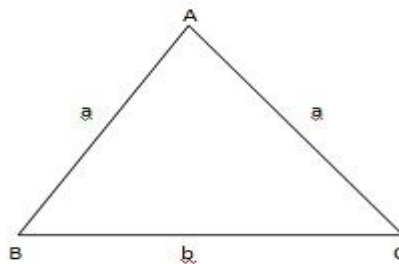


Fig. No. – 2

Draw perpendicular AD on BC.

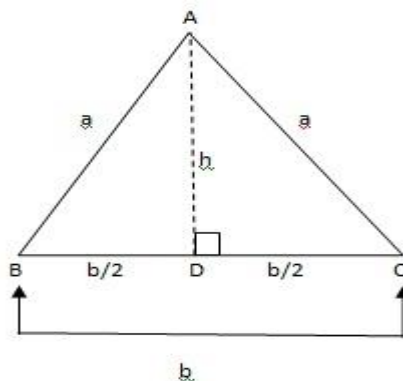


Fig. No. - 3

$\triangle ABC$ is an isosceles triangle and it is an acute angle also.

In $\triangle ABC$,

Let us represent the lengths of the sides of a triangle with the letters a,a,b. Side AB and side AC are congruent side. Third side BC is the base. AD is perpendicular to BC.

Hence, BC is the base and AD is the height.

Here, taking $AB=AC = a$

Base , $BC = b$ Height, $AD = h$

In $\triangle ABC$, two congruent right angled triangle are also formed by the length of perpendicular AD drawn on the side BC from the vertex A. By the length of perpendicular AD drawn on the side BC, Side BC is divided into two equal parts of segment. Therefore, these two equal segments are seg DB and seg DC. Similarly, two a right angled triangles are also formed, namely, $\triangle ADB$ and $\triangle ADC$ which are congruent.

Thus,

$$DB = DC = 1/2 \times BC$$

$$DB = DC = 1/2 \times b = b/2$$

$\triangle ADB$ and $\triangle ADC$ are two congruent right angled triangle.

Taking first right angled $\triangle ADC$,

In $\triangle ADC$, Seg AD and Seg DC are both sides forming

The right angle. Seg AC is the hypotenuse.

Here, $AC = a$

Height, $AD = h$

$DC = b/2$ and $m \angle ADC = 90^\circ$

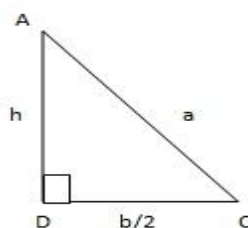


Fig. No - 4

According to Pythagoras Theorem,

$$(\text{hypotenuse})^2 = (\text{one side forming the right angle})^2 + (\text{second side forming the right angle})^2$$

In short,

$$(\text{Hypotenuse})^2 = (\text{one side})^2 + (\text{second side})^2$$

$$AC^2 = AD^2 + DC^2$$

$$AD^2 + DC^2 = AC^2$$

$$h^2 + (b/2)^2 = a^2$$

$$h^2 = a^2 - (b/2)^2$$

$$h^2 = a^2 - \frac{b^2}{4}$$

$$h^2 = \frac{a^2 \times 4}{4} - \frac{b^2}{4}$$

$$h^2 = \frac{4a^2}{4} - \frac{b^2}{4}$$

$$h^2 = \frac{4a^2 - b^2}{4}$$

Taking the square root on both side,

$$\sqrt{h^2} = \sqrt{\frac{4a^2 - b^2}{4}}$$

$$\sqrt{h^2} = \sqrt{\frac{1 \times (4a^2 - b^2)}{4}}$$

$$\sqrt{h^2} = \sqrt{\frac{1}{4}} \times \sqrt{4a^2 - b^2}$$

The square root of h^2 is h and the square root of $\frac{1}{4}$ is $\frac{1}{2}$

$$\therefore h = \frac{1}{2} \times \sqrt{4a^2 - b^2}$$

$$\therefore \text{Height, } h = \frac{1}{2} \sqrt{4a^2 - b^2}$$

$$\therefore AD = h = \frac{1}{2} \sqrt{4a^2 - b^2}$$

Thus,

$$\begin{aligned} \text{Area of } \triangle ABC &= \frac{1}{2} \times \text{Base} \times \text{Height} \\ &= \frac{1}{2} \times BC \times AD \end{aligned}$$

$$= \frac{1}{2} \times b \times h$$

But Height, $h = \frac{1}{2} \sqrt{4a^2 - b^2}$

∴ Area of $\triangle ABC = \frac{1}{2} \times b \times \frac{1}{2} \sqrt{4a^2 - b^2}$

∴ Area of $\triangle ABC = \frac{b}{2} \times \frac{1}{2} \sqrt{4a^2 - b^2}$

$$= \frac{b \times 1}{2 \times 2} \times \sqrt{4a^2 - b^2}$$

$$= \frac{b}{4} \sqrt{4a^2 - b^2}$$

∴ Area of an isosceles $\triangle ABC = \frac{b}{4} \sqrt{4a^2 - b^2}$

For example- Now consider the following examples:-

Ex. (1) If the sides of an isosceles triangle are 10 cm, 10 cm and 16 cm.

Find it's area

$\triangle DEF$ is an isosceles triangle.

In $\triangle DEF$ given alongside,

$$\angle (DE) = 10 \text{ cm.}$$

$$\angle (DF) = 10 \text{ cm.}$$

$$\angle (EF) = 16 \text{ cm}$$

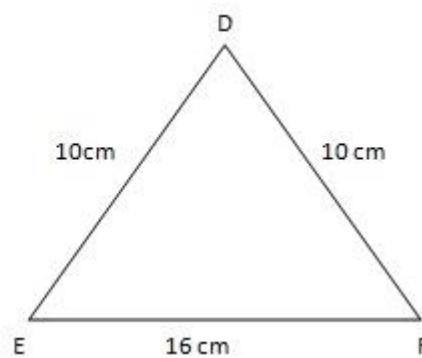


Fig No- 5

Let,

$$a = 10 \text{ cm}$$

$$\text{Base, } b = 16 \text{ cm.}$$

By using The New Formula of an isosceles triangle,

∴ Area of an isosceles $\triangle DEF = A (\triangle DEF)$

$$\begin{aligned}
 &= \frac{b}{4} \sqrt{4a^2 - b^2} \\
 &= \frac{16}{4} \times \sqrt{4(10)^2 - (16)^2} \\
 &= 4 \times \sqrt{4 \times 100 - 256} \\
 &= 4 \times \sqrt{400 - 256} \\
 &= 4 \times \sqrt{144}
 \end{aligned}$$

The square root of 144 is 12

$$= 4 \times 12 = 48 \text{ sq.cm.}$$

∴ Area of an isosceles $\triangle DEF = 48 \text{ sq.cm.}$

Verification :-

☞ Here,

$$l(\text{DE}) = a = 10 \text{ cm.}$$

$$l(\text{EF}) = b = 16 \text{ cm.}$$

$$l(\text{DF}) = c = 10 \text{ cm.}$$

By using the formula of Heron's

Perimeter of $\triangle DEF = a + b + c$

$$= 10 + 16 + 10 = 36 \text{ cm}$$

Semiperimeter of $\triangle DEF$,

$$S = \frac{a + b + c}{2}$$

$$S = \frac{36}{2}$$

$$S = 18 \text{ cm.}$$

$$\begin{aligned}
 \therefore \text{Area of an isosceles } \triangle DEF &= \sqrt{s(s-a)(s-b)(s-c)} \\
 &= \sqrt{18 \times (18-10) \times (18-16) \times (18-10)} \\
 &= \sqrt{18 \times 8 \times 2 \times 8} \\
 &= \sqrt{(18 \times 2) \times (8 \times 8)} \\
 &= \sqrt{36 \times 64} \\
 &= \sqrt{36} \times \sqrt{64}
 \end{aligned}$$

The square root of 36 is 6 and the square root of 64 is 8

$$= 6 \times 8 = 48 \text{ sq.cm}$$

∴ Area of $\triangle DEF = 48 \text{ sq.cm}$

Ex. (2) In $\triangle GHI$, $GH = 5 \text{ cm}$, $HI = 6 \text{ cm}$ and $GI = 5 \text{ cm}$.

Find the area of $\triangle GHI$.

✍

$\triangle GHI$ is an isosceles triangle.

In $\triangle GHI$ given alongside,

$$\angle(GH) = 5 \text{ cm.}$$

$$\angle(HI) = 6 \text{ cm.}$$

$$\angle(GI) = 5 \text{ cm}$$

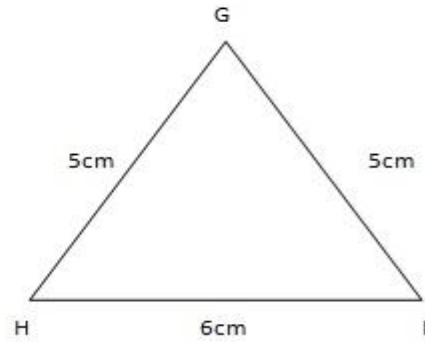


Fig No- 6

Let,

$$a = 5 \text{ cm}$$

Base, $b = 6 \text{ cm}$.

By using The New Formula of area of an isosceles triangle,

$$\begin{aligned} \therefore \text{Area of an isosceles } \triangle GHI &= \frac{b}{4} \sqrt{4a^2 - b^2} \\ &= \frac{6}{4} \times \sqrt{4 \times (5)^2 - (6)^2} \end{aligned}$$

The simplest form of $\frac{6}{4}$ is $\frac{3}{2}$

$$\begin{aligned} &= \frac{3}{2} \times \sqrt{(4 \times 25) - 36} \\ &= \frac{3}{2} \times \sqrt{100 - 36} \\ &= \frac{3}{2} \times \sqrt{64} \end{aligned}$$

The square root of 64 is 8

$$= \frac{3}{2} \times 8 = \frac{3 \times 8}{2} = \frac{24}{2}$$

$$= 12 \text{ sq.cm.}$$

∴ Area of an isosceles $\triangle GHI = 12 \text{ sq.cm.}$

Verification :-

Here,

$$l(GH) = a = 5 \text{ cm.}$$

$$l(HI) = b = 6 \text{ cm.}$$

$$l(GI) = c = 5 \text{ cm.}$$

By using the formula of Heron's

Perimeter of $\triangle GHI = a + b + c$

$$= 5 + 6 + 5$$

$$= 16 \text{ cm}$$

Semiperimeter of $\triangle GHI$,

$$S = \frac{a + b + c}{2}$$

$$S = \frac{16}{2}$$

$$S = 8 \text{ cm.}$$

$$\begin{aligned} \therefore \text{Area of an isosceles } \triangle GHI &= \sqrt{s(s-a)(s-b)(s-c)} \\ &= \sqrt{8 \times (8-5) \times (8-6) \times (8-5)} \\ &= \sqrt{8 \times 3 \times 2 \times 3} \\ &= \sqrt{(8 \times 2) \times (3 \times 3)} \\ &= \sqrt{16 \times 9} \\ &= \sqrt{144} \end{aligned}$$

The square root of 144 is 12

$$= 12 \text{ sq.cm}$$

∴ Area of an isosceles $\triangle GHI = 12 \text{ sq.cm.}$

Explanation:-

We observe the above solved examples and their verifications, it is seen that the values of solved examples by using the new formula of an isosceles triangle and the values of their verifications are equal.

Hence, the new formula of the area of an isosceles triangle is proved.

$$\text{Area of an isosceles triangle} = \frac{b}{4} \times \sqrt{4a^2 - b^2}$$

III. CONCLUSIONS

From the above new formula , we can find out the area of an isosceles triangle. This new formula is useful in educational curriculum, building and bridge construction and department of land records. This new formula is also useful to find the area of an isosceles triangular plots of lands, fields, farms, forests, etc. by drawing their maps.

REFERENCES

- [1] Geometry concepts and Pythagoras theorem.

Modeling and Simulation of Different Gas Flows Velocity and Pressure in Catalytic Converter with Porous

¹K.Mohan Laxmi, ²V.Ranjith Kumar, ³Y.V.Hanumantha Rao

¹M.Tech Student, Mechanical Engineering Department, KL University, Vijayawada.

²Assistant Professor, Mechanical Engineering Department, KL University, Vijayawada.

³Professor, Head of The Department, Mechanical Engineering, KL University, Vijayawada.

ABSTRACT

Stringent emission regulations around the world necessitate the use of high-efficiency catalytic converters in vehicle exhaust systems. Experimental studies are more expensive than computational studies. Also using computational techniques allows one to obtain all the required data for the Catalytic Converter, some of which could not be measured. In the present work, Geometric modeling ceramic monolith substrate with square shaped channel type of Catalytic converter and coated platinum and palladium using fluent software. In this software we are using crate inlet-outlet flanges and housing of the catalytic converter. After design of modeling us done different parameters in Fluent Pre-process like Analysis Type, Domain Type etc. This project studies the different porosity of porous medium how to affect to flow pressure and velocity field under the conditions of different inlet velocity and same ceramic diameter by CFD method. Geometric model of the catalytic converter has been establish and meshed by the pre-processing tool of FLUENT. The flow pressure simulation filled contours and curve of center line static pressure distribution of the ceramic porous material show that in the case of other conditions remain unchanged, the less the porosity of the ceramic porous material, the higher the inlet pressure and the more the pressure loss of the porous material. The more Porosity of ceramic is beneficial to exhaust catalytic converter.

Keywords: Catalytic Converter. Ceramic material. Velocity. Pressure. FLUENT. Porous.

I. INTRODUCTION

Porous material made with ceramic can be used into two way catalytic converter .The gas speed distribution in the converter is an important factor in the catalytic ability and the effect of catalytic materials. The paper studies on the variation of the gas flow pressure the converter by the computational fluid dynamics methods. There are many CFD commercial software such as PHOENICS, CFX, STAR-CD, FIDIP and FLUENT etc. FLUENT software has a very wide range of applications flexible characteristics of the grid, the strong capabilities of numerical solution comprehensive functionality. This article will study the fluid dynamics of the catalytic converters using the FLUENT software. Air pollution and global warming is a major issue nowadays. For this reason, emission limits are introduced around the world and continually being made stricter every year. The enforcement of this regulation has led to the compulsory utilization of catalytic converter as an emission treatment to the exhaust gas of vehicles.

1.1. History

In 1973, General Motors faced new air pollution regulations and needed a way to make its cars conform to the stricter standards. Robert C. Stempel, who at the time was a special assistant to the GM president, was assigned to oversee development of a technology capable of addressing the problem. Under Stempel's guidance, GM built on existing research to produce the first catalytic converter for use in an automobile. Catalytic converters were first installed in vehicles made in 1975 in response to EPA regulations passed two years earlier tightening auto emissions and requiring a gradual decrease in the lead content of all gasoline. Since the introduction of stringent emission regulations in the US in the 1970s, car manufacturers have modified their exhaust systems to incorporate catalytic converters for the removal of NOx, CO and hydrocarbons.

All new cars registered throughout the European Union from 1st January 1993 have to be fitted with catalytic converters. Platinum, palladium and rhodium are the main active components. A potential problem appears with the release of platinum group metals (PGMs) from the converters into the environment. There is

now convincing evidence for the release of platinum group metals (PGMs) into the environment, possibly by abrasion of the autocatalyst. As a result, PGMs are found to have increased in the environment. In recent study, we found that PGMs have increased in road dust since 1984 and particularly 1991.

II. PROBLEM DESCRIPTION

Catalytic converters are used on most vehicles on the road today. They reduce harmful emissions from internal combustion engines (such as oxides of nitrogen, hydrocarbons, and carbon monoxide) that are the result of incomplete combustion. Most new catalytic converters are the ceramic monolith substrate with square channels type and are usually coated with platinum, rhodium, or palladium.

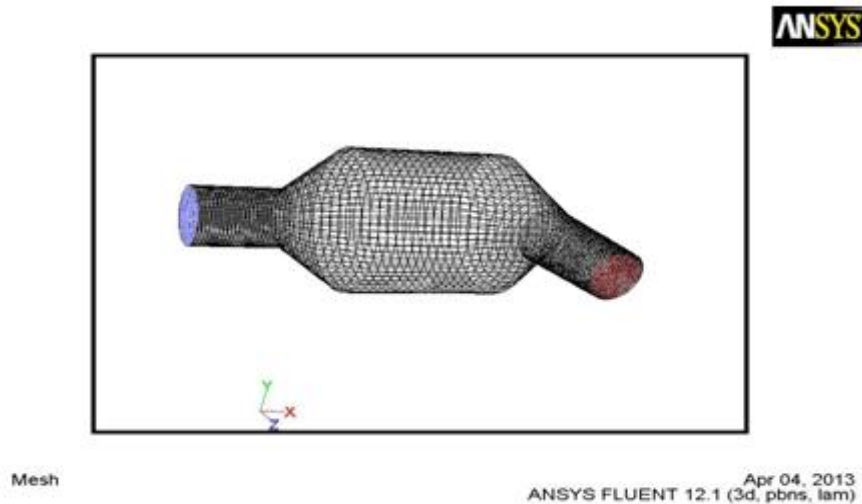


Figure: 2.1. Mesh geometry of Catalytic Converter

In this project Set up a porous zone for the substrate with appropriate resistances. Calculate a solution for gas flow through the catalytic converter using the pressure- based solver. Plot pressure and velocity distribution on specified planes of the geometry. Determine the pressure drop through the substrate and the degree of non-uniformity of flow through cross sections of the geometry using X-Y plots and numerical reports and also measure the Mass-Weighted Average of the Pressure .

III. PROBLEM FORMULATION AND MODELLING

The catalytic converter modeled here is shown in Figure. The nitrogen gas flows in through the inlet with a different uniform velocities like 20m/s, 22.6 m/s,25m/s,27.5m/s,30m/s, passes through a ceramic monolith substrate with square shaped channels, and then exits through the outlet.

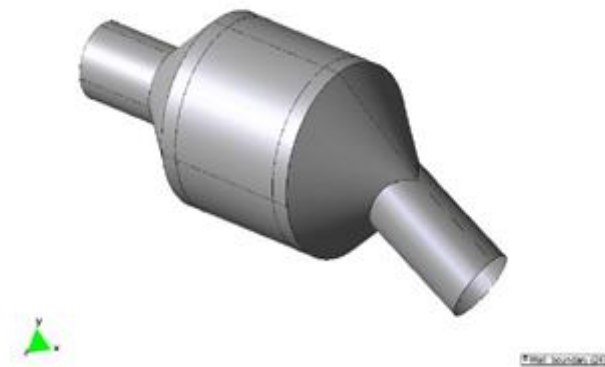


Figure: 3.Geometry of Catalytic Converter

While the flow in the inlet and outlet sections is turbulent, the flow through the substrate is laminar and is characterized by inertial and viscous loss co-efficients in the flow (X) direction. The substrate is impermeable in other directions, which is modeled using loss coefficients whose values are three orders of magnitude higher

than in the X direction.

3.1. Input Parameters:

- user mode: General Model
- Analysis Type: Steady State
- Domain Type: Multiple Domain
- Fluid Type: Nitrogen Gas
- Turbulence Model : K-Epsilon
- Heat Transfer: Thermal Energy
- Boundary Conditions: Inlet (Subsonic), outlet (Subsonic),Wall :No slip
- Domain Interface: Fluid-Porous

3.2. Modelling:

Modeling of flows through a porous medium requires a modified formulation of the Navier-Stokes equations, which reduces to their classical form and includes additional resistance terms induced by the porous region. The incompressible Navier-Stokes equations in a given domain Ω and time interval $(0,t)$ can be written as

$$\rho\left(\frac{\partial u}{\partial t} + (u \cdot \nabla)u\right) - \mu \nabla^2 u + \nabla p = f \text{ on } \Omega \times (0,t)$$

$$\nabla \cdot u = 0 \text{ on } \Omega \times (0,t)$$

where $u = u(x,t)$ denotes the velocity vector, $p = p(x,t)$ the pressure field, ρ the constant density, μ the dynamic viscosity coefficient and f represents the external body forces acting on the fluid (i.e. gravity).

In the case of solids, small velocities can be considered and $(u \cdot \nabla)u$ term is neglected. Therefore, assuming an incompressible flow (constant density) in a certain domain Ω and considering the mass conservation equation, also called continuity equation, the Navier-Stokes equation can be written as follows:

$$\rho \frac{\partial u}{\partial t} - \mu \nabla^2 u + \nabla p = f \text{ on } \Omega \times (0,t)$$

$$\nabla \cdot u = 0 \text{ on } \Omega \times (0,t)$$

The general form of the Navier-Stokes equation is valid for the flow inside pores of the porous medium but its solution cannot be generalized to describe the flow in porous region. Therefore, the general form of Navier-Stokes equation must be modified to describe the flow through porous media. To this aim, Darcy's law is used to describe the linear relation between the velocity u and gradient of pressure p in the porous medium. It defines the permeability resistance of the flow in a porous media:

$$\nabla p = - \mu D u \text{ in } \Omega_p \times (0,t)$$

Where Ω_p is the porous domain, D the Darcy's law resistance matrix and u the velocity vector. In the case of considering an homogeneous porous media, D is a diagonal matrix with coefficients $1/\alpha$, where α is the permeability coefficient.

The Reynolds number is defined as:

$$Re = \frac{\rho U L}{\mu}$$

Where U and L a characteristic velocity and a characteristic length scale, respectively. In order to characterize the inertial effects, it is possible to define the Reynolds number associated to the pores:

$$Rep = \frac{\rho U \delta}{\mu}$$

Where δ is the characteristic pore size. Whereas Darcy law is reliable for values of $Re_p < 1$, otherwise it is necessary to consider a more general model which accounts also for the inertial effects, such as:

$$\nabla p = - (\mu D u + \frac{1}{2} \rho C u |u|) \text{ in } \Omega_p \times (0,t)$$

Where C the inertial resistance matrix.

Considering a modified Navier-Stokes equation in the whole domain including the two source terms associated to the resistance induced by the porous medium (linear Darcy and inertial loss term), the momentum equations become:

$$\rho \frac{\partial u}{\partial t} - \mu \nabla^2 u + \nabla p - (\mu D u + \frac{1}{2} \rho C u |u|) = 0 \text{ in } \Omega \times (0,t)$$

In the case of considering an homogeneous porous media, D is a diagonal matrix with coefficients $1/\alpha$, where α is the permeability coefficient and C is also a diagonal matrix. Therefore, a modified Darcy's resistance matrix should be used in Tdyn, as follows

$$\rho \frac{\partial u}{\partial t} - \mu \nabla^2 u + \nabla p = \mu D^* u \text{ in } \Omega \times (0,t)$$

$$D^* = D + \frac{1}{2} \mu \rho u |u|$$

where I is the identity matrix. It should be noted that in laminar flows through porous media, the pressure p is proportional to velocity u and C can be considered zero ($D^* = D$). Therefore, the Navier-Stokes momentum equations can be rewritten as:

$$\rho \frac{\partial u}{\partial t} - \mu \nabla^2 u + \nabla p = - \mu D u \text{ in } \Omega x(0,t)$$

These momentum equations are resolved by Tdyn in the case of solids, where $(u \cdot \nabla)u$ term vanishes due to small velocities. If $(u \cdot \nabla)u = 0$ can't be neglected in the modelization (i.e. high velocities), then Tdyn should resolve the following momentum equations in a fluid instead of in a solid:

$$\rho \left(\frac{\partial u}{\partial t} + (u \cdot \nabla)u \right) - \mu \nabla^2 u + \nabla p = - \mu D u \text{ in } \Omega x(0,t)$$

In order to add the Darcy's resistance matrix D an appropriate function should be inserted in Tdyn. See the figure below and "Function syntax" in the Help manual of Tdyn for more details about defining functions

3.3 Geometry and Boundary Conditions :

The following Conditions concerns the analysis of a gas flowing through a catalytic converter. The main objective is to determine the pressure gradient and the velocity distribution through the porous media that fills the catalytic element. This model is intended to exemplify the use of Tdyn capabilities to solve problems involving flow through porous media. The boundary conditions are applied as shown in the figures below. First, a Wall/Body condition with a Y-Plus wall boundary type is applied to the external surface of the catalytic converter.

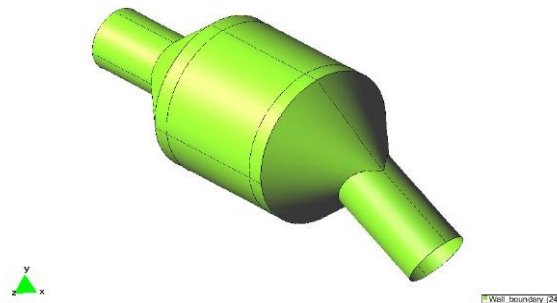


Figure: 3.3. External Surface of the Catalytic Converter

A Fix Velocity condition is further applied to the inlet surface of the model (in blue in the figure below) so that the velocity vector is fixed there to the value like 20m/s,22.6m/s,25m/s,27.5m/s,30m/s. Finally, a Pressure Field condition is used to fix the the dynamic pressure to zero at the outlet surface of the control volume (in red in the figure below).

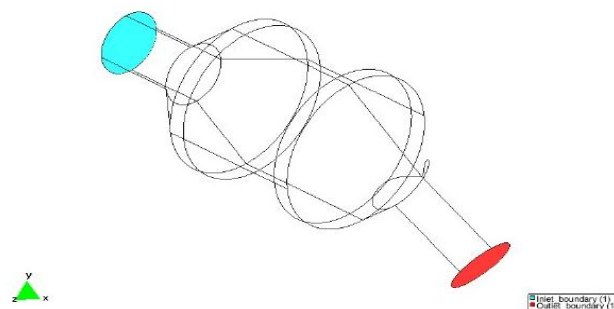


Figure: 3.3.1. Control Volumes of Catalytic Converter

3.4. Materials:

Two different materials are used in order to simulate the gas flowing through the catalyst converter. Fluid flow properties, density and viscosity, are the same in both materials and correspond to those of nitrogen gas. The two materials only differ on the values of the Darcy's law matrix. While the first one has a null matrix, the second one has assigned a Darcy matrix incorporating the resistance and inertial effects of the porous media. Hence, the first material is applied to the inlet and outlet channel regions of the catalyst converter (in blue in the figure below), while the second one is applied to the intermediate volume corresponding to the porous media (in yellow in the figure below).

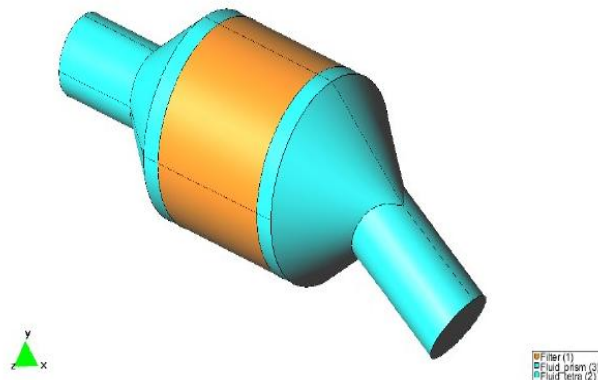


Figure: 3.2.2.Materials of the catalytic Converter

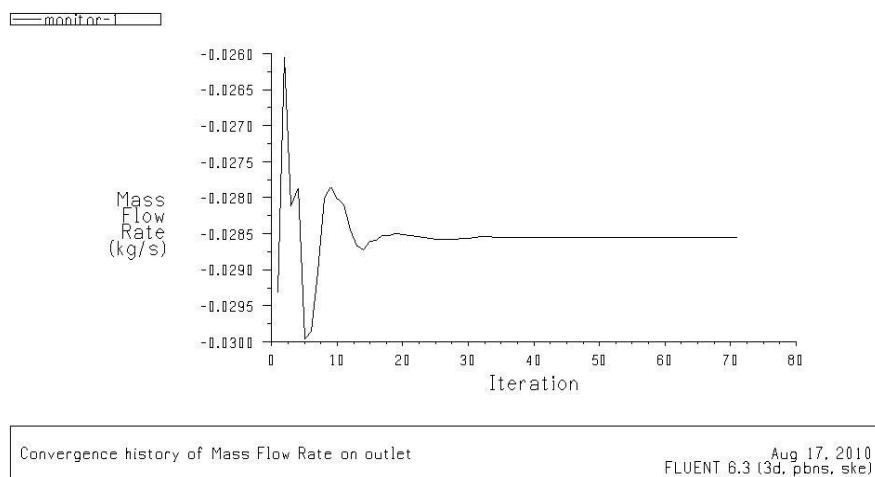
The Darcy's law matrix used to model the porous media is taken to be diagonal but anisotropic. The corresponding values of the viscous (D) and inertial (C) resistance terms are those in the table below Note that the components of the Darcy's matrix are given with respect to the global axis system (X, Y, Z) Note that the components of the Darcy's matrix are given with respect to the global axis system (X, Y, Z) so that the geometry must be conveniently oriented.

IV. RESULTS AND DISCUSSIONS

4.1. Graphical Results:

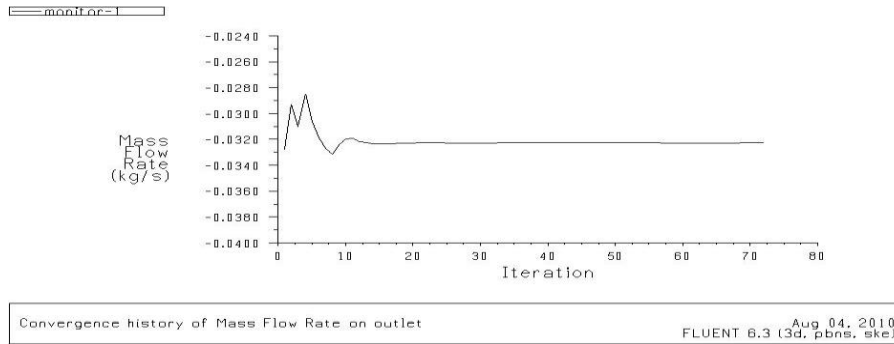
4.1.1. Mass Flow Rate Graphs at different Velocities:

After running fluent software The nitrogen gas flows through the inlet with a uniform velocity at 20 m/s the values of mass flow rate changes at different iteration we can observe in the Graph.



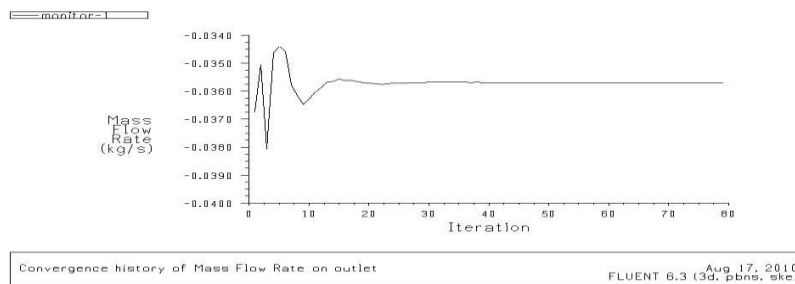
Graph: Surface Monitor Plot of Mass Flow Rate at Velocity 20 m/s

After running fluent software The nitrogen gas flows through the inlet with a uniform velocity at 22.6 m/s the values of mass flow rate changes at different iteration we can observe in the Graph.



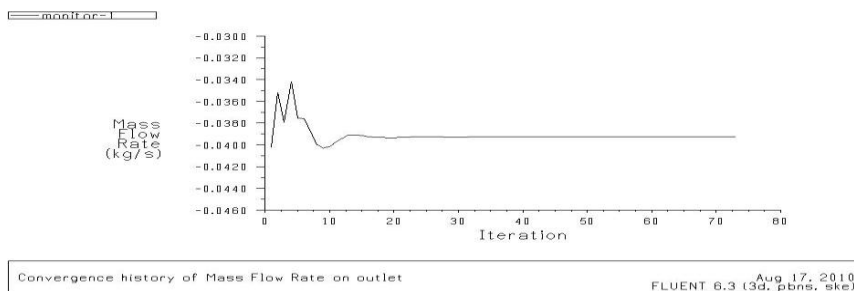
Graph: Surface Monitor Plot of Mass Flow Rate at Velocity 22.6 m/s

After running fluent software The nitrogen gas flows through the inlet with a uniform velocity at 25 m/s the values of mass flow rate changes at different iteration we can observe in the Graph.



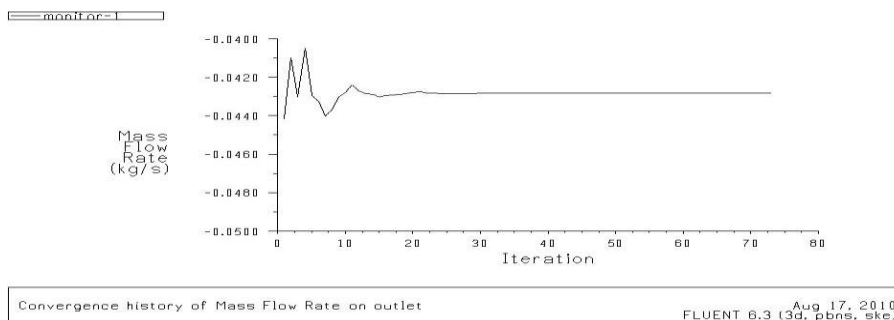
Graph: Surface Monitor Plot of Mass Flow Rate at Velocity 25 m/s

After running fluent software The nitrogen gas flows through the inlet with a uniform velocity at 27.5 m/s the values of mass flow rate changes at different iteration we can observe in the Graph.



Graph: Surface Monitor Plot of Mass Flow Rate at Velocity 27.5 m/s

After running fluent software The nitrogen gas flows through the inlet with a uniform velocity at 30 m/s the values of mass flow rate changes at different iteration we can observe in the Graph.



Graph: Surface Monitor Plot of Mass Flow Rate at Velocity 30 m/s

4.1.2.Static Pressure Graphs at Different Velocity Flows:

The Graph shown the Static Pressure vs Position of the flow in the porous medium. The porous-cl Line Surface the pressure drop across the porous substrate with respect to position at velocity at 20 m/s. The pressure drop Changes from 525 pa to 250 pa in the porous substrate

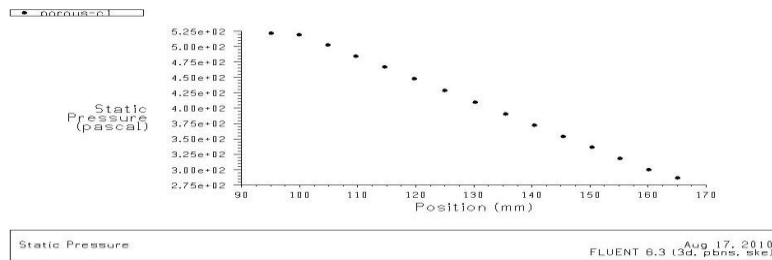


Figure:Pressure Droplet on the porous-cl Surface at velocity 20 m/s

The Graph shown the Static Pressure vs Position of the flow in the porous medium. The porous-cl Line Surface the pressure drop across the porous substrate with respect to position at velocity at 22.6 m/s. The pressure drop Changes from 650pascal to 300pa in the porous substrate.

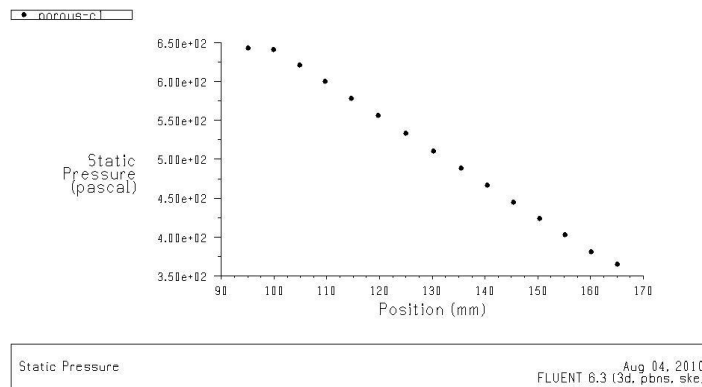


Figure:Pressure Droplet on the porous-cl Surface at velocity 22.6 m/s

The Graph shown the Static Pressure vs Position of the flow in the porous medium. The porous-cl Line Surface the pressure drop across the porous substrate with respect to position at velocity at 25 m/s. The pressure drop Changes in the porous substrate from 800 Pa to 400pa.

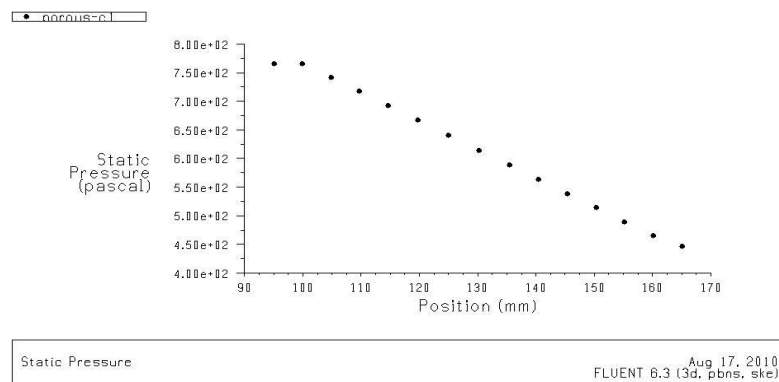
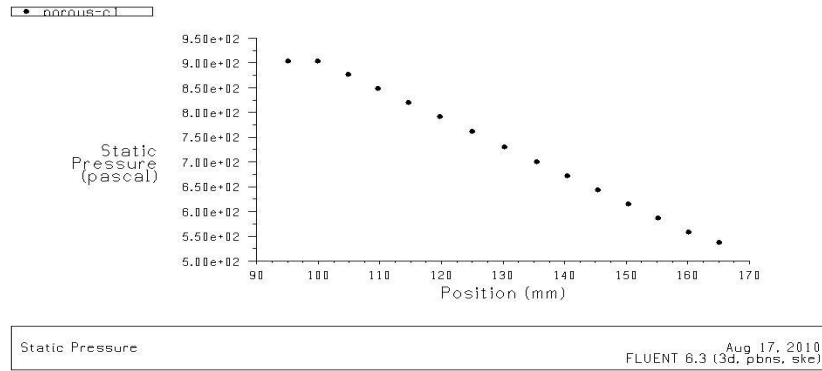


Figure:Pressure Droplet on the porous-cl Surface at velocity 25 m/s

The Graph shown the Static Pressure vs Position of the flow in the porous medium. The porous-cl Line Surface the pressure drop across the porous substrate with respect to position at velocity at 27.5 m/s. The pressure drop Changes from 950pa to 500 pa in the porous substrate.



Graph:Pressure Droplet on the porous-cl Surface at velocity 27.5 m/s

The Graph shown the Static Pressure vs Position of the flow in the porous medium. The porous-cl Line Surface the pressure drop across the porous substrate with respect to position at velocity at 30 m/s. The pressure drop Changes from 1100 pa to 600pa in the porous substrate

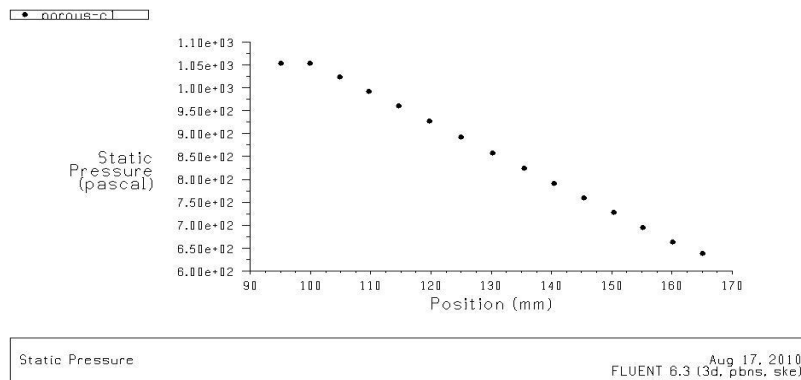


Figure: Pressure Droplet on the porous-cl Surface at velocity 30 m/s

4.2. Simulation Results:

5.2.1.Simulation Results at Velocity 20 m/s:

The pressure field distribution is shown in the picture below at velocity 20 m/s. There, it can be observed that an important pressure drop occurs within the porous region.

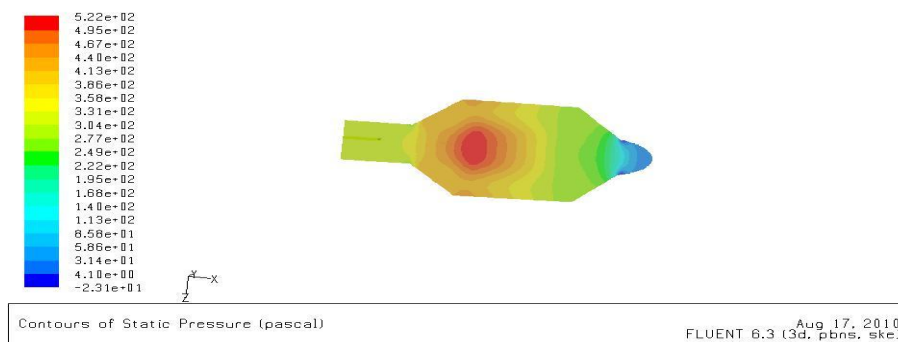


Figure:5.1. Contours of the Static Pressure on the y=0 plane

The pressure changes rapidly in the middle section, where the fluid velocity changes as it passes through the porous substrate. The pressure drop can be high, due to the inertial and viscous resistance of the porous media. The X-velocity component distribution of the fluid flow. In this picture, it becomes evident how the fluid decelerates rapidly when entering to the porous region. It can also be observed how the fluid recirculates before entering the central region of the catalyst (negative values of X-velocity component in dark blue) due to the resistance exerted by the porous media.

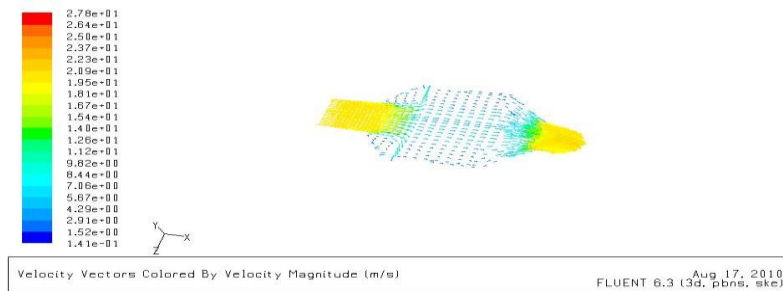


Figure: Velocity Vectors on the y=0 Plane

The flow pattern shows that the flow enters the catalytic converter as a jet, with recirculation on either side of the jet. As it passes through the porous substrate, it decelerates and straightens out, and exhibits a more uniform velocity distribution. This allows the metal catalyst present in the substrate to be more effective.



Figure:5.3. Contours of the X Velocity on the x=95, x=130, and x=165 Surfaces

The velocity profile becomes more uniform as the fluid passes through the porous media. The velocity is very high at the center (the area in red) just before the nitrogen enters the substrate and then decreases as it passes through and exits the substrate. The area in green, which corresponds to a moderate velocity, increases in extent.

5.2.1.Simulation Results at Velocity 22.6 m/s:

The pressure field distribution is shown in the picture below at velocity 22.6 m/s. There, it can be observed that an important pressure drop occurs within the porous region.

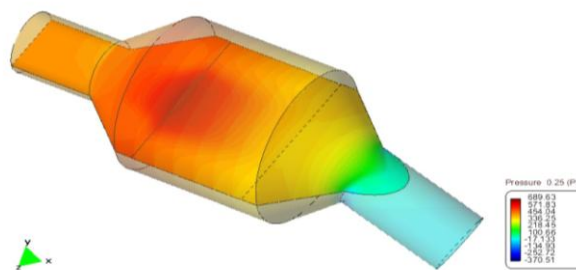


Figure:5.1. Contours of the Static Pressure on the y=0 plane

The pressure changes rapidly in the middle section, where the fluid velocity changes as it passes through the porous substrate. The pressure drop can be high, due to the inertial and viscous resistance of the porous media. The X-velocity component distribution of the fluid flow. In this picture, it becomes evident how the fluid decelerates rapidly when entering to the porous region. It can also be observed how the fluid recirculates before entering the central region of the catalyst (negative values of X-velocity component in dark blue) due to the resistance exerted by the porous media

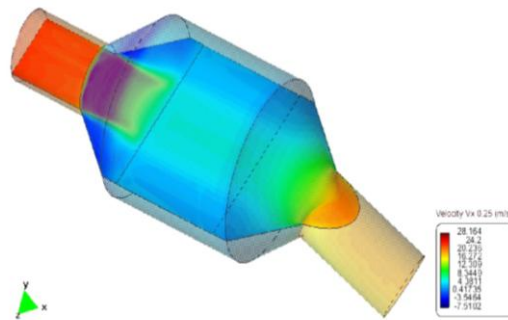


Figure: Velocity Vectors on the $y=0$ Plane

The flow pattern shows that the flow enters the catalytic converter as a jet, with recirculation on either side of the jet. As it passes through the porous substrate, it decelerates and straightens out, and exhibits a more uniform velocity distribution. This allows the metal catalyst present in the substrate to be more effective.

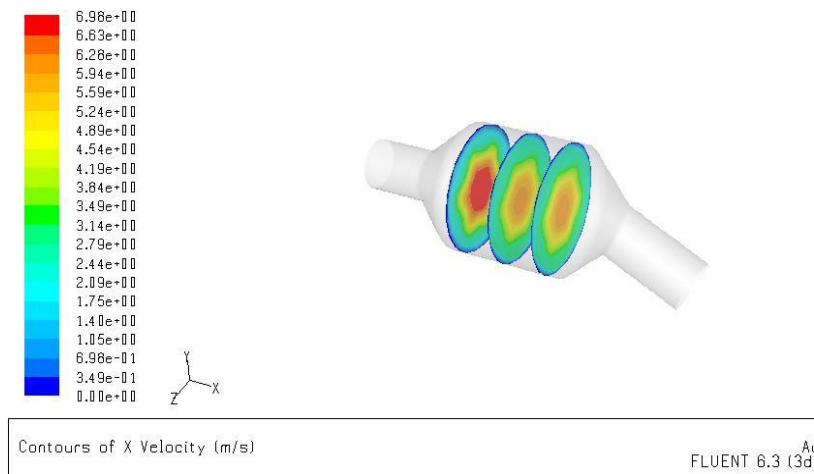


Figure: Contours of the X Velocity on the $x=95$, $x=130$, and $x=165$ Surfaces

The velocity profile becomes more uniform as the fluid passes through the porous media. The velocity is very high at the center (the area in red) just before the nitrogen enters the substrate and then decreases as it passes through and exits the substrate. The area in green, which corresponds to a moderate velocity, increases in extent.

5.2.1. Simulation Results at Velocity 25 m/s:

The pressure field distribution is shown in the picture below at velocity 25 m/s. There, it can be observed that an important pressure drop occurs within the porous region.

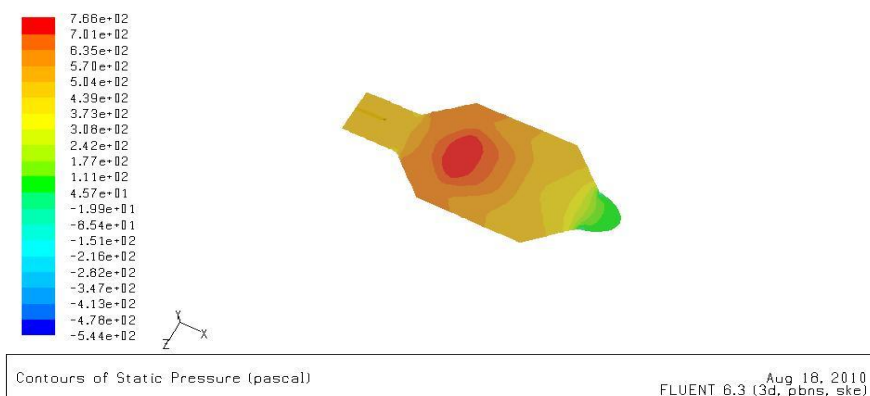


Figure: Contours of the Static Pressure on the $y=0$ plane

The pressure changes rapidly in the middle section, where the fluid velocity changes as it passes through the porous substrate. The pressure drop can be high, due to the inertial and viscous resistance of the porous media. The X-velocity component distribution of the fluid flow. In this picture, it becomes evident how the fluid decelerates rapidly when entering to the porous region. It can also be observed how the fluid recirculates before entering the central region of the catalyst (negative values of X-velocity component in dark blue) due to the resistance exerted by the porous media

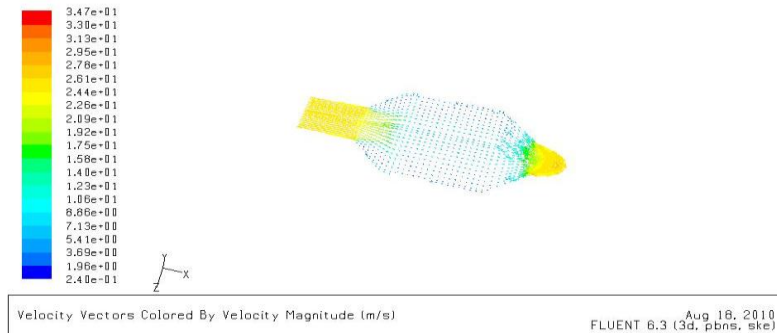


Figure: Velocity Vectors on the $y=0$ Plane

The flow pattern shows that the flow enters the catalytic converter as a jet, with recirculation on either side of the jet. As it passes through the porous substrate, it decelerates and straightens out, and exhibits a more uniform velocity distribution. This allows the metal catalyst present in the substrate to be more effective.

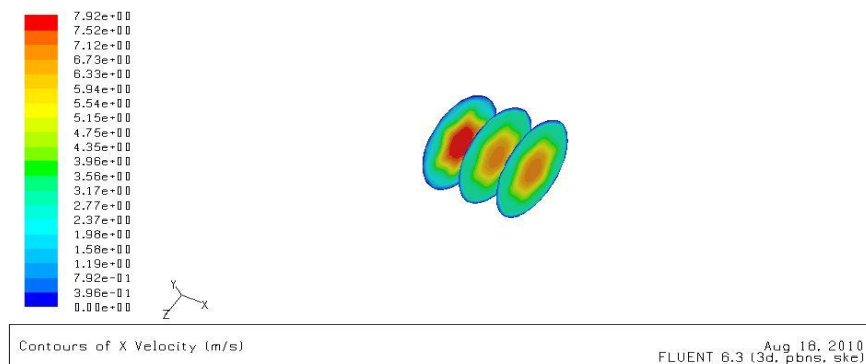


Figure: Contours of the X Velocity on the $x=95$, $x=130$, and $x=165$ Surfaces

The velocity profile becomes more uniform as the fluid passes through the porous media. The velocity is very high at the center (the area in red) just before the nitrogen enters the substrate and then decreases as it passes through and exits the substrate. The area in green, which corresponds to a moderate velocity, increases in extent.

5.2.1. Simulation Results at Velocity 27.5 m/s:

The pressure field distribution is shown in the picture below at velocity 27.5 m/s. There, it can be observed that an important pressure drop occurs within the porous region.

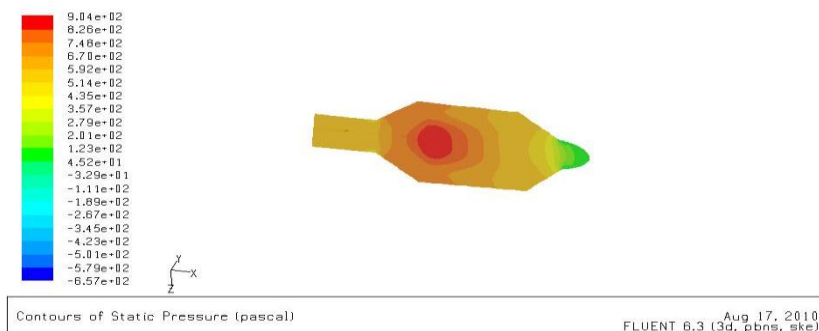


Figure:Contours of the Static Pressure on the y=0 plane

The pressure changes rapidly in the middle section, where the fluid velocity changes as it passes through the porous substrate. The pressure drop can be high, due to the inertial and viscous resistance of the porous media. The X-velocity component distribution of the fluid flow. In this picture, it becomes evident how the fluid decelerates rapidly when entering to the porous region. It can also be observed how the fluid recirculates before entering the central region of the catalyst (negative values of X-velocity component in dark blue) due to the resistance exerted by the porous media

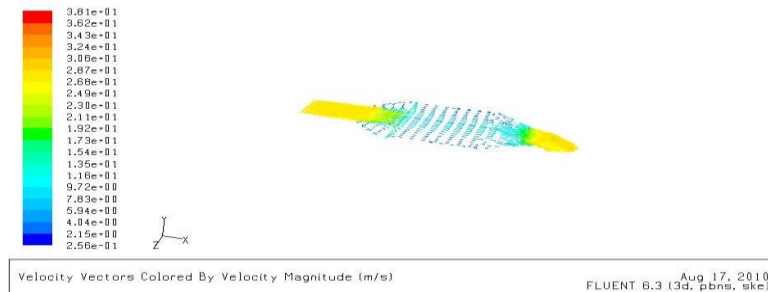


Figure: Velocity Vectors on the y=0 Plane

The flow pattern shows that the flow enters the catalytic converter as a jet, with recirculation on either side of the jet. As it passes through the porous substrate, it decelerates and straightens out, and exhibits a more uniform velocity distribution. This allows the metal catalyst present in the substrate to be more effective.

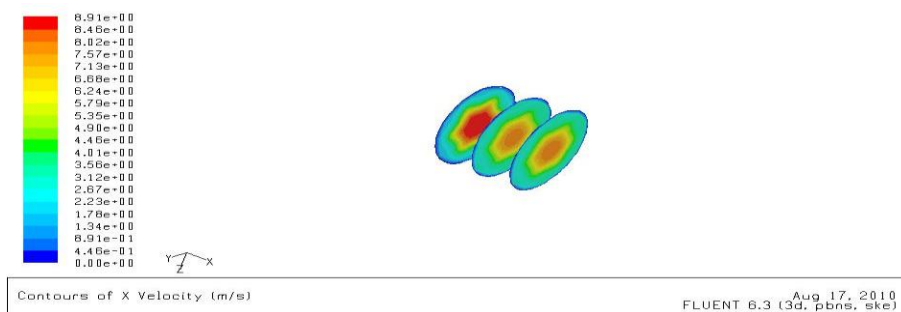


Figure:5.3. Contours of the X Velocity on the x=95, x=130, and x=165 Surfaces

The velocity profile becomes more uniform as the fluid passes through the porous media. The velocity is very high at the center (the area in red) just before the nitrogen enters the substrate and then decreases as it passes through and exits the substrate. The area in green, which corresponds to a moderate velocity, increases in extent.

5.2.1.Simulation Results at Velocity 30 m/s:

The pressure field distribution is shown in the picture below at velocity 30 m/s. There, it can be observed that an important pressure drop occurs within the porous region.

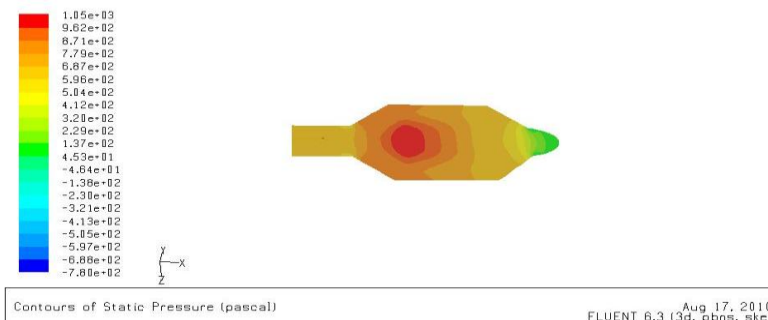


Figure: Contours of the Static Pressure on the y=0 plane

The pressure changes rapidly in the middle section, where the fluid velocity changes as it passes through the porous substrate. The pressure drop can be high, due to the inertial and viscous resistance of the porous media. The X-velocity component distribution of the fluid flow. In this picture, it becomes evident how the fluid decelerates rapidly when entering to the porous region. It can also be observed how the fluid recirculates before entering the central region of the catalyst (negative values of X-velocity component in dark blue) due to the resistance exerted by the porous media

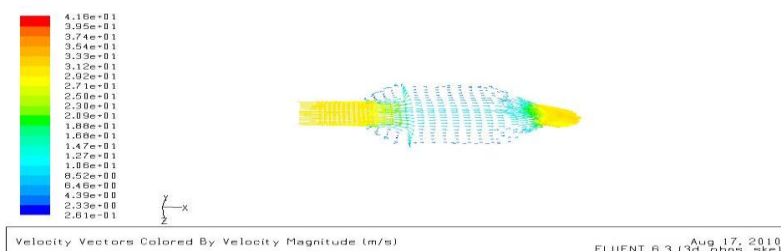


Figure: Velocity Vectors on the y=0 Plane

The flow pattern shows that the flow enters the catalytic converter as a jet, with recirculation on either side of the jet. As it passes through the porous substrate, it decelerates and straightens out, and exhibits a more uniform velocity distribution. This allows the metal catalyst present in the substrate to be more effective.



Figure: Contours of the X Velocity on the x=95, x=130, and x=165 Surfaces

The velocity profile becomes more uniform as the fluid passes through the porous media. The velocity is very high at the center (the area in red) just before the nitrogen enters the substrate and then decreases as it passes through and exits the substrate. The area in green, which corresponds to a moderate velocity, increases in extent.

4.3. Numerical Results:

S.No	Velocities (m/s)	Mass-Weighted Average for Static Pressure (pascal)		
		X=95	X=165	Net
1	20	451.81	296.27	373.65
2	22.6	555.06	376.41	465.29
3	25	660.68	459.52	559.65
4	27.5	778.68	553.27	665.975
5	30	907.28	656.75	782.015

Table: Mass-Weighted Average For Static Pressure for Different Velocities

Flow Velocities	20m/s		22.6m/s		25m/s		27.5m/s		30m/s	
	x=95	x=165	x=95	x=165	x=95	x=165	x=95	x=165	x=95	x=165
Mass-Weighted Average	4.4757	3.4783	5.1743	3.9932	5.8397	4.4830	6.5519	5.0072	7.2836	5.5460
Minimum of Facet Values	0.3873	2.2579	0.4121	2.4476	0.4333	2.6060	0.4532	2.7578	0.4702	2.8463
Maximum of Facet Values	6.6052	5.2475	7.6576	6.1421	8.6566	6.9978	9.7184	7.9142	10.8005	8.8569

Table: Numerical Results of Velocities in X-direction

S.No	Velocitys (m/s)	Standard Deviation Static Pressure (pascal)		Flow Rate for Static Pressure (pascal)(Kg/s)	
		X=95	X=165	X=95	X=165
1	20	32.5497	3.9365	12.7645	8.4686
2	22.6	40.9167	4.9620	17.7622	12.1649
3	25	49.3878	6.0080	23.4094	16.4273
4	27.5	58.9203	7.1900	30.3767	21.7551
5	30	69.2027	8.4804	38.6441	28.1697

Table: Standard Deviation and Flow Rates of Static Pressure for Different Velocities

V. CONCLUSION

In this paper Set up a porous zone for the substrate with appropriate resistances. In this paper we concluded the mass flow rate can be reduces at different iterations and also static pressure can be changes inlet of the catalytic converter to outlet of the catalytic converter. We concluded the pressure drop across the porous media and non-uniformity of the velocity distribution as the fluid goes through the porous media. Calculate a solution for gas flow through the catalytic converter using the pressure- based solver .Plot pressure and velocity distribution on specified planes of the geometry. The model approach gives better agreement in pressure drop. This present method also possesses lower computational cost based on the less computing time and Different number of Velocity's and Pressures are simulation. A ceramic monolith substrate with square shaped channels model having the parametric studies of wall thicknesses, cell densities, hydraulic diameter, and specific surface areas. A porous media having the different parametric studies of wall thicknesses, cell densities, hydraulic diameter, and specific surface areas. The results also show that a Square -shaped zone gives a good mechanical performance (lower pressure drop)

REFERENCES

- [1]. Shahrin Hisham Amirnordin, Suzairin Md Seri, Wan Saiful-Islam Wan Salim, Hamimah Abd Rahman, and Khalid Hasnan "Pressure Drop Analysis of Square and Hexagonal Cells and its Effects on the Performance of Catalytic Converters" International Journal of Environmental Science and Development, Vol. 2, No. 3, June 2011
- [2]. Shahrin Hisham Amirnordin, Suzairin Md Seri, Wan Saiful-Islam Wan Salim, Hamimah Abd Rahman, and Khalid Hasnan "Pressure Drop Prediction of Square-cell Honeycomb Monolith Structure" 2011 International Conference on Environment Science and Engineering IPCBEE vol.8 (2011) © (2011) IACSIT Press, Singapore
- [3]. CaiZhanjun, Kang Weimin, Chang Bowen, LiYabin "Study on *characteristics of gas flow pressure in catalytic converter with porous*" Applied Mechanics and Materials Vol.235 (2012) PP:30-33
- [4]. CaiZhanjun, Kang Weimin, Chang Bowen, LiYabin "Study on *characteristics of gas flow Velocity in catalytic converter with porous*" Applied Mechanics and Materials Vol.229-231 (2012) PP:391-394
- [5]. F.M. White, "Fluid Mechanics." Singapore: Mc-Graw Hill, Inc. 295- 334. 2003.
- [6]. M. Luoma, M. Harkonen, R. Lylykangas and J.Sohlo, "Optimisation of the Metallic Three-Way Catalyst Behaviour." SAE International. 971026. 1997.
- [7]. E. Abu-Khiran, R. Douglas, and G. McCullough, "Pressure loss characteristics in catalytic converters," SAE International, 2003-32- 0061, 2003.
- [8]. Manual of ANSYS Fluent, 2005.

Heat transfer enhancement in domestic refrigerator using R600a/mineral oil/nano- Al_2O_3 as working fluid

¹R. Reji Kumar , ²K. Sridhar , ³M.Narasimha

^{1,2,3}Lecturer, School of Mechanical and Industrial Engineering Bahirdar University, Bahirdar, Ethiopia

ABSTRACT

The experimental apparatus was build according to the national standards of India.. The performance of the refrigeration system depends upon the heat transfer capacity of the refrigerant. Normally R12, R22, R600, R600a and 134a are used as a refrigerant. This refrigerant heat transfer capacity is not so good and increase power consumption. Due to these limitation nanofluids are enhanced with the normal lubricant and increases the heat transfer capacity and reduces the power consumption. Aluminium oxide nanofluid is used for enhancing the heat transfer capacity of the refrigerant in the refrigeration System. In this experiment heat transfer enhancement was investigated numerically on the surface of a refrigerator by using Al_2O_3 nano-refrigerants, where nanofluids could be a significant factor in maintaining the surface temperature within a required range. The addition of nanoparticles to the refrigerant results in improvements in the thermophysical properties and heat transfer characteristics of the refrigerant, thereby improving the performance of the refrigeration system. Stable nanolubricant has been prepared for the study. The experimental studies indicate that the refrigeration system with nano-refrigerant works normally. It is found that the freezing capacity is higher and the power consumption reduces by 11.5 % when POE oil is replaced by a mixture of mineral oil and Aluminium oxide nanoparticles. Thus using Aluminium oxide nanolubricant in refrigeration system is feasible.

Key words: Aluminium oxide nanoparticle, nano-refrigerant, Thermal conductivity, freezing capacity COP, Energy consumption.

List of symbols

Symbol	Description	Unit
Nomenclature		
A	Cross sectional area	m^2
C_p	Specific heat	J/Kg k
D	Diameter	m
h	Enthalpy	KJ/Kg
h_{fg}	Latent heat of vapourisation	w/m k
K	Thermal conductivity	w/m k
m	Mass flow rate	Kg/s
T	Temperature	$^\circ\text{C}$
v	Velocity	m/s
Greek symbols		
σ	Surface tension	N/m
ρ	Density	Kg/m^3
μ	Dynamic viscosity	Kg/ms
ω	Nanoparticle concentration in the nanoparticle oil suspension	
ψ	Volume fraction of nanoparticle in the nanoparticle/oil suspension	
Subscripts		
f	liquid	
g	gas	

n	nanoparticle
o	oil
r	refrigerant
n,o	nanoparticle and oil
r,o	refrigerant and oil
r,n,o	refrigerant, nanoparticle and oil

Abbreviation

HTC	Heat transfer coefficient
TR	Tonne of refrigeration
COP	Coefficient of performance
HRF	Heat rejection factor
COP	Coefficient of performance
TR	Tonne of refrigeration

I. INTRODUCTION

It is true that rapid industrialization has led to unprecedented growth, development and technological advancement across the globe. It has also given rise to several new concerns. Today global warming and ozone layer depletion on the one hand and spiraling oil prices on the other hand have become main challenges. Excessive use of fossil fuels is leading to their sharp diminution and nuclear energy is not out of harm's way. In the face of imminent energy resource crunch there is need for developing thermal systems which are energy efficient. Thermal systems like refrigerators and air conditioners consume large amount of electric power. So avenues of developing energy efficient refrigeration and air conditioning systems with nature friendly refrigerants need to be explored. The rapid advances in nanotechnology have lead to emerging of new generation heat transfer fluids called nanofluids.

Nanofluids are prepared by suspending nano sized particles (1-100nm) in conventional fluids and have higher thermal conductivity than the base fluids. Nanofluids have the following characteristics compared to the normal solid liquid suspensions. i) higher heat transfer between the particles and fluids due to the high surface area of the particles ii) better dispersion stability with predominant Brownian motion iii) reduces particle clogging iv) reduced pumping power as compared to base fluid to obtain equivalent heat transfer. Based on the applications, nanoparticles are currently made out of a very wide variety of materials, the most common of the new generation of nanoparticles being ceramics, which are best split into metal oxide ceramics, such as titanium, zinc, aluminum and iron oxides, to name a prominent few and silicate nanoparticles, generally in the form of nanoscale flakes of clay. Addition of nanoparticles changes the boiling characteristics of the base fluids. Nanoparticles can be used in refrigeration systems because of its remarkable improvement in thermophysical and heat transfer capabilities to enhance the performance of refrigeration systems. In a vapour compression refrigeration system the nanoparticles can be added to the lubricant (compressor oil). When the refrigerant is circulated through the compressor it carries traces of lubricant + nanoparticles mixture (nanolubricants) so that the other parts of the system will have nanolubricant -refrigerant mixture.

II. LITERATURE SURVAY

Recently, some investigators have conducted studies on vapour compression refrigeration systems, to study the effect of nanoparticle in the refrigerant/lubricant on its performance. [1] Pawel et al. (2005) conducted studies on nanofluids and found that there is the significant increase in the thermal conductivity of nanofluid compared to the base fluid. They also found that addition of nanoparticles results in significant increase in the critical heat flux. [2] Bi et al. (2007) conducted studies on a domestic refrigerator using nanorefrigerants. In their studies R134a was used the refrigerant, and a mixture of mineral oil TiO₂ was used as the lubricant. They found that the refrigeration system with the nanorefrigerant worked normally and efficiently and the energy consumption reduces by 21.2%. When compared with R134a/POE oil system. Later, [3] Bi et al. (2008) found that there is remarkable reduction in the power consumption and significant improvement in freezing capacity. They pointed out the improvement in the system performance is due to better thermo physical properties of mineral oil and the presence of nanoparticles in the refrigerant.

[4] Jwo et al. (2009) conducted studies on a refrigeration system replacing R-134a refrigerant and polyester lubricant with a hydrocarbon refrigerant and mineral lubricant. The mineral lubricant included added Al₂O₃ nanoparticles to improve the lubrication and heat-transfer performance. Their studies show that the 60% R-134a and 0.1 wt % Al₂O₃ nanoparticles were optimal.

Under these conditions, the power consumption was reduced by about 2.4%, and the coefficient of performance was increased by 4.4%. [5]Peng et al. (2010) conducted experimental on the nucleate pool boiling heat transfer characteristics of refrigerant/oil mixture with diamond nano particles. The refrigerant used was R113 and the oil was VG68. They found out that the nucleate pool boiling heat transfer coefficient of R113/oil mixture with diamond nanoparticles is larger than the R113/oil mixture. They also proposed a general correlation for predicting the nucleate pool boiling heat transfer coefficient of refrigerant/oil mixture with nanoparticles, which well satisfies their experimental results.

[6]Henderson et al. (2010) conducted an experimental analysis on the flow boiling heat transfer of R134a based nanofluids in a horizontal tube. They found excellent dispersion of CuO nanoparticle with R134a and POE oil and the heat transfer coefficient increases more than 100% over baseline R134a/POE oil results. [7]Bobbo et al. (2010) conducted a study on the influence of dispersion of single wall carbon nanohorns (SWCNH) and TiO₂ on the tribological properties of POE oil together with the effects on the solubility of R134a at different temperatures. They showed that the tribological behaviour of the base lubricant can be either improved or worsen by adding nanoparticles. On the other hand the nanoparticle dispersion did not affect significantly the solubility. [8]Bi et al. (2011) conducted an experimental study on the performance of a domestic refrigerator using TiO₂-R600a nanorefrigerant as working fluid. They showed that the TiO₂-R600a system worked normally and efficiently in the refrigerator and an energy saving of 9.6%. They too cited that the freezing velocity of nano refrigerating system was more than that with pure R600a system. The purpose of this article is to report the results obtained from the experimental studies on a vapour compression system.

Lee et al. [9] investigated the friction coefficient of the mineral oil mixed with 0.1 vol.% fullerene nanoparticles, and the results indicated that the friction coefficient decreased by 90% in comparison with raw lubricant, which lead us to the conclusion that nanoparticles can improve the efficiency and reliability of the compressor. Wang and Xie [10] found that TiO₂ nanoparticles could be used as additives to enhance the solubility between mineral oil and hydrofluorocarbon (HFC) refrigerant. The refrigeration systems using the mixture of R134a and mineral oil appended with nanoparticles TiO₂, appeared to give better performance by returning more lubricant oil back to the compressor, and had the similar performance compared to the systems using polyol-ester (POE) and R134a. In the present study the refrigerant selected is R600a and the nanoparticle is alumina. Isobutane (R600a) is more widely adopted in domestic refrigerator because of its better environmental and energy performances. In this paper, a new refrigerator test system was built up according to the National Standard of India. A domestic R600a refrigerator was selected. Al₂O₃-R600a nano-refrigerant was prepared and used as working fluid. The energy consumption test and freeze capacity test were conducted to compare the performance of the refrigerator with nano-refrigerant and pure refrigerant so as to provide the basic data for the application of the nanoparticles in the refrigeration system..

III. PHYSICAL PROPERTIES OF NANOFUIDS

3.1. Thermophysical properties of base refrigerant.

Its numerical designation is R600a or Isobutane. Its chemical formula (CH ₃) ₃ CH.	
Normal boiling point	= 260-264 °K at atm pressure
Critical Temperature	= 135°C
Critical pressurer	= 3.65 MPa
Vapour pressure	= 204.8 KPa at 21°C
Specific heat of liquid	= 2.38 KJ/Kg°C at 25°C
Molar mass	= 58.12 g mol ⁻¹
Density	= 2.51 kg/m ³ , gas (15 °C, 1atm) 593.4 kg/m ³ , liquid
Melting point	= -159.6 °C, 114 K, -255 °F
Boiling point	= -11.7 °C, 261 K, 11 °F
Solubility in water	= Insoluble
Ozone depletion potential (ODP)	= 0
Global warming potential (GWP)	= 3
Flash point	= Flammable gas
Latent heat of evaporation	= 362.6 KJ/Kg at atm pressure
Specific Heat Ratio Cp/Cv	= 1.091(atm, 25°C).
Assigned colour code	= Colorless gas

3.2. Thermophysical properties of nanoparticles.

Its molecular formula is Al_2O_3 .

Melting Point	=	2072°C
Boiling Point	=	2977°C
Flash Point	=	non-flammable
Colour	=	Ivory / White
Density	=	0.26 g/cm ³
Specific heat.	=	880 J/KgK
Thermal conductivity	=	30 W/mK
Molecular mass	=	101.96 g/mol
Specific Surface Area	=	0.5- 50 m ² /g
Average Primary Particle size	=	50nm
Appearance	=	White powder
PH	=	7-9

Properties

It is insoluble in water.

Stable under normal, temperature and pressures.

It is odorless

3.3. Thermophysical properties of nanofluid.

In order to estimate the heat transfer coefficient in the refrigerant side of the evaporator the thermophysical properties of the nanorefrigerant have to be calculated. The thermophysical properties of the nanorefrigerant are calculated in two steps.

Firstly thermophysical properties of the nanoparticles oil mixture is calculated and this data is used to calculate the properties of nanorefrigerant.

3.3.1. Calculation of thermophysical properties of nanolubricant

The following correlations are used to calculate the thermophysical properties of nanolubricant

$$[11,12,13] \text{ Specific heat of nanolubricant } C_{p,n,o} = (1-\psi_n) C_{p,o} + \psi_n C_{p,n} \quad (2)$$

$$(1) \text{ Thermal conductivity nanolubricant, } K_{n,o} = K_o [(K_n + 2K_o - 2\psi_n(K_o - K_n)) / (K_n + 2K_o + \psi_n(K_o - K_n))] \quad (2)$$

$$\text{Viscosity of nanolubricant, } \mu_{n,o} = \mu_o [1 / (1 - \psi_n)^{2.5}] \quad (3)$$

$$\text{Density of nanolubricant, } \rho_{n,o} = (1 - \psi_n) \rho_o + \psi_n \rho_n \quad (4)$$

Volume fraction of nanoparticle in the nanoparticle-oil suspension,

$$\psi_n = \omega_n \rho_o / [\omega_n \rho_o + (1 - \omega_n) \rho_n] \quad (5)$$

$$\text{Mass fraction in the nanoparticle oil suspension, } \omega_n = m_n / (m_n + m_o) \quad (6)$$

3.3.2. Calculation of thermophysical properties nanorefrigerant

The following correlations are used to calculate the thermophysical properties of nanorefrigerant [14,15,16]

$$\text{Specific heat of the nanorefrigerants } C_{p,r,n,o,f} = (1 - X_{n,o}) C_{p,r,f} + X_{n,o} C_{p,n,o} \quad (7)$$

$$\text{Viscosity of the nanorefrigerants } \mu_{r,n,o,f} = \exp(X_{n,o} \ln \mu_{n,o} + (1 - X_{n,o}) \ln \mu_{r,f}), \quad (8)$$

Thermal conductivity of the nanorefrigerants

$$K_{r,n,o,f} = K_{r,f}(1 - X_{n,o}) + (K_{n,o} X_{n,o}) - (0.72 X_{n,o} (1 - X_{n,o})(K_{n,o} - K_{r,f})), \quad (9)$$

$$\text{Density of the nanorefrigerants } \rho_{r,n,o,f} = [(X_{n,o} / \rho_{n,o}) + ((1 - X_{n,o}) / \rho_{r,f})]^{-1} \quad (10)$$

$$\text{Nanoparticle/oil suspension concentration, } X_{n,o} = m_{n,o} / (m_{n,o} + m_r) \quad (11)$$

$$\text{The theoretical C.O.P is calculated using the equation } C.O.P_{th} = (h_1 - h_4) / (h_2 - h_1) \quad (12)$$

h_1 – enthalpy of refrigerant at the inlet of the compressor

h_2 – enthalpy of refrigerant at the outlet of the compressor

h_4 – enthalpy of refrigerant at the inlet of the evaporator

the values of the enthalpy are taken from refrigerant tables.

$$\text{The actual C.O.P is calculated using relation } C.O.P_{act} = \text{cooling load} / \text{power input} \quad (13)$$

IV. EXPERIMENTAL SETUP AND TEST PROCEDURE

This section provides a description of the facilities developed for conduction experimental work on a refrigerator. The technique of charging and evacuation of the system is also discussed here.

4.1. Experimental methodology

The temperature of the refrigerant inlet/outlet of each component of the refrigerator was measured with copper – constantan thermocouples (T type). The thermocouple sensors fitted at inlet and outlet of the compressor, condenser, and thermocouples/temperature sensors were interfaced with a HP data logger via a PC through the GPIB cable for data storage. Temperature measurement is necessary to find out the enthalpy in and out of each component of the system to, investigate the performance. The inlet and outlet pressure of refrigerant for each of the component is also necessary to find out their enthalpy at corresponding state.

The pressure transducer was fitted at the inlet and outlet of the compressor and expansion valve as shown in Fig.1. The pressure transducers were fitted with the T-joint and then brazed with the tube to measure the pressure at desired position. The range of the pressure transducer is -1 to + 39 bars. The pressure transducers also been interfaced with computer via data logger to store data. A service port was installed at the inlet of expansion valve and compressor for charging and recovering the refrigerant. The location of the service port is shown in Fig. 1. The evacuation has also been carried out through this service port. A power meter was connected with compressor to measure the power and energy consumption.

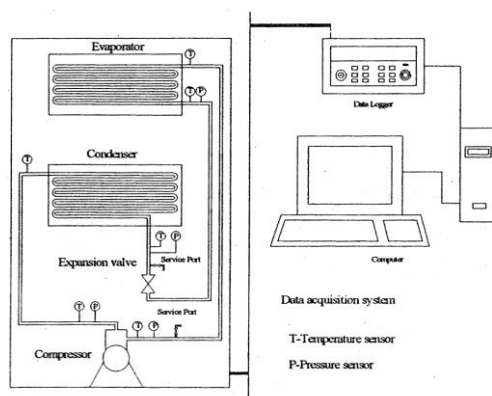


Fig. 1. Experimental apparatus

4.2. Preparation of nanolubricants

Preparation of nanolubricants is the first step in the experimental studies on nanorefrigerants. Nanofluids are not simply liquid solid mixtures. Special requirements are even, stable and durable suspension, negligible agglomeration of particles, and no chemical change of the fluid. Nanofluids can be prepared using single step or two step methods. In the present study two step procedure is used. Commercially available nanoparticles of aluminium oxide (manufactured by Sigma Aldrich) with average size <50nm and having density 0.26 g/cc were used for the preparation of nanolubricant. Mass fraction of nanoparticles in the nanoparticle–lubricant mixtures is 0.06%. An ultrasonic vibrator (Micro clean 102, Oscar Ultrasonics) was used for the uniform dispersion of the nanoparticles and it took about 24 hours of agitation to achieve the same. Experimental observation shows that the stable dispersion of alumina nanoparticles can be kept for more than 3 days without coagulation or deposition.

4.3. System Evacuation

Moisture combines in varying degree with most of the commonly used refrigerants and reacts with the lubricating oil and with other materials in the system, producing highly corrosive compound. The resulting chemical reaction often produces pitting and other damage on the valves seals, cylinder wall and other polished surface of the system. It may cause the deterioration of the lubricating oil and the formation of sludge that can gum up valves, clog oil passages, score bearing surface and produce other effect that reduce the life of the system. Moisture in the system may exist in solution or as free water. Free water can freeze into the ice crystals inside the metering device and in the evaporator tubes of system that operate below the freezing point of the water. This reaction is called freeze up. When freeze up occurs, the formation of ice within the orifice of the metering device temporarily stops the flow of the liquid refrigerant .To get rid of the detrimental effect of moisture Yellow jacket 4cfm vacuum pump was used to evacuate the system. This system evacuates fast and better which is deep enough to get rid of contaminant that could cause system failure. The evacuation system consists of a vacuum pump, a pressure gauge and hoses. The hoses were connected with the service port to remove the moisture from the system. When the pump is turned on the internal the pressure gauge shows the pressure inside the refrigerator system.

4.4. System Charging

Yellow jacket digital electronic charging scale has been used to charge R600a into the system. This is an automatic digital charging system that can charge the desired amount accurately and automatically. The charging system consists of a platform, an LCD, an electronic controlled valve and charging hose. The refrigerant cylinder was placed on the platform which measures the weight of the cylinder. The LCD displays the weight and also acts as a control panel. One charging hose was connected with the outlet of the cylinder and inlet of the electronic valve and another one was connected with the outlet of electronic valve and inlet of the service port. Using this charging system refrigerants were charged into the system according to desired amount.

4.5. Test Procedure:

The system was evacuated with the help of vacuum pump to remove the moisture and charged with the help of charging system. The pressure transducers and thermocouples fitted with the system were connected with the data logger. The data logger was interfaced with the computer and software has been installed to operate the data logger from the computer and to store the data. The data logger was set to scan the data from the temperature sensor and pressure sensor at an interval of 5 minutes. A power meter was connected with the refrigerator and interfaced with the computer and power meter software was installed. The power meter stores the instantaneous power and cumulative energy consumption of the refrigerator and cumulative energy consumption of the refrigerator. The pressures and temperatures of the refrigerants from the data logger were used to determine the enthalpy of the refrigerant. All equipments and test unit was installed inside the environment control chamber where the temperature and humidity was controlled. The dehumidifier has been used to maintain desired level of humidity at the control chamber. The experiment has been conducted of the refrigeration test rig.

V. RESULTS AND DISCUSSION

In the present experimental study, three cases have been considered. The hermetic compressor filled with i) pure POE oil ii) mineral oil and iii) mineral oil + alumina nanoparticles as lubricant. The mass fraction of the nanoparticles in the nanolubricant is 0.06 %.

5.1. The cooling load temperature – time chart

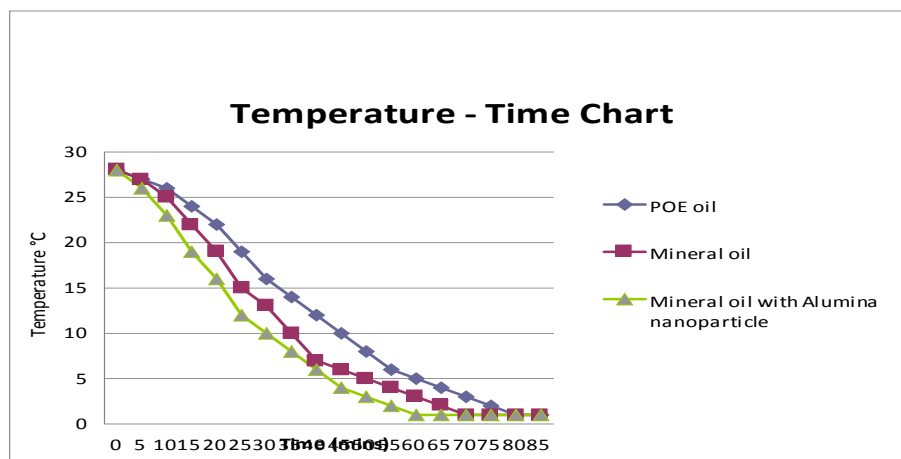


Fig.2. Temperature - Time chart

The cooling load temperature – time history is shown in figure.2 and the freezing capacity for the three cases is shown in Figure.3. In all the cases the condenser pressure is 5.6 bar and the evaporator pressure is 0.58 bar. No appreciable pressure drops due to friction were observed in the condenser and evaporator. From the figure it is clear that, the time required for reducing cooling load temperature is less for the mineral oil + alumina nanoparticle mixture. For example, with mineral oil + alumina nanoparticle, the time required to bring the cooling load temperature from 28°C to 5°C is 42 minutes where as that with mineral oil and POE oil is 50 and 60 minutes respectively. It is clear that, the freezing capacity of the mineral oil + Alumina nanoparticle mixture is higher when compared with the other two cases The time taken to reduce the temperature of the cooling load from 28°C to 1 °C with POE oil is 85 minutes and it reduces by 29 % if mineral oil + alumina nanoparticle is used. This is due to the fact the nanoparticles present in the refrigerant enhances the heat transfer rate in the refrigerant side of the evaporator

5.2. Effect of nanoparticle on the freezing capacity

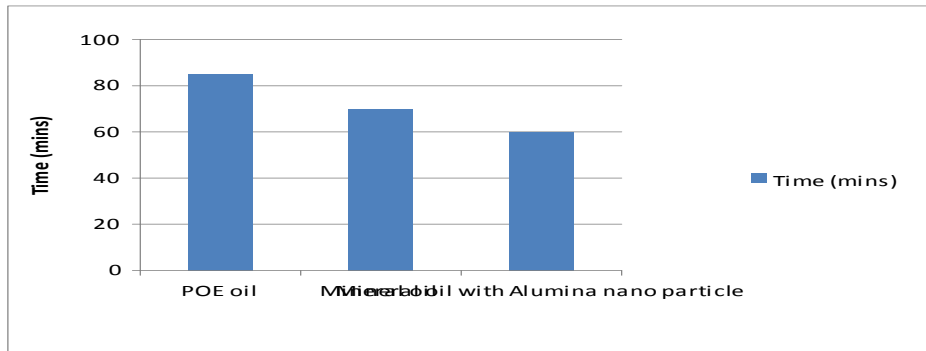


Fig.3 Effect of nanoparticle on the freezing capacity

5.3. Reduction in refrigerant temperature while passing through the condenser

Figure 4 shows drop in the refrigerant temperature in the condenser of the refrigeration system. Temperature drop of the refrigerant is high with nanorefrigerant when compared with the other cases. The temperature of the refrigerant at the inlet of the condenser is in the range 69 – 65°C. The saturation temperature of R600a corresponding to the condenser pressure of 5.6 bar is 42°C. In the case of mineral oil nanoparticle mixture the temperature at the exit of the condenser is 39°C and the subcooling obtained is 3 °C. In fact there is no subcooling when POE oil is used as the lubricant. The enhanced heat transfer rate in the condenser is due to the presence of nanoparticles in the refrigerant.

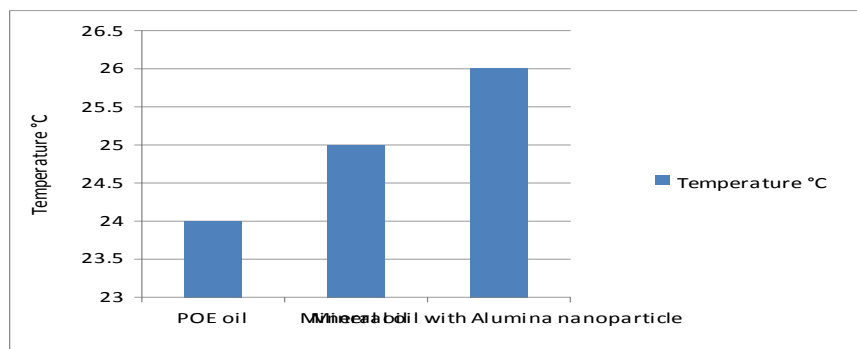


Fig.4. Reduction in refrigerant temperature while passing through the condenser

5.4. Energy Consumption By The Compressor

Table. 1. Energy consumption results

	POE oil	Mineral oil	Mineral oil with Alumina nanoparticle
Energy consumption kw hr	0.635	0.614	0.572
Energy saving %	-	6.0	11.5

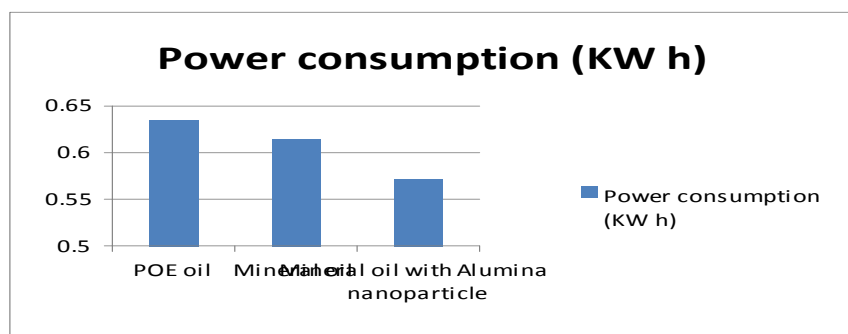


Fig.5. Comparison of power consumption

Figure 5 shows the comparison of power consumption of the compressor. The reduction in power consumption is 6 % if the mineral oil is used instead of POE Oil and a reduction of 11.5 % is observed when mineral oil is mixed nanoparticles. [8]Shengshan B (2010) reported that for a refrigeration system using R600a as refrigerant the power consumption can be reduced by 9.6 % if mineral oil with TiO₂ nanoparticle is used instead of POE oil.

5.5. Temperature of salient points

Table 2. Temperature of salient points

Quantity	POE oil °C	Mineral oil	Mineral oil with Al ₂ O ₃ nanoparticle
Temperature at inlet of the compressor	20	19	17
Temperature at inlet of the condenser	69	67	65
Temperature at outlet of the condenser	45	42	39
Temperature at outlet of the expansion valve	-20	-20	-21
Temperature at inlet of the evaporator	-19	-19	-20

5.6. Comparison of Coefficient of performance

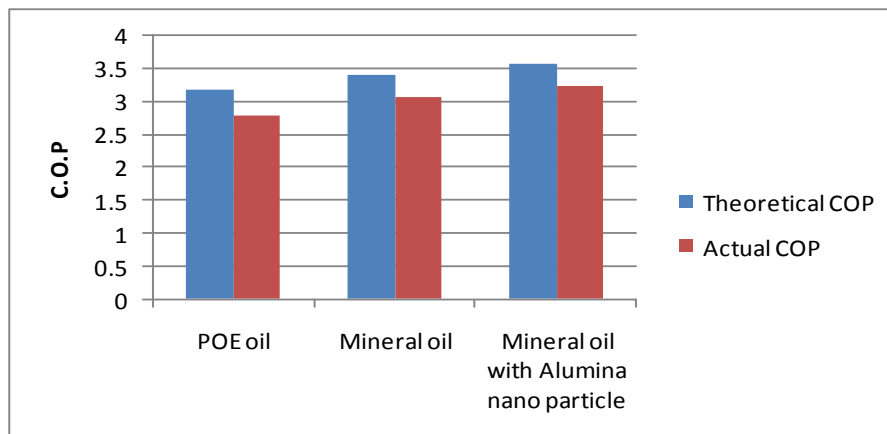


Fig. 6. Comparison of Coefficient of performance of the three cases

Figure 6 shows the coefficient of performance (COP) calculated using the experimental data. The actual COP is calculated using the cooling load and the power input. The theoretical values are also shown for comparison. In all cases the actual COP is less than the theoretical COP. The condenser pressure is 5.6 bar and the evaporator pressure is 0.58bar. The temperatures at the salient points of the refrigeration system are shown in Table 2. It is very much clear from the histogram shown below that the mineral oil + alumina nanoparticle mixture has the highest COP when compared with the other cases. The advantages of adding nanoparticle to the lubricant is manifold. It reduces the power consumption of the compressor and there is sub cooling of the nano-refrigerant in the condenser which in turn increases the COP. The Actual COP is calculated using the energy meter reading and the cooling load. For the calculation of theoretical COP the enthalpy values at the salient points are taken from P-h chart for R600a.

VI. CONCLUSION

Extensive experimental studies have been conducted to evaluate the performance parameters of a vapour compression refrigeration system with different lubricants including nanolubricants. The conclusions derived out of the present study are (i) The R600a refrigerant and mineral oil mixture with nanoparticles worked normally

(ii) Freezing capacity of the refrigeration system is higher with mineral oil + alumina nanoparticles oil mixture compared the system with POE oil

- (iii) The power consumption of the compressor reduces by 11.5% when the nanolubricant is used instead of conventional POE oil (iv) The coefficient of performance of the refrigeration system also increases by 19.6 % when the conventional POE oil is replaced with nanorefrigerant

REFERENCES

- [1] Pawel K. P., Jeffrey A.E. and David G.C., 2005. Nanofluids for thermal transport. *Materials Today*, pp. 36-44
- [2] Bi S., Shi L. and Zhang L., 2007. Performance study of a domestic refrigerator using R134a/mineral oil/nano-TiO₂ as working fluid. *ICR07-B2-346*.
- [3] Bi S., Shi L. and Zhang L., 2008. Application of nanoparticles in domestic refrigerators. *Applied Thermal Engineering*, Vol. 28, pp.1834-1843.
- [4] Jwo et.al, 2009. Effect of nano lubricant on the performance of Hydrocarbon refrigerant system. *J. Vac. Sci. Techno. B*, Vol.27, No. 3, pp. 1473-1477.
- [5] Hao Peng et.al., 2010. Nucleate pool boiling heat transfer characteristics of refrigerant/oil mixture with diamond nano particles. *International Journal of Refrigeration*, Vol.33, pp. 347-358.
- [6] Henderson et al. (2010) Experimental analysis on the flow boiling heat transfer of R134a based nanofluids in a horizontal tube. *IJHMT* , Vol. 53, pp. 944-951
- [7] Bobbo S. et.al, 2010. Influence of nanoparticles dispersion in POE oils on lubricity and R134a solubility. *International Journal of Refrigeration*, Vol.33, pp. 1180-1186.
- [8] Shengshan Bi, Performance of a Domestic Refrigerator using TiO₂-R600a nano-refrigerant as working fluid, *Int J of Energy Conservation and Management*, Vol. 52, 2011, 733-737.
- [9] Lee K, Hwang YJ, Cheong S, Kwon L, Kim S, Lee J. Performance evaluation of nano-lubricants of fullerene nanoparticles in refrigeration mineral oil. *Curr Appl Phys* 2009;9:128–31.
- [10] Wang RX, Xie HB. A refrigerating system using HFC134a and mineral lubricant appended with N-TiO₂(R) as working fluids. In: *Proceedings of the 4th international symposium on HAVC*, Tsinghua University; 2003.
- [11] Pak B.C., Cho, Y.I., 1998. Hydrodynamic and heat transfer study of dispersed fluids with submicron metallic oxide particles. *Experimental Heat Transfer*, Vol. 11, No. 2, pp. 151–170.
- [12] Hamilton, R.L., Crosser, O.K., 1962. Thermal conductivity of heterogeneous two-component systems. *Industrial and Engineering Chemistry Fundamentals*, Vol. 1, No. 3, pp. 187–191.
- [13] Brinkman, H.C., 1952. The viscosity of concentrated suspensions and solution. *The Journal of Chemical Physics*, Vol.20, pp. 571– 581.
- [14] Jensen, M.K., Jackman, D.L., 1984. Prediction of nucleate pool boiling heat transfer coefficients of refrigerant–oil mixtures. *Journal of Heat Transfer*, Vol. 106, pp. 184–190
- [15] Kedzierski, M.A., Kaul, M.P., 1993. Horizontal nucleate flow boiling heat transfer coefficient measurements and visual observations for R12, R134a, and R134a/ester lubricant mixtures. In: *Proceedings of the 6th International Symposium on Transport Phenomena in Thermal Engineering*, Vol. 1, pp. 111–116.
- [16] Baustian, J.J., Pate, M.B., Bergles, A.E., 1988. Measuring the concentration of a flowing oil–refrigerant mixture: instrument test Facility And Initial Results. *Ashrae Transactions*, Vol. 94, No. 1, Pp167–177.

AUTHORS BIBLIOGRAPHY:



R.Rejikumar Received His B.E., Degree In Mechanical Engineering From Anna University, Chennai. He Received M.E. Degree From Anna University, Thiruchirapalli. Currently Working As Teaching Faculty In The School Of Mechanical And Industrial Engineering, Institute Of Technology, Bahir Dar, University, Bahir Dar, Ethiopia



K.Sridhar Received His B.E., Degree In Mechanical Engineering From Anna University, Chennai. He Received M.E. Degree From Anna University, Coimbatore. Currently Working As Teaching Faculty In The School Of Mechanical And Industrial Engineering, Institute Of Technology, Bahir Dar, University, Bahir Dar, Ethiopia.



M.Narasimha Received His B.Tech. Degree In Mechanical Engineering From Jntu, Hyderabad. He Received M.E. Degree From Vmu, Tamilnadu. Currently Working As Teaching Faculty In The School Of Mechanical And Industrial Engineering, Institute Of Technology, Bahir Dar University, Bahir Dar, Ethiopia.

Geoidal Map and Three Dimension Surface Model Part of Port Harcourt Metropolis from “Satlevel” Collocation Model

Olaleye J. B.¹, J. O. Olusina¹, O. T. Badejo¹ and K. F. Aleem^{2, 3}

¹Department of Surveying and Geoinformatics, University of Lagos, Akoka - Lagos, Nigeria

²Department of Geomatics Engineering Technology, Yanbu Industrial College, Yanbu Industrial City, Saudi Arabia

³Surveying and Geoinformatics Programme, Abubakar Tafawa Balewa University, Bauchi Nigeria

Abstract:

Geoidal map depicts the geoid configuration of the area under study. Data acquisition for the production of such maps has been very tedious, time consuming and expensive with the use of conventional methods. "Satlevel" Collocation is a new method of geoid determination in which the ellipsoidal height from any satellite based system is combined with orthometric height from geodetic levelling to model the geoid. The method enables the geoid to be determined in patches. Geoid so determined can be applied with ellipsoidal height to get orthometric height which height users

O

e

T

rt

Harcourt metropolis. The generated data was used to produce the Contour map of the study area using SURFER software. The map was overlaid on the Local government map of Rivers State of Nigeria. The production of Geoidal map from "Satlevel" Collocation is easier than the conventional methods, when the initial geoidal coefficients have been determined. This method can be extended to other parts of Nigeria and the world at large.

Keywords: O

S

S

P

R

I. INTRODUCTION

1.1 Geoidal Map:

A Geoidal map is similar to contour map which is made up of contour lines depicting the value of geoid for any point. For producing contour map, geoidal values at different points are used for producing geoidal map. Therefore, any line on a geoidal surface is an imaginary line drawn on the geoidal map to connect points of the same geoidal height on, above or below the earth surface. The accuracy required for such maps necessitates the knowledge of the accurate and precise geoid at the same area. (Amin et al, 2005)

1.2. Geoid

The geoid is the surface which coincides with that surface to which the oceans would conform over the entire earth, if free to adjust to the combined effects of the earth's mass attraction (gravitation) and the centrifugal force of the Earth's rotation. Specifically, it is an equipotential surface, meaning that it is a surface on which the gravitational potential energy has the same value everywhere with respect to gravity. The geoid surface is irregular, but considerably smoother than earth's physical surface. Sea level, if undisturbed by tides, currents and weather, would assume a surface equal to the geoid when the observation is carried out for a numbers of years, usually 18.61years. (Deakin, 1996, Olaleye et al, 2010; Aleem, 2013)

Determination of the geoid has been one of major challenges of geodesists. Gravity data have been used in the past with stokes integration and other approaches to determine the geoid. One of such conventional methods was used by Hirvonen (1934) to carry out the first computation on a worldwide scale. He computed the geoidal undulation for 62 points distributed in an East West band encircling the entire earth surface. For the first time, Tanni (1948 and 1949) used large quantity of gravity data to compute the global geoidal heights. He employed the Pratt-Densities method. Also, Heiskanen (1957) computed the gravimetric geoid of Columbus using Free Air anomalies.

According to Heiskanen and Moritz (1967), five times gravity data more than Tanni (1934) was available in the work of Heiskanen (1957), who also used electronic compute for numerical integration of O ga 5b i h 5Pda5ca e lfi 5 5 a 5 5 a e 5 da5ca e lfi jæ e j5 h e a 5 i e j5 a 5 lfi (2005) predicted the gravimetric geoid and produce the precise geoidal map of the Toshka sector in Southern part of Egypt using least square collocation. Also, Geodesy Group of University of Lagos (GGU, 2006) produced the geoidal map of Nigeria as part of their submissions for the Optimum geoid for Nigeria using classical method (Gravimetric and Earth Geopotential Model 1996 (EGM 96)).

However, it was observed that the classical and conventional methods are time consuming, expensive and laborious. Also, Amin et al, (2005) noted the common defects of all classical techniques for geoid determination such as the inadequate and inhomogeneous distribution of the used geodetic data. The disadvantages have prevented the widespread use of these methods and hence the advent of simpler and convenient methods such as the use of Global Navigation Satellite System (GNSS) combined with geodetic levelling. GNSS provide WGS84 ellipsoidal heights and when compared with orthometric heights, from geodetic levelling, it allows for the computation of the geoid, or the geoid-ellipsoid separation in the region of the survey (Aleem, 1996; Olaleye et al, 2010; Aleem et al, 2011). These height differences were used to derive da5ca e lfi ah5 lha 5 lha ah5 lh e j5i al5 5 hai 5 . , 5The geoid model will give geoidal undulation at every point of observation. This can be substituted with the ellipsoidal height from GNSS observation to get the orthometric height as given in Equation 1:

$$N = h - H \quad (1)$$

Where:

H = Orthometric height
h = Ellipsoidal height
N = geoidal height

From Equation 1, geoidal height can be computed which can be plotted on the map in form of spot heights. The geoidal at each point can be interpolated to produce the Geoidal map.

1.3 Interpolation of Geoidal Values:

Interpolations of geoidal undulations follow the same procedures as interpolations of contours which are often done by rough estimate. The procedure is to first plot all the available geoidal heights as point data on the map and estimate the point for the undulation. However, a more accurate but time consuming method used to be adopted is to use the formula for drafting contour which can be adopted for geoidal map as given by Aleem (2011):

$$PC = \frac{D}{Z} i \quad (2)$$

Where:

PC is distance from one of the spot height to the point of geoidal line will pass.
D is the distance between two spot heights
Z is the difference between the two spot heights
i is the difference between the geoidal line and one of the Spot heights.

Distance PC will then be scaled and marked on the map, which are later connected to form the geoidal line.

1.4 Significance

Geoidal maps are effective for displaying the geoidal configuration of a place. This is significance in geophysical study as it portrayed the geopotential configuration of the area under study. Therefore, it enhances the analysis of geological structures of the area.

This study is also significant because it reduces the rigour of data acquisition each time the geoidal map of the area is to be produced, when the geoidal coefficients have been determined. The use of software developed by the Author will enhance the productivity.

1.5 Software Adopted for Geoidal Map:

There are different types of software in the market for production of contour, digital terrain and three dimensional surface model. Any of these software can be used for production of geoidal map. This study used Surfer software.

1.5.1 Surfer.

Surfer is a Contouring and 3D surface mapping software package from Golden Software Incorporation can transform random surveying data, using interpolation engine. A sophisticated interpolation engine transforms your XYZ data into publication-quality maps. It is provided with eighteen different gridding/trend surface algorithms. The methods were grouped into smoothing and exact interpolators. Smoothing interpolators are: Inverse Distance to a Power, Kriging, Polynomial Regression, Radial Basis Function, Modified Shepard's Method, Local Polynomial, Moving Average; while the exact interpolators are: Inverse Distance to a Power, Kriging, Nearest Neighbor, Radial Basis Function, Modified Shepard's Method, Triangulation with Linear Interpolation, and Natural Neighbor. Any of these interpolation methods can be used to approximate the geoid in an area, if adequate data are available. Surfer provides more gridding methods and more control over gridding parameters. Recent edition has added conversion and combination of maps with different coordinate systems.

1.5.2 Other Contour Map Software for Production of Geoidal Map

Other Contour Map Software that can be adopted for production of geoidal map may include: 3DField, Garmin Basemap, mapviewer, Contour storyteller, Function Grapher, Auto plotter, Visual data, Filter test, AutoDEM Li Contour and several other software are available for production of Contour map. Any of these software can also be used for the production of geoidal map of the study area.

II. THE STUDY AREA

Port Harcourt lies on Latitude: $4^{\circ}45'N$ and $5^{\circ}02'N$ and Longitude: $6^{\circ}52'E$ and $7^{\circ}09'E$. It is the seat of Rivers State Government in oil rich Niger delta. Many companies, business organizations and government agencies locate and operate their corporate offices. Many of these organisations have used the services of surveyors for projects that needed height information. The surveyors, unable to get a bench mark to connect, will simply establish a local datum to do the work. This practice has created a situation where many different height values, which are irreconcilable, exist in the area. Therefore, this work reviews the need for simple method of obtaining values for the benchmark, which this study is trying to solve. The points used for the study were plotted on the local government map of Rivers State to show the distribution of points (Figure 1).

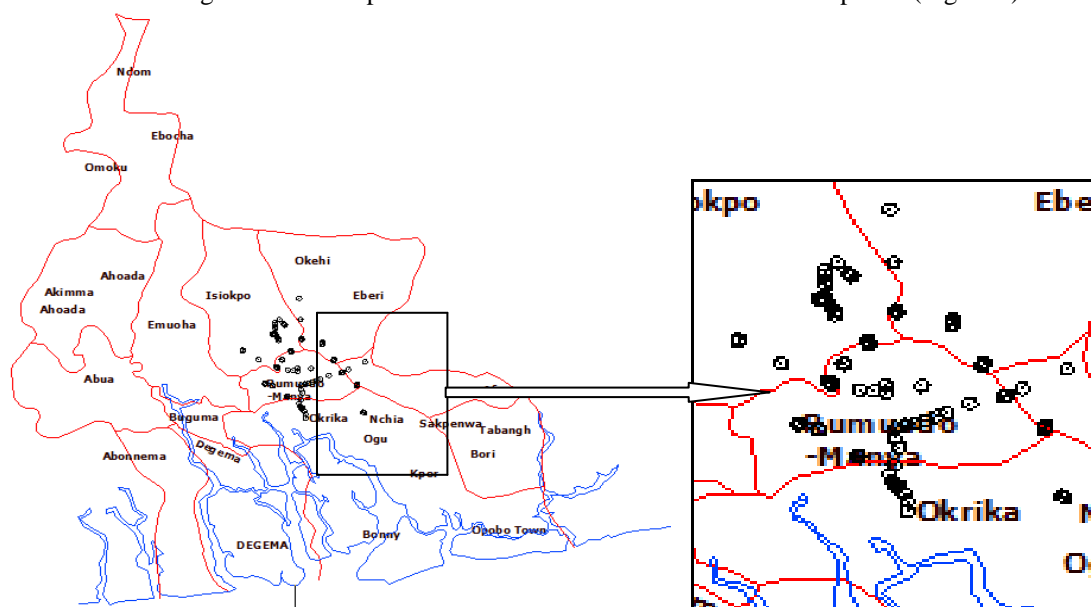


Figure 1: The Distribution of Points Used for the Study in Port Harcourt

III. METHODOLOGY

3.1 Materials and Data

The equipment needed for the exercise are:

- GNSS receiver and its accessories to acquire data for ellipsoidal height
- Level and its accessories to acquire data for orthometric height
- Computer and its accessories for computation and analysis

- Surfer software for plotting the geoidal values.
 - Any software or program that can implement least square adjustment.
- In this work Microsoft Office excel was used for all the computations, However Aleem, (2013) has validate the results.

3.2 Data Acquisition

Levelling operation was carried out to obtain data for orthometric height. GNSS observation was carried out to acquire geodetic coordinates which includes the geodetic latitude (), ca a e 5h jce a5) and ellipsoidal height (h). 86 points with good spatial distribution within the study area were covered. Other relevant data such constant for semi major axis, flattening and other parameter for the World Geodetic System WGS84 referenced ellipsoid were collected from various literatures and INTERNET websites for data analysis and processing.

3.3 Data Processing

Levelling reduction was carried; to obtain height of each point. These heath data were assumed to be the orthometric height. GNSS observation was processed to get the three dimensional coordinates, the geodetic latitude (), geodetic h jce a5 5 j 5a h e h d a e d 5 d 5 de d 5 a a5 a 5 j 5 a ah 5 h e j 5 ah

3.4 “Satlevel” Collocation Model:

O h a ah 5 h e j 5 a h 5 a ah a 5 5 h a i 5 . , P d a 5 a h e 5 h d a 5 b i 6

$$N_i = N_L + A_1 (\cos^3 \phi_i \cos \lambda_i + \sin^2 \phi_i \cos \phi_i \cos \lambda_i + \cos^3 \lambda_i \cos \phi_i + \sin^2 \lambda_i \cos \phi_i \cos \lambda) + A_2 (\cos^3 \phi_i \sin \lambda_i + \sin^2 \phi_i \cos \phi_i \sin \lambda_i + \cos^2 \lambda_i \cos \phi_i \sin \lambda_i + \sin^3 \lambda_i \cos \phi_i) + A_3 (\cos^2 \phi_i \sin \phi_i + \sin^3 \phi_i + \cos^2 \lambda_i \sin \phi_i + \sin^2 \lambda_i \sin \phi_i) + r_i \tag{3}$$

Where:

- N_L is the long wavelength part of the geoid undulation in the area.
- A₁, A₂ and A₃ are the geoidal coefficients which are unknown coefficients to be determined.
- j 5 5 a 5 d a 5 5 C O 5 4 0 5 c a a e 5 e j a 5 H e a s and Longitudes)
- r_i is residue at an observation point.

P d a 5 h a ah 5 h e j 5 a h 5 a ah a 5 5 h a i 5 . , P d a 5 a h e 5 h d a 5 b i 6 a 5 a a 5 i a 5 e j c 5 h a 5 a 5 f i a j 5 observation equation method.

P d a 5 h a ah 5 h e j 5 a h 5 a ah a 5 5 h a i 5 . , P d a 5 a h e 5 h d a 5 b i 6 a e used to compute the geoidal undulation (Table 1) of each point in the area.

The geoidal undulations were plotted into a chart (Figure 3) to form the geoidal surface.

P d a 5 c a e h j h e j 5 c a j a a 5 b i 5 h a ah 5 h e j 5 j 5 d a 5 c a a e 5 e j e s of the area were plotted into geoidal map using Surfer software (Figure 4).

Three dimensional geoid surface model (Figure 5) was plotted using the geoidal undulation and the Geodetic coordinates (Table 1)

IV. Results and Discussions

4.1 Results

The results of the orthometric heights acquired from the geodetic levelling and ellipsoidal heights from GNSS observation were substituted into Equation 1 to obtain the values of the geoidal undulation as shown in Tables 1.

Stations	Latitude [°]	Longitude [°]	Ellipsoidal Heights (h) [m]	Orthometric Heights (H) [m]	Geoid (N) [m]
GPS 02	4.988341858	7.005441514	42.542	23.638	18.904
GPS 03	4.981133603	6.949840522	40.065	21.24	18.825
GPS 04	4.972244803	6.951180808	38.771	19.938	18.833
GPS 05	4.988165797	6.959676808	41.357	22.523	18.834
GPS 06	4.976870211	6.950525386	39.485	20.657	18.828
GPS 07	4.968417417	6.950765697	38.351	19.516	18.835
GPS 08	4.956065461	6.949389547	36.427	17.585	18.842
GPS 60	4.91610835	6.881154569	20.982	02.189	18.793
XSV 662	4.873506919	6.99841315	27.603	08.648	18.955
ZVS 3003	4.847971022	7.047811589	32.308	13.282	19.026

Table 1: Sample of Orthometric heights and Geoidal Undulations of some of the Stations

Ca e h j h e j 5 b 5 da 5 O h a h 5 h e j 5 P h a 5. Si a h 5 i a 5 eng Equation 3 for Port Harcourt metropolis.

Table 2: Sample of Local and “Satlevel” Collocation Geoidal Undulations

STATIONS	Geoidal Undulation computed from Equation (1) [m]	O h a h 5 C a e h j h e j 5 i a 5 b i 5 A e j 5 [m]	Residuals
GPS 02	18.9040	18.8910	0.013
GPS 03	18.8250	18.8288	-0.0038
GPS 04	18.8330	18.8368	-0.0038
GPS 05	18.8340	18.8360	-0.002
GPS 06	18.8280	18.8327	-0.0047
GPS 07	18.8350	18.8390	-0.004
GPS 08	18.8420	18.8457	-0.0037
GPS 60	18.7930	18.7817	0.0113
XSV 662	18.9550	18.9548	0.0002
ZVS 3003	19.0260	19.0229	0.0031

The data acquired Table (1) were used to plot chart (Figure 2):

The values of the Geoidal coefficients computed using least square adjustment observation equation as:

$N_L = -5477.15802$
 $A_1 = 2714.485748$
 $A_2 = 375.21354$
 $A_3 = 214.34789$

Pda 5 a h 5 b da 5 h a h 5 h e j 5 C a e h j h e j 5 a a 5 h a 5 e j 5 d 5 e a 5 6

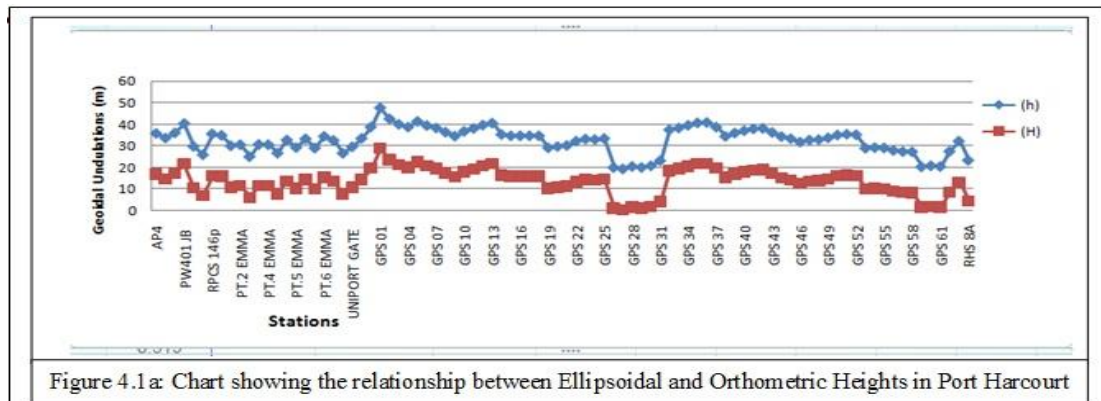


Figure 4.1a: Chart showing the relationship between Ellipsoidal and Orthometric Heights in Port Harcourt

Figure 2: Chart showing the relationship between Ellipsoidal and Orthometric Heights in Port Harcourt

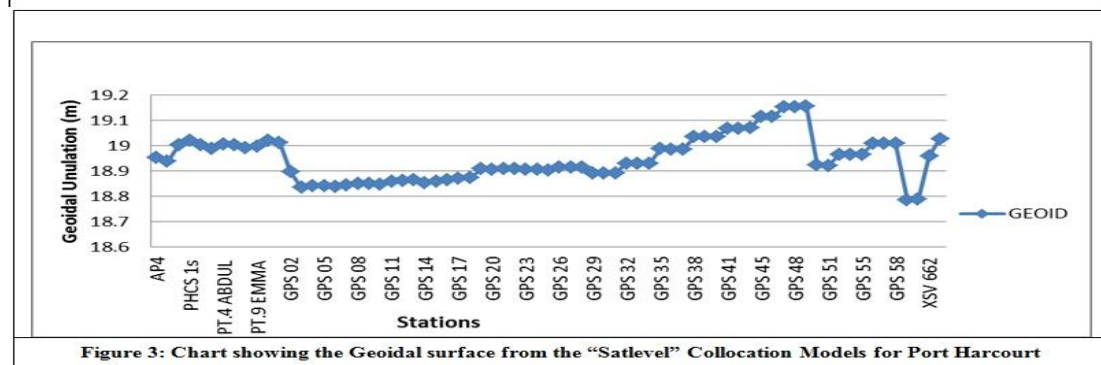


Figure 3: Chart showing the Geoidal surface from the “Satlevel” Collocation Models for Port Harcourt

Pda 5 O h a h 5 h e j 5 C a e h 5 e a 5 6

The geoidal map from geoidal undulation in Table 1 of Port Harcourt was plotted and overlaid on the Local Government map of Rivers State

Figure 4: Geoidal Map Plotted From “Satlevel” Collocation Model for Port Harcourt

The 3-D Geoid surface Model (Figure 5) was also plotted using Surfer software.

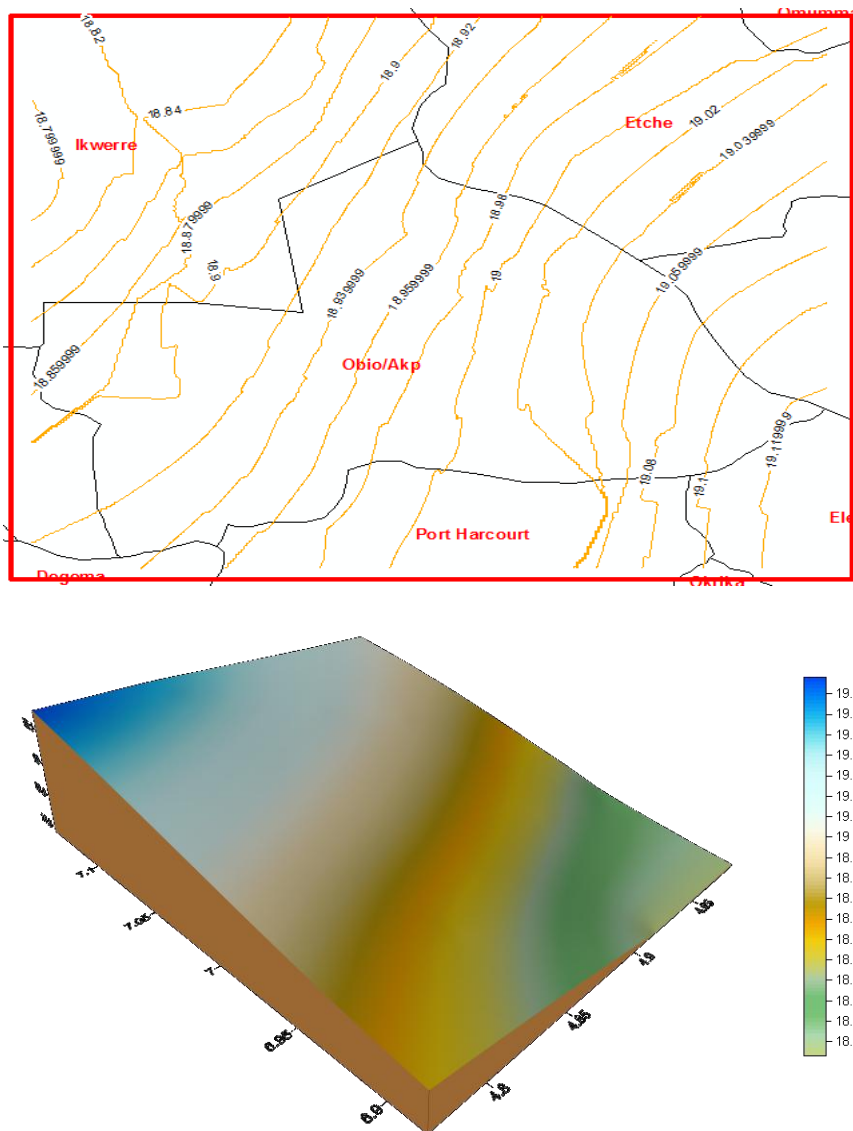


Figure 5: Three Dimensional Geoid Surface Model of part of Port Harcourt Metropolis

4.2 Discussion

Data Quality Validation. Verification of data quality is an important part of any geodetic and scientific research, as it helps to be ensuring that the data used in the models are accurate enough to satisfy the requirement of the application at hand. Data validation will assist in identification of suspicious and invalid cases such as outliers, variables, and data values in the active data set. Data acquisition for Geodetic levelling and DGPS were carried out by experienced surveyors, specifications for first order accuracy were strictly followed. The data were checked and the mean of height differences were taken as the most probable value of measurements. Therefore, the good quality of the data was guaranteed (Aleem, 2013). Ellipsoidal and orthometric heights were plotted inform of chart (Figure 4). The chart displayed that ellipsoidal and orthometric height follows the same pattern, which is an indication that the two surfaces are true representation of the same terrain.

The geoidal surface (Figure 3) of the area was plotted of Port Harcourt Presence of outliers were noted in the initial data were removed because they are more than 3 standard deviations (Heliani et al, 2004). The removals of outliers make the chart to be smoother. The geoidal map was produced using SURFER software and overlaid on the Local Government map of the Rivers State using Arc GIS software (Figure 4).

V. CONCLUSION AND RECOMMENDATION

5.1 Conclusion

In this study, levelled heights were established along with GPS observation in some parts of Port Harcourt to model the geoid in the study area. We have coordinated some of the points collocated with both GNSS and levelling in the area. 'Satlevel' Collocation Model was used to get the geoidal coefficients, which were used to get the geoidal undulation for each of the points. Ellipsoidal heights from GNSS observation were used to get the orthometric heights, and used to plot the geoidal map with surfer software.

5.2 Recommendations

The area of coverage needs to be extended and more data should be acquired to improve the results. Contracts for the production of maps should be awarded to the Institutions of Higher learning in the Nigeria. This will enable the participating staff to acquire more experience and impart same to the students, so as to improve the qualities of graduates for future challenges.

REFERENCES

- [1] K. F. Aleem. CLC j 5 ai a5Qaj ejc5 bAj e ji aj 5The Graduate Surveyors. Journal of NISS University of Nigeria, Enugu Campus. 12(1) 24 - 29. 1996
- [2] K. F. Aleem. Drafting and Mapping (GET 102). *Lecture Notes*. Department of Geomatics Engineering Technologies, Yanbu Industrial College, Kingdom of Saudi Arabia. UNPUBLISHED. 2011
- [3] K. F. mai 5 e j5 b 5Ch b d i a e 5 5H bDaacd 5 i 5 ejc5 O ha ah5 lh e j5l ah 5 5Ld 5 Thesis. Department of Surveying and Geoinformatics, University of Lagos Nigeria. UNPUBLISHED. 2013.
- [4] K. F. Aleem, J. B. Olaleye, O. T. Badejo and J. O. Olusina 5 5 i ej e j5 bAlte e bDaacd 5b i 5O alte a5l a d 5 j 5 Orthometric Height for Geoid Modelling *M S d S d* 2011. <http://ignss.org/Conferences/PastPapers/2011ConferencePastPapers/2011PeerReviewedPapers/tabid/108/Default.aspx>
- [5] M. M. Amin, S. M. El- e 5 j 5 5l 5D j 55 L a ese Geoidal Map of the Southern Part of Egypt by Collocation Toshka Ca e 5From Pharaohs to Geoinformatics. *FIG Working Week 2005* Cairo, Egypt April 16-21, 2005
- [6] Geodesy Group University of Lagos (GGU). Determination of an Optimum Geoid for Nigeria. A *Project Report* Sponsored by Centre for Geodesy and Geodynamics (CCG) and the National Space Research and Development Agency (NASRDA) Abuja, Nigeria. 2006.
- [7] C h aj5O b a 5Ej 5. , . 5 Surfer 11: Powerful Contouring, Gridding, and 3D Surface Mapping Software for Scientists and Engineers 5 j leja5 e ha5 a a 5 j5 .th November 2012 <http://www.goldensoftware.com/products/surfer/surfer.shtml>
- [8] L. S. Heliani, Y. Fukuda, and S 5P gai 5 Qa h e j5 b da5Ej ja e j5H j 5C e 5 5 ejc5 5 œe bPa ej5l alf Data. *Earth Planets Space* 52 6 l 24. 2004
- [9] W. A. Heiskanen. The Columbus Geoid. *Trans. Am. Geophys. Union*, 38:841-848. 1957
- [10] Heiskanen, W.A., and H. Moritz. *Physical Geodesy*. San Francisco, California: W.H. Freeman and Co. 1967
- [11] J. B. Olaleye.,; K. F. Aleem, J. O. Olusina and O. E. Abiodun . Establishment of an empirical Geoid Model for a Small Geographic Area: A Case Study of Port Harcourt, Nigeria. *Surveying and Land Information Science*. 70(1): 39-48(10). 2010 <http://www.ingentaconnect.com/content/nsps/salis/2010/00000070/00000001/art00006>
- [12] Tanni, L. On the Continental Undulation of the Geoid as Determined from Present Gravity Materials:. Helsinki Publishers Isostatic institute. International Association of Geodesy. No. 18. 1948
- [13] Tanni, L. (1949). *The Regional Rise of Geoid in Central Europe Materials*. Helsinki Publishers Isostatic institute. International Association of Geodesy. No. 22.

Design and development of Optical flow based Moving Object Detection and Tracking (OMODT) System

Ms. Shamshad Shirgeri¹, Ms. Pallavi Umesh Naik², Dr.G.R.Udupi³,
Prof.G.A.Bidkar⁴

^{1,2}Student of M.Tech in Industrial Electronics, ³Principal, ⁴Asst.prof & HOD E&C Dept
KLS's VDRIT, Haliyal affiliated to VTU, Belgaum, and Karnataka, India.

ABSTRACT:

Moving object detection and tracking is often the first step which has attracted a great interest from computer vision researchers due to its applications in areas, like video surveillance, traffic monitoring and image recognition. Moving object detection involves identification of an object in consecutive frames where as object tracking is used to monitor the movements with respect to the region of interest. We propose, Optical Flow Based Lucas - Kanade algorithm using different smoothing techniques for a single and multiple object detection and tracking have been developed. Lukas – Kanade algorithm with Sobel, Sobel and Gaussian smoothing techniques is used in this paper to compute Optical Flow vectors. Single object and multiple object movements in an frame with respect to the computed vectors are segmented with the help of Threshold which is specified depending on the value mentaioned. The extracted movements are tracked using Sobel edge and Centroid information. This paper describes an smoothing algorithm to estimate Moving object detection using image processing technique using Matlab Software.

Keywords - Image Pyramid Segmentation, Optical Flow Method, Sobel edge detection, Thresholding value, tracking.

I. INTRODUCTION

Motion detection and tracking has attracted a great interest from computer vision researchers due to its promising applications in areas, like video surveillance, traffic monitoring and image recognition. Motion detection can be used to study a large variety of motions like motion with respect to moving observer and static objects, static observer and moving objects or movement with respect to both [1]. There are several techniques for moving object detection, commonly used approaches are based on Optical Flow and background subtraction techniques. Based on existing work [1] suggests that the method by Lucas - Kanade is consistent in computing Optical Flow vectors. In this work analysis on Lucas - Kanade algorithm based on smoothing techniques has been performed for better accuracy in computed Optical Flow vector. The computation time has been reduced using image pyramid concept.

II. BLOCK DIAGRAM OF MOVING OBJECT DETECTION AND TRACKING

Figure1 depicts the block diagram of a method.

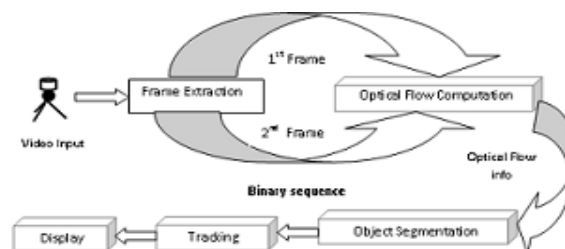


Figure 1 Optical Flow based Moving object detection and tracking method

Figure 1 contains mainly three parts they are:

- **Optical Flow Computation**
- **Object Segmentation**
- **Object Tracking**

In Optical Flow computation frame to frame Optical Flow vectors can be calculated. Object Segmentation includes multiple Object Segmentation in which computed Optical Flow Vectors are used to determine whether the pixels in the frame belong to movement or not. The Object Tracking part involves overlapping of edge information or building Boundary box over the segmented image to highlight the movement has been carried out.

2.1. The steps involved in motion detection and tracking system are as follows

- Extraction of image sequences from the input video
- Finding the moving objects for consecutive frames using Lucas - Kanade and background subtraction algorithm.
- Segmenting the regions where there is movement using thresholding operation
- Enhancing the segmented result using morphological operations.
- Highlighting the multiple objects tracking using edge or boundary box over centroid.

III. LITERATURE REVIEW

The following points has been summarized by referring journals, manuals and related documents

- The Lucas - Kanade Optical Flow works with the assumption of local flow at constant rate and the intensity of each point is constant between frames.
- The first order local differential methods are the most reliable ones that produce accurate vectors.
- The differential method does not generate Optical Flow in case of stationary moving objects (same intensity) with respect to stationary camera.
- The filtering and segmentation algorithm needs to be improved with respect to computation time suitable for real time applications.
- Use of multi resolution techniques such as image pyramid concepts, the computation time can be reduced.
- The work with respect to moving background with moving object (dynamic) has not been discussed in the most of literatures.
- Software's used with respect to the development of Optical Flow based application are MATLAB, SIMULINK, Visual C++ and Open CV.

IV. OPTICAL FLOW MOTION ANALYSIS

Optical Flow methods can be computed by using two images taken at time t and $t + \delta t$; since they deal with the Taylor series, they're also called as differential methods, as they work with the spatial $I(x, y)$ and temporal $I(t)$ derivatives. Assume that the image intensity of each visible scene point is unchanging over time.

$$I(x, y, t) = I(x+\delta x, y+\delta y, t+\delta t) \tag{1}$$

Assuming that the movement is small, the image constraint at $I(x, y, t)$ with Taylor series can be derived to give:

$$I(x + \delta x, y + \delta y, t + \delta t) = I(x, y, t) + \frac{dI}{dx} \delta x + \frac{dI}{dy} \delta y + \frac{dI}{dt} \delta t + H.O.T \tag{2}$$

From equation (2), by ignoring high order terms, we will get

$$\frac{dI}{dx} \delta x + \frac{dI}{dy} \delta y + \frac{dI}{dt} \delta t = 0 \tag{3}$$

Dividing equation (3) by δt results in

$$\frac{dI}{dx} (\delta x / \delta t) + \frac{dI}{dy} (\delta y / \delta t) + \frac{dI}{dt} = 0 \tag{4}$$

Rewriting the equation (4)



$$\frac{dI}{dx} V_x + \frac{dI}{dy} V_y + \frac{dI}{dt} = 0 \quad (5)$$

The obtained equation (5) is the Optical Flow constraint equation, which expresses a constraint on the components V_x and V_y of the Optical Flow lying on the X axis and on the Y axis respectively and (dI/dx) , (dI/dy) , (dI/dt) are the derivatives of the image at (x,y,t) . The Optical Flow constraint equation can be rewritten as shown in equation (6 and 7):

$$I_x V_x + I_y V_y = -I_t \quad (6)$$

Or, equivalently

$$[I_x \ I_y] \begin{bmatrix} V_x \\ V_y \end{bmatrix} = -I_t \quad (7)$$

The Optical Flow algorithms are mostly based on correlation, gradient and frequency information respectively. Some common algorithms for computing Optical Flow vectors are block matching for correlation, Lucas-Kanade and Horn –Schunck for gradient and phase- based filtering for frequency. Barron et al. In their work compared the accuracy of different Optical Flow techniques both real and synthetic method based on Lucas and Kanade method is consistent in producing accurate depth maps with good noise tolerance. Hence we will delve into Lucas-Kanade algorithm.

V. LUCAS KANADE OPTICAL FLOW ALGORITHM

The Lucas-Kanade algorithm assumed that motion vectors in any a given region do not change but merely shift from one position to another. Assuming that the flow (V_x, V_y) is constant in a small window of size $m \times m$ with $m > 1$, which is centered at (x, y) and numbering the pixels as $1..n$, a set of equations can be derived [1].

$$\begin{aligned} I_{x1} V_x + I_{y1} V_y &= -I_{t1} \\ I_{x2} V_x + I_{y2} V_y &= -I_{t2} \\ &\vdots \\ I_{xn} V_x + I_{yn} V_y &= -I_{tn} \end{aligned} \quad (8)$$

It is seen from equation (8); the system is over-determined since there are more than three equations for the three unknowns [1]. Hence equation can be rewritten as;

$$\begin{bmatrix} I_{x1} & I_{y1} \\ \vdots & \vdots \\ I_{xn} & I_{yn} \end{bmatrix} \begin{bmatrix} V_x \\ V_y \end{bmatrix} = \begin{bmatrix} -I_{t1} \\ \vdots \\ -I_{tn} \end{bmatrix} \quad (9)$$

Or

$$A \vec{V} = (-b) \quad (10)$$

To solve the determined system of equations, the least squares method is used [1].

$$(A)^T A \vec{V} = (A)^T (-b) \quad (11)$$

$$\vec{V} = (A^T A)^{-1} A^T (-b) \quad (12)$$

Or

$$\begin{bmatrix} \sum I_x^* I_x & \sum I_x^* I_y \\ \sum I_x^* I_y & \sum I_y^* I_y \end{bmatrix} \begin{bmatrix} u \\ v \end{bmatrix} = \begin{bmatrix} \sum I_x^* I_t \\ \sum I_y^* I_t \end{bmatrix} \quad (13)$$

Equation (13) is written as

$$A^T A = \begin{bmatrix} \sum I_x^2 & \sum I_x I_y \\ \sum I_x I_y & \sum I_y^2 \end{bmatrix} \quad (14)$$

VI. IMAGE ACQUISITION

First stage of vision system is the image acquisition stage. After the image has been obtained, some processing methods can be applied to the image to perform different vision tasks. If the image has not been acquired satisfactorily then the intended tasks may not be achievable, even with some form of image enhancement. Video Signal must be digitised. Digitises the incoming video signal Samples signal into discrete pixels at appropriate intervals -- line by line. Samples signal into a (8 bit) digital value. Stores sample frame own memory. Frame easily transferred to computer memory or a file.

VII. COMPUTATION OF SPATIAL AND TEMPORAL DERIVATIVE

In this section we discuss about the methods used to compute derivatives needed in order to estimate Optical Flow vectors. Sobel operator are used here to compute the spatial and temporal derivative.

7.1. Sobel Operator

A widely used technique for spatial derivatives computing is the convolution by using the Sobel Operator. It is a differential operator computing an approximation of the gradient of the image intensity and it's very fast to apply since it's based on a small window (3x3 kernels) to convolve with the full image. Which is also used to detect edges of a image, because by using it we'll obtain some white where the intensity changes abruptly and black when it does not have any changes. We refer to two matrices, one for the gradient over the X axis, and one for the gradient over the Y axis; consider an image I, convolving it two times in order to obtain Gx and Gy, that are the images containing the approximation of spatial derivatives. The temporal derivative (It) is calculated by subtracting the frame taken at time t + δt (second frame) from t (first frame) [1].

$$G_x = \begin{bmatrix} 1 & 0 & -1 \\ 2 & 0 & -2 \\ 1 & 0 & -1 \end{bmatrix} * A \quad \& \quad G_y = \begin{bmatrix} -1 & -2 & -1 \\ 0 & 0 & 0 \\ 1 & 2 & 1 \end{bmatrix} * A \quad (15)$$

VIII. OPTICAL FLOW VECTORS COMPUTATION

The spatial and temporal derivatives I(x, y, t) using Sobel operator are found. The Optical Flow vectors with the components 'u' and 'v' for each region are calculated by applying windowing concept over these. Since Lucas - Kanade hypothesis assumes that all the pixels in an m×m window have the same velocity components, this parameter allows us to choose how big is the windows size and as direct consequence, the density of Optical Flow vectors. To achieve good results and to avoid noise, neighborhood window must be tuned in both Least squares windowing approach. Figure 2 shows block diagram of Lucas - Kanade Optical Flow computation.

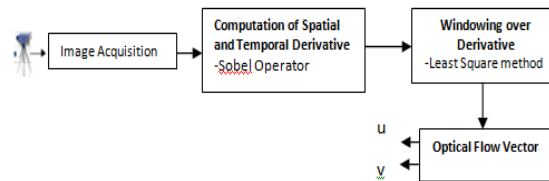


Figure 2 Figure shows the block diagram of Optical Flow based Lucas – Kanade computation

8.1. Least Square method

After finding the derivatives that is spatial and temporal I(x; y; t) from Sobel edge detection. The optic flow vectors with the components u and v for each region are calculated using equation 19 (Least squares method) and equation is as follows:

$$\begin{bmatrix} u \\ v \end{bmatrix} = \begin{bmatrix} \sum I_x * I_x & \sum I_x * I_y \\ \sum I_x * I_y & \sum I_y * I_y \end{bmatrix}^{-1} \begin{bmatrix} \sum I_x * I_t \\ \sum I_y * I_t \end{bmatrix} \quad (16)$$

IX. IMAGE PYRAMID

Image pyramid is used for reducing the resolution of the image. By using the concept of Image pyramid, the size of the image gets reduced by 1/4th and which helps in avoiding dense vectors resulting in smooth vector computation with reduction in computational time.

X. OBJECT SEGMENTATION

In order to segment the moving object, the resultant Optical Flow vectors are used to determine whether the pixels in the frame belong to movement or not. Thresholding over the Optical Flow vectors has been performed to separate the moving region. The threshold is a dynamic parameter and its value may change from one frame to the next due to several factors including weather, illumination and camera settings. The main challenge within the segmentation block is the handling of small Optical Flow vectors. These may be associated with either background noise or with slow moving, but relevant objects. The threshold equation is given by

$$of_s = \left(\left| \sqrt{u^2} + \sqrt{v^2} \right| \right) \quad (17)$$

Where “ofn” is the absolute value for Optical Flow and threshold is set as mean(mean(abs(of))); to eliminate background noise or with slow moving, median filter and morphologic processing is used, and the segmented object is given to tracking [2].

$$y_n = \begin{cases} 255 & \text{if } (of_n > \text{threshold}) \\ 0 & \text{otherwise} \end{cases} \quad (18)$$

XI. OBJECT TRACKING

Optical Flow vectors are used for tracking. Objects trajectories are represented by edges and Centroid based object tracking. In multiple objects tracking part, the overlapping of edge information or building of boundary box over the segmented image to highlight the movement has been carried out.

XII. EXPERIMENTAL RESULTS

This section provides the details about the results of motion detection and tracking. It also describes the use of image pyramid concept in real time applications like video surveillance. Implementation of developed algorithm has been tested under MATLAB platform.

12.1. Test Input and results for with and without Image Pyramid

Image pyramid is used for reducing the resolution of the image. By using the concept of Image pyramid, the size of the image gets reduced by 1/4th and which helps in avoiding dense vectors resulting in smooth vector computation with reduction in computational time. Figure 2 shows input sequences of car, captured by static camera with resolution of 160x120 pixels and frame rate of 15fps.

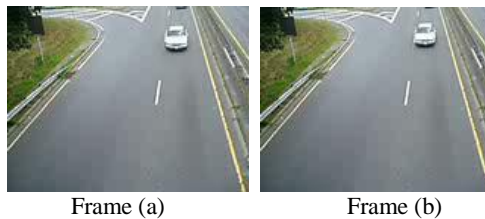


Figure 3 Input sequence of car

The expected Optical Flow vectors of the car will be as in the direction of car rotation, as camera and the background is static.

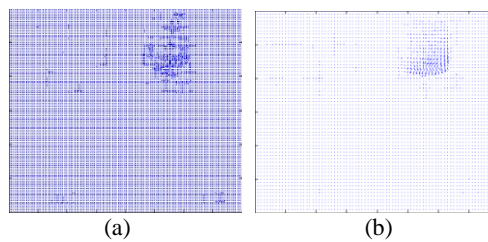


Figure 4 Optical Flow vectors for with and without image pyramid.

Figure 4 (a) shows the Optical Flow vectors obtained using Lucas – Kanade without using image pyramid over the input sequence. Figure 4 (b) shows Optical Flow vectors obtained using Lucas – Kande algorithm with 2 level image pyramid respectively. The Optical Flow vectors obtained without image pyramid has more density, which leads to overlap of the information’s and increase the computation time. Image Pyramid results to overcome these problems and provide smoother vector results with less density, high accuracy and better computation time.

XIII. MATLAB IMPLEMENTATION FOR MOVING OBJECT DETECTION AND TRACKING USING STATIC CAMERA WITH STATIONARY BACKGROUND

A test case Image sequence with 360x240 pixel resolution has been taken. This has movement with respect to a person with static background and stationary camera. The two image sequences with respect to test case are shown in Figure 5.



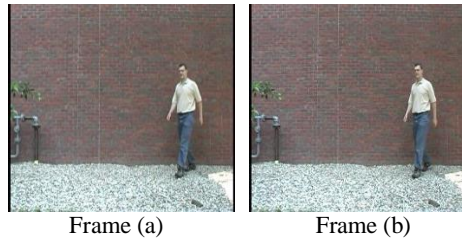


Figure 5 Input sequences of man

Optical Flow vectors will be in the direction of movement of the person. The identified movements have been segmented by using Thresholding operation. The segmented movements are tracked using edge based method. The Optical Flow vectors using Sobel based Lucas – Kanade approach without image pyramid is shown in the Figure 6.

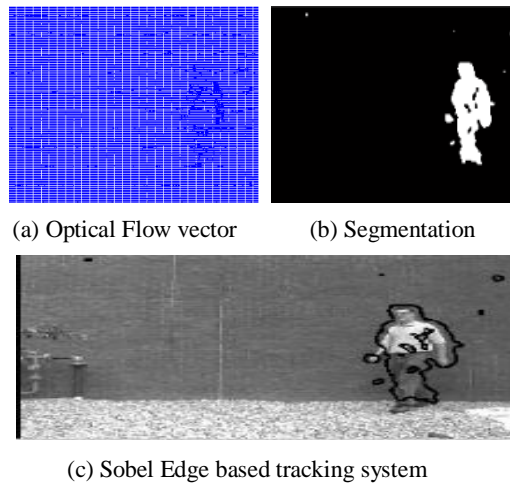


Figure 6 Detection and Tracking of moving object using Sobel Operator based Lucas – Kanade Optical Flow based algorithm without image pyramid implemented on MATLAB.

Figure 6 (a) shows Optical Flow vector of person movement. Figure 6 (b) shows selecting suitable threshold over the Optical Flow vector result. The Edge based information for the input sequence is shown in Figure 6 (c).

The Optical Flow vector using Sobel based Lucas – Kanade approach with image pyramid is shown in the Figure 7.

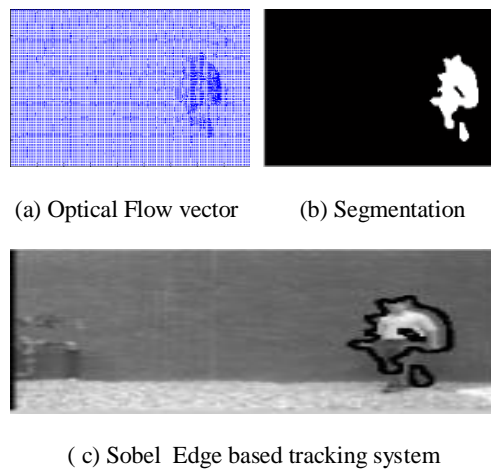


Figure 7 Detection and Tracking of moving object using Sobel Operator based Lucas – Kanade Optical Flow based algorithm with image pyramid implemented on MATLAB.

The Optical Flow vectors with image pyramid has more density, leads to overlap of the information and increases computation time.

10. MATLAB IMPLEMENTATION OF MULTIPLE MOVING OBJECTS DETECTION AND TRACKING USING STATIC CAMERA WITH STATIONARY BACKGROUND

A test case Image sequence with 160x120 pixel resolution has been taken. This has movement with respect to a car with static background and stationary camera. The two image sequences with respect to test case are shown in Figure 8.

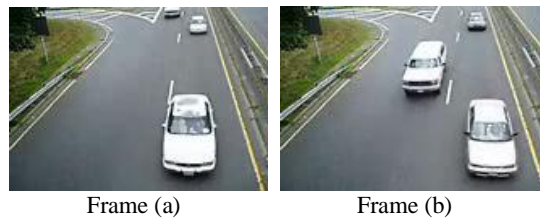


Figure 8 Input sequences using static camera with static background

Optical Flow vectors will be in the direction of movement of the person. The identified movements have been segmented by using Thresholding operation. The segmented movements are tracked using edge based method. The Optical Flow vectors using Sobel based Lucas – Kanade approach without image pyramid is shown in the Figure 9.

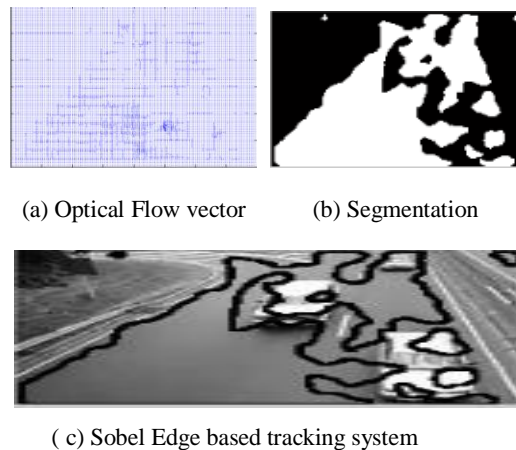
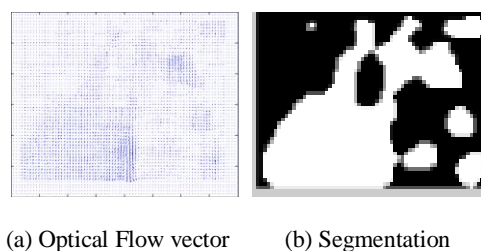


Figure 9 Detection and Tracking of moving object using Sobel Operator based Lucas – Kanade Optical Flow based algorithm without image pyramid implemented on MATLAB.

Figure 9 (a) shows Optical Flow vector of person movement. Figure 9 (b) shows selecting suitable threshold over the Optical Flow vector result. The Edge based information for the input sequence is shown in Figure 9 (c).

The Optical Flow vector using Sobel based Lucas – Kanade approach with image pyramid is shown in the Figure 10.





(c) Sobel Edge based tracking system

Figure 10 Detection and Tracking of moving object using Sobel Operator based Lucas – Kanade Optical Flow based algorithm with image pyramid implemented on MATLAB.

The Optical Flow vectors with image pyramid has more density, leads to overlap of the information and increases computation time. The Optical Flow vector result using Sobel operator based Lucas Kanade approach is shown in Figure 10(a) gives the details of cars movement. Figure 10(b) is obtained by selecting suitable threshold value over the Optical Flow result obtained. The extracted edge information with respect to the segmented movement is overlapped over the input sequence and shown in Figure10(c).

XIV. Conclusion

The obtained Optical Flow vectors without image pyramid has more density, which leads to overlap of the information's and increases the computation time. Image pyramidal results overcome these problems and provide smoother vector results with less density, high accuracy and better computation time Image pyramid in low resolution test sequence results in loss of information because the input image size is too small and contains very low resolution data. Hence the application of image pyramid should be selected always based on the input image resolution. The obtained results using Sobel operator based Lucas Kanade approach gives better accuracy in vectors with reduced computation time.

REFERENCES

- [1]. Motion Detection Based on Accumulative optical Flow and double background Filtering”, By Nan Lu, Henry Wu .
- [2]. Fonseca, A., Mayron, L., Socek, D., and Marques, O., “Design and Implementation of an Optical Flow-Based Autonomous Video Surveillance System”.
- [3]. Image Processing using Genetic Algorithm (GA)”, International Conference on Image Processing and Pattern Recognition, By Dr.G.R.Udupi [May 24th,2000].
- [4]. Arvind Ananthan and Joseph Tarkoff, Targetting Analog Devices Blackfin and SHARC from MATLAB, http://www.mathworks.com/webex/recordings/AnalogDevices_072909/index.html [accessed January 4, 2011]
- [5]. ANN Based SVC switching at Distribution Level for Minimal Injected harmonics”, IEEE India International Conference POWERCON, By Dr.G.R.Udupi, [Oct 2008].
- [6]. Sener Yilmaz and Mete Severcan, complex discrete wavelet transform based motion estimation for vision-based tracking of targets, [accessed January 4, 2011]
- [7]. Sivabalakrishnan M., and Dr.Manjula D, An Efficient Foreground Detection Algorithm for Visual Surveillance System.
- [8]. Vivek Anand and Taruja Borker, Real Time Video Processing, University of Florida.
- [9]. Sergey M Sokolov, Andrey A. Boguslavsky and Felix A. Kuftin, Vision System for Relative Motion Estimation from Optical Flow, Russia.
- [10]. Giuseppe Catalano, Alessio Gallace, Bomi Kim, Sergio Pedro and Francesco Bomi Kim, Optical Flow.
- [11]. VIDEO IMAGE PROCESSING TO CREATE A SPEED SENSOR by D.J. Dailey and L. Li ITS Research Program.
- [12]. The Autonomous Detection and Tracking of Moving Objects - A Survey Work P Sanyal, S K Bandyopadhyay.
- [13]. Audio Visual Speaker Association for Embodied Conversational Agents Trent Lewis, M. Luerksen, Sean Fitzgibbon, David Powers.

Design and Development of Medium Access Control Scheduler in LTE eNodeB

Ms. Pallavi Umesh Naik¹, Ms. Shamshad Shirgeri², Dr.G.R.Udupi³,
Prof. Plasin Francis Dias⁴

^{1, 2} Student, M.Tech in Industrial Electronics, ³Principal, ⁴Assistant.Professor, E&CE Department
^{1, 2, 3,4} VDRIT, Haliyal affiliated to VTU, Belgaum, Karnataka, India.

ABSTRACT

Long Term Evolution (LTE) is a major step in mobile radio communications, and is beyond
L FDMA as its radio access
G technology with advanced antenna technologies such as Multi-Input Multi-Output (MIMO), for both
downlink and uplink. LTE is a system with complex hardware and software. In case of Long Term
Evolution (LTE), the scheduler in the Medium Access Control (MAC) layer of the eNodeB allocates the
available radio resources among different UEs in a cell through proper handling. LTE schedulers are
part of layer 2 protocol stack and are one such module which can dramatically increase or decrease
the performance of the system. In this paper, we are presenting various types of scheduling schemes of
LTE and their advantages. The output conditions such as memory usage and execution time for varying
number of users are investigated for three of the scheduling methods: Proportional Fair (PF),
Modified-Largest Weighted Delay First (MLWDF) and EXP-Proportional Fair (EXP-PF) scheduling
algorithm. Developed algorithms are tested for single-cell/multi-cell with multiple-user scenarios in
both TDD/FDD frame structure.

Keywords: Evolved Packet Core (EPC), Evolved UMTS (Universal Mobile Telecommunication System) Terrestrial Radio Access Network (EUTRAN), Long Term Evolution (LTE), and Medium Access Control (MAC) layer Scheduling.

I. INTRODUCTION

LTE of UMTS is just one of the latest steps in an advancing series of mobile telecommunications systems and introduced in 3rd Generation Partnership Project (3GPP) Release8. LTE uses orthogonal Frequency Division Multiplexing (OFDM) and Single-Carrier Orthogonal Frequency Division Multiple Access (SC-FDMA) as its radio access technology with advanced antenna technologies such as Multi-Input Multi-Output (MIMO). Duplexing is a method for two-way transmission in either frequency domain or time domain. Downlink carries information from eNodeB to UE while uplink carries information from UE to eNodeB. Frequency Division Duplexing (FDD) and Time Division Duplexing (TDD) are two duplexing schemes used in LTE. TDD uses single channel for both downlink and uplink transmission. Separate time slots are allocated for downlink and uplink. FDD and TDD both require guard band or guard interval for effective operation and to
H stack of LTE for both uplink and downlink. Uplink supports the SC-FDMA technology whereas downlink supports OFDMA technology as an access method [1].

OFDMA facilitates distribution of subcarriers to different users at the same time. In practice group of contiguous subcarriers are allocated to single user. OFDM is a popular multicarrier scheme in which closely spaced subcarriers are used to carry data in LTE downlink. LTE uses novel SC-FDMA scheme in uplink which has lower power amplification ratio compared to OFDMA and thus facilitating low-complexity and frequency-domain equalization at the receiver. One of the major drawbacks of using OFDM is high power amplification ratio [2]. Power amplification ratio is the measure of high dynamic range of input amplitude.

II. LTE ACCESS NETWORK ARCHITECTURE

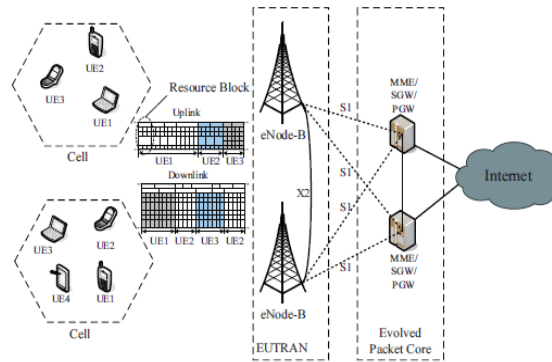


Figure1: 3GPP LTE access network (E-UTRAN) architecture

Figure1 shows an architecture of LTE network. Its functionality is divided into 3 main domains: User Equipment (UE), Evolved UMTS(Universal Mobile Telecommunication System) Terrestrial Radio Access Network (EUTRAN), and System Architecture Evolution (SAE) core also known as Evolved Packet Core (EPC). EUTRAN consists of eNodeBs which are connected by another eNodeBs by the X2 interface, and they connect to EPC networks by S1 interface. The EPC network serves as the equivalent GPRS network via 3 components: Mobility Management Entity(MME) which provides tracking and paging for idle mode UEs , Serving Gateway (SGW) which provides switching and routing for user data packets and PDN(packet data network) gateway(PGW) which provides access to external networks such as internet.

In LTE DL(downlink) and UL(uplink), the systems bandwidth is divided into separable chunks denoted as Resource Blocks(RBs) in figure1. It is considered as the minimum scheduling resolution in the time-frequency domain. The frequency domain packet scheduling(FDPS) allocates different RBs to individual users according to their current channel conditions. This FDPS policy is conducted during each Transmission Time Interval (TTI) which is 1ms.

III. THE EPC NETWORK ELEMENTS

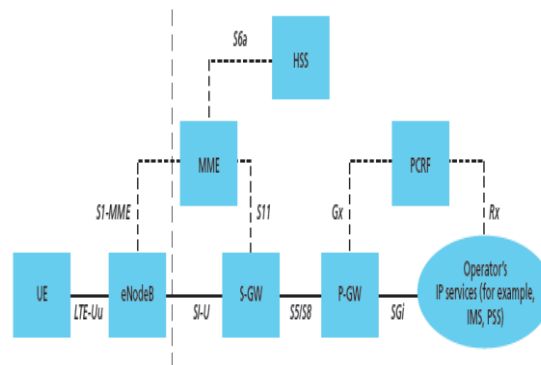


Figure2: The EPS network elements

EPC provides the user with IP connectivity to a PDN for accessing the Internet, and also for running services such as Voice over IP (VoIP). An EPC bearer is typically associated with a QoS. Many bearers can be established for a user in order to provide different QoS streams or connectivity to different PDNs. As an example we consider, a user might be engaged in a voice (VoIP) call while at the same time performing web browsing or FTP download. The network must also provide sufficient security and privacy for the user and protection for the network against fraudulent use. This is achieved by means of several EPC network elements that have different roles. Figure2 shows the overall network architecture, which includes the network elements. The network is comprised of the Core Network (CN) EPC and the access network E-UTRAN. CN consists of many logical nodes, but the access network is made up of essentially just one node, the evolved NodeB (eNodeB), which connects to the UEs.

The logical CN nodes are shown in Figure2 consists of:

PCRF C The Policy Control and Charging Rules Function (PCRF) is responsible for policy control decision-making and for controlling the flow-based charging functionalities in the Policy Control Enforcement Function (PCEF), which resides in the P-GW. The PCRF provides the QoS authorization that decides how a certain data flow will be treated in the PCEF and ensures that this is in accordance

H

HSS C The Home Subscriber Server (HSS) contains users SAE subscription data such as the EPS subscribed QoS profile and any access restrictions for roaming. It contains information about the PDNs to which the user can connect. It could be in the form of an access point name (APN) (which is a label according to DNS naming conventions describing the access point to the PDN) or a PDN address indicating subscribed IP address. In addition the HSS holds dynamic information such as the identity of the MME to which the user is currently attached. The HSS may also integrate the authentication centre (AUC), which generates the vectors for authentication and security keys.

P-GW C The PDN Gateway is responsible for IP address allocation for the UE, QoS enforcement and flow-based charging. It is responsible for the filtering of downlink user IP packets into the different QoS-based bearers which is performed based on Traffic Flow Templates (TFTs). The P-GW performs QoS enforcement for guaranteed bit rate (GBR) bearers which also serves as the mobility anchor for interworking with non-3GPP technologies such as CDMA2000 and WiMAX networks.

S-GW C All user IP packets are transferred through the Serving Gateway (S-GW) which serves as the local mobility anchor for the data bearers when the UE moves between eNodeBs. S-GW retains the information about the bearers when the UE is in the idle state and temporarily buffers downlink data while the MME initiates paging of the UE to reestablish the bearers. The S-GW performs some administrative functions in the visited network such as collecting information for charging. It also serves as the mobility anchor for interworking with other 3GPP technologies such as general packet radio service (GPRS) and UMTS.

MME C The Mobility Management Entity (MME) is the control node that processes the signalling between the UE and the CN and the protocols running between the UE and the CN are known as the Non Access Stratum (NAS) protocols.

IV. E-UTRAN LAYERED ARCHITECTURE

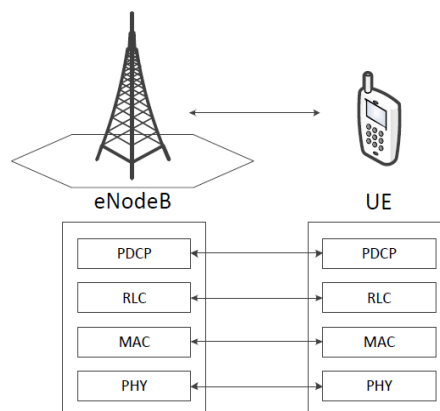


Figure 3: E-UTRAN architecture

Figure3 provides an overall illustration of the protocol architecture at the E-UTRAN level . The top three protocols are the sublayers of the TCP/IP Layer 2, while the PHY layer forms LTE's TCP/IP Layer 1.

- Layer 2 (L2)
 - Packet Data Convergence Protocol (PDCP)
 - Radio Link Control (RLC)
 - Medium Access Protocol (MAC)
- Layer 1 (L1)
 - Physical Layer(PHY)

PDCP Layer:

PDCP layer is mainly responsible for header compression/decompression of IP packets that are received from/transmitted to IP layer above, respectively. The header compression is critical in reducing the overhead of data communication over the wireless interface, which in turn increases the system's spectral efficiency. PDCP also ensures in-sequence delivery of data packets either up to the IP layer or down to the RLC layer. This sequential delivery mechanism ensures that PDCP detects missing packets for which it can initiate retransmissions, or duplicate packets that are to be discarded. PDCP also performs packet ciphering and packet encryption to ensure the secure delivery of data packets over the radio interface.

RLC Layer:

RLC layer facilitates the transfer of data units between PDCP and MAC sublayers. In doing so, RLC performs tasks similar to PDCP, such as in-sequence packet delivery and duplicate packet detection. RLC performs error correction of data packets received from MAC layer below through window-based Automatic Repeat reQuest (ARQ) operation. RLC also performs segmentation and re-assembly of data units that are passed down to/received from MAC sublayer below. To perform such a task, RLC layer contains the transmit/receive data buffers for different traffic flows, which are alternatively known as Radio Bearers (RBs). RB refers to a traffic flow, or a group of traffic flows, between a UE and the eNodeB over the radio interface that is characterized with certain QoS attributes. It ensures that RLC tailors its services to RBs according to their QoS needs, such as providing ARQ services to RBs with best effort traffic low very tolerance to packet loss.

MAC Layer:

The main task of MAC sublayer in LTE is to map between logical channels and PHY's transport channels. The Logical channels are services provided by MAC to RLC sublayer above to accommodate different types of data exchange. Logical channels can be categorized into data traffic channels (for transferring data traffic), and control channels, for transferring control signals between UE and eNodeB. Each logical channel service is provided to a certain RB from RLC layer to ensure proper RB prioritization according to their QoS requirements.

MAC sublayer performs priority handling operation to map user and control data flows from different RBs to their appropriate physical channels on PHY layer via PHY's transport channels interface. The priority handling mechanism is performed either on RBs from different UEs, or between RBs within the same UE. In addition, MAC layer is responsible for, detecting data transmission errors and correcting them via allocating time and frequency resources for data retransmissions. Data retransmissions are handled at the MAC sublayer through a process termed as Hybrid ARQ (HARQ), which is a combination of forward error-detection and correction via decoding process.

PHY Layer:

HSPA employs Wideband Code Division Multiple Access (WCDMA) as the transmission method over HSPA's physical wireless channels within a 5 MHz spectrum. When it comes to LTE, WCDMA is a non-valid choice for fulfilling LTE requirements due to the difficulty of supporting bandwidth sizes larger than 5 MHz using single carrier radio interface like WCDMA. LTE targets flexible spectrum allocations up to 20 MHz, so the use of WCDMA would require a high Signal-to-Noise-Ratio (SINR) and more complex filter design and equalization schemes at the receiving antennas. Henceforth, WCDMA, as well as almost any single-carrier transmission scheme, becomes a poor choice for LTE. The 3GPP directed its attention to the use of multiple-carrier transmissions for providing high data rates as efficiently as possible in terms of SINR. Hence, OFDM modulation scheme was a more appropriate choice for LTE due to the multicarrier nature of OFDM that provides significant advantages in terms of high data rate support. According to the 3GPP standard, Orthogonal Frequency Multiple Access (OFDMA) was chosen for the downlink direction, while Single Carrier Frequency Division Multiple Access (SC-FDMA) was chosen for the uplink.

V. E-UTRAN ARCHITECTURE

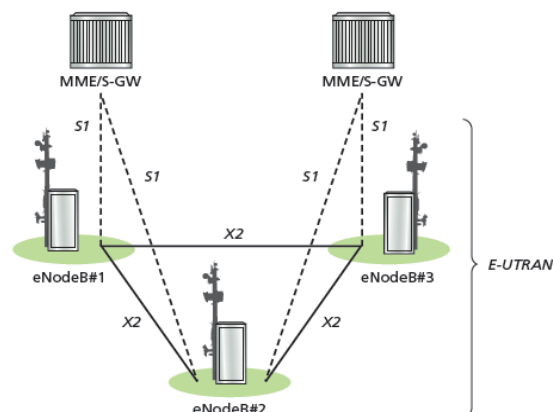


Figure 4: E-UTRAN architecture

In Figure4 we can see that eNodeBs are normally interconnected with each other by means of an interface known as E F S1 interface by means of the S1-MME interface and to the S-GW by means of the S1-U interface.

The E-UTRAN is responsible for all radio-related functions, which can be given as:

Radio resource management (RRM) C This covers all functions related to the radio bearers, such as radio bearer control, radio admission control, radio mobility control, scheduling and dynamic allocation of resources to UEs in both uplink and downlink.

Header Compression C This helps to ensure efficient use of the radio interface by compressing the IP packet headers that could otherwise represent a significant overhead, especially for small packets such as VoIP.

Security C All data sent over the radio interface is encrypted.

Connectivity to the EPC C This consists of the signalling toward MME and the bearer path toward the S-GW.

VI. SCHEDULING IN LTE

Scheduling is defined as allocating pre-determined number of sub-carriers for a fixed time to each requesting UEs. There are various methods of scheduling, such as channel dependent or channel aware scheduling methods and channel unaware scheduling. LTE scheduler algorithm need to be designed at layer2 (called as MAC layer) stack of LTE for both uplink and downlink. Schedulers are one such module which can dramatically increase or decrease the performance of the system. Uplink supports the SC-FDMA technology whereas downlink supports the OFDMA technology as an access method. LTE supports for advanced antenna techniques such as MIMO. Since Uplink supports the SC-FDMA technique as its access technology, each users need to be allocated a contiguous resource blocks (RBs) which leads to the complexity of the system.

Uplink scheduling determines which UEs is allowed to transmit and with which resource blocks during a given time interval. However, unlike downlink scheduling, uplink scheduling cannot automatically know the transmission demand from a UE. Thus, before the UE can transmit data to the eNodeB, it first sends a Scheduling Request (SR) to request the transmission permit. When the scheduler in the eNodeB receives the SR, it replies with a scheduling grant for the request [6]. In addition, the scheduler determines the time/frequency resource which the UE should use as well as transport format. After the UE has received the information of assignment, it can transmit data with required parameters over a sub-frame when the grant is valid. In this, LTE uplink scheduler module will be designed to handle both real and non real time data supporting both TDD and FDD frame structure for improving performance.

VII. DESIGN AND DEVELOPMENT OF SCHEDULING ALGORITHMS

This section discuss about the system development phase of the uplink scheduling algorithms using open source framework of LTE simulator. It contains requirement gathering, requirement analysis and system structure design using block diagram. *LTE-Sim* has been written in C++.

Design of Proportional Fair Scheduling Algorithm

Proportional fair is a compromise-based scheduling algorithm. It is basically Based upon maintaining a balance between two competing interests: Trying to maximize total wireless network throughput while at the same time allowing all users at least a minimal level of service which is done by assigning each data flow a data rate or a scheduling priority (depending on the implementation) that is inversely proportional to its anticipated resource consumption.

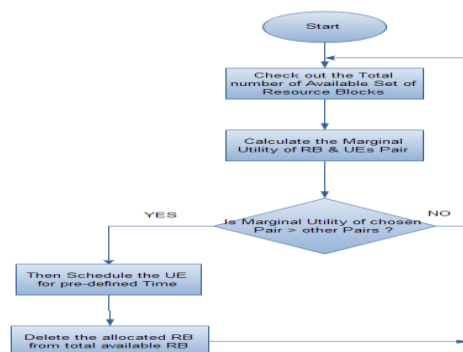


Figure5: Flow Chart of Proportional Fair Algorithm

Design of M-LWDF Scheduling Algorithm

The Modified-Largest Weighted Delay First (MLWDF) algorithm belongs to the LWDF family. It tries to meet delay guarantees by prioritizing data according to the queuing delay the packets have experienced. A delay guarantee violation occurs when the packets of user i experience a steady-state delay T_i , which exceeds some delay threshold D_i . The value of D_i is one of the defining characteristics of the different data types and depends on the negotiation process initiated before any data is transmitted. QoS guarantees require that the probability of such violations must be smaller than some pre-fixed threshold ϵ . The M-LWDF is a very attractive scheduling protocol used for wireless networks, as it varies the transmission rates of packets, depending on the channel condition.

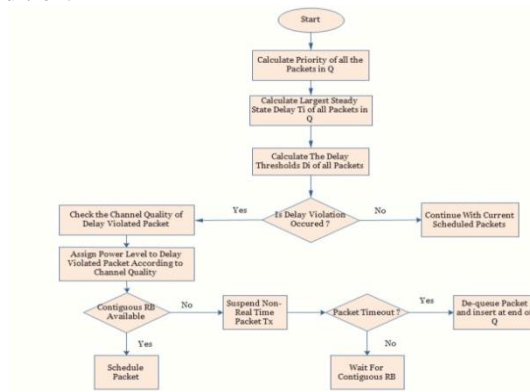


Figure6: Flow Chart of MLWDF Algorithm

Design of EXP-PF Scheduling Algorithm

H

to the number of allocated slots for transmission. Hence, it is easy to reserve system resource for real time service users in a wireless system. However, in an adaptive modulation and coding (AMC/TDM) system, the system capacity is time varying and depends on the service times of users, so that it is hard to find optimum priority rule for real and non-real time services. An AMC/TDM system cannot reserve service slots enough to satisfy QoS of real time service since the transmission rates per slot changes with respect to time. The EXP rule algorithm can support both real time and non-real time service users in an AMC/TDM system, but the throughput of a non-real time user is not maximized. The EXP-PF algorithm optimizes the throughput of non-real time service users and the EXP rule for real time service users.

VIII. RESULTS

The output conditions such as memory usage and execution time for varying number of users are investigated for all the three scheduling methods: Proportional Fair (PF), Modified-Largest Weighted Delay First (MLWDF) and EXP-Proportional Fair (EXP-PF) scheduling algorithm. The results are shown in Figure8 and Figure9.

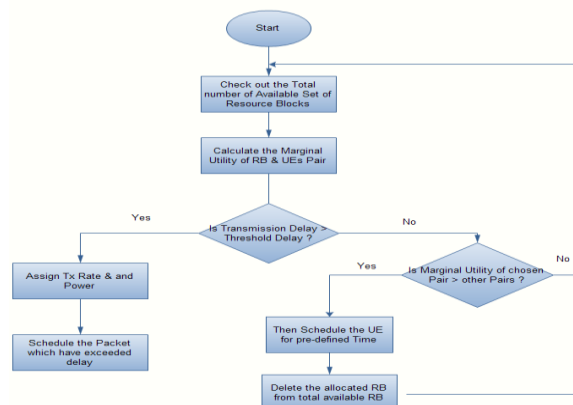


Figure7: Flow Chart of EXP-PF Algorithm

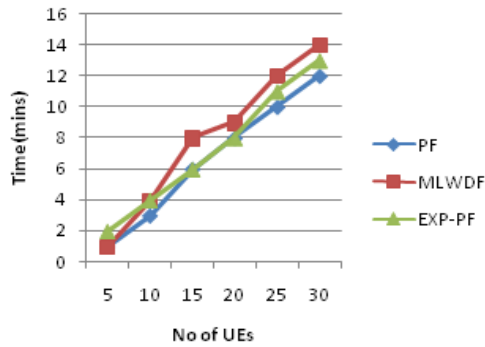


Figure 8: No:of UEs vs Time(mins)

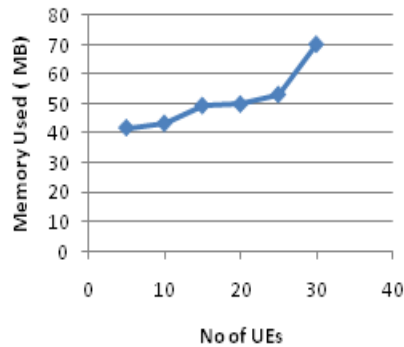


Figure 9: No:of UEs vs Memory Used MB

IX. CONCLUSION

Memory used to simulate the process increases from 40 Mb to 70 Mb with the increase in number of UEs from 10 to 30 and it is independent on the scheduling algorithm used by the eNodeB. The time required to execute the simulation increases from 1 minute to 14 minutes with the increase in number of UEs from 10 to 30; it depends on the scheduling algorithm used by the eNodeB. In fact, the PF algorithm requires less time than other scheduling strategies due to its very simple implementation.

REFERENCES

[1] *LTE The UMTS Long Term Evolution*, John Wiley & Sons Ltd.

[2] Hyung G. Myung, Single Carrier Orthogonal Multiple Access Technique for Broadband Wireless Communications, PhD Dissertation, 2007.

[3] Hongkun Yang, Fengyuan Ren, Chuang Lin, Jiao Zhang, Frequency-Domain Packet Scheduling for 3GPP LTE Uplink, Tsinghua University, Dissertation of PhD, 2008.

[4] 3GPP Technical specification , Evolved Universal Terrestrial Radio Access (E-UTRA) and Evolved Universal Terrestrial Radio Access (E-UTRAN).

[5] 3GPP TS 36.302, Evolved Universal Terrestrial Radio Access (E-UTRA); Services provided by the physical layer, Release 8, version 8.0.0, www.3gpp.org, 2008.

[6] Yifen Tan, Active Queue Management for LTE uplink in eNodeB, Helsinki University of Technology, Espoo, 2009.

[7] E. Dahlman, S. Parkvall, J. Skold, and P. Beming, 3G Evolution, Second Edition:HSPA and LTE for Mobile Broadband. Academic Press, 2008.

[8] F -c F -710, Apr.2010.

[9] F - Frd Generation Partnership Project (3GPP), Mar.2010.

[10] Giuseppe piro, Luigi Alfredo Grieco, Gennaro Boggia and Francesco Capozzi, Pietro Camarda Simulating LTE Cellular Systems: an Open Source framework, IEEE TRANS. VEH. Technology, 2010.

[11] E F Yang, Jiao Zhang and Chuang Lin.

Development, Carbonation and Characterization of Local Millet Beverage (Kunu)

¹Otaru, A.J., ²Ameh, C.U., ³Okafor, J.O., ⁴Odigure, J.O., ⁵Abdulkareem, A.S and ⁶Ibrahim, S.

^{1, 3, 4&5}(Department of Chemical Engineering, Federal Univeristy of Technology, PMB 065, Gidan Kwanu, Minna, Niger State, Nigeria).

²(Chevron Nigeria Limited, 2 Chevron Drive, Lekki, Nigeria)

⁶(Ovecon Engineering and Consultancy, P.O. Box 1730, Zaria, Nigeria)

ABSTRACT

The need to improve on the quality of local millet beverage (kunu) and the widespread effort in developing countries like Nigeria to develop carbonated drink from locally source materials gave birth to this research work. The aim of this research is to analyze the shelf-life of the product to see if carbonation could extended the shelf-life of the product giving the drink a more refreshing sensation without interfering with the properties of the drink. Because the production of local millet beverage is not standardized, the local traditional technology was used in preparing the drink and carbonation was done using a pure CO₂ extinguisher. Four (4) samples of the drink were made; sample 1 contained CO₂ and citric acid, sample 2 contained CO₂, sample 3 contained citric acid and sample 4 contained nothing (still sample). The products were analyzed for total solid, pH, protein, ash, acidity, moisture content and trace elements. Sensory evaluation and microbiological analysis were also carried out for each sample. In analyzing the product shelf-life which started fermenting after 72 hours, followed by the sample containing CO₂ only (sample 2). The samples analyzed were not refrigerated during the period of storage. It was found that the sample with the highest gas volume has the best shelf-life and the non-carbonated sample yielded easily to microbial growth. Therefore, this research work clearly shows that the development of a carbonated millet drink is practically possible, cost effective and has numerous advantages with other available carbonated drinks.

Keywords: Kunu, Carbonation, Shelf life, Nigeria.

I. INTRODUCTION

Millet drink (Kunu), is a nutritious non-alcoholic drink that is produced from various cereal grains such as millet. Kunu is a drink that has found great appeal in the northern part of Nigeria, its consumption is spread over every class of personality and it is consumed either as a food supplement or thirst quencher. The availability of kunu as an alternative for carbonated drinks products which have little to nutritional benefits that is cheaply available for every class of individual. Kunu is one of the complex mixtures which contain macromolecules such as protein, carbohydrates and lipids (Gafa et al, 2002). The major important cereals which are used in the preparation of kunu are millet, maize, guinea corn and rice. During the preparation of kunu, the ingredients needed are ginger (zingiber officimals), alligator pepper (afromonium melegueta), red pepper (capsicum species), black pepper (piper guineense) and kakandoru or eru. All these ingredients perform one function or the other in the course of the preparation. The most abundant constituents of kunu is water and it acts as the medium in which all other constituents are dissolved and contain only traces amount of in-organic substances. The high nutritive value of kunu is attributed due to the presence of protein, carbohydrates and in particular, vitamin B (Wakil, 2004).

Kunu is taken after meal as a supplement or to quench thirst. Kunu is widely accepted as food drink in some urban centres especially in the Hausa land. The quality and quantity of the products depend largely on the quality of the ingredients and handling technique in the course of production by the producer. The product could be obtained quantitatively after 2 days and it could be stored for another 3 days when refrigerated (Wakil, 2004). It has however been reported that, if kunu is kept overnight in hot season without being refrigerated, its quality begins to deteriorate and this may lead to the spoilage which when consume could constitute danger to health (Adebayo et al, 2010). Spoilage of this product from observation occurs from improper handling, constant fermentation of the ingredients especially the carbohydrates and enzymatic action on the substrates (Wakil,

2004). Hence there is need for proper formulation and carbonation of the product. Carbonated drinks are desired and preferred because of its sharp, unique and refreshing taste. Carbonated drinks are non-alcoholic beverages that consist of CO₂, water, flavouring and some other types of sweet syrup (Abdulkareem et al, 2010). The CO₂ when introduced increases the acidity level of the drink, thereby keeping some micro-organisms from growing. The thrives of microbes in a drink is what usually reduces the shelf-life of the product (Julio et al, 2011). Carbonated millet beverages (kunu) are expected to make a lot of difference when compared to other available carbonated drinks because of its nutritive values among many other properties which include:

- [1] Its ability to aid digestion and absorption of components into the body system.
- [2] Boosting the immune system of the body against microbial attack.

Currently in Nigeria, soft drinks are very expensive to buy. A bottle of 50cl costs an average price of ₦80.00. The soft drinks have little or no nutritive value because they contained high concentration of sugar and artificial concentrates (The Nation, 2012). Kunu however seem to be highly nutritious with relatively low cost of production and consumption. It is being prepared from our local cereals which are very common and are part of our stable food substances. The problem facing the satisfaction derived from kunu comes from its fast deterioration due to microbial activities causing its spoilage. Therefore, the need to enhance the shelf-life of kunu and to make it more refreshing and appealing gave birth to this research study aimed at the development and characterization of carbonated local millet beverage (kunu).

II. EXPERIMENTAL METHODOLOGY

This section presents a step by step account of experimental procedure carried out in the determination of the properties necessary or that must be possessed by carbonated millet beverage (kunu).

Collection of sample materials

The raw materials for the preparation of the kunu were purchased from a major market in Minna, Nigeria. These materials include millet, alligator pepper, kakandoru, sweet potatoes.

Sample preparation

1kg of millet grains were cleaned and steeped in twice its volume of water (2L) for 24h. Thereafter the steeped grains were washed and spices added. The spices added were ginger, red pepper, cloves and black pepper. The steeped millet grains and spices were then milled in a grinding machine and sieved to remove the shafts after which the supernatant was decanted from the slurry. The slurry was divided into two equal halves with one half added to boiling water while stirring for 2 minutes, cooled to a temperature of 35°C and subsequently added to the remaining half slurry. Adequate amount of water was added to the mixture, stirred and left to settle. After which, the mixture was sieved using a muslin cloth and the filtrate was sweetened with granulated sugar and mixed properly to obtain the freshly processed millet beverage. The product was bottled in plastic bottles.

Carbonation of the products

Carbonation is often one of the last processes in the production of carbonated soft drinks and beer. Thus the carbonation process is critical not only to the final taste and appearance of the product, but influences the filling of the final beverage. To carbonate the product, it was first pre-chilled in a refrigerator to lower the temperature of the product to about 2-4°C for easy absorption of CO₂. Due to the unavailability of a carbonating machine in the laboratory, carbonation of the product was done using a pure CO₂ fire extinguisher. One end of a hose was attached to the mouth of the extinguisher and the other end attached to the bottle mouth of the product. The extinguisher lever was gently pressed to release CO₂ gas into the product and the bottle was sealed immediately for freshness. Sample 1, 2, 3 and 4 were made; sample 1 contained CO₂ and citric acid, sample 2 contained CO₂, sample 3 contained citric acid and sample 4 contained nothing (still sample). Samples 3 and 4 are the drinks that were not carbonated and sample 1 and 2 were the carbonated drinks.

Physiochemical Characteristics of Kunu Beverage

Determination of pH

10ml of the millet drinks was shaken with 100ml of water and allowed to stand for a period of 30minutes. The material was filtered and the pH of the filtrate was determined with a pH meter.

Determination of Titratable Acidity

100ml of the millet drink was shaken with 200ml of CO₂ in a conical flask and placed in a water bath at 40°C for one hour with the flask loosely stopper. It was filtered and 100ml of the clear filtrate was titrated with 0.05M of NaOH solution with phenolphthalein indicator. The acidity of water extracts increases during storage

Determination of Total Solid

10g of the millet drink was weighed (W_1) into a flat-bottomed metal dish and placed on boiling water for about 30 minutes until the liquid evaporated leaving the solid. It was then transferred into an oven maintained at 100°C for $2\frac{1}{2}$ h and weighed as W_2 . It was then desiccated, cooled and weighed. It was heated in the oven again for 1 hour, cooled and weighed. The process was continued until constant weight W_3 .

Determination of Protein

20g of the sample was weighed and placed into a Kjeldahl digestion tube. A Kjeldahl tablet of selenium catalyst and 20cm^3 of concentrated H_2SO_4 were added into the tube. The tube was then placed in the digestion block and pre-heated in a fume cupboard until a clear solution was obtained. After digestion, the tube was removed from the digester cooled and the resulting aliquot solution was diluted with distilled water to 50cm^3 . 10cm^3 aliquot of the diluted solution was pipette into the distillation flask containing 20cm^3 of 40% NaOH solution. The content diluted with 40cm^3 water and was distilled using micro-Kjeldahl distillation apparatus. The distillate was retrieved into a receiving flask containing 25cm^3 of boric acid indicator solution. The distillate was titrated with 0.10M HCl solution to purple grey end point.

CO_2 Gas Volume Determination

The sample is equilibrated by gently inverting the sample 20 times in 30 seconds, then wait for bubbles to settle in the liquid. The sample is then placed under the Zahm Nagel tester and align crown with the piercing device. The snifter valve is then closed in front of the tester. Grasp springs and crossbar were carefully lowered until the piercing needle rests on the crown. The crown is then pierced by forcing the crossbar down with a firm and rapid motion. The head pressure is then released by carefully opening the snifter valve, allow the pressure drop and close the valve quickly. The maximum pressure is then recorded and the crossbar is removed, and a thermometer is inserted immediately and the temperature is recorded. The pressure and temperature recorded were converted gas volume by using a gas volume chart.

Determination of Ash Content

The crucible dish was cleaned, dried ignited, cooled and weighed as W_1 . 24.4g of the millet drink was weighed accurately and directly in the dish i.e. W_2 . The substance was dried on a boiling water bath and the charred over a Bunsen flame or hot plate in fume cupboard until no more soot was given out. Then, it was then ashed with a muffle furnace at 500°C to obtain W_3 .

Determination of Trace Elements

The determination of trace metal contaminants in millet drink was carried out. These trace metals are lead, copper, zinc, manganese and calcium. The organic matter of the food was first destroyed dry ashing 24.4g of Kunu sample between $400\text{--}500^\circ\text{C}$ for 5h. This was followed by acid digestion by adding 20ml of H_2SO_4 and 10ml of HNO_3 (2:1). The mixture was heated on Bunsen burner until the brown fumes subsided. Another 10ml of H_2SO_4 was continued at 10 minutes interval and heating continued until the solution becomes colourless. The digestion sample was then analyzed for lead, zinc, calcium, manganese and copper using AAS.

Determination of Moisture Content

10g of millet drink was weighed into a pre-weighted flat dish W_1 and dried at an oven temperature of 105°C for 3h as W_2 . It was allowed to cool in an airtight desiccator and reweighed. It was heated in the oven again for half an hour, cooled and weighed. The process was repeated until constant weight was obtained W_3 .

III. MICROBIOLOGICAL ANALYSIS OF THE PRODUCT

Determination of Yeast and Mould

These were carried out by the pour plate method as described by Nigeria Distilleries Limited (NDL) using nutrient agar and potato dextrose agar for total aerobic bacteria and total yeast count respectively. Nutrient agar was inoculated with a 0.1ml of appropriately 10ml diluted millet drink by spread-plate technique and incubated at 37°C for 24h. Colonies were counted and multiplied by the dilution factor. Colony counts were done after the appropriate period of incubation. Distinct colonies from the poured plate were streaked to fresh sterile nutrients agar plates to obtain pure colonies of bacterial and transferred to agar slants as stock culture for later use.

Sensory Evaluation

The available sample of the millet beverage is given to the respondents with a copy questionnaire to be filled based on the sample with preferred taste, colour, texture, flavour, and general acceptability.

Shelf-Life Determination

Within the period of storage the following analysis were carried out;
 Periodic pH determination
 Fermentation rate

Table 1. Sample Description

Sample	Specification
1	CO ₂ + citric acid
2	CO ₂ only
3	Citric acid
4	Still

Results and Discussion

Experiments carried out in the development and characterization of carbonated local millet beverage (kunu) and various results obtained are presented.

Table 2 Physical Analysis of Local Millet Beverage

Moisture content (%)	86.6
Total solid (mg/l)	853
Protein (%)	1.75
Ash content (%)	0.20

Table 3 pH Variation and CO₂ Content

Samples	pH	Titrateable Acidity	Gas volume (cm ³)
1	2.38	0.110	3.0
2	2.42	0.097	2.5
3	2.75	0.083	0
4	3.83	0.063	0

Table 4 Mineral Analysis of Millet Drink

Minerals	Quantity (ppm)	Maximum Permissible Limit in ppm (WHO)
Lead	0.001	0.01
Copper	1.070	100
Zinc	3.100	300
Calcium	4.200	No limit
Manganese	1.020	0.36

Table 5 Microbiological Analysis of Millet Drink

Samples	1	2	3	4
Bacteria count	30	44	54	70
Yeast and mould	1	2	3	4

Table 6 Sensory Evaluation of Millet Drink

Samples	1	2	3	4	Total number of respondent
Respondent	7	4	2	2	15

Table 7 Shelf-life Determination cm³

1 st DAY (24 HOURS)			
Samples	Time (hrs)	Vol. Increase (cm ³)	pH
1	6	-	2.38
	12	-	2.38
	18	-	2.38
	24	-	2.38
2	6	-	2.42
	12	-	2.42
	18	-	2.42
	24	-	2.42
3	6	-	2.75
	12	-	2.75
	18	-	2.75
	24	-	2.75
4	6	-	3.83
	12	-	3.83
	18	-	3.83
	24	-	3.83

IV. DISCUSSION

The various results obtained in the analysis of carbonated local millet beverage (kunu) are presented in Tables 2-6

Table 2 shows the results obtained in the physical analysis of the final product.

2 nd DAY (48 HOURS)			
Samples	Time (hrs)	Vol. Increase (cm ³)	pH
1	6	-	2.38
	12	-	2.38
	18	-	2.38
	24	-	2.38
2	6	-	2.20
	12	-	2.20
	18	-	2.20
	24	3.4	2.20
3	6	-	2.30
	12	-	2.30
	18	-	2.30
	24	4.2	2.30
4	6	-	3.41
	12	-	3.41
	18	-	3.41
	24	5.1	3.41
3 rd DAY (72 HOURS)			
Samples	Time (hrs)	Vol. Increase (cm ³)	pH
1	6	-	2.10
	12	-	2.10
	18	-	2.10
	24	2.7	2.10
2	6	4.3	1.90
	12	4.8	1.90
	18	5.0	1.90
	24	5.8	1.90
3	6	5.1	1.52
	12	5.8	1.52
	18	6.2	1.52
	24	6.9	1.52
4	6	6.0	1.30
	12	6.8	1.30
	18	7.4	1.30
	24	9.1	1.30

The percentage moisture content of the samples was found to be 86.6%, this is attributed to the fact that water is the most abundant constituent of the product and it acts as the medium in which all other constituents are dissolved. The percentage moisture content also shows the level of the viscosity of the samples as the slurry was diluted with water during preparation. The total solids in the samples, was found to be 853mg/l. The high percentage value of the total solids could be attributed to various ingredients used in the preparation of the samples. It may also reflect the volatile composition of the samples. The percentage protein in the samples was found to be 1.75%. The protein content of the product (kunu) made it to more nutritious than any of the carbonated soft drinks which seem to have contained no protein content. Their major components are sugar, colouring and carbonated water. The percentage ash in the sample was 0.2%. The importance of the ash content is that it gives an idea of the amount of minerals elements present in the samples. It has also been reported that the value of ash is a useful and quality or grading assessment of certain edible materials (AOAC, 1990). This result was also supported by the level of trace elements in the samples.

Table 3 shows the results obtained from the chemical analysis of the final product. The pH of the samples 1, 2, 3, and 4 were found to be 2.38, 2.42, 2.75, and 3.83 respectively. Sample 1 (sample containing CO₂ and citric acid) gave a pH of 2.38 which slightly more acidic compared to the other samples (2, 3, and 4). This is due to the presence of CO₂ and citric acid.

CO₂ when added to the product dissolves in water (the major constituents of the product) forming carbonic acid (H₂CO₃) which in turn increases the acidity of the product. Sample 2 (sample containing only CO₂) gave a pH of 2.43, which is acidic compared to sample 3 and 4 due to the formation of carbonic acid between CO₂ and water, but a little less acidic than sample 1 because sample 1 contains citric acid which also influences the pH of the product. Sample 3 (sample with citric acid) gave a pH of 2.75 more acidic than sample 4 due to the presence of citric acid. And sample 4 (still sample) gave a pH of 3.83 which is less acidic than the other samples because it contains no CO₂ or citric acid.

The percentage titratable acidity was found to be 0.11%, 0.097%, 0.083%, and 0.063% for sample 1, 2, 3 and 4 respectively. The varying values obtained for each sample is attributed to the presence of CO₂ or citric acid or both. It was observed that the percentage titratable acidity decreases as the pH increases from sample 1 to 4. This implies that the more acidic the sample is the more NaOH volume it would require to neutralize it. Table 4 shows the results obtained for the major, essential trace and toxic elements. The major element is calcium while the trace elements are zinc, copper and manganese and toxic element is lead. The result revealed that calcium has the highest concentration (4.20ppm) followed by zinc (3.10ppm), then copper (1.07ppm), then manganese (1.02ppm) and the least is lead (0.001ppm). The quantity of trace elements were relatively low for lead (0.001ppm), copper (1.07ppm), manganese (1.02ppm) compared with their tolerant limit. This is very good results from the biological point of view. However, calcium which is essential requirement for bone development and strong teeth and zinc which aid digestion and body functions were relatively high (zinc, 3.10ppm), (calcium, 4.20ppm). The concentration of manganese is relatively moderate because it becomes poisonous when taken in high concentration.

Table 5 shows the results of the microbial analysis of the final product. For the bacteria, yeast and mould count, the non – carbonated sample 4 has the highest count of 70 and 4 respectively probably because of its low acidic content and a gradual decrease in the bacteria, yeast and mould count was observed for the carbonated samples 1 and 2. Carbonated sample 1 has the lowest bacteria; yeast and mould count of 30 and 1 respectively. This could be attributed to high acidic medium which inhibits the growth of micro organisms. The presence of some of the bacteria may be due to contamination from the substrate, the environment during production, the hygienic state of the processing of the sample. While the presence of fungi may be attributed to the acidic nature of the sample since it has been observed that yeast and mould are capable of utilizing organic acids. Also the presence of fungi in the food may lead to poisoning and contaminated fungi result in the production of undesirable odour, colour changes and even the taste of the sample will be changed. The general observation from the microbial analysis shows that as the medium becomes more acidic the concentration of micro-organisms continues to reduce.

Table 6 shows the results of the sensory evaluation of the final product. A total number of 15 respondents were recorded for all the samples. The non-carbonated sample 3 and 4 has the lowest acceptance number of 2 respondents while carbonated sample 1 has the highest number of respondents of 7. This was considered the most acceptable because of the fizzling and refreshing taste produced by the CO₂ gas. However, carbonated sample 2 also recorded 4 respondents. This was considered to be so perhaps because of the low carbonic acid concentration present.

Table 7 shows the evaluation for the shelf-life of the final product carried out at six hours interval. Kunu as it is known as a very short shelf-life and it would be still acceptable after approximately 48hours without refrigeration. The short shelf-life is attributed to the microbial activities causing fermentation in the final product which will eventually cause spoilage of the product. In this study, the fermentation rate of each of the samples is observed by the swelling (volume increase) of the bottles in which the samples are kept. The swelling or volume increase of the sample bottles with time is the same as the rate of fermentation. The general observations from the tables show that as pH decreases for each sample, the rate of fermentation increases implying that the rate of fermentation is invariably proportional to the pH of the product. Results as presented also indicate that as the pH decreases the titratable acidity of the samples increased. During the first 24hours of storage all samples recorded no volume increase and their pH were still stable. In the second 24hours (48hours) of storage, sample 1 (sample containing CO₂ and citric acid) recorded no volume increase and its pH was still stable. But the rest of the sample 2, 3, and 4 (sample 2 containing CO₂, sample 3 containing citric acid, and sample 4 the still sample) recorded volume increase of 3.4cm³, 4.2cm³, and 5.1cm³ with pH drop of 2.20, 2.31, and 3.41 respectively at the end of the second 24hours.

This indicated that fermentation had begun in the samples. Sample 1 recorded a volume increase of 2.7cm³ and a pH drop of 2.10 after 72 hours of storage while the rest of the samples recorded steady volume increase and pH drop within the 72 hours of storage. This implies that sample 1 is the best among all the samples, it is presumed to last for over 72hours. Therefore, the shelf-life of the developed carbonated millet beverage was extended by roughly another 24hours.

V. CONCLUSION AND RECOMMENDATION

In this study, carbonated millet drinks was developed and characterized to determine the suitability of the drink as an alternative carbonated source from local materials. Results obtained revealed that both chemical and microbial characterization of the millet drink (kunu) reflects that the product contained no harmful micro-organisms or by-product. The micro-organisms encountered in this study of indigenous fermented food drink (kunu) was as a result of contamination from one source or the other which include water, air, equipment or utensils used in processing, personal hygiene etc. These bacterial are non pathogenic and human commensalisms, hence they cannot transfer disease. It was found that the sample with the highest gas volume has the best shelf-life and the non-carbonated sample yielded easily to microbial growth. Therefore, this research work clearly shows that the development of a carbonated millet drink (kunu) is practically possible.

REFERENCES

- [1] Adebayo, G.B., Otunola, G.A., & Ajao, T.A., (2010). Physicochemical, Microbiological and Sensory Characteristics of Kunu Prepared from Millet, Maize and Guinea Corn and Stored at Selected Temperatures. *Advance Journal of Food Science and Technology* 2(1):41-46, 2010. ISSN: 2042-4876. Maxwell Scientific Organization, 2009.
- [2] Abdulkareem, A.S., Uthman, H., and Jimoh, A., (2011). Development and Characterization of a Carbonated Ginger Drink. Department of Chemical Engineering. Federal University of Technology, Minna.
- [3] Gaffa, T., Jideani, I.A., & Nkama, I. (2002). Traditional Production, Consumption and Storage of Kunu – A non-alcoholic cereal beverage. *Plant Foods for Human Nutrition*. Vol. 57, Number 1; Pp 73-81.
- [4] Julio, A., (2011). Fermented Foods and Beverages of the North-East India. *Food Processing, Dried Food, Frozen Food, Juice and Beverage*. (www.agrifoodGateway.com)
- [5] The Nigerian Nation, 2012 (www.issuu.com/thenation/dosc/april-13-2012)
- [6] Wakil, S., (2004). Isolation and Screening of Antimicrobial Producing Lactic Acid. University of Ibadan, Nigeria.
- [7] Ingredients Used and Popular Method of Preparation of Kunu (www.ifood.tv/20-12-2010).
- [8] WHO, EU & EPA Standard (2012).
- [9] journal.chemistrycentral.com/content

Study on the Effectiveness of Phytoremediation in the Removal of Heavy Metals from Soil Using Corn

¹Otaru, A.J., ²Ameh, C.U., ³Okafor, J.O., ⁴Odigure, J.O., ⁵Abdulkareem, A.S and ⁶Ibrahim, S.

^{1, 3, 4&5}(Department of Chemical Engineering, Federal Univeristy of Technology, PMB 065, Gidan Kwanu, Minna, Niger State, Nigeria).

²(Chevron Nigeria Limited, 2 Chevron Drive, Lekki, Nigeria)

⁶(Ovecon Engineering and Consultancy, P.O. Box 1730, Zaria, Nigeria)

ABSTRACT:

The research study aimed at determining the effectiveness of phytoremediation in the removal of heavy metals using corn. Soil sample collected at a depth of 20 cm were taken from Gidan Kwanu area of Niger state, Nigeria. The experiment consists of 12 treatments each containing 4 kg of soil including soil without concentrations of Zn, Fe and Pb to serve as the control. 3 pots each were contaminated with 2.5 g/dm³ concentration of Zn, Fe and Pb. The initial analysis of the soil indicates that the uncontaminated soil sample contained 1.55 mg/kg of Zn, 31 mg/kg of Fe and 0.13 mg/kg of Pb while the contaminated soil sample contained 15.33 mg/kg of Zn, 45.7 mg/kg of Fe and 4.16 mg/kg of Pb. 4 corn seeds were planted on each of the soil sample at a depth of 4cm and the setup was monitored properly in an isolated place. Samples were taken for analysis at 2 weeks interval in a period of 8 weeks. Results show that at the end of the 8 weeks, there was reduction in the concentration of the heavy metals in the soil and there was an increase in the level of heavy metals in the plant leaves and stems. The plants were tolerant of the heavy metals as they had a fast growth, therefore it was concluded that corn is a hyper accumulator and it is effective in the removal and detoxification of soil contaminated with heavy metals.

Keywords: Phytoremediation, Heavy metals, Corn, Soil, Nigeria.

I. INTRODUCTION

Farming, military and industrial activities are responsible for contamination of large areas of developed countries with high concentrations of heavy metals and organic pollutants (Peuke and Renneberg, 2005). In addition to the negative effects of accumulation of heavy metals on ecosystems and other natural resources, they also pose a great danger to public health because pollutants can enter food chain through agricultural product or leach into drinking water (Peuke and Renneberg, 2005). Soil located in Industrialized regions have been identified as the most affected area due to the heavy metals they used for production and manufacturing. Soil pollution spread to other parts of the natural environment because soil lies at the confluence of many natural systems (Mohammad *et al.*, 2008). Many human diseases result from the buildup of toxic metals in soil, making remediation of these areas crucial in the protection of human health (Shaylor *et al.*, 2009). Risk reduction can be through a process of removal, degradation or containment of contaminants. In Nigeria and other developing countries in the world, farmers are commonly using untreated industrial and municipal wastewater for irrigation, particularly in the suburbs of large cities and in the vicinity of major industrial estates (Ghafoor *et al.*, 2008). However long term application of heavy metals such as cadmium (Cd), chromium (Cr), Lead(Pb), and Zinc (Zn), in soil causes decline in soil microbial activity, soil and groundwater contamination, reduction in soil fertility and contamination of human food chain (Cynthia and David, 1997).

Current methods of soil remediation such as soil washing, mechanical separation, extraction and storage do not really solve the problem. Hence the need for alternative, cheap and efficient methods to clean up heavily contaminated industrial areas. The current remediation techniques of heavy metal from contaminated soil water are expensive, time consuming and environmentally destructive. Unlike organic compounds, metals cannot degrade and therefore effective cleanup requires their immobilization to reduce or remove toxicity. In recent years, scientist and engineers have started to generate cost effective technologies such as adsorbents. Plants are an effective means of removal of contaminants from soil (Wenzel *et al.*, 1999). Phytoremediation is a

general term for using plants to remove, degrade or contain soil pollutants such as heavy metals, pesticides, solvents, crude oil, polyaromatic hydrocarbon and landfill leachates.

For instance wild flowers were recently used to degrade hydrocarbons from an oil spill in Kuwait (Brady and Weil, 1999). Phytoremediation is therefore an emerging technology for cleaning up of contaminated and is now a widely supported green technology which may provide an alternative to cleaning wastewater and contaminated soil. It is a cost effective, environmentally friendly and aesthetically pleasant nature and equal applicability for the removal of both organic and inorganic pollutants present in soil, water and air (Yu *et al.*, 2001). Plants which can accumulate high concentration of metals in the harvestable biomass are termed hyperaccumulators. According to and Proctor (1990), the plants that can accumulate $>100 \text{ mg Cd kg}^{-1}$ or $>500 \text{ mg Cr kg}^{-1}$ in dry leaf tissue are termed hyperaccumulators. Reeves and Baker (2000) also identified hyperaccumulator plants for elements including Cd, Cr, Ni, Pb, Zn and (Hajar, 1997). However such plants are typically slow growing small and weedy plants that produce only limited amount of biomass and therefore takes significance time to decontaminate polluted sites (Cherian and Oliveira, 2005). Therefore fast growing tree species that guarantee high biomass yield have a tendency for higher heavy metal accumulation, a deep root system and a strong evapotranspiration system are preferred for phytoremediation over conventional hyperaccumulator (Sebastiani, et al., 2004).

A major factor influencing the efficiency of phytoremediation is the ability of plants to absorb large quantities of metal in a short period of time. Corn (*Zea mays*) planted on the contaminated soil had higher levels of heavy metals than the one planted on the uncontaminated soil. The difference indicates that they have been absorbed away from the contaminated soil (Kumar et al., 1995). *Zea mays* is thus a hyper accumulator of heavy metal, tolerant of the targeted metals and also had a fast growth rate (Cunningham, et al., 1995). This present study focus on evaluating the performance of corn as an hyperaccumulator in the removal of heavy metals from soil.

II. RESEARCH METHODOLOGY

Soil Sampling

Soil sample was collected from Gidan Kwanu area of Minna, Niger state, Nigeria at a depth of 20cm. Four fresh corn seeds were planted in pots containing 4 kg of the soil at a depth of 4 cm. The experiment consists of 4 treatments, each of these treatment were divided into 3 replicates to give a total of 12 pots. 3 pots without zinc, iron and lead to serve as control, 3 pots contaminated with 2.5 g/dm^3 concentration of Zinc, 3 pots contaminated with 2.5 g/dm^3 concentration of Iron and 3 pots contaminated with 2.5 g/dm^3 concentration of Lead. All the soil samples were taken for initial analysis. The set up was placed in Crop Production Departmental garden of Federal University Technology Minna, Nigeria and monitored properly. After 8 weeks of seed planting and germination, samples from the contaminated soil and the control were analyzed at two weeks interval for heavy metal content. At the end of the 8 weeks, the plants were uprooted and the stems and leaves were also analyzed for the heavy metal uptake.

Soil preparation

Soil preparation before analysis involves two major steps: soil pre-treatment and soil digestion.

Soil Pre-treatment

The soil samples were properly grounded using Agate mortar to enhance the oxidation of soil samples and it was passed through a 0.25 mm sieve mesh to obtain a fine particle.

Soil Digestion

There are various methods of digesting soil such as nitric acid digestion, nitric acid-sulphuric acid digestion, nitric acid-perchloric acid digestion, wet ashing digestion and microwave digestion. In this experiment the nitric acid-perchloric acid digestion was utilized. 0.5g of the finely grounded soil sample was accurately weighed using a digital weighing balance and placed in a 50ml beaker. 20ml of a mixture of nitric acid and perchloric acid in 1:1 molar ratio was poured into the soil in the beaker and the content was placed on a hot plate and heated gently at low temperature until dense white fumes of HClO_3 appears. The digested sample was allowed to cool before it was filtered into a 50ml standard volumetric flask which was made up to mark with distilled water and the sample ware placed in storage containers and taken for analysis using atomic absorption spectrometer.

Soil Analysis

The soil was analysed using an atomic absorption spectrometer (AAS). The Sample was aspirated into a flame, atomized and a light beam was directed through the flame into a monochromator and a detector measured the amount of light absorbed by the atomized element in the flame. The radiation was passed through a filter or monochromator which tuned the line of interest but screened the others. The photo detector then received the resonance line, diminished by simple absorption and finally the concentration was displayed.



Plate 1: Experimental Set up

III. RESULTS AND DISCUSSIONS

The study is focus on evaluating the effectiveness of corn as a phytoremediating agent in the removal of heavy metal from soil. The results of the study conducted in period of 8 weeks are presented in tables and figures. The concentrations of Zn, Fe and Pb over a period of 8 weeks at 2 weeks interval are presented in table 1- 5 while the results obtained on the leaves and stems after 8weeks are presented in table 6 and 7. The result of the percentage absorbance of the heavy metal in the leaves and stems of the plant at the end of the 8 week period are presented as Figure 1-4.

Table 1: Sample at Initial Stage

Treatments	Zn(mg/kg)	Fe(mg/kg)	Pb(mg/kg)
CONTROL	1.55	31	0.13
T1	14.9	47	4.16
T2	15.7	47.2	4.22
T3	16	42.9	4.09

Table 2: Sample at 2nd Week

Treatments	Zn(mg/kg)	Fe(mg/kg)	Pb(mg/kg)
CONTROL	0.70	14.30	0.11
T1	12.33	25.78	3.17
T2	13.16	34.80	3.10
T3	11.59	36.11	3.11

Table 3: Sample at the 4th Week

Treatment	Zn(mg/kg)	Fe(mg/kg)	Pb(mg/kg)
CONTROL	0.36	11.04	0.10
T1	9.05	18.02	1.65
T2	10.17	20.24	1.42
T3	9.24	19.26	1.73

Table 4: Sample at the 6th Week

Treatment	Zn(mg/kg)	Fe(mg/kg)	Pb(mg/kg)
CONTROL	0.25	8.56	0.06
T1	4.79	13.56	1.17
T2	5.12	14.02	0.98
T3	4.24	15.73	1.32

Table 5: Sample at the 8th Week

Treatment	Zn(mg/kg)	Fe(mg/kg)	Pb(mg/kg)
CONTROL	0.22	8.13	0.03
T1	4.33	8.88	0.91
T2	4.59	12.24	0.77
T3	3.99	13.51	1.02

Table 6: Results of Levels of Heavy Metal in Leaves of the Corn after 8 Weeks

Treatment	Zn(mg/kg)	Fe(mg/kg)	Pb(mg/kg)
CONTROL	0.32	4.34	0.02
T1	1.94	6.12	0.62
T2	1.91	6.18	0.54
T3	1.85	7.26	0.57

Table 7: Results of Levels of Heavy Metal in Stems of the Corn after 8 Weeks

Treatment	Zn(mg/kg)	Fe(mg/kg)	Pb(mg/kg)
CONTROL	0.39	4.57	0.03
T1	2.27	7.75	0.71
T2	1.98	8.26	0.67
T3	2.06	8.85	0.59

Percentage Absorbance in Leaves and Stems

The percentage absorbance of Zn, Fe and Pb into the plants and stems of the corn planted on both the control and contaminated soil was calculated after 8 weeks. The results are as follows:

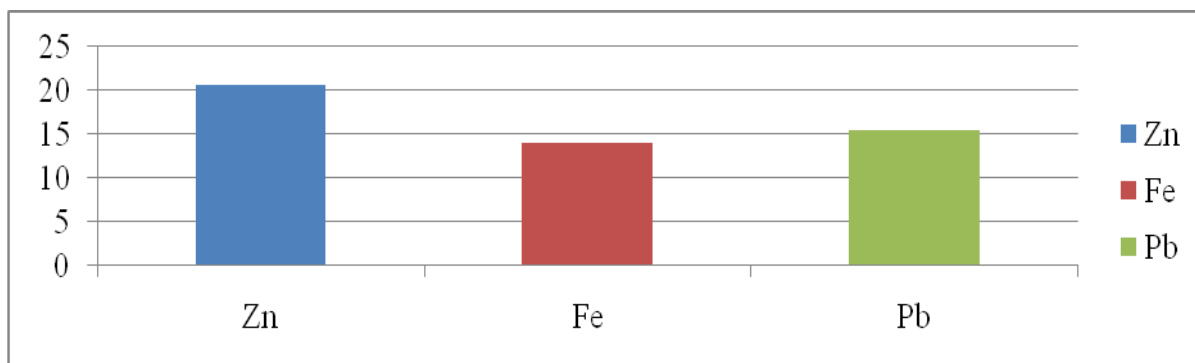


Figure 1: Percentage Absorbance of Heavy Metals in leaves of Corn on Controlled soil sample after 8 weeks

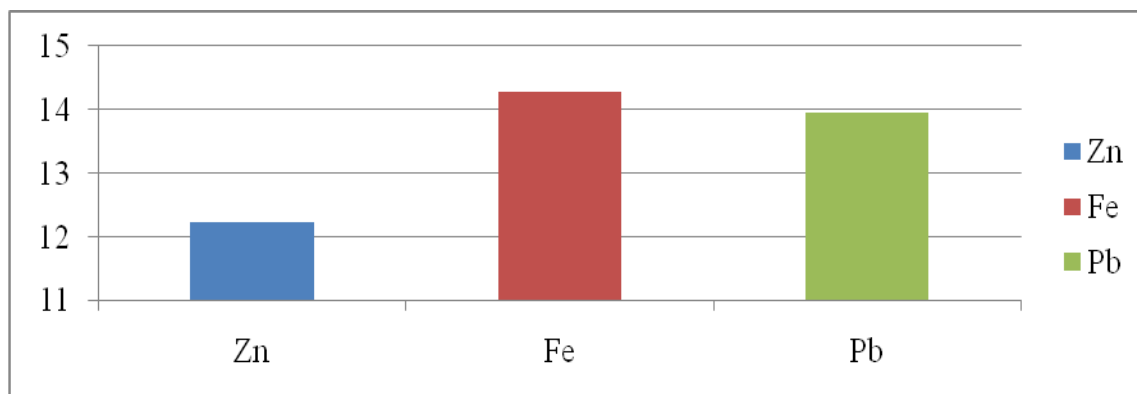


Figure 2: Percentage Absorbance of Heavy Metals in leaves of Corn on Contaminated soil sample after 8 weeks

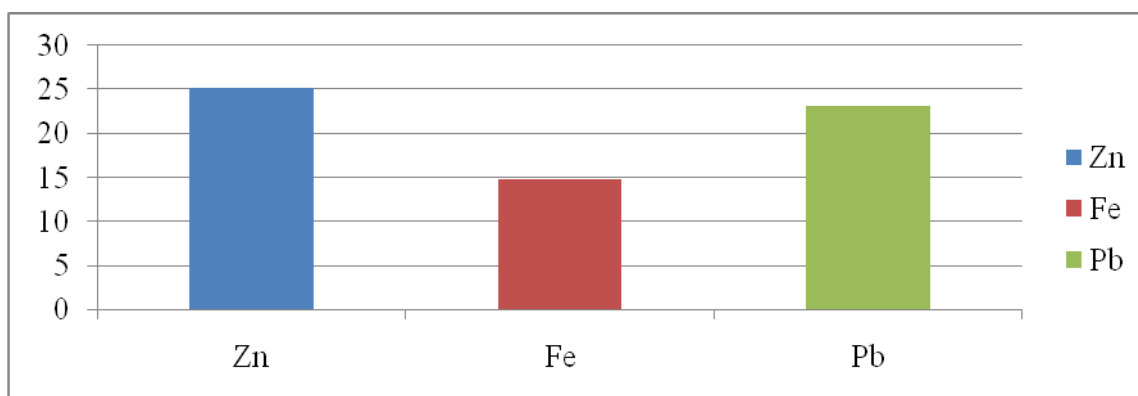


Figure 3: Percentage Absorbance of Heavy Metals in Stems of Corn on Controlled soil sample after 8 weeks

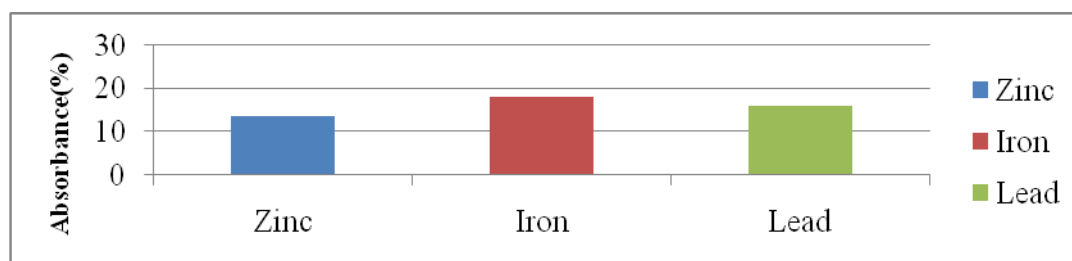


Figure 4: Percentage Absorbance of Heavy Metals in Stems of Corn on Contaminated soil sample after 8 weeks

Discussion of Results

Table 1 to 5 shows the level of heavy metals concentration found in the control and contaminated soil samples in 2 weeks interval in a space of 8 weeks. Table 6 and 7 shows the level of heavy metal in the stem and leaf of the harvested plant sample. Figure 1 to 4 shows the comparative reduction in the level of heavy metals in soil over the study period of 12 weeks. Table 1 shows the average concentration of Zn, Fe and Pb at the initial stage was 1.55 mg/kg, 31 mg/kg and 0.13 mg/kg respectively which shows their level in a soil that is not contaminated and from the result it can be deduce that iron has a high concentration in an uncontaminated soil. Also, the average concentration of Zn, Fe and Pb at the initial stage in the contaminated soil was 15.53 mg/kg, 45.7 mg/kg and 4.16 mg/kg respectively which is considerably high for a contaminated soil. Table 2 shows the result of the sample at the end of the 2nd week of experiment.

The concentration of Zn, Fe and Pb in the uncontaminated soil is 0.7 mg/kg, 14.3 mg/kg and 0.11 mg/kg respectively and their average levels in the contaminated soil are 12.36 mg/kg, 32.23 mg/kg and 3.12 mg/kg respectively. These indicate a comparative reduction of the heavy metals ion both the controlled and contaminated soil which can be attributed to the transport of the heavy metal into the roots of the plant. Table 3 shows the result of the sample at the end of the 4th week of experiment. The concentration of Zn, Fe and Pb in the uncontaminated soil is 0.36 mg/kg, 11.04 mg/kg and 0.10 mg/kg respectively and their average levels in the contaminated soil are 9.48 mg/kg, 19.17 mg/kg and 4.18 mg/kg respectively. These also indicates a comparative reduction of the heavy metals in both the controlled and contaminated soil which show more amount of the heavy metals have been absorbed in the corn (*Zea Mays*). Table 4 shows the result of the sample at the end of the 6th week of experiment. The concentration of Zn, Fe and Pb in the uncontaminated soil is 0.25 mg/kg, 8.56 mg/kg and 0.06 mg/kg respectively and their average levels in the contaminated soil are 4.72 mg/kg, 14.44 mg/kg and 1.16 mg/kg respectively.

These also indicates a comparative reduction of the heavy metals in both the controlled and contaminated soil which show more amount of the heavy metals have been absorbed in the corn (*Zea Mays*). Table 5 shows the result of the sample at the end of the 8th week of experiment. The concentration of Zn, Fe and Pb in the uncontaminated soil is 0.22 mg/kg, 8.13 mg/kg and 0.03 mg/kg respectively and their average levels in the contaminated soil are 4.30 mg/kg, 11.54 mg/kg and 0.9 mg/kg respectively. The result at the end of the 8th week also indicates a comparative reduction of the heavy metals in both the controlled and contaminated soil which show more amount of the heavy metals have been absorbed in the plant without affecting the development of the corn (*Zea Mays*). In summary, it can be deduced that the level of Zn, Fe and Pb in both the controlled and contaminated sample reduce over time of 8 weeks. From Figure 1, the percentage absorbance of Zn, Fe and Pb into the leaves of the plant is 20.65 %, 14.00 % and 15.38 % respectively of their initial concentration from the controlled soil sample into the leaves. In Figure 2, there was an uptake of 12.23 % Zn, 14.3 % Fe and 13.9 % Pb of the initial concentration from the contaminated soil sample into the leaves of the corn. From these results, it can be deduce that Zn has the highest absorption rate into the leaves from the controlled soil sample and Fe has the highest absorption rate into leaves of the contaminated soil sample.

From figure 3, there was an uptake of 25.16 % Zn, 14.74 % Fe and 23.08 % Pb of the initial concentration from the controlled soil sample into the stem of the plant. Also, in Figure 4 there was an uptake of 13.52 % Zn, 18.14 % Fe and a 15.87 % Pb of the initial concentration from the contaminated soil sample into the stem of the corn plant. From these results, it can be deduce that Zn has the highest absorbance rate into the stem from the controlled soil sample and Fe has the highest absorbance rate into the stem from the contaminated soil sample. The results also pointed out that the level of the heavy metals in the stem were more than their amount in the leaves which can be attributed to the further transportation of the heavy metals from the stem to the leaves. The highest removal of Zn concentration in the contaminated soil sample was in the sixth week period and the highest removal of Fe and Pb was in the Fourth week.

From all these result obtained, it shows there was a steady decrease in the levels of the heavy metals in both the controlled and contaminated soil sample and an increase in the levels of these heavy metals in the leaves and stem of the corn accompanied by their corresponding decrease in soil sample indicate that they are accumulating into the corn through its root. The increase in the levels of these heavy metals in the corn sample can be attributed to two major transport mechanisms: convection and diffusion. There is a transport of soluble metal ions from the soil solid to the root surface due to convection because as water is being lost by the leaves due to transpiration. There is need of replacement of these water from the soil, these water loss to the atmosphere create a concentration gradient thereby driving the diffusion of ions towards the depleted layer of the plant thereby creating a movement from the soil into the roots, stems and leaves. Some ions are absorbed by roots faster than the rate of the supply.

IV. CONCLUSION

From the results obtained in the cause of this study, it was deduced that there was an uptake of 25.16 % Zn, 14.74 % Fe and 23.08 % Pb of the initial concentration from the controlled soil sample and an uptake of 13.52 % Zn, 18.14 % Fe and a 15.87 % Pb of the initial concentration from the contaminated soil sample into the stem of the corn plant. Therefore it can be concluded that corn (*Zea Mays*) is a hyper accumulator of heavy metal, tolerant of the targeted metals and also had a fast growth rate and is a good phytoremediation agent.

REFERENCES

- [1] Brady, N.C., & R.R. Weil. (1999). The nature and properties of soils. 12th Ed. Prentice Hall. Upper Saddle River, NJ.
- [2] Cherian, S. & Oliveira, M.M. (2005). Transgenic plants in phytoremediation: recent advance and new possibilities. *Environ Sci Technol.* 2005; 39(24):9377-9390. Doi: 10.1021/es051134I.
- [3] Cunningham, S.D., Berti, W.R. & Huang, J.W. (1995). Phytoremediation of contaminated soils: A broad review of the phytoremediation of metals and organic. *Trends Bioethanol* 1995, 13:393±397.
- [4] Cynthia, R.E & David, A.D. (1997). Remediation of metals-contaminated soils and groundwater. Department of Civil and Environmental Engineering, Camegie Mellon University, Pittsburgh, PA 15238. GWRTAC.
- [5] Ghafoor A., Rauf, A., Arif, M. & Muzaffar, W. (2008). Chemical composition of wastewaters from different industries of the Faisalabad city. Pg 367–369.
- [6] Hajar A.S.M. (1997.) Comparative ecology of *Minuartia Verna* (L.) Hiern and *thlaspi alpestre* in Southern Pennines, with special reference to heavy metal tolerance. University of Sheffield, Sheffield UK
- [7] Kumar, P., Dushenkov, V., Motto, H. & Raskin, I. (1995). Phytoextraction: the use of plants to remove heavy metals from soils. *Environ Sci Tech* 1995, 29:1232±1245.
- [8] Mohammed, I.L., Zhen-li, H., Peter, J.S. & Xiao-e, Y. (2008). Phytoremediation of Heavy Metal Polluted Soils and Water: Progress and Perspectives. *Journal of Zhejiang. Univ Sci B.* 2008 March; 9 (3): 210-220. Doi: 10.1631/jzus.B0710633 PMID: PMC2266886.
- [9] Peuke, A. D. & Rennenberg, H. (2005). Phytoremediation with transgenic trees. 199 – 207.
- [10] Proctor J. (1990). The influence of cadmium, copper, lead, and zinc on the distribution and evolution of metallophytes in the British Isles. Pg 91-108.
- [11] Reeves, R.D. & Baker, A.J.M. (2000). Metal-accumulating plants. In: *Phytoremediation of toxic metals: using plant to clean up the environment.* Raskin, I. and Ensley, B.D. (Eds). Wiley, New York, pp: 190 – 200.
- [12] Sebastiani, L., Scebba, F. & Tognetti, R. (2004). Heavy metal accumulation and growth response in poplar clones *Eridano* (*Populus deltoids x maximowiczii*) and I-214 (*P. x euramericana*) exposed to industrial waste. *Environmental and Experimental Botany.* Vol. 52. No. 1, pp. 70-71.
- [13] Shaylor, H., McBride, M., & Harrison, E. (2009). Guide to soil testing and interpreting results. Ithaca, NY: Cornell University, Department of Crop and Soil Sciences, Waste Management Institute. Retrieved June 12, 2011 from <http://cwmi.css.cornell.edu/guide%20to%20soil.pdf>.
- [14] Wenzel, W.W., Maria, N., & Dos Santos, U. (1999). Phytoextraction of metal polluted soils in Latin America. Department of Forest- and Soil Science. University of Natural Resources and Applied Life Sciences, Vienna. Peter-Jordan-Str. 82, A-1190 Vienna.
- [15] Yu, B., Zhang, Y., Shukla, A., Shukla, S.S & Dorris, K.L. (2001). The removal of heavy metals from aqueous solutions by sawdust adsorption-removal of lead and comparison of its adsorption with copper. Harzard, J. Mater., A and B Environmental Service, Houston, TX, USA. B84: 83 – 95.
- [16] Mater., A and B Environmental Service, Houston, TX, USA. B84: 83 – 95.

Design of Vibration Isolator for Machine-tool

Komma.Hemamaheshbabu¹, Tippa Bhimasankara Rao², D.Muralidhar yadav³

¹PG Student, Department of Mechanical Engineering, Nimra Institute of Science and Technology

² HOD, Department of Mechanical Engineering, Nimra Institute of Science and Technology, Vijayawada, AP, INDIA

³ associate Professor, Dr.Samual George Institute Of Engineering & Technology, Markapur

ABSTRACT

Our project work mainly deals with design of vibration isolator for milling machine, which is being vibrated due to transmission of vibration from its neighbouring machine tool through ground. The vibration signature of the vibrating machine and its attenuation during transmission through ground is considered and the resultant exciting force amplitude is determined. The vibration isolator is designed to isolate the milling machine from that exciting force considering maximum allowable amplitude for cutter of milling machine. The result is also analysed and verified using Ansys.

Keywords: ANSYS. Amplitude. Milling machine. Pro-E. Vibration isolator.

I. INTRODUCTION

Vibration is a term that describes oscillation in a mechanical system. It is defined by the frequency (or frequencies) and amplitude. Either the motion of a physical object or structure or, alternatively, an oscillating force applied to a mechanical system is vibration in a generic sense. Conceptually, the time-history of vibration may be considered to be sinusoidal or simple harmonic in form. The frequency is defined in terms of cycles per unit time, and the magnitude in terms of amplitude (the maximum value of a sinusoidal quantity). The vibration encountered in practice often does not have this regular pattern. It may be a combination of several sinusoidal quantities, each having a different frequency and amplitude. If each frequency component is an integral multiple of the lowest frequency, the vibration repeats itself after a determined interval of time and is called periodic. If there is no integral relation among the frequency components, there is no periodicity and the vibration is defined as complex. Vibration isolation concerns means to bring about a reduction in a vibratory effect. A vibration isolator in its most elementary form may be considered as a resilient member connecting the equipment and foundation. The function of an isolator is to reduce the magnitude of motion transmitted from a vibrating foundation to the equipment or to reduce the magnitude of force transmitted from the equipment to its foundation. Our project work mainly deals with design of vibration isolator for milling machine, in which is being vibrated due to transmission of vibration from its neighboring machine tool through ground. The vibration signature of the vibrating machine and its attenuation during transmission through ground is considered and the resultant exciting force amplitude is determined. The vibration isolator is designed to isolate the milling machine from that exciting force considering maximum allowable amplitude for cutter of milling machine. And the result is also analysed and verified using Ansys.

II. CONCEPT OF VIBRATION ISOLATION

The concept of vibration isolation is illustrated by consideration of the single degree-of-freedom system illustrated in Fig. 1. This system consists of a rigid body representing equipment connected to a foundation by an isolator having resilience and energy dissipating means; it is unidirectional in that the body is constrained to move only in vertical translation. The performance of the isolator may be evaluated by the following characteristics of the response of the equipment-isolator system of Fig. 1 to steady-state sinusoidal vibration.

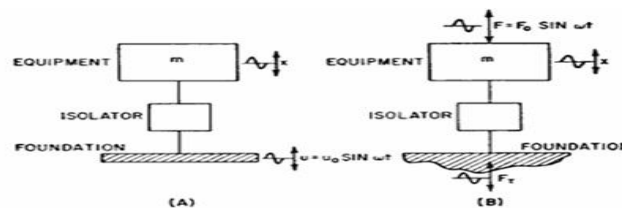


Fig.1 vibration isolation

- **Absolute transmissibility:** Transmissibility is a measure of the reduction of transmitted force or motion afforded by an isolator. If the source of vibration is an oscillating motion of the foundation (motion excitation), transmissibility is the ratio of the vibration amplitude of the equipment to the vibration amplitude of the foundation. If the source of vibration is an oscillating force originating within the equipment (force excitation), transmissibility is the ratio of the force amplitude transmitted to the foundation to the amplitude of the exciting force.
- **Relative transmissibility:** Relative transmissibility is the ratio of the relative deflection amplitude of the isolator to the displacement amplitude imposed at the foundation. A vibration isolator effects a reduction in vibration by permitting deflection of the isolator. The relative deflection is a measure of the clearance required in the isolator. This characteristic is significant only in an isolator used to reduce the vibration transmitted from a vibrating foundation.
- **Motion response:** Motion response is the ratio of the displacement amplitude of the equipment to the quotient obtained by dividing the excitation force amplitude by the static stiffness of the isolator. If the equipment is acted on by an exciting force, the resultant motion of the equipment determines the space requirements for the isolator, i.e., the isolator must have a clearance at least as great as the equipment motion.

III. VIBRATION IN MACHINE TOOLS AND THEIR ISOLATION

Machining and measuring operations are invariably accompanied by relative vibration between work piece and tool. These vibrations are due to one or more of the following causes: (1) in homogeneities in the work piece material; (2) variation of chip cross section; (3) disturbances in the work piece or tool drives; (4) dynamic loads generated by acceleration/deceleration of massive moving components; (5) vibration transmitted from the environment; (6) self-excited vibration generated by the cutting process or by friction (machine-tool chatter). The tolerable level of relative vibration between tool and work piece, i.e., the maximum amplitude and to some extent the frequency, is determined by the required surface finish and machining accuracy as well as by detrimental effects of the vibration on tool life and by the noise which is frequently generated.

IV. CASE STUDY OF MACHINE-TOOL VIBRATIONS

A heavy machine tool mounted on the first floor of a building has been modeled as a three degree of freedom system.

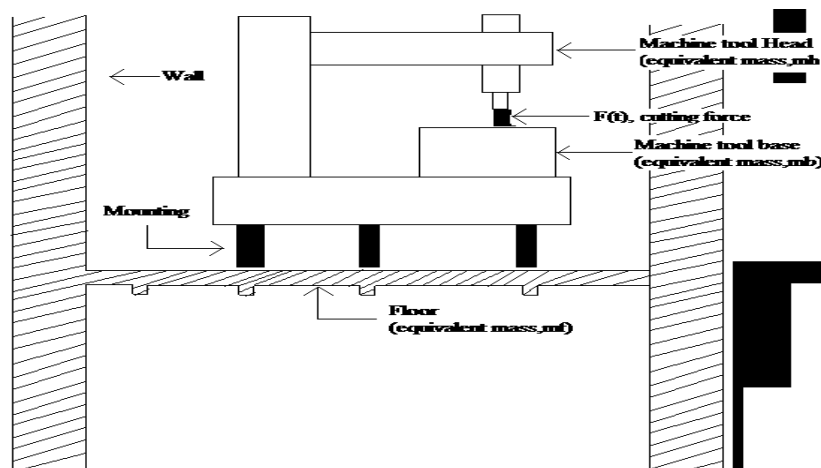


Fig 2 Diagram of drilling machine

V. ISOLATION OF MILLING MACHINE

Ground vibrations from an air compressor is transmitted to a nearby milling machine and is found to be detrimental to achieving specified accuracies during precision milling operations.

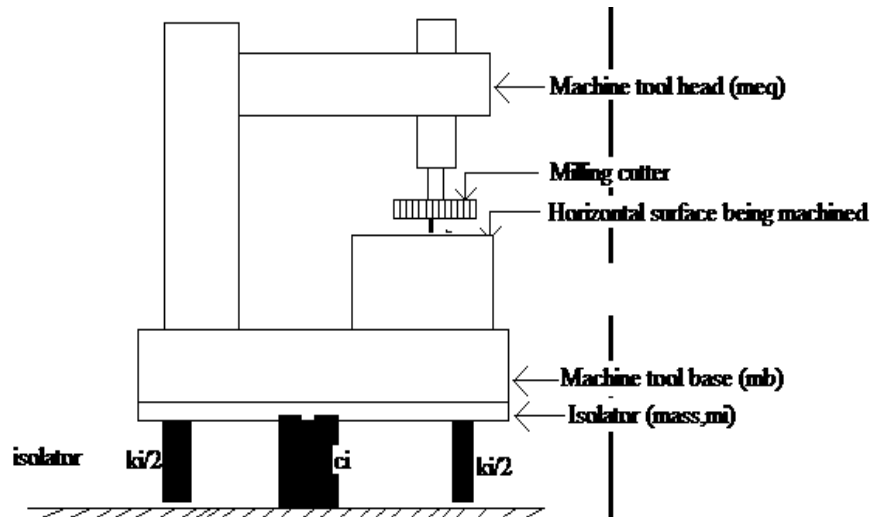


Fig 3 Diagram of milling machine

VI. VERIFICATION USING ANSYS

The result is verified using Ansys. The following are the procedural steps to be followed to perform harmonic analysis.

- **Starting with Ansys**

1. File → clear & start new → Do not read file → OK → Yes.
2. File → change job name → vibration analysis → OK.
3. File → change title → harmonic analysis → OK.
4. Main menu → Preferences → structural → h-method → OK

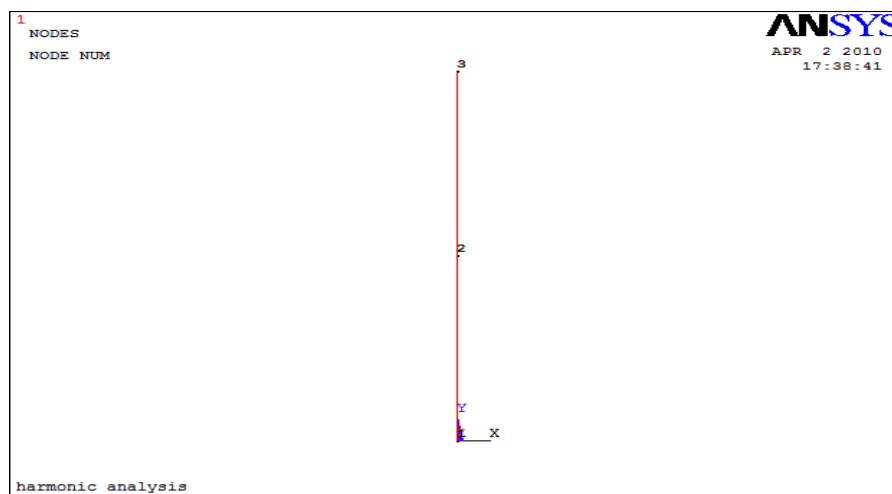


Fig.4 Nodal diagram

- **Specify the analysis type, MDOF, and load step specifications**

- [1] Main menu → solution → Analysis type → New analysis.
- [2] Click once on “Harmonic” and click on OK.
- [3] Main menu → solution → Analysis type → Analysis options
- [4] Click on “Full” to select the solution method.
- [5] Click on “amplitude-phase” to select the DOF printout format and click on OK.
- [6] Main menu → solution → Load step opts → Time/Frequenc → Freq and substeps.
- [7] Enter 0 & 20 for the harmonic frequency range.
- [8] Enter 30 for the number of substeps.
- [9] Click once on “stepped” to specify stepped boundary conditions.
- [10] Click on OK.

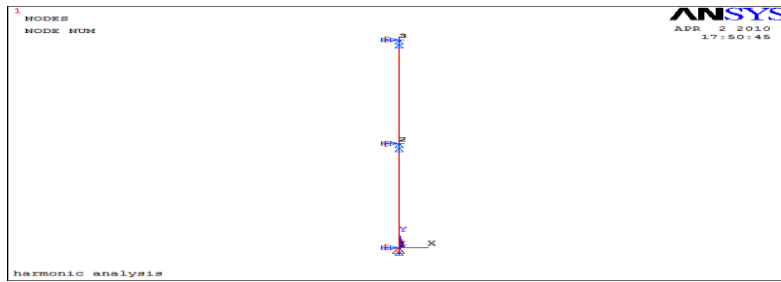


Fig .5 Application of load on nodes

• Solving the Model

- [1] Main menu → solution → solve → current LS
- [2] Review the information in the status window and click on close.
- [3] Click on OK on the solve current Load step dialog box to begin the solution.
- [4] When the solution is finished, a dialog box starting “Solution is done!” appears.
- [5] Click on close.

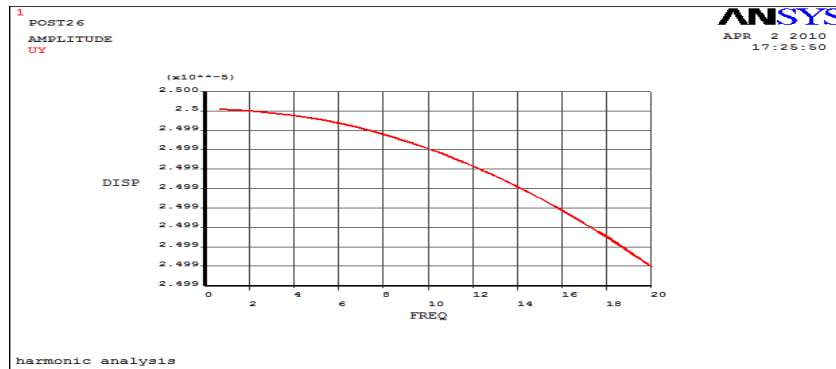


Fig 6 Frequency Vs Amplitude

VII. RESULTS AND DISCUSSION

We have designed a vibration isolator for milling machine. Theoretically we designed the isolator whose mass is obtained as 4060Kg with the help of given displacement of cutter as 2.5×10^{-6} m. We solved the same using harmonic analysis in Ansys an analysis package. In Ansys we gave the mass and found the displacement of cutter axis. We got the graph as shown in the figure below.

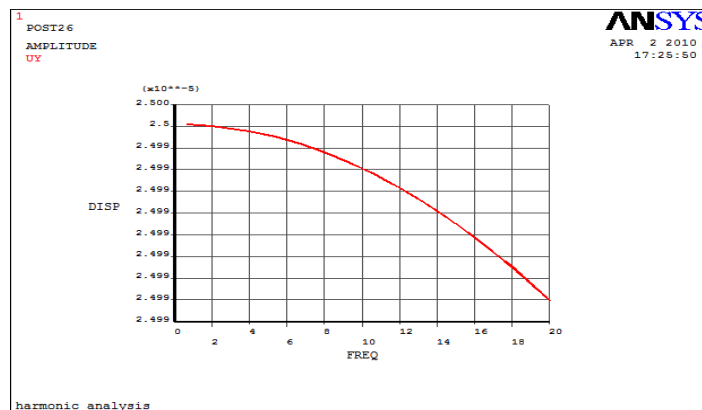


Fig 7 Frequency Vs Amplitude

From the graph it is clear that the maximum amplitude is 2.5×10^{-6} m. From above it is clear that the results obtained in both the cases i.e. theoretical value as well as the value obtained by Ansys are same.

VIII. CONCLUSION

The vibration isolator for a milling machine being excited by neighboring machine was designed successfully theoretically, and is verified using ANSYS software. A vibration isolator for milling machine is designed. Theoretically designed isolator has a mass of 4060Kg with the help of given displacement of cutter as 2.5×10^{-6} m. The same was verified using harmonic analysis in Ansys an analysis package. In Ansys the displacement of cutter axis is found and the graph is plotted, from which it is clear that the maximum amplitude is 2.5×10^{-6} m. Thus, the results obtained in both the cases i.e. theoretical value as well as the value obtained by Ansys are same.

REFERENCES

- [1]. Machine design by r.s. khurmi
- [2]. Psg, 2008."design data," kalaikathir achchagam publishers, coimbatore, india
- [3]. Intelligent Systems": A Comparative StudyHindawi Publishing Corporation Applied Computational Intelligence and Soft Computing Volume 2011, Article ID 183764, 18 pages.
- [4]. Abbas Fadhel Ibraheem, Saad Kareem Shather & Kasim A. Khalaf, "Prediction of Cutting Forces by using Machine Parameters in end Milling Process", Eng.&Tech. Vol.26.No.11, 2008.
- [5]. S. Abainia, M. Bey, N. Moussaoui and S. Gouasmia." Prediction of Milling Forces by Integrating a Geometric and a Mechanistic Model", Proceedings of the World Congress on Engineering 2012 Vol III WCE 2012, July 4 - 6, 2012, London, U.K.
- [6]. Md. Anayet u patwari, a.k.m. nurul amin, waleed f. Faris, 'prediction of tangential cutting force in end milling of Medium carbon steel by coupling design of experiment and Response surface methodology'. Journal of mechanical engineering, vol. Me 40, no. 2, December 2009 Transaction of the mech. Eng. Div., the institution of engineers, Bangladesh.
- [7]. Smaoui, M.; Bouaziz,z. &Zghal,A., 'Simulation of cutting forces for complex surfaces in Ball-End milling', Int j simul model 7(2008) 2,93-105.

Power Systems Generation Scheduling and Optimization Using Fuzzy Logic Techniques

Yogesh Sharma¹, Kuldeep Kumar Swarnkar²

¹M.E. Student, Electrical Engineering Department MITS, Gwalior (M.P)

²Asst. Professor, Electrical Engineering Department MITS, Gwalior (M.P)

ABSTRACT

In this, paper solving the unit commitment problem is usual in a generation scheduling such that the overall generating cost can be at least while satisfying a variety of constraints. The four-generating units are using for the thermal power plant as a case study. The dynamic programming, dynamic graphical programming and fuzzy logic algorithm apply a solution to the unit commitment problem that is logical, possible and with affordable cost of operation which is the main goal of unit commitment. The results procured by the fuzzy logic algorithm are tabular, graphed and compared with that obtained by the dynamic programming and dynamic graphical programming. The result shows that the implementation of fuzzy logic provides a possible solution with significant savings order to obtain preferable unit combinations of particular load demand of at each time period. the commitment is such that the total cost is minimizing. The total cost includes both the production cost and the costs associated with start-up and shutdown of units. Dynamic programming, dynamic graphical programming is an optimization technique which gives the optimal solution.

Keywords : Generation scheduling, Unit commitment, fuzzy-logic, dynamic programming, dynamic graphical programming and optimization

I. INTRODUCTION

In the early days the power system consisted of isolated stations and their individual loads. Unit commitment is one of the decision-making levels in the hierarchy of power system operations management. The optimization problem is posed over Time horizons that vary from 24 hours to one week. The objective is to determine the set of generating units, among those owned by a utility that should be connected to the power grid on an hourly basis to supply the demand at minimum operating cost over the scheduling horizon. This optimization problem is constrained by the unit characteristics and other operation limitations. Since the objective of the unit commitment is to determine a cyclic schedule that will meet the system constraints at minimum cost, the economic operation of a power system may be formulated as a dynamic optimization problem[2]. The problem is dynamic in the sense that decisions to startup and/or shutdown units at any stage cannot be made without considering the states of the system at some other stages. The problem of UC is nothing but to determine the units that should operate for a particular load. To 'commit' a generating unit is to 'turn it on', i.e., to bring it up to speed, synchronize it to the system, and connect it, so that it can deliver power to the time network. The unit commitment is commonly formulated as a non-linear, large scale, mixed integer combination optimization problem.

Review of UCP may be developed. The dynamic Programming (DP) method as in [2] Based on priority list is flexible, but the computational time suffers from dimensionality. As Lagrangian relaxation (LR) for UCP was superior to DP due to its higher solution quality and faster computational time. However, numerical convergence and solution quality of LR are not satisfactory when identical units exist [6]. With the advent of heuristic approaches, genetic algorithm (GA) [7], evolutionary programming (EP) [8], simulated annealing (SA) [6], and tabu search (TS) [8] have been proposed to solve the UC problems. The results obtained by GA, EP, TS and SA require a considerable amount of computational time especially for large system size.

The use of fuzzy logic has received increased attention in recent years because of its worth in dropping the requirement for difficult mathematical models in problem solving. , in comparison fuzzy logic employing linguistic condition, which deal with the practicable relationship between input and output variables. For this cause, fuzzy logic algorithm makes it easier to manipulate and solve several problems, particularly where the mathematical model is not explicitly known, or is hard to solve.

Moreover, fuzzy logic as a new technique approximates reasoning while allowing decisions to be made efficiently. To achieve a good unit commitment planning under fuzzy approach, generation cost and load demand are all specified as a fuzzy set notation. Fuzzy Logic Technique is then applied to yield the desired commitment schedule.[1] In order to demonstrate the superiority of this proposed approach, the power plant of four-thermal generating units is chosen as a test system.

II. THE UNIT COMMITMENT PROBLEM

The unit commitment problem can be mathematically described as given in equation (1).

$$\text{Min } F_i(P_i^t, U_i^t) = \sum t \sum i [(a_i P^2 + b_i P + c_i)] + SC_i^t(1 - U_i^{t-1})U_i^t \quad (1)$$

Where $F_i(P_i^t)$ is the generator fuel cost function in quadratic form, a_i , b_i and c_i are the coefficients of unit i , and P_i^t is the power generation of unit i at time t . [1]

A. Problem Constrains

The minimization of the objective function is subjected to two kinds of constraints, namely: system and unit Constraints and these can be summarized as follows:

B. System Constraints

(i) **Power Balance Constraints:** to satisfy the load balance in each stage, the forecasted load demand should be equal to the total power generated for every feasible combination. Equation (2) represents this constraint where P_D^t represents the total power load demand at a certain period [3].

$$\sum_{i=1}^N P_i^t U_i^t - (P_D^t) = 0 \quad (2)$$

For each time period (T), the spinning reserve requirements R must be met and this can be mathematically Formulated as in equation (3) [3]:

$$\sum_{i=1}^N P_i^{max} U_i - (P_D) = R \quad t = 1, 2, 3, \dots, T \quad (3)$$

C Unit constraints

(i) **Generation Limits:** Each unit must satisfy its generation range and this certain rated range must not be violated. This can be accomplished through satisfying the formula in equation (4) [3]:

$$P_i^{min} U_i^t \leq P_i \leq P_i^{max} U_i^t \quad i = 1, 2, 3, \dots, N \quad (4)$$

Where: P_i^{min} and P_i^{max} are the generation limits of unit i .

(ii) **Ramp-Up and Ramp-Down Constraints:** To avoid damaging the turbine, the electrical output of a unit cannot be changed by more than a certain amount over a period of time. For each unit, the output is limited by ramp up/down rate at each time period the unit is turned on/off and this can be formulated as in equations (5) and (6)

$$P_i^{t-1} - P_i^t \leq RD_i \text{ if } (U_i^t = 1) \text{ and } (U_i^{t-1} = 1) \quad (5)$$

$$P_i^t - P_i^{t-1} \leq RU_i \text{ if } (U_i^t = 1) \text{ and } (U_i^{t-1} = 1) \quad (6)$$

Where: RD_i and RU_i is respectively the ramp down and ramp up rate limit of unit i . [3]

III. DYNAMIC PROGRAMMING

Dynamic programming acts as an important optimization technique with broad usage areas. It decomposes a problem for a series of smaller problems, solves them, and develops an optimal solution to the original problem step-by-step. The optimal solution is developed from the sub problem recursively. In its fundamental form, the dynamic programming algorithm for unit commitment problem examines every possible state in every space. Some of these states are found to be infeasible and hence they are rejected immediately. But even, for an average size utility, a large number of feasible states will exist and the requirement of execution time will stretch the capability of even the largest computers. [2] Hence many proposed techniques use only some part of simplification and approximation to the fundamental dynamic programming algorithm. Dynamic programming has many advantages over the enumeration scheme.

The chief advantage being the reduction in the dimensionality of the problem. Suppose we have found units in a system and any combination of them could serve the single load. A maximum of 2^N-1 combinations are available for testing. If:-

- [1] No load costs are zero.
- [2] 2. Unit input-output characteristics are linear between zero output and full load.
- [3] There are no other restrictions.
- [4] Start-up costs have a fixed amount.

In the dynamic programming approach that types, it is approved that:

- [1] A state consists of an array of units with only specified units operating at a Time and rest off-line.
- [2] The start-up cost of a unit is independent of the time it has been off-line (i.e., it is a fixed amount).
- [3] There are constant costs for shutting down a unit.
- [4] There is a strict priority order, and in each space a specified lower reaches Amount of capacity must be operating.

A thinkable state is one in which of the committed units can be supply the required load and that meets the amount of capacity at each period [2]

IV. FUZZY LOGIC IMPLEMENTATION

Fuzzy logic has sharply become one in every of the foremost among the current technologies for developing advanced control systems. Fuzzy logic addresses applications dead because it resembles human higher cognitive process power. it's the ability to get precise solutions from bound or rough detail. It fills a vital gap in engineering design strategies that was left vacant by the foremost mathematical approaches (e.g. linear control design), and strictly logic-based approaches (e.g. expert systems) in system design. Whereas alternative approaches require accurate equations to model real-world behaviors, fuzzy design will work well with the ambiguities of real-world human language and logic. Fuzzy logic may be a superset of conventional (Boolean) logic that has been extended to handle the construct of partial true values between "completely true" and "completely false". As its name suggests, it's the logic underlying modes of reasoning that are approximate instead of exact. [10] The importance of fuzzy logic comes from the actual fact that almost all modes of human reasoning, wisdom reasoning, are approximate in nature.

The essential characteristics of fuzzy logic as supported by Zadeh Lotfi as follows:

- In fuzzy logic, precise reasoning is viewed as a limiting case of approximate reasoning.
- In fuzzy logic, matter of degree plays an important role. Any system is fuzzified.
- In fuzzy logic, information is interpreted as a group of elastic or, equivalently, fuzzy constraint on a group of variables
- Inference is viewed as a process of propagation of elastic constraints

V. UNIT COMMITMENT USING FUZZY LOGIC

A. Fuzzy Model for the Unit Commitment Problem

The target of all electrical utility is to control at minimum cost whereas meeting the load demand and spinning reserve needs. Within the gift formulation, the fuzzy variables related to the unit commitment downside are the load capability of generator (LCG), the Incremental fuel cost (IC), the start-up cost (SUC) because the input parameters and also the generation cost (GRC) because the output parameter. These fuzzy variables are given and shortly explained within the following:

- **The load capability of generator** is taken into account to be fuzzy, because it relies upon the load demand at amount of your time.
- **Incremental fuel cost is taken to be fuzzy**; as a result of the cost of fuel could amendment over the amount of your time, and since the cost of fuel for every unit is also completely different.
- **Start-up costs** of the units area unit assumed to be fuzzy, as a result of some units are on-line et al are offline. And it's necessary to say that we tend to embody the beginning costs, closedown costs, maintenance costs and crew expenses of every unit as a set worth that's start-up cost. So, start-up cost of a unit is freelance of the time it's been off line.[1]
- **Generating cost** of the system is treated as a fuzzy variable since it's directly proportional to the hourly load.

B. Fuzzy Sets Associated with Unit Commitment

After characteristic the fuzzy variables related to the unit commitment, the fuzzy sets process these variables area unit hand-picked and normalized between 0 and 1. [1] This normalized cost may be increased by a particular multiplier factor to adjust any desired variable.

The sets process the load capability of generator (LCG) area unit as follows:

LCG (MW) = Low (Lo), Below Average (BAV), Average (Av), above Average (AAV), High (H)

The Incremental cost (IC) is declared by the subsequent sets,

IC (Rs) = {low, small, large}

The Startup cost (SUC) is outlined by the subsequent sets

SUP (Rs) = {Zero, Medium, High}

The cost, chosen because the objectives perform is given by,

GRC (Rs) = Low (Lo), Below Average (BAV), Average (Av), above Average (AAV), High (H)

Suitable ranges area unit hand-picked for the fuzzy sets hand-picked from the given problem [1]

C Membership function

Based on the fuzzy sets, the membership functions are chosen for every fuzzy input and output variables. Triangular membership function is chosen for all the fuzzy variables.

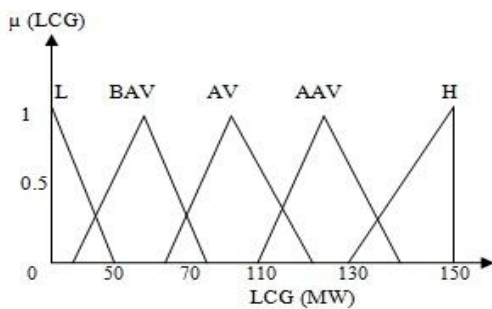


Figure.1 Membership function of load capacity of Generators

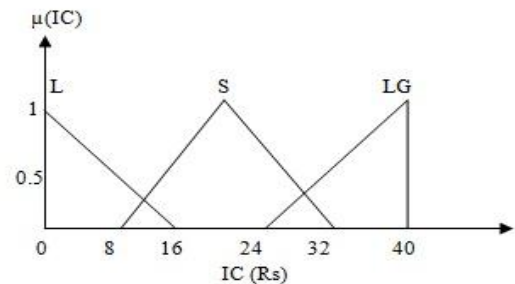


Figure.2 Membership function of Incremental Cost

D Fuzzy If - Then Rules

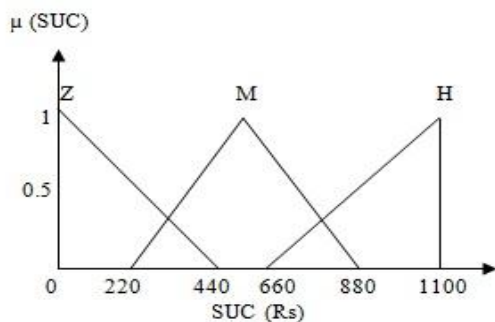


Figure (3): Membership function of Start-up Cost

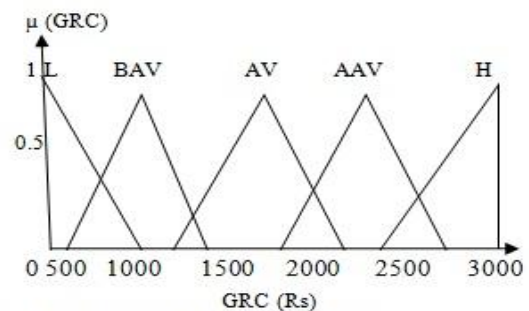


Figure (4): Membership function of generation cost

In a fuzzy-logic-based approach, choices area unit created by forming a series of rules that relate the input variables to the Output variable victimization if-then statements. [1] The If (condition) is an antecedent to the Then (consequence) of each rule. Each decree general can be diagrammatical in the following manner:If (antecedent) then (consequence) Load capacity of generator, marginal cost, and startup cost area unit thought-about as input variables and cost is treated because the output variable. This relation between the input variables and the output variable is given as:

$$\text{Generation cost} = \{(\text{Load capacity of Generator}) \text{ and } (\text{Incremental Cost}) \text{ and } (\text{start-up Cost})\}$$

In fuzzy set notation this is often written as

$$\text{GRC} = \mu_{\text{LCG}} \cap \mu_{\text{IC}} \cap \mu_{\text{SUP}} \text{ Or } \text{GRC} = \min \{ \mu_{\text{LCG}}, \mu_{\text{IC}}, \mu_{\text{SUP}} \} \tag{7}$$

Using the above notation, fuzzy rules area unit written to associate fuzzy input variables with the fuzzy output variable. primarily based Upon these relationships, and with relation to, a total of forty five rules are often composed (since there are a unit five subsets for Load capability of generator, 3 subsets for differential cost, and three subsets for start-up cost (5×3×3=45).[1] Following If (the load capability of a generator is low, and the incremental fuel cost is massive and the start–up cost is zero),then the production cost is low. other rule area unit show in table1 for fuzzification and the fuzzy results should be defuzzified by a definite defuzzification methodology once relating the input variable to the output variable as listed in Table 1. that's referred to as a defuzzification method to realize crisp numerical values.

E Defuzzification Process

Defuzzification is the transformation of the fuzzy signals back to crisp values. One of the most normally used ways of defuzzification ways Mean of maxima (MOM) methodology. Mistreatment this methodology, the generation cost is obtained as in equation (8):

RULE	LCG	IC	SUC	GRC	RULE	LCG	IC	SUC	GRC
1	L	L	Z	L	24	AV	S	H	AV
2	L	L	M	L	25	AV	LG	Z	AV
3	L	L	H	L	26	AV	LG	M	AV
4	L	S	Z	L	27	AV	LG	H	AV
5	L	S	M	L	28	AAV	L	Z	AAV
6	L	S	H	L	29	AAV	L	M	AAV
7	L	LG	Z	L	30	AAV	L	H	AAV
8	L	LG	M	L	31	AAV	S	Z	AAV
9	L	LG	H	L	32	AAV	S	M	AAV
10	BAV	L	Z	BAV	33	AAV	S	H	AAV
11	BAV	L	M	BAV	34	AAV	LG	Z	AAV
12	BAV	L	H	BAV	35	AAV	LG	M	AAV
13	BAV	S	Z	BAV	36	AAV	LG	H	AAV
14	BAV	S	M	BAV	37	H	L	Z	H
15	BAV	S	H	BAV	38	H	L	M	H
16	BAV	LG	Z	BAV	39	H	L	H	H
17	BAV	LG	M	BAV	40	H	S	Z	H
18	BAV	LG	H	BAV	41	H	S	M	H
19	AV	L	Z	AV	42	H	S	H	H
20	AV	L	M	AV	43	H	LG	Z	H
21	AV	L	H	AV	44	H	LG	M	H
22	AV	S	Z	AV	45	H	LG	H	H
23	AV	S	M	AV					

$$\text{GENERATION COST} = \sum_{i=1}^n \frac{GRC_i}{\mu(GRC)_i} \tag{8}$$

Where: $\mu(GRC)_i$ is the membership value of the clipped output and $(GRC)_i$ is the quantitative value of the clipped output and n is the number of the points corresponding to quantitative value of the output.

Table (1): Fuzzy Rules Relating Input/output Fuzzy Variable [1]

VI. CASE STUDY

Plant in Turkey with four generating units has been thought-about as a case study. A daily load demand divided into eight periods (three hours for each) is taken into account. Table two contains this load demand [12] whereas Figure (5) bar graphs this demand. The unit commitment drawback are going to be resolved applying the dynamic programming and dynamic graphical programming and fuzzy logic approaches and therefore the results are going to be compared. The parameters of those four generating units as well as the value coefficients, the most and therefore the minimum real power generation, the start-up cost, and therefore the ramp rates of every unit are given in Table 2. As mentioned, the generation cost (GRC) is taken into account because the output variable whereas the load capability of a generator (LCG), the incremental fuel cost(IC) and therefore the start-up cost (SUC) is taken as input variables. It's vital to notice that the ranges of every set are selected once some experiments in an exceedingly subjective manner. As an example, if the loads vary which will be served by the biggest generator is between 0 to 150 MW, Then low LCG can be chosen at intervals the vary of 0–35 MW. [1]This enables a relative and virtual analysis of the linguistic definitions with the numerical values. Similarly, the subsets for different variables are often lingually outlined and it's clear that the vary of LCG and GRC is wider than IC and SUC. Thus 5 zones area unit created for each LCG and GRC fuzzy variables and 3 zones for the slim variables (IC and SUC)

Unit No	Generation Limits		Running cost			Start-up cost		Ramp Rates	
	P _{min} (MW)	P _{max} (MW)	A (\$/MW ² .h)	B (\$/MW.h)	C (\$/h)	SC (\$)	SD (\$)	RU (MW/h)	RD (MW/h)
1	8	32	0.515	10.86	149.9	60	120	6	6
2	17	65	0.227	8.341	284.6	240	480	14	14
3	35	150	0.082	9.9441	495.8	550	1100	30	30
4	30	150	0.074	12.44	388.9	550	1100	30	30

Table (2): Parameters for the Four-Unit Tuncbilek Thermal Power Plant [12]

Table (3): Daily Load Demand (MW)

Period hour	Demand(MW)
1-3	168
3-6	150
6-9	260
9-12	275
12-15	313
15-18	347
18-21	308
21-24	231

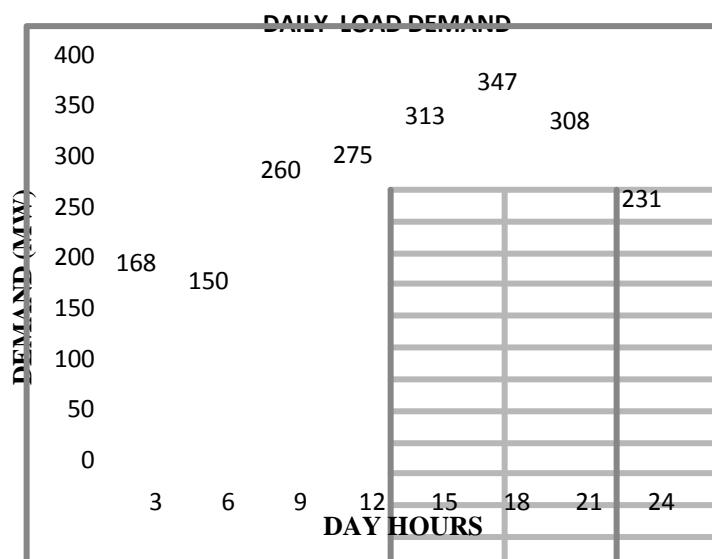


Figure (5): daily load demand in Mega Watt (MW)

VII. SIMULATION RESULT

There is fuzzy logic algorithmic rule victimization for the unit commitment drawback of the four-generating units at the Tuncbilek thermal power station in Turkey is developed. A Matlab bug to supply an answer to the matter is additionally developed. The results obtained by the fuzzy logic rule give crisp values of the generation cost in every amount for each given fuzzy input variables. The whole set of results obtained for the four-generating units are summarized in Table 4. The fuzzy logic approach provides a logical and possible answer for each period. For every amount, the ad of the unit commitments equals the load demand. The generation costs obtained by the dynamic programming (DP), dynamic graphical programming (DGP) for victimization to the finding of the start-up cost and therefore the fuzzy logic (FL) comparison result given within the Table 4. There are simulation results of generation cost given in figure 6 is feeding the fuzzy variable knowledge and figure 7 is output of generation cost and figure 8 show the considering with the incremental cost and generation cost with the generating limits of the thought knowledge.

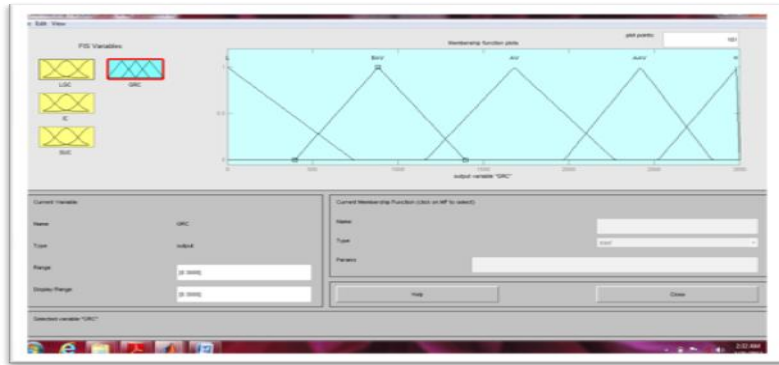


Figure (6): Feeding values to the variables

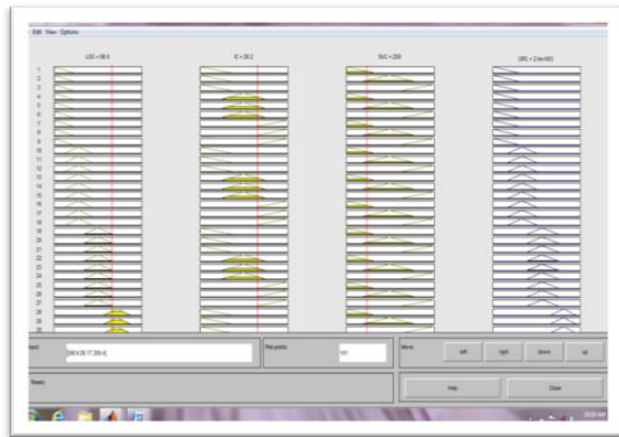


Figure (7): Output of fuzzy in terms of Generation cost

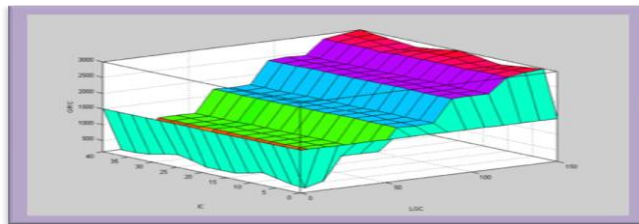


Figure (8): Incremental Cost Vs Generation cost considering Generator limit

Table (4): Comparison between Generation Costs in Rs Obtained From Fuzzy Logic with DP and DGP Method

Period	Load demand(MW)	Unit commitment				IC	Generation cost in Rs		
		Unit 1	Unit 2	Unit 3	Unit 4		DP	DGP	FL
1	168	0	0	87.6920	80.3090	24.32	4413.38	4342.56	3520
2	150	0	0	79.16342	70.83658	22.92	3438.38	3431.38	3460
3	260	0	43.5162	110.7908	105.5932	28.09	6750.17	6734.40	5750
4	275	16.7403	43.1677	110.0306	105.0614	27.98	6849.95	6840.98	6075
5	313	18.9320	48.4999	124.4773	121.0907	30.35	7747.65	7747.65	6130
6	347	20.9916	53.1725	137.3329	135.5031	32.48	8851.98	8851.98	8125
7	308	18.7391	47.8028	122.5849	118.9731	30.04	7596.66	7596.66	6600
8	231	0	39.2739	98.85776	92.66834	26.17	5544.93	5544.93	5420
						TOTAL	51193.1	51090.54	45080.00

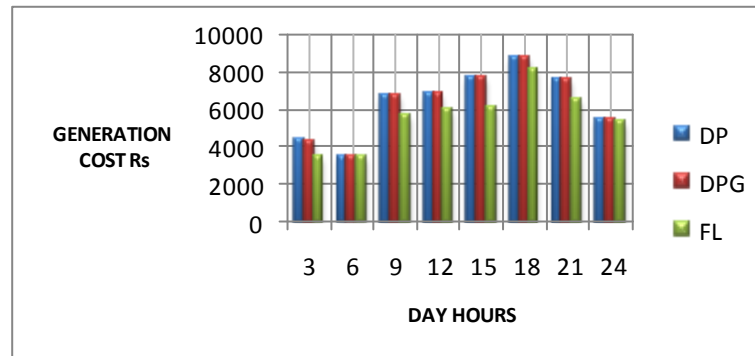


Figure 9 Generation cost of each period

VIII. CONCLUSION

The primary objective has been to demonstrate that if the method of the unit commitment downside will be delineate lingually, then such linguistic descriptions will be translated to resolution an answer that yields a logical and a possible solution to the matter with higher results compared to dynamic programming and dynamic graphical programming. This answer to the unit commitment downside victimization formal logic is with success obtained and also the best set up from a group of fine possible commitment selections has been accomplished. The output Results show that it's doable to urge some enhancements by fuzzy logic approach. Moreover, the results show that the fuzzy logic provides a legitimate and a possible answer to the unit commitment downside whereas satisfying all constraints for every period. For an equivalent unit commitments and also the same incremental fuel cost, the. Within the generation cost obtained by the fuzzy logic area unit less than those obtained by the dynamic programming and dynamic graphical programming. For the eight-time periods, the generation cost is lower once the fuzzy logic approach is used. The savings within the generation cost of the little capability thermal station of Tuncbilek in someday is **6010.54** rupees and monthly **180316** rupees and this makes the annual savings to achieve concerning **2163794.40** rupees. It's powerfully believed that because the capability of the facility plant will increase the savings within the cost conjointly will increase and this justifies the utilization of fuzzy logic to handle the unit commitment downside.

REFERENCES

- [1] Assad Abu-Jasser" Solving the Unit Commitment Problem Using Fuzzy Logic" International Journal of Computer and Electrical Engineering, Vol. 3, No. 6, December 2011.
- [2] Allen J Wood and Bruce F Wallenberg, "power generation, operation and Control", John Wiley and sons, New York.
- [3] S. Saleem, "Unit Commitment Solution Methods", Proceedings of World Academy of Science, Engineering and Technology, Vol-26, ISSN 1307-6884, December 2007, pp 600-605.
- [4] Ahmed Yusuf Saber, Tomonobu Senjyu, Naomitsu Urasaki "Fuzzy Unit Commitment Scheduling Using Absolutely Stochastic Simulated Annealing" IEEE transactions on power systems, VOL. 21, NO. 2, MAY 2006, pp 953-964.
- [5] N. P. Padhy "Unit Commitment – A Bibliographical Survey." IEEE Transactions on Power Systems, vol 9, no 2, pp 1196 – 1205, May 2004.
- [6] N. J. Redondo and A. J. Conejo. "Short-term Hydro-thermal Coordination by Lagrangian Relaxation: Solution of the Dual Problem." IEEE Transactions on Power Systems, vol 14, pp 89 –95, February 1999
- [7] S. Dekranjanpetch, G. B. Sheble and A. J. Conejo. "Auction Implementation Problems using Lagrangian Relaxation." IEEE Transactions on Power Systems, vol 14, pp 82–88, February 1999.
- [8] S. A. Kazarlis, A. G. Bakirtzis and V. Petridis. "A Genetic Algorithm Solution to the Unit Commitment Problem." IEEE Transactions on Power Systems, vol 11, pp 83–92, February 1996.
- [9] K. A. Juste, H. Kita, E. Tanaka and J. Hasegawa. "An Evolutionary Programming Solution to the Unit Commitment Problem." IEEE Transactions on Power Systems, vol 14, pp 1452–1459, November 1999.
- [10] S. Rajasekaran, g. A. Vijayalakshmi pai "neural networks, fuzzy logic and genetic algorithm" prentice-hall of India private limited, new delhi-2013
- [11] A. H. Mantawy, Y. L. Abdel–Magid and S Z Selim Shokri. "Integrating Genetic Algorithm, Tabu Search and Simulated Annealing for the Unit Commitment Problem." IEEE Transactions on Power Systems, vol 14, no 3, pp 829–836, August 1999
- [12] Ü. B. Filik and M. Kurban, "Solving Unit Commitment Problem Using Modified Sub gradient Method Combined with Simulated Annealing Algorithm," Mathematical Problems in Engineering, Hindawy Publishing Corporation, May 2010, Article ID 295645, 15 pages, Doi: 10.1155/2010/295645

Static and Modal Analysis of Leaf Spring using FEA

Meghavath. Peerunaik¹, Tippa Bhimasankara Rao², K.N.D.Malleswara Rao³

¹PG Student, Department of Mechanical Engineering, Nimra Institute of Science and Technology

² HOD, Department of Mechanical Engineering, Nimra Institute of Science and Technology, Vijayawada, AP, INDIA

³asst. Prof, Department Of Mechanical Engineering, Vikas College Of Engineering & Technology, Nunna, Ap, India

ABSTRACT

The objective of this present work is to estimate the deflection, stress and mode frequency induced in the leaf spring of an army jeep design by the ordinance factory. The emphasis in this project is on the application of computer aided analysis using finite element concept. The component chosen for analysis is a leaf spring which is an automotive component used to absorb vibrations induced during the motion of vehicle. It also acts as a structure to support vertical loading due to the weight of the vehicle and payload. Under operating conditions, the behaviour of the leaf spring is complicated due to its clamping effects and interleaf contact, hence its analysis is essential to predict the displacement, mode frequency and stresses. The leaf spring, which we are analyzing, is a specially designed leaf spring used in military jeeps. This spring is intended to bare heavy jerks and vibrations reduced during military operations. A model of such jeep has been shown in this project report. In analysis part the finite element of leaf spring is created using solid tetrahedron elements, appropriate boundary conditions are applied, material properties are given and loads are applied as per its design, the resultant deformation, mode frequencies and stresses obtained are reported and discussed.

Keywords: ANSYS, bending moment, leaf spring, torsional moment, Pro-E.

I. INTRODUCTION

Semi-elliptic leaf springs are almost universally used for suspension in light and heavy commercial vehicles. For cars also, these are widely used in rear suspension. The spring consists of a number of leaves called blades. The blades are varying in length. The blades are usually given an initial curvature or cambered so that they will tend to straighten under the load. The leaf spring is based upon the theory of a beam of uniform strength. The lengthiest blade has eyes on its ends. This blade is called main or master leaf, the remaining blades are called graduated leaves. All the blades are bound together by means of steel straps. The spring is mounted on the axle of the vehicle. The entire vehicle load rests on the leaf spring. The front end of the spring is connected to the frame with a simple pin joint, while the rear end of the spring is connected with a shackle. Shackle is the flexible link which connects between leaf spring rear eye and frame. When the vehicle comes across a projection on the road surface, the wheel moves up, this leads to deflecting the spring. This changes the length between the spring eyes.

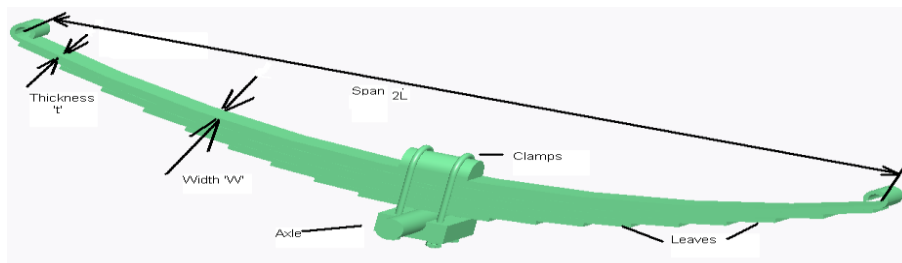


Fig.1 Elements of Leaf spring

1. Geometric properties of leaf spring

Camber = 80mm
Span = 1220mm
Thickness = 7mm
Width = 60mm

Number of full length leaves $n_F = 2$
 Number of graduated leaves $n_G = 8$

II. MATERIAL PROPERTIES OF LEAF SPRING

Parameter	Value
Material selected – Steel	55Si2Mn90
Tensile strength (N/mm ²)	1962
Yield strength (N/mm ²)	1470
Young’s modulus E (N/mm ²)	$2.1 \cdot 10^5$
Design stress (σ_b) (N/mm ²)	653
Total length (mm)	1190
The arc length between the axle seat and the front eye (mm)	595
Arc height at axle seat (mm)	120
Spring rate (N/mm)	32
Normal static loading (N)	3850
Available space for spring width (mm)	60 – 70
Spring weight (kg)	26

Table.1 material properties

Material = Manganese Silicon steel
 Density = $7.86E-6$ kg/mm²
 Poisson’s ratio = 0.3

III. MODELING OF LEAF SPRING

Pro Engineer software was used for this particular model and the steps are as follows:

- [1] Start a new part model with Metric units set.
- [2] Draw the sketches of the trajectories of each leaf of spring with the radius obtained from calculations with span 1220mm camber 80.
- [3] Using sweep command draw a section 60 mm X 7 mm thick sweep along the above drawn curves of leaf.
- [4] According the spring design manual the eye diameter is formed on the first leaf.
- [5] Thickness of leaves = 7mm.
- [6] After all the features of all leaves as are modeled, generate family table for each leaf.
- [7] Generate models for u-clams, axle rod, top support plate etc.
- [8] Assemble each of the leaf in an assembly model and assemble all other models.
- [9] Provide a 1/2 inch dia hole in the leaf spring for bolt.
- [10] Export the model to iges – solid – assembly – flat level.

IV. COMPOSITE MONO LEAF SPRING

The steps for modeling are as follows:

- [1] Start a new part model with Metric units set.
- [2] Draw the sketch of the trajectory with dimensions of first leaf of spring of steel spring assembly without eyes, span is same as 1220mm and camber 80.
- [3] The geometrical dimensions are carried forward from the steel leaf spring except for the number of plates and thickness in order to maintain the required cross section area. Generate sketches cross section dimensions at center and ends as mentioned in table follows:
- [4] Using swept blend
- [5] Select trajectory
- [6] Pivot direction
- [7] Select plane for pivot direction
- [8] Select origin trajectory
- [9] Select cross section sketches. The model is ready.
- [10] Export the model to iges – solid – part – flat level.



Fig.2 Model of mono composite leaf spring

V. ANALYSIS OF LEAF SPRING

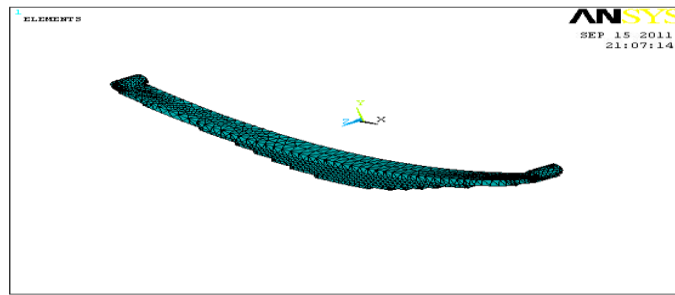


Fig.3 meshed model of leaf spring

VI. RESULTS & DISCUSSION

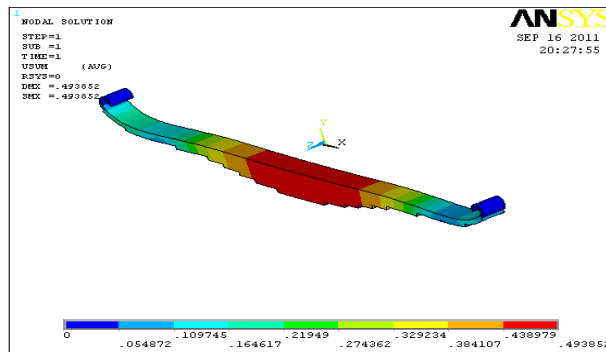


Fig.4 Distribution of Displacements plots at a load of 2000 N on steel leaf spring

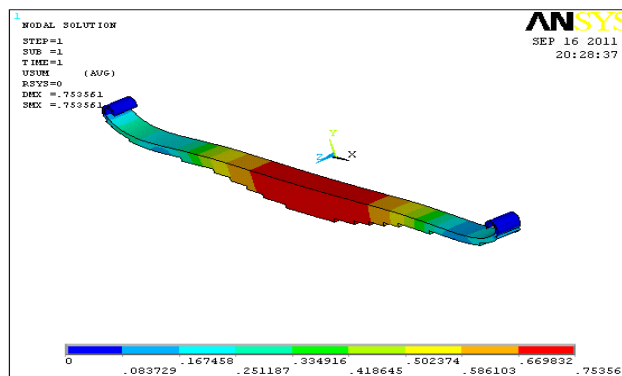


Fig.5 Distribution of Displacements plots at a load of 3000 N on steel leaf spring

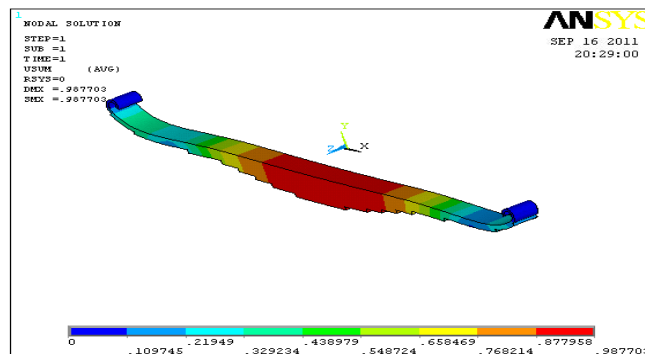


Fig.6 Distribution of Displacements plots at a load of 4000 N on steel leaf spring

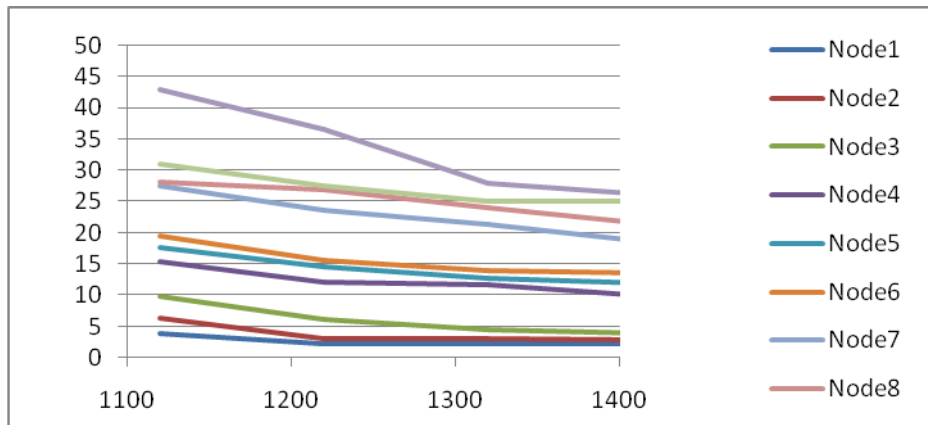


Fig.7 Comparative chart of variation of natural frequency with span

VII. CONCLUSION

The leaf spring has been modeled using solid tetrahedron 4 – node element. By performing static analysis it is concluded that the maximum safe load is 4000 N for the given specification of the leaf spring.

These static analysis results of mono composite Carbon Epoxy leaf springs are compared to steel leaf spring. The results show:

- [1] The stresses in the composite leaf spring are much lower than that of the steel spring.
- [2] The composite spring can be designed to strengths and stiffness much closer to steel leaf spring by varying the layer configuration and fiber orientation angles.
- [3]

The strength to weight ratio is higher for composite leaf spring than conventional steel spring with similar design. The major disadvantages of composite leaf spring are the matrix material has low chipping resistance when it is subjected to poor road environments which may break some fibers in the lower portion of the spring. This may result in a loss of capability to share flexural stiffness. But this depends on the condition of the road. In normal road condition, this type of problem will not be there. Composite leaf springs made of polymer matrix composites have high strength retention on ageing at severe environments. The steel leaf spring width is kept constant and variation of natural frequency with leaf thickness, span, camber and numbers of leaves are studied. It is observed from the present work that the natural frequency increases with increase of camber and almost constant with number of leaves, but natural frequency decreases with increase of span. The natural frequencies of various parametric combinations are compared with the excitation frequency for different road irregularities. The values of natural frequencies and excitation frequencies are the same for both the springs as the geometric parameters of the spring are almost same except for number of leaves.

REFERENCES

- [1]. Machine design by S.Md.Jalaludeen, Anuradha agencies.
- [2]. Machine design by R.K. Jain
- [3]. Machine design by 'R.S. Kurmi'
- [4]. Design of machine elements by 'Bandri'
- [5]. Machine design by R.K. Rajput
- [6]. Design data book by Md.jalaludeen
- [7]. Design data book by P.S.G. College
- [8]. www.cs.cmu.edu/People/rapidproto/mechanisms/references.html
- [9]. Mechanical Engg design – Joseph E. Shigley.
- [10]. Design data book – P.S.G. College of technology.
- [11]. Design data book – K.Mahadevan & K.Balaveera Reddy.
- [12]. Analysis and approximation of contact problem By Mircea Sofonia and Weimin Hann
- [13]. Elastic contact analysis by boundary elements By Susumu Takahashi
- [14]. "A comprehensive analysis of fillet and contact stresses in straight spur gears" By M.A. Alfares
- [15]. www.cs.cmu.edu/People/rapidproto/mechanisms/references.html
- [16]. Mechanical Engg design – Joseph E. Shigley.
- [17]. Design data book – P.S.G. College of technology.
- [18]. Design data book – K.Mahadevan & K.Balaveera Reddy.
- [19]. Analysis and approximation of contact problem
- [20]. By Mircea Sofonia and Weimin Hann
- [21]. Elastic contact analysis by boundary elements
- [22]. By Susumu Takahashi
- [23]. "A comprehensive analysis of fillet and contact stresses in straight spur gears" By M.A. Alfares
- [24]. International Journal of Computer Applications in Technology 2001 - Vol. 14, No.1/2/3 pp. 109-116

Facial Emotion Recognition in Videos Using Hmm

Rani R. Pagariya¹, Mahip M. Bartere²

¹ M.E (2nd sem. CSE), GHRCEM, Amravati,

² Lecturer in CSE Dept. at GHRCEM, Amravati

ABSTRACT:

Human computer interaction is an emerging field in computer science. It is said that for a computer to be intelligent it must interact with human the way human and human interact. Human mainly interact through speech along with that it interact through physical gestures and postures which mainly include facial expressions. This paper discusses what the facial expressions are, the needs of recognizing the facial expression, and how to recognize the facial expression? Two such methods of recognizing the facial expressions using HMM are provided. One is Emotion Recognition from Facial Expressions using Multilevel HMM and another one compute a derivative of features with histogram differencing and derivative of Gaussians and model the changes with a hidden Markov model.

Keywords: Derivatives, Emotion, Facial expression, Features, Hidden Markov Models, State sequence, ML classifier.

I. INTRODUCTION

Emotion plays an important role in human life. At different movements of time human faces reflects differently with different intensity, which reflects there mood. Facial features and expressions are critical to everyday communication. Besides speaker recognition, face assists a number of cognitive tasks: for example, the shape and motion of lips forming visemes can contribute greatly to speech comprehension in a noisy environment. While intuition may imply otherwise, social psychology research has shown that conveying messages in meaningful conversations can be dominated by facial expressions, and not spoken words. This result has led to renewed interest in detecting and analyzing facial expressions in not just extreme situations, but also in everyday human-human discourse. [1] There are different six facial expressions considered over here: happy, angry, surprise, disgust, fear, sad. And evaluate using HMM.

II. LITERATURE SURVEY:

The origins of facial expression analysis go back into the 19th century, when Darwin originally proposed the concept of universal facial expressions in man and animals. Since the early 1970s, Ekman and Friesen (1975) have performed extensive studies of human facial expressions, providing evidence to support this universality theory. These 'universal facial expressions' are those representing happiness, sadness, anger, fear, surprise, and disgust. To prove this, they provide results from studying facial expressions in different cultures, even primitive or isolated ones. These studies show that the processes of expression and recognition of emotions on the face are common enough, despite differences imposed by social rules. Ekman and Friesen used FACS to manually describe facial expressions, using still images of, and usually extreme, facial expressions. This work inspired researchers to analyze facial expressions by tracking prominent facial features or measuring the amount of facial movement, usually relying on the 'universal expressions' or a defined subset of them. In the 1990s, automatic facial expression analysis research gained much interest, mainly thanks to progress, in the related fields such as image processing (face detection, tracking and recognition) and the increasing availability of relatively cheap computational power.

In one of the ground-breaking and most publicized works, Mase and Pentland (1990) used measurements of optical flow to recognize facial expressions. In the following, Lanitis et al. used a flexible shape and appearance model for face identification, pose recovery and facial expression recognition. Black and Yacoob (1997) proposed local parameterized models of image motion to recover non-rigid facial motion, which was used as input to a rule-based basic expression classifier; Yacoob and Davis (1996) also worked in the same framework, this time using optical flow as input to the rules. Local optical flow was also the basis of Rosenblum's work, utilizing a radial basis function network for expression classification. Otsuka and Ohya utilized the 2D Fourier transform coefficients of the optical flow as feature vectors for a hidden Markov model(HMM).

Regarding feature-based techniques, Donato, Bartlett, Hager, Ekman, and Sejnowski (1999) tested different features for recognizing facial AUs and inferring the facial expression in the frame. Oliver et al. tracked the lower face to extract mouth shape information and fed them to an HMM, recognizing again only universal expressions [1].

III. HIDDEN MARKOV MODEL

The Hidden Markov Model (HMM) is a powerful statistical tool for modeling generative sequences that can be characterized by an underlying process generating an observable sequence. HMMs have found application in many areas interested in signal processing, and in particular speech processing, but have also been applied with success to low level NLP tasks such as part-of-speech tagging, phrase chunking, and extracting target information from documents. Andrei Markov gave his name to the mathematical theory of Markov processes in the early twentieth century, but it was Baum and his colleagues that developed the theory of HMMs in the 1960[2]. A hidden Markov model (HMM) is a statistical Markov model in which the system being modeled is assumed to be a Markov process with unobserved (*hidden*) states. An HMM can be considered as the simplest dynamic Bayesian network.

Markov Processes fig1 depicts an example of a Markov process. The model presented describes a simple model for a stock market index. The model has three states, Bull, Bear and Even, and three index observations up, down, unchanged. The model is a finite state automaton, with probabilistic transitions between states. Given a sequence of observations, example: up-down-down we can easily verify that the state sequence that produced those observations was: Bull-Bear-Bear, and the probability of the sequence is simply the product of the transitions, in this case $0.2 \times 0.3 \times 0.3$ [2].

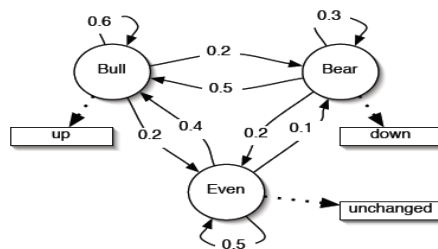


Figure 1: Markov process example[1]

The Markov property guarantees that the future evolution of the process depends only on its present state, and not on its past history [3].Hidden Markov Models Diagram 2 shows an example of how the previous model can be extended into a HMM. The new model now allows all observation symbols to be emitted from each state with a finite probability. This change makes the model much more expressive and able to better represent our intuition, in this case, that a bull market would have both good days and bad days, but there would be more good ones.

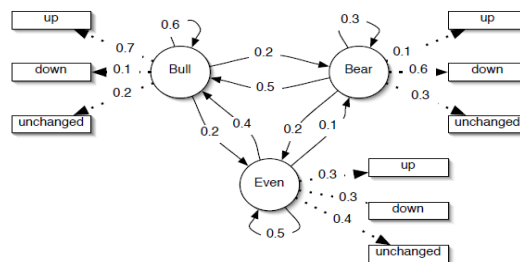


Figure 2: hmm

The key difference is that now if we have the observation sequence up-down-down then we cannot say exactly what state sequence produced these observations and thus the state sequence is ‘hidden’. We can however calculate the probability that the model produced the sequence, as well as which state sequence was most likely to have produced the observations. The next three sections describe the common calculations that we would like to be able to perform on a HMM. The formal definition of a HMM is as follows:

$$\lambda = (A, B, \pi) \tag{1}$$

S is our state alphabet set, and V is the observation alphabet set:

$$S = (s_1, s_2, \dots, s_N) \quad (2)$$

$$V = (v_1, v_2, \dots, v_M) \quad (3)$$

We define Q to be a fixed state sequence of length T, and corresponding observations O:

$$Q = q_1, q_2, \dots, q_T \quad (4)$$

$$O = o_1, o_2, \dots, o_T \quad (5)$$

A is a transition array, storing the probability of state j following state i. Note the state transition probabilities are independent of time:

$$A = [a_{ij}], a_{ij} = P(q_t = s_j | q_{t-1} = s_i) \quad (6)$$

B is the observation array, storing the probability of observation k being produced from the state j, independent of t:

$$B = [b_i(k)], b_i(k) = P(x_t = v_k | q_t = s_i) \quad (7)$$

π is the initial probability array:

$$\pi = [\pi_i], \pi_i = P(q_1 = s_i) \quad (8)$$

Two assumptions are made by the model. The first, called the Markov assumption, states that the current state is dependent only on the previous state, this represents the memory of the model:

$$P(q_t | q_1^{t-1}) = P(q_t | q_{t-1}) \quad (9)$$

The independence assumption states that the output observation at time t is dependent only on the current state, it is independent of previous observations and states:

$$P(o_t | o_1^{t-1}, q_1^t) = P(o_t | q_t) \quad (10) [3].$$

IV. METHODOLOGIES

4.1. Expression Recognition Using Emotion-Specific HMMs

Since the display of a certain facial expression in video is represented by a temporal sequence of facial motions it is natural to model each expression using an HMM trained for that particular type of expression. There will be six such HMMs, one for each expression: * *happy, angry, surprise, disgust, fear, sad* . There are several choices of model structure that can be used. The two main models are the left-to-right model and the ergodic model. In the left-to-right model, the probability of going back to the previous state is set to zero, and therefore the model will always start from a certain state and end up in an ‘exiting’ state. In the ergodic model every state can be reached from any other state in a finite number of time steps. Otsuka and Ohya used left-to-right models with three states to model each type of facial expression. The advantage of using this model lies in the fact that it seems natural to model a sequential event with a model that also starts from a fixed starting state and always reaches an end state. It also involves fewer parameters, and therefore is easier to train. However, it reduces the degrees of freedom the model has to try to account for the observation sequence. There has been no study to indicate that the facial expression sequence is indeed modeled well by the left-to-right model. On the other hand, using the ergodic HMM allows more freedom for the model to account for the observation sequences, and in fact, for an infinite amount of training data it can be shown that the ergodic model will reduce to the left-to-right model, if that is indeed the true model. In this work both types of models were tested with various numbers of states in an attempt to study the best structure that can model facial expressions. The observation vector O_t for the HMM represents continuous motion of the facial action units. Therefore, B is represented by the probability density functions (pdf) of the observation vector at time t given the state of the model. The Gaussian distribution is chosen to represent these pdf’s, i.e.

$$B = \{b_i(O_t)\} \sim N(\mu_j, \Sigma_j), 1 \leq j \leq N \quad (11)$$

Where μ_j and Σ_j are the mean vector and full covariance matrix, respectively.

The parameters of the model of emotion-expression specific HMM are learned using the well-known Baum- Welch re estimation formulas For learning, hand labeled sequences of each of the facial expressions are used as ground truth sequences, and the Baum algorithm is used to derive the maximum likelihood (ML) estimation of the model parameters (λ)Parameter learning is followed by the construction of a ML classifier. Given an observation sequence O_t , where $t \in (1, T)$, the probability of the observation $P(O_t | \lambda_j)$ given

each of the six models is computed using the forward backward procedure .The sequence is classified as the emotion corresponding to the model that yielded the highest probability, i.e.

$$c^* = \underset{1 \leq c \leq 6}{\operatorname{argmax}} [P(O|\lambda_c)] \quad (12) [4, 5].$$

4.2. Automatic Segmentation and Recognition of Emotions Using Multilevel HMM.

The main problem with the approach taken in the previous section is that it works on isolated facial expression sequences or on presegmented sequences of the expressions P from the video. In reality, this segmentation is not available, and therefore there is a need to find an automatic way of segmenting the sequences. Concatenation of the HMMs representing phonemes in conjunction with the use of grammar has been used in many systems for continuous speech recognition. Dynamic programming for continuous speech has also been proposed in different researches. It is not very straightforward to try and apply these methods to the emotion recognition problem since there is no clear notion of language in displaying emotions. Otsuka and Ohya [4] used a heuristic method based on changes in the motion of several regions of the face to decide that an expression sequence is beginning and ending. After detecting the boundaries, the sequence is classified to one of the emotions using the emotion-specific HMM. This method is prone to errors because of the sensitivity of the classifier to the segmentation result. Although the result of the HMM's are independent of each other, if we assume that they model realistically the motion of the facial features related to each emotion, the combination of the state sequence of the six HMM's together can provide very useful information and enhance the discrimination between the different classes. Since we will use a left-to-right model (with return), the changing of the state sequence can have a physical attribute attached to it (such as opening and closing of mouth when smiling), and therefore there we can gain useful information from looking at the state sequence and using it to discriminate between the emotions at each point in time.

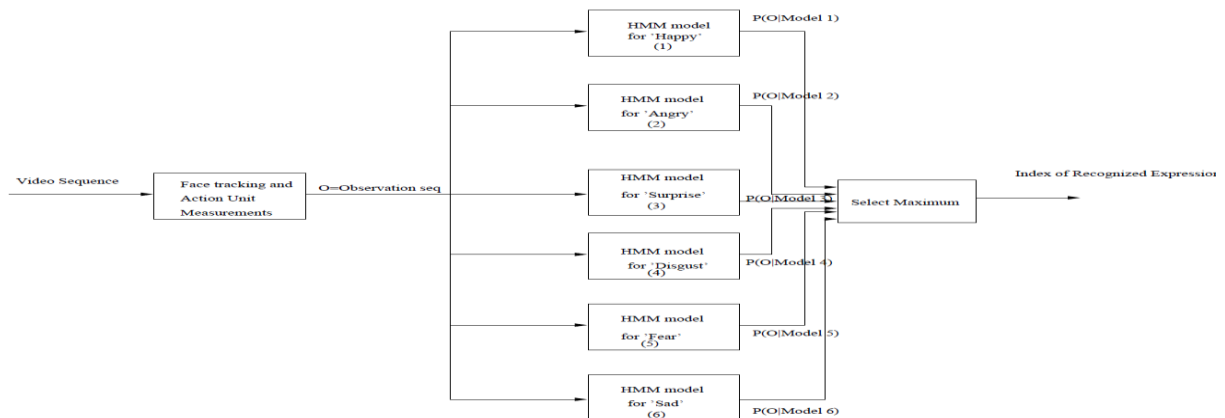


Figure 3: Maximum likelihood classifier for emotion specific HMM

To solve the segmentation problem and enhance the discrimination between the classes, a different kind of architecture is needed. Figure 4 shows the proposed architecture for automatic segmentation and recognition of the displayed expression at each time instance. As can be seen, the motion features are fed continuously to the six emotionsspecific HMMs. The state sequence of each of the HMMs is decoded and used as the observation vector for the high- level HMM. The high-level HMM consists of seven states, one for each of the six emotions and one for *neutral*. The *neutral* state is necessary as for the large portion of time, there is no display of emotion on a person's face. The transitions between emotions are imposed to pass through the *neutral* state since it is fair to assume that the face resumes a neutral position before it displays a new emotion. For instance, a person cannot go from expressing happy to sad without returning the face to its neutral position (even for a very brief interval). The recognition of the expression is done by decoding the state that the high-level HMM is in at each point in time since the state represents the displayed emotion. To get a more stable recognition, output of the classifier will actually be a smoothed version of the state sequence, i.e., the high-level HMM will have to stay in a particular state for a long enough time in order for the output to be the emotion related to that state.

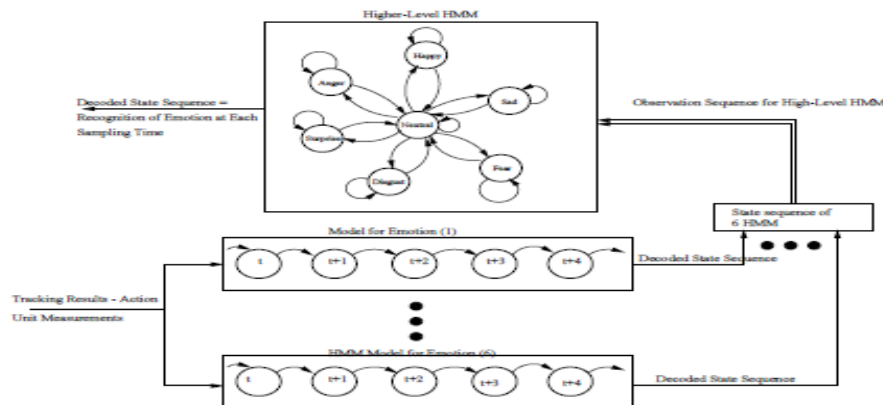


Figure4: Multilevel HMM architecture for automatic segmentation and recognition of emotion

The training procedure of the system is as follows:

- Train the emotion-specific HMMs using a hand segmented sequence as described in the previous section.
- Feed all six HMMs with the continuous (labeled) facial expression sequence. Each expression sequence contains several instances of each facial expression with *neutral* instances separating the emotions.
- Obtain the state sequence of each HMM to form the six-dimensional observation vector of the higher-level HMM,

$$O_t^h = [q_t^{(1)}, \dots, q_t^{(6)}]^T \quad (13)$$

where q_t^i is the state of the i th emotion-specific HMM. The decoding of the state sequence is done using the Viterbi algorithm [8].

- Learn the probability observation matrix for each state of the high-level HMM using $P(q_j^{(i)}|S_k) = \{ \text{expected frequency of model } i \text{ being in state } j \text{ given that the true state was } k \}$ and,

$$B^{(h)} = \{b_k(O_t^h)\} = \left\{ \prod_{i=1}^6 (P(q_j^{(i)}|S_k)) \right\} \quad \text{where } j \in (1, \text{Number of States for Lower Level HMM}). \quad (14)$$

- Compute the transition probability $A = \{a_{kl}\}_l$ of the high-level HMM using the frequency of transiting from each of the six emotion classes to the *neutral* state in the training sequences and from the *neutral* state to the other emotion states. For notation, the *neutral* state is numbered 7, and the other states are numbered as in the previous section. It should be noted that the transition probabilities from one emotion state to another that is not *neutral* are set to zero.
- Set the initial probability of the high-level HMM to be 1 for the *neutral* state and 0 for all other states. This forces the model to always start at the *neutral* state and assumes that a person will display a *neutral* expression in the beginning of any video sequence. This assumption is made just for simplicity of the testing.

The steps followed during the testing phase are very similar to the ones followed during training. The face tracking sequence is fed into the lower-level HMMs and a decoded state sequence is obtained using the

Viterbi algorithm. The decoded lower-level state sequence O_t^h is fed into the higher-level HMM and the observation probabilities are computed using equation. Note that in this way of computing the probability, it is assumed that the state sequences of the lower-level HMMs are independent given the true labeling of the sequence. This assumption is reasonable since the HMMs are trained independently and on different training sequences. In addition, without this assumption, the size of B will be enormous, since it will have to account for all possible combinations of states of the six lower-level HMMs, and it would require a huge amount of training data. Using the Viterbi algorithm again for the high-level HMM, a most likely state sequence is produced. The state that the HMM was in at time t corresponds to the expressed emotion in the video sequence at time t . To make the classification result robust to undesired fast changes, a smoothing of the state sequence is done by not changing the actual classification result if the HMM did not stay in a particular state for more than T times,

where T can vary between 1 and 15 samples (assuming a 30-Hz sampling rate). The introduction of the smoothing factor T will cause a delay in the decision of the system, but of no more than T sample times [4].

4.3. Facial Emotion Recognition by Computing Derivatives of Features.

The system overview is shown in Fig:

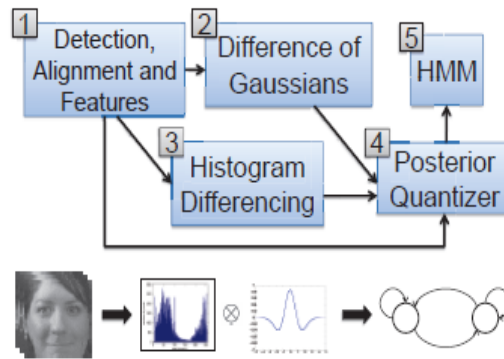


Figure 5: overview of system.

(1)Face ROI is detected with a boosted cascade of Haar-like features, aligned with SIFT Flow to a reference image, and Local Phase Quantization (LPQ) texture features are extracted. The derivatives of features are estimated with two methods: (2) with a fine spatial granularity with Difference of Gaussians (DoG) and (3) with a course spatial granularity with histogram differencing (HD) of LPQ histograms. (4) A support vector machine (SVM) outputs posterior probabilities for emotion labels from each of the three feature vectors and yhe posterior probabilities are quantized into a single observation vector. (5) A hidden Markov model computes the optimal emotion labels, taking of advantage of the co-occurrences between $x(t)$ and $x'(t)$. Where T is the length of the video. U has m_i observable symbols.

4.3.1. Detection, Alignment and Features

Faces are extracted with a boosted cascade of Haar-like features. After extraction, faces are aligned with SIFT Flow to the Avatar Reference Image . The parameters of this algorithm are the number of iterations I . After alignment, LPQ histograms are extracted in each of $n \times n$ local regions and the histograms are concatenated to form the feature vector (this process is also called cells, or gridding).

4.3.2. Modeling Temporal Changes

The derivative of features $x'(t)$ is approximated by two methods: convolution with a DoG filter and difference of feature histograms. DoG has a fine spatial granularity, in that it captures local changes happening at the pixel. Histogram differencing has a course spatial granularity, in that captures global changes happening between the histograms of each cell. **Local derivatives with DoG:** A DoG filter is employed as opposed to a finite difference because the finite difference is sensitive to noise. The i -th feature $\langle x(t) \rangle_i$ is convolved with the DoG filter to approximate the gradient of $x(t)$ with the following equation:

$$\langle x'_{DoG}(t) \rangle_i \approx \langle x(t) \rangle_i \otimes h(t) \quad (15)$$

Where $h(t) \sim N(0, \sigma_1) - N(0, \sigma_2)$ and $\sigma_1 = 4\sigma_2$.

The effect of Eq. 1 is a 1-D temporal gradient of $\langle x(t) \rangle_i$ that has been low-pass filtered to remove noise. $h(t)$ is discretized to $2l$, where $3\sigma_2 = l$, retaining approx. 99% of the energy of the larger Gaussian.

Global derivatives with HD: Let the feature vector $x(t)$ be composed of a set of n^2 histograms $\{H_1(t), H_2(t), \dots, H_{n^2}(t)\}$. The histogram difference is computed with the L_1 metric, for each histogram, between $t - \delta$ and $t + \delta$. This is similar to shot transition detection for key frames, except the histogram of features is used, as opposed to color histograms. A new feature vector $x'_{HD}(t) \in \mathbb{R}^{1 \times n^2}$ is generated where:

$$\langle x'_{HD}(t) \rangle_i = \|H_i(t - \delta) - H_i(t + \delta)\|_1 \quad (16)$$

Where $H_i(t)$ is the i -th histogram at time t , and δ is a spacing parameter.

Observation quantization: A linear SVM is trained to output posterior probabilities. Let $\tilde{w}_i(t)$ be the estimated label at time t from a matcher using the i -th feature set. We hypothesize that a co-occurrence exists,

where the feature derivatives perform better when emotion is weak or transitioning, e.g. $\tilde{w}_{DoG}(t)$ would properly classify t_0 in Fig. 1, and $\tilde{w}_{LPQ}(t)$ would not. The output of the SVM must be fused in such a way as to capture the combination of outputs of the SVM. First, the posterior probabilities across all videos for each matcher are quantized into m bins with k -means clustering. Let $v_i(t)$ be the set of membership of $\tilde{w}_i(t)$ at time t , ranging from 0 to $m - 1$. Second, the quantized probabilities $v_i(t)$ of each matcher are combined into a single observation matrix. Let $u(t)$ be the combined, quantized observation at time t :

$$u(t) = \sum_{i=1}^n m^{(i-1)} v_i(t) \quad (17)$$

Where n is the number of different matchers. Let U be the observation sequence defined as:

$$U = \{\mathbf{u}(t) : 0 < t \leq T\} \quad (18)$$

Hidden Markov Model: Co-occurrence aware fusion is realized with a Hidden Markov model (HMM). We formulate out HMM as follows: given the observation sequence U , and the HMM, optimal corresponding state sequence $Y = y(0) y(1) \dots y(T)$ must be chosen. Y is taken to be the estimated labels; the number of states of the model is equal to the number of classes p . The state transition probability distribution matrix A and observation probability distribution matrix B are estimated from training data. We assign labels with:

$$Y = \operatorname{argmax}_{y(0) \dots y(T)} p(y(0) \dots y(T), \dots) \quad U | \lambda(A, B) \quad (19)$$

Where λ is the model. Above equation is solved with dynamic Programming, with the Viterbi algorithm. Because the joint probabilities of the matchers are estimated, the model can fuse information from each matcher in a more meaningful way, as opposed to simply aggregating the labels [6].

V. APPLICATIONS

Facial emotion recognition has applications in: Facial emotion recognition has applications in medicine [6] in treatment of Asperger. Asperger syndrome (AS), is an autism spectrum disorder (ASD) that is characterized by significant difficulties in social interaction, alongside restricted and repetitive patterns of behavior and interests. It differs from other autism spectrum disorders by its relative preservation of linguistic and cognitive development. Although not required for diagnosis, physical clumsiness and atypical (peculiar, odd) use of language are frequently reported. So it is easy to recognize the facial expressions than language. It has application in video games [6] such as Xbox Kinect. Kinect is a motion sensing input device by Microsoft for the Xbox 360 video game console and Windows PCs. Based around a webcam-style add-on peripheral for the Xbox 360 console, it enables users to control and interact with the Xbox 360 without the need to touch a game controller, through a natural user interface using gestures and spoken commands. Most important use of any facial emotion technique is human-computer interaction to make intelligent tutoring systems and Affective computing [6] is the study and development of systems and devices that can recognize, interpret, process, and simulate human affects. The machine should interpret the emotional state of humans and adapt its behavior to them, giving an appropriate response for those emotions.

VI. CONCLUSION:

In this paper method for emotion recognition from video sequences of facial expression were explored. For facial emotion recognition where a subject can freely express emotions, a derivative of features was more suitable than using the features themselves. While Emotion-specific HMM, relied on segmentation of a continuous video into sequences of emotions (or neutral state), multilevel HMM, performed automatic segmentation and recognition from a continuous signal. By giving feedback to the computer, a better interaction can be achieved. This can be used in many ways. For example, it can help in education by helping children learn effectively with computers. Among the both above methods multilevel HMM is easy as compared to derivative of features.

REFERENCES

- [1] Spiros V. Ioannou, Amaryllis T. Raouzaoui, Vasilis A. Tzouvaras, Theofilos P. Mailis, Kostas C. Karpouzis, Stefanos D. Kollias "Emotion recognition through facial expression analysis based on a neurofuzzy network". Special Issue, Greece, 2005.
- [2] "Phil Blunsom." Hidden Markov Models" August 19, 2004.
- [3] Ramon van Handel "Hidden Markov Models" Lecture Note July 28, 2008.
- [4] Ira Cohen, Ashutosh Garg, Thomas S. Huang Beckman Institute for Advanced Science and Technology "Emotion Recognition from Facial Expressions using Multilevel HMM".

- [5] Ira Cohen, Nicu Sebe , Larry Chen , Ashutosh Garg, Thomas S. Huang. Beckman Institute for Advanced Science and Technology, University of Illinois at Urbana “Facial Expression Recognition from Video Sequences: Temporal and Static Modeling”.
- [6] Albert Cruz, Bir Bhanu and Ninad Thakoor.” Facial Emotion Recognition in Continuous Video” 21st International Conference on Pattern Recognition (ICPR 2012) November 11-15, 2012. Tsukuba, Japan.
- [7] L. S. Chen. “Joint processing of audio-visual information for the recognition of emotional expressions in human-computer interaction.”PhD thesis, University of Illinois at Urbana-Champaign, Dept. of Electrical Engineering, 2000.
- [8] Dilbag Singh “Human Emotion Recognition System” I.J. Image, Graphics and Signal Processing, 2012, 8, 50-56 Published Online August 2012 in MECS.
- [9] V.V. Starovoitov, D.I Samal, D.V. Briliuk “Three Approaches For Face Recognition” The 6-th International Conference on Pattern Recognition and Image Analysis October 21-26, 2002, Velikiy Novgorod, Russia, pp. 707-711.
- [10] Kwang-Eun Ko, Kwee-Bo Sim “Development of a Facial Emotion Recognition Method based oncombining AAM with DBN” 2010 International Conference on Cyberworlds.
- [11] Mohammad Ibrahim Khan and Md. Al-Amin Bhuiyan “Facial Expression Recognition for Human-Robot Interface” IJCSN, VOL.9 No.4, April 2009.
- [12] Mayur S. Burange, S. V. Dhopte “Neuro Fuzzy Model for Human Face Expression Recognition” IJEAT ISSN: 2249 – 8958, Volume-1, Issue-5, June 2012.

Unique and Low Cost Airport Multi-Application Control System

¹,Adnan Affandi , ²Mubashshir Husain

^{1,2},Electrical and Computer Engineering Department, King Abdul Aziz University P.O. BOX: 80204, Jeddah 21589

ABSTRACT

This paper presents the design and implementation of an integrated computer based multi-purpose control system for airports. The system provides three main functions for the airport uthorities. The first function is the Airport Paging System which is an automatic paging system that will automatically announce user specified messages at specified times relating to the departure and arrival times of flights. This function will also allow for manual use of the paging system. The second function is the Airport Gate Monitor which is an automatic system that will monitor the airport gate and take photos of each person entering the gate. These photos are then are archived with date and time tag for security needs. The third function is the Passport Line Control which allows the airport authorities to monitor and activate the passport lines according to their needs. This paper consist of the software part which is developed using MATLAB and the hardware witch is developed using a personal computer, electronic circuits, and USB camera.

I. INTRODUCTION

Computer based control systems are very useful in our everyday life. We can use computer to control almost everything around us. It is also possible to use the computer to monitor an area for some critical situation. An example of such a situation is the main gate of an airport where it is important to keep photos of the persons entering the airport for security reasons. Another example is to use the computer based control system to control the sound paging system in the airport where departure and arrival flight information need to be announced at specific times. Computer based control systems are also useful for control of queue lines. The system can be used to activate any line by clicking a button on the computer screen. This paper presents the design and implementation of an integrated computer based multi-purpose control system for airports. The system provides 3 main functions for the airport authorities. The first function is the AIRPORT PAGING SYSTEM which is an automatic paging system that will automatically announce user specified messages at specified times relating to the departure and arrival times of flights.

This function will also allow for manual use of the paging system. The second function is the AIRPORT GATE MONITOR which is an automatic system that will monitor the airport gate and take photos of each person entering the gate. These photos are then archived with date and time tag for security needs. The third function is the PASSPORT LINE CONTROL which allows the airport authorities to monitor and activate the passport lines according to their needs.

The paper consist of the software part which is developed using MATLAB and the hardware witch is developed using a personal computer, electronic circuits, and USB camera. The control programs will provide the users of this system with graphical user interfaces (GUIs) that allow the users to operate the different functions of this system easily.

II. AIRPORT PAGING SYSTEM

The AIRPORT PAGING SYSTEM which is an automatic paging system that will automatically announce user specified messages at specified times relating to the departure and arrival times of flights. In order to implement this function, the system will require both hardware and software parts. Figure 1.1 shows a diagram that illustrates the function of the AIRPORT PAGING SYSTEM.

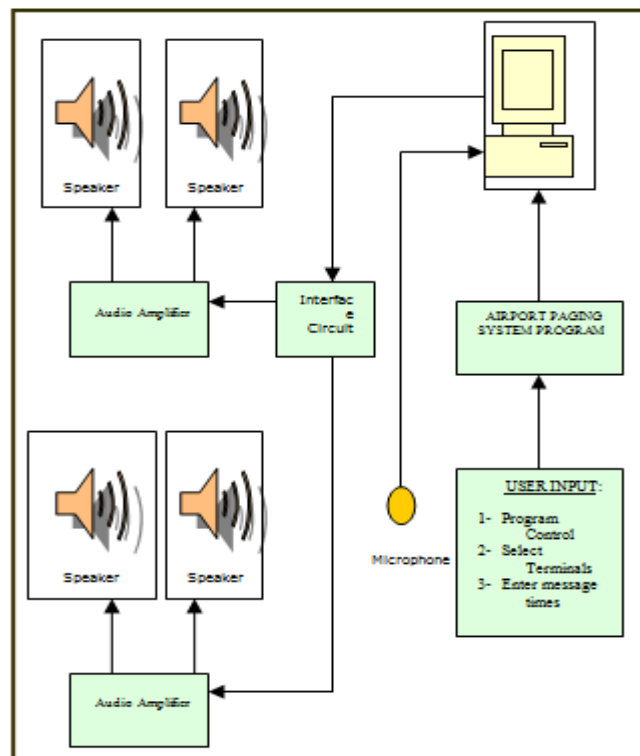


Figure 1.1: Airport Paging System

The AIRPORT PAGING SYSTEM will consist of 2 audio amplifiers each driving two speakers. One pair of speakers is located in the departure terminal and the other pair is located in the arrival terminal. The audio amplifiers are controlled by the computer so that they can be turned ON/OFF at the required times. The audio signals are produced at the sound card of the computer and fed to the inputs of the audio amplifiers. The user can select the terminals to which each message is directed and the time at which the message is played. An alternative solution for the Automatic Airport Paging System is to use manual functions for example the paging system can be operated by a person who will announce the different messages by himself according to the flights schedule. This solution will require an operator.[2]

III. AIRPORT GATE MONITOR SYSTEM

The AIRPORT GATE MONITOR which is an automatic system that will monitor the airport gate and take photos of each person entering the gate. These photos are then archived with date and time tags for security needs. Figure 1.2 shows a diagram of the AIRPORT GATE MONITOR SYSTEM.[1]

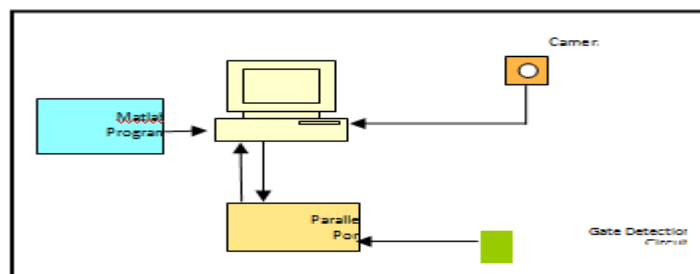


Figure 1.2: Airport Gate Monitor System

An alternative solution to the Gate Monitor System is to use a video camera with recording capabilities to continuously record the movement at the gate and record it for security use. This solution will need expensive video camera and video recording sets with expensive recording tapes.

IV. PASSPORT LINE CONTROL SYSTEM

The PASSPORT LINE CONTROL which allows the airport authorities to monitor and activate the passport lines according to their needs. Figure 1.3 shows a diagram of the PASSPORT LINE CONTROL SYSTEM.

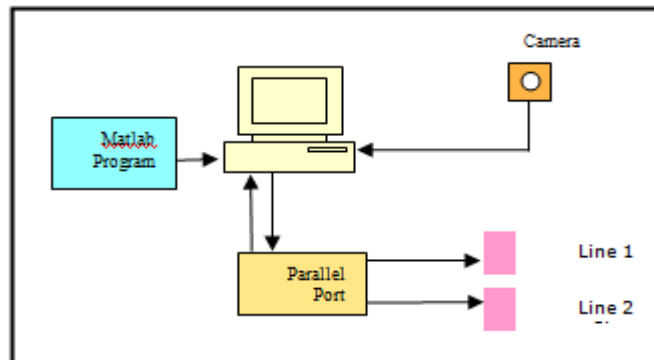


Figure 1.2: Airport Gate Monitor System

An alternative solution to the Passport Line Control System is to operate the lines manually by watching the number of people in the queue and switching the line sign accordingly.

V. PAPER ELEMENTS AND STEPS

The following work steps were performed during the course of this paper.

5.1 Hardware Part:

- [1] Test and understand the computer parallel port, its pin out, and the different voltage levels appearing on them
- [2] Test and understand the image acquisition functions required to control the USB camera.
- [3] Design, build and test interface between the computer parallel port and the other parts in the system.
- [4] Design, build and test the interface circuits needed to control the audio amplifiers used in the paper.
- [5] Design and build a gate pass detection circuit using infrared transmitter and receiver and make necessary interfacing for them.
- [6] Build a complete working prototype model for the system for the purpose of testing and demonstration.

5.2 Software Part:

- [1] Review of Matlab programming and control functions using the Digital Input/Output functions from the Data Acquisition tool box. The different functions used to operate the camera and the audio output were tested and verified to work correctly.
- [2] Design, write, and test a complete set of programs that will provide automatic monitoring of the gate and the USB camera. And, provide the control functions of the camera.
- [3] Design and test a graphical user interface program (GUI) that provides an easy interface to the user where the user orders are executed by clicking on pushbuttons on the computer screen.
- [4] Obtain a suitable USB camera with its driver to be used in the paper as the monitoring camera.

5.3 Hardware Part

The hardware requirements for each of the three parts of this paper are listed below.

5.3.1 AIRPORT PAGING SYSTEM

- [1] Two audio power amplifier with 4 speakers and connections
- [2] Interface circuit to control the audio amplifiers by switching them ON / OFF
- [3] Microphone
- [4] Power supply circuit.

5.3.2 AIRPORT GATE MONITOR

- [1] Gate Pass Detection Circuit which is an infrared detection circuit that will be used to detect if the gate is passed by someone along with the circuit interface to the computer parallel port.
- [2] Power supply circuit including a voltage regulator.
- [3] USB camera with driver and connections to be used in image acquisition.

5.3.3 PASSPORT LINE CONTROL

- [1] LED indicator for both lines with connections to the parallel port.
- [2] Parallel port connection that gives access to the required lines of the parallel port (Data and Status). This will allow the outside circuits to be interfaced to the parallel port

5.3.4 Audio Amplifier Circuit

The audio amplifier circuit is required to take the audio signal from the sound card and produce a higher power at the speakers. The larger the area to be covered by the audio the higher the required power of the audio amplifier needed. There are several audio power amplifier options. One option is to use an integrated circuit to build an audio amplifier. A famous chip for this purpose is the LM386. The LM386 is a power amplifier designed for use in low voltage consumer applications. The gain is internally set to 20 to keep external part count low, but the addition of an external resistor and capacitor between pins 1 and 8 will increase the gain to any value from 20 to 200. The inputs are ground referenced while the output automatically biases to one-half the supply voltage. The quiescent power drain is only 24 milliwatts when operating from a 6 volt supply, making the LM386 ideal for battery operation. Figure 5.1 shows a block diagram and pin configuration of the LM386 audio amplifier chip and figure 5.2 show the internal circuit diagram of the LM386 chip.

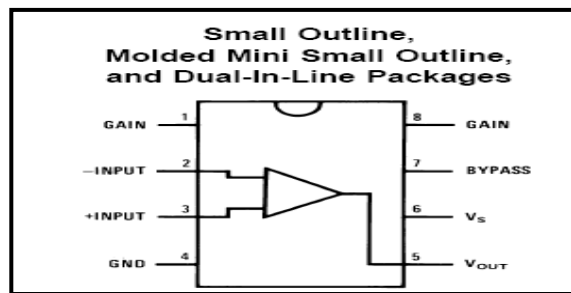


Figure 5.1: LM386 Audio Amplifier Chip

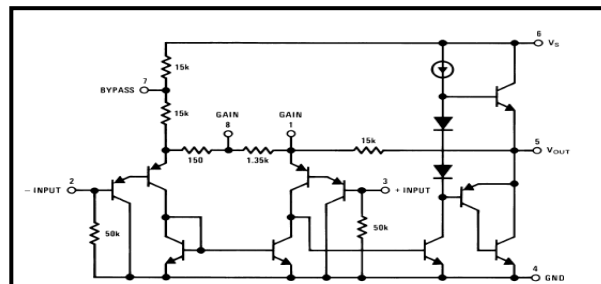


Figure 5.2: LM386 Audio Amplifier Circuit Diagram

Another option is to use a pre built audio amplifier circuits. This option will save time and will represent the actual situations in the airport because there will already be audio amplifier for the announcement of sound messages in the airport. Figure 5.3 shows a photo of the audio amplifier board used in this paper.



Figure 5.3: Audio Amplifier Board

5.3.5 Gate Pass Detection Circuit

An infrared detection circuit was designed and built to detect the presence or passage of a person through the airport gate. The detection signal will be connected to the parallel port of the computer for further processing. The circuit for the infrared detector is depicted in figure 5.4.

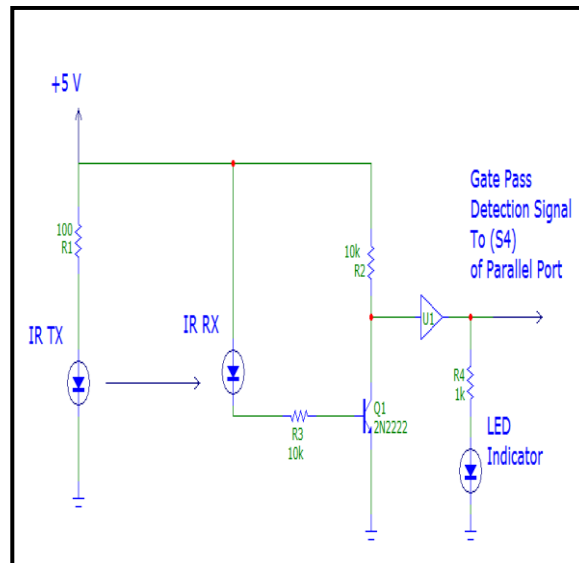


Figure 5.4: Circuit for Gate Pass Detection

The circuit consists of 2 parts, the infrared transmitter and the infrared receiver. The infrared transmitter section consists of a series connection of an infrared transmitter LED (IR transmitter) and a current limiting resistor. When current passes through the circuit, the IR transmitter will be ON and will produce an infrared beam. The infrared receiver section consists of an IR receiver LED that will drive a transistor circuit. The transistor used is the 2N2222A or any of its equivalence like the BCY 58. When power is ON and no IR ray, the IR receiver will not produce any current. This will keep the transistor OFF because no base current will flow and the collector will be at (HIGH) voltage. When IR ray is present at the IR receiver, a current will flow in the base of the transistor which will turn the transistor ON. This will take the collector point of the transistor to approximately 0 volt (LOW). The output of the IR detector will be taken at the collector of the transistor through a buffer gate which will prevent loading to the circuit and provide suitable interface for the digital input of the computer parallel port. A low voltage at the output indicates infrared path is not broken which means no body is detected. The presence of a body between the transmitter and the receiver will break the infrared path and the output will be high. The following table summarizes the output signal indication of the IR detector.

STATUS	IR Detector Output	LED Indicator
Body Present	High	ON
Body not present	Low	OFF

Table 5.1: IR Detector Output

5.3.6 Power Supply Circuit

The power supply circuit consists of a 5 volt voltage regulator and a non regulated power supply board. The power supply board provides 12 volts DC unregulated. Figure 5.5 shows a photo of the power supply board.



Figure 5.5: Power Supply Board

Since the circuits of this paper require regulated 5 volts DC supply, a voltage regulator is used. The voltage regulator used for this purpose is the AN7805 which is a 5 volt regulator from the 78xx series of regulators. The AN78xx series are 3-pin fixed positive output type monolithic voltage regulators. Stabilized fixed output voltage is obtained from unstable DC input voltage without using any external components. 11 types of fixed output voltage are available; 5V, 6V, 7V, 8V, 9V, 10V, 12V, 15V, 18V, 20V, and 24V. They can be used widely in power circuits with current capacity of up to 1A. Figure 5.6 shows the pi diagram of the 7805 regulator.

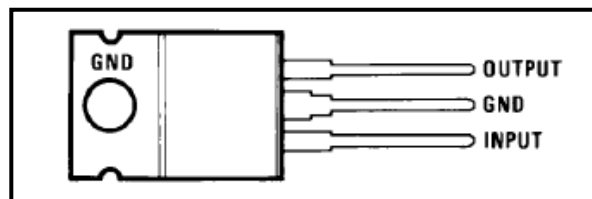


Figure 5.5: 7805 Regulator Pin Diagram

And figure 5.7 and 5.8 show a block diagram of the 7805 and a circuit diagram that shows how the 7805 regulator can be connected in a practical circuit.

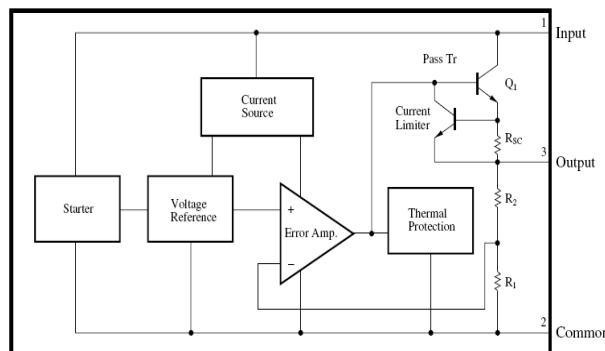


Figure 5.6: Block Diagram for The 7805 Regulator

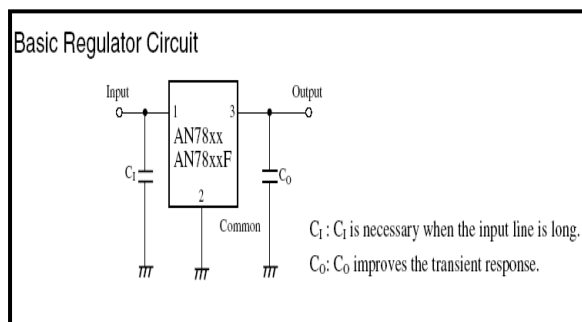


Figure 5.7: Connection Diagram for The 7805 Regulator

The complete power supply circuit is shown in figure 5.8. The capacitors used at the input and output of the regulator are to smooth and improve the DC. An LED indicator circuit is connected at the output of the regulator to provide indication of power ON or OFF.

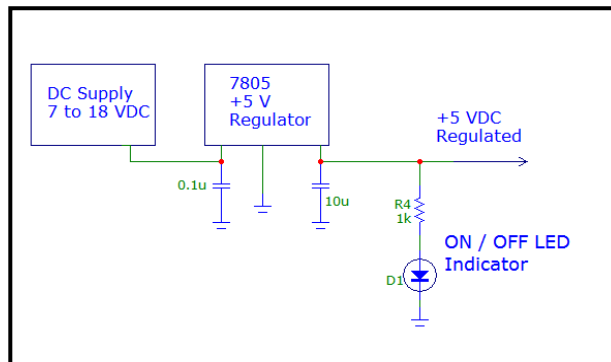


Figure 5.8: Power Supply and Regulator Circuit

5.3.7 Switching Circuit

Two switching circuits are used in this paper. The switching circuits are used to turn the Audio Amplifiers ON and OFF using logic signals from Pins D1 and D2 of the parallel port.

Figure 5.9 shows the switching circuit for the two audio amplifiers.

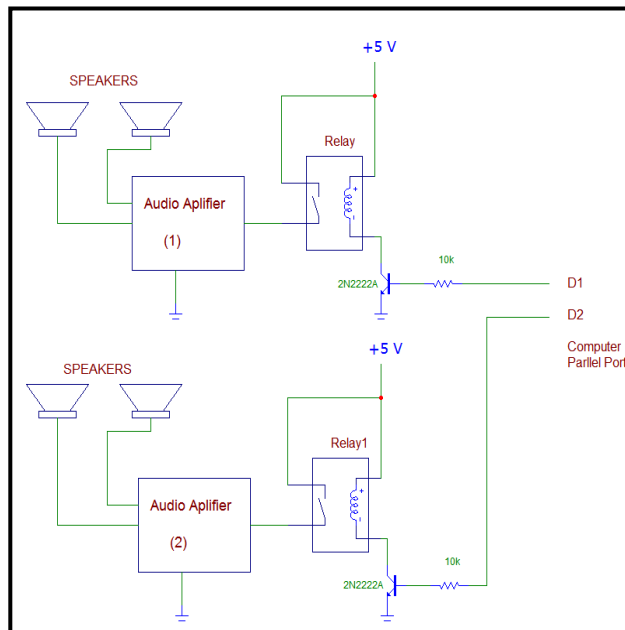


Figure 5.9: Switching Circuit for Audio Amplifiers

It is clear from the circuit diagram that when the input to the circuit from the parallel port is logic HIGH, the transistor will turn ON passing current through the relay magnet which will turn ON the audio amplifier. When the input to the circuit is logic LOW, the transistor is turned OFF which will turn OFF the relay and the relay contacts will be open turning the audio amplifier OFF. The relay used is a 5 V relay with contacts capable of handling the load.

5.3.8 Line Control Circuit

The passport line control circuit consists of two LED indicators with current limiting resistors. These two indicators are turned ON or OFF by the logic level coming from D3 and D4 of the parallel port. Figure 5.10 shows the circuit diagram for the Passport Line Control.

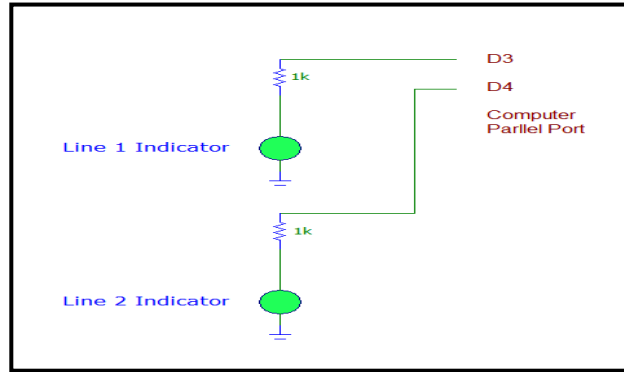


Figure 5.10: Line Control Circuit

The USB camera is also connected to the USB port to be controlled by the computer as needed.

5.3.9 Building paper Circuits

The complete paper circuit was built and each part is tested and verified to be working correctly. The circuits were built according to the design in the above sections. All electronic parts were obtained from local market. Figures 5.11 to 5.13 show the built circuits and model.

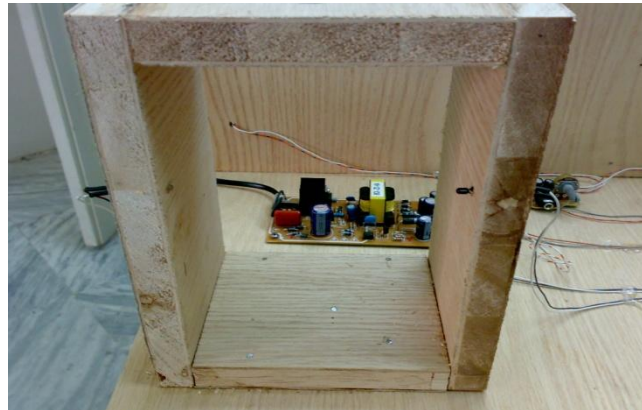


Figure 5.11: Prototype of Gate Pass Detection



Figure 5.13(a):Top view of a Part of Model

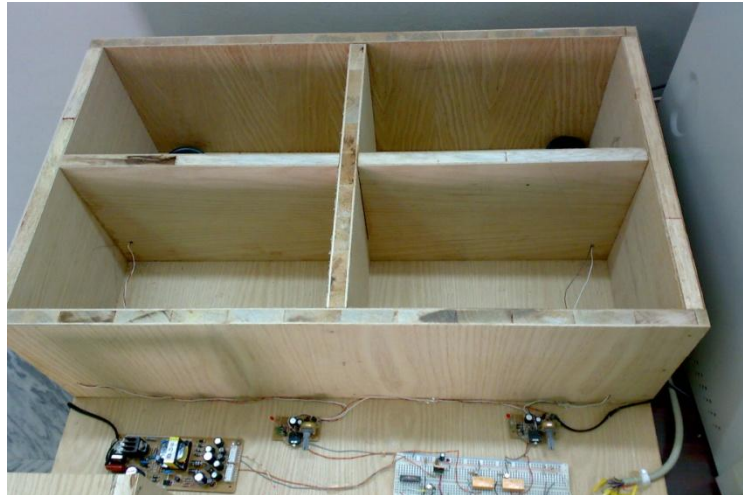


Figure 5.13(b): Top view of other part of Model

VI. SOFTWARE PART

6.1 Airport Control Program Requirement

The Airport Control Program has 4 Graphical User Interface parts that must be designed to provide the user with the following functions:

- [1] The first GUI (AIRPORT CONTROL SYSTEM) is the main one and its function is to allow the user to select one of the following functions:
(AIRPORT PAGING SYSTEM)
(AIRPORT GATE MONITOR)
(PASSPORT LINE CONTROL)
- [2] The second GUI (AIRPORT PAGING SYSTEM) allows the user to fully control the paging system of the airport.
- [3] The third GUI (AIRPORT GATE MONITOR) allows the user to fully control the gate monitoring system of the airport.
- [4] The fourth GUI (PASSPORT LINE CONTROL) allows the user to fully control the passport lines of the airport.

The following sections describe each of the GUIs and shows snapshots of them.

6.2 GUI (AIRPORT CONTROL SYSTEM)

The first GUI (AIRPORT CONTROL SYSTEM) is the main one and its function is to allow the user to select one of the function provided by this paper model.

Figure 6.1 shows a snapshot of the GUI.



The GUI allows the user to select one of the following functions: (AIRPORT PAGING SYSTEM), (AIRPORT GATE MONITOR), or (PASSPORT LINE CONTROL) by a bush button.

6.3 GUI (AIRPORT PAGING SYSTEM)

The (AIRPORT PAGING SYSTEM) GUI provide the user with full control of the airport paging system.

Figure 6.2 shows a snapshot of the GUI in its idle state.

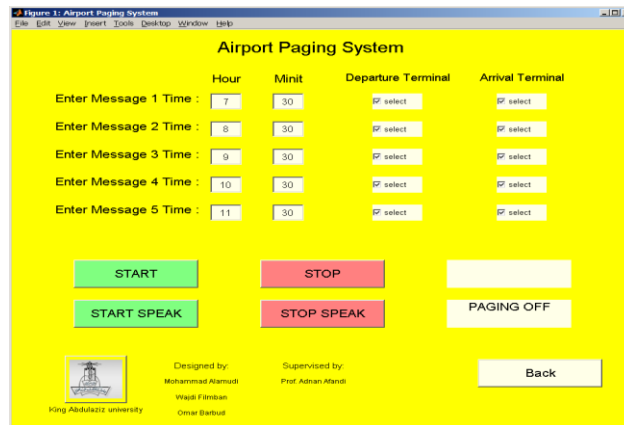


Figure 6.2: (AIRPORT PAGING SYSTEM) GUI – Idle

The (AIRPORT PAGING SYSTEM) GUI allows the user to select the terminals to which each of the five audio messages is directed. The two terminals are the Departure Terminal and the Arrival Terminal. The GUI has input fields to enter the time at which each of the messages is played. The GUI has push button to turn the automatic paging ON and OFF as shown in figure 6.2.



Figure 6.3: (AIRPORT PAGING SYSTEM) GUI – Auto Running

When the Start is pressed the system will continuously monitor the computer clock. When any of the message times is due, the system will play the corresponding message. In addition, the system will play the Azan when any of prayer time is due. The prayer times are calculated using a special prayer function. Figure 6.3 shows a snapshot of the (AIRPORT PAGING SYSTEM) GUI while running.

The GUI also allows the user to speak directly into the paging system if he wants. The (START SPEAK) (STOP SPEAK) buttons turn ON and OFF this feature. Figure 6.4 shows a snapshot of the GUI in the (START SPEAK) state.

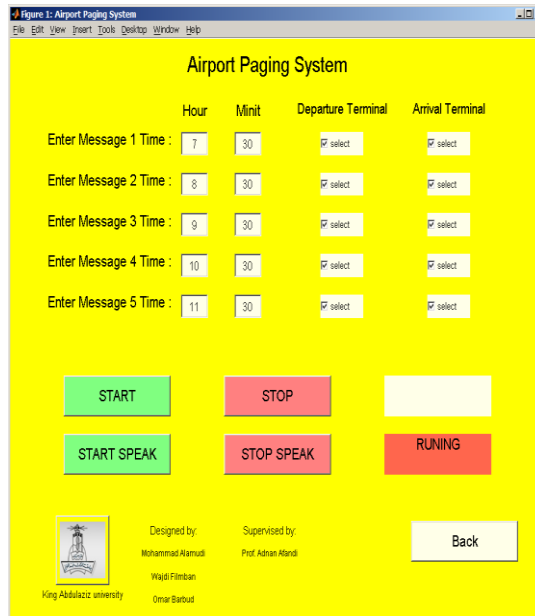


Figure 6.4: (AIRPORT PAGING SYSTEM) GUI – Start Speak

6.4 GUI (AIRPORT GATE MONITOR)

The (AIRPORT GATE MONITOR) GUI provide the user with full control of the airport gate monitor system. Figure 6.5 shows a snapshot of the GUI in its OFF state.

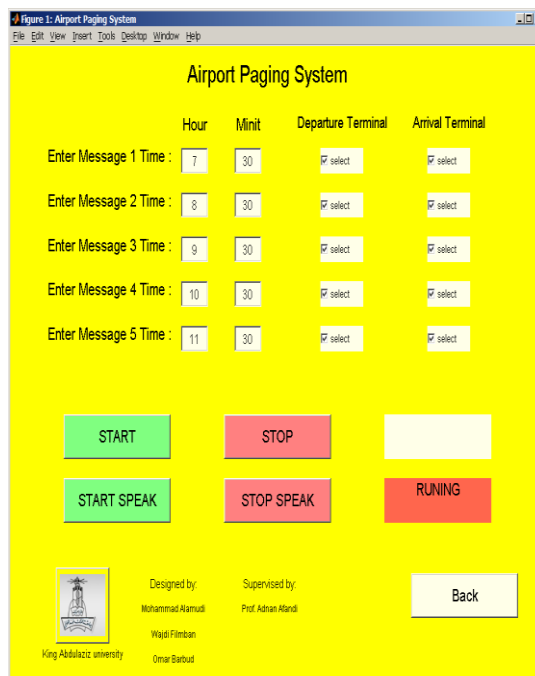
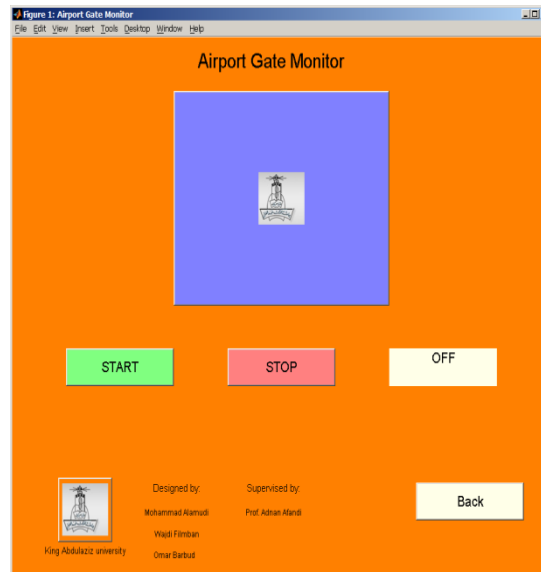


Figure 6.5: (AIRPORT GATE MONITOR) GUI – OFF State

When the (AIRPORT GATE MONITOR) is running, the computer will continuously monitor the gate pass circuit. When a person enters the gate, a digital signal is detected at the parallel port and the USB camera is turned ON.

The program will take a photo of the person entering the gate and post it in the GUI figure as shown I figures 6.6 to 6.8.



6.5 GUI (PASSPORT LINE CONTROL)

The (PASSPORT LINE CONTROL) GUI provide the user with full control of the passport lines. In this paper, 2 passport lines are assumed to exist. Each line has a light sign to indicate if it is active. The two signs are controlled by the user through the GUI. The GUI has 3 pushbuttons. 2 of them the (connect and disconnect) are used to activate the program or deactivate it. The third pushbutton is to turn ON the camera and see a live view of the passport lines so that the user can decide which line to activate. The GUI also provides 2 activation boxes, one for each line. Figure 6.10 shows a snapshot of the GUI at disconnect state and figure 6.11 shows a snapshot of the GUI at connect state with both lines activated.

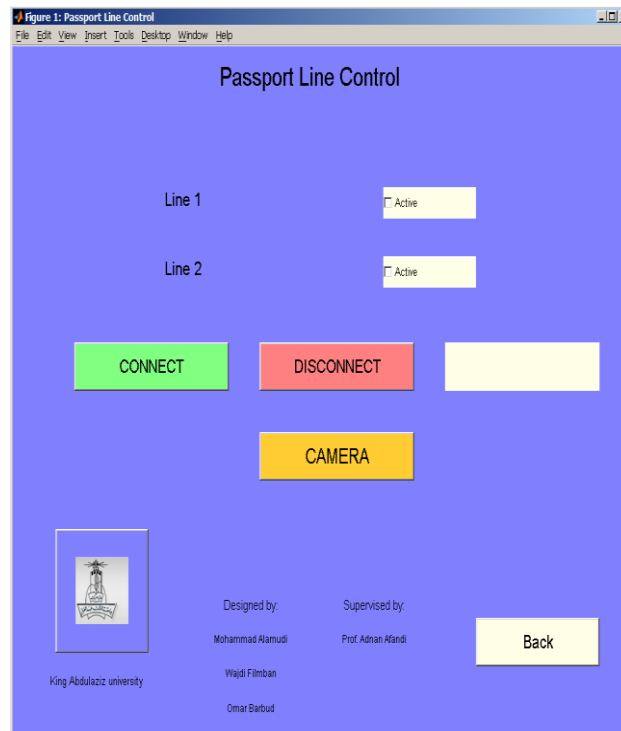


Figure 6.10: (PASSPORT LINE CONTROL) GUI – Disconnected State

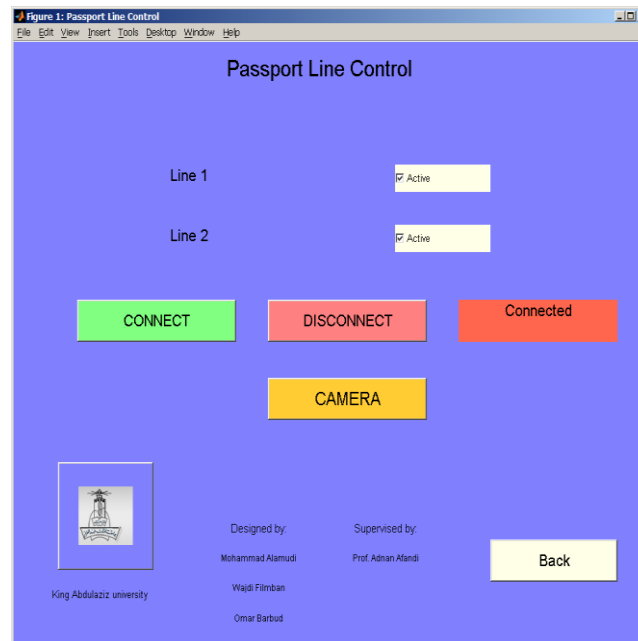


Figure 6.11: (PASSPORT LINE CONTROL) GUI – Connected

VII. CONCLUSION AND FUTURE DEVELOPMENT

This paper presents the design and implementation of an integrated computer based multi-purpose control system for airports. The system provides 3 main functions for the airport authorities. The first function is the AIRPORT PAGING SYSTEM which is an automatic paging system that will automatically announce user specified messages at specified times relating to the departure and arrival times of flights. This function will also allow for manual use of the paging system. The second function is the AIRPORT GATE MONITOR which is an automatic system that will monitor the airport gate and take photos of each person entering the gate. These photos are then archived with date and time tag for security needs. The third function is the PASSPORT LINE CONTROL which allows the airport authorities to monitor and activate the passport lines according to their needs. The paper consist of the software part which is developed using MATLAB and the hardware witch is developed using a personal computer, electronic circuits, and USB camera. A final demonstration model is built to test and verify the functionality of the system. As a future development, the system can be expanded to cover more passport lines. Other functions can be added to control airport systems.

REFERENCES :

- [1] Gunawan Sugiarta YB , Riyanto Bambang , Hendrawan And Suhardi, "Feature Level Fusion Of Speech And Face Image Based Person Identification System," Second International Conference On Computer Engineering And Applications ,2010
- [2] ANDREW S. ROBBINS,, "Operating And Maintenance Experiences With Automated People-Mover Microprocessor-Based Train Control" IEEE TRANSACTIONS ON INDUSTRY APPLICATIONS, VOL. 1A-22, NO. 3, MAY/JUNE 1986
- [3] [Http://Home.Cogeco.Ca/~Rpaisley4/Atdetir.Html](http://Home.Cogeco.Ca/~Rpaisley4/Atdetir.Html)
- [4] [Http://Www.Tkk.Fi/Misc/Electronics/Circuits/Irdetector.Html](http://Www.Tkk.Fi/Misc/Electronics/Circuits/Irdetector.Html)
- [5] [Http://Www.Airport-Int.Com/Categories/Airport-Security-System/Airport-Security-System.Asp](http://Www.Airport-Int.Com/Categories/Airport-Security-System/Airport-Security-System.Asp)
- [6] [Http://Www.Rose-Hulman.Edu/~Herniter/Data_Sheets/2N2222A.Pdf](http://Www.Rose-Hulman.Edu/~Herniter/Data_Sheets/2N2222A.Pdf)
- [7] [Http://Www.Lvr.Com/Parport.Htm](http://Www.Lvr.Com/Parport.Htm)
- [8] [Http://Www.Lvr.Com/Files/Ibmlpt.Txt](http://Www.Lvr.Com/Files/Ibmlpt.Txt)
- [9] Www.Findernet.Com/En/Products/Profiles.Php?Serie=30&Lang=En